SOVIET PHYSICS

JETP

A translation of the Journal of Experimental and Theoretical Physics of the USSR.

SOVIET PHYSICS JETP VOL. 35 (8), NO. 3, pp. 387-576 March, 1959

ENERGY DEPENDENCE OF THE ANGULAR CORRELATION OF POSITRONS FROM $\pi \to \mu \to e$ DECAY

Kh. P. BABAIAN, N. A. MARUTIAN, K. A. MATEVOSIAN, and M. G. SARINIAN

Physics Institute, Academy of Sciences, Armenian S.S.R.

Submitted to JETP editor February 13, 1958; resubmitted June 6, 1958

J. Exptl. Theoret. Phys. (U.S.S.R.) **35**, 561-564 (September, 1958)

The energy dependence of the angular correlation of positrons was investigated for 405 $\pi \to \mu \to e$ decay events in nuclear emulsion. The experimental energy dependence of the backward-forward ratio for the emitted positrons agrees with the predictions of the two-component neutrino theory.

LEE and Yang[1] have shown that nonconservation of parity leads to angular correlation in meson and hyperon decays and in various Fermi interactions. Landau[2] has suggested that in these interactions conservation of parity and of charge conjugation do not occur independently; instead we have conservation of "combined inversion," which is the product of space reflection and charge conjugation. The discovery of parity nonconservation has led to the two-component theory of the neutrino.[2-4]

Parity nonconservation in $\pi \to \mu$ decay results in polarization of the muon spin parallel or antiparallel to the direction of motion. Subsequent decay of the muon leads to angular asymmetry of positrons as a function of energy; this is given in the two-component neutrino theory by

$$dN = 2N\varepsilon^2 [(3-2\varepsilon) + \lambda \cos\theta\, (2\varepsilon - 1)]\, d\varepsilon\, d(\cos\theta), \qquad (1)$$

where ϵ is the ratio of the positron energy to the maximum possible energy, θ is the angle between the muon and positron directions, and λ is a theoretical constant ranging from -1 to $+1$.

The first article by Garwin and his coworkers[5] reported a slight increase of the asymmetry parameter with energy. The results given in their second article[6] are in quite good quantitative agreement with the two-component neutrino theory.

Vaisenberg and Smirnitskii[7] investigated the energy dependence of the asymmetry parameter in 120 $\pi \to \mu \to e$ decay events in the Ilford G5 emulsion and found qualitative agreement with the theory. In the second article by the same workers,[8] where 580 events have been studied, it is shown that the asymmetry parameter increases rapidly as the positron energy increases.

The present work was performed on part of a 9-liter stack of 600-μ Ilford G5 emulsions which were exposed in Italy for 6 to 7 hours at a height of ~27 km. We had previously[9] studied the angular distribution of positrons in 2160 $\pi \to \mu \to e$ decay events completed in a single layer, where the $\mu \to e$ decay occurred not less than 30 μ below the surface of the developed emulsion and the projection of the positron track in the plane of the emulsion was $\geq 15\,\mu$. The solid angle between the muon and positron tracks was determined to within 2°. For the asymmetry parameter we obtained

$$A = -(0.135 \pm 0.043).$$

For the purpose of determining the energy dependence of the asymmetry parameter, we selected events with positron tracks longer than 1000 μ, which were more than 1 cm distant from the edges of the plates (to avoid edge distortions). For 405 events which satisfied these requirements the dis-

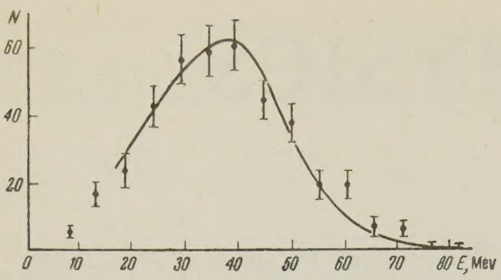

FIG. 1

tribution of positron track lengths was as follows:

Track length, mm	1–2	2–3	3–4	4–5	5–6	6–7	7–8	>8
Number of tracks	194	91	54	26	18	10	8	4

In determining positron energies by the multiple-scattering method for tracks $\leq 2000\,\mu$ the cell length was $50\,\mu$, while for longer tracks the cell length was $100\,\mu$. The positron energy was determined with an error which varied from 25% to 10% at the beginning and end of the distribution, respectively.

For an approximate evaluation of the Michel parameter ρ, it has been assumed that our experiment involves the same smearing of the theoretical spectra ($\rho = 0$, 0.25, 0.5, 0.75) as in reference 10. The χ^2 method gave $\rho = 0.62 \pm 0.14$. Figure 1 shows the experimental distribution and "smeared" theoretical curve for $\rho = 0.62$ plotted as the average of the curves for $\rho = 0.5$ and $\rho = 0.75$. The good agreement between the experimental points and the curve is an argument in favor of the assumption mentioned above.

Figures 2a and 2b represent the experimental distributions of positrons emitted forward ($0° \leq \theta \leq 90°$) and backward ($90° \leq \theta \leq 180°$), respectively. In 218 events the positron was emitted backward, while in the remaining 187 events it was emitted forward. These spectra show a small shift of the distribution peaks, which also results from the energy dependence of asymmetry.

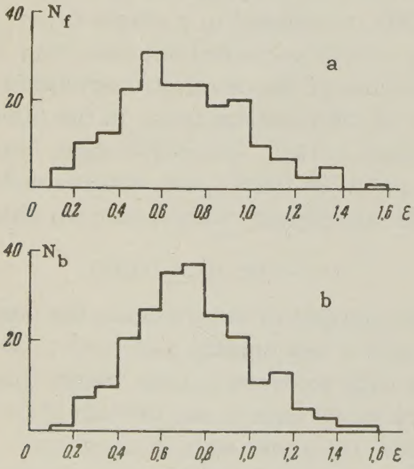

FIG. 2

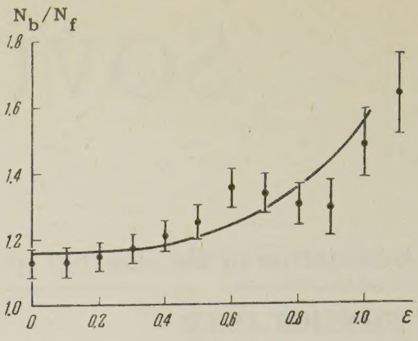

FIG. 3

Figure 3 shows the theoretical curve (calculated without taking into account the spread of measured values and bremsstrahlung) for the energy dependence of the ratio between N_b, the number of positrons emitted backward, and N, the number of positrons emitted forward; the mean weighted asymmetry parameter was $A = -(0.141 \pm 0.013)$ and its theoretical increase with energy was taken into account. The mean weighted value was obtained from the articles listed in the table. Figure 3 also shows the experimental points normalized to their theoretical values for $\epsilon = 0.3$.

Source	Number of events	$-A$
Rome,[11] cosmic rays	1028	0.222 ± 0.067
Bristol,[12] cosmic rays	1562	0.08 ± 0.05
Copenhagen,[13] cosmic rays	817	0.17 ± 0.07
Moscow,[8] 〃 〃	2000	0.120 ± 0.039
Erevan,[19] 〃 〃	2160	0.135 ± 0.043
Chicago,[14] accelerators	2000	0.174 ± 0.038
Göttingen,[15] 〃	2003	0.095 ± 0.044
Rochester,[16] 〃	1048	0.19 ± 0.06
Cambridge,[17] 〃	3021	0.149 ± 0.033

The asymmetry parameter for the investigated 405 $\pi \rightarrow \mu \rightarrow e$ decay events increases from $A = -(0.153 \pm 0.086)$ for $\epsilon = 0.1$ to $A = -(0.400 \pm 0.220)$ for $\epsilon = 1.0$. These results also support the two-component neutrino theory.

With experimental errors taken into account the correlation sign is observed to change in the energy range $\epsilon = 0.4$ to 0.7.

The authors wish to thank A. I. Alikhanian for his interest and I. I. Gol'dman for valuable suggestions. They are also indebted to L. N. Tatevosian for assistance with some of the measurements.

---

[1] T. D. Lee and C. N. Yang, Phys. Rev. **104**, 254 (1956).

[2] L. D. Landau, J. Exptl. Theoret. Phys. (U.S.S.R.) **32**, 405 (1957), Soviet Phys. JETP **5**, 336 (1957).

[3] T. D. Lee and C. N. Yang, Phys. Rev. **105**, 1671 (1957).

[4] A. Salam, Nuovo cimento **5**, 299 (1957).

[5] Garwin, Lederman and Weinrich, Phys. Rev. **105**, 1415 (1957).

[6] Berley, Garwin, Coffin, Lederman, and Weinrich, Phys. Rev. **106**, 835 (1957).

[7] A. O. Vaisenberg and V. A. Smirnitskii, J. Exptl. Theoret. Phys. (U.S.S.R.) **32**, 1340 (1957), Soviet Phys. JETP **5**, 1093 (1957).

[8] A. O. Vaisenberg and V. A. Smirnitskii, J. Exptl. Theoret. Phys. (U.S.S.R.) **33**, 621 (1957), Soviet Phys. JETP **6**, 477 (1958).

[9] Babaian, Marutian, Matevosian, and Sarinian, Dokl. Akad. Nauk Arm. SSR (in press).

[10] Bonetti, Levi-Setti, Panetti, Rossi, and Tomasini, Nuovo cimento **3**, 33 (1956).

[11] Castagnoli, Franzinetti, and Manfredini, Nuovo cimento **5**, 684 (1957).

[12] Bhomik, Evans, and Prowse, Nuovo cimento **5**, 1663 (1957).

[13] M. F. Kaplon, Rochester Conference on High-Energy Nuclear Physics, 1957.

[14] J. I. Friedman and V. L. Telegdi, Phys. Rev. **106**, 1290 (1957).

[15] Biswas, Ceccarelli, and Crussard, Nuovo cimento **5**, 756 (1957).

[16] Fournet-Davis, Engler, Goebel, Hoang, Kaplon, and Klarmann, Nuovo cimento **6**, 311 (1957).

[17] Chadwick, Durrani, Eisberg, Jones, Wignall, and Wilkinson, Phil. Mag. **2**, 684 (1957).

Translated by I. Emin
120

ON THE APPLICABILITY OF MASSEY'S ADIABATIC HYPOTHESIS TO DOUBLE CHARGE EXCHANGE

Ia. M. FOGEL', R. V. MITIN, V. F. KOZLOV, and N. D. ROMASHKO

Physico-Technical Institute, Academy of Sciences, Ukrainian S.S.R.

Submitted to JETP editor March 15, 1958

J. Exptl. Theoret. Phys. (U.S.S.R.) **35**, 565-573 (September, 1958)

The question of the applicability of Massey's adiabatic hypothesis to double charge exchange processes is considered. An analysis of the ion-velocity dependence of the cross sections for double charge exchange of some types of ions in inert gases shows that the positions of the maxima of the respective curves correspond to Massey's adiabatic criterion. In carrying out the analysis it is necessary to take into account the existence of excited ions in the primary beam as well as of the formation of slow excited doubly-charged ions. As in the case of ordinary charge exchange the constant a in the case of double charge exchange varies slightly from one ion-molecule system to another. The mean value of a for double charge exchange in inert gases is 1.5 A. The value of a for double charge exchange in molecular gases differs greatly from this value.

INTRODUCTION

AT the present time the cross sections for inelastic processes in heavy-particle collisions can be calculated quantum-mechanically for only a very limited number of cases — for particles with a small number of outer orbital electrons in slow collisions, when $v \ll v_0$, and in fast collisions, when $v \gg v_0$ (v is the relative velocity of the colliding particles and v_0 is the velocity of the electrons in the colliding particles). The theoretical literature is reviewed in reference 1.

The effective electron capture (charge exchange) cross section can also be calculated in the few instances when the potential energy curves are known for the initial and final states of the colliding particles. For such cases the cross sections are calculated by the method proposed in references 2 to 4. In all other cases the experimental results can be treated only on the basis of general theoretical considerations associated with Massey's "adiabatic hypothesis."[5] According to this hypothesis the principal quantity that determines the dependence of the cross section on the relative velocity of the particles is the adiabatic parameter $a|\Delta E|/hv$, where a is the distance at which the particles interact, ΔE is the "resonance defect" (the change of internal energy of the particles when they interact) and h is Planck's constant. For small velocities, when the condition $a|\Delta E|/hv \gg 1$ holds, inelastic cross sections are very small and increase rapidly with the velocity. The maximum cross section is reached when

$$a|\Delta E|/hv_{\max} \approx 1. \tag{1}$$

After passing through the maximum the cross section decreases monotonically as the velocity increases.

The available experimental data show that in many instances the curves of $\sigma(v)$ are what would be expected from the adiabatic hypothesis. Thus, for example, in reference 6 it was shown that for ordinary charge exchange of singly-charged positive ions (capture of a single electron) the maximum of $\sigma_{10}(v)$* for many ion-molecule systems is given by (1), if it is assumed that the particles are in their ground states before and after the collision. a varies very little for these processes in the case of many ion-molecule systems. For some processes, however, the curve of $\sigma(v)$ is clearly not in accord with the adiabatic hypothesis. There is disagreement in two ways: (1) Two and sometimes even three maxima are observed[7] instead of a single maximum. (2) The cross sections are anomalously large at small velocities.

The fact that $\sigma(v)$ has more than one maximum does not actually conflict with the adiabatic hypothesis and results from the fact that excited particles may participate in the process in ques-

---

*σ_{ik} is the cross section for the process in which a particle with charge ie is transformed into a particle with charge ke.

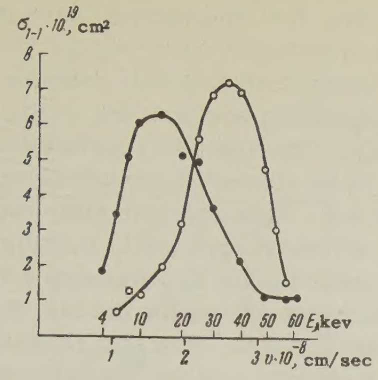

FIG. 1. ○ – H⁺ – He, ● – H⁺ – Ne.

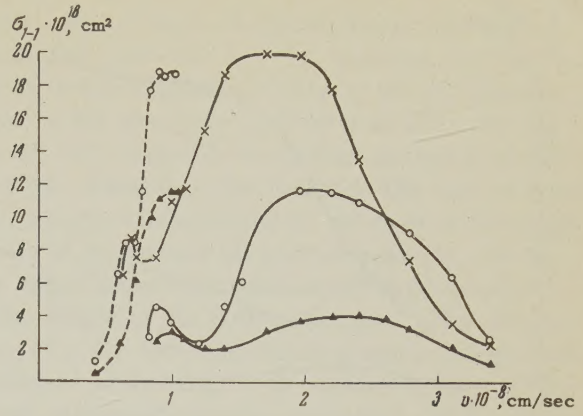

FIG. 2. —— – H⁺, – – – – C⁺, ▲ – Ar, ▼ – Kr, × – Xe.

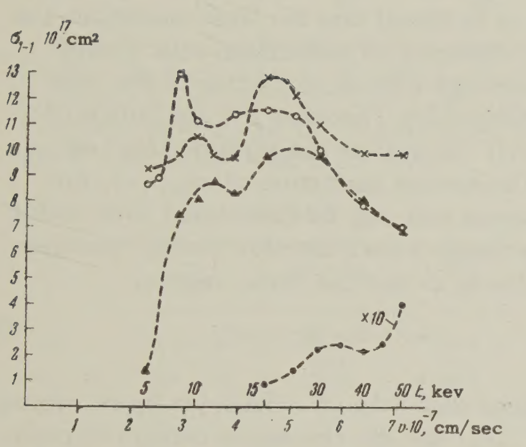

FIG. 3. ● – F⁺ – Ne, ▲ – F⁺ – Ar, ○ – F⁺ – Kr, × – F⁺ – Xe.

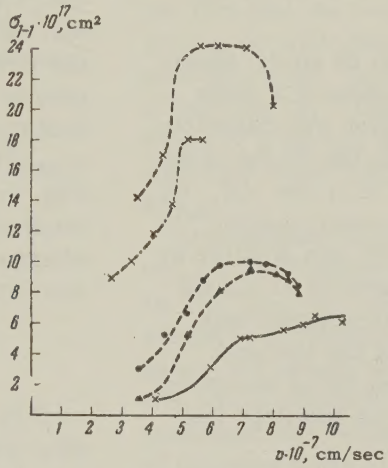

FIG. 4. —— – C⁺, – – – – O⁺, —·— – Cl⁺, ▲ – Ar, ● – Kr, × – Xe.

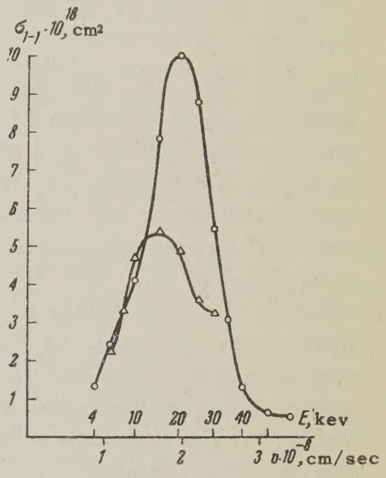

FIG. 5. ○ – H⁺ – H₂, Δ – N₂.

tion as well as particles which are in their ground state.

The anomalously large inelastic cross sections at low velocities result from violations of the adiabatic condition $a\,|\Delta E\,|/hv \gg 1$. Such violations can occur when the potential energy curves of the initial and final states of the colliding-particle system are so close at some internuclear separation R_n that the minimum potential energy difference $\Delta U(R_n)$ becomes very small. Bates and Massey[8] have considered the cases in which violation of the adiabatic condition is probable for slow collisions.

It is of interest to determine to what extent the adiabatic hypothesis can be applied to the capture of two electrons by singly-charged positive ions, that is to processes of the type

$$A^+ + B \rightarrow A^- + B^{++}. \qquad (2)$$

The available experimental data on double charge exchange of H_1^+,[9] C_1^+, O_1^+,[10] and Cl_1^+[11] has been insufficient to determine whether the adiabatic hypothesis can be applied to these processes, because the cross sections were measured in a relatively narrow energy range. In the present article for the purpose of determining the maximum of $\sigma_{1-1}(v)$ we have measured the cross sections for a number of ion-molecule systems in a wider energy range than was used in earlier work. We have also measured the double charge exchange cross section of F^+. The next section presents these results and a discussion based on Massey's adiabatic hypothesis.

EXPERIMENTAL RESULTS

We measured the cross sections of the process $H_1^+ \rightarrow H_1^-$ in the gases He, Ne, Ar, Kr, Xe, H_2, and N_2 over the energy interval from 3 to 65 kev, $C_1^+ \rightarrow C_1^-$ in Ar, Kr, and Xe (50 to 65 kev), $O_1^+ \rightarrow O_1^-$ in Ar and Kr (50 to 65 kev), $Cl_1^+ \rightarrow Cl_1^-$ in Xe (50 to 60 kev) and $F_1^+ \rightarrow F_1^-$ in He,

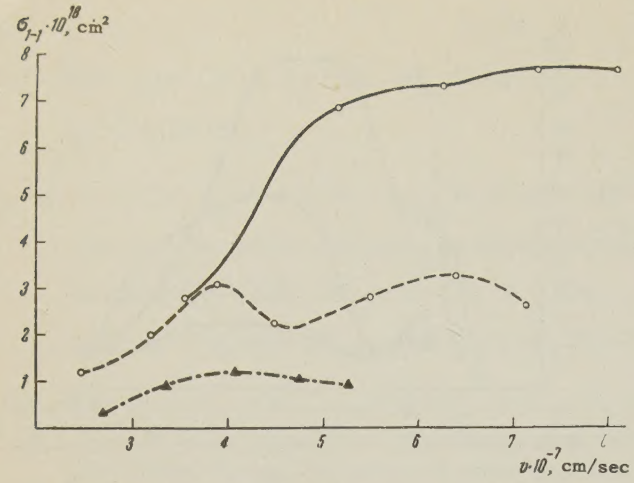

FIG. 6. ----F⁺, —— O⁺, —·—— Cl⁺, ▲–N₂, ○ – H₂.

Ne, Ar, Kr, Xe, and H_2 (5 to 50 kev). Measurements were performed by means of a mass spectrometer similar to that which was described in detail in reference 12. Within the limits of experimental error our values of σ_{1-1} for C_1^+, O_1^+, and Cl_1^+ agreed with earlier measurements.[10,11] Our values of σ_{1-1} for $H_1^+ \rightarrow H_1^-$ are smaller by a factor of 1.5 or 2 than in reference 9. As we have shown, the cause of this discrepancy was contamination of the capillary of the McLeod gauge used in reference 9, which led to incorrect values for the pressure of the gas admitted into the collision chamber.

Figures 1 to 6 show curves of $\sigma_{1-1}(v)$ for ion-molecule systems when maxima are observed. In some figures two maxima of $\sigma_{1-1}(v)$ are observed.

We shall first analyze the curves of $\sigma_{1-1}(v)$ for double charge exchange of ions in inert gases. We shall naturally begin with the simplest case, H_1^+ and He, where the particles that participate in the double charge exchange can be only in their ground states, so that the curve of $\sigma_{1-1}(v)$ for this process can have only a single maximum, the position of which is given by (1), as is actually found to be the case. By determining v_{max} from $\sigma_{1-1}(v)$ in Fig. 1 and calculating the resonance defect of the process $H_1^+ + He \rightarrow H_1^- + He^{++}$ we can use (1) to calculate a, which for $H_1^+ - He$ is 1.6 A.

Let us now consider double charge exchange for other ion-molecule systems. When a is identical for different systems it follows from (1) that $v_{max} \sim |\Delta E|$. We shall assume that the maxima of $\sigma_{1-1}(v)$ for the indicated systems represent double charge exchanges with all participating particles in their ground states. $v_{max}(|\Delta E|)$ as plotted under this condition is shown in Fig. 7.* The vertical bars indicate the errors in determination of v_{max}. When the curve of a cross section only reaches a plateau, the corresponding vertical line in Fig. 7 has no upper limit. The systems represented in Fig. 7 are seen to be clustered around the straight line for a = 1.5 A. This approximately constant value of a for different systems is in definite agreement with the results given in reference 6 for ordinary charge exchange except for the fact that in the latter case a ≈ 8 A. This is a reasonable result since it is obvious that for the capture of two electrons the particles must approach closer than for the capture of a single electron.

Consider the systems $H_1^+ - Ar$, $H_1^+ - Kr$, and $H_1^+ - Xe$, for which $\sigma_{1-1}(v)$ has two maxima. If it is assumed that the first maximum (at the lower velocity) is associated with double charge exchange without excitation of the slow doubly-charged ion (process 2), the points of $v_{max}(|\Delta E|)$ fit well on the straight line† of Fig. 7. The second maximum of $\sigma_{1-1}(v)$ for these systems can only be associated with double charge exchange where the slow doubly-charged ion remains in an excited state, that is,

$$H_1^+ + B \rightarrow H_1^- + B^{++*}. \qquad (3)$$

It is clear that $|\Delta E_2| - |\Delta E_1| = E_{B^{++}}$, where ΔE_1 and ΔE_2 are the resonance defects of processes (2) and (3) and $E_{B^{++}}$ is the excitation energy of B^{++}. Assuming that a is identical for processes (2) and (3), we can use the adiabatic criterion (1) to calculate $|\Delta E_2|$ and thus $E_{B^{++}}$. It was found that for the systems $H_1^+ - Ar$, $H_1^+ - Kr$, and $H_1^+ - Xe$ $E_{B^{++}}$ agrees within the limits of experimental error with the third ionization potential of Ar, Kr, and Xe atoms (Table I). On the basis of the foregoing postulate we can thus assume that the second maximum of $\sigma_{1-1}(v)$ for the indicated systems results from the process

---

*In plotting $v_{max} = f(|\Delta E|)$ the points for $F_1^+ - Ar$, $F_1^+ - Kr$ and $F_1^+ - Xe$ were determined on the assumption that the maximum at the higher velocity corresponds to double charge exchange when all particles are in their ground states. For $H_1^+ - Ar$, $H_1^+ - Kr$ and $H_1^+ - Xe$ it was assumed that the maximum at the smaller velocity represents this process. The justification for this procedure will appear in the discussion which follows.

†If it is assumed that the second maximum (at the higher velocity) is associated with a process for particles in their ground states, the origin of the first maximum cannot be explained by the adiabatic hypothesis since in the present instance the primary beam cannot contain excited ions.

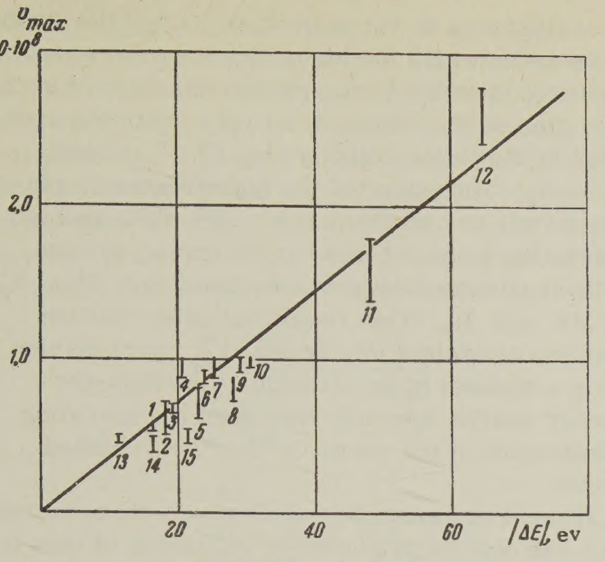

FIG. 7. v_{max} as a function of the resonance defect. 1 – Cl^+ – Xe; 2 – O^+ – Xe; 3 – H^+ – Xe; 4 – C^+ – Xe; 5 – O^+ – Kr; 6 – H^+ – Kr; 7 – C^+ – Kr; 8 – O^+ – Ar; 9 – H^+ – Ar; 10 – C^+ – Ar; 11 – H^+ – Ne; 12 – H^+ – He; 13 – F^+ – Xe; 14 – F^+ – Kr; 15 – F^+ – Ar.

TABLE I

System	$\Delta E_2 - \Delta E_1$, ev	V_{iB}^{III}, ev
H_1^+ — Xe	30.0	31.3
H_1^+ — Kr	33.5	35.7
H_1^+ — Ar	39.0	40.9

$$H_1^+ + B \rightarrow H_1^- + B^{+++} + e. \qquad (4)$$

Using the terminology of reference 13, process (4) can be called ionization with capture when of the three electrons separated from particle B two are captured by a proton while the third electron passes into the continuum. The ion B^{+++} can also be produced by ordinary ionization ($H_1^+ + B \rightarrow H_1^+ + B^{+++} + 3e$) so that the cross section for the production of triply-charged ions as determined by the method developed in reference 13 is actually the sum of the cross sections for ordinary ionization and process (4), which must be kept in mind in interpreting experiments on the ionization of Ar, Kr, and Xe by protons.

It is striking that (1) for Kr and Xe the second maximum is higher than the first maximum while for Ar they are of approximately the same height, (2) the relative height of the second maximum diminishes with decreasing atomic number of the gas, and (3) there is no second maximum for Ne. At first glance the first of these facts seems incomprehensible since it is difficult to imagine that process (4), which possesses a considerably larger resonance defect than process (2), can have greater probability than the latter process. But it must be remembered that the shape of the curve of $\sigma_{1-1}(v)$ between the two maxima is determined not only by the processes (2) and (4) but evidently also by a number of processes (3) with different excitation energies of the B^{++} ions. Therefore the height of the second maximum, which is determined by the sum of the probabilities of processes (3) and process (4), can be of the same order of magnitude or even greater than the height of the first maximum. The shape of $\sigma_{1-1}(v)$ for the considered systems shows that the relative probability of processes (3) and (4) decreases compared with the probability of the principal process (2) as the atomic number of the gas decreases. This may possibly be associated with the fact that the resonance defects of processes (3) and (4) will with decreasing atomic number increase more rapidly than the resonance defect of process (2). This appears to explain the absence of a second maxima of $\sigma_{1-1}(v)$ for Ne, which we would have had to observe around 70 kev.

Our present interpretation of the shape of $\sigma_{1-1}(v)$ for double charge exchange of protons in Ne, Ar, Kr, and Xe on the basis of the adiabatic hypothesis can be justified by investigating the energy loss which occurs when a positive ion is converted into a negative ion.* Such investigations, which will provide direct proof of the possibility of applying the adiabatic hypothesis to double charge exchange, are planned for a later and more thorough state in the study of these processes.

Two maxima of the $\sigma_{1-1}(v)$ curve are also observed for the process $F_1^+ \rightarrow F_1^-$ in the gases Ar, Kr, and Xe (Fig. 3).

When it is assumed that for the systems H_1^+ — Ar, H_1^+ — Kr, and H_1^+ — Xe the maximum at the lower velocity represents process (2), the subsequent calculation of the constant a gives a value much below 1.5 A (for example, for F_1^+ — Kr the value is 0.67 A). On the other hand, the excitation energies of slow ions which are calculated from the position of the maximum at the higher velocity differ greatly from the tabulated values.† When

---

*It is easily shown that when $\theta = 0$ and $\Delta E \ll T_0$ we have $\Delta E = m_2/m_1 + m_2(\Delta T + 2\, m_1/m_2\, T_0)$, where θ and ΔT are the scattering angle and energy loss in double charge exchange, m_1 and m_2 are the mass of the ion and gas atom, respectively, T_0 is the kinetic energy of the ion. This relation enables us to use the measured value of ΔT to calculate ΔE; from ΔE we can then determine the character of the process that has resulted in the given energy loss.

†For $F_1^+ - H_2$ the maximum at the higher velocity cannot be interpreted in this manner.

TABLE II

System	Calculated excitation energy in ev	Ion state	Energy of state in ev
$F^+ - Xe$	3.6±0.9	$2s^2\,2p^4\,{}^3P_{2,1,0}$	0
$F^+ - Kr$	6.5±1.6	$2s^2\,2p^4\,{}^1D_2$	2.6
$F^+ - Ar$	6,9±1.9	$2s^2\,2p^4\,{}^1S_0$	5.6
$F^+ - Ne$	20.4±2.5	$2s^2\,2p^4\,3s\,{}^5S_2{}^0$	22.0

we assume that the maximum at the higher velocity represents process (2), the value of a does not differ greatly from 1.5 A (see the points for $F_1^+ - Ar$, $F_1^+ - Kr$, and $F_1^+ - Xe$ in Fig. 7). The maxima at the lower velocity for these systems can be explained by the presence of metastable excited ions in the primary beam. The excitation energy E_{A^+} can be calculated as the difference $|\Delta E_1| - |\Delta E_2|$, where ΔE_1 is the resonance defect of process (2) and ΔE_2 is the resonance defect of the process $A^{+*} + B \rightarrow A^- + B^{++}$.

Assuming that the value of a for double charge exchange of an excited ion is the same as for process (2), we can calculate ΔE_2 and the excitation energy E_{A^+}. The excitation energy of F_1^+ corresponding to the maximum of $\sigma_{1-1}(v)$ for $F_1 -$ Ne can be calculated if we assume that a for this system is the same as for $F_1^+ - Ar$, $F_1^+ - Kr$, and $F_1^+ - Xe$. For $F_1^+ - Ne$ we use a = 1.2 A, which is the average for the systems that have been mentioned, and obtain $E_{F^+} = 20.4$ ev. Table II gives the calculated fast-ion excitation energies compared with the tabulated excitation energies of F_1^+.* These values are seen to agree within the limits of experimental error. The $\sigma_{1-1}(v)$ curve for $F_1^+ - Xe$ shows an additional maximum associated with the fact that the beam contains F_1^+ in the state $2s^22p^4\,{}^1D$, additional maxima for $F_1^+ - Ar$ and $F_1^+ - Kr$ associated with the excited state $2s^22p^4\,{}^1S$ of F_1^+ and, finally, a maximum for $F_1^+ - Ne$ associated with the excited state $2s^22p^33s^5S$ (the state $2s2p^5\,{}^3P$ is not metastable). The fact that the curves of $\sigma_{1-1}(v)$ for $F_1^+ - Ar$ and $F_1^+ - Kr$ do not contain a maximum for the state $2s^22p^4\,{}^1D$ evidently means that this maximum is not distinct from the principal maximum.

Thus the data in Table II do not disagree with the hypothesis that the low-velocity maxima of $\sigma_{1-1}(v)$ for the systems given in the table are associated with the presence of excited ions in the primary beam. Keeping in mind the fact that the shape of $\sigma_{1-1}(v)$ can depend on the fraction of excited ions in the beam,* we varied the conditions under which the high-frequency ion source operated in order to determine the effect of such variation on the shape of $\sigma_{1-1}(v)$ near the maximum at the lower velocity for $F_1^+ - Ar$ and $F_1^+ - H_2$. The power of the high-frequency generator was varied from 150 to 300 watts and the extracting potential was varied from 2 to 4 kv without affecting the cross sections for $F_1^+ - F_1^-$ in Ar and H_2. This result indicates that the fraction of excited ions in the F_1^+ beam issuing from a channel in the cathode of the high-frequency source does not depend on the operating parameters of the source within the indicated limits.

It must be remembered, however, that excited ions can also be produced by collisions of ions in the primary beam with molecules of residual gas. In order to determine the influence of the composition of the primary beam on the shape of $\sigma_{1-1}(v)$ it would be desirable to investigate the shape of these curves when it is definitely known that the beam from the source does not contain excited ions (a thermionic source), for comparison with the curves obtained in the present work. We shall continue our work in this direction.

Maxima of $\sigma_{1-1}(v)$ are also observed for some cases of double charge exchange in molecular gases (see the curves for $H_1^+ - H_2$, $O_1^+ - H_2$, $F_1^+ - H_2$, $H_1^+ - N_2$, and $Cl_1^+ - N_2$ in Figs. 5 and 6). In discussing double charge exchange in molecular gases it must be remembered above all that this process can take two different forms represented schematically by the formulas

$$A^+ + B_2 \rightarrow A^- + B_2^{++}; \qquad (5)$$

$$A^+ + B_2 \rightarrow A^- + B^+ + B^+. \qquad (6)$$

The resonance defect of process (5), in which a slow doubly-charged molecular ion† is produced, can be calculated in the usual way (reference 12). The resonance defect of process (6) can be calculated from

$$\Delta E = V_{iA}^I + S_A - (E_{\text{dis}} + 2V_{iB}^I + E_{\text{п}}), \qquad (7)$$

where E_{dis} is the dissociation energy of molecule B_2 and E_p is the potential energy of the two B^+ ions which are produced. It is easily seen that double charge exchange in hydrogen can occur only according to (6). The resonance defect in this case can be calculated unambiguously since E_p is known for the two protons formed from the unexcited H_2 molecule.[15] For other molecular gases E_p is unknown, so that the resonance defect can be calculated only for process (5) and then only when the first and second ionization potentials of B_2 are known.

---

*The excitation energy of F_1^+ was taken from reference 14.

*If the primary beam contains excited ions with only a single excitation energy, it is easily shown that the measured cross section σ_{1-1}' is expressed by $\sigma_{1-1}' = k\sigma_{1-1}^* + (1-k)\sigma_{1-1}$, where k is the fraction of excited ions in the beam and σ_{1-1}^* and σ_{1-1} are the cross sections for double charge exchange of excited and unexcited ions, respectively.

†Process (5) can naturally occur only when B_2^{++} is stable.

TABLE III

Ion-molecule system	*a*, Angstroms
$H^+ - H_2$	2.3
$O^+ - H_2$	0.9
$F^+ - H_2$	0.9
$H^+ - N_2$	2.0
$Cl^+ - N_2$	0.5

Table III gives the values of a calculated from (1) for the cases of double charge exchange in molecular gases when a maximum of $\sigma_{1-1}(v)$ is observed.* For $H_1^+ - N_2$ and $Cl_1^+ - N_2$ it was assumed that the double charge exchange proceeded according to (5), and in calculating the resonance defect we used the potential for the appearance of N_2^{++} which was determined in reference 16.

Table III shows that a for double charge exchange in molecular gases varies within broad limits and is considerably different from the average value, 1.5 A, which is characteristic of atomic gases. The calculation of the excitation energy of F_1^+ from the maxima of $\sigma_{1-1}(v)$ for $F_1^+ - H_2$ yields 11.1 ev, which does not agree with any of the actual excitation energies of this ion (Table II). The hypothesis that a is constant for double charge exchange of unexcited and excited F_1^+ ions in hydrogen is clearly not confirmed.

It follows from the foregoing discussion that the study of the true shape of the curve $\sigma_{1-1}(v)$ at low velocity is complicated by the presence of excited ions in the primary beam, which leads to additional maxima that distort the curve for $\sigma_{1-1}(v)$ in this region. However, there are some double charge exchange processes, namely $H_1^+ \rightarrow H_1^-$ in He and H_2 as well as $Li^+ \rightarrow Li^-$ with a Li^+ beam from a thermionic source,[17] for which we can assume that $\sigma_{1-1}(v)$ is undistorted at low velocities. In all of these cases, the cross section σ_{1-1} is observed to decrease rapidly as the velocity decreases, as can be expected from the adiabatic hypothesis.

For these cases we can affirm that the potential curves of the initial and final states of the system of colliding particles do not intersect. In order to determine whether this is a general law, we must continue the study of double charge exchange at low velocities as far as the threshold for those cases in which we can eliminate the possibility of the presence of excited ions in the primary beam.

In conclusion, we wish to thank Professor A. K. Val'ter for his continued interest.

---

*For $F_1^+ - H_2$, a was calculated for the maximum at the higher velocity, and for $O_1^+ - H_2$ the lower limit of a was determined since $\sigma_{1-1}(v)$ only reaches a plateau.

[1] E. B. Armstrong and A. Dalgarno, The Airglow and the Aurora, London, 1955, p. 328.

[2] L. D. Landau, Sow. Phys. **1**, 88 (1932).

[3] C. Zener, Proc. Roy. Soc. (London) **A137**, 696 (1932).

[4] E. C. G. Stueckelberg, Helv. Phys. Acta **5**, 370 (1932).

[5] H. S. W. Massey, Rep. Progr. Phys. **12**, 248 (1948).

[6] J. B. Hasted and J. B. H. Stedeford, Proc. Roy. Soc. (London) **A227**, 466 (1955).

[7] H. B. Gilbody and J. B. Hasted, Proc. Roy. Soc. (London) **A238**, 334 (1956).

[8] D. R. Bates and H. S. W. Massey, Phil. Mag. **45**, 111 (1954).

[9] Ia. M. Fogel' and R. V. Mitin, J. Exptl. Theoret. Phys. (U.S.S.R.) **30**, 450 (1956), Soviet Phys. JETP **3**, 334 (1956).

[10] Fogel', Mitin, and Koval', J. Exptl. Theoret. Phys. (U.S.S.R.) **31**, 397 (1956), Soviet Phys. JETP **4**, 359 (1957).

[11] Ia. M. Fogel' and R. V. Mitin, Тр. физ.-мат. фак-та, ХГУ (Trans. Phys.-Math. Fac., Khar'kov State Univ.) **7**, 165 (1958).

[12] Ia. M. Fogel' and L. I. Krupnik, J. Exptl. Theoret. Phys. (U.S.S.R.) **29**, 209 (1955), Soviet Phys. JETP **2**, 252 (1956).

[13] Fedorenko, Afrosimov, and Kaminker, J. Tech. Phys. (U.S.S.R.) **26**, 1929 (1956), Soviet Phys. JTP **1**, 1861 (1956).

[14] C. E. Moore, Atomic Energy Levels, National Bureau of Standards, 1949.

[15] Handbuch der Physik **23**, Part I, 1933, p. 114.

[16] H. D. Hagstrum and J. T. Tate, Phys. Rev. **59**, 354 (1941).

[17] Ia. M. Fogel' and A. D. Timofeev, Тр. физ.-мат. фак-та, ХГУ (Trans. Phys.-Math. Fac. Khar'kov State Univ.) **7**, 147 (1958).

Translated by I. Emin
121

SOVIET PHYSICS JETP VOLUME 35(8), NUMBER 3 MARCH, 1959

INVESTIGATION OF THE ANGULAR DISTRIBUTION OF SECONDARY PARTICLES IN SHOWERS PRODUCED BY HIGH-ENERGY NUCLEONS

L. A. SAN'KO, Zh. S. TAKIBAEV, and Ts. I. SHAKHOVA

Submitted to JETP editor March 15, 1958

J. Exptl. Theoret. Phys. (U.S.S.R.) **35**, 574-583 (September, 1958)

The angular distribution of secondary shower particles produced in the stratosphere by nucleons with energies above 50 Bev is investigated. An analysis of the distribution is carried out on basis of the theory of multiple meson production in nucleon-nucleon collisions and collisions between several nucleons according to the tunnel effect model.

THE angular distribution of shower particles reflects the processes taking place in the target nucleus in interaction with the incident nucleon. In order to study such interactions, we examined showers produced by protons. The showers were selected from a large number of stars produced in emulsion stacks exposed in the atmosphere at the latitudes of Moscow and Italy in 1955. (Stacks I – f – 55 and R).

The particle detection efficiency was determined from the $\pi \rightarrow \mu \rightarrow e$ decay sensitivity and the emulsion was calibrated by measuring the grain density of electron tracks.[1] The angular distribution of thin tracks (shower particles) was determined for all showers.

The space angle θ_i between the direction of the primary and the i-th shower particle was determined by the formula:

$$\cos\theta_i = \cos\varphi_i \cos\varphi_0 (\tan\varphi_i \tan\varphi_0 + \cos\lambda_i),$$

where φ_i is the angle between the direction of the i-th shower particle and the emulsion plane, φ_0 is the angle between the direction of the primary (or the shower axis) and the emulsion plane, and λ_i is the angle between the i-th shower particle and the primary (or the shower axis) in the plane of emulsion.

For showers produced by neutral particles we determined the mean direction (axis) of the shower, with respect to which the spatial angle θ_i was measured. For that case

$$\sin\varphi_0 = Z / \sqrt{X^2 + Y^2 + Z^2};$$

$$\sin\lambda_0 = X / \sqrt{X^2 + Y^2 + Z^2}\cos\varphi_0,$$

$$X = \sum_{i=1}^{n_s} \cos\varphi_i \sin\lambda_i'; \quad Y = \sum_{i=1}^{n_s} \cos\varphi_i \cos\lambda_i'; \quad Z = \sum_{i=1}^{n_s} \sin\varphi_i;$$

where λ_0 and λ_i', are the angles in the emulsion plane of the shower axis and the i-th particle, respectively, with the direction of any arbitrarily chosen track near the axis.

The energy of the primary particles was determined from the angular distribution of shower particles; it was assumed that the incident particle interacts either with a single nucleon or with a column of nuclear matter. For nucleon-nucleon interactions, the primary particle energy was determined in first approximation[2] from the formula

$$E = 2Mc^2 / \tan^2 \theta_{1/2},$$

where $\theta_{1/2}$ is the angle containing a half of the shower particles.

For interactions between a nucleon and nucleons of the tunnel l/d long, the energy was found from the equation

$$E = Mc^2 \times [l/d + \sqrt{(l/d)^2 + \tan^2\theta_{1/2}(\tan^2\theta_{1/2} + (l/d)^2 + 1)}] / \tan^2\theta_{1/2}. \quad (1)$$

Such an energy estimate corresponds to the assumption that the produced particles are monoenergetic in the center-of-mass system (c.m.s.). ($\beta_\pi^* = v_\pi^*/c = 1$, where v_π^* is the velocity of π mesons in the c.m.s.). The energy spectrum of shower particles was accounted for in the estimate of the primary energy according to reference 2, and the energy spectrum of the primary particles — according to Ref. 3. Both refinements strengthen our conclusions on the role of secondary interactions inside the nucleus.

1. INTEGRAL AND DIFFERENTIAL ANGULAR DISTRIBUTIONS OF SHOWER PARTICLES

In the study of the angular distribution of shower particles in the laboratory system of coordinates* (l.s.) it is assumed that the distribution in the c.m.s. is symmetric with respect to the plane perpendicular to the line joining the interacting nucleons. The relation between the angle θ^* in the c.m.s. and θ in the l.s. is given by the equation

$$\gamma_c \tan\theta = \sin\theta^* / (m + \cos\theta^*), \quad m = \beta_c/\beta_\pi^*; \quad (2)$$

where γ_c is the primary energy in the c.m.s. and β_c is the velocity of the center-of-mass system.

If the particles produced are monoenergetic ($\beta_\pi^* = 1$) then, knowing the angular distribution function in the c.m.s. $N(\theta^*)$, it is easy to find the distribution function in the l.s. $N(\theta)$.

In fact, for an isotopic distribution of shower particles in the c.m.s. we have

$$N(\theta^*) = \mathrm{const}\cdot d\Omega$$

the angular distribution function in the l.s. is of the form[4]

$$N(\theta) = \frac{N\gamma_c\alpha[m + \sqrt{1-(m^2-1)\alpha^2}]^2}{2\cos^2\theta\,(\alpha^2+1)^2\sqrt{1-(m^2-1)\alpha^2}}$$

for $m \le 1$, or

$$N(\theta) = \frac{N\gamma_c\alpha}{2\cos^2\theta\,(\alpha^2+1)^2}\left[\frac{m \pm \sqrt{1-(m^2-1)\alpha^2}}{\sqrt{1-(m^2-1)\alpha^2}}\right]$$

for $m \ge 1$, where $\alpha = \gamma_c \tan\theta$.

The fraction of shower particles f contained in the angle θ_f is defined as

$$f = \frac{1}{N}\int_0^{\theta_f} N(\theta)\,d\theta, \quad (3)$$

where N is the total number of particles. Substituting $N(\theta)$ and integrating, we find:

$$f = \frac{1}{2}\left[1 + m - \frac{m + \sqrt{1-(m^2-1)\alpha^2}}{\alpha^2+1}\right] \quad \text{for } m \leqslant 1, \quad (4)$$

$$f = 1 - \frac{\sqrt{1-(m^2-1)\alpha^2}}{\alpha^2+1} \quad \text{for } m \geqslant 1. \quad (5)$$

Accounting for the energy spectrum of shower particles in the c.m.s., we can find in an analogous way, for a given $N(\theta^*)$, the corresponding integral distribution in the l.s.

The differential angular distribution in the l.s., for an isotropic distribution in the c.m.s. and $m = 1$, is

$$\frac{df}{dy} = \frac{df}{d\alpha}\frac{d\alpha}{dy} = \frac{2\cdot 10^{2y}}{(10^{2y}+1)^2}\ln 10; \quad y = \log\alpha. \quad (6)$$

For an anisotropic distribution in c.m.s., e.g., for $N(\theta^*) \sim \cos^2\theta^*$, we have

$$df/dy = 4\cdot 10^{2y}(10^{2y}-1)(10^{2y}+1)^{-3}\ln 10.$$

The above expression, however, tends to zero for $y \to 0$, which is not observed experimentally. We shall consider therefore the following distribution function of shower particles:

$$N(\theta^*) = a^2\cos^2\theta^* + \sin^2\theta^*;$$

which is proportional to the radius vector of the ellipsoid of rotation with the major axis parallel to the line joining the colliding nucleons. The total number of particles is then

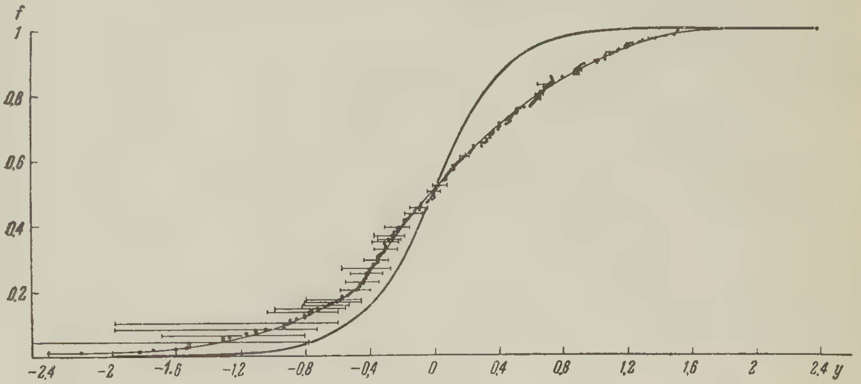

FIG. 1. Summary integral angular distribution of showers with $E_0 \geq 1000$ Bev. The solid curve shown for comparison represents an isotopic distribution of shower particles in the c.m.s. for $m = 1$. Experimental errors are shown in the figure. The abscissa represents $y = \log\gamma_c \tan\theta_f$.

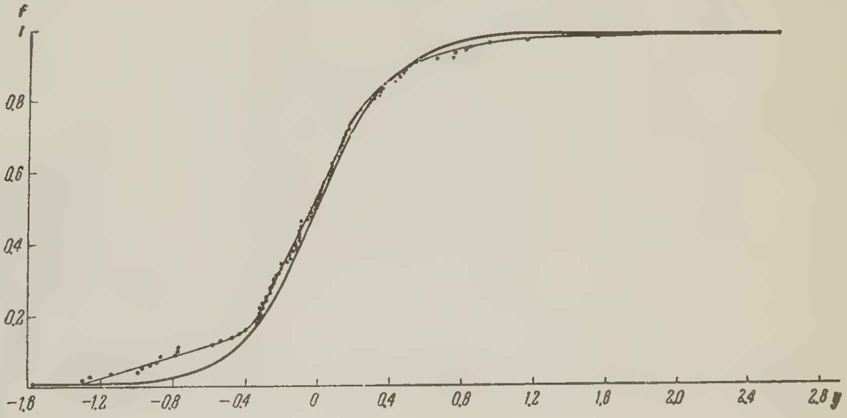

FIG. 2. Same as Fig. 1, only for $E_0 \leq 100$ Bev.

$$N = \int_0^\pi C\,(a^2\cos^2\theta^* + \sin^2\theta^*)^{1/2}\sin\theta^* d\theta^*,$$

$$C = \frac{N}{a + \ln(a + \sqrt{a^2+1})/\sqrt{a^2-1}},$$

where a is the ratio of the axes of the ellipsoid of rotation.

The differential angular distribution in the l.s. is given by the following expression:

$$\frac{\partial f}{\partial y} = \frac{4C}{N}\left\{\left(\frac{1-10^{2y}}{1+10^{2y}}\right)^2 (a^2-1)+1\right\}^{1/2}\frac{10^{2y}\ln 10}{(10^{2y}+1)^2}. \qquad (7)$$

In the analysis of showers we constructed the curves of the integral angular distribution, which should be symmetric about f = ½ for m = 1. The majority of experimental curves are asymmetric. This means either that m ≠ 1 or that the assumption about a symmetric emission is incorrect. It is possible that the deviations from symmetry are a consequence of multiple collisions of the primary nuclear inside the nucleus.

2. COMPARISON WITH EXPERIMENTAL DATA

Showers initiated by primaries with energy $E_0 \leq 10^{11}$ ev and $E_0 \geq 10^{12}$ ev were selected from a large number of showers (over 200) for a study of the differences in the shower production mechanism at different energies.

The summary experimental integral angular distributions are shown in Figs. 1 and 2; curves corresponding to a symmetric distribution of shower particles in the c.m.s. are also included. Comparison shows that the angular distribution in the region $E_0 \leq 10^{11}$ ev is isotropic. Showers from references 5 and 6 have been included in the group $E_0 \geq 10^{12}$ ev together with showers detected and reduced in our laboratory.

It can be seen from Fig. 1 that, for $E_0 \geq 10^{12}$ ev, the distribution of shower particles in the c.m.s. is anisotropic.

For the energy region 5×10^{10} to 10^{11} ev we also studied the differential angular distribution of a summary shower with $n_s = 161$ particles. The curves, shown in Fig. 3, were calculated according to Eq. (7) for a = 1 and a = 1.4. The fit between experimental and theoretical curves was examined by the χ^2 test. An analysis of the differential angular distribution shows that it is almost totally isotropic in c.m.s.

3. ANALYSIS OF SHOWERS FROM THE POINT OF VIEW OF THE MULTIPLE MESON PRODUCTION THEORY

The theory of a pure multiple production of mesons assumes that all mesons are produced in a single interaction between the incident nucleon and a nucleon or a group of nucleons of the target nucleus (tunnel effect). It is assumed that the nucleon group forms a continuous amorphous mass of nuclear matter, since the collisions between the incident nucleon and the nucleons of the nucleus are not sharply divided in time. In the instant of collision, the nucleons of the nucleus are not in the same state with respect to the incident nucleon; the shape of the tunnel may, therefore, not be cylindrical. For small energies (< 50 Bev) the deviation from such a shape may be large, but for the region > 50 Bev we assume that the tunnel shape is almost cylindrical. In the following we assume that a nucleon incident upon the nucleus interacts with a column of nuclear matter in a tunnel whose length depends on the impact parameter. If M (column)/M (nucleon) = l/d nucleons of the nucleus take part in the collision, one can estimate[7] the energy of the primary nucleon $\gamma = E/Mc^2$ by means of Eq. (1). In the

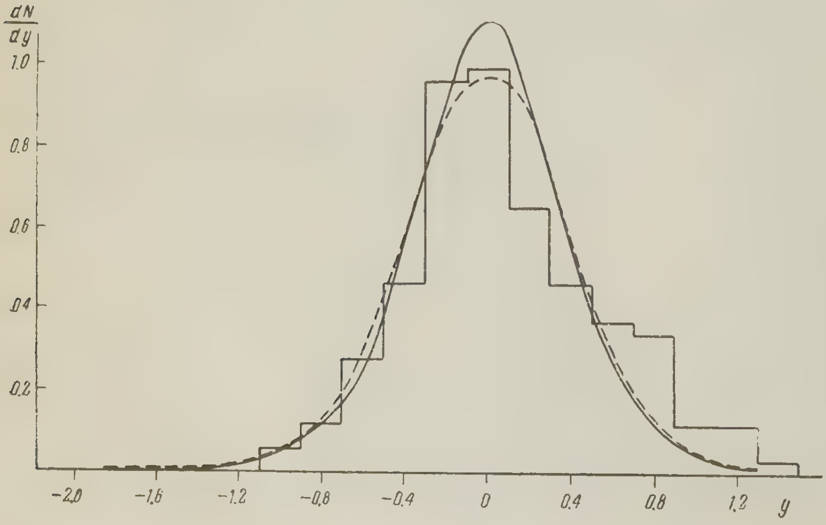

FIG. 3. Differential angular distribution for 161 shower particles. The solid and dashed curves correspond to Eq. (7) for a = 1 and a = 1.4 respectively.

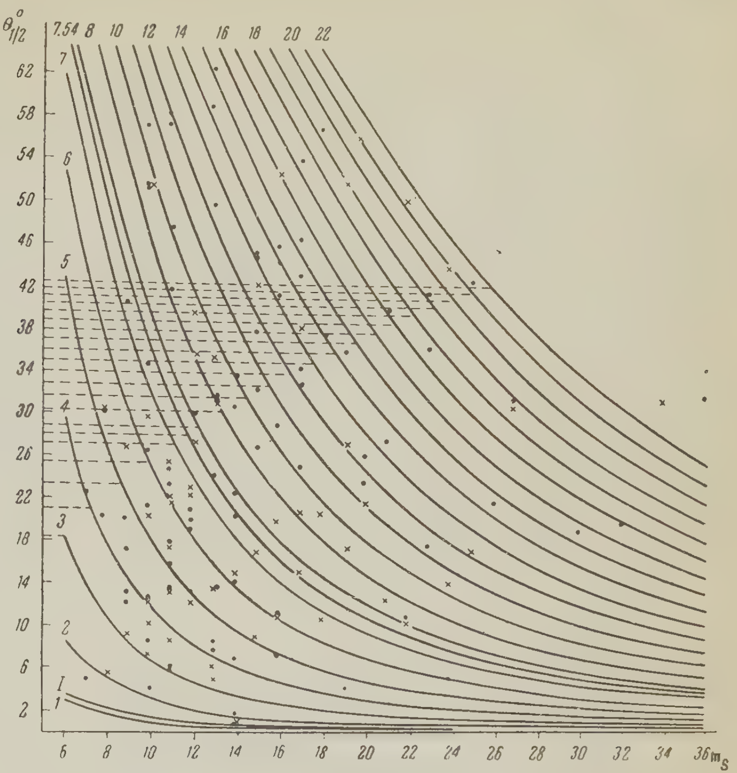

FIG. 4. Dependence of $\theta_{1/2}$ on n_s for different l/d. Experimental points for 138 showers (● – showers of the stack I – f; × – showers of the stack R). The region below dashed lines corresponds to $E_0 > 50$ Bev for each l/d.

derivation of (1) it has been assumed that (a) the number of particles is large (b) the emission of particles in c.m.s. is symmetric, and (c) all particles are relativistic in c.m.s., i.e. $\beta^*_\pi = 1$, $m = \beta_c$.

The angle $\theta_{1/2}$ is found from Eq. (1) as a function of γ and l/d:

$$\tan^2\theta_{1/2} = \frac{1 + 2\gamma l/d + (l/d)^2}{\gamma^2 - 1}\ . \qquad (8)$$

The total number of particles N taking part in the interaction and produced in it is determined from the hydrodynamical theory:[8]

$$N = 0.84\,(l/d + 1)\,\gamma^{1/4} \text{ for } l/d \leqslant 3.7, \qquad (9)$$

$$N = 1.55\,(l/d - 0.25)^{3/4}\gamma^{1/4} \text{ for } l/d > 3.7. \qquad (10)$$

On the other hand, depending on the nature of the primary particle (p, n), we have

$$(p)\ \ N = 3n_s/2 + l/4d - {}^{1}/_{2};$$
$$(n)\ \ N = 3n_s/2 + l/4d + 1;$$
$$(p,\, n)\ \ N = 3n_s/2 + l/4d + {}^{1}/_{2}.$$

The value of γ was found by substituting N into Eqs. (9) and (10), and $\tan\theta_{1/2}$ was then obtained from Eq. (8).

The analysis of all reduced showers (138 in all) was carried out from the point of view of the interaction with a column of nucleons in the tunnel. The dependence of $\theta_{1/2}$ on n_s was plotted for different tunnel lengths l/d (Fig. 4). Curves for proton-produced stars were used (for stars with primary neutrons the curves are flatter and lie lower) and experimental points were marked in coordinates $\theta_{1/2}$, n_s for showers produced by protons and neutrons. The diameters of emulsion nuclei range from 1 to 7.54 in units of d. The parameter l/d can, therefore, vary for emulsion from 0 to 7.54.

If the tunnel-effect model is correct, the experimental points should all lie below the curve corresponding to $l/d = 7.54$. In reality it was found that a considerable part of the points fell above the curve (cf. Fig. 4).

The large scatter of experimental points cannot be explained by fluctuations of n_s and $\theta_{1/2}$. In fact, allowing for fluctuations, the number of particles in the forward and backward cones in the c.m.s. is

$$n_s/2 \pm \sqrt{n_s/2}.$$

The angle $\theta_{1/2}$ also fluctuates from $\theta_{1/2\min}$ to $\theta_{1/2\max}$, representing the angles that contain $n_s/2 \mp \sqrt{n_s/2}$ particles (in the c.m.s.).

For an isotropic distribution of particles in the c.m.s. we know, on one hand, that the fraction of particles f contained within the angle $\theta^*_f = \pi/2 \mp \Delta\theta$ is $f = (1 - \cos\theta^*_f)/2$. On the other hand,

$$f = (n_s/2 + \sqrt{n_s/2})/n_s.$$

It follows hence that $\cos\theta^*_f = \mp\sqrt{2/n_s}$. Substituting this values into Eq. (2) we obtain

$$\tan\theta_{1/2}\binom{\min}{\max} = \frac{\sqrt{n_s - 2}}{\sqrt{n_s} \pm \sqrt{2}} \frac{\tan\theta_{1/2}}{\sqrt{1 + \tan^2\theta_{1/2}}} \cdot \qquad (11)$$

It can be seen from Fig. 5 that the width of fluctuation strips does not include the expected amount of experimental points and, consequently, fluctuations of the multiplicity and of the angle $\theta_{1/2}$ cannot explain the observed relatively large number of showers corresponding to tunnel lengths > 7.54. We therefore plotted curves for larger l/d (up to $l/d = 22$), in order to encompass all showers studied. The points corresponding to these showers lie below the curve $l/d = 7.54$; in extensive showers one must assume, for agreement with the theory, that $\theta_{1/2}$ may in some cases be 3 to 5 times larger. Such an increase may be due to secondary interactions in the target nucleus.

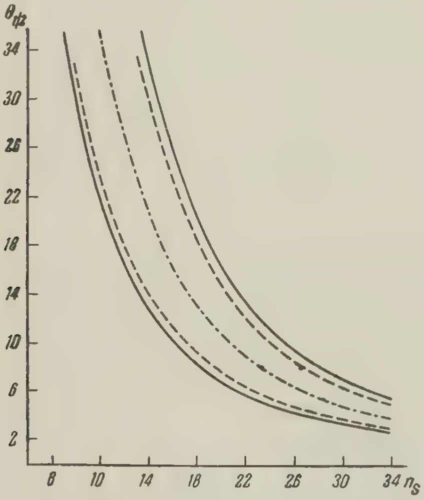

FIG. 5. Dependence of $\theta_{1/2}$ on n_s for $l/d = 7.54$ and fluctuation curves: dashed – for fluctuations of $\theta_{1/2}$, solid – for fluctuation of n_s.

The experimental points in Fig. 4 for showers with $E_0 > 50$ Bev were divided with respect to tunnel length (points lying above dotted curves were not taken into account). A histogram was then constructed of the distribution of showers with respect to l/d and compared with the computed histogram of the tunnel-length distribution of the relative number of interactions with emulsion nuclei.

If the interaction cross section is equal to the geometrical one $\sigma = \sigma_0 A^{2/3}$, then the number of interactions with a given nucleus is $n = \sigma q S t$, where q is the number of nuclei per unit volume, S is the flux of primary nucleons with a given primary energy, and t is the time. The total number of interactions can be obtained by integrating over the nuclei of all elements of the emulsion. The relative number of interactions with each nucleus is as follows:

I	Ag	Br	S	O	N	C	H
0.0082	0.3068	0.3815	0.0032	0.1037	0.0273	0.1154	0.0542

If we represent the nucleus by a spherical continuous body of radius $r_0 A^{1/3}$, we can relatively easily calculate the relative number of interactions in the emulsion for different tunnel lengths. The results of the calculation for Ilford G-5 emulsion are:

$l/d =$ 0–1	1–2	2–3	3–4	4–5	5–6	6–7	7–7.54
0.089	0.104	0.173	0.182	0.139	0.168	0.132	0.013

These data served as the basis for the histogram and were compared with the experimental histograms (Figs. 6 and 7).

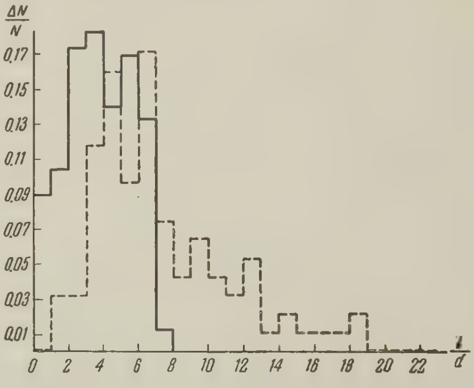

FIG. 6. Histograms of the tunnel-length distribution $(0 \le l/d \le 7.54)$ of interactions. (Solid line – theoretical). Experimental histogram (dashed) includes errors. $E_0 > 50$ Bev. (94 showers).

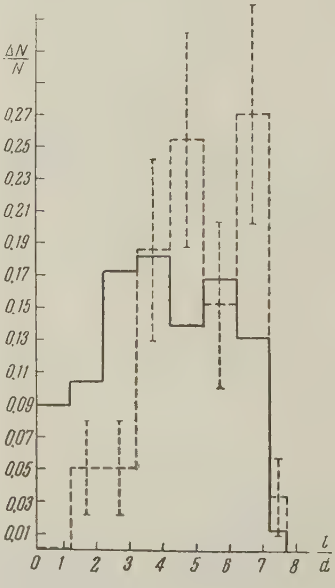

FIG. 7. Histograms of the tunnel-length distribution $(0 \le l/d \le 22)$ of showers with $E_0 > 50$ Bev. Solid line – theoretical, dashed – experimental (59 events).

It can be seen that the experimental histogram is shifted towards longer tunnels. The same result follows from an estimate of the ratio of the number of interactions N_1 for longer tunnels

$(7.54 \geq l/d > 3.6)$ to the number of interactions N_2 involving shorter tunnels $(3.6 \geq l/d \geq 0)$: the calculated ratio in emulsion is $N_1/N_2 = 1.45$, while the observed is $N_1/N_2 = 5.39 \pm 0.30$ for $E_0 > 50$ Bev and $N_1/N_2 = 2.92 \pm 0.31$ for $E_0 > 100$ Bev.

We have studied the variation of Eq. (1) and the form of dependence of $\theta_{1/2}$ on n_s when conditions (b) and (c) are not satisfied.

Let the condition (a) be satisfied, i.e., let the showers have a large multiplicity. We shall find γ for the case when the emission of particles in the c.m.s. is asymmetric with respect to the plane passing through the center of mass and perpendicular to the direction of the nucleon, but is symmetric in the system of equal velocities. In such a system the velocity of the incident nucleon (v_1'), of a tunnel nucleon (v_2'), and of the system (v_p') are equal.

The energy of a tunnel nucleon γ' is given, for $\beta_\pi' = 1$, by the expression:

$$\gamma' = 1/\sqrt{1-\beta_p'^2},\ \beta_p' = v_p'/C = 1/\sqrt{1+\tan^2\theta_{1/2}}.$$

The nucleon velocity v in the laboratory system and v_1' in the equal-velocity system are connected by the relation:

$$\beta = 2\beta_p'/(1+\beta_p'^2).$$

The primary particle energy in l.s. is then

$$\gamma = 1 + 2/\tan^2\theta_{1/2}.$$

If $\beta_\pi' \neq 1$ and $m = \beta_p'/\beta_\pi'$, we have

$$\gamma = 2/m^2\tan^2\theta_{1/2} - 1.$$

and the relation between $\theta_{1/2}$ and n_s is:

$$N^4/[0.84(l/d+1)]^4 = 2/m^2\tan^2\theta_{1/2} - 1 \quad \text{for } l/d \leqslant 3.7,$$
$$N^4/[1.55\,(l/d-0.25)^{3/4}]^4 = 2/m^2\tan^2\theta_{1/2} - 1 \quad \text{for } l/d > 3.7. \tag{12}$$

The dependence of $\theta_{1/2}$ on n_s for different m, calculated according to Eq. (12) for $l/d = 7.54$, is shown in Fig. 8. For comparison, analogous curves for the c.m.s. are shown in the figure as well, the energy of the primary for a symmetric distribution in the c.m.s. being defined by the formula

$$\gamma = \frac{(l/d)\,(1-m^2\tan^2\theta_{1/2}) + \sqrt{(l/d)^2 + m^2\tan^2\theta_{1/2}\,(1-l/d)^2}}{m^2\tan^2\theta_{1/2}}. \tag{13}$$

The curves, obtained under the assumption of a symmetric emission in the equal-velocity system, lie below the corresponding curves in the c.m.s. since $\beta_p' \geq \beta_c'$. If we drop conditions (b) and (c), a still larger number of experimental points will fall above the curve for $l/d = 7.54$ and, consequently, will not be explained by the multiple meson production theory.

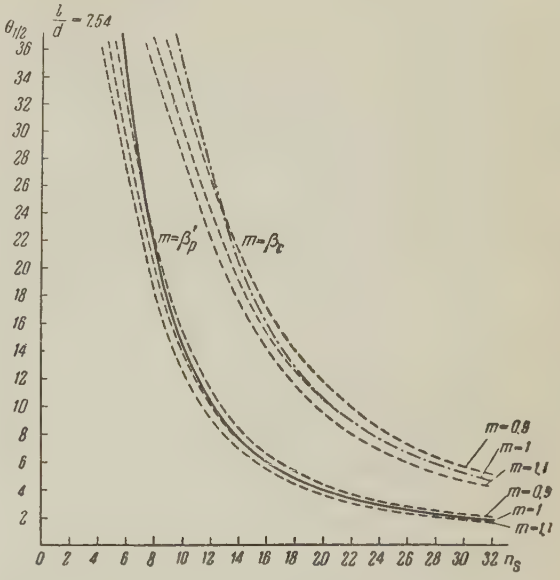

FIG. 8. Dependence of $\theta_{1/2}$ on n_s for different m. Top curves calculated assuming symmetry in c.m.s., bottom – assuming symmetry in the equal velocity system.

In the above calculations the energies were estimated neglecting the energy spectrum of shower particles. Such a procedure decreases the primary energy. If we correct the value of γ_c according to reference 2, the calculated curves fall lower, as can be seen in Fig. 9.

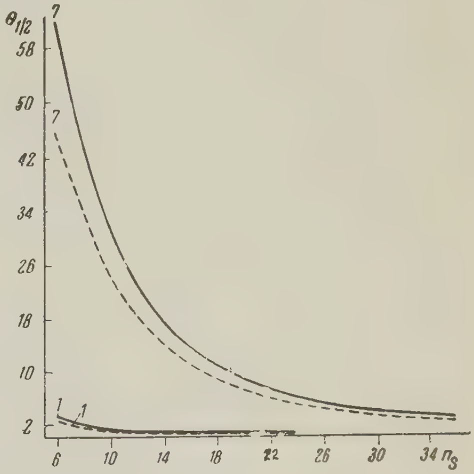

FIG. 9. Curves for $l/d = 1$ and 7, calculated assuming a power energy spectrum of shower particles (dashed), and assuming that the particles are monoenergetic ($\beta_\pi^* = 1$) (solid).

CONCLUSION

The integral angular distribution of shower particles in stars produced by 5×10^{10} to 10^{12} ev primaries is asymmetric about $f = \frac{1}{2}$. An analysis of the symmetry of the integral-distribution curve shows that the angular distribution of shower particles in the c.m.s. is nearly isotropic. The experimentally observed relation between n_s and $\theta_{1/2}$ is greatly different from that calculated on basis of the multiple meson production theory. The discrepancy cannot be explained by fluctuations of multiplicity and angle $\theta_{1/2}$.

The observed values of n_s and $\theta_{1/2}$ can be explained if one assumes the production of mesons in secondary interactions in about 40% of showers produced in the stratosphere at 30 to 33 km altitude.

---

[1] M. Baldo-Ceolin and B. Sechi, Nuovo cimento **2**, 6 (1955).

[2] Castagnoli, Cortini, Franzinetti, Manfredini, and Moreno, Nuovo cimento **10**, 1539 (1953).

[3] Zh. S. Takibaev, J. Exptl. Theoret. Phys. (U.S.S.R.) **35**, 277 (1958), Soviet Phys. JETP **8**, 191 (1959).

[4] Bradt, Kaplon, and Peters, Helv. Phys. Acta, **23**, 24 (1950).

[5] Schein, Glasser, and Haskin, Nuovo cimento **2**, 647 (1955).

[6] Debenetti, Garelli, and Tallone, Nuovo cimento **4**, 1142 (1956).

[7] Zh. S. Takibaev, Вестн. АН КазССР (Bull. Acad. Sci. Kazakh S.S.R.) **1**, 69 (1957); Takibaev, Usik, and Antonova, Dokl. Akad. Nauk SSSR **111**, 341 (1956), Soviet Phys. "Doklady" **1**, 666 (1956).

[8] S. Z. Belen'kii and L. D. Landau, Usp. Fiz. Nauk **56**, 309 (1955).

Translated by H. Kasha
122

SOVIET PHYSICS JETP VOLUME 35(8), NUMBER 3 MARCH, 1959

ON THE THERMAL STABILITY OF THE DOMAIN STRUCTURE IN SILICON-IRON CRYSTALS

L. V. KIRENSKII and I. F. DEGTIAREV

Institute of Physics, Siberian Branch, Academy of Science, U.S.S.R.

Submitted to JETP editor April 1, 1958

J. Exptl. Theoret. Phys. (U.S.S.R.) **35**, 584-586 (September, 1958)

The longitudinal magneto-optical Kerr effect is applied to the examination of the domain structure of 3% silicon iron in the temperature range from 20° to 700°C. It is shown that the domain structure possesses high stability in this temperature range.

INTRODUCTION

A very great number of investigations, both theoretical and experimental, have been devoted to the study of the domain structure of ferromagnets. Such interest in their domain structure is fully justified insofar as the basic properties of ferromagnets in weak and intermediate fields are determined by the domain structure, and the magnetization process proceeds by way of the motion of domain boundaries.[1]

At the present time there are many methods for the study of domain structure. The principal, well-developed method is that of powder patterns.[2] The application of the powder-pattern method, however, is limited to relatively low temperatures. Besides, an examination of the dynamics of a domain structure by means of cinematography and powder patters is possible only for slowly varying fields or elastic stresses.[3]

Thus, attempts to find other methods of investigation of the domain structure of ferromagnets, free from the drawbacks indicated above, are quite natural. Among such methods, one must cite the electron-optical methods,[4] the permalloy-probe method,[5] and methods that utilize the magneto-optical Kerr effect.[6] As regards the last method, the polar Kerr effect has been successfully employed in the investigation of the domain structure of uniaxial crystals, in particular MnBi crystals. Application of this method is possible only in the presence of a magnetization component normal to the surface of the specimen.

There are comparatively few works employing the longitudinal Kerr effect with the magnetization vector in the plane of the surface of the specimen and in the plane of incidence of the light beam, and the investigation itself involves considerable technical difficulties. These difficulties are due to the fact that the angle of rotation of the plane of polarization upon reflection of light from a ferromagnetic mirror is small (maximum up to 5′) for the aforementioned Kerr effect. Besides, a major experimental difficulty lies in overcoming the effect of microrelief of the surface. Surface microrelief gives significantly more difference between intensities of beams reflected from different regions than between neighboring zones of spontaneous magnetization.

The small rotation of the plane of polarization in the longitudinal Kerr effect makes visual observation of the domain structure impossible on account of insufficient contrast. The authors of the works referred to above surmounted the effect of surface microrelief by applying a photographic method. The specimen under investigation was photographed in a state of magnetic saturation. The true surface microrelief was obtained in the negative obtained. From the negative, a transparent positive was prepared which was exactly superposed on the negatives taken with the specimen in the investigated state. This made it possible to disclose the domain structure.

The literature contains indications that the Kerr effect is reinforced by dielectric and semiconducting films.[7] This effect was utilized to develop a method for examining the domain structure. This method has no time delay and is applicable over a considerably broader temperature range.

EXPERIMENTAL PORTION

The basic idea of the experiment consists in employing the properties of the iron oxide film to increase the magnitude of Kerr effect observed, making possible visual observation of the domain structure along with still and motion picture recording.

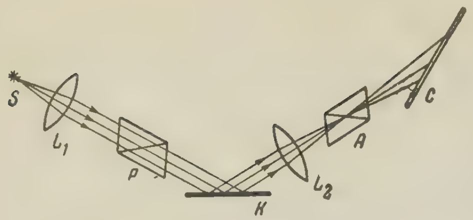

FIG. 1. Arrangement of apparatus for observation of a domain structure by means of the longitudinal Kerr effect.

The diagram of the arrangement is shown in Fig. 1. Light from the source S (a prefocused incandescent lamp) is converted into a parallel beam by means of lens L_1. The polarizer P polarizes the light in a plane perpendicular to the plane of incidence. After reflection from the surface of the examined specimen K, the lens L_2 forms an image of the surface in the plane C, where the photographic plate is placed. The analyzer A is located at the point of maximum convergence of the reflected rays.

Before photographing, the polarizer and analyzer are adjusted for minimum light transmission. The analyzer is then turned through a small angle and, if visually observed through the ocular, the domains emerge clearly in the form of dark and bright bands. Since this method is instantaneous, the stroboscope effect can be used to observe the process of boundary displacement in applied fields of frequency 50 cps and higher.

It has been found possible also to study the domain structure over a very broad temperature range. For this, the specimen K was placed together with a heater H in a chamber which could be evacuated (Fig. 2). The chamber had two glass windows positioned normal to the incident and reflected beams. The heater was mounted in a porcelain tube D so that no shifting of the specimen occurred during a change in temperature. The temperature was measured by means of a nichrome-constantan thermocouple

At temperatures above 500°C the specimen began to glow, but for exposures up to ten seconds this natural radiation did not essentially affect the photographic film up to 700°C.

Studies were carried out on single crystals of 3% silicon iron, cut in strips $25 \times 4 \times 0.3$ mm. in the (110) plane. The specimens, prepared in the same way as for observation of powder patterns, were annealed in vacuum on the order of 10^{-3} mm. Hg at a temperature near 1000°C for three hours. The annealing removed the mechanical strains and covered the surface of the specimen with a fine film of iron oxide. With an appropriate film thickness, the visual observation spoken of above was made possible.

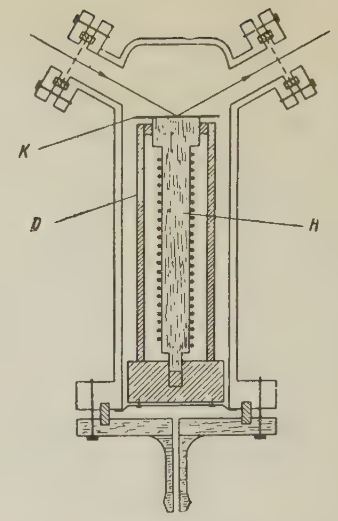

FIG. 2. Diagram of apparatus for the investigation of domain structure at various temperatures.

The photographs of Fig. 3 illustrate the change in the domain structure during the application of an increasing magnetic field. The broadening of the domains most advantageously oriented with respect to the field at the expense of those less favorably oriented suggests that both the domain structure itself and its change with the field are recorded sufficiently reliably.

Photographs of the domain structure in the absence of a field at various temperatures from 20 to 700°C are presented in Fig. 4. It is seen that the domain structure of silicon iron is characterized by an unusually high thermal stability. In fact, the width of the domain strips is maintained strictly constant over the indicated temperature interval.

The domain structure shown can be called "normal." By "normal" domain structure in a given case we understand such a domain struc-

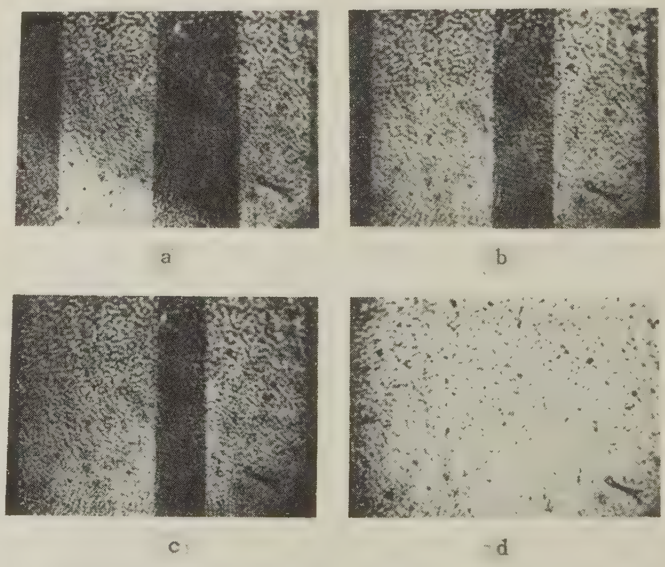
a
b
c
d

FIG. 3. Change of the domain structure during application of a field. a) H = 0, b) H = 15 Oe, c) H = 25 Oe, d) H = 60 Oe.

ture as is obtained by demagnetizing the specimen with an alternating field whose amplitude decreases to zero. In case of a specimen with some other prior magnetic history, the domain structure can be substantially different from normal. Visual observations made at temperatures from 20 to 500°C have shown that such an abnormal domain structure likewise remains unchanged with variation of temperature.

SUMMARY

1. Utilization of an iron-oxide film in the study of the domain structure of ferromagnets by means of the longitudinal Kerr effect allows visual observation of the domain structure and its still- and motion-picture photography.

2. Because of the absence of time delay, the magneto-optical Kerr effect method permits the conducting of examinations at substantial rates of change of the magnetic field and of the elastic stresses.

3. The magneto-optical Kerr effect allows investigations to be carried out over a broad range of temperatures.

4. The domain structure of silicon iron in the (110) plane is distinguished by high thermal stability.

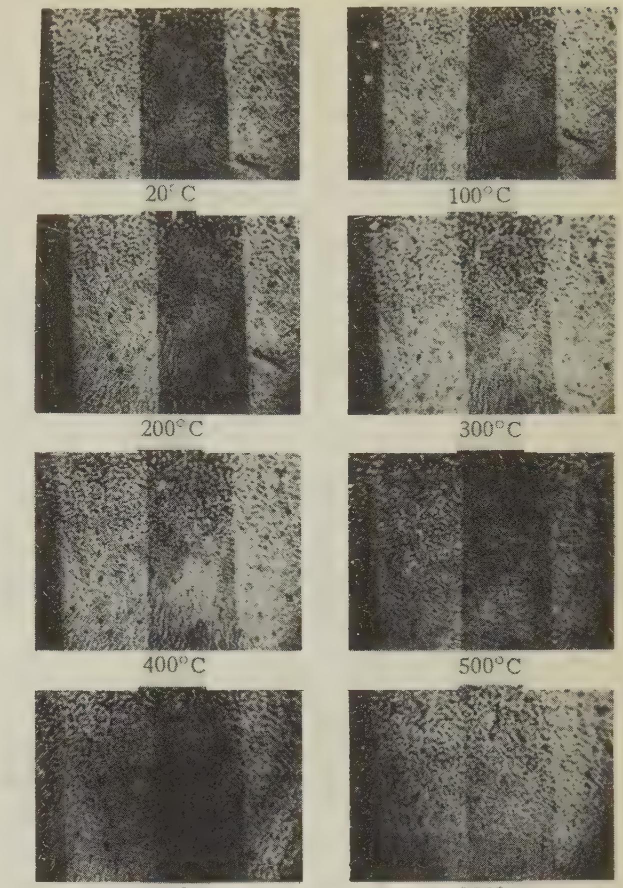

FIG. 4. Normal domain structure of silicon iron crystals in the absence of a magnetic field at various temperatures.

---

[1] L. D. Landau and E. M. Lifschitz, Sow. Phys. **8**, 153 (1935).

[2] F. Bitter, Phys. Rev. **38**, 1903 (1931); N. Akulov and M. Dehtiar, Ann. Physik **15**, 750 (1932).

[3] L. V. Kirenskii and V. D. Dylgerov, Физика металлов и металловедение (Phys. of Metals and Metal Research) **3**, 216 (1956); Kirenskii, Dylgerov, and Savchenko, Izv. Akad. Nauk SSSR, Ser. Fiz. **21**, 1168 (1957) [Columbia Tech. Transl. **21**, 1157 (1957)].

[4] Spivak, Kanavina, Sbitnikova, and Dombrovskaia, Dokl. Akad. Nauk SSSR **105**, 706 (1955); Spivak, Prilezhaeva, and Azovtsev, ibid. **105**, 965 (1955).

[5] J. Kaczer, C. S. Fysik casopis. (Czechoslovak J. Phys.) **5**, 239 (1955).

[6] C. A. Fowler, Jr. and E. M. Fryer, Phys. Rev. **94**, 52 (1954); B. W. Roberts and C. P. Bean, Phys. Rev. **96**, 1494 (1954).

[7] M. M. Noskov and A. V. Sokolov, J. Exptl. Theoret. Phys. (U.S.S.R.) **17**, 969 (1947).

Translated by R. Eisner
123

SOVIET PHYSICS JETP VOLUME 35(8), NUMBER 3 MARCH, 1959

TRITIUM PRODUCTION IN METALS BY 120 TO 660-Mev PROTONS

V. V. KUZNETSOV and V. N. MEKHEDOV

Joint Institute for Nuclear Research

Submitted to JETP editor April 2, 1958

J. Exptl. Theoret. Phys. (U.S.S.R.) **35**, 587-591 (September, 1958)

Results of an investigation of tritium production in various elements by 660-Mev protons are presented. Excitation functions are given for tritium production in the 120 to 660 Mev range.

EXPERIMENTAL METHOD

THE present investigation was undertaken to supplement the results of references 1 to 6 and to determine additional characteristics of tritium production in metals by protons.

Specimens of metals measuring 2×6×15 mm were bombarded with protons in the internal beam of the synchrocyclotron of the Joint Institute for Nuclear Research. Four to six specimens were irradiated simultaneously while fastened in a massive aluminum holder. The proton beam was directed parallel to the 6-mm side. The bombarding energy was varied by changing the target radius in the synchrocylotron. Irradiation times were 2 to 5 min in an internal beam of 10^{11} to 10^{12} protons/sec.

The quantity of tritium in a bombarded target was determined by means of a special vacuum system which is shown diagramatically in Fig. 1. The apparatus consists of a tubular furnace 1 with a quartz tube 2 for melting the targets 3; a palladium thimble 4 with an electric heater 5 to separate the hydrogen-tritium mixture from the other gaseous reaction products; traps containing activated charcoal 6 cooled by liquid nitrogen (a trap was used to produce a pressure drop during passage of the active gas); and a Geiger counter 7 in a lead shield 8 (40 mm thick). The apparatus also included several reservoirs — for hydrogen 9, pure argon 10, alcohol 11, and a tank 12 for diluting the highly active mixture.

Bombarded targets were melted in a quartz tube of 140 cm^3 volume, in a hydrogen atmosphere* at 50 mm Hg. The melting time was 1.5 to 2 hours at 900 to 1050°C.† About 90% of the tritium was separated from the specimens. A second melting process under the same conditions gave 8 or 9% and a third process yielded 1 to 2% of the total tritium activity. A special check of the yield of the active mixture by activated charcoal showed that the charcoal yields practically all of the gas at room temperature.

The vacuum system enabled us to send into the counter from 0.057 to 0.1 of the hydrogen-tritium mixture at 1 to 6 mm Hg. The β-particle detector was a cylindrical glass counter of 60 cm^3 volume with a copper cathode. The counter was filled with alcohol vapor at 15 mm and argon at 95 to 100 mm in addition to the hydrogen-tritium mixture. Under these conditions, the Geiger counter had the following operating characteristics: a counter plateau from 100 to 150 v, a plateau slope not greater than 10% at 100 v, and a background of 80 to 100 pulses per minute. The tritium activity was measured at 1000 to 10000 pulses per minute. The efficiency of the counter for registering beta particles from tritium decay is estimated at about 90%.

The proton beam was monitored by a 20μ aluminum foil in which the specimens were wrapped during bombardment. The dependence of the yields of the $Al^{27}(p, 3pn)Na^{24}$ reaction on the proton energy was taken from references 7 and 8. After bombardment the aluminum foil was dissolved in 1 ml of HCl, after which the decay of activity was measured in the fraction 0.01 of the solution. The activity of the monitor was measured by an end-window counter with mica windows 3 mg/cm^2 thick. The detector recorded 18% of the entire activity of the monitor.

EXPERIMENTAL RESULTS

The table contains the cross sections of various elements for tritium production by 120 to 660 Mev protons. The values in the table are the averages of not less than 3 measurements, except that for magnesium, tin, gold and bismuth single

---

*The hydrogen used experimentally as a carrier first passed through the palladium thimble.

†The experiments were performed with elements whose melting points did not exceed 1100°C.

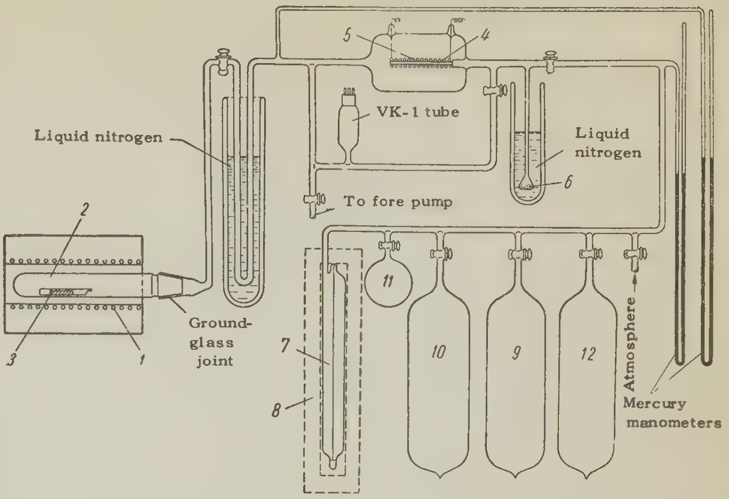

FIG. 1. Diagram of the vacuum system for determining the amount of tritium produced in various elements by high-energy protons.

measurements are sometimes given. The total error in determining each value is estimated at ± 30%. This is double the half-width of the curve of deviations from the average experimental values for all of the experiments; the curve was almost Gaussian in shape.

The tritium production cross sections σ_{H3} of aluminum and lead at 120 Mev are almost identical. Considerable increase of σ_{H3} for heavy elements is observed as the proton energy is increased. In the 300 to 500 Mev range the increase of the cross section is slowed down, but above 550 Mev it increases sharply. At 660 Mev the σ_{H3} of lead and bismuth is almost twice as large as on the plateau (300 to 500 Mev) and reaches 10% of the geometric cross section. This relation is clear for lead and bismuth. For aluminum and magnesium the relation is almost linear. The values for tin lie between the values for lead and aluminum.

The dependence of σ_{H3} on atomic weight at 660 Mev is shown in Fig. 2, where the dashed line shows the dependence of the excitation energy on atomic number at 450 Mev. The figure also shows the cross sections which we obtained experimentally at 450 Mev or by means of interpolation of the energy relations (triangles), and gives results taken from reference 1 (open circles). There is good agreement between our results and reference 1 for aluminum and lead at 450 Mev. Figure 2 is marked by a steady increase of σ_{H3} with A. At 660 Mev σ_{H3} of aluminum and bismuth increases ~ 3 times as A increases ~ 8 times.

DISCUSSION

It is interesting to observe how the tritium production cross section depends on proton energy at still higher energies. Fig. 3 gives data on tritium production in aluminum and lead by fast protons; the data were obtained in the present work or from the literature.[1,4,6] Experimental values

Target material	Proton energy, Mev	Average cross section	Number of experiments
Magnesium	660	43 ± 13	2
Aluminum	660	46 ± 14	17
Copper	660	74 ± 22	6
Zinc	660	67 ± 20	7
Silver	660	76 ± 23	4
Cadmium	660	95 ± 28	3
Tin	660	122 ± 37	3
Antimony	660	88 ± 26	2
Gold	660	139 ± 41	1
Lead	660	186 ± 56	11
Bismuth	660	167 ± 50	4
Aluminum	600	44 ± 13	2
Tin	600	86 ± 26	1
Lead	600	157 ± 47	3
Magnesium	550	26 ± 8	2
Aluminum	550	33 ± 10	6
Tin	550	69 ± 21	1
Lead	550	87 ± 26	3
Bismuth	550	75 ± 22	1
Aluminum	500	37 ± 11	5
Magnesium	450	30 ± 9	1
Aluminum	450	24 ± 7	3
Lead	450	91 ± 27	3
Magnesium	300	19 ± 6	2
Aluminum	300	25 ± 7	3
Tin	300	38 ± 11	2
Lead	300	73 ± 22	4
Bismuth	300	73 ± 22	1
Aluminum	200	18 ±6	3
Aluminum	120	16 ± 5	3
Lead	120	17 ± 5	3

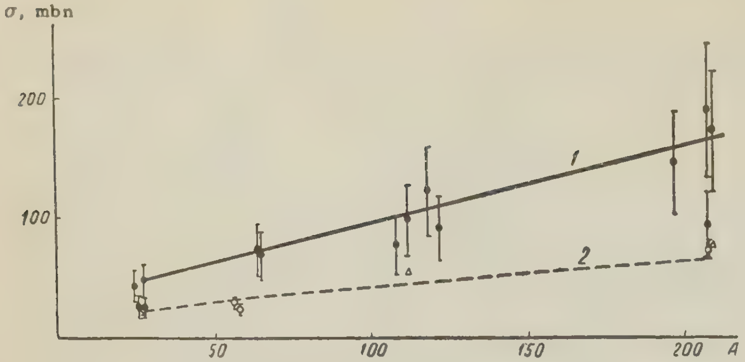

FIG. 2. Dependence of the tritium production cross section on the atomic weight of the target material at 1) 660 Mev and 2) 450 Mev.

taken from the literature are indicated in Fig. 3 by open circles and squares. The crosses denote cross sections in iron for the proton energies 0.16, 1.0, 3.0 and 6.2 Bev (reference 4) and 50 to 170 Mev.[6] The figure shows that the observed growth of σ_{H3} in lead above 550 Mev is continued. For 2.05 Bev σ_{H3} exceeds the cross section at 300 to 500 Mev by a factor of more than 5 and reaches 25% of the geometric cross section. In the case of aluminum σ_{H3} is almost unchanged up to 2.05 Bev. σ_{H3} increases steadily in iron with proton energy, but the curve for iron is closer to the curve for aluminum than for lead. Only for the energy region from 0.1 to 0.17 Bev is σ_{H3} in iron below the value for aluminum. Thus with increasing proton energy the heavy elements show a relatively greater rise of the tritium production cross section than the light elements.

In Fig. 3 the solid curves give the dependence of the variation of the probability of tritium emission from lead and aluminum as calculated by evaporation theory in the 120 to 500 Mev proton energy range. The calculated curves were adjusted to experimental results so as to provide coincidence of the greatest possible number of points. The calculation was performed by means of the formulas given by Hagedorn and Mackay,[9] using the excitation energies given in reference 10. (For lead we used the excitation energy calculated for bismuth.) The relation which gives the temperature of a nucleus at a given excitation energy was taken from reference 11. The effective barrier for tritium emission was $V'_{H^3} = V_0/2 = 8.1$ Mev for lead and $V_{H^3} = V_0/2 = 2.3$ Mev for aluminum. We see that the evaporation theory gives a relation between σ_{H^3} and proton energy which is about the same as the experimental result.

The relative probability of tritium emission, $\gamma_{H^3}/\gamma_{tot}$, where γ_{tot} is the total evaporation probability of neutrons, protons, alpha particles etc. ($\gamma_{tot} = \gamma_n + \gamma_p + \gamma_d + \gamma_{H^3} + \gamma_{He^3} + \gamma_{He^4}$), also agrees with the experimental ratio $\sigma_{H^3}/\sigma_{geom}$ for 120- and 500-Mev protons. For aluminum $\gamma_{H^3}/\gamma_{tot}$ was 10^{-2} and 3×10^{-2}, whereas $\sigma_{H^3}/\sigma_{geom}$ is 2.5×10^{-2} (neglecting the transparency of the nucleus). For lead $\gamma_{H^3}/\gamma_{tot}$ was 3×10^{-3} and 1.1×10^{-2} with the same proton energies. $\sigma_{H^3}/\sigma_{geom}$ (neglecting transparency) was 8×10^{-3} and 4×10^{-2}, respectively. Thus the relative probability of tritium emission varies in the same direction as the experimental ratio $\sigma_{H^3}/\sigma_{geom}$, differing by a factor of not more than 3. This discrepancy is not significant in view of the approximate character of the calculations.

The agreement of the proton-energy dependence of σ_{H^3} (Fig. 3) and of $\sigma_{H^3}/\sigma_{geom}$ with evaporation theory indicates that in our experiments we recorded mainly tritium nuclei which

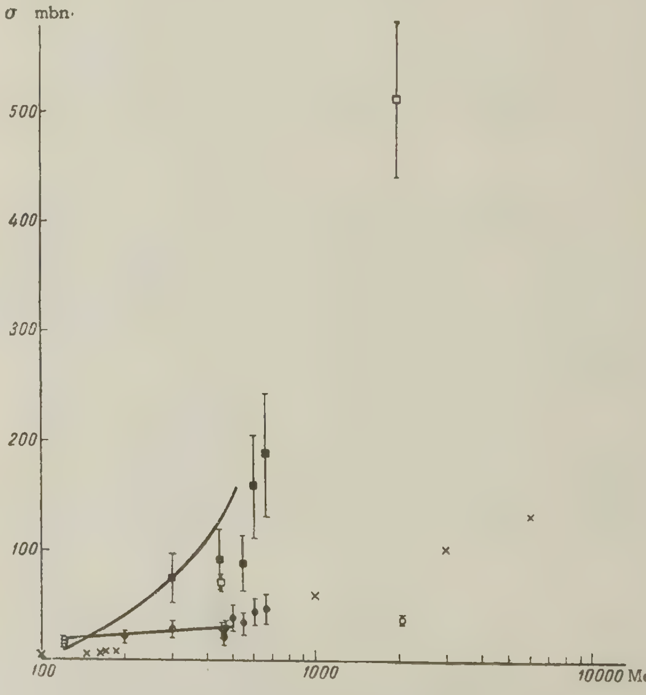

FIG. 3. Dependence of the tritium production cross section of aluminum, lead and iron on proton energy. ■, □ – Pb; ●, ○ – Al; × – Fe; solid curve – calculation by evaporation theory.

had been evaporated. This conclusion is also supported by the shapes of the curves for the excitation energy and production cross section σ_{H^3} in different elements with 450-Mev protons (Fig. 2).

For proton energies above 500 Mev evaporation theory gives a probability of tritium emission which is notably above the experimental cross sections, although the ratio $\gamma_{H^3}/\gamma_{tot}$ remains approximately unchanged. If we assume that theory agrees with experiment in the 120 to 500 Mev energy range, then for 2 Bev the probability of tritium emission exceeds the experimental value by ~ 7 times in aluminum and ~ 13 times in lead. These excessive calculated values are evidently due to the fact that at such high proton energies the evaporation theory cannot be applied.

The authors wish to thank V. A. Khalkin, M. Ia. Kuznetsova, and V. I. Salatskii for their assistance, and Iu. D. Prokoshkin for valuable suggestions.

---

[1] Currie, Libby, and Wolfgang, Phys. Rev. **101**, 1557 (1956).

[2] E. L. Fireman and F. S. Rowland, Phys. Rev. **97**, 780 (1955).

[3] E. L. Fireman, Phys. Rev. **97**, 1303 (1955).

[4] E. L. Fireman and J. Zähringer, Phys. Rev. **107**, 1695 (1957).

[5] Wade, Gonzalez-Vidal, Glass and Seaborg, Phys. Rev. **107**, 1311 (1957).

[6] K. Goebel, CERN 58-2 (1958).

[7] Iu. D. Prokoshkin and A. A. Tiapkin, J. Exptl. Theoret. Phys. (U.S.S.R.) **32**, 177 (1957), Soviet Phys. JETP **5**, 148 (1957).

[8] L. Winsberg, Radiochemical Studies of High-Energy Nuclear Reactions at Berkeley. Report at Gordon Conference on Nuclear Chemistry, 1957.

[9] Kosmische Strahlung, edited by W. Heisenberg (Springer, Berlin, 1953), second edition.

[10] Metropolis, Rivius, Storm, Turkevich, Miller, and Friedlander, Monte-Carlo Calculations on Intranuclear Cascades I. Low energy studies, 1957.

[11] G. Fujimoto and J. Yamaguchi, Progr. Theoret. Phys. **5**, 787 (1950).

Translated by I. Emin
124

GAMMA RADIATION FROM RADIATIVE CAPTURE OF THERMAL NEUTRONS BY Mo^{95}, Ag^{107}, Te^{123}, *AND* Cs^{133} *NUCLEI*

L. F. KALINKIN, A. S. MELIORANSKII, and I. V. ESTULIN

Scientific Research Institute for Nuclear Physics, Moscow State University

Submitted to JETP editor April 5, 1958

J. Exptl. Theoret. Phys. (U.S.S.R.) **35**, 592-598 (September, 1958)

A single-crystal scintillation spectrometer adjusted for operation at high counting rates was used to measure the energies and absolute intensities of γ rays in the region of 20 to 1000 kev, emitted after radiative capture of neutrons in samples enriched in isotopes of Mo^{95}, Ag^{107}, Te^{123}, and Cs^{133}. The observed γ rays come from transitions between low lying states of these nuclei.

MEASURING TECHNIQUE

THE present paper is a continuation of previous work of the authors[1] on the investigation of the γ radiation emitted by nuclei after capture of thermal neutrons. The measurements were carried out in the range of γ-ray energies from 20 to 1000 kev. The neutron source was the modernized heavy-water reactor of the Academy of Sciences, U.S.S.R.[2] The increased power of the reactor and the use of more complete neutron collimation than in the previous experiments enabled us to obtain a flux of the external beam in the region of the target of $\sim 10^8$ neutrons/sec cm^2.

In measurements of neutron-capture gamma rays using magnetic spectrometers,[3-5] the shielding of the neutron beam from pile γ rays was accomplished by means of thick layers (~ 10 cm) of lead or bismuth. In the present work it turned out that it was sufficient to cover the neutron beam inside the collimator with a thin combined filter (1.7 mm of lead, 1.5 mm of tin, and 0.5 mm of zinc), which strongly absorbed the soft γ rays and produced a negligible weakening of the neutron flux.

The γ-ray detector was a single crystal scintillation spectrometer with a NaI (Tl) crystal 30 mm in diameter and 19.7 mm high. The use of photomultiplier FEU-11, a non-saturating pulse amplifier,[6] and a fast acting non-saturating single-channel analyzer enabled us to work with high integral counting rates (up to $\sim 10^5$ pulses/sec) without any change in the resolution and the energy calibration of the spectrometer. The window width of the analyzer corresponded to energy intervals of 2.4, 6, and 20 kev for measurements in the energy ranges $E_\gamma \leq 50$, $E_\gamma \leq 400$, and $E_\gamma \geq 400$ kev, respectively. The line shape, the photopeak efficiency, and the resolution of the spectrometer were determined experimentally, under the geometrical conditions existing in the capture gamma-ray measurements, for γ rays of 22, 25, 27, 31, 59, 72 kev (the K radiations of Ag, Sn, Te, Cs, W, and T, respectively), 159 kev (Te^{123M}), 279 kev (Hg^{203}), 323 kev (Cr^{51}), 480 kev (γ-rays from the $B^{10}(n, \alpha) Li^{7*}$ reaction), 662 kev (Cs^{137}), 762 kev (Nb^{95}), and 1120 kev (Zn^{65}). The resolving power of the spectrometer in the energy region E_γ = 279 to 1120 kev can be written as

$$\eta = (240/\sqrt{E_\gamma}) + 0.2. \quad (1)$$

where the resolution η is in percent and E_γ is in kev. For $E_\gamma < 279$ kev, the values of $\eta(E_\gamma)$ are somewhat smaller than those given by formula (1). Figure 1 shows the dependence of the photopeak efficiency ϵ_Φ of the spectrometer on E_γ:[1] (1) for a NaI (Tl) crystal with h = 10 mm, d = 28 mm; (2) for the crystal with h = 19.7 mm,

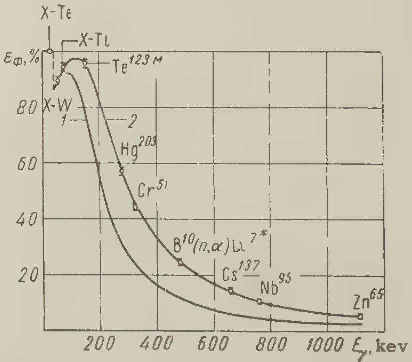

FIG. 1. Photopeak efficiency of spectrometer with NaI (Tl) crystal: 1) crystal with h = 10 mm, d = 28 mm; 2) crystal with h = 19.7 mm, d = 30 mm.

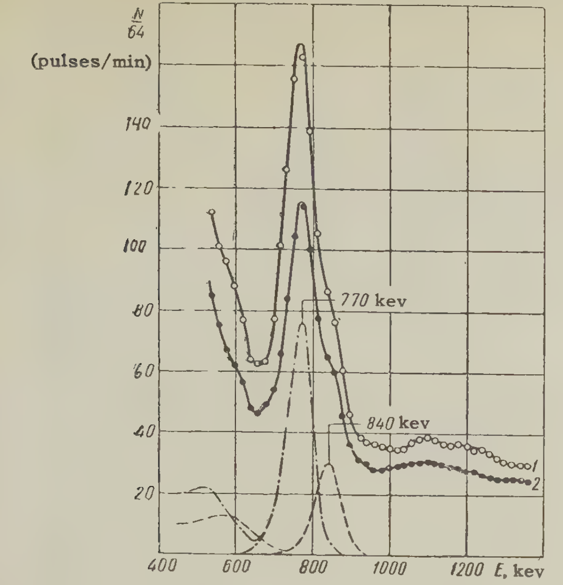

FIG. 2. Spectrum of pulsed from Mo^{96} γ rays: 1) measurements without filter, 2) measurements with 5.490 g/cm² filter.

d = 30 mm, which was used in our work. The reduction in ϵ_Φ for $E_\gamma < 100$ kev, which is shown in curve 2, is caused by the increased probability of escape of iodine K radiation from the crystal and the consequent increase in the "escape" peak at the expense of reducing the area under the peak corresponding to the full energy of the γ rays.

For $E_\gamma < 33$ kev (the binding energy of the electrons in the iodine K-shell), $\epsilon_\Phi \approx 100\%$.

The intensity of the measured γ rays, in numbers of quanta per neutron capture, was determined as previously[1] by comparison with the known γ-ray intensity from the $B^{10}(n, \alpha)Li^{7*}$ reaction, which is 0.935 quanta per capture.[7] The values of the effective neutron capture cross sections were taken from Hughes.[8]

The details of the technique for measurement of neutron capture γ rays (the geometry of the experiment; the extraction of the effect of neutrons from the $(n\gamma)$ reaction; the measurement of the spectra with thin lead filters to absorb the soft radiation for the purpose of reducing the background from hard γ rays; the resolution of the spectra into components; the determination of the intensity of γ-ray lines, etc) have been described earlier.[1]

RESULTS OF MEASUREMENTS

Molybdenum. A sample of metallic molybdenum weighing 0.666 g was enriched to 88.8% of the Mo^{95} isotope, so that 99.4% of the neutron captures occurred in this isotope. Figure 2 shows the spectrum of pulses from Mo^{96} γ rays in the energy region from 550 to 1350 kev. Curve 1 corresponds

Radiating nucleus	Present work		Results of other authors	
	γ-ray energy E_γ, kev	Number of quanta per neutron capture n_γ, in%	γ-ray energy E_γ, kev	Number of quanta per neutron capture n_γ, in%
Mo^{96}	360±10 770±10 840±10 1100—1240	~2 91±14 43±8 18		
Ag^{108}	22±2* 83±2 117±3 202 {197±3 215±4 (266±4) ** (302+5)	10±6 18±3 9±2 43 {21±4 22±4 12±3 18±4	82±2 [10] 117±2 [10] 199+3 [10] 187 [11]	20±4 [10] 11±2 [10] 34±6 [10]
Te^{124}	360±10 605±10 725±10	2.5±0.5 58±9 17±4	625±10 [15]; 609 [11]	54+14[15]
Cs^{184}	31±2* 120±3 184±3 (215±4) (258±4) (310±5)	27±6 20±3 9±2 7±2 5±1 4±1	Spectrum not resolved[11]	

*K x-radiation.

**The energies of γ lines whose existence has not been reliably established are given in parenthesis.

to measurements without a lead filter in the collimator, curve 2 to measurements with a 5.490 g/cm^2 lead filter. The dotted curves are the individual lines resolved from curve 2, whose energy and intensity are given in the table. In the 1100 to 1240 kev energy region there is an unresolved maximum from Mo^{96} γ rays with a total γ-ray intensity of ~18%. In the region $E_\gamma < 770$ kev we observed a small peak from 360-kev γ rays, but this peak is not present in the spectrum of the filtered radiation.

The hard γ rays from radiative capture of neutrons in molybdenum were measured by Kinsey and Bartholomew.[3] From their work, the energy of the first two excited states of Mo^{96} is 760 ± 15 and 1610 ± 20 kev. The 840- and 770-kev γ rays found in the present work are the cascade transition from the second excited state of Mo^{96} at 1610 kev, which is well known from the decay of Nb^{96} and Tc^{96}.[9] Apparently the (360 ± 10)-kev γ rays result from a transition between levels lying higher than the first two excited levels.

In the decay of Nb^{96} and Tc^{96} the Mo^{96} nucleus is excited to an energy ~2.7 Mev. The ground state of Mo^{96} is then reached only by cascade transitions through the first excited level. In neutron capture one produces an excited state of Mo^{96} with an excitation energy of 9.15 Mev.[3] However, in this case also the ground state of the nucleus is reached mainly by transitions through the first excited level (in 91 ± 14% of the cases of neutron capture).

Silver. A metallic silver sample weighing 0.455 g was enriched to 97.8% in the Ag^{107} isotope, so that 94% of the neutron captures took place in this isotope. Figure 3 shows the spectrum of Ag^{108} γ rays absorbed in 2.205 g/cm^2 of lead, and the resolution of the spectrum into components. The energies and intensities of the γ lines are given in the table. It should be mentioned that the half-width of the 202-kev peak exceeds by 30% the half-width for a monochromatic line of the same energy (which is shown by the dashed curve in Fig. 3). This allows us to postulate the presence in the region of the peak of at least two γ lines with energies 197 ± 3 and 215 ± 4 kev, with intensities of 21 ± 4 and 22 ± 4% respectively. This resulution is not unique since there are no reliable arguments for assuming that this maximum consists of two and not more than two lines. However these γ rays with their assigned energies fit well into the γ-ray transition scheme (Fig. 4) discussed below.

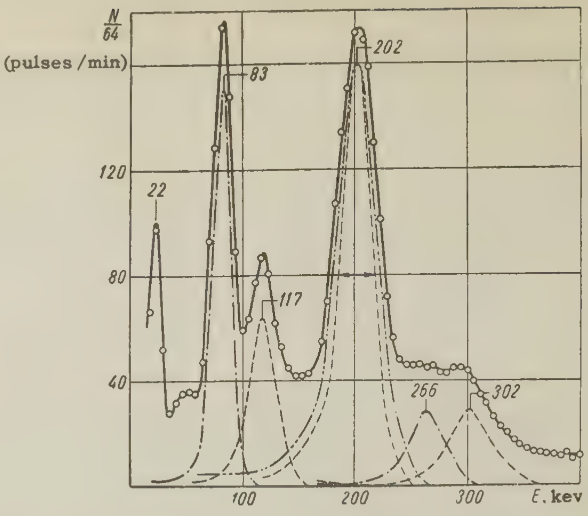

FIG. 3. Spectrum of pulses from Ag^{108} γ rays, absorbed in 2.205 g/cm^2 Pb.

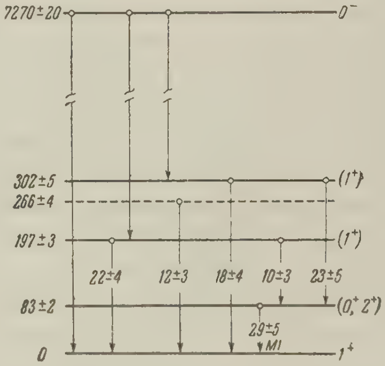

FIG. 4. γ-ray transitions in Ag^{108}. The numbers in the breaks in the arrows give the intensities of the transitions in percent per neutron capture, taking account of conversion $(n_\gamma + k_\gamma)$.

According to the data of Skliarevskii, Stepanov, and Obiníakov,[10] the γ rays from radiative capture of neutrons in the Ag^{107} and Ag^{109} isotopes include lines with energies close to one another. The intensities of the Ag^{108} γ lines found in the present work were corrected for the contribution of the radiation following neutron capture in Ag^{109} in the sample (6% of the captures) by using the intensities from reference 10. The values of energy and intensity for those γ lines which occur in both our work and in reference 10 are in good agreement. The 187-kev γ rays found by Hamermesh and Hummel[11] in the radiation accompanying neutron capture in natural silver are apparently due to a superposition of neighboring lines of Ag^{108} and Ag^{110}.[10]

The γ rays at 22 ± 2 kev are naturally interpreted as Ag K radiation, which could result from internal conversion in the K shell and from self-absorption of the γ rays in the target via the photoeffect. Of the observed 22 ± 4 x-ray photons per hundred neutron captures, 12 ± 2 photons are due to the effect of self-absorption. The self-absorption was computed for the target thickness 0.283 g/cm^2 employed in the experiment by using the intensities of the Ag^{108} γ lines given in the table. Thus 10 ± 6 x-ray photons are associated with internal conversion. After correcting for the K-fluorescence yield $f = 0.82$,[12] the number of cases of conversion of all the γ rays will be equal to $K = \Sigma K_{\gamma_i} = (12 \pm 7\%)$ per neutron capture, where K_{γ_i} refers to a single γ line. The "thick" target used in our experiments limited the accuracy in determining K.

The hard γ quanta from the Ag (n, γ) reaction which were found in reference 4 indicate the presence of levels in Ag^{108} with excitation energies of 0.32 ± 0.03 and 0.21 ± 0.03 Mev. The soft γ rays observed in the present work fix more precisely the energies of these levels which serve as the basis for setting up a possible scheme of γ transitions (Fig. 4). In this scheme, which includes the γ lines found by us, excited levels at 83 ± 2 and 266 ± 4 kev are introduced in addition to the levels mentioned above.

The state of Ag^{108} which is produced as a result of capture of a thermal neutron (from now on we call it the initial state) can be either 0^- or 1^- The direct transition to the ground state is an E1 transition. The transitions with comparable intensities to the 197- and 302-kev levels, which were found in reference 4, should also be E1. Thus these levels can be 0^+, 1^+, 2^+.

Using the known intensity of the 83-kev γ rays and theoretical values of the K-shell conversion coefficients taken from the work of Sliv and Band,[13] we can predict the number of cases of conversion K_{83} for radiative transitions of various multiplicities: 133 (M2), 37 (E2), 11.4 (M1), and 43 (E1) (in % per neutron capture). The quadrupole transitions contradict the experimental value of K as determined in the present work from the intensity of the x-rays. We have a choice between the dipole transitions M1 and E1 for the 83-kev γ transition. If we assign this transition to be E1, the state at 83 ± 3 kev must have negative parity. If this is the case, the intensities of the competing transitions of opposite parity from the 302- and 197-kev levels to the 83-kev level and to the ground state (cf. diagram) should be markedly different, whereas the experiments show them to be comparable (cf. table). In addition, in order to make the intensity of the transitions leading to the 83-kev state agree with the intensity of the transitions which deexcite this state, it is preferable to assign the (83 ± 3)-kev transition to M1. Thus this transition should be taken to be magnetic dipole, and the characteristics of the corresponding excited level can be 0^+, 1^+ or 2^+. In reference 4 no γ quanta corresponding to the transition from the initial state to the 83 kev level were found, which can be understood if the initial Ag^{108} state is 0^- and the 83-kev state is 0^+ or 2^+. The 0^- assignment for the initial state in Ag^{108} is directly established by the results of reference 14, in which the first resonance level of Ag^{107} at $E_p = 16.6$ ev was found to have $I = 0$. The excited levels at 197 and 302 kev will be 1^+, and the γ transitions shown in Fig. 4 will be either M1 or E2, which does not contradict the experimental value of K.

Tellurium. The 72.8-mg sample of metallic tellurium used in the experiment was enriched to 28% in Te^{123}, so that 97% of the neutron captures took place in this isotope. In 2.4% of the cases, the neutrons were captured by Te^{124} which constituted 41.5% of the sample. The energies and intensities of the observed γ rays are given in the table. Figure 5 shows the spectrum of γ lines absorbed in a 4.39 g/cm lead filter, in the region of well-resolved lines (shown dotted in the figure). The energy and intensity of the (605 ± 10)-kev γ quanta determined in the present work agrees, within the limits of error, with the results of previous work.[11,15]

The γ quanta with energies of 775 and 605 kev can only come from Te^{124}, because of their high intensity. Similar γ rays are observed in the radioactive decay of Sb^{124} and I^{124},[9] where they correspond to transitions between the first two levels of Te^{124}. The 360-kev γ lines with 2.5% intensity could belong to Te^{125} since the target contains Te^{124}. But in that case the high intensity of this line (~100% per neutron capture in Te^{124})

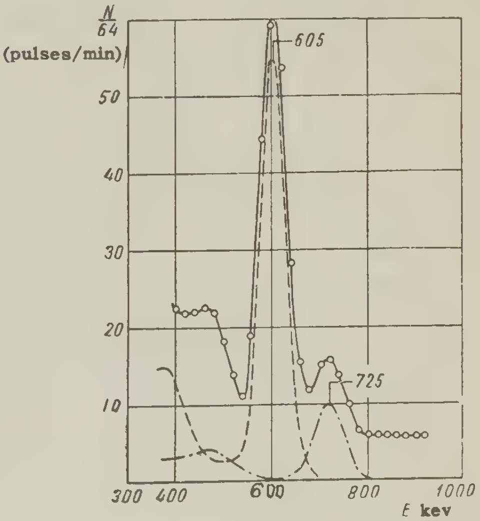

FIG. 5. Spectrum of pulses from Te^{124} γ rays absorbed in 4.386 g/cm^2 Pb.

would require its assignment as a transition from one of the lower lying levels. But it is known from the decay of Sb^{125} (reference 9) that no γ quanta of such energy are emitted in transitions between the low lying states of Te^{125}. Thus the 360-kev γ quanta observed here probably belong to Te^{124} and correspond to transitions between levels with excitation energies greater than 1380 kev.

The intensities of the transitions between the first two excited states of the even-even nuclei Te^{124} and Mo^{96} differ somewhat. In Te^{124} the majority of the cascade transitions from the initial state lead to the ground state, passing over the first two excited states.

Cesium. In the measurements with cesium, we used targets of cesium fluoride weighing 0.540, 2.486, and 8.200 g. The first of these targets was used for the measurements in the region $E_\gamma \leq 50$ kev, where the absorption of the γ rays in the source material is especially important. Figure 6 shows the spectrum of the γ rays, absorbed in 2.205 g/cm^2 of lead, for the 2.486-g target, and its resolution into components (only the photopeaks are shown). The energies and intensities of the γ lines are given in the table. The Cs^{134} nucleus has a level at 10.5 kev whose quantum numbers (5^+) are close to those of the 4^+ ground state.[9] The γ transitions from higher levels to this level and to the ground state can have comparable probabilities. It is possible that the spectrum is poorly resolved in the region $E_\gamma > 180$ kev because of overlapping of γ lines due to such transitions. The neutron capture γ rays of cesium were measured earlier by Hamermesh and Hummel,[11] but the spectrum was not resolved. The γ lines found in the present work are not to be associated with the decay of the three-hour isomer of Cs^{134}, since the cross section for activation of this isomer is small $(2 \times 10^{-2}$ barn). The intense γ radiation with energy 120 ± 3 kev probably corresponds to a transition from a (120 ± 3)-kev state to the ground state. The less intense γ quanta with energy 184 ± 4 kev are possibly due to transitions between levels with excitation energies of 310 ± 5 and 120 ± 3 kev, while the 310-kev γ rays come from the direct transition from the excited state to the ground state.

The softest γ radiation with energy 31 ± 2 kev is the x-radiation of cesium, emitted mainly after internal conversion of the γ quanta in the K shell. For the thin target of cesium fluoride, the correction for self-absorption through the photoeffect amounted to 10% of the observed x-ray intensity. Taking into account the K-fluorescence yield $f = 0.89$,[12] the total number of cases of conversion will be $K = (30 \pm 6)\%$ per neutron capture. The value of K was compared with the intensities of the γ lines, using theoretical values of the K-shell internal conversion coefficients,[13] in a way similar to that which we described in our discussion of the measurements on silver. This analysis leads to the conclusion that the 120-kev γ transition is E2, while the 184 and 215 kev transitions are M2. In this case we get a value of $K = 25 \pm 5$, in satisfactory agreement with the experimental data. The large number of soft γ rays in the spectrum from the $Cs^{133}(n, \gamma)$ reaction indicates that the odd-odd nucleus Cs^{134} has a high level density even near the ground state.

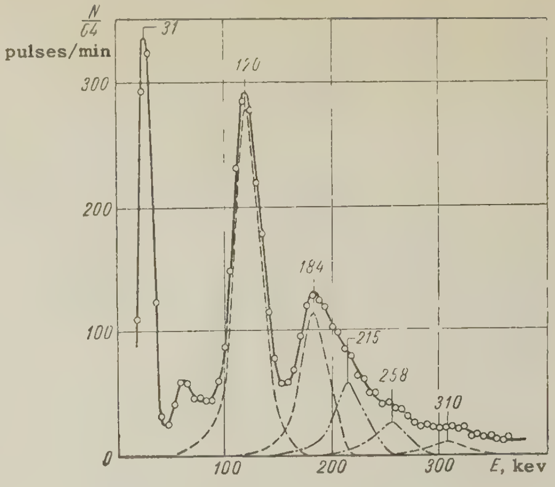

FIG. 6. Spectrum of pulses from Cs^{134} γ rays absorbed in 2.205 g-cm^2 Pb.

The authors thank I. S. Shapiro for his interest in the work and discussion of the results; S. A. Gavrilov, A. P. Shilov, and the entire operating crew of the physics reactor, and also Ia. A. Kleiman, A. M. Safronov and V. F. Tsarakaev for assistance in carrying out the experiment.

---

[1] Estulin, Kalinkin, and Melioranskii, J. Exptl. Theoret. Phys. (U.S.S.R.) **32**, 979 (1957), Soviet Phys. JETP **5**, 801 (1957).

[2] Short communication in Атомная энергия (Atomic Energy) **3**, 276 (1957).

[3] B. B. Kinsey and G. A. Bartholomew, Can. J. Phys. **31**, 1051 (1953).

[4] G. A. Bartholomew and B. B. Kinsey, Can. J. Phys. **31**, 1025 (1953).

[5] Ad'iasevich, Groshev, and Demidov, Сессия АН СССР по мирному использованию атомной энергии 1—5 июля 1955 г. (Session of the Academy of Sciences of the USSR on peaceful uses of atomic energy, July 1-5, 1955). Session of the Division of Physical and Mathematical Sciences, Acad. Sci. Press, p. 270, 1955.

[6] A. S. Melioranskii and Iu. M. Ostanevich, **Приборы и техника эксперимента** (Instrum. and Meas. Engg.) (in press).

[7] J. A. DeJuren and H. Rosenwasser, Phys. Rev. **93**, 831 (1954).

[8] D. J. Hughes, Pile Neutron Research, Addison-Wesley, 1953.

[9] V. S. Dzhelepov and L. K. Peker, **Схемы распада радиоактивных изотопов** (Decay Schemes of Radioactive Isotopes), Acad. Sci. Press, Moscow-Leningrad, 1957.

[10] Skliarevskii, Stepanov, and Obiniakov, **Атомная энергия** (Atomic Energy) (in press).

[11] B. Hamermesh and V. Hummel, Phys. Rev. **88**, 916 (1952).

[12] C. E. Roos, Phys. Rev. **105**, 931 (1957).

[13] L. A. Sliv and I. M. Band, **Таблицы коэффициентов внутренней конверсии гамма-излучения** (Tables of Internal Conversion Coefficients of Gamma Radiation), Part 1. Acad. Sci. Press, Moscow-Leningrad, 1956.

[14] Rae, Collins, Kinsey, Lynn, and Wiblin, Nucl. Phys. **5**, 89 (1958).

[15] Fenstermacher, Bennett, Walters, Bockelman, and Schultz, Phys. Rev. **107**, 1650 (1957).

Translated by M. Hamermesh
125

SOVIET PHYSICS JETP VOLUME 35(8), NUMBER 3 MARCH, 1959

INELASTIC INTERACTION BETWEEN COSMIC RAY PROTONS OF KINETIC ENERGY ABOVE 7 Bev AND CARBON AND HYDROGEN NUCLEI

K. I. ALEKSEEVA and N. L. GRIGOROV

Moscow State University

Submitted to JETP editor April 8, 1958

J. Exptl. Theoret. Phys. (U.S.S.R.) **35**, 599-611 (September, 1958)

Inelastic interaction between cosmic ray protons of kinetic energy above 7 Bev (mean energy ~ 20 Bev) and carbon and hydrogen nuclei was investigated at a geomagnetic latitude of 31° N in the stratosphere. The measurements were made with a telescope containing absorbers of lead and of the investigated graphite and paraffin. A system of hodoscopic counters surrounded the telescope and the absorbers. A value of 315 ± 50 millibarns was obtained for the proton-carbon inelastic-interaction cross section. The proton-proton inelastic interaction cross section was 32 ± 10 millibarns. The average number of charged penetrating particles was found to be 4.2 ± 0.5 particles per shower in carbon and ~ 3.4 particles per shower in hydrogen.

1. INTRODUCTION

THE study of absorption of beams of nuclear-active particles in cosmic rays[1] and of the formation of various secondary cosmic-ray components in the atmosphere[2] has led in its time to the conclusion that the interaction between nucleons and light nuclei have low inelasticity in the energy range from 2 to 1,000 Bev. In connection with this, it has been suggested by Vernov[3] that the observed low inelasticity of the interaction discloses a certain structural feature of the nucleon, namely that it has a denser central portion and less dense peripheral portion. Experiments on the scattering of 1.4-Bev pions by protons, performed in 1955,[4] lead to similar conclusions.

A study of the inelasticity of interaction between nucleons and nuclei is thus found to be one of the effective means of investigating the structural properties of the interacting particles. It must be emphasized here that the value of the coefficient of inelasticity of interaction obtained in references 1 and 2 depends substantially on the effective cross section for inelastic interaction between the nucleons and the nuclei of the atoms in the atmosphere. This cross section was assumed to equal the geometric cross section. It was therefore quite important to measure this cross section for cosmic-ray particles in the region of energies, for which collisions with light nuclei were found to be of low inelasticity.

Directly connected with problems in the interaction of high-energy particles with light nuclei is the study of the dependence of the number of particles generated upon interaction on the atomic weight of the nucleus and on the energy of the incident particle. It is equally important to determine the effective cross section of inelastic proton-proton interaction and its energy dependence.

In the present article we report the measured effective cross sections of inelastic interaction between primary cosmic rays (protons with kinetic energy greater than 7 Bev) with carbon and hydrogen nuclei[5-8] and the measured number of particles generated in these interactions. The experiments were performed in the stratosphere at an altitude of 20 to 25 km and a geomagnetic latitude 31°N, for there the proton energy spectrum is cut off on the low side of 7 Bev, and diminishes as the 1.5 power with increasing energy (integral spectrum). The apparatus developed made it possible to measure the interaction cross section by two different methods, to measure the number of particles produced by interaction, and to determine the current of primary particles with greater procedural reliability than previously.

2. MEASUREMENT METHOD AND APPARATUS

Two methods were used in this work to determine the inelastic-scattering cross section.

Method I. The cross section was determined from the reduced flux of single shower-producing protons as the latter pass through the investigated absorber. The flux is reduced by inelastic interactions between the protons and the atomic nuclei of the investigated matter. The relative reduction in the flux is determined in this method by the

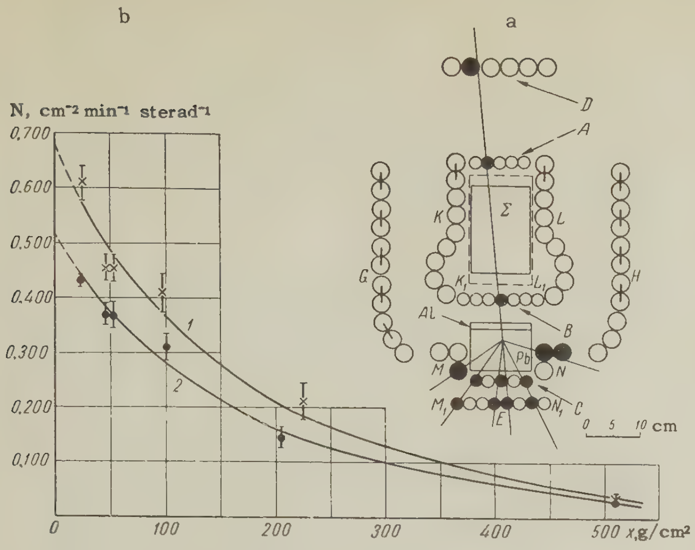

FIG. 1. a) Arrangement of counters and absorbers in the instrument and counter operation in the shower, b) Number of showers of lead measured as follows: 1) without graphite absorber in telescope, 2) with 16.8 g/cm² graphite in the telescope.

change in the number of electron-nuclear showers from a lead indicator over which the investigated absorber is placed.

Method II. The cross section is determined by directly measuring the number of electron-nuclear showers occurring in the investigated matter when nuclear-active particles pass through the latter.* To determine the cross section by this method it is necessary to know, in addition to the number of electron-nuclear showers from the investigated substance, also the flux of shower-producing protons I_x at a given depth of the atmosphere x. This flux can be determined if we know the flux I_0 of the primary protons, arriving from cosmic space at the boundary of the atmosphere, and we know the absorption range of the shower-producing component in the air, L_{abs}^{air} (L_{abs}^{air} is determined from the altitude dependence of the electron-nuclear showers in lead).[6]

Thus, to solve our problem with the aid of the above two methods, we had to measure in the stratosphere, as accurately as possible, the number of electron-nuclear showers in paraffin, graphite, and lead. It was also necessary to determine the altitude dependence of the particle flux of the hard component which, when extrapolated to the

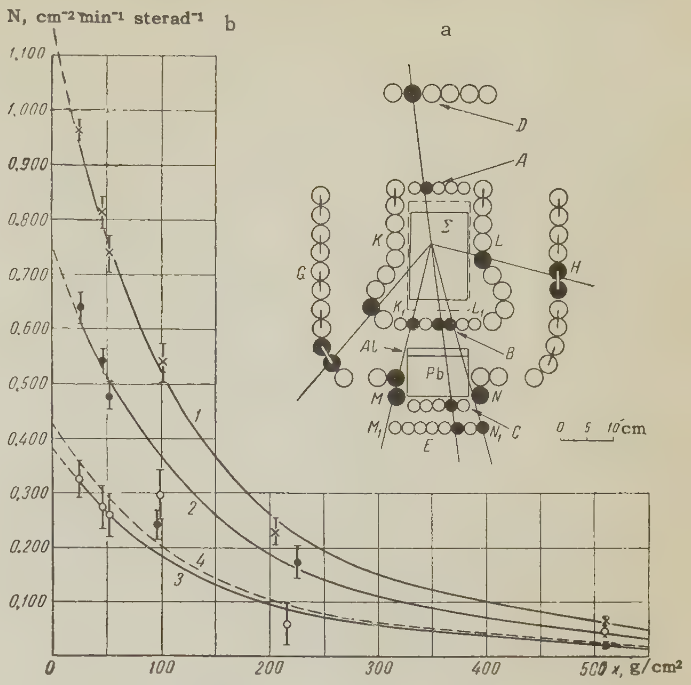

FIG. 2. a) Arrangement of counters and absorber in the instrument and counter operation in the shower. b) Curves: 1) number of showers in upper part of the instrument when measured with graphite absorber (16.8 g/cm²); 2) the same without graphite absorber (background); 3) difference between curves 1 and 2; 4) number of interactions in carbon N_{intC}, with allowance for corrections.

top of the atomosphere, yields the flux* I_0 of the primary protons. Based on these requirements, we selected apparatus that separated, the hard component of cosmic rays with the aid of lead. To obtain good geometrical conditions with respect to separation of the hard components, we placed the lead indicator of our instrument in the lower portion of a rather long telescope, thanks to which the possibility of registering the so-called "additional" showers in lead due to particles moving outside the solid angle of the instrument.†

The placement of the counters and absorbers in the instruments used to determine the cross section of inelastic interaction is shown in Figs. 1a and 2a. The vertical telescope consisted of three rows A, B, C of self-quenching Geiger-Mueller counters, (five counters in each row) connected for three-fold coincidence. Row D of hodoscopic counters, placed at a certain distance above the Geiger counters, covered almost the entire solid angle of the instrument. An absorber comprising 8 cm of lead and 0.9 cm of aluminum was placed between rows B and C of the telescopic counters. Absorber Σ of the investigated substance was placed between rows A and B of the telescopic counters. The solid lines in the diagram show the placement of an absorber made of powdered graphite (volume density $d \approx 1.0$ to 1.1 g/cm^3; density per unit absorber surface $d_1 = 16.0$ g/cm^2). The dotted line shows the position of a paraffin absorber ($d \approx 0.95$ g/cm^3; $d_1 = 18.8$ g/cm^2). The absorbers were interchanged automatically every three minutes. The telescope and the absorbers were surrounded by a large number of counters (K, K_1, L, L_1, M, M_1, N, N_1, E, G, H),* which served to register the charged particles produced by interaction between the protons and carbon, hydrogen, and lead nuclei. All counters,† including the telescopic ones, were connected to a vacuum-tube hodoscope.

---

*Owing to the large extent of the atmosphere at low density of matter, the nuclear-active components in the stratosphere with energies below 10^{11} ev are almost exclusively nucleons, since the charged pions with energies less than 10^{11} ev decay before they interact with the nuclei of the air atoms.

*By extrapolating to the top of the atmosphere we found the flux of primary particles at latitude 31°N (longitude 73°E) to be $I_0 = 2.0$ to 2.1 particles/cm²-min-sterad.[6] Winkler et al[9] found at a depth of 15 g/cm² (geomagnetic latitude 30°N) a value $I_{x=15} \approx 2.7$ to 2.8 particles/cm²-min-sterad with a 3-cm lead absorber. Extrapolation of Winkler's data to the top of the atmosphere where the flux of the primary particles at the boundary of the atmosphere at latitude 30°N a value $I_0 = 2.1$ to 2.2 particles/cm²-min-sterad, i.e., a value very close to ours.

† The "additional" showers due to particles traveling outside the solid angle of the instrument cause coincidences of discharges in telescopic counters only because shower particles enter into these counters.

The pulse controlling the operation of the instrument was produced by three-fold coincidence of the discharges and counters A, B, and C. However, when processing the measurement results, we took into account only those cases where the triple coincidence was accompanied by operation of one of the counters in row D, i.e., four-fold coincidences. The instrument readings were telemetered to the earth and recorded on motion-picture film by a photoregister. The resolution of the telescope was 3×10^{-6} seconds; the resolution of the hodoscopic numbers (which was different for different counter groups) ranged from 1×10^{-5} to 2×10^{-5} seconds. The instruments, their characteristics, the method of hodoscope data processing, and the methods used to introduce various corrections in the measurement results are all described in references 6 to 8.

The results published in this article were obtained by launching five instruments in pilot balloons into the stratosphere in September 1955. Two of these instruments contained a graphite absorber and an absorber comprising 8 cm lead and 0.9 cm aluminum in the telescope, two contained absorbers of paraffin and graphite and a Pb + Al absorber, and one contained absorbers of paraffin and graphite without a Pb + Al absorber in the telescope.

3. USE OF METHOD I TO DETERMINE THE RANGE AND CROSS SECTION FOR INELASTIC INTERACTION BETWEEN A PROTON AND A CARBON NUCLEUS

Using hodoscopic counters, we were able to investigate cases where a singly-charged particle (proton) traversed the upper portion of the telescope (through absorber Σ) without interacting and without experiencing inelastic interaction in the lead block. We selected here the events in which the particles of the shower produced in the lead entered only into counters C, E, M, M_1, N, and N_1, located in the lower portion of the instrument around the lead (showers produced in lead without upward-moving particles). The selection method employed is illustrated by the shower in lead shown in Fig. 1a (the counters operated by the passage of the particles are denoted by the filled-in circles). The number of such showers in lead is proportional to the flux of single shower-producing particles incident on the lead. When the graphite is placed in the telescope the flux diminishes in accordance with the reduction in the flux of single shower-producing particles. An analysis of the counters operated in the showers has shown that these showers contain practically no non-local shower impurities (not more than 4%).

Figure 1b shows the measured number of showers in lead in the presence of graphite in the telescope, (N^C_{sPb}, curve 2) and without graphite (N^b_{sPb}, curve 1) at different depth x of the atmosphere. The curves were corrected for random coincidences and for δ showers (the correction for the δ showers in lead was the same with and without graphite in the telescope and its numerical value was (6.85 ± 0.12)% of the number of single particles registered at a given altitude[6-8]). The statistical errors are indicated for all points of the curves. To increase the statistical accuracy of the determined cross section for the interaction with carbon we also used, when plotting the curves, the results of a series of measurements with graphite and paraffin with an approximate account of the shower production in hydrogen. The effective thickness of the graphite absorber, for the

---

*In the processing of the results we disregarded the counter rows G, and H, which were used only to monitor the operation of counters K and L.

†The dimensions of the counters are given in reference 6. The counters were filled with a mixture of argon and ethylene. The negative electrode was a thin graphite layer deposited on the inner surface of the glass walls of the counters. The counter glass wall was 1.0 to 1.5 mm thick.

TABLE I. Range and cross section of inelastic p-C interaction as measured by method I.

Depth of atmosphere, x, g/cm²	Showers in lead			L_p^C, g/cm²	σ_p^C, mbn
	without graphite in telescope N_{sPb}^b, cm⁻² min⁻¹ sterad⁻¹	with graphite* in telescope N_{sPb}^C cm⁻² min⁻¹ sterad⁻¹	$\frac{N_{sPb}^C}{N_{sPb}^b}$		
53.0	0.452 ± 0.026	$0,369\pm0.024$	$0,816\pm0.070$		
46.7	$0.454\pm0,024$	$0,370\pm0.019$	0.815 ± 0.059		
25.0	0.609 ± 0.029	$0.431\pm0,012$	0.709 ± 0.039		
Average 33.7			0.754 ± 0.030	63^{+12}_{-9}	315 ± 50

*Effective thickness of graphite 16.8 g/cm².

combined data, was 16.8 g/cm². From the data given in Fig. 1b it is possible to determine the range L_p^C for the inelastic interaction between a proton and carbon nucleus, using a formula that accounts for the fraction of α particles in the primary cosmic radiation:

$$N_{sPb}^C / N_{sPb}^b = p \exp\{-16.8/L_p^C\} + \alpha \exp\{-16.8/L_\alpha^C\}. \tag{1}$$

Here p and α are the fractions of the protons and α particles at altitudes 20 to 25 km, and L_α^C is the interaction range of an α particle in a light substance, assumed here as 40 g/cm². The number of primary α particles at the top of the atmosphere was assumed to be 20% of the total number of primary particles. The correction for the interaction due to α particles was approximately 5% of the value of the cross section.

The range L_p^C and the cross section σ_p^C for inelastic interaction between protons and carbon nuclei, obtained by the above method in the altitude range from 20 to 25 km, was found to be (see Table I):

$$L_p^C = 63^{+12}_{-9} \text{ g/cm}^2; \ \sigma_p^C = 315 \pm 50 \text{ millibarns}.$$

It must be noted that the cross section of inelastic interaction as determined by the above method includes automatically interactions with proton charge exchange and with formation of only neutral fast particles; it also includes events of shower production by charged particles with a wide angle of divergence, when not one charged particle enters the lower row of telescopic counters.

4. USE OF METHOD II TO DETERMINE THE RANGE AND CROSS SECTION OF INELASTIC INTERACTION BETWEEN A PROTON AND A CARBON NUCLEUS

The showers of the particles that are produced by interaction between protons and carbon nuclei are identified by operation of the counters that are immediately adjacent to the graphite filter (counters K, K_1, B, L_1, L) independently of the operation of the counters located near the lead, i.e., they are classified as showers registered in the upper portion of the instrument.[6] An example is the event shown in Fig. 2a.

We determine the range of inelastic interaction from the relation

$$N_{\text{int C}} = I_x p (1 - \exp\{-16.8/L_p^C\}) + I_x \alpha (1 - \exp\{-16.8/L_\alpha^C\}). \tag{2}$$

Here $I_x = I_0 \exp(-x/L_{\text{abs}}^{\text{air}})$ is the flux of shower-producing particles at a given depth x of the atmosphere, I_0 is the flux of primary particles on the top of the atmosphere at the geomagnetic latitude 31°N, $L_{\text{abs}}^{\text{air}}$ is the absorption range of the shower-producing component in the air, and $N_{\text{int C}}$ is the number of nuclear interactions in carbon.

Figure 2b shows the altitude dependence of the showers registered in the upper portion of the instrument by the counters that surround directly the graphite absorber, obtained with a graphite absorber (N_s^C, curve 1) and without it (N_s^b, curve 2). These curves have been corrected for random coincidences and for δ showers (the corrections are respectively (7.00 ± 0.20)% and (3.00 ± 0.15)% of the total number of registered single particles with and without graphite in the telescope[6-8]). The statistical errors are indicated for all points of the curves. Curve 3 of Fig. 2b represents the difference between curves 1 and 2. Curve 4 was obtained from curve 3 by introducing corrections for the change in the number of showers in lead with upward-directed particles, when changing from measurements with graphite to measurements without graphite (correction for the variation in the "backward current," see references 6 and 7), and for the entrance of shower

TABLE II. Measured range and cross section for inelastic p-C interaction by method II.

Depth of atmosphere, x, g/cm²	Showers in upper portion of instrument			Flux of shower-producing particles I_x for $I_0 = 2.0$	$\frac{N_s^C - N_s^b}{Ix}$	Correction for change in "backward current"	Correction for slits	$\frac{N_s^C - N_s^b}{I_x}$ with corrections	L_p^C, g/cm²	σ_p^C, mbn
	with graphite* N_s^C cm⁻² min⁻¹ sterad⁻¹	without graphite (background) N_s^b cm⁻² min⁻¹ sterad⁻¹	$N_s^C - N_s^b$							
53.0	0.741±0.034	0.482±0.027	0.258±0.043	1.402	0.184±0.030					
46.7	0.815±0.028	0.542±0.026	0.274±0.038	1.467	0.186±0.026					
25.0	0.964±0.018	0.638±0.029	0.326±0.034	1.683	0.193±0.020					
Average 33.7					0.190±0.014	+0.015	+0.010	0.215±0.014	76±7	264±24

*Effective thickness of graphite 18.8 g/cm².

particles into the slit between counters (see Table II). To determine the cross section with our data, we took the flux of primary particles on the top of the atmosphere of latitude 31°N to be $I_0 = 2.0$ particles/cm²-min-sterad (reference 6) and the range of absorption of a shower-producing component in air to be L_{abs}^{air} 150 g/cm² (reference 6).

Using this method we obtain the following values for the range and for the cross section of inelastic p-C interactions (see Table II):

$$L_p^C = 76 \pm .7 \text{ g/cm}^2; \sigma_p^C = 264 \pm 24 \text{ millibarns.}$$

The cross section obtained by direct observation of showers in graphite thus turned out to be some 20% less than the value obtained from the reduction in the flux of single shower-producing particles. It is possible that this difference is explained essentially by the fact that when the protons interact with the carbon nuclei, approximately 10 or 15% of the events are accompanied by interactions without a shooting off of high energy charged particles (π^0 mesons and fast neutron).[10,11] It is also possible that charged-particle showers with wide divergence angles are produced, so that not a single charged particle enters into the lower row C of the telescopic counters. These events are missed by the instrument in the direct observation of showers in the graphite, but are registered by the first of the methods described. The indicated fraction of such interactions is quite probable, if we consider that the showers observed in graphite consist in approximately 30% of the cases of two charged particles. Comparison with the measured values of the cross section, obtained by other authors[12-14] by diverse methods, also indicates a possible error in counting the interactions in determination of the proton-carbon nucleus cross section by direct observation of showers in graphite.

5. CROSS SECTION OF INELASTIC PROTON-PROTON INTERACTION

We investigated the inelastic proton-proton interaction as the difference between proton interactions in paraffin and in graphite. Both aforementioned methods were used to determine the cross section for inelastic proton-proton interactions. Production of a shower that consists of only neutral fast particles is considerably less probable in proton-proton interactions than in collisions between a proton and a complex nucleus. The method of direct observation of showers on hydrogen can therefore be considered practically free of interaction counting errors due to production of fast neutral particles alone. This is in contrast

TABLE III. Results of measurement of range and cross section of inelastic p-p interaction

Instrument	Method	Average depth of atmosphere, x, g/cm²	Ratio of fluxes I_{par}/I_{gr}	L_p^H, g/cm^{-2}	σ_p^H, mbn
No. 3 with absorber 8 cm Pb + 0.9 cm Al	II	36.4	0.905 ± 0.033		
No. 5 with absorber Pb + Al	II	25.9	0.948 ± 0.030		
No. 7 without lead absorber	II	42.5	0.981 ± 0.028		
No. 3 with absorber 8 cm Pb + 0.9 cm Al	I	36.4	0.866 ± 0.058		
No. 5 with Pb + Al absorber	I	25.9	1.000 ± 0.060		
	Average	34.0	0.947 ± 0.060	51^{+23}_{-12}	32 ± 10

Note: Amount of hydrogen in paraffin 2.8 g/cm².

with what takes place in the determination of the cross section for the interaction between protons and carbon nuclei. We have determined the cross section from flight data with two instruments (Nos. 3 and 5) with paraffin, graphite, and lead absorbers and with one instrument (No. 7) with paraffin and graphite absorbers, but without a lead absorber in the telescope.

For approximate standardization of the conditions of registration of the electron-nuclear showers produced in the paraffin and graphite, we used powdered graphite. The graphite and paraffin absorbers were placed in the telescope with their centers aligned (see Figs. 1a and 2a). The thickness of the graphite absorber, in g/cm², was equivalent to the amount of carbon, in the paraffin absorber, also in g/cm².

We have calculated the cross section for inelastic proton-proton interaction from the ratio of the fluxes of single shower-producing particles obtained with paraffin and graphite in the telescope (I_{par} and I_{gr} respectively). This ratio is related to the range L_p^H of inelastic proton-proton interaction by the equation

$$I_{par}/I_{gr} = \exp(-2.8/L_p^H); \qquad (3)$$

where 2.8 is the amount of hydrogen in paraffin (g/cm²). The interaction due to primary α particles was negligible.

In the method of direct observation of showers in paraffin (N_s^{par}) and in graphite (N_s^{gr}), the flux ratio is obtained by measuring the quantity $(N_s^{par} - N_s^{gr})/I_{gr}$, since $I_{par}/I_{gr} = 1 - (N_s^{par} - N_s^{gr})/I_{gr}$. Here $I_{gr} = I_x \exp(-x'L_p^C) = I_0 \exp(-x/L_{abs}^{air}) \exp(-x'L_p^C)$ is the flux of single shower-producing particles at a given depth x of the atomosphere, attenuated by interaction with carbon nuclei in the paraffin absorber, and x′ is the carbon in the paraffin in g/cm². To determine I_{gr} we used our following data: 1) $I_0 = 2.0$ particles/cm²-min-sterad;[6] 2) $L_{abs}^{air} = 150$ g/cm²;[6] 3) $L_p^C = 63$ g/cm² (sec. 3; see also reference 7).

In the method that makes use of the reduction in the flux of single shower-producing particles, the flux ratio is obtained by measuring the number of showers in lead in the presence of paraffin (N_{sPb}^{par}) and graphite (N_{sPb}^{gr}) in the telescope: $I_{par}/I_{gr} = N_{sPb}^{par}/N_{sPb}^{gr}$.

Table III shows the values of the ratio of fluxes of single shower-producing particles, I_{par}/I_{gr}, obtained with various instruments and diverse methods. These values include the corrections (see references 6 and 8). The statistical errors are indicated in all cases.

After averaging all the data given in the table, with allowance for the statistical weights, the range L_p^H and cross section σ_p^H of inelastic proton-proton interaction become:

$$L_p^{II} = 51^{+23}_{-12} \text{ g/cm}^2 \quad \sigma_p^H = 32 \pm 10 \text{ millibarns}$$

Figure 3 shows the cross section for inelastic

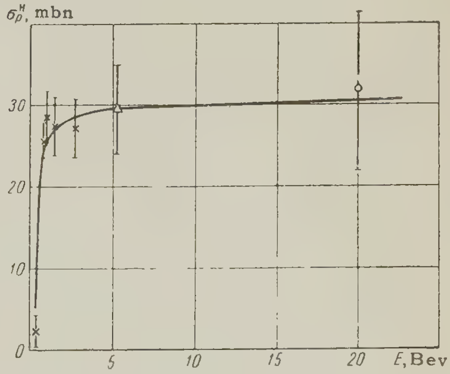

FIG. 3. Effective cross section of proton-proton inelastic integration vs. kinetic energy of incident proton. × – data of reference 15, obtained with accelerators, △ – Wright et al.[16] o – Alekseeva and Grigorov.[5,8]

proton-proton interaction as a function of the kinetic energy of the incident proton, plotted from data obtained with accelerators[15,16] and from our own data obtained with cosmic-ray protons of kinetic energy > 7 Bev ($\bar{E} \approx 20$ Bev). This curve shows that, within the limits of statistical experimental errors, no considerable change in the cross section for inelastic proton-proton interaction is observed in the energy interval from 1 or 2 to approximately 20 Bev.

At energies on the order of several Bev we can estimate the nucleon interaction in peripheral collisions from a calculation of the interaction of their π-meson fields by the Weizsaecker-Williams method. Such an estimate was made by Bubelev,[17,18] who used experimental[3,4] values of the scattering cross section and of the radius of the nucleon core.[15] In the energy range from 1 to 10 Bev, Bubelev's calculations yield a constant effective cross section for inelastic peripheral nucleon collisions. If we take Bubelev's calculations, then our experimental data, which suggests a constant effective cross section for inelastic interactions up to energies of ≈ 20 Bev, lead to the conclusion that, in the energy range from 1 or 2 to ~ 20 Bev, the contribution of central collisions to the value of the cross section remains constant and does not exceed $\sim 20\%$.

6. NUMBER OF PARTICLES IN ELECTRON-NUCLEON SHOWERS, OBTAINED ON LIGHT NUCLEI AT ENERGIES 10^{10} ev.

By analyzing the operation of the counters directly adjacent to the investigated absorber Σ (counters K, K_1, B, L_1, and L; Fig. 2a) we were able to determine the distribution of the showers of particles in carbon and hydrogen from the number of operating counters; we were also able to determine the average number of counters operated per shower. The shower particles registered by the counters consisted essentially of penetrating particles (the energy of the π mesons registered by the counters surrounding the absorber Σ was $E_\pi \gtrsim 50$ Mev).

Figure 4 shows the distributions of the electron-nuclear showers over the number n of counters operated per shower (over the number of particles in the shower), obtained by us and by the authors of reference 20, as a percentage of the total number of registered electron-nuclear showers with $n \geq 2$. Curve 1 gives the distribution of electron-nuclear showers in carbon, as obtained from the number of counters operated in the shower,* for an altitude of 20 to 25 km at geomagnetic latitude 31°N. To improve the statistics in plotting this curve, we used the combined data of all the instruments lifted to the stratosphere, both with graphite absorbers and with graphite and paraffin absorbers, with a lead absorber in the telescope. The measurement results were corrected for random coincidences and for δ showers. Curve 2 of Fig. 4 gives the measured number of penetrating particles in showers in beryllium, obtained by Baradzei, Smorodin et al.[20] with the aid of a cloud chamber at an altitude of 9 km and geomagnetic latitude 51°N. These results are free of the influence of the control signal on the shower selection, since the chamber would operate by passage of even one charged particle through the instrument. We see that our shower spectrum differs substantially from the spectrum obtained in reference 20 (curve 2). This difference in spectra cannot be attributed to the difference in the atomic weights of the investigated substances (carbon and beryllium), since these atomic weights are close to each other. There is also little likelihood that the difference in the spec-

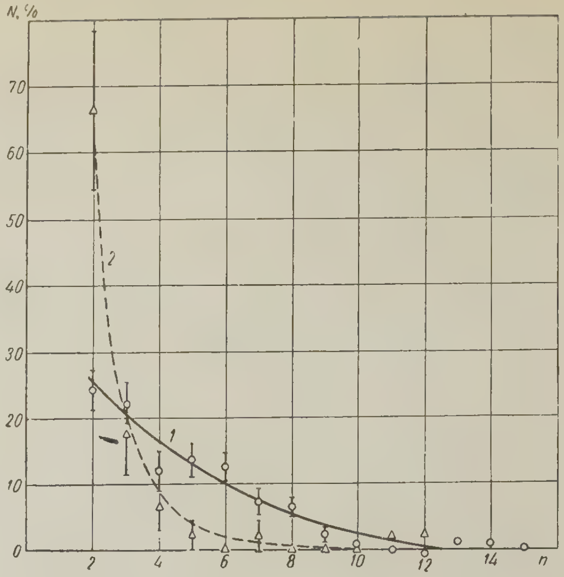

FIG. 4. Distribution of electron-nuclear showers with more than 2 charged particles with respect to the number of particles n in the shower, as a percentage of the total number of counted showers. 1) showers in carbon, according to Alekseeva and Grigorov; 2) showers in beryllium according to Baradzei, Smorodin, et al.[20]

---

*In those cases when two counters in rows K and L could be operated by passage of a single particle (operation of two in-line counters in the middle of rows K and L), these two counters were regarded as a single counter.

tra is due to differences in the apparatus.*

The difference between our spectrum and that obtained by the authors of reference 20 (see Fig. 4) is apparently due to difference in the energy spectra of the shower-producing protons.

We obtained the following values for the average number of operated counters (average number of penetrating particles) in showers with $n \geq 2$ particles at an average energy of shower-producing protons $\bar{E} \sim 20$ Bev: $\bar{n} = 4.2 \pm 0.5$, and $n \approx 3.4$ particles per shower for carbon and hydrogen, respectively (see Table IV).

Comparison of the average number of charged π mesons in showers with $n \geq 2$ in beryllium, at an average kinetic energy of shower-producing protons $\bar{E} \sim 6$ Bev (reference 20 and 21), with the value we obtained for the average number of charged π mesons in showers from carbon at an average proton energy $\bar{E} \sim 20$ Bev (see Table IV) gives an approximate dependence $\bar{n} = k\bar{E}^m$, where $m \sim 0.3$.

At energies $\sim 10^{10}$ ev, the production of π mesons by nucleon-nucleon interactions is treated by the statistical theory of multiple-particle production. The principal conclusions of this theory, with allowance for the nucleon isobar states that arise during the interaction, are discussed in reference 22. It would be interesting to compare our experimental data on the number of particles produced in p-C and p-p interactions with the deductions of the statistical theory of multiple-particle production in nucleon-nucleon interactions. Inasmuch as we deal in stratosphere measurements with proton spectra that are different at different altitudes, we have calculated, for the sake of comparing the experimental results with the theoretical deductions, the average number of charged particles (p, π^+, π^-) per shower in p-p interactions for the primary-proton spectrum in the stratosphere at geomagnetic latitudes 31°N $(\bar{E}_{kin} \sim 20$ Bev) and 51°N $(\bar{E}_{kin} \sim 6$ Bev). The calculations were based on the results obtained by the authors of reference 22, with allowance for the fluctuation in the number of charged particles produced in the shower.* This number was found to be, respectively, 3.8 and 3.0 particles (p, π^+, π^-) per shower. The number of protons per shower, according to the calculations, was 1.1. Unfortunately, the presence of additional apparatus-induced fluctuations in the experimentally-obtained distribution of showers with respect to the number of particles has made it impossible to make a correct comparison between the theoretical and experimental particle-number spectra of showers.

The calculated values of the average number of charged π mesons produced in p-p interaction, and also the experimental data on the average number of charged particles and charged π mesons in showers with $n \geq 2$, are compared in Table IV for hydrogen,[16] beryllium,[20] and carbon and hydrogen (our data). It follows from the table that, within the limit of the statistical accuracy of the experiment, the experimentally-determined average number of charged π mesons produced by p-p interaction agrees, for the energy spectra of the primary protons at latitudes 31°N and 51°N with the number calculated on the basis of the statistical theory of multiple particle production with account of the isobar states of the colliding nucleons. Going from hydrogen to the light nuclei Be and C, the number of charged π mesons in the shower (shown in the last column of Table IV), for interactions between nucleons and light nuclei, is approximately 1.2 or 1.3 times the number of charged π mesons in nucleon-nucleon interac-

---

*The effect of errors in counting showers with $n = 2$ particles, resulting from shower particles entering into the same counter, was relatively small in our experiments, since for the cosmic-ray proton spectrum at the latitude 31°N the production of showers with $n = 2$ charged particles is less probable than production of showers with $n \geq 3$ (for the proton spectrum at latitude 51°N to the contrary, a shower with $n = 2$ is more probable). In addition, for each class of showers, the loss in showers due to transition to a class with a smaller number of particles n is compensated for, to a considerable extent, by the showers from classes with higher values of n.

*Since the theoretical curves of the relative probability of production of n particles by inelastic proton collision in the energy range from 1 to 20 Bev are well approximated by the normal-distribution curve with a constant $h = 0.32 \pm 0.58 E_{kin}^{-0.5}$ Bev, the average number of charged particles were determined for the proton spectra indicated above by graphically integrating the expression:

$$\bar{n}_{p\pi^\pm} = \sum_{n=2}^{n=1} n F_1(n)/F_2, \tag{4}$$

where

$$F_1(n) = \int_{E_{kin}^{min}}^{\infty} \frac{Ah}{(E_{kin}+1)^{2.5}\sqrt{\pi}} \exp\left\{-h^2\left[n - \bar{\bar{n}}(E_{kin})\right]^2\right\} dE_{kin},$$

$$F_2 = \int_{E_{kin}^{min}}^{\infty} \frac{A}{(E_{kin}+1)^{2.5}} dE_{kin};$$

A is a constant, and $\bar{\bar{n}}(E_{kin})$ is the most probable number of particles per shower for a given proton energy E_{kin}. All the supplementary data of the theoretical investigations of S. Z. Belen'kiy, V. M. Maksimenko, A. I. Nikishov, and I. L. Rozental' needed for these calculations, were graciously supplied by V. M. Maksimenko.

TABLE IV. Average number of particles in showers with n ≥ 2 particles, produced by interaction between a proton and a light nucleus and between two protons

Average proton energy	$\overline{E}_{kin}$ ~ 6 Bev		$\overline{E}_{kin}$ ~ 20 Bev	
Interaction	p – p	p – Be	p – p	p – C
Experimentally-obtained average number of charged particles in shower (π mesons and protons)	3.2 ± 0.6[16]	3.0 ± 0.5[20]	~ 3.4*	4.2 ± 0.5*
Correction for protons	– 1.1**	– 0.6***	–0.8***	– 0.8***
Average number of charged π mesons in shower (experiment)	2.1	2.4	2.6	3.4
Average number of charged π mesons in shower, according to statistical-theory data for the energy spectra of incident protons	1.9		2.7	
Ratio of number of charged π mesons in shower in interactions between a nucleon and a light nucleus and in nucleon-nucleon interactions	1.26		1.26	

*Our data.

**Correction in accordance with statistical-theory data.

***Correction in accordance with Smorodin's data for showers in beryllium.[21]

tions at the same energy. From a comparison of the experimental data with the results of the statistical-theory calculations it follows apparently that at energies ~ 10^{10} ev there is little likelihood of considerable production of independent successive nucleon-nucleon interactions within the light nucleus.

CONCLUSIONS

1. The measured values of the range and of the cross section for inelastic interactions between protons and carbon nuclei are, respectively $L_p^C = 63^{+12}_{-9}$ g/cm^2 and $\sigma_p^C = 315 \pm 50$ millibarns. This means that, within the limits of experimental accuracy, the latter equals the geometric cross section of the carbon nucleus.

2. The respective values obtained for proton-proton interactions are $L_p^H = 51^{+23}_{-12}$ g/cm^2 and $\sigma_p^H = 32 \pm 10$ millibarns. In the energy range from 1 or 20 Bev, there is no noticeable change in the proton-proton inelastic cross section, within the limits of experimental accuracy.

3. The average number of penetrating particles in electron-nuclear showers is 4.2 ± 0.5 ~ 3.4 particles per shower, in carbon and hydrogen respectively, at an average proton energy of ~ 20 Bev. The dependence of the average number of π mesons in the shower on the average energy of the incident proton varies approximately as the 0.3 power of the energy, in the range from 6×10^9 to 2×10^{10} ev. The calculated number of charged π mesons produced in p-p interactions, calculated on the basis of the statistical theory of multiple particle production which account of the isobar states of the colliding nucleons, equals the experimentally-determined number.

The authors express their gratitude to S. I. Brikker, F. D. Savin, N. A. Shcherbakov, M. M. Dubrovin, and V. A. Sobiniakov, who participated in the preparation of the instruments and in their operation in the scientific expedition of 1955.

---

[1] G. T. Zatsepin, J. Exptl. Theoret. Phys. (U.S.S.R.) 19, 1104 (1949).

[2] N. L. Grigorov, Usp. Fiz. Nauk **58**, 599 (1956).

[3] Vernov, Grigorov, Zatsepin, and Chudakov, Izv. Akad. Nauk SSSR, Ser. Fiz. **19**, 493 (1955) [Columbia Techn. Transl. **19**, 445 (1955)].

[4] Eisberg, Fowler, Lea, Shepard, Shutt, Thorndike, and Whittemore, Phys. Rev. **97**, 797 (1955). W. D. Walker and J. Crussard, Phys. Rev. **98**, 1416 (1955).

[5] K. I. Alekseeva and N. L. Grigorov, J. Exptl. Theoret. Phys. (U.S.S.R.) **32**, 404 (1957), Soviet Phys. JETP **5**, 339 (1957).

[6] Alekseeva, Brikker, Grigorov, Savin, and Shcherbakov, Dokl. Akad. Nauk SSSR **115**, 71 (1957), Soviet Phys. "Doklady" **2**, 303 (1957).

[7] K. I. Alekseeva and N. L. Grigorov, Dokl. Akad. Nauk SSSR **115**, 259 (1957), Soviet Phys. "Doklady" **2**, 317 (1957).

[8] K. I. Alekseeva and N. L. Grigorov, Dokl. Akad. Nauk SSSR **117**, 593 (1957), Soviet Phys. "Doklady" **2**, 514 (1957).

[9] Winkler, Stix, Dwight, and Sabin, Phys. Rev. **79**, 656 (1950).

[10] Camerini, Davies, Fowler, Franzinetti, Muir-

head, Lock, Perkins, and Yekutieli, Phil. Mag. **42**, 1241 (1951).

[11] Kocharin, Saakian, Aivazian, Kirakosian, and Aleksanian, Izv. Akad. Nauk SSSR, Ser. Fiz. **19**, 515 (1955) [Columbia Techn. Transl. **19**, 463 (1955)].

[12] R. R. Brown, Phys. Rev. **87**, 999 (1952).

[13] Walker, Duller, and Sorrels, Phys. Rev. **86**, 865 (1952).

[14] J. G. Askowith and K. Sitte, Phys. Rev. **97**, 159 (1955).

[15] Proceedings of the VI Rochester Conference, April 1956.

[16] Wright, Saphir, Powell, Maenchen, and Fowler, Phys. Rev. **100**, 1802 (1955).

[17] E. G. Bubelev, J. Exptl. Theoret. Phys. (U.S.S.R.) **33**, 539 (1957), Soviet Phys. JETP **6**, 421 (1958).

[18] E. G. Bubelev, Joint Institute for Nuclear Research, Laboratory of Theoretical Physics, 1956.

[19] D. I. Blokhintsev, CERN Symposium, Geneva, 1956.

[20] Baradzei, Rubtsov, Smorodin, Slov'ev, Tolkachev, and Tulinov, Izv. Akad. Nauk SSSR, Ser. Fiz. **19**, 502 (1955) [Columbia Techn. Transl. **19**, 453 (1955)].

[21] Iu. A. Smorodin, Dissertation, Moscow, Phys. Inst. Acad. Sci. 1958.

[22] Belen'kii, Maksimenko, Nikishov, and Rozental', Usp. Fiz. Nauk **62**, 1 (1957).

Translated by J. G. Adashko
126

SOVIET PHYSICS JETP VOLUME 35(8), NUMBER 3 MARCH, 1959

PARAMAGNETIC RELAXATION IN POTASSIUM CHROMIUM SULFATE AND AMMONIUM IRON SULFATE

N. S. GARIF'IANOV

Physico-Technical Institute, Kazan' Branch, Academy of Sciences, U.S.S.R.

Submitted to JETP editor April 9, 1958

J. Exptl. Theoret. Phys. (U.S.S.R.) **35**, 612-617 (September, 1958)

A phase transition in the interval from 90 to 300°K was detected by the paramagnetic relaxation method in single crystals of chromium potassium sulfate and ammonium iron sulfate.

THE author has shown earlier[1,2] that the 546-Mcs spin-spin absorption in parallel fields at room temperature diminishes monotonically in certain salts of Mn^{++} and Gd^{+++} with increasing constant magnetic field $H_{||}$. The experimental curves obtained fit well the approximate formula

$$\chi''/\chi_0 = (1-F)^2 \rho_S \nu, \quad F = \frac{b/c}{[(b/c) + H_{||}^2]}, \qquad (1)$$

where ν is the frequency of the alternating magnetic field H_ν, and ρ_S is the isothermal spin-spin relaxation time, independent of $H_{||}$. Formula (1) follows from the general theory of Shaposhnikov[3] provided $1/\rho_S < \nu < 1/\rho_L$. Formula (1) leads to a relation for b, the constant of the magnetic heat capacity of the spin system:

$$b = (1+\sqrt{2})\, C\, (\Delta H_{||})^2, \qquad (2)$$

where C is the Curie constant and $\Delta H_{||}$ is the half-width of the absorption curve $\chi^{||}(H_{||})$. A good agreement between the Shaposhnikov theory and experiment was also reported in references 4 to 6.

1. MEASUREMENT PROCEDURE

A point-by-point measurement consumes much time and does not always disclose the details of complicated $\chi''(H_{||})$ curves. In the present work we used, instead of a static magnetic field, a 50-cycle magnetic field of amplitude up to 2500 Oe. The $\chi''(H)$ curves were displayed on an oscillograph screen. The magnetic field was calibrated by resonance from the free radical of $\alpha\alpha$-diphenyl-β pycril-hydrazil at a frequency of 600 Mcs. The measurement procedure was described in detail in reference 7 and verified with Tutton's salt ($MnNH_4SO_4 \cdot 6H_2O$). The $\chi''(H_{||})$ curve obtained for this salt in the frequency range from 600 to 300 Mcs and in the temperature interval from 300 to 90°K diminishes monotonically with increasing field $H_{||}$. In this case $\Delta H_{||}$ remains constant as the temperature is varied from 90 to 300°K. The experimental $\chi''(H_{||})$ curve fits formula (1) with ρ_S = const and $b/c = 0.61 \times 10^6$ Oe^2. At T = 90°K the intensity of $\chi''(H_{||})$ is approximately three times the intensity at room temperature.

We used $CuCl_2 \cdot 2H_2O$ to verify that H_ν and $H_{||}$ are parallel. In this salt, $T_1 = T_2 = 8.1 \times 10^{-10}$ sec, owing to the large exchange interactions in the perpendicular field, and the absorption $\chi''(H_{||})$ is independent of $H_{||}$ in parallel fields.[8]

When measuring the paramagnetic relaxation and the proton resonance in single crystals of the alums, the magnetic field $H_{||}$ was oriented along one of the diagonals of the elementary cube.

2. MEASUREMENT RESULTS

$CrK(SO_4)_2 \cdot 12H_2O$

This salt was investigated in detail in a wide range of temperatures, using both the paramagnetic-relaxation method in parallel fields,[4,9,10] and the method of resonant absorption in the microwave band.[11-13]

Paramagnetic-resonance measurements[13] have shown that there is a phase transition in potassium chromium sulfate, and that therefore the initial splitting of spin doublets depends on the temperature (see Table I).

Investigations[10] of paramagnetic relaxation T = 90°K give a value $b/c = 0.64 \times 10^6$ Oe^2 and a spin-lattice relaxation time $\rho_L(H_{||} = 0) = 2.5 \times 10^{-7}$ sec. Since ρ_L is on the order of 10^{-7} sec, the spin-spin relaxation plays the predominant role in the frequency range from 600 to 50 Mcs. The experimental $\chi''(H_{||})$ curve (see Fig. 1a) which we obtained at 545 Mcs and T = 90°K, does not fit the theoretical $\chi''(H_{||})$ curve, calculated with formula (1) for ρ_S = const and $b/c = 0.64 \times 10^6$

TABLE I

T° K	293	193	90	20
δ, cm⁻¹	0.12	0.055	{ 0.15 0.26±0.01	{ 0.15±0.01 0.27±0.003

Oe^2. In this case the theoretical curve for $H_{||} \neq 0$ passes above the experimental $\chi''(H_{||})$ curve. Our experimental $\chi''(H_{||})$ curve also fails to fit formula (1) for $b/c = 0.79 \times 10^6$ Oe^2, determined from the structure of the microwave magnetic-resonance spectra[13,14] under the assumption that the potassium chromium sulfate contains approximately 80% Cr^{+++} ions with $\delta = 0.15$ cm^{-1} and 20% with $\delta = 0.27$ cm^{-1}.

When $\Delta H_{||} = 370$ Oe relation (2) gives $b/c = 0.33 \times 10^6$ Oe^2. This low value of b/c is in contradiction with the b/c values given above. At 200°K and 545 Mcs, the $\chi''(H_{||})$ curve (see Fig. 1b) corresponds to spin-lattice absorption. At this frequency, spin-lattice relaxation is observed only when ρ_L is on the order of 10^{-9} sec.

When the temperature is raised to room temperature (295°K) the spin-lattice absorption is seen to weaken and spin-spin absorption appears. It follows hence that the time ρ_L is on the order of 10^{-8} sec. Further increase of the temperature, to 320°K, increases the time further to an order of 5×10^{-8} sec. This is why spin-spin absorption plays a predominant role at this frequency, while the absorption due to the spin-lattice relaxation is vanishingly small. A maximum absorption is seen now in $\chi''(H_{||})$ at $H_{||} = 480$ Oe (see Fig. 1c). It is impossible to calculate b/c from relation (2), owing to the presence of a maximum on $\chi''(H_{||})$.

At 75 Mcs and 90°K the maximum of $\chi''(H_{||})$ in $CrK(SO_4)_2 \cdot 12H_2O$ occurs at $H_{||} = 260$ Oe. An analogous $\chi''(H_{||})$ curve was reported earlier in reference 14.

In efflorescent potassium chrom alum, which contains $5H_2O$, on the average, the phase transition disappears and at $\nu \sim 540$ to 75 Mcs, in the temperature range of approximately 320 to 90°K, one observes absorption which decreases monotonically with increasing $H_{||}$. The pattern of the phase transition does not change when D_2O replaces H_2O in single crystals of potassium chrome alum.

$FeNH_4(SO_4)_2 \cdot 12H_2O$

Ammonium iron sulfate is the most thoroughly investigated salt.[4,9,15] Investigations[10] of paramagnetic relaxation in parallel fields at T = 90°K have yielded $b/c = 0.27 \times 10^6$ Oe^2 and $\rho_L(H_{||} = 0) = 4 \times 10^{-8}$ sec.

The $\chi''(H_{||})$ absorption curve, which we have for $\nu = 540$ Mcs and T = 90°K, corresponds to spin-spin relaxation (see Fig. 2a). Relation (2) for $\Delta H = 480$ Oe gives $b/c = 0.55 \times 10^6$ Oe^2. In view of this, the theoretical curve will be considerably below the experimental curve when $\rho_S =$ const and $b/c = 0.27 \times 10^6$ Oe^2 for $H_{||} \neq 0$.

At 200°K the $\chi''(H_{||})$ absorption curve (see Fig. 2b) is due to the spin-lattice relaxation. It follows therefore that ρ_L is on the order of 10^{-9} sec. A further increase of the temperature to 295°K again results in a spin-spin absorption curve (see Fig. 2c), indicating a lengthening of ρ_L to approximately 10^{-8} sec.

When $\Delta H = 300$ Oe, relation (2) yields $b/c = 0.22 \times 10^6$ Oe^2. The theoretical curve, calculated for $b/c = 0.27 \times 10^6$ Oe^2 for $H_{||} \neq 0$ lies above the experimental curve of $\chi''(H_{||})$ at T = 295°K. At 75 Mcs and 90°K, spin-spin absorption is observed with a maximum of $\chi''(H_{||})$ at $H_{||} = 600$ Oe. In efflorescent salts, containing $4H_2O$ on the average, the phase transition vanishes and an absorption maximum of $\chi''(H_{||})$ is observed in the range

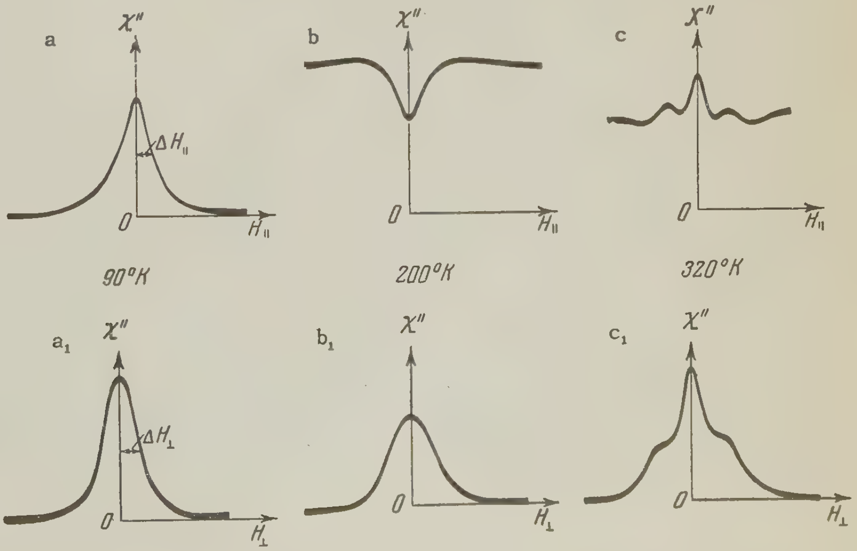

FIG. 1. $CrK(SO_4)_2 \cdot 12H_2O$; $\nu = 545$ Mcs; a, b, c) curves of $\chi''(H_{||})$; a_1, b_1, c_1) curve of $\chi''(H_{\perp})$; χ'' in arbitrary units

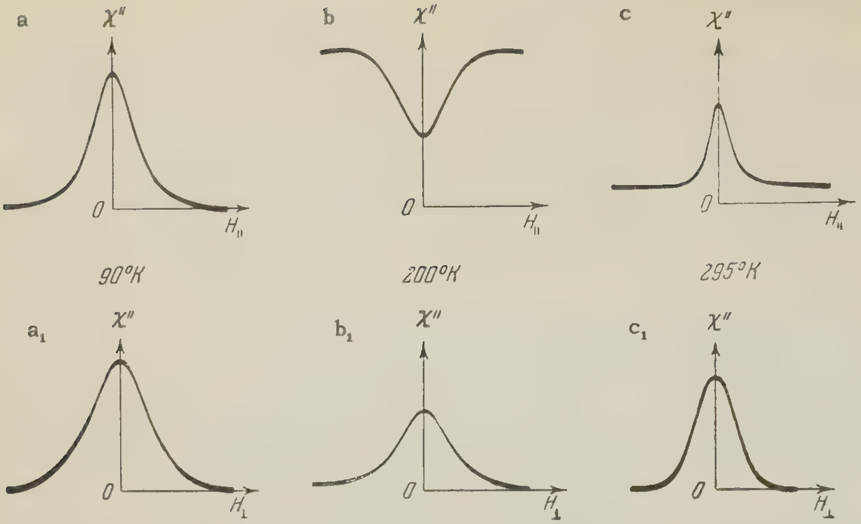

FIG. 2. $FeNH_4(SO_4)_2 \cdot 12H_2O$; $\nu = 540$ Mcs; a, b, c) curves of $\chi''(H_{\parallel})$; a_1, b_1, c_1) curve of $\chi''(H_{\perp})$; χ'' in arbitrary units.

$\nu \sim 600$ to 200 Mcs. The position of the maximum of $\chi''(H_{\parallel})$ is independent of the temperature and shifts towards the lower magnetic fields $H_{\parallel}$ with diminishing frequency of the alternating magnetic field H_{ν}.

3. PHASE TRANSITION IN PERPENDICULAR FIELDS

In perpendicular fields, the phase transition in undiluted potassium-chrome (see Figs. $1a_1$, $1b_1$, and $1c_1$) and iron-ammonium (Figure $2a_1$, $2b_1$, and $2c_1$) alums is also accompanied by a change in the shape of the absorption curves $\chi''(H_{\perp})$ in the temperature range from 90 to 300°K (see Table II).

TABLE II

Substance	$\Delta H_{\perp}$, Oe		
	90° K	200° K	295° K
$CrK(SO_4)_2 \cdot 12\ H_2O$	400	500	—
$FeNH_4(SO_4)_2 \cdot 12\ H_2O$	730	670	520

In single crystals of $CrK(SO_4)_2 \cdot 12H_2O$ and $FeNH_4(SO_4)_2 \cdot 12H_2O$, diluted respectively by $AlK(SO_4)_2 \cdot 12H_2O$ and $AlNH_4(SO_4)_2 \cdot 12H_2O$ in a ratio of 1 : 10, fine-structure spectra corresponding to intermediate fields ($\delta \gtrsim h\nu$) are observed at 540 Mc and 90 and 295°K. The spectra at 90°K differ from those at room temperature, and in the vicinity of the phase-transition point, $T \sim 200$°K, the fine-structure peaks spread out, leaving one broad line.

An unsuccessful attempt was also made to study the phase transition in dilute chromium-potassium and iron-ammonium phosphates and in pure aluminum-potassium and aluminum-ammonium sulfates with the aid of proton resonance. At 15 Mcs we obtained temperature-independent fine-structure proton lines consisting of four components for potassium sulfates and five components for ammonium sulfates.

4. DISCUSSION OF THE RESULTS

In one of the first investigations devoted to the absorption maxima in parallel fields, Gorter and Frijer[14] suggested that this maximum in $CrK(SO_4)_2 \cdot 12H_2O$ at 20°K is due to relaxation between two spin systems ("second spin-spin relaxation"). They observed furthermore that at liquid-air temperature the second relaxation in the spin system of $CrK(SO_4)_2 \cdot 12H_2O$ does not permit exact determination of b/c from measurements of paramagnetic dispersion and absorption.

During phase transitions in chromium-potassium and iron-ammonium sulfates, conditions are apparently set up for the appearance of second relaxation in the spin system. This second relaxation causes the half-width $\Delta H_{\parallel}$ of the $\chi''(H_{\parallel})$ curves that result from spin-spin relaxation to broaden in iron-ammonium sulfates at 90°K and ~ 540 Mcs and to narrow down in chromium-potassium sulfates at the same temperature. The second relaxation is sometimes the cause of the maxima that appear on these curves.

We now proceed to a discussion of the results obtained in perpendicular fields. Since the line width in a perpendicular field is determined, in the case of dilute single crystals, by the spin-lattice interactions, then the short time ρ_L at 200°K leads to such a strong broadening of the lines that the peaks of the fine structure spread out at 540 Mcs, leaving a single broad line. On the other hand, in undiluted single crystals the widths of the lines are determined by magnetic-dipole interactions and therefore the shortening of ρ_L of 200°K barely affects the width $\Delta H_\perp$ of the $\chi''(H_\perp)$ curve.

5. PRINCIPAL RESULTS

1. The paramagnetic-relaxation method was used for the first time to observe the phase transition in the iron-ammonium sulfate in the temperature range from 90 to 300°K.

2. The same method was used to confirm the existence of a phase transition in chromium-potassium sulfates.

3. The phase transition in both alums is accompanied by variations in ρ_L, $\Delta H_\perp$, $\Delta H_\parallel$ and b/c. Here ρ_L becomes shorter as the temperature drops from 300 to 200°K and reaches a value $\rho_L \sim 10^{-9}$ sec at $T \sim 200°K$. Upon further cooling ρ_L again lengthens, as expected.

4. The shortest time ρ_L corresponds to the minimum value of δ for $CrK(SO_4)_2 \cdot 12H_2O$. To reconcile this result with the Van Vleck theory[16] it is natural to assume that the variation in the splitting of the orbital levels in a cubic field, resulting from the phase transition, has a greater effect on the relaxation time ρ_L than the variation in the initial splitting of the spin sublevels.

In conclusion, the author thanks B. M. Kozyrev for an evaluation of the results and E. I. Semenova for preparation of the specimens.

---

[1] N. S. Garif'ianov, Dissertation, Kazan' State University, 1953.

[2] N. S. Garif'ianov, J. Exptl. Theoret. Phys. (U.S.S.R.) **25**, 359 (1953).

[3] I. G. Shaposhnikov, J. Exptl. Theoret. Phys. **18**, 533 (1948).

[4] K. P. Sitnikov, Dissertation, Kazan' State University, 1954.

[5] A. I. Kurushin, Izv. Akad. Nauk SSSR, Ser. Fiz. **20**, 1232 (1956) [Columbia Techn. Transl. **20**, 1122 (1956)].

[6] T. I. Volokhova, J. Exptl. Theoret. Phys. (U.S.S.R.) **31**, 889 (1956), Soviet Phys. JETP **4**, 918 (1957).

[7] N. S. Garif'ianov and B. M. Kozyrev, J. Exptl. Theoret. Phys. (U.S.S.R.) **30**, 272 (1956), Soviet Phys. JETP **3**, 255 (1956).

[8] B. M. Kozyrev, Doctoral dissertation, Moscow, Phys. Inst. Acad. Sci., 1957.

[9] T. I. Volokhova, J. Exptl. Theoret. Phys. (U.S.S.R.) **33**, 856 (1957), Soviet Phys. JETP **6**, 661 (1958).

[10] C. J. Gorter, Paramagnetic Relaxation, Amsterdam, 1947 (Russ. Transl. IIL, M., 1949).

[11] E. K. Zavoiskii, J. Phys. (U.S.S.R.) **10**, 170 (1946).

[12] B. Bleaney, Phys. Rev. **75**, 1962 (1949).

[13] B. Bleaney, Proc. Roy. Soc. **A204**, 204 (1950).

[14] F. W. Frijer and C. J. Gorter, Physica **18**, 549 (1952).

[15] C. A. Whitmer and R. T. Weidner, Phys. Rev. **84**, 159 (1951).

[16] J. H. Van Vleck, Phys. Rev. **57**, 426 (1949).

Translated by J. G. Adashko
127

SOVIET PHYSICS JETP VOLUME 35(8), NUMBER 3 MARCH, 1959

INVESTIGATION OF EXTENSIVE COSMIC RAY SHOWERS UNDER DENSE SUBSTANCES

S. I. NIKOL' SKII and A. A. POMANSKII

P. N. Lebedev Physical Institute, Academy of Sciences, U.S.S.R.

Submitted to JETP editor April 10, 1958

J. Exptl. Theoret. Phys. (U.S.S.R.) **35**, 618-630 (September, 1958)

The absorption of extensive air shower particles in an absorber of low atomic number was investigated at the altitude of 3860 m above sea level. Analysis of the data shows that in the lower third part of the atmosphere about 60% of the energy of the nuclear-active component is transferred to μ mesons and neutrinos. Some of the data seem to indicate that the absorption of shower particles increases in showers with total number of particles $N > 10^5$.

INTRODUCTION

NUMEROUS experimental data on extensive air showers (EAS) of cosmic radiation, obtained at various altitudes, lead to the conclusion that the shower structure i.e., its lateral distribution and composition, is independent of the level of observation, within the limits of experimental errors, for altitudes from 0 to 5000 m above the sea level. On the other hand, the study of the dependence of EAS on the altitude shows that the variation of the recorded number of showers with altitude of observation depends only to a small extent on the total number of particles and, consequently, cannot be explained by the electromagnetic cascade theory. There are two possible ways of explaining these experimental facts:

1. An extensive atmospheric shower is produced by a nuclear cascade event[1] that takes place when ultra-high-energy primary cosmic ray particles pass through the atmosphere. The electron-photon component of the shower is in equilibrium with nuclear-active particles that constitute the foundation of the shower. The energy flux of these particles has the following absorption coefficient in the atmosphere

$$\mu \approx 1/200 \text{ cm}^2/\text{g}.$$

2. It is possible[2] that, because of the still-unknown value of the effective nucleon interaction cross-section, or of the fluctuations of energy distribution among secondary particles in interactions of ultra-high-energy nucleons, the mean free path of particles that initiate EAS is equal to or greater than ~ 120 g/cm^2, and that the flux of nucleons (and of other nuclear-active particles) of corresponding energies decreases with the altitude with an absorption coefficient $\sim 1/120$ cm^2/g. The shower characteristics are then independent of the observation level because of the biased detection of showers produced at a certain effective height above the place of observation.

There are still no sufficient data for a definite choice between the two alternatives. Two ways of solving the problem are possible. The first is to determine experimentally the effective cross-section for the transfer of a given energy fraction to secondary particles in nuclear interactions of nucleons and $\pi^\pm$ mesons of 10^{12} to 10^{15} ev. So far, such data are not available even for $\sim 10^{11}$ ev. The second way is to measure the particle absorption of an individual EAS. The absorption of an individual shower in the atmosphere can be studied by simultaneous measurement of Cerenkov-light pulses produced by the passage of shower particles through the atmosphere and of the number of particles at the observation level.[3] One can also measure the absorption of EAS of a given size in a dense medium. The results of such measurements, made with ionization counters and a counter hodoscope, are presented in this article. The measurements were carried out at 3860 m above sea level (Pamir) in the autumn of 1955.

EXPERIMENTAL SETUP

The results given below were obtained by means of a large and complex array described in reference 4. A general diagram of the part of the array essential for the present work is given in Fig. 1.

We recorded all EAS, the particles of which produced four-fold coincidences of counters placed around the center of the array in two groups 2 m apart. The area of the master counters in each channel amounted to 500 cm^2. Thirty-nine groups of hodoscoped counters, the position of which is shown in the diagram, were used for core location and determination of the number of charged particles. Thirty-three hodoscope-counter groups contained each 24 counters of 100 cm^2 area each, three groups placed 19 m from the array center consisted each of 36 counters, 330 cm^2 in area each; three other groups at 19 m from the array center consisted each of 24 counters 22 cm^2 in area each. The flux density of charged particles incident on a hodoscope-counter group was determined from the ratio of the number of counters struck to that of counter's missed.

The method of core location was similar to that used in reference 5. The lateral distribution function of charged particles was taken from reference 6. Errors in axis location using such a method amounted to 5 or 6 m near the center of the array and increased to ~15 to 20 m at distances of ~60 m from the center. In case when the shower axis fell in the central part of the array where 33 counter groups were placed, the axis was located by our earlier method.[6] The accuracy increased then to 0.8 m.

For the subsequent determination of the total number of shower particles we made use of many hodoscope points, obtaining an accuracy of 6 to 15% for showers with axes incident on the central part of the array. In that case, the error in axis location does not influence the measured number of particles in the shower, since the array is symmetric. In other cases the error of the determination of the shower size amounted to 40%. The showers recorded were divided into seven size groups. The distribution of showers in these groups, for showers with axes passing near the array center, is shown in Fig. 2. It should be noted that the distribution in Fig. 2 does not include showers with less than 10^4 and more than 10^6 particles, since the described hodoscope array was not suitable for detection of such showers. The relative number of showers of > 10^6 particles with axis near the array center was, however, small because of the energy spectrum of primary particles, and showers with < 10^4 particles practically did not produce four-fold coincidences in the master counter groups.

Twenty-four cylindrical ionization chambers* were used to measure the number of shower particles under the absorber. Twelve of these were 18.5 cm in diameter and had a working-volume length of 42 cm. The remaining chambers were 22.5 cm in diameter and a working-volume length of 96 cm. The chambers were filled with pure argon at 4 atmos. The chambers were calibrated both by measuring the ionization produced by the passage of a μ meson along the chamber axis and by comparing the ionization burst in non-shielded chambers with the number of discharged hodoscope counters during the passage of an EAS. Allowing for the transition effect in chamber walls (2 g/cm^2 Cu) and for the angular distribution of shower electrons, both methods of calibration give practically identical results which are also in agreement with the calculated size of bursts.

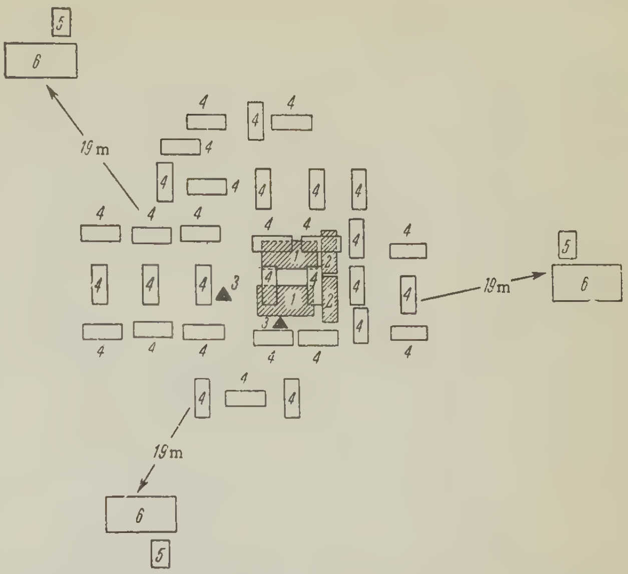

FIG. 1. General diagram of the array: 1) groups of large ionization chambers, 2) groups of small ionization chambers, 3) master counters, 4, 5, 6) hodoscope-counter group.

An absorber made of aluminum and graphite was placed above the chambers for a measurement of the absorption of EAS in dense substances. The relative amounts of aluminum and graphite were chosen so that the absorber had absorption characteristics similar to air (neglecting the $\pi^{\pm} \to \mu^{\pm} + \nu$ decay). The thickness used was equal to 230 g/cm^2, which amounted to 7.7 cascade units and 3.5 nuclear units, or, assuming that the effective cross section for nuclear interactions is equal to the geometrical cross sec-

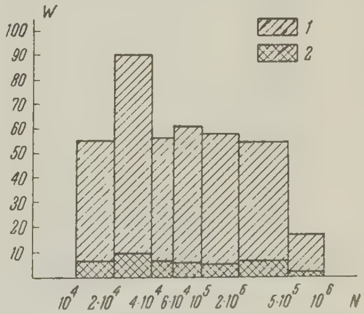

FIG. 2. Size distribution of EAS: 1) recorded near the array center 2) showers, the axis of which traversed ionization chambers.

---

*The authors thank L. A. Razorenov who took part in the development and testing of the ionization chambers.

tion, 3.45 nuclear units. A layer of air 230 g/cm^2 thick is equal to 7 cascade units and 3.5 nuclear units. Since the mean atomic numbers of the lower graphite layer and of the air are similar, the transition effect in walls of the chambers was practically identical in chamber calibration and in measurements of the number of particles under the absorber. An increase of the ionization per shower particle, caused by the scattering of shower particles, which leads to an increase of the "mean" chord of the chamber, was also independent of the fact whether the absorber was placed above the chamber. It is possible that the mean ionization per shower particle was somewhat lower under the absorber, in view of the zenith-angle distribution of shower axes. This effect, which could lead to a decrease of the number of particles observed under the absorber, has been neglected, but its magnitude is clearly small. In view of the fact that the $\pi^{\pm}$ decay mean free path is much larger than the nuclear interaction mean free path in a dense medium, the fraction of nuclear-active particles in a shower is larger under a dense absorber than at a corresponding altitude in air. The contribution of ionization due to heavily ionizing particles to the total ionization measured under a dense substance increases proportionally to the flux of nuclear-active particles. However, the uncertainty about the composition of ionizing particles under a dense absorber does not influence the determination of the energy flux carried by shower particles, since it is immaterial in which way the energy of the shower is dissipated on ionization.

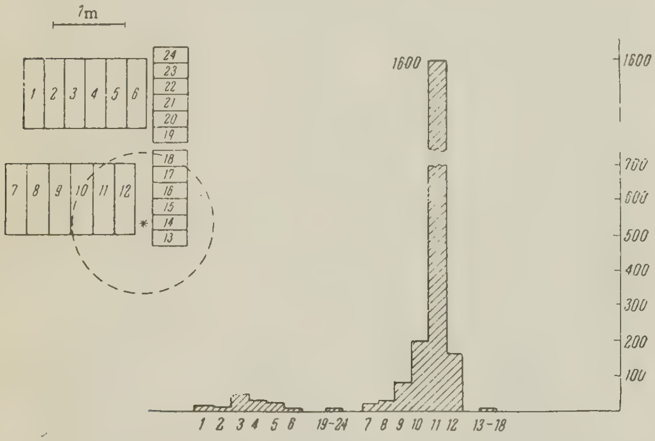

FIG. 3. A single-core shower with $\bar{N} = 4.2 \times 10^4$. Position of ionization chambers appear in the diagram (upper left). The position of the axis is indicated by a star. The numbers of the ionization chambers are indicated on the x axis. The y axis represents the number of particles.

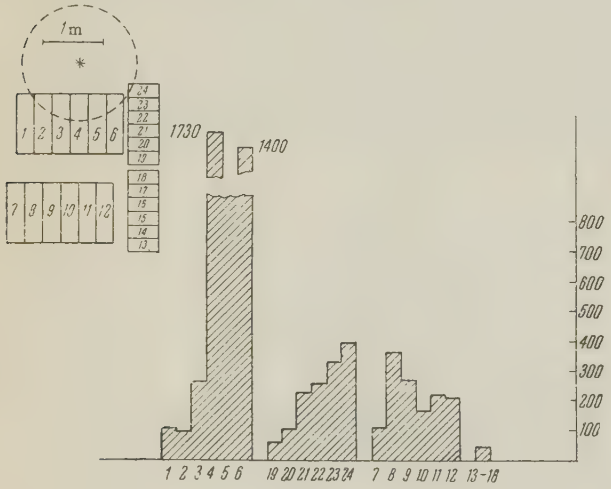

FIG. 4. A multicore shower, with $\bar{N} = 4.7 \times 10^5$. Notation as in Fig. 3.

OBSERVATION OF THE CORES OF EXTENSIVE AIR SHOWERS

It was already mentioned that the error in shower-axis location by means of the hodoscope was 0.8 m when the axis passed near ionization chambers. Since the ionization chambers and the counters were placed in different horizontal planes, and the shower-arrival angle was measured in a few cases only, the error in finding the point of intersection of the axis with the ionization-chamber plane increased to ~1 m. It was therefore impossible to tell, on the basis of the hodoscope data only, through which of the chambers the core passed.

The distribution of pulse heights of the ionization chambers was analyzed for each case in order to increase the accuracy in core location. It was found from the pulse-height distribution that the number of cores passing through the chambers is approximately equal to that expected from statistical considerations. The size distribution of showers given in Fig. 2 consists of all events in which the axis fell not further than 3.5 m from the geometrical center of the ionization-chamber positions. The collecting area was equal to ~37 m^2. Out of 400 showers, the axes of which fell in that area, 43 axes passed through the chambers, the total area of which amounted to ~3.5 m^2. The shower size distribution of these events is shown in Fig. 2. It can be seen that the distribution is analogous to that of all 400 showers. One cannot, however, attribute much weight to this fact in view both of the existence of multicore showers and of the diffuseness of the core.

Typical histograms of the ionization-burst size distributions for showers incident on an area covered by ionization chambers are shown in Figs. 3

and 4. Since there is no sharp limit between the record of showers with single cores and those having multiple ones, we classify as multicore showers all events in which the largest pulses, differing by no more than a factor of two, were observed at least in two non-adjacent or any three ionization chambers. We analyzed all events in which the shower axis passed through ionization chambers, using this criterion for multicore showers. The results are given in Table I.

TABLE I

Total number of particles in showers of the group	Number of axes observed	Number of axes with two or more cores
$1.5 \cdot 10^4$	7	2
$2.9 \cdot 10^4$	10	3
$5 \cdot 10^4$	8	2
$8 \cdot 10^4$	6	2
$1.5 \cdot 10^5$	5	2
$3.5 \cdot 10^5$	6	5
$5.8 \cdot 10^5$	1	1

It can be seen that the relative number of multicore showers amounts to ~ 30% of showers with total number of particles $N \leq 10^5$. Multicore showers are more frequent among EAS with $N > 10^5$, their fraction being ~ 70%.

MEASUREMENT OF THE SHOWER PARTICLE FLUX UNDER AN ABSORBER

To determine the shower particle flux under an absorber in EAS with a given number of particles $\overline{N}$ at a given distance $\overline{r}$ from shower axis, we measured the mean ionization produced in ionization chambers by showers with mean number of particles between N_1 and N_2 $(N_1 < \overline{N} < N_2)$ the axes of which fell in the ring $r_1 < \overline{r} < r_2$. The chosen intervals of the total number of shower particles are shown in the histogram in Fig. 2.

The mean number of particles in EAS of a given group was defined as $\overline{N}_0 = (1/n) \sum_i^n N_{0i}$, where N_{0i} is the total number of particles in the i-th shower, and n is the number of showers in the group. The mean distance was defined for a given ring as $\overline{r} = (1/n) \sum_i^n r_i$. The corresponding particle flux density under an absorber can be defined as $\rho(\overline{r}, \overline{N}_0) = \frac{i}{n\sigma} \sum_i^n J_i$, where σ is the area of the ionization chambers and J_i is the sum of ionization bursts in chambers under the absorber, expressed in numbers of shower particles. The results are given in Table II. It should be noted that all said above is correct for distances larger than 2 or 3 m, where we can neglect the dimensions of the ionization chamber array and the error in axis location. For smaller distances, the axis location was found more accurately by comparing the ionization bursts in various chambers and taking the chamber position into account. In addition, for distances in the 0 to 0.3 m range, when the dimensions of separate chambers were larger than the region under consideration, the number of particles

TABLE II. Mean ionization, expressed as the number of relativistic particles per m^2 for shower groups with different number of particles $\overline{N}_0$

Distance from axis, $\overline{r}$	$1.5 \cdot 10^4$	$2{,}9 \cdot 10^4$	$5 \cdot 10^4$	$8 \cdot 10^4$	$1{,}5 \cdot 10^5$	$3.5 \cdot 10^5$	$5.8 \cdot 10^5$
0.03	1750 ±650	3000 ±1000	5300 ±1600	6300 ±500	6700 ±400	18000 ±7000	58000
0.3—1	230 ±120	360 ±60	630 ±130	1000 ±250	1400 ±600	5000 ±2200	11000
1—2	25 ±13	125 ±25	200 ±60	500 ±230	540 ±220	1150 ±450	2500
2—3	23 ±5	79 ±16	126 ±24	260 ±70	320 ±80	470 ±120	630 ±160
3—5	18 ±7	37 ±15	44 ±19	71 ±16	89 ±21	120 ±30	400 ±120
5—8	6.3 ±2.3	12.5 ±4.5	23 ±10	45 ±10	37 ±9	90 ±25	250 ±70
8—20	—	3.1 ±0.9	6.3 ±1.7	7.4 ±2.5	9.1 ±2.6	8.3 ±2,2	—
20—40	—	—	0.83 ±0.27	2 ±0.6	2.9 ±1.1	2.5 ±0.8	8 ±1.5
40—70	—	—	—	—	—	1 ±0.25	1.75 ±0.3
Number of particles within the radius of 0.3 m	500 ±180	850 ±280	1500 ±450	1800 ±140	1900 ±110	5100 ±2000	16000

under an absorber in a circle of 0.3 m radius, given in the lowest row of Table II, was actually measured instead of the mean density $\rho(\overline{r}, \overline{N}_0)$. This number was assumed to be equal to $N'(r) = (1/n) \sum_{i=1}^{n} J'_i$, where J'_i is the measure of ionization in the chamber with the largest burst or the sum of ionizations in two adjacent chambers with the largest bursts. In part of the events, the value of $N'(r)$ was slightly higher in view of the fact that particles not belonging to the core passed through the chambers. However, by extrapolating the lateral distribution of shower particles under a dense absorber (Fig. 5) for the smallest distances, we can see that the increase is not larger than 25% of the value measured. The errors given in Table II are standard deviations of the arithmetic mean for the given shower group.

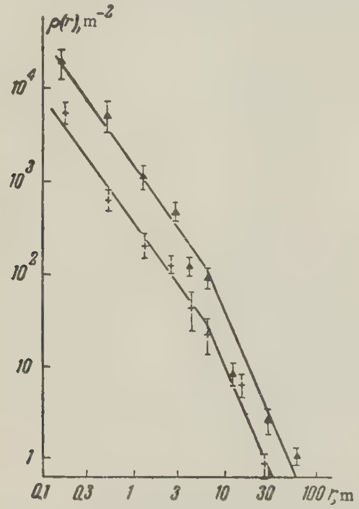

FIG. 5. Lateral distribution of the particle density of charged particles under an absorber in EAS of different size. Δ – showers with $\overline{N} = 3.5 \times 10^5$ particles, × – with $\overline{N} = 5 \times 10^4$. Solid curves represent an analytical approximation.

The data of Table II can be regarded as the result of measurements of the mean particle flux density at various distances from the axis of the EAS under an infinitely extended absorber. Consequently, one can talk about the lateral distribution function of the effective particle flux under an absorber. An analysis of Table II shows that, within the limits of experimental errors, the function is independent of shower size in the region from 0 to 6.5 m and can be written in the form

$$f(r) \sim r^{-(1.37 \pm 0.04)}.$$

The lack of experimental data on the flux of particles at large distances form the axis for showers with $N < 10^5$ does not permit us to determine the dependence of the lateral distribution function on shower size at distances above 6.5 m. However, the fact that function does not change at small distances from the axis gives grounds for expecting that the lateral distribution of particle flux under dense substances is independent of shower size also at large distances from the axis. For showers with $N > 10^5$, the lateral distribution function in the 6.5 to 70 m region can be written in the form

$$f(r) = r^{-(2.3 \pm 0.1)}.$$

Figure 5 illustrates the fit between this approximate expression and the observed lateral distribution of particle flux in EAS under a dense substance.

ABSORPTION OF EXTENSIVE AIR SHOWERS IN A DENSE SUBSTANCE

The data on particle flux density under a dense substance obtained by us made it possible to calculate the total number of particles in EAS under an absorber 230 g/cm^2 in thickness. The number of particles was directly measured in the 0 to 0.3 m region, while for larger distances we used the approximations discussed above.

An estimate of the ionization produced by shower μ mesons and electrons in equilibrium with each other shows that the ionization measured under the absorber can be explained by μ mesons traversing the absorbers only at distances > 1000 m from shower axis, i.e., at distances where the particle-density observed in air coincides with the density of the μ-meson component. We limited ourselves therefore to distances < 1000 m from shower axis in calculating the number of particles in a shower under the absorber. Results of the calculation are given in Table III.

TABLE III

Total number of shower particles above the absorber	Total number of shower particles underneath the absorber	Number of particles underneath the absorber within the radius of 40 m
$1.5 \cdot 10^4$	$(7.8 \pm 1.4) \cdot 10^3$	—
$2.9 \cdot 10^4$	$(1.7 \pm 0.23) \cdot 10^4$	—
$5 \cdot 10^4$	$(2.8 \pm 0.43) \cdot 10^4$	$(2.2 \pm 0.3) \cdot 10^4$
$8 \cdot 10^4$	$(4.3 \pm 0.54) \cdot 10^4$	$(3.9 \pm 0.46) \cdot 10^4$
$1.5 \cdot 10^5$	$(4.6 \pm 0.6) \cdot 10^4$	$(4.5 \pm 0.6) \cdot 10^4$
$3.5 \cdot 10^5$	$(1.1 \pm 0.17) \cdot 10^5$	$(7.3 \pm 0.9) \cdot 10^4$
$5.8 \cdot 10^5$	$(2.5 \pm 0.6) \cdot 10^5$	

The result of a straightforward summation of the number of particles in rings at distances 0 to 40 m from the shower axis is given in column 3 for several shower groups. It can be seen that particles at distances larger than 40 m contribute little to the total number of particles.

The ratio of the number of particles observed under the absorber N to the total number of charged particles of the same showers at the observation level in air N_0 is given in Fig. 6. The values of that ratio calculated for an electron-photon cascade with age parameter $s = 1.2$, neglecting the nuclear-active shower component, are also shown in the figure. This value of s follows from the altitude dependence and from the electron lateral distribution function of EAS at 3860 m altitude.[7] The marked discrepancy between experimental data and cascade theory calculations indicates a substantial contribution of the electron-photon component, produced in the absorber by nuclear-active particles to the total flux of shower particles under the absorber.

It is of interest to compare the absorption of shower particles in the dense substance used as the absorber with the absorption of EAS particles in air. The ratio of shower particles at an altitude corresponding to the pressure of 880 g/cm^2 to the number of particles at our observation level (650 g/cm^2) is also shown in Fig. 6. The absorption of shower particles in air is calculated from the longitudinal development of EAS[8] and the data on the barometer effect.[9] The discrepancy between the values of the absorption coefficient of EAS with $N_0 > 10^5$ at sea level given by references 8 and 9 is shown in Fig. 6 by the shaded area.

DISCUSSION OF RESULTS

A striking feature of Fig. 6 is the observed difference in the absorption of EAS of various size. For showers with $N_0 < 10^5$ the ratio of particles under the absorber N to the number above the absorber N_0 is equal to 0.55 ± 0.035. For showers with $N_0 > 10^5$ that ratio is 0.33 ± 0.032. The deviations from the mean $\overline{N/N_0} = 0.47 \pm 0.025$ are large enough to be significant. The question arises whether the observed absorption variation is limited to a narrow range of primary energies which follows directly from Fig. 6, or whether shower absorption varies all over the investigated range, increasing monotonically with shower size. It must be mentioned that the increase of the shower absorption coefficient with the primary energy contradicts both the electromagnetic cascade theory and any nuclear cascade theory of development of EAS, which assumes that the character of elementary nuclear interactions is independent of the energy of interacting particles.

We shall write the dependence of N/N_0 on N_0 as

$$N/N_0 = \log(\alpha / N_0^\beta).$$

The values of α and β can be determined by the least-squares method. At the statistical accuracy of the experimental data, the proposed relation cannot be rejected, although the probability that it is correct is less than 25%. The fit between the experiment and the proposed relation $N/N_0 = f(N_0)$ is especially bad near $N_0 \approx 10^5$. The spread of the values N/N_0 observed over the range $N_0 = 5 \times 10^4$ to $N_0 = 1.5 \times 10^5$ at the seven measured points would be expected to occur with a probability of 6%, the proximity of the values N_0 indicating that the problem lies not in a successful choice of the relation $N/N_0 = f(N_0)$, but in the validity of that relation on the whole range of N_0 from 1.5×10^4 to 5.8×10^5. It is therefore very probable that the experimentally-observed variation of the absorption of EAS in dense substances for showers of $N_0 \geq 1.5 \times 10^5$ and $N_0 \leq 8 \times 10^4$ actually exists. This variation could be due to a variation of the character of the elementary act of nuclear interaction for particles with energy corresponding to EAS with $N_0 \sim 10^5$ at 3860 m altitude.

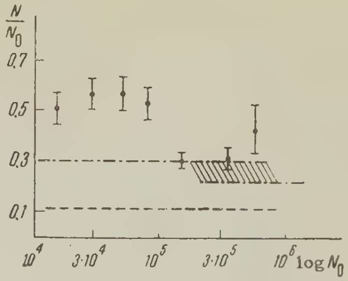

FIG. 6. Dashed line represents the ratio N/N_0 calculated for an electron-photon cascade with $s = 1.2$; dot-dash – N/N_0 calculated from the altitude dependence of showers. The points represent the values of N/N_0 measured in the experiment.

Let us consider our results on the absorption of EAS with $N_0 \leq 10^5$ in connection with two possible interpretations of experimental data on EAS. If we assume that the showers recorded at any observation level are initiated at different heights above that level by primary cosmic ray particles as the result of nuclear interactions accompanied by a transfer of the whole energy of the primary to secondary particles (π mesons), and that the variation of the recorded number of showers with the altitude of observation is associated with the absorption of primary cosmic ray particles, then the age of the electron-photon component of EAS $s = 1.2$ to 1.3, observed in measurements, is an average characteristic of the showers selected by the array.

Under such assumptions, secondary nuclear-active particles are not an important component of EAS. To estimate the further absorption of the group of showers recorded by the array, we consider the absorption of the electron-photon shower, which is a superposition of all showers recorded* and which can, therefore, be assigned the value $s \sim 1.2$. It can be seen from Fig. 6 that the absorption of a shower with $s \sim 1.2$ is markedly different from the absorption measured, which shows that one cannot neglect the nuclear-active component. Production of the electron-photon component by nuclear-active particles lengthens the range of the cascade.

If the range increase is such that the cascade absorption corresponds in the mean to the altitude dependence then, on the average, an equilibrium is reached between the electron-photon and the nuclear-active shower components. This fact rules out nuclear interactions with full energy transfer to secondary particles, since such events cannot lead to equilibrium cascades, absorbed with a mean free path of ~ 180 to 200 g/cm^2.

We shall consider now our results from the point of view of an equilibrium between the electron-photon component and the nuclear-active shower particles. In that case the observed altitude dependence of EAS corresponds to the absorption of the particles in an individual shower. It can be seen from Fig. 6 that the absorption of showers with $N_0 < 10^5$ in a dense substance, measured in our experiments, is much less than the absorption in an equivalent layer of air. This result can be explained by the transition effect, in view of the fact that no decay of 10^9 to 10^{10}-ev $\pi^{\pm}$ mesons occurs in dense substances.

We shall now analyze quantitatively the energy balance in EAS with $N_0 = 10^5$. The energy E_e dissipated by the shower electrons, from the observation level (3860 m altitude) until the shower is totally absorbed, is derived from the energy carried by the electron-photon component at the observation level $E_{e\text{-}p}$ and from the energy E_{π^0} transferred to π^0 mesons in nuclear interactions below the observation level. $E_{e\text{-}p}$ can be determined from the electromagnetic cascade theory under the assumption that $s = 1.2$.[7] For a shower with $N_0 = 10^5$, $E_{e\text{-}p}$ equals $\sim 2.6 \times 10^{13}$ ev.

Furthermore,

$$E_e = \int_0^\infty N_0 \beta \exp\{-x/200\}\, dx = 4.2\cdot 10^{13} \text{ ev}.$$

where β is the ionization-energy loss of a relativistic particle traversing 1 g/cm^2 of air, and x is the thickness of air in g/cm^2 traversed. We have, therefore,

$$E_{\pi^0} = E_e - E_{e\text{-}p} = 1.6\cdot 10^{13} \text{ ev}.$$

Since the absorption of a nuclear cascade in dense substances, as well as in air, is determined essentially by the absorption of particles having the highest energy we can expect that, after the transition processes have ended, the absorption of EAS particles in a dense substance follows the same law as in air (cf. Fig. 7). However, in a dense substance the total energy of the nuclear-active component is transferred to the electron-photon component, $E_e = E_{e\text{-}p} + E_{n\text{-}a}$. We shall now determine E'_e. According to Fig. 7 we have

$$E'_e = \int_0^\infty N_0 \beta f(x)\, dx = 1.1 N_0 \beta 120$$

$$+ \int_{120}^\infty \beta\cdot 5.5 N_0 \exp\{-x/200\}\, dx \approx 7\cdot 10^{13} \text{ ev}.$$

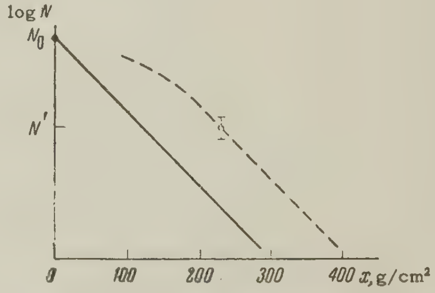

FIG. 7. Absorption of shower particles in the lower third of the atmosphere (solid line) and in an equivalent dense substance (dashed).

It follows that $E_{n\text{-}a} = 4.4 \times 10^{13}$ ev. In the atmosphere a larger part of this energy ($E_{n\text{-}a} - E_{\pi^0} \sim 2.8 \times 10^{13}$ ev) is carried away by μ mesons and neutrinos in the $\pi^{\pm} \rightarrow \mu^{\pm} + \nu$ decay. If that fact were neglected, the energy of the nuclear-active component would be underestimated. The energy distribution among the various components of a shower with $N_0 = 10^5$ at 3860 m altitude is as follows:

Energy of the electron-photon component	2.6×10^{13} ev
Energy of the nuclear-active component:	
carried by π^0 mesons	1.6×10^{13} ev
carried by $\mu^{\pm}$ mesons and neutrinos	2.8×10^{13} ev
Energy of μ mesons	4×10^{13} ev

It can be seen from the above that the energy fraction of the nuclear-active component, transferred to the electron-photon component in the passage of EAS with $N_0 < 10^5$ through the lower part of the atmosphere, is practically identical to the number of π^0 mesons relative to that of all the mesons produced in nuclear interactions. This means that most nuclear-active particles in EAS with $N_0 < 10^5$ are nucleons, owing to the instability of $\pi^\pm$ mesons. In fact, according to Ref. 4, the most energetic nuclear-active particle in EAS with $N_0 = 10^5$ has an energy of 2 to 4×10^{12} ev and transfers in a nuclear interaction about 4×10^{12} ev per secondary π meson, which is close to the energy at which the decay of $\pi^\pm$ mesons at 3860 m in air becomes predominant over secondary nuclear interactions. The main flux of nuclear-active particles in EAS with $N_0 = 10^5$ has an even lower energy. Calculations* carried out by us using the consecutive-generation method[12] lead to the same result: 60% of the energy of the nuclear-active component is carried away by μ mesons. The calculations were based upon the following assumptions: (1) The energy spectrum of nucleons of the depth of 500 g/cm^2 is of the form $\sim dE/E^{1.8}$ for $E \leq 10^{13}$ ev, high-energy particles are absent; (2) in nuclear interactions a nucleon carries away 0.6 of the primary nucleon energy; (3) such a particle is not produced in nuclear interactions of π mesons; (4) 0.25 of the secondary π mesons carry away 75% of the energy transferred to π mesons; the remaining π mesons carry away the remaining energy fraction, the assumed total number of π mesons being $\sim 4(E_0/2Mc^2)^{1/4}$, where E_0 is the primary-particle energy and M the nucleonic mass. The mean free path for nuclear interactions was taken as 70 g/cm^2. It should be noted that the conclusion about the predominantly nucleonic composition of the nuclear-active component of EAS is in agreement with the observed ratio between the neutral and charged nuclear-active particles.[13]

---

*Such a procedure is permissible when the number of showers with $s < 1$ amounts to not more than 20 to 25% of the total number of showers in the group.

CONCLUSION

1. The measurements indicate that in EAS with total number of particles $10^4 < N < 10^5$ an equilibrium is attained, at least in the mean, between the nuclear-active and electron-photon components. This fact contradicts the hypothesis that EAS are produced in the depths of the atmosphere as the result of nuclear interactions in which the total energy of the primary particle is dissipated. It indicates also that fluctuations play a comparatively unimportant part in the development of EAS of the above size.

2. The energy carried by the nuclear-active component in EAS with $N < 10^5$ in the lower third of the atmosphere is 1.7 times that carried by the electron-photon component. However, a larger part ($\sim 60\%$) of this energy is dissipated in μ-meson production.

3. The variation of the absorption coefficient of EAS, as well as the change in the core structure observed in the passage from showers with $N < 10^5$ to showers with $N > 10^5$, is consistent with the assumption, proposed earlier,[14] that the character of the nuclear interaction changes at the energy $E_0 \approx 3 \times 10^{14}$ ev.

A large group of workers of the Physical Institute of the Academy of Sciences U.S.S.R. and of senior students of the Physical Faculty of Moscow State University took part in the measurements. The authors consider it their duty to express their gratitude to all these persons.

The authors thank Prof. S. N. Vernov, Prof. N. A. Dobrotin, and Prof. G. I. Zatsepin for helpful discussion of results.

---

*The energy carried away by μ mesons was estimated according to references 10 and 11. In view of the lack of experimental data on the energy region above 10^{10} ev and on their lateral distribution at distances > 1000 m from the shower axis, these estimates are very rough.

[1] G. T. Zatsepin, Dokl. Akad. Nauk SSSR **67**, 993 (1949).

[2] V. I. Zatsepin, J. Exptl. Theoret. Phys. (U.S.S.R.) **33**, 190 (1957), Soviet Phys. JETP **6**, 150 (1958).

[3] N. M. Nesterova and A. E. Chudakov, J. Exptl. Theoret. Phys. (U.S.S.R.) **28**, 384 (1955), Soviet Phys. JETP **1**, 388 (1955).

[4] Dovzhenko, Zatsepin, Murzina, Nikol'skii, Rakobol'skaia, and Tukish, Dokl. Akad. Nauk SSSR **118**, 899 (1958), Soviet Phys. "Doklady" **3**, 122 (1958).

[5] R. W. Williams, Phys. Rev. **74**, 1689 (1948).

[6] Vavilov, Nikol'skii, and Tukish, Dokl. Akad. Nauk SSSR **93**, 233 (1954).

[7] S. I. Nikol'skii, and V. M. Seleznev, J. Exptl. Theoret. Phys. (U.S.S.R.) **32**, 1250 (1957), Soviet Phys. JETP **5**, 1019 (1957).

[8] Dobrotin, Zatsepin, Rozental', Sarycheva, Khristiansen, and Eidus, Usp. Fiz. Nauk **49**, 185 (1953).

[9] Cranshaw, Galbraith, Porter, de Beer, and Hillas, Proceedings of the Varenna Conference on Cosmic Rays, 1957.

[10] Vavilov, Evstigneev, and Nikol'skii, J. Exptl. Theoret. Phys. (U.S.S.R.) **32**, 1319 (1957), Soviet Phys. JETP **5**, 1078 (1957).

[11] Dovzhenko, Nelepo, and Nikol'skii, J. Exptl. Theoret. Phys. (U.S.S.R.) **32**, 463 (1957), Soviet Phys. JETP **5**, 391 (1957).

[12] G. T. Zatsepin and I. L. Rozental', Dokl. Akad. Nauk SSSR **99**, 369 (1954).

[13] H. L. Kasnitz and K. Sitte, Phys. Rev. **94**, 977 (1954).

[14] Nikol'skii, Vavilov and Batov, Dokl. Akad. Nauk SSSR, **111**, 71 (1956), Soviet Phys. "Doklady" **1**, 625 (1956).

Translated by H. Kasha
128

SOVIET PHYSICS JETP VOLUME 35(8), NUMBER 3 MARCH, 1959

TRIPLE DISINTEGRATIONS OF URANIUM NUCLEI

N. A. PERFILOV and G. F. DENISENKO

Radium Institute, Academy of Sciences, U.S.S.R.

Submitted to JETP editor April 12, 1958

J. Exptl. Theoret. Phys. (U.S.S.R.) 35, 631-634 (September, 1958)

A study was made of the disintegration of uranium by 460-Mev and 660-Mev protons into three multiply-charged particles: two particles of the heavy fragment type and the third with considerably smaller mass and charge. The yield for given proton energies, the angular distribution of the light multiply-charged particles (front-to-back ratio), and their distribution in charge and energy were determined for such triple disintegrations. A mechanism is proposed for the triple disintegrations and the fragmentation cross section of uranium is estimated on this basis.

1. INTRODUCTION

In scanning plates with uranium-loaded emulsion which have been irradiated with high-energy protons, one observes disintegrations with emission of three multiply charged particles (cf. the figure in the insert). Such events occur approximately once in 200 or 220 cases of normal binary fission for incident proton energies of 660 Mev, and once in 400 cases for protons of 460 Mev. Up to now, 43 such disintegrations have been found and studied.

These disintegrations can be divided into two types. Type I consists of those disintegrations in which the ranges of all three multiply-charged particles are approximately equal. The equality of the ranges implies approximate equality of the masses.

The disintegrations of type II are those in which one of the three multiply-charged particles has considerably greater range in the emulsion and consequently much lower mass than the other two. The yield of triple disintegrations of type II is greater than that for type I by a factor of 5 or 6. It should be mentioned that in the majority of disintegrations of type II, in addition to the three multiply-charged particles one also observes tracks of protons and α particles, with an average of 1.6 charged particles per disintegration, whereas none of the disintegrations of type I are accompanied by emission of charged particles.

The present paper describes the results of a study of disintegrations of type II. The reason for this restriction is that up to the present time a satisfactory method for determining the nature of particles in nuclear emulsions has been developed for charge values up to $Z = 11$,[1] whereas there is no reliable method for identifying multiply-charged particles from their tracks in emulsion for larger values of the charge. Thus all the subsequent statements will refer to disintegrations of type II.

2. EXPERIMENTAL RESULTS

The main results are the following.

(a) The yield of triple disintegrations increases with incident proton energy; for example it doubles when the proton energy is changed from 460 to 660 Mev.

(b) The light multiply-charged particle in the triple disintegrations is emitted preferentially in the forward direction relative to the incident proton beam. The front-to-back ratio is ≈ 5.

(c) We give below the charge distribution of the light multiply charged particles. The charge was determined by the photometering method[1] in 22 cases:

Charge of particle:	4	5	6	7	8	9	10	11
Number of particles:	8	5	1	4	0	2	1	1

From these data the average charge is ~ 6.

(d) The table gives the energy of the light multiply-charged particles as determined from the range-energy curve[2,3] and the energy of the Coulomb interaction* between the light multiply charged particle and the residual nucleus. The charge of the residual nucleus was taken to be $Z = Z_t - (Z_l + \Delta Z)$, where Z_t is the charge of the uranium nucleus, Z_l is the charge of the light multiply-charged particle, and ΔZ is the change of charge

---

*In computing the Coulomb interaction we set $r_0 = 1.45 \times 10^{-13}$ cm.

Z	4	5	6	7	9	10	11
E_{exp}, Mev	17	21	48	52	80	55	70
	30	78		65	40		
	28						
	22	57		78			
	48	25		54			
	32	34					
	25						
	36						
E_{Coul}, Mev	42	51	60	71	85	92	102

associated with emission of protons and α particles in the particular disintegration.

3. DISCUSSION OF EXPERIMENTAL RESULTS

The data on dependence of yield on incident proton energy, angular distribution of the light-multiply charged particles, and their charge distribution are not in contradiction with the assumption that these disintegrations occur as the result of the superposition of two processes: emission of a light multiply-charged particle (a fragment) by the nucleus, and subsequent normal fission of the residual nucleus. Assuming this mechanism for the production of triple disintegrations, we can evaluate the cross section for fragmentation of uranium or the ratio of the fragmentation cross section to the cross section for inelastic processes, and compare the result with the similar ratio obtained for a nucleus in the middle of the periodic table, such as silver, since the fragmentation cross section has been determined for this element.[4] We have:

$$\frac{\sigma_{fr}(U)}{\sigma_{in}(U)} = \frac{N_{fr}(U)}{N_{int}} = \left(N_T \frac{\sigma_{in}(86)}{\sigma_f(86)}\right) \Big/ \left(N_f \frac{\sigma_{in}(U)}{\sigma_f(U)}\right).$$

Here N_T is the number of disintegrations of type II (30 for $E_p = 660$ Mev) observed for N_f binary fissions ($= 6300$); $\sigma_f(U)$ is the uranium fission cross section[5] ($= 1.1$ barns); $\sigma_{in}(U)$ is the cross section for inelastic interaction of uranium[6] ($= 0.9\,\sigma_{geom}$ or 2.2 barns); $\sigma_f(86)$ is the fission cross section of the residual nucleus. This last cross section was taken to be 0.4 barn in the computation; this value was based on the assumption that in the interval from bismuth (for which [7]$\sigma_f(Bi) \approx 0.2$ barn) to uranium the fission cross section changes proportionally to the change in Z. On substituting these values, we get:

$$(\sigma_{fr}/\sigma_{in})_U \approx 0.01 = (\sigma_{fr}^{*}/\sigma_{in})_{Ag}$$

and consequently $\sigma_{fr}(U) \approx 22$ millibarns (for incident proton energy $E_p = 660$ Mev).

The result obtained on the basis of our assumptions shows that the fragmentation cross section increases proportionally to the geometric cross section. This value for the fragmentation cross section of uranium (22 millibarns) was obtained under the assumption that the emission of the fragment from the target nucleus does not affect the probability of fission of the residual nucleus. If, however, the preceding fragmentation changes (increases or decreases) the probability of fission of the residual nucleus, we obtain a correspondingly increased or lowered value for the fragmentation cross section of uranium.

However, not all of the experimental data can be made understandable from the point of view of our assumption of superposition of the two processes — fragmentation and subsequent fission of the residual nucleus. Comparing the values of the experimentally observed energy and the Coulomb interaction energy given in the table, we see that in most cases $E_{exp} < E_{Coul}$, whereas for fragmentation of silver nuclei[1] the values of E_{exp} cluster around the values of the Coulomb interaction energy, and $E_{exp} \gg E_{Coul}$ in several cases. As mentioned previously, we computed the Coulomb energy for a spherical nucleus, assuming $r_0 = 1.45 \times 10^{-13}$ cm. However, if we compute E_{Coul} for a deformed nucleus, assuming for example $\Delta R/R = 0.2$, the values of E_{Coul} are decreased by approximately 10 Mev, which brings many of the values of E_{Coul} close to E_{exp}. But if in the

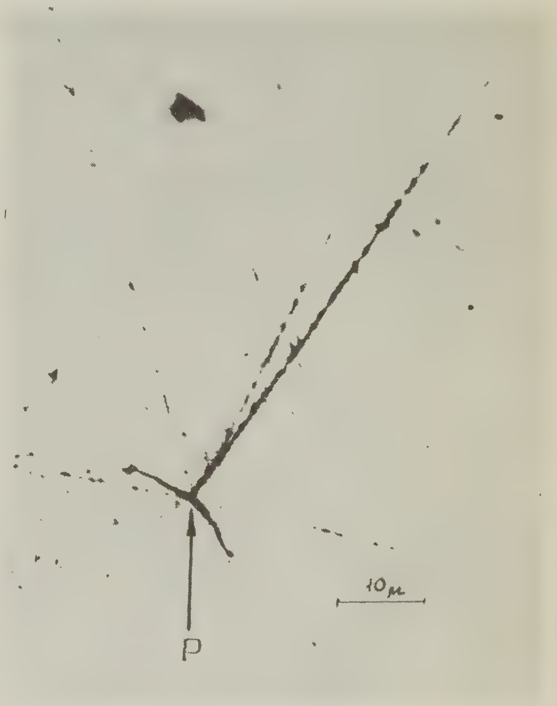

FIG. 1

majority of cases E_{exp} is actually less than E_{Coul} computed on the assumption of interaction of two charges (even taking account of nuclear deformation), this may indicate that there is simultaneity in the disintegration of uranium into three particles. Such events can be treated as triple fissions, but it is then not clear why the light multiply charged particle is emitted preferentially into the forward hemisphere.

For a more detailed study of the phenomenon of fragmentation of uranium nuclei, it would be interesting to study this phenomenon in pure form, i.e., not only to study disintegrations with three multiply charged particles, two of which may be assigned as fission products, but also to study disintegrations with one fragment. However, such a study is not possible if the emulsion is loaded with uranium by soaking the plate in a water solution of some uranium compound. With such a loading procedure, it is not possible to separate fragment-containing stars from disintegration of uranium from similar stars from disintegration of silver nuclei. Besides, there will be more fragment-containing stars from disintegration of silver nuclei because the number of Ag nuclei in the emulsion is approximately two orders of magnitude greater than the number of uranium nuclei loaded into the emulsion.

One solution to this problem is to introduce the element in which fragmentation is to be studied in the form of grains of dimension 3 to 6 μ into the middle layer of a three-layer plate.[8] However such a method requires a very long time of searching for disintegrations, in view of the low probability for producing a disintegration containing a fragment in such grains.

In our laboratory, the fragmentation of bismuth nuclei is being studied by the method of introducing elements into the emulsion in the form of grains. The results will be published later.

---

[1] O. V. Lozhkin, J. Exptl. Theoret. Phys. (U.S.S.R.) **32**, 208 (1957), Soviet Phys. JETP **5**, 293 (1957).

[2] A. Papineau, Compt. rend. **242**, 2933 (1956).

[3] Parfanovich, Semchinova, and Flerov, J. Exptl. Theoret. Phys. (U.S.S.R.) **33**, 343 (1957); Soviet Phys. JETP **6**, 266 (1958).

[4] O. V. Lozhkin and N. A. Perfilov, J. Exptl. Theoret. Phys. (U.S.S.R.) **31**, 913 (1956); Soviet Phys. JETP **4**, 790 (1957). O. V. Lozhkin, J. Exptl. Theoret. Phys. (U.S.S.R.) **33**, 354 (1957), Soviet Phys. JETP **6**, 273 (1958).

[5] Perfilov, Ivanova, Lozhkin, et al. Сессия АН СССР по мирному использованию атомной энергии (Session of the Academy of Sciences, U.S.S.R., on Peaceful Uses of Atomic Energy) Session of the Chemical Sciences Division, Acad. Sci. Press, 1955. N. S. Ivanova, J. Exptl. Theoret. Phys. (U.S.S.R.) **31**, 413 (1956); Soviet Phys. JETP **4**, 365 (1957).

[6] V. I. Moskalev and B. V. Gavrilovskii, Dokl. Akad. Nauk SSSR **110**, 972 (1956), Soviet Phys. "Doklady" **1**, 607 (1956).

[7] P. Kruger and N. Sugarman, Phys. Rev. **99**, 1450 (1955). L. G. Jodra and N. Sugarman, Phys. Rev. **99**, 1470 (1955).

[8] Perfilov, Gerling, Prokof'eva, and Solov'eva, Тр. РИАН (Trans., Radium Institute Acad. Sci.) **7**, 265 (1956).

Translated by M. Hamermesh
129

SOVIET PHYSICS JETP VOLUME 35(8), NUMBER 3 MARCH, 1959

ON THE SIZE SPECTRUM OF EXTENSIVE AIR SHOWERS

G. V. KULIKOV and G. B. KHRISTIANSEN

Moscow State University

Submitted to JETP editor April 22, 1958

J. Exptl. Theoret. Phys. (U.S.S.R.) 35, 635-640 (September, 1958)

Experimental data are presented on the size spectrum of extensive air showers in the region 10^5 to 2×10^6 particles. An analysis of these and other data available in the literature indicates that there is, very probably, an irregularity in the shower size distribution curve in the region between 10^6 and 10^7 particles. This is considered to constitute an argument in favor of the metagalactic origin of cosmic rays with energies above 10^{16} ev.

IN connection with the problem of a change in the character of the elementary interaction in the ultra high energy range, Vernov[1] suggested the idea that such a change could reflect itself as an irregularity in the size spectrum of extensive air showers (EAS). On the other hand, the study of the size spectrum of EAS is of considerable interest for the investigation of the primary component of cosmic radiation.

In the majority of experiments carried out so far the density spectrum of EAS was actually measured, and the size spectrum was calculated on its basis. Such a method of obtaining the size spectrum of an EAS has, however, many disadvantages. In fact, it is known that the density spectrum is the result of an integration of the size spectrum over a wide range, in which the number of particles varies by 2 or 3 orders of magnitude. As the result, the density spectrum cannot reflect all details of the size spectrum.

In the present work the size spectrum of EAS has been studied directly. The measurements were carried at sea level in May 1954.

EXPERIMENTAL SETUP AND METHOD

The measurements were carried out using the array described in reference 2, by the method of correlated hodoscopes[3] which, in principle, permits it to study each shower individually.

The size and position of the hodoscope counter groups are shown in Fig. 1. The array permitted us to locate the shower axis and find the number of particles in showers in the range from 2×10^4 to 2×10^6 particles. The hodoscope arrangement displayed the number of discharged counters in various counter groups for each shower. Knowing the position of counters struck in the plane of observation, one can find the total number of particles N and the coordinates of the axis X_0, Y_0 of the recorded shower, under the assumption that (1) the shower is axially symmetric and (2) the trajectories of the shower particles are distributed according to the Poisson law and possible fluctuations of the lateral distribution function in a shower with given N are governed only by that law.

The probability that, when m_i out of n_i counters are struck at the i-th point with coordinates X_i, Y_i, the recorded shower consists of N particles and its axis has coordinates X_0, Y_0, is proportional to

$$C_{n_i}^{m_i}\,[1-\exp(-\sigma_i\rho_i)]^{m_i}\exp[-\sigma_i\rho_i(n_i-m_i)],$$

where σ_i is the area of a single counter in the i-th group, and

$$\rho_i = kNf(|\mathbf{r}_i-\mathbf{r}_0|),\ k=2\cdot 10^{-3}\ \mathrm{m}^{-1}\ [2],$$

$$f(|\mathbf{r}_i-\mathbf{r}_0|)=\frac{1}{|\mathbf{r}_i-\mathbf{r}_0|}\exp\left(-\frac{|\mathbf{r}_i-\mathbf{r}_0|}{58}\right),$$

$$|\mathbf{r}_i-\mathbf{r}_0| = [(X_i-X_0)^2+(Y_i-Y_0)^2]^{1/2}.$$

The probability that, for an occurring combination (m_i, n_i), the recorded shower will have individual characteristics N, X_0, Y_0, is then given (to a normalization constant) by the following expression:

$$W(X_0, Y_0, N) \approx \prod_{i=1}^{56} C_{n_i}^{m_i}\,[1-\exp(-\sigma_i\rho_i)]^{m_i}\exp[-\sigma_i\rho_i(n_i-m_i)]. \quad (1)$$

Determination of the shower size and its axis location is therefore reduced to the following extremum problem: find the maximum of Eq. (1) with respect to the variables N, X_0, and Y_0, knowing the value of other parameters in the expression. The problem was solved with the electronic computer of the Computing Center of Moscow State University.

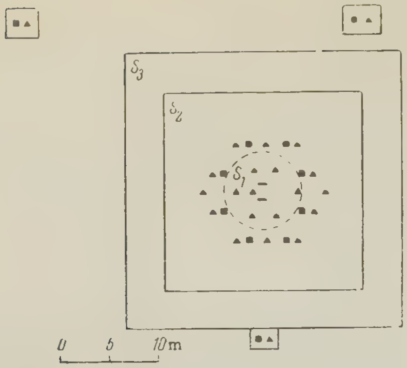

FIG. 1. Diagram of the hodoscope array used for the study of the size spectrum of EAS. ■ — group of 24 hodoscope counters, 330 cm² in area each: ▲ — group of 48 hodoscope counters, 24 of area of 100 cm² each, and 24 of area of 24 cm² each, ■ — master groups.

N was found with an accuracy of 10%, and X_0 and Y_0 with an accuracy of 0.5 m for shower axes falling within the area S_1. The errors were 15% and 1.0 m respectively when the axis fell within the area S_3.

The axis location and the number of particles for each individual shower being known, it is possible to find the absolute rate of showers of a given size. The dimensions of the collecting area were different for showers of different size, being determined not only by the position of hodoscope points but also by the probability of shower detection using the chosen six-fold counter coincidence arrangement.

RESULTS AND DISCUSSION

The experimental results which are made use of in the present article were gathered during 285 hours of operation of the array. The number of showers of a size above given value, the axes of which fell in the area $S_1 = 78\ \text{m}^2$ for $N > 8 \times 10^4$, $S_2 = 400\ \text{m}^2$, for $N > 1.6 \times 10^5$, and $S_3 = 576\ \text{m}^2$, for still larger N (the relative position of these areas is shown in Fig. 1), used for constructing the spectrum, are given in the table. The probability that a shower incident upon the above areas was recorded by the array was greater than 95%.

The integral size spectrum constructed from using the data is shown in Fig. 2. The ordinate represents the number of showers above certain size in $\text{cm}^{-2}\ \text{sec}^{-1}\ \text{sterad}^{-1}$. It was shown[4] that the rate of showers arriving vertically per unit solid angle F(N, 0) is related to the total F(N) for the given array by

$$F(N, 0) = F(N)(\nu + 1)/2\pi,$$

when the zenith angle distribution of shower axes incident upon the array is proportional to $\cos^2\theta$, with $\nu = 8$.[5]

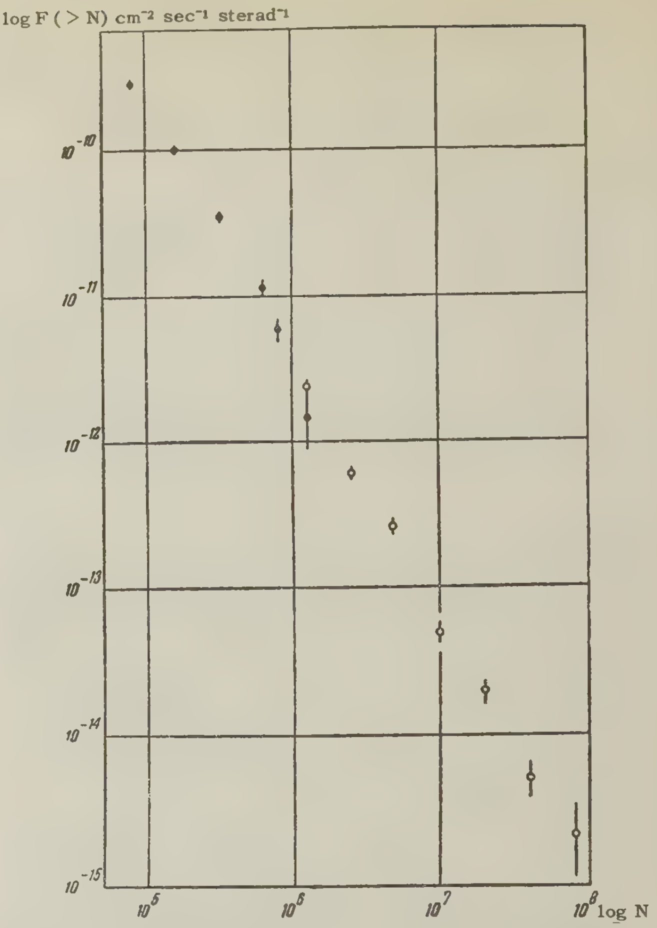

FIG. 2. Integral size spectrum of EAS. ● — measurements of the present experiment, ○ — measurements of reference 7.

The data indicate with a high probability that a change in the character of the spectrum may occur in the investigated region $N = 8 \times 10^4$ to 1.5×10^6. In the region $N = 8 \times 10^4$ to 8×10^5 the integral spectrum can be approximated by a power law with an exponent $\kappa = 1.5 \pm 0.1$. For $N > 8 \times 10^5$ the spectrum is steeper. For a quantitative determination of the exponent κ in that region we used the data of reference 6, in which each shower was measured individually.* These data are also shown in Fig. 2. For the region $N = 8 \times 10^5$ to 3×10^6 we then obtain $\kappa = 2.2 \pm 0.3$. Using the results of reference 6, for the region $N = 10^7$ to 10^8 we have $\kappa = 1.5 \pm 0.2$.†

The exponent of the size spectrum of EAS was

---

*It should be mentioned that the lateral distribution function used in reference 6 does not differ from that used by us by more than 25%.

†In reference 6 the size-spectrum exponent was determined for the whole range of measurements $N = 8 \times 10^5$ to 10^8 and was found to be $\varkappa = 1.84 \pm 0.15$. A χ^2 test shows, however, that the probability that the spectrum has two exponents $\varkappa = 2.2 \pm 0.3$ and $\varkappa = 1.5 \pm 0.2$ is three times higher then the probability of a single exponent $\varkappa = 1.84 \pm 0.15$. The probabilities are 75 and 25% respectively.

Number of particles in shower, N	$0.8\cdot10^5$	$1.6\cdot10^5$	$3.2\cdot10^5$	$6.4\cdot10^5$	$8.0\cdot10^5$	$12.8\cdot10^5$
Number of showers with number of particles > N	157	276	138	46	24	6

measured earlier using arrays with widely spaced counters connected in coincidence.[7,8] It is well known that such arrays select effectively showers with size varying by two orders of magnitude. The values of the exponent $\kappa \approx 1.9$ to 2.0 obtained in these experiments for the range $10^6 < N < 10^8$ do not contradict the above data on variation of the exponent in that range.

The observed variation of the size spectrum is evidently related to a corresponding variation of the spectrum of the primary ultra-high-energy cosmic radiation that initiates the EAS.* We shall make the simplest assumption that the total number of particles N in EAS is connected with the primary energy E by the following relation:

$$E = k_0 N,$$

where k_0 is almost independent of N and, at sea-level, equals about 10^{10} ev.[9] To the size range $N = 10^5$ to 10^8 corresponds, therefore, the primary energy range $E = 10^{15}$ to 10^{18} ev.

The observed variation of the primary cosmic-ray spectra can be explained by the following model of propagation from their point of origin to the point of observation: we shall assume that sources of primary cosmic radiation exist in the galaxy, producing particles with energy E, up to the highest experimentally observed[10] ones, integral spectrum of this particle being $\sim E^{-\kappa}$. In view of the presence of regions with a higher magnetic field (magnetic clouds) in the galaxy, the particles are diffused when their energy is $E \leq 300\ Hl \approx 10^{16}$ ev, where l is the size of magnetic clouds and H is the magnetic field intensity ($H \sim 10^{-5}$ Oe and l is on the order of several light-years). As the result of the diffusion, the particles are accumulated in the galaxy, the storage factor being on the order of $\sim 10^3$ to 10^4.[11] Particles with energy $E > 10^{16}$ ev are diffused to a lesser extent, so that their concentration is strongly dependent on the energy. One can expect therefore a rather sharp variation of the primary-energy spectrum, namely that it becomes steeper for $E > 10^{16}$ ev. Particles of $> 10^{16}$ ev, propagating practically in straight lines, leave the galaxy. If we assume that a similar process takes place in other galaxies as well, it is evident that the particles with $E \geq 10^{16}$ ev may have a metagalactic origin.

We shall estimate now the contribution of other galaxies to the flux of particles with $E > 10^{16}$ ev. We shall asume that the concentration of galaxies in the universe is n. If S is the emission intensity per unit volume of each galaxy then the total flux of particles I through surface ω will be given by the expression

$$I = SV2\pi \int_0^R r^2 dr n 2 \int_0^{\pi/2} \frac{\omega \cos\theta}{r^2} \sin\theta d\theta, \qquad (2)$$

where V is the galactic volume and R is the maximum distance traversed by the particles without interaction.* The flux of particles of similar energies through surface ω produced by our galaxy I_G is

$$I_G = S2\pi \int_0^{R_0} r^2 dr 2 \int_0^{\pi/2} \frac{\omega \cos\theta}{r^2} \sin\theta d\theta,$$

where R_0 is the radius of galaxy (assuming that the galaxy is spherical). The ratio of these fluxes is $I/I_G = nVR/R_0$. Assuming that $n = 10^{-18}$ cubic light years, $V \sim 10^{14}$ per cubic light year, $R = 10^{12}$ light years (reference 12), and $R_0 = 10^5$ light years, we obtain $I/I_G = 10^3$.

The ratio of the particle flux produced by other galaxies to that produced by our galaxy is, in its order of magnitude, equal to the "storage factor" due to diffusion.

It is natural to assume that the energy spectrum of particles of metagalactic origin will be characterized by the same exponent κ. Since the intensity of the galactic and metagalactic radiation is of the same order of magnitude, the observed spectrum is a superposition of the spectra of particles of galactic and metagalactic origin.

Finally, we should like to mention that the conclusions of the present work with respect to the irregularity in the size spectrum of EAS cannot be regarded as final, since the experimental data on which they are based do not possess a sufficient statistical accuracy. The results, however, stress the great urgency of further experiments on the size spectrum of EAS.

---

*With regard to another possible interpretation, cf. reference 1.

*In connection with the presence of magnetic fields of $\sim 10^{-7}$ Oe in the metagalactic space,[11] the upper limit of integration in Eq. (2) will be limited by smaller values of R; it is then necessary, however, to account for the storage factor of the metagalactic space.

The authors wish to thank Prof. S. N. Vernov for valuable advice and discussion of the results, G. S. Rosiakov who lead the computing team in the computation center of Moscow State University, V. I. Solov'eva who took part in several stages of the work, and D. S. Stel'makh who executed a large amount of work in preliminary reduction of the data.

---

[1] Vernov, Zatsepin, Khristiansen, and Chudakov, Сообщение на Всесоюзной конференции по космическим лучам (Report at the All Union Conference on Cosmic Rays), Tbilisi, 1956.

[2] Abrosimov, Zatsepin, Solov'eva, Khristiansen, and Chikin, Izv. Akad. Nauk SSSR, Ser. Fiz. **19**, 677 (1955) [Columbia Techn. Transl. **19**, 616 (1955)].

[3] Dobrotin, Zatsepin, Nikol'skii, Sarycheva, and Khristiansen, Izv. Akad. Nauk SSR, Ser. Fiz. **19**, 666 (1955) [Columbia Techn. Transl. **19**, 605 (1955)].

[4] Abrosimov, Goriunov, Dmitriev, Solov'eva, Khrenov, and Khristiansen, J. Exptl. Theoret. Phys. (U.S.S.R.) **34**, 1077 (1958), Soviet Phys. JETP **7**, 746 (1958).

[5] Abrosimov, Goman'kov, Ivanovskaia, and Sarycheva, J. Exptl. Theoret. Phys. (U.S.S.R.) **33**, 1110 (1957), Soviet Phys. JETP **6**, 856 (1957).

[6] Clark, Earl, Kraushaar, Linsley, Rossi, and Scherb, Nature **180**, 406 (1957).

[7] Eidus, Adamovich, Ivanovskaia, Nikolaev, and Tuliankina, J. Exptl. Theoret. Phys. (U.S.S.R.) **22**, 440 (1952).

[8] Antonov, Vavilov, Zatsepin, Kutuzov, Skvortsov, and Khristiansen, J. Exptl. Theoret. Phys. (U.S.S.R.) **32**, 227 (1957), Soviet Phys. JETP **5**, 172 (1957).

[9] K. Greisen, Progress in Cosmic Ray Physics, vol. III, ch. I, Amsterdam 1956.

[10] V. L. Ginzburg, Usp. Fiz. Nauk **62**, 37 (1957).

[11] A. Unsold, Phys. Rev. **82**, 857 (1951).

[12] G. Cocconi, Nuovo cimento **3**, 1433 (1956).

Translated by H. Kasha
130

SOVIET PHYSICS JETP VOLUME 35 (8), NUMBER 3 MARCH, 1959

ANOMALY IN THE MAGNETIC ANISOTROPY OF $K_3Fe(CN)_6$ *SINGLE CRYSTALS AT LOW TEMPERATURES*

G. SHOFFA, O. RISTAN, and K. RUCKPAUL

Institute for Biology and Medicine, Academy of Sciences, German Democratic Republic

Submitted to JETP editor April 25, 1958

J. Exptl. Theoret. Phys. (U.S.S.R.) 35, 641-644 (September, 1958)

The anomalous behavior in the magnetic anisotropy of $K_3Fe(CN)_6$ single crystals near 126°K, apparently due to the interaction between paramagnetic ions, is described.

THE temperature dependence of the anisotropic magnetic susceptibility of $K_3Fe(CN)_6$ single crystals has been studied experimentally[1-4] and theoretically[5-7] by a number of investigators. The new measurements reported in this paper were motivated by the recently published paper of Stephenson and Morrow[8] in which an anomaly in the specific heat of $K_3Fe(CN)_6$ was reported at 131°K. The authors attribute this anomaly to a magnetic transition of some kind but do not consider the effect in detail.

All the presently available measurements of the magnetic anisotropy in $K_3Fe(CN)_6$ single crystals at low temperatures have been performed over large temperature ranges[1, 2, 4] or have not included the temperature indicated above.[3] In no case has there been a detailed investigation in the temperature region in which the specific-heat anomaly has been observed. Moreover, the experimental results reported by different authors are not consistent. Up to this time no account has been taken of x-ray studies of the structure of $K_3Fe(CN)_6$ carried out by Barkhatov and Zhdanov,[9-11] although these would be useful in interpreting the experimental results. In addition paramagnetic resonance measurements carried out in recent years[12, 13] furnish valuable new data which should be exploited. Inasmuch as potassium ferricyanide serves as a classical example of a so-called covalent complex, it is hoped that the present work will be of value.

EXPERIMENTAL RESULTS

Large $K_3Fe(CN)_6$ single crystals were grown in water solutions; a few especially well-formed crystals were used. The morphology of potassium ferricyanide crystals is described by Groth.[14] The crystal structure has been studied by Barkhatov and Zhdanov.[9-11] The elementary cell contains two parts by weight of $K_3Fe(CN)_6$. The relation between the external crystallographic axes (a, b, c), the molecular axes (α, β, γ) and the molecular magnetic axes (x, y, z) in the ab plane are shown in Fig. 1. These crystallographic data were used in analyzing the magnetic anisotropy.

The measurements of the magnetic anisotropy were carried out by the Krishnan technique, using the system which has been described in detail in reference 15; this system can be used to measure the anisotropies over small temperature ranges (1 to 2 degrees) in the temperature region 90 to 300°K. Thus, it was possible to make a detailed study of the region near 130°K of interest to us. The strength of the uniform magnetic field was measured by a nuclear-resonance method. The torsional constant of the quartz fiber was determined by measuring the torsional period of a suspended body whose moment of inertia was known. The crystals were suspended and measured along all three crystallographic axes; this procedure was necessary since the angle between the crystallographic and magnetic axes in potassium ferricyanide is temperature dependent, especially at low temperatures. The difference between the results of the present measurements and the paramagnetic-resonance measurements[13] and the results obtained by Guha[4] is explained by the fact that this factor was not taken into account.

To compute the magnetic susceptibilities along all three magnetic axes one must know the temperature dependence and the mean value of the susceptibility. These measurements were performed at the same temperatures using the method described by Guha.

The results of measurements of the magnetic susceptibilities χ_1, χ_2, and χ_3 and the mean susceptibility are shown in Fig. 2. Although the measurements were performed at every 2 or 3 degrees, for clarity the points in the figure are

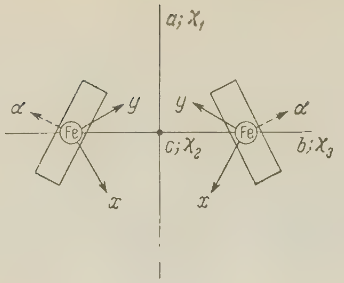

FIG. 1

given at every 10 degrees, except for the points of interest in the neighborhood of the transition. As is apparent from the figure, χ_1 and χ_3 are essentially the same at the higher temperatures. This result indicates that the tetragonal crystallographic field predominates in potassium ferricyanide. Frequently, there is a rotational effect when the crystals are suspended by the c axis since it is difficult to determine the position of this axis accurately from the external shape of the crystal. As we have already indicated, the crystals must be measured in all directions; that is to say, we must have more measured quantities than there are unknowns in the computation formulas. It is necessary to eliminate the uncertainty in the determination of the crystallographic axes. The positions of the magnetic axes with respect to the external axes of the crystal (a, b, c), the molecular axes in the elementary cell (α, β, γ) and the molecular magnetic axes (x, y, z) in the ab plane are shown in Fig. 1. The magnetic axes of the crystal coincide with the crystallographic axes. The molecular magnetic axes x and y form angles of 30 and 60 degrees with the magnetic axis χ_1 in the ab plane. The molecular magnetic z axis is perpendicular to the χ_1 and χ_3 axes and is parallel to the χ_2 axis; thus, this axis is perpendicular to the plane of the figure.

The most interesting results of these measurements are those for the temperature dependence of the magnetic anisotropy near 126°K. As is apparent from Fig. 2, at this temperature χ_1 increases considerably, χ_2 decreases, and χ_3 remains unchanged. Measurements by the Guha method in polycrystalline samples, show a discontinuity at this same temperature in the slope of the susceptibility-vs.-temperature curve. The existence of this anomaly in the magnetic anisotropy was verified many times in several crystals. The measurements in the transition region are not as accurate as those at the other points because there was a temperature variation during the measurement. This variation was a result of the large angle of rotation of the quartz fiber. It is difficult to determine the location of the peak. However, the effect is so large that there can be no doubt as to its existence. The absolute accuracy in the temperature measurements is ± 2°; the relative accuracy for the series of measurements is ±0.5°. The error in the measurements is due chiefly to the fact that the temperature is not measured in the crystal itself, but rather in the vicinity of the crystal.

It is interesting to note that after the anisotropy transition the magnetic axis χ_3, which is along the crystallographic axis, is characterized by a higher magnetic susceptibility than the χ_1 axis. A change in the direction of the axis of highest magnetization has been also observed by Bleaney and O'Brien[7] in paramagnetic-resonance measurements.

DISCUSSION OF THE RESULTS

The anomaly in the magnetic anisotropy in the present work is observed at approximately the same point as the anomaly in the specific heat which has been observed by Stephenson and Morrow in polycrystalline potassium ferricyanide. The present measurements verify the assumption made by these authors that the anomaly is due to a magnetic transition. Furthermore, we have shown that the transition is anisotropic. Since it is almost entirely compensated along the χ_1 and χ_2 axes the effect on the mean magnetic susceptibility and specific heat is very small.

It is difficult to interpret this anomaly on the basis of the experimental and theoretical data available at this time. Bleaney and O'Brien have observed in paramagnetic-resonance measurements that the highest susceptibility is along the a axis at 90°K and along the b axis at 20°K.

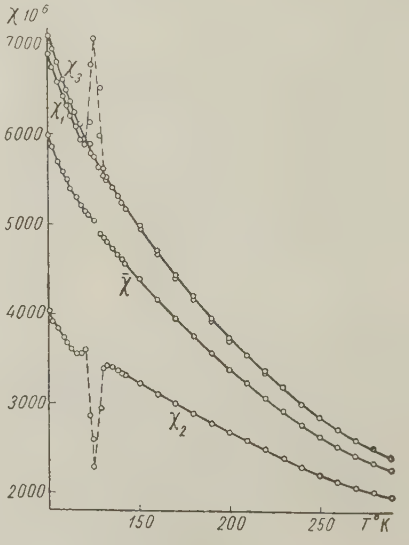

FIG. 2

The effect observed by these authors is not characteristic of diamagnetic dilution; hence, it is reasonable to assume that the effect is due to exchange interactions between neighboring paramagnetic ions. Apparently the anomaly reported here is of the same nature. It would seem that the interaction between magnetic ions in the present case is highly anisotropic and is related to the change in direction of the magnetic axes of the individual molecules. This is to be associated with a change in the direction of the axes of the crystal as a whole. A theoretical analysis indicates that in $K_3Fe(CN)_6$ a small change in the crystalline field must lead to a marked change in the anisotropy.[7] The exchange forces between neighboring paramagnetic ions are found in ions with five or more d-electrons.

The problems considered here have been studied recently in many experimental and theoretical papers concerned with problems in antiferromagnetism.[16] The relation between the effects reported here and this work will be examined in subsequent papers.

---

[1] L. C. Jackson, Proc. Roy. Soc. (London) **A140**, 695 (1933).

[2] L. C. Jackson, Proc. Phys. Soc. (London) **50**, 707 (1938).

[3] H. Masson, Compt. rend. **224**, 1277 (1947).

[4] B. C. Guha, Proc. Roy. Soc. (London) **A206**, 353 (1951).

[5] J. B. Howard, J. Chem. Phys. **3**, 813 (1935).

[6] M. Kotani, J. Phys. Soc. Japan **4**, 293 (1949).

[7] B. Bleaney and M. C. M. O'Brien, Proc. Phys. Soc. (London) **B69**, 1216 (1956).

[8] C. C. Stephenson and J. C. Morrow, J. Am. Chem. Soc. **78**, 275 (1956).

[9] V. I. Barkhatov and G. S. Zhdanov, Acta Phys. Chim. U.R.S.S. **16**, 43 (1942).

[10] V. I. Barkhatov, Acta Phys. Chim. U.R.S.S. **16**, 123 (1942).

[11] V. I. Barkhatov, J. Phys. Chem. (U.S.S.R.) **18**, 445 (1944).

[12] B. Bleaney and D. J. E. Ingram, Proc. Phys. Soc. (London) **A65**, 953 (1952).

[13] Baker, Bleaney, and Bowers, Proc. Phys. Soc. (London) **B69**, 1205 (1956).

[14] P. Groth, Chemische Kristallographie, Bd. 1, Leipzig (1906).

[15] G. Schoffa and G. Mai, Exp. Technik der Physik (in press).

[16] Антиферромагнетизм Antiferromagnetism (Collection of Russ. Transl.) IIL, M. 1956.

Translated by H. Lashinsky
131

ANGULAR CORRELATION FOR LOW-ENERGY POSITRONS EMITTED IN $\pi^+-\mu^+-e^+$ *DECAY*

A. O. VAISENBERG, V. A. SMIRNITSKII, E. D. KOLGANOVA, Z. V. MINERVINA, E. A. PESOTSKAIA, and N. V. RABIN

Submitted to JETP editor May 31, 1958

J. Exptl. Theoret. Phys. (U.S.S.R.) **35**, 645-648 (September, 1958)

The energies of 1099 positrons from $\pi^+-\mu^+-e^+$ decays in photographic emulsions and the angles ϑ between the muon and positron tracks have been measured. It is shown that in the energy regions $\epsilon = (0 \text{ to } 0.3)$, $(0.3 \text{ to } 0.6)$ and (> 0.9), the value of $\overline{\cos\vartheta}$, which is proportional to the asymmetry parameter, is $+0.18 \pm 0.10$, 0.00 ± 0.04 and -0.09 ± 0.04, respectively. (ϵ is the positron energy as a fraction of its maximum energy.) 201 low-energy positrons ($\epsilon < 0.3$) were selected and measured out of a total of 8000 $\pi^+-\mu^+-e^+$ decays. For these positrons $\overline{\cos\vartheta} = +0.07 \pm 0.05$. A χ^2 test shows that the probability of positive asymmetry in the 0 to 0.3 energy range is close to 95%.

AFTER the discovery of parity nonconservation in weak interactions, the energy dependence of the angular correlation of positrons in $\pi^+-\mu^+-e^+$ decay was studied by several groups. In references 1 and 2 it was shown that the asymmetry parameter increases with positron energy. This is in qualitative agreement with the two-component neutrino theory.

The measurements of the Columbia group[3] and of Mukhin, Ozerov, and Pontecorvo,[4] which were performed by electronic methods, showed that above 20 or 25 Mev the energy dependence of asymmetry agrees with the two-component theory to within a statistical error of 5 to 10%. In this theory the average cosine of the angle ϑ between the spin direction of the muon and the direction of positron emission in μ^+-e^+ decay is related to the positron energy ϵ as follows:

$$\overline{\cos\vartheta} = \frac{\alpha\lambda}{3}\frac{2\varepsilon-1}{3-2\varepsilon}. \qquad (1)$$

Here ϵ is the positron energy as a fraction of its maximum energy; λ is a parameter of the theory, defined as the ratio between the vector and axial-vector interaction constants; α is a coefficient that indicates the fraction of muons which preserve their polarization before decay. It follows from (1) that the asymmetry is large for ϵ close to 1, that it vanishes at the middle of the spectrum ($\overline{\cos\vartheta} = 0$ for $\epsilon = \frac{1}{2}$), and that its sign is reversed at low energies ($\epsilon < \frac{1}{2}$). Since it is known from experiment that at high energies $\overline{\cos\vartheta} < 0$ ($\lambda < 0$), we may expect for $\epsilon < \frac{1}{2}$ a positive value of $\overline{\cos\vartheta}$.

Asymmetry at low energies was the principal subject of the present investigation. NIKFI-P emulsions $400\,\mu$ thick were exposed to a π^+-meson beam in the synchrocyclotron of the Joint Institute for Nuclear Research. Positron tracks from $\pi^+-\mu^+-e^+$ decays in the emulsions were selected according to the criteria given in reference 2. As a result of these criteria we can assume that we were investigating correlation in a plane rather than in space. This increases $\overline{\cos\vartheta}$ appreciably since for correlation in a plane we have

$$\overline{\cos\vartheta} = \frac{\alpha\lambda}{2}\frac{2\varepsilon-1}{3-2\varepsilon}. \qquad (2)$$

But due to the finite thickness of the emulsions the geometry of the measurements is somewhat different from plane geometry. Appropriate corrections are easily introduced. The values of $\overline{\cos\vartheta}$ must be 7 to 10% smaller than those obtained by means of (2).

Positron energies were determined from third differences by the usual multiple scattering method with a signal-to-noise ratio which was considerably larger than 2.5 on the average. The mean error of our energy measurements was close to 15%. The angle ϑ was measured to within 1 or 2 degrees.

In the first of two series of measurements we obtained the energies and angles ϑ for 1099 positron tracks which satisfied the selection criteria. These included the data for 580 tracks given in reference 2. The results are given in Table I, which shows the energy intervals of the positrons and the total numbers of tracks observed in these intervals. The fourth line of the table gives the experimental value of $\overline{\cos\vartheta}$ obtained by examin-

TABLE I

Angle ϑ		Interval of energy ε			
		0—0.3	0.3—0.6	0.6—0.9	0.9
0—180°	Number of particles n	46	333	440	280
	$\overline{\cos\vartheta} \pm 0.7/\sqrt{n}$	+0.18±0.10	0.00±0.04	—0.05±0.03	—0.09±0.04
0—60°; 120—180°	Number of particles n	34	231	300	198
	$\overline{\cos\vartheta} \pm 0.85/\sqrt{n}$	+0.30±0.15	0.00±0.06	—0.06±0.05	—0.16±0.06

ing all angles from 0 to 180°. The last line gives the values of $\overline{\cos\vartheta}$ for angles from 0 to 60° and from 120 to 180°. In the last case $\overline{\cos\vartheta}$ must be 1.4 times greater than the value obtained by using all angles. From these data we see that in agreement with theory the asymmetry parameter or $\overline{\cos\vartheta}$, which is proportional to it, is close to zero near $\epsilon = \frac{1}{2}$ $(0.3 < \epsilon < 0.6)$. In the region 0 to 0.3, the sign of the asymmetry is reversed: $\overline{\cos\vartheta} = +0.18 \pm 0.10$ for all 46 particles and $\overline{\cos\vartheta} = +0.30 \pm 0.15$ for 34 of these 46 particles for which ϑ is between the limits 0 to 60° and 120 to 180°. The data thus indicates that at low energies $\overline{\cos\vartheta}$ is positive although the statistical reliability of this result is small.

The second set of measurements was obtained for the purpose of improving the statistical accuracy of the results at low energies. In a systematic scan of $\pi^+ - \mu^+ - e^+$ decays about 8000 tracks were selected according to the selection criteria; low-energy positron tracks were selected from among these. A preliminary scan of the 8000 tracks was performed to select those which in three lengths of 180μ (the field of view of an ocular micrometer with 40 × 15 magnification) give an average deviation that exceeds 5μ from a straight line. This preliminary scan yielded about 500 tracks on which multiple scattering was then measured by ordinary methods. Of these tracks, 155 had energies below $\epsilon = 0.3$; we thus increased the number of positrons in the initial spectral region from 46 to 201. The energies of the other particles selected in this way did not exceed $\epsilon = 0.8$.

Table II summarizes the asymmetry data from both sets of measurements at low energies. For $\epsilon = 0.3 - 0.6$ asymmetry is absent as previously, whereas for the energy interval $0 - 0.3$, where the number of particles is almost four times greater than in the first series of measurements, positive asymmetry is observed as previously.

In comparing the experimental and theoretical values of $\overline{\cos\vartheta}$ we must calculate $\overline{\cos\vartheta}$ in the energy interval of interest. The two-component theory easily yields a value of +0.11 for $\overline{\cos\vartheta}$ in the 0 to 0.3 energy interval. It must be taken into account that in emulsions the observed asymmetry is greatly reduced by depolarization; the asymmetry parameter in emulsion averaged over the entire spectrum is close to 0.1 (reference 5) instead of 0.33 for $\alpha = 1$. The corresponding value of $\overline{\cos\vartheta}$ will then be +0.03. Finally, it must be taken into account that the dispersion of scattering and bremsstrahlung measurements of electrons in emulsion transfers high-energy electrons to the low-energy region and thus reduces the positive value of $\overline{\cos\vartheta}$ in this region. The correction for dispersion obtained by suitable "smearing" of the theoretical spectra leads to a reduction of $\overline{\cos\vartheta}$ by 25 or 30% in the 0 to 0.3 energy interval. We must, moreover, consider the reduction of $\overline{\cos\vartheta}$ which results from radiative corrections to the spectrum.[6] In first approximation the two corrections are added and reduce the theoretical value of $\overline{\cos\vartheta}$ by about 40%. The final theoretical value of $\overline{\cos\vartheta}$ is ~ +0.02 for 0 to 180° and, correspondingly, ~ +0.03 for 0 to 60° and 120 to 180°. The measurements (Table II) are $\overline{\cos\vartheta} = +0.07 \pm 0.05$ $+0.13 \pm 0.07$, respectively.

TABLE II

Angle ϑ		Interval of energy ε	
		0—0.3	0.3—0.6
0—180°	Number of particles	201	499
	$\overline{\cos\vartheta}$	+0.07±0.05	+0.01±0.03
0—60°; 120—180°	Number of particles	141	337
	$\overline{\cos\vartheta}$	+0.13±0.07	+0.01±0.05

A χ^2 test of the result shows that the probability of positive asymmetry in the 0 to 0.3 energy region is close to 95%. The result obtained is considerably larger than the theoretical asymmetry.

The statistical accuracy of the measurements will have to be considerably improved, however, to provide a quantitative test of the theory at low energies.

Measurements similar to ours have recently been performed by Pershin and others using a propane bubble chamber. The results obtained by these workers are close to ours.[7]

The authors wish to thank A. I. Alikhanov for his interest and A. P. Birzgal for calculating the "smearing" of the theoretical spectra. The authors also wish to thank the scanning group for the scans of a large number of emulsions.

---

[1] A. O. Vaisenberg and V. A. Smirnitskii, J. Exptl. Theoret. Phys. (U.S.S.R.) **32**, 1340 (1957), Soviet Phys. JETP **5**, 1093 (1957).

[2] A. O. Vaisenberg and V. A. Smirnitskii, J. Exptl. Theoret. Phys. (U.S.S.R.) **33**, 621 (1957), Soviet Phys. JETP **6**, 477 (1958).

[3] Berley, Coffin, Garvin, Lederman, and Weinrich, Phys. Rev. **106**, 835 (1957).

[4] Mukhin, Ozerov, and Pontecorvo, Publ. No. 159, Joint Institute for Nuclear Research, 1958.

[5] I. I. Gurevich et al., J. Exptl. Theoret. Phys. (U.S.S.R.) **34**, 265 (1957), Soviet Phys. JETP **7**, 185 (1958).

[6] T. Kinoshita and A. Sirlin, Phys. Rev. **107**, 593 (1957).

[7] Barmin, Pershin, Kanavets, and Morozov, J. Exptl. Theoret. Phys. (U.S.S.R.) **35**, 542 (1958), Soviet Phys. JETP **8**, 374 (1959).

Translated by I. Emin
132

SOVIET PHYSICS JETP VOLUME 35(8), NUMBER 3 MARCH, 1959

FORMATION OF HYDROGEN MESIC MOLECULES

Ia. B. ZEL'DOVICH and S. S. GERSHTEIN

Institute for Physical Problems, Academy of Sciences, U.S.S.R.

Submitted to JETP editor June 19, 1958

J. Exptl. Theoret. Phys. (U.S.S.R.) **35**, 649-654 (September, 1958)

An effective mechanism is described for the formation of hydrogen mesic molecules. It consists of dipole transitions from S-wave repulsive states to the $K = 1$ rotational level with energy transfer to a conversion electron. The calculations give 1.5×10^6 sec^{-1} for the probability of formation of a mesic molecule $(pp)_\mu^+$ in liquid hydrogen. The process under consideration is relevant to the meson catalysis of the $p + d$ nuclear reaction as well as to the $\mu^- + p \rightarrow n + \nu$ process in liquid hydrogen.

THE formation of μ-mesic hydrogen molecules is of interest in the theory of μ-mesonic catalysis[1] of nuclear reactions for two reasons. First, the yield of the nuclear reaction depends on the probability of formation of mesic molecules since the mesic molecules are the initial stage for the nuclear reaction. Second, formation of the mesic molecule $(pp)_\mu^+$ (as well as the decay of the μ-meson) depletes the supply of μ mesons available for catalysing the nuclear reactions; this explains the dependence of the reaction yield on the concentration of deuterium. The formation of $(pp)_\mu^+$ is also of interest in the study of the elementary interaction $(pn\mu\nu)$, which is one of the more important problems in the theory of weak interactions. It has been shown[2] that the probability of formation of mesic molecules can be considerably increased by the resonance phenomena if the transition is from an initial state (in which the meson function is Σ_g and the nuclei are in a relative S state) to an excited vibrational level of the mesic molecule with $K = 0$ (a 0-0 transition). However, even in this case the probability of formation of mesic molecules during the μ-meson lifetime is not more than 30 to 40%.*

A rather effective mechanism, as was already noted,[4] for the formation of mesic molecules from various nuclei is provided by electric dipole transitions to the rotational $K = 1$ level accompanied by electron conversion.

The dipole moment of the mesic ion relative to its center of mass (this is necessary since the total charge is different from zero) is

$$\mathbf{d} = -\frac{e}{2}\left\{\frac{M_2 - M_1}{M_2 + M_1}\,\mathbf{R} + (\mathbf{r}_1 + \mathbf{r}_2)\right\}, \tag{1}$$

where $\mathbf{R} = \mathbf{R}_2 - \mathbf{R}_1$, $\mathbf{r}_1 = \mathbf{r} - \mathbf{R}_1$, $\mathbf{r}_2 = \mathbf{r} - \mathbf{R}_2$; $\mathbf{R}_1$, $\mathbf{R}_2$, $\mathbf{r}$ are the coordinates of the nuclei and the μ meson, M_2 and M_1 are the nuclear masses.

The computation of the probability of formation of mesic molecules with transfer of the binding energy to the electron of the hydrogen atom is analogous to the computation of the probability of internal conversion in nuclear transitions since the dimension of a mesic molecule is small compared to atomic dimensions. Taking the exact hydrogenic Coulomb functions for the electron wave function in the initial and final states (neglecting the fact that the mesic atom combines with a proton, which in turn is bound in a normal H_2 molecule) and integrating over the electron coordinates and the direction of electron emission, we obtain for the probability of formation of the mesic molecule

$$W = \frac{16}{3}(Na_e^3)\left(\frac{m_e}{m_\mu}\right)^5 \eta\zeta^2 \frac{e}{a_e\hbar} \sum_{M_K} \left| \int \Psi_{\mathrm{mol}}^{(f)*}\mathbf{d}\Psi_{\mathrm{mol}}^{(i)}\,(d\mathbf{R})\,(d\mathbf{r}) \right|^2, \tag{2}$$

where

$$\eta = \frac{e^2}{\hbar v_e}, \quad \zeta = \left[\frac{2\pi\eta}{(1 - e^{-2\pi\eta})(1 + \eta^2)}\right]^{1/2} \exp\{-2\eta \cot^{-1} \eta\},$$

$N = 4.2 \times 10^{22}$ is the number of nuclei in cm^3, a_e the Bohr radius, and v_e the electron velocity. The integral in (2) is written in mesic atom units ($e = 1$,

---

*We note that in reference 3 the probability for formation of mesic molecules in 0 – 0 transitions is overestimated by three orders of magnitude in comparison with reference 2. In calculating the Coulomb interaction (D.6) Jackson[3] stopped at the first term, independent of the mesic molecule coordinates, which would give a transition probability of exactly zero if the orthogonality of the initial and final state wave functions were taken into account. The calculation (D.6) in higher orders would give, as it should for a 0 – 0 transition, $\Sigma e_i r_i^2$.

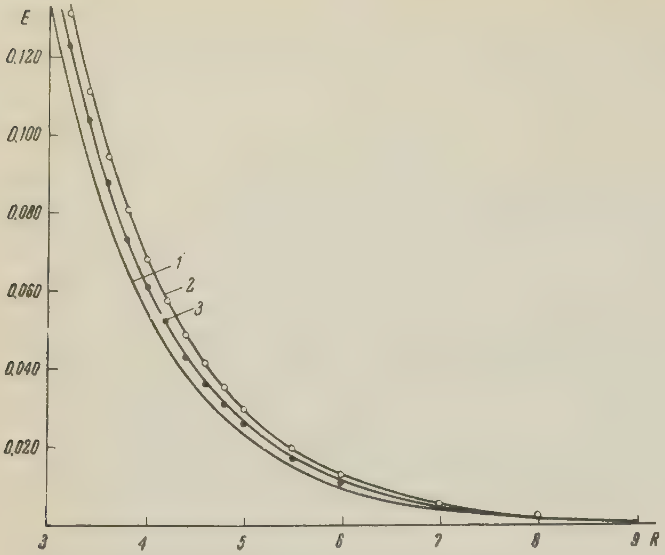

FIG. 1. The potential $E_u(R)$ in the repulsive Σ_u state (from reference 5) – curve 1. The effective potential in the Σ_u state including the corrections (computed in reference 6) due to nuclear motion, for protons – curve 2, for deuterons – curve 3. Values of the approximating exponential: ○ – $V_u = 1.850\ e^{1 \cdot 826 R}$ (for protons), ● – $V_u = 2.017\ e^{-0 \cdot 873 R}$ (for deuterons). (E and R in mesic atom units).

$\hbar = 1$, $m_\mu = 1$) assuming that $\Psi_{\text{mol}}^{(i)}$ is normalized to unit probability density in the incident wave. The summation in (2) is over all possible final states of the mesic molecule.

The first term in the expression (1) for the dipole moment (it is nonzero for different nuclei only, e.g., for the $(pd)_\mu^+$ mesic molecule) takes part only in transitions in which the parity of the meson function is unchanged ($\Sigma_g \to \Sigma_g$). The second term, whose role in conversion has not been considered previously,* is relevant for different [$(pd)_\mu^+$, $(dt)_\mu^+$, $(pt)_\mu^+$] as well as for identical nuclei [$(pp)_\mu^+$, $(dd)_\mu^+$, $(tt)_\mu^+$] and gives rise to transitions of the type $\Sigma_u \to \Sigma_g$.

An approximate analytic expression may be given for $\Psi_{\text{mol}}^{(i)}$ and $\Psi_{\text{mol}}^{(f)}$ in the case of identical nuclei.

The initial state wave function, corresponding to a dissociated mesic molecule, is of the form

$$\Psi_{\text{mol}}^{(i)} = \frac{f(R)}{R}\,\Sigma_u(R, r_1, r_2). \tag{3}$$

The relative motion of the nuclei is described by an S wave, since formation of mesic molecules takes place only after mesic atoms have been slowed down to thermal velocities. The function $f(R)$ is determined from the Schrödinger equation with a known repulsive potential $E_u(R)$. The numerical values of $E_u(R)$,[5] including corrections ΔE_u which take into account the motion of the nuclei accurate to terms of order $\sim m_\mu/M$,[6] may be approximated by an exponential in the region R of interest in this problem (see Fig. 1):

$$V_u = E_u(R) + \Delta E_u(R) \simeq B \exp(-\beta R). \tag{4}$$

The Schrödinger equation with the potential (4) may be transformed into the Bessel equation by a change of variable. The function $f(R)$ (including normalization) for the energy of relative motion tending to zero is of the form

$$f(R) = \frac{2}{\beta} K_0\left(\frac{2\sqrt{MB}}{\beta}\,e^{-\beta R/2}\right) \tag{5}$$

[$K_0(z)$ is the Bessel function of the third kind, M is the mass of one of the nuclei]. $f(R)$ falls off rapidly for small R, and for $R \geq 8$ it goes over into the wave function corresponding to free motion.

The mesic molecule final state wave function, corresponding to the rotational $K = 1$ level, has the form

$$\Psi_{\text{mol}}^{(f)} = \frac{g(R)}{R}\,Y_{1,M_K}(\theta, \varphi)\,\Sigma_g(R, r_1, r_2). \tag{6}$$

The numerical values of the attractive potential $E_g(R)$ (taken from reference 5) together with the corrections ΔE_g (calculated in reference 6) and the centrifugal potential are well approximated near the minimum R_e by the Morse function (Fig. 2)

$$V_g = E_g(R) + \Delta E_g(R) + \frac{2}{MR^2} \simeq D \times [e^{-2\alpha(R-R_e)} - 2e^{-\alpha(R-R_e)}]. \tag{7}$$

The solution of the Schrödinger equation for the potential (7) gives, in the case of the mesic molecule $(pp)_\mu^+$, only one $K = 1$ level with an energy $E \simeq -109$ ev. The corresponding wave function is

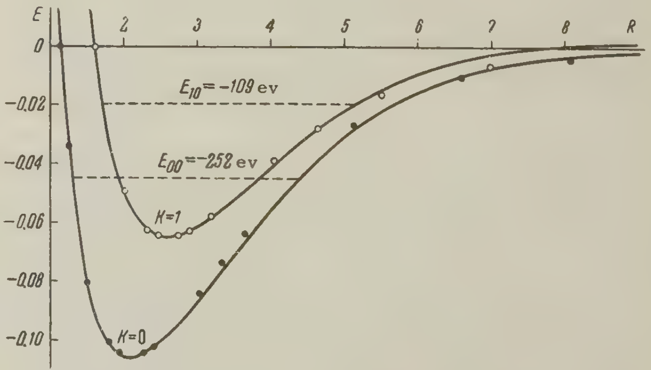

FIG. 2. Mesic molecule $(pp)_\mu$. Effective potentials in the Σ_g state for K = 0 and K = 1 including corrections due to nuclear motion.[6] Values of the approximating Morse function (7): ● – $R_e = 2.15$, $D = 0.1055$, $\alpha = 0.67$; ○ – $R_e = 2.62$, $D = 0.065$, $\alpha = 0.69$, (E and R in mesic atom units).

---

*It has been mentioned in radiative transitions.[2]

of the form

$$g(R) = [\alpha/\Gamma(2s)]^{1/2} e^{-\xi/2} \xi^{s}, \tag{8}$$

where

$$\xi = \frac{2\sqrt{MD}}{\alpha} e^{-\alpha(R-R_e)}; \quad s = \frac{\sqrt{-ME}}{\alpha}.$$

The deviations of the interaction potential from the Morse function (7) at large and small R do not substantially affect the magnitude of the energy level since in these regions of R the wave function is exponentially small.* The influence of these deviations on the form of the wave function at large R is also insignificant since for $R \gtrsim 5$, $e^{-\xi/2}$ is already $\simeq 1$, and the wave function corresponds to free motion: $g(R) \sim \exp\{-R\sqrt{-ME}\}$.

Since $f(R)$ falls off rapidly for small R only the region $R > 4$ is important in the integral (2). The following approximation is good enough for such R†

$$\Sigma_{g,u} = [2\pi(1 \pm S)]^{-1/2} (e^{-r_1} \pm e^{-r_2}), \tag{9}$$

where

$$S = \frac{1}{\pi} \int e^{-r_1} e^{-r_2} d\tau = \left(1 + R + \frac{R^2}{3}\right) e^{-R}.$$

Integration in (2) over the μ-meson coordinates then gives for the dipole moment matrix element

$$\langle d \rangle_{gu} = -(1 - S^2)^{-1/2} R/2 \simeq -R/2.$$

The integration in (2) over the angles of the mesic molecule and the summation over the orbital angular-momentum projections M_K is simple to carry out. The remaining integral over the radial functions is computed easily with the help of (3), (5), (6), and (8).‡ By multiplying (2) by $\frac{3}{4}$, which represents the probability that the spin wave function of the protons is in the state Σ_u, $K = 0$ ("ortho-mesic-hydrogen"), we finally obtain for the probability of formation of mesic molecules $(pp)_\mu^+$

$$W \approx 1.5 \cdot 10^6 \text{ sec}^{-1}$$

(i.e., three times the probability for the decay $\mu \to e + \nu + \tilde{\nu}$). Consequently the formation of $(pp)_\mu^+$ must be considered in the discussion of the dependence of the rate of the nuclear reaction $p + d \to He^3$ on the concentration of deuterium. The qualitative agreement with experiment obtained in reference 4 is, however, not upset since the cross section for μ-meson capture by deuterons[7] turns out to be larger than was assumed in reference 4.* The probability of formation of a deuterium mesic atom in natural hydrogen and in hydrogen containing 0.3% deuterium was found experimentally[1] to be 24 and 80% respectively (the calculation gives 44 and 94%). Apparently the probability of formation of $(pp)_\mu^+$ is even greater, or (and) the probability of the exchange $p_\mu + d \to d_\mu + p$ is less than our calculations indicate.

The probability of formation of the mesic molecule $(pd)_\mu^+$ will be substantially larger than the probability of formation of $(pp)_\mu^+$ due to transitions Σ_g, $K = 0 \to \Sigma_g$, $K = 1$, caused by the first term in the expression (1) for the dipole moment. Furthermore, the resonance[2] may play a significant role if the mesic molecule $(pd)_\mu^+$ has a vibrational level close to the energy of the $p + d_\mu$ system infinitely separated; it could lead to an increase in the amplitude of the wave function near the nuclei. (The resonance plays no role in the repulsive Σ_u state.)

It has been shown[8] that, given a quantity of deuterium sufficient for all mesons to form d_μ atoms, the number of nuclear reactions would be 0.36 ± 0.06 per meson. The measured rate equals $0.36 = W_1 W_2/(W_1 + W)(W_2 + W)$ where W_2 is the probability of formation of the molecule, W_1 the probability of a nuclear reaction in the molecule and W the probability of the decay of a μ-meson per second. On the other hand, the time dependence of the nuclear reaction measured in reference 8 was given by the difference of two exponentials $[\exp(-\lambda_2 t) - \exp(-\lambda_1 t)]$ where $\lambda_1 = W_1 + W$, $\lambda_2 = W_2 + W$. The experiment gives $0.19 \times 10^6 < \lambda_1 < 0.88 \times 10^6$; $0.55 \times 10^6 < \lambda_2 < 2 \times 10^7$. Only $W_2 > 1.4 \times 10^6$ and $0.24 \times 10^6 < W_1 < 0.43 \times 10^6$ are consistent with the observed reaction probability, which is in agreement with our calculations and other experiments. (The second solution $W_1 > 1.4 \times 10^6$ and $0.24 \times 10^6 < W_2 < 0.43 \times 10^6$ is unreasonable.)

The formation of mesic molecules changes the conclusions drawn in reference 9 on total polarization of neutrons formed in the process $\mu + p \to n + \nu$, since in liquid hydrogen this process proceeds to a large extent from the mesic molecule state. In the mesic molecule $(pp)_\mu^+$ the $K = 1$

---

*The level shift caused by these deviations may be calculated numerically using perturbation theory: $\Delta E = \int g^2(R) (V_g - V_{Morse}) dR$.

†We recall that mesic atom units are being used.

‡We note that the integrand $f(R)\, Rg(R)$ has, in the case of $(pp)^+\mu$, a maximum at $R \approx 8.5$; a comparatively good result is thus obtained by replacing $f(R)$ and $g(R)$ by their asymptotic expressions for large R, and the integration can then be carried out analytically.

*In the final result in reference 7 there is a misprint; the actual capture cross section is $\sigma \approx 6\pi a_\mu^2 k_0/k_1$.

state is possible only for a parallel spin orientation $I = 1$ for the two protons ("ortho-mesic-hydrogen"). Owing to fast transitions to the lowest hyperfine-structure state[9] the initial state of the mesic atom is $F = 0$ and the mesic molecules $(pp)^+_\mu$ are formed in the $K = 1$ state with a total spin $J = 1/2$, so that the μ-meson spin is antiparallel to both protons. Although the transition probability from the metastable "ortho-mesic-hydrogen" state into "para-mesic-hydrogen" is small, already in the state with parallel spin protons $I = 1$ and antiparallel μ-meson spin $(J = 1/2)$ we get the product $\mathbf{i}_1 \cdot \mathbf{s} + \mathbf{i}_2 \cdot \mathbf{s} = -1$ ($\mathbf{i}_1$, $\mathbf{i}_2$, $\mathbf{s}$ are the protons and μ-meson spins respectively), while in the mesic atom we get $\mathbf{i}_1 \cdot \mathbf{s} = -3/4$ for $F = 0$ and $\mathbf{i}_1 \cdot \mathbf{s} = 1/4$ for $F = 1$. Thus the mesic molecule in the ortho-state with spin $J = 1/2$ is equivalent to a mixture of atoms consisting of 75% $(F = 0)$ and 25% $(F = 1)$. In spite of this, owing to the interaction between the rotation of the molecule and the spins, the $K = 1$, $J = 1/2$ state is partially transformed into the $K = 1$, $J = 3/2$ state (corresponding to a pure $F = 1$ state). The process $\mu^- + p \rightarrow n + \nu$ in the $F = 0$ state without admixtures of $F = 1$ can be observed at hydrogen densities 20 or more times smaller than the density of liquid hydrogen.* At that the transition probability in $F = 0$ state remains sufficiently large $(10^9\ \text{sec}^{-1})$ and the probability of formation of mesic molecules during the meson lifetime will be 15% or less. The influence of the relative proton — μ-meson spin orientation on the process $\mu + p \rightarrow n + \nu$ will be discussed in a subsequent note.

---

*Gaseous hydrogen of that density has a pressure of 40 atmos at room temperature.

---

[1] Alvarez, Bradner, Crawford, et al., Phys. Rev. **105**, 1127 (1957).

[2] Ia. B. Zel'dovich, Dokl. Akad. Nauk S.S.S.R. **95**, 493 (1954).

[3] J. D. Jackson, Phys. Rev. **106**, 330 (1957).

[4] Ia. B. Zel'dovich and A. D. Sakharov, J. Exptl. Theoret. Phys. (U.S.S.R.) **32**, 947 (1957), Soviet Phys. JETP **5**, 775 (1957).

[5] P. R. Bates, et al., Phil. Trans. Roy. Soc. **A246**, 215 (1956).

[6] A. Dalgarno and R. McCarroll, Proc. Roy. Soc. **237**, 383 (1956).

[7] S. S. Gershtein, Dokl. Akad. Nauk S.S.S.R. **117**, 956 (1957), Soviet Phys. "Doklady" **2**, 559 (1957).

[8] Ashmore, Nordhagen, Strauch, and Townes, Proc. Phys. Soc. **71**, 161 (1958).

[9] S. S. Gershtein, J. Exptl. Theoret. Phys. (U.S.S.R.) **34**, 463 (1958), Soviet Phys. JETP **7**, 318 (1958).

Translated by A. Bincer
133

SOVIET PHYSICS JETP VOLUME 35(8), NUMBER 3 MARCH, 1959

INTERACTION BETWEEN A CHARGED CURRENT-CONDUCTING JET MOVING IN A CIRCLE AND A FERRITE

A. N. DIDENKO

Moscow State University

Submitted to JETP editor January 18, 1958; resubmitted May 22, 1958

J. Exptl. Theoret. Phys. (U.S.S.R.) 35, 655-661 (September, 1958)

The radiation spectrum of a current-conducting jet which moves in a circle in a homogeneous space is considered. Asymptotic expressions for Bessel and Neumann functions, which yield good approximations even at relatively low values of the indices and arguments, are used to study the radiation spectrum and the transverse forces exerted by the ferrite in cases of non-uniform media.

1. INTRODUCTION. METHOD OF CALCULATION

THE interaction between current-conducting jets, moving with high velocities, and a ferrite was first considered by Morozov.[1] The ramifications of this problem were noted by this author: in studying earlier cases of practical importance the interaction could be analyzed in a quasi-stationary approximation. It now becomes apparent, however, that there are a number of physical problems in which one deals with objects which are not true currents or charges, and which move as a unit with velocities greater than the phase velocity of light in many materials (high-current accelerators, new methods of generating radio waves). In reference 1 the analysis was made assuming rectilinear motion of the jet. In this case the "trajectories" are planes parallel to one of the Cartesian coordinate planes. The entire space was assumed to be made up of layers characterized by different values of ϵ and μ, all parallel to the same coordinate plane.

However, great interest attaches to the case in which the jet moves in a circle. In this case the "trajectories" are cylindrical surfaces and the space is divided into cylindrical layers characterized by different values of ϵ and μ, which are coaxial with the trajectory cylinders (this situation is considered in greater detail in Sec. 3). An investigation of this configuration is of interest in its own right from the point of view of general radiation theory because at certain critical velocities the total radiation loss is determined by the Cerenkov effect as well as the finite radius of curvature of the trajectory.

In the present paper we consider several cases in which a charged current-conducting jet moving in a circle interacts with a ferrite medium or media. We assume that the different parts of space are media characterized by different ϵ and μ. We assume that a charged current-conducting jet moves in the aximuthal direction in a circle of radius a with a velocity $\mathbf{v}(0, v, V_z)$ in one of these media; it is also assumed that the jet is infinitesimally thin and unbounded in the z direction and that it traces out a cylinder of radius a in its motion (cf. Fig. 1). We denote the strength of the current which flows in the jet by I_0; the linear charge density is denoted by ρ. The current components are given by the following expressions:

$$\begin{gathered} j_r = 0;\ \ j_\varphi = \rho v \frac{\delta(r-a)}{r}\,\delta(\varphi-\omega_0 t); \\ j_z = I\,\frac{\delta(r-a)}{r}\,\delta(\varphi-\omega_0 t)\ \ \left(\omega_0 = \frac{v}{a}\right). \end{gathered} \tag{1}$$

It can be shown that the electromagnetic field described by Maxwell equations can be broken up into two independent fields: one of these is determined by the total current $I = I_0 + \rho V_z$ and the other by the charge ρ. As in reference 1, we call the first the I-field and the second the ρ-field.

Substituting Eq. (1) in Maxwell equations and solving the system of homogeneous equations with appropriate boundary conditions (cf., e.g., reference 2) we find the field components and the forces which act on the jet in several particular cases.

In order to obtain definite results we assume that $\epsilon(\omega)$ and $\mu(\omega)$ are real in all media; this assumption is not entirely justified since it is necessary to take account of absorption in considering dispersive media.

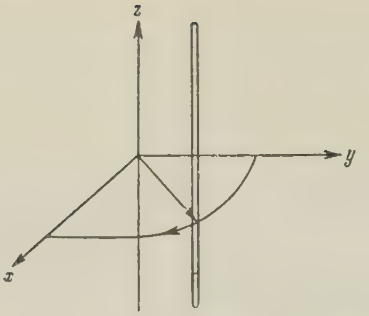

FIG. 1

2. MOTION IN HOMOGENEOUS SPACE

We first consider the motion of a charged current filament (infinite along the z axis) in a medium characterized by ϵ and μ which fills the entire space (Fig. 1). Carrying out the calculation in accordance with the scheme given above, we find the field components and the radiation losses for the I-field and the ρ-field; the latter is taken as the scalar product of the force which acts on the jet and its velocity, with sign reversed:[3]

$$W = -\mathbf{v}\cdot\mathbf{F} = W^I + W^\rho = \sum_{n=1}^{\infty} W_n^I + \sum_{n=1}^{\infty} W_n^\rho,$$

where

$$W_n^\rho = (2\pi\mu k\rho^2 v^2 / c)\, J_n'^2 (\sqrt{\varepsilon\mu}\, ka), \tag{2}$$

$$W_n^I = (2\pi\mu k I^2 / c)\, J_n^2 (\sqrt{\varepsilon\mu}\, ka). \tag{3}$$

It is easy to show that $-\mathbf{v}\cdot\mathbf{F} = \partial U/\partial t$ where $\partial U/\partial t$ is the energy flux computed from the Poynting theorem. A discussion of this result, which is not completely obvious for the jet case, is given in reference 1.

We now consider the motion of the jet in empty space ($\epsilon = \mu = 1$). In the nonrelativistic case it is easily shown that the maximum radiation of the I-field and the ρ-field occurs at the first harmonic (dipole radiation). In the relativistic case, which is of greatest interest, W_n^ρ and W_n^I are expressed in terms of Bessel functions $J_n(x)$ and their derivatives for which $n \sim x$ $(n-x)/n = \xi$; $\xi \ll 1$). Thus, to study the radiation spectra we introduce the asymptotic expansion for $J_n(x)$ and $J'(x)$; these can give good approximations even at small values of the indices and arguments ($n \sim x$). Without considering this procedure in detail, we may note that the method given in reference 4 gives a comparatively simple way of finding the following asymptotic expressions:

$$J_n(x) = \frac{1}{\pi}\sqrt{\frac{2\xi}{3}}\, K_{1/3}\left[\frac{n}{3}(2\xi)^{3/2}\right] e^{-\sigma},$$

$$J_n'(x) = \frac{2\xi}{\pi\sqrt{3}}\, K_{2/3}\left[\frac{n}{3}(2\xi)^{3/2}\right] e^{-\sigma}, \tag{4}$$

$$\xi = \frac{n-x}{n} \ll 1; \quad \sigma = \frac{B_1}{2n} - \frac{B_2}{12n^3} + \ldots;$$

where K is the MacDonald function and B_i is the Bernuolli number (cf. reference 5). The asymptotic expressions for the Neumann functions are given in this same paper; these forms will be required for analysis of other particular cases and are better than the asymptotic expressions given by Fock.[6]

Substituting the expressions for $J_n(x)$ and $J'_n(x)$ from Eq. (4) in Eqs. (2) and (3) we obtain the following expressions for the radiation of the I-field and the ρ-field:

$$W^\rho = \sum_{n=1}^{\infty} \frac{2}{3\pi}\frac{\rho^2 n\beta^3 c}{a}\left(\frac{mc^2}{E}\right)^4 K_{2/3}^2\left[\frac{n}{3}\left(\frac{mc^2}{E}\right)^3\right] e^{-2\sigma}, \tag{5}$$

$$W^I = \sum_{n=1}^{\infty} \frac{2}{3\pi}\frac{I^2 n\beta}{ac}\left(\frac{mc^2}{E}\right)^2 K_{1/3}^2\left[\frac{n}{3}\left(\frac{mc^2}{E}\right)^3\right] e^{-2\sigma}. \tag{6}$$

It is apparent from Eqs. (5) and (6) that in the relativistic case there is a difference in the spectral energy distribution for the I-field and the ρ-field. From Eq. (5) it follows that the radiation intensity of the n-th harmonic of the ρ-field is inversely proportional to $n^{1/3}$ when $n \ll 3(E/mc^2)^3$ and falls off exponentially when $n \gg 3(E/mc^2)^3$, i.e., the strongest radiation in the relativistic case is at the first harmonic. We may note that in the relativistic case the total radiation intensity of the ρ-field is independent of the energy of the jet. On the other hand, the radiation intensity of the I-field, as is apparent from Eq. (6), is directly proportional to $n^{1/3}$ when $n \ll 3(E/mc^2)^3$, is a maximum when $n = 3(E/mc^2)^3$ and falls off exponentially when $n \gg 3(E/mc^2)^3$. For the high harmonics $n \gg 1$ (in the present case these harmonics make the main contribution to the total radiation energy) and we may assume that the radiation frequency ω is continuous. Thus, the summation over n is replaced by integration; using the value of the integral computed by Klepikov:

$$\int_0^\infty K_\nu(x) K_\rho(x)\, x^{\mu-1} dx = \frac{2^{\mu-3}}{\Gamma(\mu)}\Gamma\left(\frac{\mu+\nu+\rho}{2}\right)\Gamma\left(\frac{\mu-\nu+\rho}{2}\right) \tag{7}$$

$$\times\Gamma\left(\frac{\mu+\nu-\rho}{2}\right)\Gamma\left(\frac{\mu-\nu-\rho}{2}\right) \quad (\operatorname{Re}\mu > |\operatorname{Re}(\nu\pm\rho)|),$$

we find the total radiation intensity per unit length of a jet characterized by a current I :

$$W^I = (2/\sqrt{3})\,(I^2\beta/ac)\,(E/mc^2)^4. \qquad (8)$$

It follows from Eq. (8) that the radiation of the I-field of a jet and the radiation of a relativistic electron which moves in a circle are strong functions of energy. Apparently, this is explained by the different directivity of the radiation of the I-field and the ρ-field. A similar result has been obtained by Morozov[1] for a current filament which oscillates in a direction perpendicular to its length.

3. INHOMOGENEOUS SPACES

We now consider the case in which the space is filled with different media. As has already been noted, the portions of space filled by media with ϵ and μ form coaxial cylindrical surfaces of different radii (cf. Fig. 2). In one of the media a charged current-conducting jet, infinite along the z axis, describes a circle of radius a and traces out a coaxial cylinder of radius a in its motion. As before we denote the total current of the jet by I and the linear density by ρ.

We consider three cases below:

(1) a jet which moves in a circle of radius a inside a cylinder of radius a_1 ($a < a_1$) characterized by ϵ_1 and μ_1, surrounded by a medium described by ϵ_2 and μ_2 (Fig. 2, I);

(2) a jet which moves in a circle of radius a in a medium described by ϵ_2 and μ_2 around a ferrite cylinder of radius a_1 characterized by ϵ_1 and μ_1 ($a_1 < a$) (Fig. 2, II);

(3) a jet which moves in a circle of radius a inside a curved channel in a medium characterized by ϵ_2 and μ_2, formed by cylindrical surfaces of radii a_1 and a_2 ($a_1 < a < a_2$); the channel is surrounded by media described by $\epsilon_{1,3}$ and $\mu_{1,3}$ (Fig. 2, III).

If we neglect absorption the radiation intensity of the ρ-field is given by the following:

$$W_i^\rho = \sum_{n=1}^{\infty} W_n^\rho\, \varphi_{n,i}^\rho \quad (i = 1, 2, 3),$$

$$\varphi_{n,1}^\rho = \frac{\chi}{\alpha_1^2 + \beta_1^2}\,\frac{4}{\pi^2 k_1 k_2 a_1^2};$$

$$\varphi_{n,2}^\rho = \frac{1}{J_n'^2(k_s a)}\,\frac{[\alpha_1 N_n'(k_s a) - \beta_1 J_n'(k_s a)]^2}{\alpha_1^2 + \beta_1^2};$$

$$\varphi_{n,3}^\rho = \frac{1}{J_n'^2(k_s a)}\,\frac{4\chi}{\pi^2 k_1 k_2 a_2^2}\,\frac{[\alpha_1 N_n'(k_s a) - \beta_1 J_n'(k_s a)]^2}{A^2 + B^2};$$

$$\alpha_1 = J_n(k_1 a_1)\, J_n'(k_2 a_1) - \chi J_n(k_2 a_1)\, J_n'(k_1 a_1);$$

$$\beta_1 = J_n(k_1 a_1)\, N_n'(k_2 a_1) - \chi N_n(k_2 a_1)\, J_n'(k_1 a_1);$$

$$\gamma_1 = N_n(k_1 a_1)\, J_n'(k_2 a_1) - \chi J_n(k_2 a_1)\, N_n'(k_1 a_1); \qquad (9)$$

$$\delta_1 = N_n(k_1 a_1)\, N_n'(k_2 a_1) - \chi N_n(k_2 a_1)\, N_n'(k_1 a_1);$$

$$\chi = \sqrt{\varepsilon_2\mu_1/\varepsilon_1\mu_2}; \quad k_{1,2} = \sqrt{\varepsilon_{1,2}\mu_{1,2}}\,k; \quad k_s = \sqrt{\varepsilon_s\mu_s}\,k;$$

$$A = \alpha_1\beta_2 - \beta_1\alpha_2; \quad B = \alpha_1\delta_2 - \beta_1\gamma_2;$$

α_2, β_2, γ_2 and δ_2 are obtained by substituting $k_1 \to k_3$; $a_1 \to a_2$ in the expressions for α_1, β_1, γ_1 and S_1; the subscript "s" on ϵ, μ, and k indicate values for the media in which the jet moves; the subscript "i" refers to the particular case considered in this section.

In a similar way we obtain expressions for the radial forces exerted on the jet by the ρ-fields (below we call these transverse forces):

$$F_{r,i}^\rho = \sum_{n=1}^{\infty} F_{r,n}^\rho f_{n,i}^\rho \quad (i = 1, 2, 3), \qquad (10)$$

where

$$F_{r,n}^\rho = \frac{2\pi\mu_s k_s \rho^2 v^2}{c^2}\left(1 - \frac{1}{\varepsilon_s\mu_s\beta^2}\right) J_n(k_s a)\, N_n'(k_s a);$$

$$f_{n,1}^\rho = -\frac{J_n'(k_s a)}{N_n'(k_s a)}\,\frac{\alpha_1\gamma_1 + \beta_1\delta_1}{\alpha_1^2 + \beta_1^2};$$

$$f_{n,2}^\rho = -\left\{\frac{[\alpha_1 N_n(k_s a) - \beta_1 J_n(k_s a)]\,[\alpha_1 J_n'(k_s a) + \beta_1 N_n'(k_s a)]}{J_n(k_s a)\, N_n'(k_s a)\,(\alpha_1^2 + \beta_1^2)} + 1\right\};$$

$$f_{n,3}^\rho = -\left\{\frac{[\alpha_1 N_n(k_s a) - \beta_1 J_n(k_s a)]}{J_n(k_s a)\, N_n'(k_s a)\,(A^2 + B^2)} \times [A(\beta_2 J_n'(k_s a) - \alpha_2 N_n'(k_s a)) + B(\delta_2 J_n'(k_s a) - \gamma_2 N_n'(k_s a))] + 1\right\}.$$

The expressions for the radiation intensities and transverse forces of the I-field can be obtained from Eqs. (9) and (10) if the following substitutions are made:

$$\rho v \to I; \quad (1 - 1/\varepsilon_s\mu_s\beta^2) \to 1,$$

$$J_n(x) \to J_n'(x); \quad N_n(x) \to N_n'(x).$$

We may note that these formulas apply at any velocity. It is easy to show that when $v \to 0$, $W_i^{\rho I} \to 0$ while $F_{ri}^{\rho I}$ becomes the expression which describes the interaction between a charged filament or a conductor and a ferrite, which is well known in electrostatics and magnetostatics. Thus, in case II (Fig. 2, II) when $v \to 0$, we obtain from Eq. (9) the force on a unit length of the charged filament in a medium characterized by ϵ_2 exerted by a dielectric cylinder characterized by ϵ_1:

$$F_{r,2}^\rho = 2\rho^2(\varepsilon_2 - \varepsilon_1)\, a_1^2/\varepsilon_2(\varepsilon_1 + \varepsilon_2)\, a\,(a^2 - a_1^2), \qquad (11)$$

from Eq. (10) we find the force which exerted on a conductor in a medium characterized by μ_2 by a

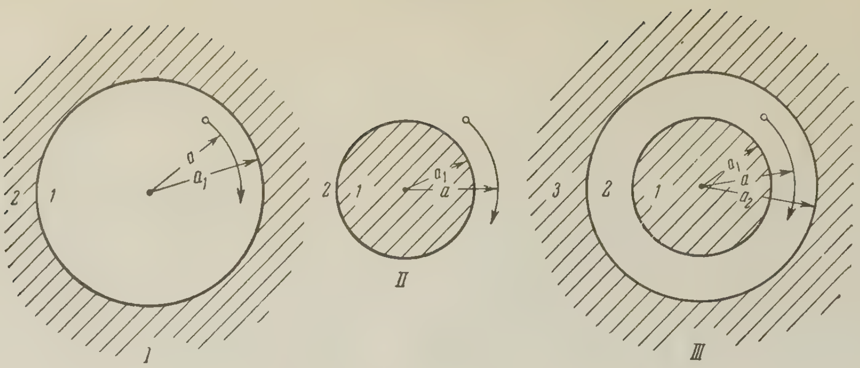

FIG. 2

cylinder characterized by a magnetic permeability μ_1:

$$F^{I}_{r,2} = 2I^2(\mu_1 - \mu_2)a_1^2/\mu_2 c^2(\mu_1 + \mu_2)a(a^2 - a_1^2) \quad (12)$$

(cf. for example, reference 8).

More interesting results are obtained for jets which move with relativistic velocities.

We consider jets which move in empty space $\epsilon_s = \mu_s = 1$) close to dense ferrite media (cases I and II), or inside a circular channel which is narrow compared with the radius of curvature, (case III) with velocities close to the velocity of light in vacuo $\{|(a_{1,2} - a)/a| = \Delta a/a;\ (\Delta a/a)^2 << 1\}$. The radiation intensity and the transverse currents are given by Bessel functions $J_n(x)$ and Neumann functions $N_n(x)$ and their derivatives for which the indices and arguments are approximately the same ($x \sim n$) or for which the arguments are considerably greater than the indices. The asymptotic formulas, which yield good approximations for these values of the indices and arguments, can be used to investigate the basic features of these cases (the asymptotic formulas for $J_n(x)$ and $N_n(x)$ when $x \sim n$ are given in references 5 and 6). We consider certain of these cases.

(a) If the jet moves in the azimuthal direction inside an empty circular channel which is narrow compared with the radius of curvature (cf. Fig. 2, III) and if $\epsilon_1 = \epsilon_3 = \epsilon$; $\mu_1 = \mu_3 = \mu$,

$$\varphi^{\rho}_{n,3} = \frac{J_n'^2(\sqrt{\varepsilon\mu}\,ka_1)}{J_n'^2(ka)}\frac{a_1\mu}{a_2}, \quad \text{if } \left(\frac{\lambda}{2\Delta a}\right) \gg \sqrt{\frac{2\Delta a}{a}}\left[\frac{\Gamma(^2/_3)}{\Gamma(^4/_3)}\right]^{3/2}, \quad (13)$$

$$\varphi^{\rho}_{n,3} = \frac{2a}{a_2}\left\{\left(\varkappa + \frac{1}{\varkappa}\right) - \left(\varkappa - \frac{1}{\varkappa}\right)\sin\left[\frac{2n}{3}\left(\frac{2\Delta a}{a}\right)^{3/2}\right]\right\}^{-1}, \quad \text{if } \left(\frac{\lambda}{2\Delta a}\right) \ll \frac{4\Delta a}{a}, \quad (14)$$

where we have introduced the notation $\kappa = \sqrt{2\epsilon\Delta a/a\mu}$ and λ is the wave length associated with the radiation of the jet.

Whence it follows that if the conditions in (13) are fulfilled, the expression for $W^{\rho}_{n,3}$ coincides with the expression for the radiation intensity of the n-th harmonic of the ρ-field of a jet which moves in a homogeneous space filled by a medium which surrounds the channel. The condition in (13) is analogous to the Ginzburg-Frank inequality[9] for a jet that moves in vacuum inside a circular region of space which is surrounded by a ferrite. It is easy to show that when (14) is satisfied the energy spectrum (maxima and minima on the curve which characterizes the spectral distribution of radiation losses) is such that the total intensity of the radiation beyond a point which corresponds to the frequency interval $\Delta\omega = (3\pi v/a)(a/2\Delta a)^{3/2}$ is equal to the radiation intensity of a charged jet that moves in vacuum [cf. Eq. (5)].

(b) In this case the transverse forces for the harmonics of the ρ-field which satisfy the condition in (14) are written in the following form:

$$F^{\rho}_{r,n,3} = \frac{2\pi k\rho^2(1 - \beta^2)J_n(ka)J_n'(ka)(\varkappa - 1/\varkappa)\cos[(2n/3)(2\Delta a/a)^{3/2}]}{(\varkappa + 1/\varkappa) - (\varkappa - 1/\varkappa)\ \sin[(2n/3)(2\Delta a/a)^{3/2}]}. \quad (15)$$

It is apparent from (15) that the transverse force of the ρ-field depends on the parameter κ. If $\kappa > 1$, the harmonics of the field for which $n < n_{cr}$ (critical harmonics are those which satisfy the condition: $^2/_3\, n_{cr}\ (2\Delta a/a)^{3/2} = 2m \pm 1/2)\pi$, $m = 0, 1, 2, \ldots\ldots$ weaken the attractive force between the jet and the inner cylinder whereas the harmonics of the field for which $n > n_{cr}$ intensify this force. On the other hand, if $\kappa < 1$, the harmonics for which $n > n_{cr}$ weaken the attractive force whereas the harmonics below the critical harmonic intensify it.

(c) The functions $\phi^{I}_{n,3}$ and $F^{I}_{r,n,3}$ which characterize the I-field are obtained from Eqs. (13), (14) and (15) by means of the following substitutions: $\rho v \rightarrow I$, $\kappa \rightarrow \sqrt{2\mu\Delta a/a\epsilon}$, $(1-\beta^2) \rightarrow -1$; thus, for the I-field the parameter which characterizes the maxima and minima on the spectral intensity curve and determines transverse forces is the quantity $\sqrt{2\mu\Delta a/a\epsilon}$.

(d) A comparison of cases I and III shows that there is no difference when (14) is satisfied.

---

[1] A. I. Morozov, Вестник МГУ (Bulletin, Moscow State Univ.) No. 1, 72 (1957) ; Dissertation, Moscow State Univ. 1957.

[2] M. I. Kaganov, Тр. физич. отделения физ.-мат. ф-та ХГУ (Trans. Phys., Div., Phys.-Math. Faculties, Khar'kov State Univ.) 4, 67 (1953).

[3] N. Bohr, The Passage of Atomic Particles Through Matter (Russ. Transl.) IIL, M. 1950.

[4] Ivanenko and Sokolov, Классическая теория поля (Classical Theory of Fields) GITTL, M.-L. 1951; A. A. Sokolov, Вестник МГУ (Bulletin, Moscow State Univ.) No. 4, 77 (1947).

[5] A. N. Didenko, Радиотехника и электроника (Radio Engineering and Electronics) (in press).

[6] V. A. Fock, Dokl. Akad. Nauk SSSR, 1, 97 (1934).

[7] N. P. Klepikov, Dissertation, Moscow State Univ. 1953.

[8] Landau and Lifshitz, Электродинамика сплошных сред (Electrodynamics of Continuous Media) GITTL, M. 1957.

[9] V. L. Ginzburg and I. M. Frank, Dokl. Akad. Nauk SSSR 56, 699 (1947).

Translated by H. Lashinsky
134

SOVIET PHYSICS JETP VOLUME 35(8), NUMBER 3 MARCH, 1959

ELASTIC SCATTERING OF PHOTONS ON EXCITED NUCLEONS

N. F. NELIPA

P. N. Lebedev Physics Institute, Academy of Sciences, U.S.S.R.

Submitted to JETP editor February 24, 1958

J. Exptl. Theoret. Phys. (U.S.S.R.) **35**, 662-667 (September, 1958)

The cross section for elastic scattering of γ quanta is computed with allowance for the excited nucleon states as described by the Markov model. The calculated cross sections are found to agree satisfactorily with the available experimental data.

1. It is well known that the cross sections of many processes (scattering and photoproduction of π-mesons etc.) have been found to show only one or a few maxima. To explain the first of these maxima, Tamm has developed a semiphenomenolgical theory involving a nucleon isobar state. In terms of this theory he analyzed π-meson[1] and γ-ray[2] scattering and the photoproduction of π mesons[3] on nucleons. He obtained a qualitative agreement with the experimental data.

Markov has given another explanation of the observed maxima of the cross sections.[4] It, too, is founded on the picture of an excited nucleon state which is identified to be a hyperon instead of an isobaric state. We have shown earlier[5] that there exist two distinct classes of excited nucleon states in Markov's model. If these excited states are identified with the hyperons, then accounting for the latter in the intermediate states leads indeed to resonance effects. In reference 5 this was illustrated with the example of π^- scattering on protons. However, in that paper a number of essential assumptions were made. They were: applicability of perturbation theory, pseudoscalar meson-nucleon interaction, and identical form of the interaction of the meson both with the nucleon and the excited state of the nucleon. This example can therefore be considered only as illustration. In this connection it is of interest to investigate the elastic scattering of photons on excited nucleons in terms of the Markov model, since the above questions can be unequivocally answered in this case. Such an investigation is furthermore of interest because some experimental data have recently been obtained on that process.

A more consequent treatment of the process should be made in terms of damping theory, since the cross section at the resonance energy is generally infinite. However, in a preliminary calculation of the differential cross section at energies differing from the resonance energy, we can limit ourselves to a perturbation-calculation treatment. We can also disregard for the time being effects due to the meson cloud around the nucleon. These simplifications are taken into account in the treatment of the problem in the present paper. Furthermore, we assume that the first excited state of the nucleon is the Λ^0-particle, and we take the excitation energy to be 140 Mev (the excitation energy in this case can lie anywhere between 140 and 180 Mev). Then the obtained cross sections are close to the experimentally-observed values.

2. In the lowest nonvanishing order of perturbation theory the process

$$\gamma + P \rightarrow \gamma' + P' \tag{I}$$

is described by the diagrams of Fig. 1. The lower diagrams correspond to the case where the intermediate state consists of the excited nucleon state. We shall perform the calculation in the laboratory system.

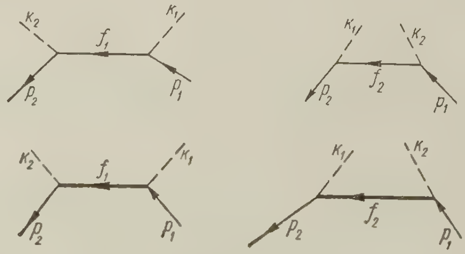

FIG. 1

The matrix elements corresponding to the lower diagrams are given (the notation is that employed by Akhiezer and Berestetskii[6]) by

$$S_{nn'} = -\frac{ie^2}{2\sqrt{\omega_0\omega}} J_{nn'}\overline{u_2}\left\{\hat{e}_2\frac{i\hat{f}_1 - M}{f_1^2 + M^2}\hat{e}_1\right\}u_1,$$
$$S'_{nn'} = -\frac{ie^2}{2\sqrt{\omega_0\omega}} J'_{nn'}\overline{u_2}\left\{\hat{e}_1\frac{i\hat{f}_2 - M}{\hat{f}_2^2 + M^2}\hat{e}_2\right\}u_1, \tag{1}$$

where $f_1 = p_1 + k_1 = p_2 + k_2$; $f_2 = p_1 - k_2 = p_2 - k_1$;

ω_0, e_1 and ω, e_2 are the energy and polarization vectors of the incoming and outgoing photon respectively; $M = m + a(n_1 + n_2 + n_3 + n_0)$ is the mass of the excited nucleon state; a is the excitation energy; n_1, n_2, n_3, n_0 are numbers that characterize the excitation of the nucleon; $J_{nn'} = (I_{nn''}I_{n''n'})_1 + (I_{nn''}I_{n''n'})_2 + (I_{nn''}I_{n''n'})_3 + \ldots$,

$$I_{nn'} = N \int H_{n_1}(\xi_1) \ldots H_{n_0'}(\xi_0)$$
$$\times \exp\left\{-\xi_\nu^2 - \frac{1}{m^2}(p_\nu \xi_\nu)^2 - \frac{1}{M^2}(f_\nu \xi_\nu)^2 - ik_\nu \xi_\nu r_0\right\} d^4\xi,$$

k is the energy-momentum vector of the photon; $I_{nn''}$ corresponds to the transition from the initial to the intermediate state, and $I_{n''n'}$ to the transition from the intermediate to the final state. The subscripts 1, 2 . . . refer to the different diagrams of a given excited state* (which, in general, is degenerate).

We have assumed that the photons interact with the excited state in the same way as with the usual nucleons.[7]

The two upper diagrams correspond to the following transition-matrix elements:

$$S_{00} = \frac{-ie^2 J_{00}}{2\sqrt{\omega_0\omega}} \bar{u}_2 \left\{\hat{e}_2 \frac{i\hat{f}_1 - m}{f_1^2 + m^2} \hat{e}_1\right\} u_1,$$
$$S_{00}' = \frac{-ie^2 J_{00}'}{2\sqrt{\omega_0\omega}} \bar{u}_2 \left\{\hat{e}_1 \frac{i\hat{f}_2 - m}{f_2^2 + m^2} \hat{e}_2\right\} u_1, \tag{1'}$$

where m is the mass of the nonexcited nucleon, while J_{00} and J_{00}' are the respective integrals over the variables of the intermediate state.

3. To calculate $J_{nn'}$ which enters the expression for the cross section, we must know $I_{nn'}$. In reference 5 we have obtained an expression for $I_{nn'}$ for the case where either the initial or final nucleon momentum vanishes. For our present purposes we must know $I_{nn'}$ also for the case when both these momenta differ from zero (this need arises in the diagrams where a photon is emitted first and absorbed afterwards).

By the same method as used in reference 5 we obtain for an arbitrary coordinate system

$$N \exp\{-t_1^2 + \ldots + t_0^2 - t_1'^2 + \ldots + t_0'^2\}$$
$$\times \int_{-\infty}^{+\infty} \exp\{-\xi_\nu\xi_\nu - (p_\nu'\xi_\nu)^2 - (f_\nu'\xi_\nu)^2 + K_\nu\xi_\nu\} d^4\xi \tag{2}$$
$$= N \sum_{n_1=0}^{\infty} \cdots \sum_{n_0'=0}^{\infty} I_{nn'} \frac{1}{n_1!} \cdots \frac{1}{n_0'!} t_1^{n_1} \ldots t_0^{n_0'},$$

where $p_\nu' = p_\nu/m$, $f_\nu' = f_\nu/M$, $K_\nu = 2(t_\nu + t_\nu') - ik_\nu r_0$.

Expressing the quadratic form in the exponent as a sum of squares, we obtain the left hand side of (2) in the form

$$N \frac{\pi^2}{\sqrt{-\Delta_4}} \exp\left[\frac{1}{2}(K_\nu a_\nu) - t_\nu^2 - t_\nu'^2\right], \tag{2'}$$

where

$$K_\nu a_\nu = \frac{1}{2}K^2 - (p_\nu K_\nu)(f_\nu K_\nu)/(p_\nu f_\nu)^2,$$
$$\Delta = -(p_\nu f_\nu)^2/m^2M^2.$$

Thus we have according to (2)

$$I_{nn'} = N \frac{\pi^2}{\sqrt{-\Delta_4}} \left\{\frac{\partial^{n_1+\ldots+n_0'}}{\partial t_1^{n_1} \ldots \partial t_0^{n_0'}} \times \exp\left[\frac{1}{2}(K_\nu a_\nu) - t_\nu^2 - t_\nu'^2\right]\right\}_{t_1=\ldots t_0'=0} \tag{3}$$

In particular, if $n_1 = n_2 = \ldots = n_0' = 0$ one sees from (3) that

$$I_{00} = J_{00} = \frac{1}{\sqrt{-\Delta}} \exp\left\{-\frac{r_0^2}{4}\left[\frac{(p_\nu k_\nu)(f_\nu k_\nu) - k^2(p_\nu f_\nu)}{-(p_\nu f_\nu)}\right]\right\}$$
$$\approx \frac{1}{\sqrt{-\Delta_4}}. \tag{4}$$

In the following we shall assume that the excited state of the nucleon has a lifetime of the order 10^{-10} sec (e.g., a Λ^0 particle). Then[8], $r_0 \sim 10^{-19}$ cm and we therefore shall neglect quantities $\sim r_0 p$.

If $N = n_1 + n_2 + n_3 = 0$, $n_0 = 0$ and $N' = 1$, $n_0' = 0$ then, for $n_1' = 1$, we have

$$I_{01} = -i\frac{r_0}{\sqrt{2}} I_{00}\left[k_1 - \frac{(f_\nu k_\nu)p_1 - (p_\nu k_\nu)f_1}{(p_\nu f_\nu)}\right] \tag{5}$$

and analogously for $n_2' = 1$, $n_3' = 1$.

If $N = n_0 = 0$ and $N' = n_0' = 1$ then, for $n_1' = 1$,

$$I_{02} = \frac{1}{2} I_{00}\left[\frac{2(p_0 f_1 + p_1 f_0)}{(p_\nu f_\nu)} + O(r_0 p)\right] \tag{6}$$

and analogously for $n_2' = 1$, $n_3' = 1$.

As can be seen, the selection rules for the transition-matrix elements with respect to the internal coordinates are in the present case the same as for $f = 0$, which was treated in reference 5. This means that the most probable transitions will be those for which $N' = n_0'$.*

---

*In diagrams where the nucleon is not excited, $M = m$.

*It is easy to verify that Eqs. (4) to (6) go over into Eqs. (10), (11) of reference 5 when $f = 0$. We use the opportunity to point out that in Eqs. (10) and (11) of reference 5 a term $2(t_0 + t_0')$ should be added in the exponent and the sign of β and of $2q_1/E$ should be inverted. The same holds for Eqs. (13) and (14). In the last expressions q signifies that q_1 stands for n_1', q_2 for n_2' etc.

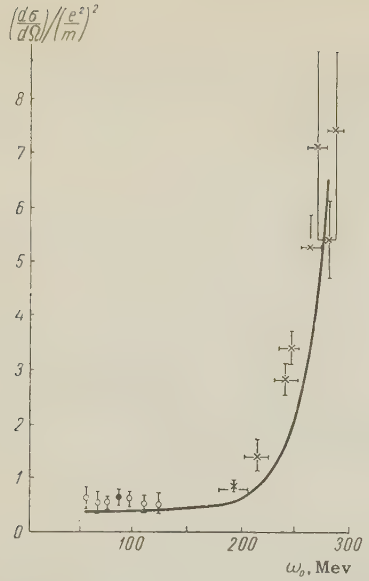

FIG. 2. Dependence of the differential scattering cross section on the energy of the incoming photon for the angle $\vartheta = 90°$ in the center-of-mass system. (The energy, ω_0, is given in the lab. system).

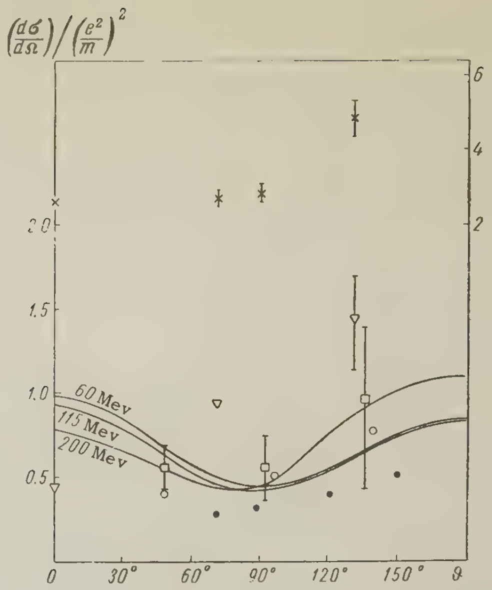

FIG. 3. Angular distributions of the scattered photons for different primary energies: calculated (solid curves) and measured: × – 239 Mev (right scale), ∇ – 193 Mev, ○ – 100 Mev, □ – 90 Mev, ● – 65 Mev.

4. We now calculate the differential cross section of the process (I).

We limit ourselves to such excitations in the intermediate state for which $N = n_0 = 1$. Then J_{02} will be made up of three contributions according to the threefold degeneracy of the diagram containing excited nucleons in the intermediate state. Thus, according to (6) we have

$$J_{02} = \frac{\dfrac{\omega_0^2 - \omega\omega_0 \cos\vartheta}{Mm}\sqrt{1 + \dfrac{\omega_0^2}{M^2} + \dfrac{\omega_0^2}{M^2}\left(1 + \dfrac{\omega_0}{m} - \dfrac{\omega}{m}\right)}}{\left(1 + \dfrac{\omega_0^2}{M^2}\right)\left[\dfrac{\omega_0^2 - \omega_0\omega\cos\vartheta}{Mm} - \sqrt{1 + \dfrac{\omega_0^2}{M^2}\left(1 + \dfrac{\omega_0}{m} - \dfrac{\omega}{m}\right)}\right]^2}, \tag{7}$$

$$J'_{02} = \frac{\dfrac{\omega^2}{M^2}\left(1 + \dfrac{\omega_0}{m} - \dfrac{\omega}{m}\right) + \dfrac{\omega^2 - \omega_0\omega\cos\vartheta}{Mm}\sqrt{1 + \dfrac{\omega^2}{M^2}}}{\left(1 + \dfrac{\omega^2}{M^2}\right)\left[\dfrac{\omega\omega_0\cos\vartheta - \omega^2}{Mm} + \sqrt{1 + \dfrac{\omega^2}{M^2}\left(1 + \dfrac{\omega_0}{m} - \dfrac{\omega}{m}\right)}\right]^2}. \tag{7'}$$

Furthermore, according to (4) we have

$$J_{00} = -\left\{\sqrt{1 + \frac{\omega_0^2}{m^2}}\left[\frac{\omega_0^2}{m^2} - \frac{\omega\omega_0\cos\vartheta}{m^2} - \sqrt{1 + \frac{\omega_0^2}{m^2}\left(1 + \frac{\omega_0}{m} - \frac{\omega}{m}\right)}\right]\right\}^{-1}, \tag{8}$$

$$J'_{00} = -\left\{\sqrt{1 + \frac{\omega^2}{m^2}}\left[\frac{\omega^2}{m^2} - \frac{\omega\omega_0\cos\vartheta}{m^2} - \sqrt{1 + \frac{\omega^2}{m^2}\left(1 + \frac{\omega_0}{m} - \frac{\omega}{m}\right)}\right]\right\}^{-1}. \tag{8'}$$

We finally obtain for the differential cross section of process (I) the expression

$$\begin{aligned}\frac{1}{r_0^2}\frac{d\sigma}{d\Omega} = \frac{1}{2}\left(\frac{\omega}{\omega_0}\right)^2 \Bigg\{&\left(1 + \frac{\omega_0}{m} + \frac{\omega_0\omega}{m^2}\right)\Phi_1^2 + \left(1 - \frac{\omega}{m} + \frac{\omega_0\omega}{m^2}\right)\Phi_2^2 \\ &+ \frac{2a^2}{m^2}\left(\frac{\omega_0}{m} + 5 - \frac{\omega}{m}\right)(\Phi_3^2 + \Phi_4^2) - \left(2 - \frac{\omega}{m} + \frac{\omega_0}{m}\right)\Phi_1\Phi_2 \\ &+ \frac{2a}{m}\left(1 - \frac{\omega}{m} - \frac{3\omega_0}{m}\right)\Phi_1\Phi_3 - \frac{2a}{m}\left(1 - \frac{\omega}{m} + 3\frac{\omega_0}{m}\right)\Phi_1\Phi_4 \\ &- \frac{2a}{m}\left(1 - 3\frac{\omega}{m} + \frac{\omega_0}{m}\right)\Phi_2\Phi_3 + \frac{2a}{m}\left(1 + 3\frac{\omega}{m} + \frac{\omega_0}{m}\right)\Phi_2\Phi_4 \\ &+ \frac{4a^2}{m^2}\left(1 + \frac{\omega}{m} - \frac{\omega_0}{m}\right)\Phi_3\Phi_4\Bigg\},\end{aligned} \tag{9}$$

where

$$r_0^2 = \left(\frac{e^2}{m}\right)^2, \quad \Phi_1 = \frac{m}{\omega_0}J_{00} + \Phi_3, \quad \Phi_2 = \frac{m}{\omega}J'_{00} + \Phi_4,$$

$$\Phi_3 = J_{02}\left(\frac{\omega_0}{m} - \frac{2a^2}{m^2} - \frac{2a}{m}\right)^{-1}, \quad \Phi_4 = J'_{02}\left(\frac{\omega}{m} + \frac{2a^2}{m^2} + \frac{2a}{m}\right)^{-1}.$$

The elastic photon-proton scattering cross section was evaluated from (9) (in units of e^4/m^2) for an angle of 90° in the center-of-mass system and for $a = 140$ Mev. It is plotted in Fig. 2 using experimental points taken from reference 9. As can be seen, there is rather good agreement between the calculations (in the range of their applicability) and the experimental data.

The dependence of the differential cross section (in units of e^4/m^2) on the center-of-mass angle, according to Eq. (9) with $a = 140$ Mev, has been plotted in Fig. 3 for several photon energies. The experimental points are from references 9 and 10.

We see that these experimental data are poor and contain large experimental errors. The experimental points evidently indicate a characteristic tendency. As the photon energy increases, almost up to the resonance energy, the backward scattering becomes more prominent.* If this is so, then the tendency of our angular distributions are in opposition with the experimental distributions up to an energy ~100 Mev but have a similar tendency at higher energies. However, a definite comparison will be possible only after the calculations have been performed in the damping theory, with account of meson effects.

It should be further noted that the cross section for the scattering of photons on nucleons has been calculated in several papers. Some have used the picture of an isobaric state (see, e.g., reference 3, where further references are given) while others have used actual meson-theoretical approaches (see, e.g., reference 12 which also contains further references). The results of the different calculations are rather contradictory.

In conclusion, I would like to thank M. A. Markov for valuable suggestions and I. A. Egorova for the numerical computations.

---

[1] Tamm, Gol'fand, and Fainberg, J. Exptl. Theoret. Phys. (U.S.S.R.) **26**, 649 (1954).

[2] V. I. Ritus, J. Exptl. Theoret. Phys. (U.S.S.R.) **30**, 1070 (1956), Soviet Phys. JETP **3**, 926 (1957).

[3] V. I. Ritus, J. Exptl. Theoret. Phys. (U.S.S.R.) **27**, 660 (1954).

[4] M. A. Markov, Гипероны и K-мезоны (Hyperons and K-Mesons) 3, Joint Inst. for Nucl. Res., 1957.

[5] N. F. Nelipa, J. Exptl. Theoret. Phys. (U.S.S.R.) **33**, 1277 (1957), Soviet Phys. JETP **6**, 981 (1958).

[6] A. I. Akhiezer and V. B. Berestetskii, Квантовая электродинамика (Quantum Electrodynamics) GITTL, Moscow (1953) [Transl. publ. by Dept. of Commerce].

[7] M. A. Markov, О систематике элементарных частиц (On the Systematics of Elementary Particles), Acad. Sci. Press, Moscow, 1955.

[8] P. S. Isaev and M. A. Markov, J. Exptl. Theoret. Phys. **29**, 111 (1955), Soviet Phys. JETP **2**, 84 (1956).

[9] G. Bernardini, Proceedings of the 7th Rochester Conference (1957).

[10] Govorkov, Gol'danskii, Karpukhin, Kutcenko, and Pavlovskaia, Dokl. Akad. Nauk (U.S.S.R.) **111**, 988 (1956), Soviet Phys. "Doklady" **2**, (1956).

[11] Pugh, Gomez, Frisch, and Janes, Phys. Rev. **105**, 982 (1957).

[12] R. H. Capps and W. G. Holladay, Phys. Rev. **99**, 931 (1955).

Translated by M. Danos
135

---

*The opposite result has been obtained in reference 11.

SOVIET PHYSICS JETP VOLUME 35(8), NUMBER 3 MARCH, 1959

OSCILLATIONS IN THE CONDUCTIVITY OF METALLIC FILMS IN MAGNETIC FIELDS

V. L. GUREVICH

Submitted to JETP editor February 3, 1958; resubmitted May 19, 1958

J. Exptl. Theoret. Phys. (U.S.S.R.) **35**, 668-677 (September, 1958)

Oscillations of the conductivity of metallic films in magnetic fields are considered for arbitrary dispersion law of the electron energy and for arbitrary orientation of the field. The oscillations are not a quantum effect and are related to the finite thickness of the film and to the diffusion character of the reflection of electrons from its surface. In contrast to the Shubnikov-de Haas effect, the conductivity in the given case oscillates as a function of H and not of H^{-1}. Measurements of the amplitudes and periods of oscillation allow us to draw conclusions on the shape of the Fermi surface in metals.

1. Oscillations of the conductivity of a metallic film due to the size of the magnetic field H perpendicular to it have been carried out by Sondheimer[1] under the assumption of an isotropic dispersion law for the electron energy. They are determined by the diffusion character of the reflection of the electrons from the surface of the film. Thanks to this, the helical electron trajectory bounded by these surfaces (the electrons move in the magnetic field H) undergoes simultaneously the effect of the electric field **E** and is cut off at some fraction of a turn, dependent on H. The value of this fraction determines the oscillating component of the current, while the complete turns give the monotonically-varying component.

In the present paper it is shown that oscillations also ought to exist for an arbitrary dependence of the electron energy ϵ on the quasi-momentum p and for an arbitrary direction of the field H, not parallel to the surface of the film. Measurements of the amplitude and period for various orientations of the field permit us to make judgments on the shape of the Fermi surface in the metal. The problem of the possibility of complete establishment of the Fermi surface by means of the oscillations is an independent problem which we shall not consider in the present paper.

Let us estimate the magnitude of the period of oscillation. The electron travels from one surface of the film to the other in the time $t \approx a/|\bar{v}_\zeta|$, where a is the thickness of the film, the ζ axis is perpendicular to the surface of the film, and v_ζ is the time average of the ζ component of the electron velocity. The period or rotation of the electron in its orbit is $T = 2\pi m^*c/eH$, where e is the electronic charge, and m^* is the effective electronic mass, introduced by Lifshitz, Azbel', and Kaganov in reference 2. It depends on ϵ and p_z — quantities which are conserved in the presence of a magnetic field (z axis directed along **H**). In this case, electrons with energies close to the Fermi energy ϵ_0 are necessary for conduction. In a time t, an electron completes $n = t/T = aeH/2\pi m^*c|\bar{v}_\zeta|$ round trips. For this number to be changed by one, the magnetic field must change by the quantity $\Delta H = 2\pi m^*c|\bar{v}_\zeta|/ea$. This also is the period of oscillation of the current created by electrons with given p_z (we consider ϵ to be equal to ϵ_0). It depends on p_z, since groups of electrons with different p_z correspond to different periods. The total current was observed experimentally; it is obvious that, generally speaking, the oscillations connected with a given group of electrons will be "smeared out" by oscillations of other groups with neighboring values of p_z, corresponding to slightly longer and slightly shorter periods. The total effect observed includes oscillations whose periods are determined by certain isolated values of p_z. They belong to two basic types.

Oscillations of the first type are connected with p_z close to p_z^*, the maximum value of p_z on the Fermi surface. They are sinusoidal, and their amplitudes fall off as H^{-4}; this result agrees with that obtained by Sondheimer.[1] However, their period is determined not by a single parameter (the limiting Fermi momentum, as in reference 1), but by the relation $\sqrt{K}/\cos\theta$, where K is the Gaussian curvature of the Fermi surface at the point $p_z = p_z^0$, and θ is the angle between the z and ζ axes. Thus, it is possible, by means of the oscillations of the first type, to determine the Gaussian curvature of the Fermi surface at all its elliptic points. This possibility of the determination of the Gaussian curvature, although it does not give very great accuracy (the amplitudes of oscillation fall off rapidly with increasing field), can be shown to be suitable, since it does not involve the use of complicated high-frequency apparatus. In this case, all the data relative to the Gaussian curvature can be obtained in principle by investigating a single specimen, cut out in a suitable manner relative to the crystallographic axes.

Oscillations of the second type are connected with such $p_z = p_{z_i}$ for which the function $\Delta H(p_z)$ has an extremum. Then, approximately the same periods ΔH correspond to a rather large group of electrons with p_z close to p_{zi}. These oscillations are not sinusoidal, and their amplitudes fall off with the field as $H^{-5/2}$.

In order that the oscillations take place and be observable, it is obvious that the inequality

$$t_0 \gtrsim a/|\bar{v}_\zeta| \gg T, \tag{1.1}$$

must be satisfied, where t_0 is the time of volume relaxation of the conduction electrons. It should be noted that it is not easy to obtain experimental conditions under which $t_0 \gtrsim a/|\bar{v}_\zeta|$. For this, we need monocrystalline films, free from stresses, and low temperatures. The difference in the film thickness at different points must be less than $|\bar{v}_\zeta|T$. However, at the present time, these difficulties are surmountable, since we now can obtain metallic samples in which the mean free path l is sufficiently large at liquid-helium temperatures. For example, in the work of Kunzler and Renton,[3] $l = 0.45$ mm (tin), while monocrystalline films 0.1 mm thick (and in some cases less) can be obtained. The magnitude of the magnetic field necessary for the observation of oscillations is determined by the thickness of the film compatible with the inequality (1.1); for $a \approx 0.1$ mm, it amounts to thousands of oersteds.

We note that the oscillations of similar origin were recently observed by Babiskin and Siebenmann[4] on a sodium specimen which, it is true, had the shape not of a film but of a thin wire. In these experiments, $l = 0.12$ mm.

2. We now return to a rigorous solution of the problem. The linearized kinetic equation for electrons in a metal in the shape assumed by Lifshitz, Azbel', and Kaganov[2] has the form (see also reference 5):

$$v_\zeta \frac{\partial f}{\partial \zeta} + \Omega_0 \frac{\partial f}{\partial \tau} + \frac{1}{t_0}\hat{S}f = e\frac{\partial F_0}{\partial \varepsilon}\sum_{\nu=1}^{3} v_\nu E_\nu. \tag{2.1}$$

Here $\Omega_0 = eH/m_0c$, τ is the dimensionless coordinate introduced in reference 2, which determines the position of the electron in the orbit ($\tau = \Omega_0 t$, where t is the time of motion of the electron along the orbit, determined from an arbitrary initial time), F_0 is the equilibrium distribution function, f is the nonequilibrium addition to it, $\hat{S}/t_0$ is the collision operator, m_0 is a quantity with the dimensions of mass, which drops out of the final results; for intermediate estimates, it is appropriate to consider it to be of the order of m^*. The function f satisfies the conditions

$$f|_{\zeta=0,\, v_\zeta>0} = f|_{\zeta=a,\, v_\zeta<0} = 0 \tag{2.2}$$

(diffusivity of reflection) and in the case of a closed trajectory,[2] which is also of interest to us, it must be a periodic function of τ with period $\theta = 2\pi m^*/m_0$ [$m^* = (2\pi)^{-1}\partial S/\partial\epsilon$, S is the area cut out of the surface $\epsilon(p) = \text{const}$ by the surface $p_z = \text{const}$]. The ζ component of the current-density vector satisfies the conditions $j_\zeta(0) = j_\zeta(a) = 0$, but, inasmuch as $\operatorname{div} j = 0$ in a stationary case, then, generally, $j_\zeta(\zeta) = 0$.

We set $f = e(\partial F_0/\partial\epsilon)\sum_{\nu=1}^{3} f_\nu$, where the functions f_ν are solutions of the equation

$$v_\zeta \partial f_\nu/\partial\zeta + \Omega_0 \partial f_\nu/\partial\tau + \hat{S}f_\nu/t_0 = v_\nu E_\nu \tag{2.3}$$

with the boundary conditions (2.2). The Fourier coefficients in the expansion

$$f(\zeta) = a^{-1}\sum_k \varphi_k^{(\nu)} \exp(2\pi ik\zeta/a) \tag{2.4}$$

satisfy the equation

$$\begin{aligned} &\partial\varphi_k^{(\nu)}/\partial\tau + (ik\alpha + \gamma\hat{S})\varphi_k^{(\nu)} \\ &= -\Omega_0^{-1}|v_\zeta|[f(0) + f(a)] + \Omega_0^{-1}v_\nu\mathcal{E}_k^{(\nu)}. \end{aligned} \tag{2.5}$$

This relation is easily obtained by substituting (2.4) in (2.3) and taking (2.2) into account. Here

$$\alpha = 2\pi v_\zeta/a\Omega_0, \quad \gamma = 1/\Omega_0 t_0,$$

$$\mathcal{E}_k^{(\nu)} = \int_0^a \exp(-2\pi ik\zeta/a)E_\nu(\zeta)\,d\zeta.$$

We carried out further calculations under the assumption that $\hat{S} = 1$, i.e., that the collision operator can be described with the help of the relaxation time $t_0(p)$. Such a simplification is valid since (as we shall see below) for $t_0 \gg a/|\bar{v}_\zeta|$ (and it is principally this case that is of interest to us), the time t_0 does not usually enter into the expression for the oscillating part of the conductivity tensor. This is natural, because the oscillations are due to those electrons which move from one surface of conductor to the other without undergoing collisions in the interior of the conductor. In this case the term which describes the volume collisions is necessary only for the intermediate calculations. If $t_0 \sim a/|\bar{v}_\zeta|$, then the relaxation time enters into the final result, since it determines the fraction of electrons which do not reach the other surface of the film and, consequently, do not take part in the oscillations. In this case the assumption on the relaxation time permits us to determine the order of magnitude of the amplitudes of the oscillations and their exact period, since the period depends only on the peculiarities of the spectrum and the relaxation time does not enter into it.

The solution of (2.5) periodic in τ has the form:

$$\varphi_k^{(\nu)}(\tau) = \Omega_0^{-1}\mathscr{E}_k^{(\nu)}\int_{-\infty}^{\tau} v_\nu(\tau)\exp\left[\int_{\tau}^{\tau'}(\gamma + ik\alpha)\,d\tau''\right]d\tau'$$
$$-a^{-1}\Omega_0^{-2}\int_{-\infty}^{\tau}|v_\zeta(\tau')|\,g_\nu(\tau')\exp\left[\int_{\tau}^{\tau'}(\gamma + ik\alpha)\,d\tau''\right]d\tau', \qquad (2.6)$$

where

$$g_\nu(\tau) = a\Omega_0[f_\nu(0) + f_\nu(0)].$$

In turn,

$$g_\nu(\tau) = 2\Omega_0\sum_k \varphi_k^{(\nu)} = 2\Phi_\nu(\tau)$$
$$-(2/a\Omega_0)\sum_k\int_{-\infty}^{\tau}|v_\zeta(\tau')|\,g_\nu(\tau')\exp\left[\int_{\tau}^{\tau'}(\gamma + ik\alpha)\,d\tau''\right]d\tau', \qquad (2.7)$$

where

$$\Phi_\nu(\tau) = \sum_k \mathscr{E}_k^{(\nu)}\int_{-\infty}^{\tau} v_\nu(\tau)\exp\left[\int_{\tau}^{\tau'}(\gamma + ik\alpha)\,d\tau''\right]d\tau'. \qquad (2.8)$$

The series on the right-hand side of (2.7) can be transformed with the aid of the identity

$$\sum_{k=-\infty}^{\infty} e^{ikx} = 2\pi\sum_{n=-\infty}^{\infty}\delta(x - 2\pi n).$$

Integrating the δ-function in (2.7), we obtain the equation for the function $g_\nu(\tau)$:

$$\sum_{\tau_n \leqslant \tau} g_\nu(\tau_n)\exp\left(-\int_{\tau_n}^{\tau}\gamma d\tau'\right) = \Phi_\nu(\tau), \qquad (2.9)$$

where the functions $\tau_n(\tau)$ are determined from the condition

$$\left|\int_{\tau_n}^{\tau}\alpha d\tau'\right| = 2\pi n \quad \text{or} \quad \int_{\tau_n}^{\tau} v_\zeta\,d\tau' = na\Omega_0\bar{v}_\zeta/|\bar{v}_\zeta| \equiv nq\bar{v}_\zeta \qquad (2.10)$$

(the bar denotes averaging over the period of θ). It is not difficult to establish that, if the velocity $v_\zeta(\tau)$ has one and the same sign for all τ, Eq. (2.10) has a unique solution $\tau_n(\tau)$ for a given n. In particular, its unique solution for $n = 0$ is $\tau_0(\tau) = \tau$. It is then quite simple to find the solution of (2.9). From the general equality

$$\int_{\tau_{n+1}}^{\tau} v_\zeta\,d\tau' = (n+1)\,q\bar{v}_\zeta$$

we subtract its value for $n = 1$. As a result we get the identity

$$\tau_n[\tau_1(\tau)] = \tau_{n+1}(\tau). \qquad (2.11)$$

From this it easily follows that

$$g_\nu(\tau) = \Phi_\nu(\tau) - \Phi_\nu(\tau_1)\exp\left(-\int_{\tau_1}^{\tau}\gamma d\tau'\right)$$
$$= \Phi_\nu(\tau) - \Phi_\nu(\tau_1)\exp\{-\bar{\gamma}(\tau - \tau_1) - \Gamma(\tau) + \Gamma(\tau_1)\}, \qquad (2.12)$$

(where $\gamma(\tau) = \bar{\gamma} + d\Gamma/d\tau$) is a solution of Eq. (2.9). The second component in (2.12) is an oscillating function of the variable q with period θ, i.e., an oscillating function of the field H. Indeed, let us set $\tau_1 = \tau - q + \Delta\tau$ and $v_\zeta = \bar{v}_\zeta + dW_\zeta/d\tau$. The function $W_\zeta(\tau)$ is a periodic function of τ with period θ. The function $\Delta\tau$ satisfies the equation

$$\Delta\tau(\tau, q) = W_\zeta(\tau)/\bar{v}_\zeta - W_\zeta(\tau - q + \Delta\tau)/\bar{v}_\zeta \qquad (2.13)$$

and is consequently a periodic function of the second argument. But $\Phi_\nu(\tau_1) = \Phi_\nu(\tau - q + \Delta\tau)$, i.e., $\Phi_\nu(\tau_1)$ [and also $\Gamma(\tau_1)$], together with $g_\nu(\tau)$, are periodic functions of q. It is clear that the functions $\varphi_k^{(\nu)}(\tau)$ determined by Eq. (2.6) are, generally speaking, oscillating functions of q with the same period. This dependence is important and leads to the observed effects if the exponent in (2.12) is $\lesssim 1$. But $\tau - \tau_1 \approx q$, and this condition takes the form $a/|\bar{v}_\zeta|t_0 \lesssim 1$, i.e., it coincides with the inequality (1.1) given originally. The period of oscillation $\theta = 2\pi m^*/m_0$ depends on ϵ and p_z. Therefore, it will frequently be of use to us to replace q by the variable $u = qm_0/m^* = aeH/m^*c|\bar{v}_\zeta|$. The quantities $\Delta\tau$ and $\Phi(\tau_\zeta)$ are oscillating functions of this variable with period 2π.

For certain values of ϵ and p_z, the function $v_\zeta(\tau)$ can be shown to be fluctuating in sign. Then for some τ, Eq. (2.10) at $n = 0$ can have several solutions, i.e., the function $\tau_0(\tau) \leq \tau$ can be nonunique. Reasoning as above, it is not difficult to show that for such τ the solution of (2.9) has the form

$$g_\nu(\tau) = \Phi_\nu(\tau) - \Phi_\nu(\tau_0)\exp\left(-\int_{\tau_0}^{\tau}\gamma d\tau'\right), \qquad (2.14)$$

where τ_0 denotes the maximum value of the function $\tau_0(\tau) \leq \tau$, different from τ. For τ such that the function $\tau_0(\tau)$ is single valued Eq. (2.12) holds as before, but now we mean by τ_1 the maximum value, generally speaking, of the multiply-valued function $\tau_1(\tau)$.

We note that (2.14) contains no oscillating dependence on the magnetic field H, inasmuch as the magnetic field does not enter at all into the equation for $\tau_0(\tau)$. The reason for this is the following. If the velocity $v_\xi(\tau)$ is a sign-alternating function of τ, then an electron leaving the surface of the film at some value of τ can, by describing a fraction of a turn, return to the same surface and experience diffuse reflection from it. For such τ, the function $\tau_0(\tau) \leq \tau$ is nonunique, but, inasmuch as the value of this fraction is independent of H, $g_\nu(\tau)$ has a non-periodic dependence on H. However, even in this case there are electrons which make a contribution to the oscillations. The fact is that if the field H is not parallel to the film surface then, in general, for arbitrary ϵ and p_z, there exist initial values of τ for which the electron reaches the opposite surface of the film. For such τ, the function $\tau_0(\tau) \leq \tau$ is single-valued and consequently, the oscillating function (2.12) is valid for $g_\nu(\tau)$.

3. The experimentally-measured components of the mean current density are *

$$\bar{j}_\mu = a^{-1}\int_0^a j_\mu(\zeta)\,d\zeta = -\frac{2e^2m_0}{ah^3}\sum_{\nu=1}^{3}\int v_\mu\varphi_0^{(\nu)}\frac{\partial F_0}{\partial\varepsilon}\,d\tau\,dp_z\,d\varepsilon$$

$$= -\frac{2e^2m_0}{ah^3}\sum_{\nu=1}^{3}\int dp_z\,d\varepsilon\,\frac{\partial F_0}{\partial\varepsilon}$$

$$\times\Big\{\frac{1}{\Omega_0}\mathscr{E}_0^{(\nu)}\int_0^\theta v_\mu(\tau)\int_{-\infty}^{\tau}d\tau'\exp\Big(\int_\tau^{\tau'}\gamma d\tau''\Big)\,v_\nu(\tau') \tag{3.1}$$

$$-\frac{1}{a\Omega_0^2}\sum_k\int_0^\theta d\tau v_\mu(\tau)\int_{-\infty}^{\tau}d\tau'\,|v_\zeta(\tau')|\int_{\tau'^{(1)}}^{\tau'}d\rho$$

$$\times\exp\Big[ik\int_{\tau'}^{\rho}\alpha d\rho' + \int_\tau^\rho\gamma d\rho'\Big]\,v_\nu(\rho)\Big\} \equiv -\frac{2e^2m_0}{a\,h^3}$$

$$\times\sum_{\nu=1}^{3}\int dp_z\,d\varepsilon\,\frac{dF_0}{\partial\varepsilon}\Big(\frac{1}{\Omega_0}\mathscr{E}_0^{(\nu)}A_{\mu\nu} + \frac{1}{a\Omega_0^2}\sum_k B_{\mu\nu}^k\,\mathscr{E}_k^{(\nu)}\Big),$$

where $\tau^{(1)}$ is equal to τ_1 or τ_0, depending on whether Eq. (2.12) or Eq. (2.14) holds. The condition $j_\xi(\xi) = 0$ permits us to establish $E_\xi(\xi)$ as a linear function of E_ξ and E_η, and to obtain an expression for the current density in the form

$$\bar{j}_\mu = \sum_{\nu=1}^{2} s_{\mu\nu}E_\nu.$$

The effective-conductivity tensor of the film $s_{\mu\nu}$ (the inverse of the tensor $r_{\mu\nu}$ above) is also determined by experiment.

In order to compute its oscillating part $\Delta s_{\mu\nu}$, we find the derivatives

$$\partial^2B_{\mu\nu}^k/\partial u^2 = (m^*/m_0)^2\,\partial^2B_{\mu\nu}^k/\partial q^2,$$

from a knowledge of which we can easily find the oscillating parts of the coefficients $B_{\mu\nu}^k$. Let us first consider the case in which the function $\tau_0(\tau) \leq \tau$ is single valued for all τ. Then

$$\frac{\partial}{\partial u}B_{\mu\nu}^k = \frac{m^*}{m_0}\frac{\partial}{\partial q}\;B_{\mu\nu}^k =$$

$$-\frac{m^*\bar{v}_\zeta}{m_0}\int_0^\theta d\tau v_\mu(\tau)\int_{-\infty}^{\tau}d\tau'\,\frac{|v_\zeta(\tau')|}{v_\zeta(\tau_1')}\times\exp\Big(\int_\tau^{\tau'}\gamma d\tau''\Big)v_\nu(\tau_1')$$

$$= -\frac{m^*|\bar{v}_\zeta|}{m_0}\int_0^\theta d\tau v_\mu(\tau)\int_{-\infty}^{\tau_1}v_\nu(\tau')\exp\Big(\int_\tau^{\tau'}\gamma d\tau''\Big)d\tau'. \tag{3.2}$$

Here we have used the identities $\partial\tau_1/\partial q = -\bar{v}_\xi/v_\xi(\tau_1)$ and $v_\xi(\tau)d\tau = v_\xi(\tau_1)d\tau_1$, which follow from the definition of the function $\tau_1(\tau)$. Then,

$$\frac{\partial^2}{\partial u^2}\;B_{\mu\nu}^k \equiv C_{\mu\nu}$$

$$= \bar{v}_\zeta^2\Big(\frac{m^*}{m_0}\Big)^2 e^{-\bar{\gamma}q}\int_0^\theta d\tau\,\frac{v_\mu(\tau)\,v_\nu(\tau_1)}{|v_\zeta(\tau_1)|}\times\exp\{\gamma\Delta\tau + \Gamma(\tau_1) - \Gamma(\tau)\}$$

$$\approx \bar{v}_\zeta^2\Big(\frac{m^*}{m_0}\Big)^2 e^{-\bar{\delta}u}\int_0^\theta d\tau\,\frac{v_\mu(\tau)\,v_\nu(\tau_1)}{|v_\zeta(\tau_1)|}. \tag{3.3}$$

We have left here only the zero-order terms in the expansion in $\gamma \ll 1$; $\delta = (m^*/m_0)\gamma$. It is clear that these terms are oscillating functions of u with period 2π; consequently, they are periodic functions of the magnetic field H. It is then not difficult to prove that the oscillating parts of the coefficients $B_{\mu\nu}$ computed to this degree of accuracy have the form $e^{-\bar{\delta}u}b_{\mu\nu}(\epsilon, p_z, u)$, where $b_{\mu\nu}$ are periodic functions of u. If $\nu = \xi$, then the $v_\xi(\tau_1)$ in the numerator and denominator of (3.3) cancel and the zero-order term (in the expansions in powers of γ) does not oscillate. Therefore, if $E_\xi(\xi)$ is of the same order as E_ξ and E_η, the contributions of the coefficients $B_{\mu\nu}(\nu \neq \xi)$ in the oscillating part of the current density $\bar{j}_\mu$ is, roughly speaking, t_0/T times larger than the contribution of the coefficients $B_{\mu\xi}$, and the latter can be neglected. Then the sum (3.1) is simplified, since only terms with $k = 0$ enter into it, inasmuch as E_ξ and E_η do not depend on ξ. It is not difficult to carry out all the calculations in the general case; however, henceforth we shall assume this simplification. We note that we can neglect the oscillations connected with E_ξ in every case if $t_0 \sim a/v_0$, where v_0 is of the order of the velocity on the Fermi surface. Such an estimate is easily obtained if we consider that the tensor $s_{\nu\mu}$ is of the order

$$\sigma_{\mu\nu}^{(\infty)} - \sigma_{\mu\zeta}^{(\infty)}\sigma_{\zeta\nu}^{(\infty)}/\sigma_{\zeta\zeta}^{(\infty)},$$

---

*After the present research was completed, a paper was published by Kaner[6] on the conductivity of metallic films in a magnetic field, in which the same expression is obtained for the current density in the film. However, the problem of the oscillating conductivity of the film was not considered there.

in this case, where $\sigma_{\mu\nu}^{(\infty)}$ is the conductivity tensor of a macroscopic sample, as computed in reference 2.

Now, if ϵ and p_z are such that the function $\tau_0(\tau) \leq \tau$ is not single valued for all τ, we can obtain Eq. (3.3) for $C_{\mu\nu}$ in the same way; in such a case, we integrate over that part of the interval from 0 to θ, where this function is single valued. We note that if $t_0 \gg a/|\bar{v}_\xi|$, then $\bar{\delta}u \ll 1$, and the relaxation time does not enter into (3.3), nor into the expression for the oscillating part of the conductivity tensor.

With the help of the identity $v_\xi(\tau)\,d\tau = v_\xi(\tau_1)\,d\tau_1$, we obtain

$$\int \frac{v_\mu(\tau)\,v_\nu(\tau_1)}{|v_\zeta(\tau_1)|}\,d\tau = \int \frac{v_\mu(\tau_{-1})\,v_\nu(\tau)}{|v_\zeta(\tau_{-1})|}\,d\tau. \qquad (3.4)$$

Here $\tau_1(\tau)$ is the solution of (2.10) for $n = -1$ [obviously, it is its own inverse function relative to $\tau_1(\tau)$]; the first integral extends over the region of single-valuedness of the function $\tau_0(\tau) \geq \tau$, while the second extends over the region of single-valuedness of $\tau_0(\tau) \geq \tau$. It is easily verified that, for a reversal of the direction of the magnetic field, we can obtain an expression for the oscillating part of the current, replacing $\tau_1(\tau)$ in (3.3) by $\tau_{-1}(\tau)$. It therefore follows from (3.4) that $\Delta s_{\mu\nu}(-\mathbf{H}) = \Delta s_{\nu\mu}(\mathbf{H})$.

4. If $u \ll \epsilon_0/kT$, we can set $\partial F/\partial\epsilon = -\delta(\epsilon - \epsilon_0)$, and then

$$\Delta s_{\mu\nu} = (2e^2 m_0 / a h^3 \Omega_0^2) \int_0^{p_z^0} a p_z L_{\mu\nu}(p_z, u)$$

$$= (2e^2 m_0 / a h^3 \Omega_0^2) \int_0^{p_z^0} dp_z e^{-Q} l_{\mu\nu}(p_z, u), \qquad (4.1)$$

where

$$l_{\mu\nu} = b_{\mu\nu}(\varepsilon_0, p_z, u) + b_{\mu\nu}(\varepsilon_0, -p_z, u), \quad Q = a\bar{t}_0^{-1}/|\bar{v}_\zeta|.$$

The quantity $L_{\mu\nu}$ depends smoothly on p_z, and oscillates like the function $u \gg 1$. This means that $L_{\mu\nu}(p_z, u)$ oscillates as a function of the field H, while the period of oscillation $\Delta H = 2\pi m^* c\,|\bar{v}_\xi|/ea$ depends on p_z, i.e., as noted earlier, different periods of oscillation correspond to groups of electrons with different p_z. Oscillations of different types entering into the total effect described by Eq. (4.1) are connected with different portions of the integration inverval. Oscillations of the first type are determined by p_z close to p_z^0. Oscillations of the second type are connected with such $p_z = p_{zi}$, for which $du/dp_z = 0$. For such p_z, the function $\Delta H(p_z)$ has an extremum.

Let us begin with the consideration of oscillations of the first type. In the vicinity of the point p_z^0, the equation of the Fermi surface $\epsilon(\mathbf{p}) = \epsilon_0$ has the form

$$v_z^0 \Delta p_z + \frac{1}{2} \sum_{i,k=1}^{3} \beta_{ik} \Delta p_i \Delta p_k = 0, \qquad (4.2)$$

$$\beta_{ik} = (\partial^2\varepsilon/\partial p_i \partial p_k)_0; \quad \Delta p_i = p_i - p_i^0.$$

We consider the point p_z^0 to be elliptic; consequently, the quadratic form $\sum_{i,k=1}^{2} \beta_{ik}\Delta p_i \Delta p_k$ is positive definite. The equations of motion of the electron in the zero approximation in the electric field have the form[2]

$$\frac{1}{m_0}\frac{dp_x}{d\tau} = -v_y, \quad \frac{1}{m_0}\frac{dp_y}{d\tau} = v_x. \qquad (4.3)$$

As will be seen later [see Eq. (4.6)], the region of integration important to the determination of the first type is the one for which $|\Delta p_z|/p_z^0 \sim 1/u \ll 1$. It is obvious that $\Delta p_x \sim \Delta p_y \sim u^{-1/2} p_z^0$ in this region. Substituting into (4.3) the expressions for the velocities v_x and v_y [obtained from (4.2)] we get (with accuracy up to quantities of order higher than $u^{-1/2}$):

$$v_x = \sqrt{2v_z^0(p_z^0 - p_z)}\,(\beta_1^{1/2}\cos\omega\tau\cos\varphi + \beta_2^{1/2}\sin\omega\tau\sin\varphi);$$

$$v_y = \sqrt{2v_z^0(p_z^0 - p_z)}\,(-\beta_1^{1/2}\cos\omega\tau\sin\varphi + \beta_2^{1/2}\sin\omega\tau\cos\varphi);$$

$$v_z = v_z^0 + \sqrt{2v_z^0(p_z - p_z)}\,(\beta_{x'z}\beta_1^{-1/2}\cos\omega\tau + \beta_{y'z}\beta_2^{-1/2}\sin\omega\tau). \qquad (4.4)$$

Here β_1 and β_2 are the principal values of the tensor β_{ik} $(i, k = 1, 2)$, φ is the angle between the xy axis and the principal axes x′, y′, and $\omega = m_0\sqrt{\beta_1\beta_2} = m_0/m^*$. It then follows that $u = \omega q = aeH\sqrt{\beta_1\beta_2}/c\,|\bar{v}_\xi|$. Now, $v_\xi = -v_y \sin\vartheta + v_z \cos\vartheta$ (we assume that the axes x and ξ coincide); therefore, if $\cos\vartheta > u^{-1/2}$, then $\tau_1 = \tau - q$ with accuracy up to quantities of the order $u^{-1/2}$, inasmuch as $w_\xi \sim v_\xi^0 u^{-1/2}$. If $\cos\vartheta > u^{-1/2}$, the function $\tau_0(\tau)$ is single valued for all significant values of p_z.

It follows from (3.3) and (4.4) that the oscillating part of the coefficients $C_{\mu\nu}$, computed with relative accuracy up to $1/u$, is proportional to the sum of integrals of the form

$$\int_0^{\theta} \cos\omega\tau \cos\omega(\tau - q)\,d\tau = \pi\omega^{-1}\cos u$$

and identical expressions with two sines or sine and cosine. It is therefore not difficult to demonstrate that the coefficients $b_{\mu\nu}$ have the form

$$b_{\mu\nu} = c_{\mu\nu} m_0^{-3} (\beta_1\beta_2)^{-1} (v_z^0)^2\,|p_z^0 - p_z|\cos(u + \lambda_{\mu\nu}), \qquad (4.5)$$

where $c_{\mu\nu}$ is a constant on the order of unity. Inasmuch as $b_{\mu\nu}(-p_z, u) = b_{\mu\nu}(p_z, u)$ in the given case, the part of the conductivity tensor connected with oscillations of the first type is

$$\Delta s_{\mu\nu}^{(1)} = \frac{4c_{\mu\nu}e^2 (v_z^0)^2}{ah^3\Omega^2} \int^{p_z^0} e^{-Q} (p_z^0 - p_z) \cos (u + \lambda_{\mu\nu}), \quad (4.6)$$

where $\Omega = eH/m^*c = eh\sqrt{\beta_1\beta_2}/c$. We expand Q and u in powers of $p_z - p_z^0$, limiting ourselves to the zero term in the former case and the linear term in the latter, and integrate by parts. We get

$$\Delta s_{\mu\lambda}^{(1)} = -\frac{4c_{\mu\nu}e^2 (v_z^0)^2}{a^3h^3\Omega^4\left(\frac{d}{dp_z}\frac{1}{|\bar{v}_\zeta|}\right)_0^2} e^{-Q_0} \cos\left[\frac{aeH\sqrt{\beta_1\beta_2}}{c\,|v_z^0|\cos\vartheta} + \lambda_{\mu\nu}\right]. \quad (4.7)$$

We note that $\sqrt{\beta_1\beta_2}/|v_z^0| = \sqrt{K}$, where K is the Gaussian curvature of the Fermi surface.

Thus, the oscillations of the first type are sinusoidal; their amplitudes fall off as H^{-4}, while their period is

$$\Delta H = 2\pi c \cos\vartheta / ae\sqrt{K}. \quad (4.8)$$

Its measurement determines the Gaussian curvature of the Fermi surface at the elliptic point, the normal to which is parallel to the direction of the magnetic field.

If the Fermi surface is nonconvex, then there can be several such points, and to each of them there will generally correspond a period of oscillation. If the Fermi surface is open (closed trajectory), then there can exist a maximum momentum p_z^0 for certain directions of H; oscillations of the first type are then lacking. In the case of closed Fermi surfaces, these oscillations are always present.

5. We now consider oscillations of the second type. For simplicity, we shall assume that there is only one point $p_z^* = p_z$ at which the derivative du/dp_z vanishes. In order to determine the oscillating part of the integral (4.1) connected with the behavior of the integrand $L_{\mu\nu}(p_z, u)$ near $p_z = p_{z1}$, we expand its second argument in powers of $p_z - p_{z1}$ as far as the quadratic term, while we set the first argument equal to p_{z1}, since $L_{\mu\nu}$ is a smooth function:

$$L_{\mu\nu}(p_z, u) \approx L_{\mu\nu}[p_{z1}, u_1 + u_1''(p_z - p_{z1})^2/2]. \quad (5.1)$$

In this case, inasmuch as we are only interested in the oscillating component in (4.1), we can consider that

$$\bar{L}_{\mu\nu}(p_{z1}) = (2\pi)^{-1}\int_0^{2\pi} L_{\mu\nu}(p_{z1}, u)\,du = 0.$$

Then the part of the conductivity tensor connected with oscillations of the second type is

$$\Delta s_{\mu\nu}^{(2)} = \frac{2e^2m_0}{ah^3\Omega_0^2}\int_{p_1}^{p_2} L_{\mu\nu}\left[p_{z1}, u_1 + \frac{1}{2}u_1''(p_z - p_{z1})^2\right]dp_z. \quad (5.2)$$

Here the upper and lower limits of the integral are so chosen that for $p_z = p_1$ and $p_z = p_2$, we can, with sufficient accuracy, limit ourselves to the quadratic terms in the expansion of (5.1). We introduce a new integration variable $\xi = \sqrt{|u_1''|} \times (p_z - p_{z1})$. If the magnetic field is large enough that $|\xi_i| = \sqrt{|u_1''|}\,|p_i - p_{z1}| \gg 1$, it is easy to show that oscillations of the second type are present, and that their amplitudes fall off as $H^{-5/2}$. Actually, limiting ourselves in accuracy to $1/|\xi_i|$, we can integrate in ξ over infinite limits and get

$$\Delta s_{\mu\nu}^{(2)} = \frac{2e^2m_0}{ah^3\Omega_0^2\sqrt{eaH/c}}\left|\frac{d^2}{dp_z^2}\frac{1}{|\bar{v}_\zeta|\,m^*}\right|_{(1)}^{-1/2} \times \int_{-\infty}^{\infty} L_{\mu\nu}(p_{z1}, u \pm \xi^2/2)\,d\xi. \quad (5.3)$$

The period of oscillation is $\Delta H = 2\pi c\,|\bar{v}_{\zeta_1}|\,m_1^*\,|\,ea$. We emphasize that these oscillations are absent in every case when the derivative does not generally vanish in the interval $0 < p_z \leq p_z^0$. In particular, we can show that this derivative does not vanish if the Fermi surface is an ellipsoid. Of, course, the presence of oscillations of the second type is evidence of a significant deviation in the shape of the Fermi surface from ellipsoidal. Therefore, the shape of these oscillations should generally be quite different from sinusoidal.

6. In addition to the two types of oscillations considered here, there is a third type connected with those values of p_z for which a non-single valuedness arises in the function $\tau_0(\tau) \leq \tau$. These oscillations are generally non-sinusoidal and their amplitudes fall off with increasing field more rapidly than was the case with the first two types (as H^{-5}). If the Fermi surface has a complicated structure (for example, if it is self-intersecting) then still other types of oscillations can exist.

It is not difficult to estimate the order of magnitude of the amplitudes of the oscillations

$$\Delta s_{\mu\nu} \approx e^2an(m^*v_0)^{-1}(v_0T/a)^k \sim H^{-k},$$

where n is the density of electrons and k = 4 or $5/2$ for oscillations of the first or second type, respectively. Estimates in such form are suitable in that they do not depend on the number of components of the tensor $\Delta s_{\mu\nu}$ and on the magnitude of the ratio t_0v_0/a (it is assumed only that $t_0v_0/a \gtrsim 1$). It is then easy to obtain estimates for the relative magnitude of the oscillating part of the specific resistance. For example, if $t_0v_0/a \sim 1$, then

$$s_{\mu\nu} \sim \sigma_{\mu\nu}^{(\infty)} - \sigma_{\mu\zeta}^{(\infty)}\sigma_{\zeta\nu}^{(\infty)}/\sigma_{\zeta\zeta}^{(\infty)},$$

and we find that when $\sin\theta \gg v_0 T/a$, while open trajectories are absent,

$$\Delta r_{\mu\nu} / r_{\mu\nu} \approx (v_0 T / a)^{k-2}.$$

We note in conclusion that the study of oscillations allows us, in a number of cases, to proceed directly to qualitative conclusions regarding the shape of the Fermi surface. The presence of oscillations of the second type points up a significant departure of its shape from the ellipsoidal. The presence of several component oscillations of the first type with different periods demonstrates that the Fermi surface is nonconvex or, that there are several surfaces. Complete disappearance of the oscillations of the first type for certain directions of the magnetic field, not lying in the plane of the film, in the case in which the inequality (1.1) is satisfied, means that the Fermi surface is open in these directions.

[1] E. H. Sondheimer, Phys. Rev. **80**, 401 (1950).

[2] Lifshitz, Azbel', and Kaganov, J. Exptl. Theoret. Phys. (U.S.S.R.) **31**, 63 (1956), Soviet Phys. JETP **4**, 41 (1957).

[3] J. E. Kunzler and C. A. Renton, Phys. Rev. **108**, 1397 (1957).

[4] J. Babkskin and P. G. Siebenmann, Phys. Rev. **107**, 1249 (1957).

[5] M. Ia. Azbel' and E. A. Kaner, J. Exptl. Theoret. Phys. (U.S.S.R.) **32**, 896 (1957), Soviet Phys. JETP **5**, 730 (1957).

[6] E. A. Kaner, J. Exptl. Theoret. Phys. (U.S.S.R.) **34**, 658 (1958), Soviet Phys. JETP **7**, 454 (1958).

Translated by R. T. Beyer
136

SOVIET PHYSICS JETP VOLUME 35(8), NUMBER 3 MARCH, 1959

POLARIZATION OF NUCLEAR MOMENTS AND NUCLEAR-RESONANCE LINE WIDTHS IN CRYSTALS OF CU^{++} ION SALTS

Sh. Sh. BASHKIROV and K. A. VALIEV

Kazan' State Pedagogical Institute

Submitted to JETP editor March 2, 1958

J. Exptl. Theoret. Phys. (U.S.S.R.) 35, 678-684 (September, 1958)

The probabilities of nuclear relaxation transitions in Cu^{++} ion salts are computed. The magnitude of nuclear polarization appearing on saturation of electron and nuclear resonance transitions is calculated. The effect of electron and nuclear relaxation on the broadening of nuclear resonance lines in paramagnetic atoms is considered.

1. INTRODUCTION

IT has been shown by many investigators[1,2] that by saturating the electron magnetic resonance it is possible to obtain polarization of nuclear magnetic moments amounting to several percent at comparatively high temperatures of 1 to 4°K. Later experiments were carried out on the polarization of nuclei by means of saturating "forbidden" electronic transitions, which arise in the second approximation if the constant and the variable magnetic fields are parallel to each other.[3] Feher[4] obtained polarized nuclei by exciting magnetic dipole transitions between energy sublevels of electronic and nuclear spins of paramagnetic atoms.

The success of the above experiments on nuclear polarization depends largely on spin-lattice relaxation processes. Such processes are characterized by the probabilities of electronic transitions $A_{M,M-1}$ (M is the magnetic quantum number of the electron spin of the atom), which occur without a change in the quantum number of nuclear spin, and by the probabilities $a_{m,m-1}$ of nuclear-relaxation transitions. The latter transitions may be accompanied by a change in the orientation of electronic spin from M to $M+1$. Calculations of nuclear polarization, taking into account both electronic and nuclear relaxation transitions, have been carried out by Abragam[2] for the case of a simple atom with $S=\frac{1}{2}$, $I=\frac{1}{2}$ in liquid solutions.

In this paper we calculate the transition probabilities $A_{M,M-1}$ and $a_{m,m-1}$ for doubly-charged copper ions in hydrated crystals. The relations obtained for the probabilities are then used to calculate the polarization of nuclei of Cu^{64} [$I=1$, $|\mu| = 0.40\,\mu_N$ (reference 5)]. It should be noted that the calculations of $a_{m,m-1}$ carried out by the authors[6,7] for a number of rare earth ions and for ions of the iron group can be used to calculate nuclear polarization in salts of these ions.

2. PROBABILITIES OF NUCLEAR RELAXATION TRANSITIONS

Relaxation transitions between hyperfine energy sublevels of the ion are due to the modulation of the hyperfine splittings of the ion by thermal vibrations of the lattice. The lattice vibrations affect directly only the orbital splittings of the ion, but through spin-orbit interactions of the form $\lambda\mathbf{L}\cdot\mathbf{S}$ this leads to a modulation of the intervals between the levels of the electron spin. Changes in the spacing between energy levels of nuclear spin arise, in turn, through the hyperfine magnetic interaction of the ion of the form $AJ_ZS_Z + B(I_XS_X + I_yS_y)$. Thus, the perturbation that gives rise to relaxation transitions between the hyperfine sublevels of the ion has the form:

$$\mathscr{H} = \mathscr{H}_{OL} + \lambda(\mathbf{L}\cdot\mathbf{S}) + AI_zS_z + B(I_xS_x + I_yS_y) \quad (1)$$

For the operator $\mathcal{H}_{OL}$, which connects the normal coordinates of the lattice oscillators q with the orbital angular momentum (electron coordinates) of the magnetic ion, we use Kronig's expression[8]

$$\begin{gathered}\mathscr{H}_{OL} = 8e\mu a^{-5}q\varphi\,[(3z^2-r^2)f_1 + 2(x^2-y^2)f_2 \\ -2xyf_{xy} - 2xzf_{xz} - 2yzf_{yz}], \\ f_1 = (u_z\lambda_z - {}^2/_3\,\lambda_xu_x - {}^2/_3\,u_y\lambda_y), \\ f_2 = (u_x\lambda_x - u_y\lambda_y), \quad f_{ij} = (u_i\lambda_j + u_j\lambda_i).\end{gathered} \quad (2)$$

Here λ, u are unit vectors in the direction of polarization and the direction of propagation of the Debye waves, $r(x, y, z)$ is the distance between the nucleus and the magnetic electron, e is the electronic charge, μ is the effective electric dipole moment of the neutral molecule closest to the

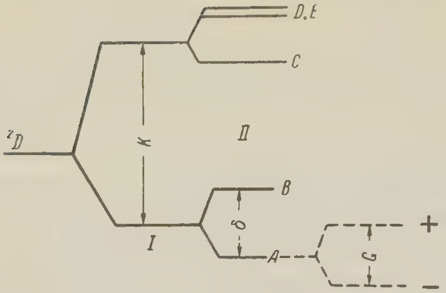

FIG. 1. Diagram of the successive splitting of the ground level of the Cu^{++} ion in an electric field of cubic (I) and tetragonal (II) symmetry. Dotted lines show the splitting of the lower Kramers doublet in an external magnetic field.

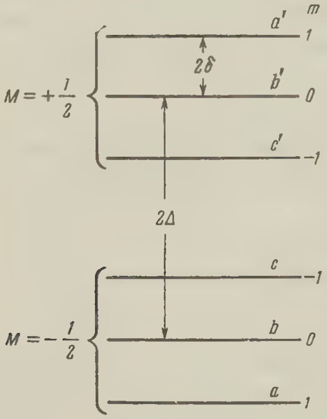

FIG. 2. Diagram of hyperfine splitting of the lower Kramers doublet of the Cu^{++} ion (isotope 64 with spin I = 1).

ion, $\varphi = 2\pi a\nu/c$, c and ν are the velocity and the frequency of the Debye wave, and a is the lattice constant.

In hydrated salts the system of orbital levels of the Cu^{++} ion (^2D ground state) can be characterized by the following wave functions[9] (Fig. 1):

$$\Phi_A = (\psi_2 + \psi_{-2})/\sqrt{2}, \quad \Phi_B \quad \psi_0, \quad \Phi_C = i(\psi_2 - \psi_{-2})/\sqrt{2},$$

$$\Phi_D = i(\psi_1 + \psi_{-1})/\sqrt{2}, \quad \Phi_E = (\psi_1 - \psi_{-1})/\sqrt{2}. \tag{3}$$

The splittings K and δ due to the cubic and tetragonal components of the crystalline field are equal respectively[10] to 12,300 and 1,400 cm^{-1}. Figure 2 shows the hyperfine splittings of the lower Kramers doublet of the ion in a strong magnetic field directed along the axis of symmetry of the crystalline field (G ≫ A, B). The wave functions of these levels have the form

$$\Psi_{M,m} = \varphi_{M,m} + \frac{B}{G} f_{M,m}\varphi_{M-1,m+1} - \frac{B}{G} f_{M+1,m-1}\varphi_{M+1,m-1}, \tag{4}$$

$$f_{M,m} = {}^1/_2[(S+M)(S-M+1)(I+m+1)(I-m)]^{1/2},$$

$$G = g\ \beta H_0.$$

The matrix elements of the perturbation (1) may be easily calculated using the functions (3) and (4). The matrix elements of (2) calculated by the method of equivalent operators are given by Bashkirov.[11]

The perturbation (1) can cause relaxation transitions in which one or two (or more) lattice phonons can take part. At temperatures down to ~1°K the probability of single-phonon processes will be small compared to the probabilities of two-phonon processes. The latter can be calculated by means of the following formula:[12]

$$a_{m,m-1} = 4\pi^2 h^{-2} \times \int_0^{k\Theta/h} H(\pm{}^1/_2, m, n, n'; \pm{}^1/_2, m-1, n-1, n'+1)|^2_{\text{av}}\rho_\nu\rho_{\nu'}d\nu, \tag{5}$$

where n and n′ are quantum numbers of the oscillators q and q′, ρ_ν is the density of lattice oscillators of frequency ν, and Θ is the Debye temperature. The matrix element appearing in (5) differs from zero in the fourth order and is equal to:

$$\mathscr{H}(\pm{}^1/_2, m; \pm{}^1/_2, m-1) = p f_{1/2, m-1}\mathscr{H}'(+{}^1/_2, n, n'; -{}^1/_2, n-1, n'+1) \tag{6}$$

$$\mathscr{H}' = \frac{3\cdot 32^2\lambda h\nu}{\delta^2 K}\left(\frac{e\mu\varphi\bar{r}^2}{a^5}\right)(f_2' f_{xz} + i f_2' f_{yz} - f_2 f_{xz}' - i f_2 f_{yz}')\, q(n, n-1)\, q'(n', n'+1). \tag{6a}$$

The quantity f′ refers to oscillator q′; p = B/G.

It is important to note that the matrix element of the transition between nuclear sublevels is proportional to the matrix element of the transition between electronic sublevels which occurs without a change in the quantum number m. The averaging of (6a) in accordance with formula (5) gives the electronic transition probability A $(\frac{1}{2}, -\frac{1}{2})$. This allows us to express the probabilities of nuclear relaxation transitions in terms of the probabilities of the electronic transitions:

$$a(\pm{}^1/_2, m; \pm{}^1/_2, m-1) = p^2 f^2_{1/2, m-1} A({}^1/_2, -{}^1/_2) = \lambda_1 A. \tag{7}$$

In addition to the relaxation transitions considered above, there are other possible nuclear-relaxation transitions, which involve the simultaneous reorientation of the electronic and nuclear spins. Calculations yield the following relation for the probabilities of such transitions:

$$a({}^1/_2, m; -{}^1/_2, m+1) = 2p^2 f^2_{1/2, m} A = 2\lambda_1 A. \tag{8}$$

The above results can also be presented in the following form (I = 1):

Transition	$\pm{}^1/_2\ m; \mp{}^1/_2\ m$	$M, 1; M, 0$	$M, 0; M, -1$	${}^1/_2, 0; -{}^1/_2, 1$	${}^1/_2, -1; -{}^1/_2, 0$
a_{ij}/A	1	λ_1	λ_1	$2\lambda_1$	$2\lambda_1$

3. POLARIZATION OF Cu^{64} NUCLEI IN PARAMAGNETIC SALTS

We have calculated the polarization of Cu^{64} nuclei in the cases listed above. This is the first time that polarization is calculated by the method of saturating electronic transitions that are forbidden in the first approximation. According to Jeffries,[3] allowance for nuclear-relaxation transitions can decrease the polarization obtained from simple considerations (without detailed account of nuclear transitions) by a factor of ~2. According to our calculations, a noticeable decrease in the polarization due to nuclear transitions is possible only at low intensities of the external field ($G \sim A, B$). The method of nuclear polarization by means of simultaneous saturation of electronic and nuclear resonance discussed below (in subsection B) is of some interest. Feher[4] excited these transitions not simultaneously, but one after the other. This makes possible nuclear polarization only in crystals with a very long electron relaxation time, when the nonequilibrium populations of levels that result from excitation of the (electronic) resonance can be preserved until the instant of excitation of the other (nuclear) resonance. In salts of paramagnetic ions of the iron group, the electronic relaxation times are of the order of $\sim 10^{-3}$ sec at $T = 4°K$ and the method described by Feher[4] cannot be used. The electronic and the nuclear resonances must therefore be excited simultaneously. The results of the calculations are discussed below.

(A) We first consider the case when two electronic resonance transitions are saturated by a radio frequency field: $a \rightarrow a'$, $b \rightarrow b'$. We denote by $a, b \ldots c'$ the relative level populations and set up the system of equations for the populations in the nonequilibrium state which has been established:[13]

$$\frac{dx_i}{dt} = \sum_j{}' (x_j W_{ji} - x_i W_{ij}) = 0, \quad x_i = a, b, \ldots, c', \tag{9}$$
$$W_{aa'} = a_{aa'} + V_{aa'}, \quad W_{bb'} = a_{bb'} + V_{bb'}, \quad W_{ij} = a_{ij}.$$

Here $V_{aa'}$ and $V_{bb'}$ are the probabilities of magnetic dipole transitions produced by the variable external field.* The probabilities of the direct and the inverse transitions are connected by the following relations:[13]

$$a_{ij} \exp(-\varepsilon_i / kT) = a_{ji} \exp(-\varepsilon_j / kT), \quad V_{aa'} = V_{a'a}. \tag{10}$$

The nonzero probabilities a_{ij} have been calculated earlier. The system (9) must be solved subject to the conditions of saturation and normalization: $a = a'$; $b = b'$; $a + b + \ldots + c' = 1$.

The constants in Eq. (9) are of the following order of magnitude: $\Delta = 0.1$, $\delta = 10^{-3}$, and $\lambda_1 = 10^{-4}$ at $T = 4°K$ and $H_0 = 3{,}000$ Oe; $\Delta = 0.4$ and $\delta = 2 \times 10^{-3}$ at $T = 1°K$. It is seen that at these temperatures we can expand the exponentials and retain only one term of the expansion. The resultant solution of (9) is of the form:

$$a = a' = b(1 + \Delta), \quad c = b(1 + \Delta/2),$$
$$c' = b(1 - 3\Delta/2), \quad b = b'. \tag{11}$$

In expressions (11) we have omitted terms proportional to λ_1, δ, and their products. For the field intensity used in the experiments ($\sim 10^{-4}$ Oe), the contribution of these terms to the polarization will be small.*

We have also considered the case of saturation of a single electronic transition: $a \rightarrow a'$. The solution which we have obtained is of the form:

$$a = a' = b(1 - \Delta/2), \; b' = b(1 - 2\Delta),$$
$$c' = b(1 - 2\Delta), \; c = b. \tag{12}$$

(B) We give the solution of equations (9) for the case of simultaneous saturation of electronic and nuclear transitions, $a \rightarrow a'$; $b' \rightarrow a'$:

$$a = a' = b' = b(1 - 2\Delta),$$
$$c' = b(1 - 2\Delta), \; c = b. \tag{13}$$

We now compare the results given by (11) to (13). It is convenient to describe the resultant polarization by the ratio $(a + a')/(b + b')$. This ratio is given in the three cases by $1 + \Delta$, $1 + \Delta/2$, $1 - \Delta$ respectively. Polarization due to saturating two electronic transitions or to simultaneous saturation of electronic and nuclear transitions is twice the polarization due to saturating a single electronic transition. It is evident that it is difficult to realize simultaneous saturation of two electronic transitions. It is easier to realize saturation of a nuclear and an electronic transition, and this would give rise to the same degree of nuclear polarization.

(C) We now give the calculated polarization of Cu^{64} nuclei by saturation of "forbidden" transitions. From the form of the wave functions given by (4) it follows that the transitions will be $a \rightarrow b'$ and $b \rightarrow c'$. We consider the case when the transition $a \rightarrow b'$ is saturated. The level populations and the polarization which are established in this case are given by:

---

*It is assumed that equilibrium in the spin system is established through the interaction of the spins with the lattice; this is the case in magnetically-diluted crystals.

*It is worth noting that the probabilities of nuclear transitions characterize the duration of the transition processes from the time of switching on the rf resonance field until the time that a stationary population of levels becomes established.

$$b' = c' = a, \; a' = a(1-2\Delta), \qquad c = a(1+2\Delta), \; b = a(1+2\Delta). \tag{14}$$

This corresponds to the appearance of nuclear polarization along directions of nuclear spin with projections $m = 0, -1$.

(D) We now discuss briefly the question of the saturation of nuclear resonance transitions. Let us ascertain which relaxation transitions, nuclear or electronic, determine whether a splitting of nuclear resonance is possible. To do this we must find the population of levels in the presence of the resonance field and we must determine the saturation parameter:[13]

$$S(\mathscr{H}_1) = (a-b)/(a_0-b_0) = (1 + V/W)^{-1}, \tag{15}$$

where a, b are the populations of the levels between which resonance takes place (the subscript zero refers to the population of the level in the absence of the resonance field $\mathscr{H}_1$): V is the probability of resonance transitions to which the field $\mathscr{H}_1$ gives rise; W is the probability of all the relaxation transitions $b \rightarrow a$. In addition to the direct relaxation transition $b \rightarrow a$ with the probability $a(0; 1)$, two other transitions via intermediate levels are possible: $b \rightarrow b' \rightarrow a$ and $b \rightarrow b' \rightarrow a' \rightarrow a$. The efficiency of these latter processes is evidently determined by the least probable of the transitions involved, i.e., by the probabilities of nuclear transitions $b' \rightarrow a$ and $b' \rightarrow a'$. It follows from this that $W \approx a_{ba} + a_{b'a} + a_{b'a'}$. Our exact calculation of W leads to the same result.

Thus, saturation of nuclear resonance in the case of paramagnetic atoms depends only on the probabilities of nuclear relaxation transitions. We also note that the degree of saturation of nuclear resonance depends strongly on the intensity of the constant field due to the quadratic decrease of the probabilities W as the field decreases.

4. WIDTH OF MAGNETIC RESONANCE LINES OF NUCLEI OF PARAMAGNETIC ATOMS

Valiev[6,7] and Bashkirov[7] have studied theoretically the possibility of experimental investigation of paramagnetic crystals by means of observing magnetic resonance of nuclei of paramagnetic atoms. It was found that the energy absorbed in nuclear resonance in the case of paramagnetic atoms is considerably larger than the energy absorbed by the resonance of nuclei of diamagnetic atoms. The possibility of directly observing the effect depends, in addition to the amount of energy absorbed, also to a large extent on the line width. Valiev[6] has given an approximate estimate of the width of the lines in question by means of the relation: $\Delta\nu_{m-1,m} = 1/a_{m,m-1}$ where $a_{m,m-1}$ is the probability of a relaxation transition between the hyperfine sublevels of the ion. However, this relation will be valid only at very low temperatures. Let us consider the example of the Cu^{++} ion.

The width of the resonance line arising as a result of transitions between a certain pair of hyperfine sublevels, for example a and b, is equal to the sum of the widths of these sublevels: $\Delta\nu_{a,b} = \gamma_a + \gamma_b$. The level width, in turn, is equal to the sum of the probabilities of all the relaxation transitions originating from that level; in our case $\gamma_a = A_{aa'} + a_{ab} + a_{ab'}$; $\gamma_b = A_{bb'} + a_{ba} + a_{bc} + a_{bc'}$. As we have shown above the ratio a_{ij}/A is of the order 10^{-4} for an external field intensity ~5,000 Oe and at relatively high temperatures. From this it follows that the line width of nuclear resonance is mainly determined by the probabilities of electronic relaxation transitions. Nuclear relaxation transitions will determine line widths only at very low temperatures, as can be seen from the following. Electronic transitions originating in the level $M = -\frac{1}{2}$ are accompanied by absorption of energy of lattice vibrations; therefore at low temperatures (when single-phonon processes predominate) the probability $A(-\frac{1}{2}, \frac{1}{2})$ is proportional to the average number of phonons of the lattice oscillator with the electronic resonance frequency $\nu_e : A \sim \bar{n}_{\nu_e} = [\exp(h\nu_e/kT) - 1]^{-1}$. On the other hand, the probabilities a_{ij} are proportional to $\bar{n}_{\nu_N} + 1$ or $\bar{n}_{\nu_N}$ (depending on whether the lattice phonon is absorbed or emitted in the transition $i \rightarrow j$; ν_N is the frequency of nuclear resonance). It can be easily seen that in the temperature region $h\nu_N/k \ll T \ll h\nu_e/k$, $\bar{n}_{\nu_e} \ll 1$ and the number of electronic transitions is sharply decreased, while $\bar{n}_{\nu_N} \gg 1$ and the number of nuclear transitions is still relatively large. Under these conditions the ratio a_{ij}/A may be greater than unity. Nevertheless, right down to temperatures ~1°K, the main contribution to the line width of nuclear resonance is made by electronic transitions.

At liquid-helium temperatures the probabilities $A \sim 10^3\ \mathrm{sec}^{-1}$ for most paramagnetic ions of the iron group, which corresponds to a line width of $\sim 10^3$ cps. Such lines may be observed by quadrupole-resonance techniques or by modulating the constant magnetic field. Spectroscopes employing field modulation are capable of detecting nuclear resonance lines 10 Oe wide.[14] To observe nuclear resonance in the case of magnetic atoms, the probabilities of electronic relaxation transitions of these atoms, expressed in oersteds (by means of the relation $hA = \gamma\beta_N\Delta H$), must therefore be of the order of 10 Oe. This is the case when A $\sim 10^4$ sec^{-1}. The probabilities A in the case of salts of ions which are in the S state (Mn^{++}, Gd^{+++}) turn out to be of the order of 10^4 sec^{-1} already at liquid hydrogen temperatures.[15] Under these conditions it is possible to observe the effect directly.

It should be noted that an important condition for observing this effect is the proper choice of resonance frequency, since it is practically impossible to attain resonance by varying the magnetic field, owing to the weak dependence of the resonance frequency on the field (it is determined by the constants A, B of the magnetic coupling between the electronic and the nuclear spins of the ion).

---

[1] A. Overhauser, Phys. Rev. **89**, 689 (1953); F. Bloch, Phys. Rev. **93** 944 (1954).

[2] A. Abragam, Phys. Rev. **98**, 1729 (1955).

[3] C. D. Jeffries, Phys. Rev. **106**, 164 (1957).

[4] G. Feher, Phys. Rev. **103**, 500 (1956); G. Feher and E. A. Gere, Phys. Rev. **103**, 501 (1956).

[5] Kiults, Kunts, and Khartman, Usp. Fiz. Nauk **55**, 537 (1955).

[6] K. A. Valiev, J. Exptl. Theoret. Phys. (U.S.S.R.) **33**, 1045 (1957), Soviet Phys. JETP **6**, 804 (1958).

[7] K. A. Valiev, Физика металлов и металловедение (Physics of Metals and Metal Research) **6**, 2 (1958); Sh. Sh. Bashkirov, Уч. зап. Каз. ун-та (Sci. Notes of Kazan' University) **117**, No. 9, 154 (1957).

[8] R. Kronig, Physica **6**, 33 (1939).

[9] A. Abragam and M. Pryce, Proc. Roy. Soc. **A206**, 164 (1951).

[10] J. Owen, Proc. Roy. Soc. **A227**, 183 (1955).

[11] Sh. Sh. Bashkirov, J. Exptl. Theoret. Phys. (U.S.S.R.) **34**, 1465 (1958), Soviet Phys. JETP **7**, 1013 (1958).

[12] J. H. Van Vleck, Phys. Rev. **57**, 426 (1940).

[13] J. P. Lloyd and G. E. Pake, Phys. Rev. **94**, 579 (1954).

[14] N. Fuschillo and C. Reuton, Nature **180**, 1063 (1957).

[15] C. J. Gorter, Paramagnetic Relaxation, Amsterdam, 1947 (Russ. transl. IIL 1949).

Translated by G. Volkoff
137

SOVIET PHYSICS JETP VOLUME 35(8), NUMBER 3 MARCH, 1959

WAVE FUNCTIONS OF MANY-ELECTRON SYSTEMS

V. I. PEREL'

Leningrad State University

Submitted to JETP editor March 26, 1958

J. Exptl. Theoret. Phys. (U.S.S.R.) **35**, 685-690 (September, 1958)

A general form has been derived for a wave function which is an eigenfunction of S^2 and S_z and satisfies the Pauli principle. An expression is given for the Schrödinger wave function of the system constructed from one-electron functions.

1. INTRODUCTION

In many problems in the quantum mechanics of many-electron systems one can in first approximation neglect the spin dependence of the Hamiltonian. Then the determination of the wave function consists in the approximate solution of the Schrödinger equation containing only spatial coordinates. However, the symmetry properties of the Schrödinger wave function depend on the total spin of the system. Fock[1] derived the symmetry conditions which the Schrödinger wave function has to satisfy in order for the total wave function of the system to be an eigenfunction of S^2 ($\mathbf{S}$ is the total spin operator) and to satisfy the Pauli principle. Fock showed that these conditions are satisfied by a product of determinants consisting of one-electron functions, if the same coordinate function is taken for every pair of electrons with opposite spins. However, there exist methods of solving the Schrödinger equation which do not introduce only one-electron functions (the method of partial separation of variables, the adiabatic method, etc.). On the other hand, even in the approximation that uses one-electron functions we cannot use the simple product of determinants in those cases when two electrons with opposite spins are known to be in different states (e.g., the case of the singlets of the alkaline-earth elements).

In these cases it is often difficult to construct from the approximate solution of the Schrödinger equation a Schrödinger function which satisfies the Fock conditions, or a total wave function of the system. The method of the Young scheme[2] and the method of Abarenkov[3] have the disadvantage that they do not give sufficiently convenient expressions for the total and the Schrödinger wave function of the system.

We shall show below that the Schrödinger and the total wave functions are most conveniently constructed from a given approximate solution of the Schrödinger equation with the help of operators transforming an arbitrary function into an eigenfunction of J^2 and J_z ($\mathbf{J}$ is the spin, orbital, or total angular momentum of the system in units of $\hbar$). We shall call them the characteristic operators for J^2 and J_z.

2. THE CHARACTERISTIC OPERATORS FOR J^2 AND J_z AND THEIR PROPERTIES

We introduce the operator A^j_{pq}, which operates on the function $g(x_1, \ldots, x_n)$ according to

$$A^j_{pq} g = \int_0^{2\pi} d\varphi \int_0^{2\pi} d\psi \int_0^{\pi} \sin\vartheta \, d\vartheta \cdot \overline{f^j_{pq}}(\varphi, \vartheta, \psi) P_{\varphi,\vartheta,\psi} g. \qquad (1)$$

Here $x_1, \ldots, x_n$ are the coordinates of the particles of the system (both spin and spatial), $P_{\varphi,\vartheta,\psi}$ is the rotation operator of the coordinate system given by the Eulerian angles φ, ϑ, ψ. It operates either on the spin or on the spatial coordinates, or on both, depending on the character of the angular momentum J. Also,

$$f^j_{pq} = (2\pi)^{-2} e^{ip\varphi} e^{iq\psi} F^j_{pq}(\vartheta); \qquad (2a)$$

$$F^j_{pq} = M^{ab}_n \left(\cos\frac{\vartheta}{2}\right)^b \left(i \sin\frac{\vartheta}{2}\right)^a G^{ab}_n(\cos\vartheta); \qquad (2b)$$

$$G^{ab}_n(x) = \frac{(-1)^n}{n!\,2^n} (1-x)^{-a} (1+x)^{-b} \frac{d^n}{dx^n} \times (1-x)^{a+n} (1+x)^{b+n}; \qquad (2c)$$

$$M^{ab}_n = \frac{a+b+2n+1}{2} \sqrt{\frac{n!\,(a+b+n)!}{(a+n)!\,(b+n)!}}; \qquad (2d)$$

$$a = |p-q|; \; b = |p+q|; \quad j = n + \frac{a+b}{2}; \; n = 0, 1, 2\ldots \qquad (2e)$$

Each of the numbers p and q may thus take any value from $-j$ to j in steps of unity, $G^{ab}_n(x)$ is the Jacobi polynomial.[4] The functions $f^j_{p,q}$ are, up to a numerical factor, the matrix elements of the irreducible representation of the rotation group.[5] In fact,

$$f^j_{pq}(\varphi, \vartheta, \psi) = \frac{2j+1}{8\pi^2} D^j(P_{\varphi, \vartheta, \psi})_{pq}.$$

We shall in the following assume that the function g may be expanded into a series in terms of eigenfunctions of J^2 and J_z, corresponding to either only integer or only half odd-integer values j. Group theory[5,6] yields the following fundamental property of the operators A^j_{pq}.

If $g^{j'}_m$ is an eigenfunction of J^2 and J_z with eigenvalues $j'(j'+1)$ and m, respectively, then

$$A^j_{pq} g^{j'}_m = \delta_{jj'} \delta_{qm} g^j_p. \tag{3}$$

From this we derive the following properties:

$$J^2 A^j_{pq} = A^j_{pq} J^2 = j(j+1) A^j_{pq}, \tag{4}$$

$$J_z A^j_{pq} = p A^j_{pq}, \tag{5}$$

$$A^j_{pq} J_z = q A^j_{pq}, \tag{6}$$

$$(J_x \pm iJ_y) A^j_{pq} = \sqrt{(j \mp p)(j \pm p + 1)}\, A^j_{p \pm 1, q}, \tag{7}$$

$$A^j_{pq}(J_x \mp iJ_y) = \sqrt{(j \pm q)(j \mp q + 1)}\, A^j_{p, q \mp 1}, \tag{8}$$

$$A_{pt} A^{j'}_{t'q} = \delta_{jj'} \delta_{tt'} A^j_{pq}, \tag{9}$$

$$\sum_{j, p} A^j_{pp} = 1, \tag{10}$$

$$A^{j+}_{pq} = A^j_{qp}. \tag{11}$$

In the last formula, A^{j+}_{pq} is the hermitian conjugate operator to A^j_{pq}. In formulas (3) to (11) the values j, j′ can be either all integers, or all odd half-integers.

If the Hamiltonian of the system H is invariant under the rotations $P_{\varphi\vartheta\psi}$, then clearly

$$H A^j_{pq} = A^j_{pq} H. \tag{12}$$

In this case the operators A^j_{pq} have the following extremal property. Let g_m be an approximate solution of the Schrödinger equation which is not an eigenfunction of J^2, but which is an eigenfunction of J_z with eigenvalues m. We can construct new functions from g_m by a rotation of the coordinate system. All functions obtained in this way give the same expectation value for the energy.

We form

$$u = \int_0^{2\pi} d\varphi \int_0^{2\pi} d\psi \int_0^{\pi} \sin\vartheta\, d\vartheta \cdot f(\varphi, \vartheta, \psi) P_{\varphi\vartheta\psi} g_m \tag{13}$$

and take $f(\varphi, \vartheta, \psi)$ such that the functional

$$I = (u, Hu) \text{ with the condition } (u, u) = 1 \tag{14}$$

has an extremal value. For this purpose we expand $f(\varphi, \vartheta, \psi)$ in a series of the functions f^j_{pq}:

$$f = \sum_{j, p, q} a^j_{pq} f^j_{pq}(\varphi, \vartheta, \psi),$$

from where we get

$$u = \sum_{j, p} a^j_{pm} A^j_{pm} g_m.$$

Taking a^j_{pm} as the variation parameters and using the properties of the operators A^j_{pm}, we can easily show that the functional (14) has an extremal value for the functions

$$u^j_{pm} = A^j_{pm} g_m / (A^j_{mm} g_m, g_m), \tag{15}$$

and the corresponding energy values are given by the expression

$$E_{jm} = (A^j_{mm} g_m, H g_m) / (A^j_{mm} g_m, g_m), \tag{16}$$

where, according to (22), $j = |m| + n$, $n = 0, 1, 2, \ldots$ This property of the operators A^j_{pq} was recently used in the theory of the nucleus.[7]

3. THE SCHRÖDINGER WAVE FUNCTION FOR THE MANY-ELECTRON SYSTEM

In this section A^s_{pq} denotes the characteristic operator for S^2 and S_z. (**S** is the vector of the spin angular momentum of the system of N electrons in units of ħ).

We introduce two functions of the z component of the spin of electron i (we call this component $\frac{1}{2}\sigma_i$):

$$u_i = \begin{matrix} 1 & \text{for } \sigma_i = -1 \\ 0 & \text{for } \sigma_i = 1 \end{matrix}, \quad v_i = \begin{matrix} 0 & \text{for } \sigma_i = -1 \\ 1 & \text{for } \sigma_i = 1 \end{matrix}. \tag{17}$$

We use the notation

$$e_{\alpha_1 \ldots \alpha_k} = u_1 \ldots u_k v_{k+1} \ldots v_N. \tag{18}$$

This is an eigenfunction of S_z with eigenvalues s, if $k = N/2 - s$.

An arbitrary function of the spin variables with a given value for the projection of the total spin can be expanded in terms of the functions $e_{\alpha_1 \ldots \alpha_k}$ with various sets $\alpha_1, \ldots, \alpha_k$. Hence, because of the properties of the operator A^s_{pq}, an arbitrary function of the spin coordinates which is an eigenfunction of S^2 and S_z with eigenvalues $s(s+1)$ and m, respectively, can be represented as a linear combination of functions $A^s_{ms} e_{\alpha_1 \ldots \alpha_k}$.

Let now $\Psi(\mathbf{r}_1, \ldots, \mathbf{r}_N)$ be an approximate solution of the Schrödinger equation which is independent of spin. The problem is now to use this solution in order to construct the total wave function for the system satisfying the Pauli principle and being an eigenfunction of S^2 and S_z (we shall in the following call a function satisfying these three conditions, a "correct" function). It follows that the most general "correct" function which can be constructed from Ψ is an arbitrary linear combination of terms

$$A^s_{ms} A \Psi(\mathbf{r}_1 \ldots \mathbf{r}_N) e_{\alpha_1 \ldots \alpha_k} \tag{19}$$

with various sets $\alpha_1 \ldots \alpha_k$ (A is the antisymmetrization operator). We may take the numbers $\alpha_1 \ldots \alpha_k$ to give the places in the function Ψ corresponding to a negative spin projection. The remaining places correspond to positive spin projection. Thus the most general "correct" function derivable from Ψ is an arbitrary linear combination of expressions obtained from

$$A^s_{ms} A \Psi(\mathbf{r}_1, \ldots, \mathbf{r}_N) e_{1 \ldots k} \tag{20}$$

by interchanging the numbers designating the places corresponding to the negative spin projection in the function Ψ.

We now consider the principal case, when Ψ is expressed as a product of one-electron functions:

$$\Psi(\mathbf{r}_1, \ldots, \mathbf{r}_N) = \Psi_1(\mathbf{r}_1) \Psi_2(\mathbf{r}_2) \ldots \Psi_N(\mathbf{r}_N). \tag{21}$$

In this case the position number of the argument coincides with the number of the one-electron function. The first k functions in (20) correspond to negative spin projection; the remaining functions, to positive spin projection. Furthermore, $h_k = A\Psi_1(r_1) \ldots \Psi_N(r_N) e_{1 \ldots k}$ is simply the Slater determinant:

$$h_k = \begin{vmatrix} \Psi_1(\mathbf{r}_1) u_1 & \ldots & \Psi_1(\mathbf{r}_N) u_N \\ \ldots & \ldots & \ldots \\ \Psi_k(\mathbf{r}_1) u_1 & \ldots & \Psi_k(\mathbf{r}_N) u_N \\ \Psi_{k+1}(\mathbf{r}_1) v_1 & \ldots & \Psi_{k+1}(\mathbf{r}_N) v_N \\ \ldots & \ldots & \ldots \\ \Psi_N(\mathbf{r}_1) v_1 & \ldots & \Psi_N(\mathbf{r}_N) v_N \end{vmatrix}. \tag{22}$$

We note that

$$P_{\varphi\vartheta\psi} u_i = \beta v_i + \delta u_i; \quad P_{\varphi\vartheta\psi} v_i = \alpha v_i + \gamma u_i,$$

where α, β, γ, δ are the Cayley-Klein parameters:

$$\begin{pmatrix} \alpha & \beta \\ \gamma & \delta \end{pmatrix} = \begin{pmatrix} \cos\frac{\vartheta}{2} e^{i(\varphi+\psi)/2} & i\sin\frac{\vartheta}{2} e^{i(\varphi-\psi)/2} \\ i\sin\frac{\vartheta}{2} e^{i(\psi-\varphi)/2} & \cos\frac{\vartheta}{2} e^{-i(\varphi+\psi)/2} \end{pmatrix}. \tag{23}$$

Using the properties of the operator A^s_{pq}, we easily obtain

$$A^s_{ms} h_k = \sqrt{\frac{(s+m)!}{(s-m)!\,(2s)!}} (S_x - iS_y)^{s-m} A^s_{ss} h_k, \tag{24}$$

$$A^s_{ss} h_k = \sum_{(\alpha)} \Phi^s_{\alpha_1 \ldots \alpha_k} e_{\alpha_1 \ldots \alpha_k}, \tag{25}$$

where we sum over all possible sets $\alpha_1 \ldots \alpha_k$, and

$$\Phi^s_{1,2\ldots k} = \frac{2s+1}{2} \int_0^{\pi} \left(\cos\frac{\vartheta}{2}\right)^{2s} \sin\vartheta \, d\vartheta \begin{vmatrix} \Psi_1(\mathbf{r}_1)\cos\frac{\vartheta}{2} \ldots \Psi_1(\mathbf{r}_k)\cos\frac{\vartheta}{2} & \Psi_1(\mathbf{r}_{k+1})\, i\sin\frac{\vartheta}{2} \ldots \Psi_1(\mathbf{r}_N)\, i\sin\frac{\vartheta}{2} \\ \ldots & \ldots \\ \Psi_k(\mathbf{r}_1)\cos\frac{\vartheta}{2} \ldots \Psi_k(\mathbf{r}_k)\cos\frac{\vartheta}{2} & \Psi_k(\mathbf{r}_{k+1})\, i\sin\frac{\vartheta}{2} \ldots \Psi_k(\mathbf{r}_N)\, i\sin\frac{\vartheta}{2} \\ \Psi_{k+1}(\mathbf{r}_1)\, i\sin\frac{\vartheta}{2} \ldots \Psi_{k+1}(\mathbf{r}_k)\, i\sin\frac{\vartheta}{2} & \Psi_{k+1}(\mathbf{r}_{k+1})\cos\frac{\vartheta}{2} \ldots \Psi_{k+1}(\mathbf{r}_N)\cos\frac{\vartheta}{2} \\ \ldots & \ldots \\ \Psi_N(\mathbf{r}_1)\, i\sin\frac{\vartheta}{2} \ldots \Psi_N(\mathbf{r}_k)\, i\sin\frac{\vartheta}{2} & \Psi_N(\mathbf{r}_{k+1})\cos\frac{\vartheta}{2} \ldots \Psi_N(\mathbf{r}_N)\cos\frac{\vartheta}{2} \end{vmatrix} \tag{26}$$

$\Phi^s_{\alpha_1 \ldots \alpha_k}$ differs from (26) in that $\cos(\vartheta/2)$ appears in those elements of the determinant which stand at the intersection of the columns with numbers $\alpha_1 \ldots \alpha_k$ and the first k rows, and also in the elements remaining after these columns and rows are crossed out. All other elements contain $i \sin(\vartheta/2)$.

Formula (26) gives an expression for the Schrödinger function corresponding to the "correct" function (24) (by Schrödinger function we mean the function of spatial coordinates which may be substituted for the total wave function in the calculation of the matrix elements of symmetric, spin-independent operators).

If the first k one-electron functions are linear combinations of the remaining N-k functions the right hand side of (26) reduces to the usual product of determinants. In the general case the right hand side of (26) may easily be written in the form of a linear combination of products of determinants, by expanding the determinant under the integral according to the minors constructed from the first k rows.

We introduce a general formula for the result of operating on the Slater determinant with the operator A^s_{pq}:

$$A^s_{pq} h_l = \sum_{(\alpha)} \Phi^{spq}_{\alpha_1 \ldots x_m} e_{\alpha_1 \ldots \alpha_m}; \quad l = \frac{N}{2} - q; \quad m = \frac{N}{2} - p, \tag{25a}$$

$$\Phi^{spq}_{\alpha_1 \ldots \alpha_m} = \int_0^{\pi} \overline{F^s_{pq}}(\vartheta) \Delta^l_{\alpha_1 \ldots \alpha_m} \sin\vartheta \, d\vartheta, \tag{26a}$$

where F^s_{pq} is given by (26), and $\Delta^l_{\alpha_1 \ldots \alpha_m}$ is a determinant differing from the determinant in (26) only in that $\cos(\vartheta/2)$ appears in the elements standing at the intersection of the columns with numbers $\alpha_1 \ldots \alpha_m$ and the first l rows, and also in the elements remaining after these columns and rows are crossed out. The other elements contain i sin $(\vartheta/2)$. $\Phi^{spq}_{\alpha_1\ldots\alpha_m}$ is the Schrödinger function for the "correct" function (25a).

$A^s_{pq}h_l$ can also be expressed as a linear combination of Slater determinants $h_{\alpha_1\ldots\alpha_m}$, which differ from h_l only in that here the spin factors u appear in the elements of the rows with numbers $\alpha_1\ldots\alpha_m$, while the elements of the remaining rows contain the spin factors v:

$$A^s_{pq}h_l = \sum_{(\alpha)} C^{st_\alpha}_{pq} h_{\alpha_1\ldots\alpha_m}, \tag{27}$$

where we sum over all sets $\alpha_1\ldots\alpha_m$. Here

$$C^{st_\alpha}_{pq} = \int\limits_0^\pi \overline{F^s_{pq}(\vartheta)} \left(\cos\frac{\vartheta}{2}\right)^{p+q+2t_\alpha} \left(i\sin\frac{\vartheta}{2}\right)^{N-p-q-2t_\alpha} \sin\vartheta\, d\vartheta; \tag{28}$$

t_α is the number of common elements in the sets $1, 2, \ldots, l$ and $\alpha_1, \ldots, \alpha_m$; l and m are related to p and q through (25a). A special case of the expansion (27) is formula (15) in Loewdin's paper.[8] We note that his projection operators ${}^{2l+1}\Theta$ are related to the operators A^s_{pq} in the following way:

$$ {}^{(2s+1)}\Theta = \sum_{p=-s}^{s} A^s_{pp}. \tag{29}$$

I am very grateful to M. I. Petrashen', E. E. Fradkin, Iu. N. Demkov, and E. D. Trifonov for discussions of this paper.

---

[1] V. A. Fock, J. Exptl. Theoret. Phys. (U.S.S.R.) **10**, 961 (1940).

[2] H. Weyl, *Gruppentheorie und Quantenmechanik*, Leipzig, 1928.

[3] I. V. Abarenkov, Вестник ЛГУ (Bulletin, Leningrad State Univ.) No. 10 (1955).

[4] D. Jackson, *Fourier Series and Orthogonal Polynomials* (Russ. Transl., M., 1948).

[5] I. M. Gel'fand and Z. Ia. Shapiro, Usp. mat. nauk **1**, 3 (1952).

[6] E. Wigner, *Gruppentheorie und ihre Anwendung auf die Quantenmechanik der Atomspektren*, Braunschweig, 1931.

[7] R. E. Peierls and J. Yoccoz, Proc. Phys. Soc. **A70**, 381 (1957).

[8] P. O. Loewdin, Phys. Rev. **97**, 1509 (1955).

Translated by R. Lipperheide
138

SOVIET PHYSICS JETP VOLUME 35(8), NUMBER 3 MARCH, 1959

ON THE THEORY OF PARAMAGNETIC RESONANCE IN METALS

M. Ia. AZBEL', V. I. GERASIMENKO, and I. M. LIFSHITZ

Physico-Technical Institute, Academy of Sciences, Ukrainian S.S.R.

Submitted to JETP editor March 29, 1958

J. Exptl. Theoret. Phys. (U.S.S.R.) **35**, 691-702 (September, 1958)

On the basis of the general theory,[1] we have investigated the dependence of the surface impedance of metals in paramagnetic resonance on the dispersion of conduction electrons and on the angle of inclination of the constant magnetic field to the surface of the metal. The case of resonance saturation is examined.

1. INTRODUCTION

PARAMAGNETIC resonance occurs in a metal the electrons of which possess paramagnetic susceptibility when the metal is placed in both a constant magnetic field H_0 and an alternating electromagnetic field H_1 with the frequency $\omega = \Omega_0 \equiv 2\mu H_0/\hbar$. Much experimental work[2] has been done in recent years on paramagnetic resonant absorption of electromagnetic waves impinging on metals.

Dyson[3] was the first to include electron diffusion from the skin layer in a theoretical examination of this effect. His theory is based on the free-electron model, that is, the conduction electrons were regarded as free particles obeying the dispersion law $\epsilon(\mathbf{p}) = p^2/2m^*$. A formula was derived for the surface impedance when the constant magnetic field H_0 is perpendicular to the metal surface and the strength of the alternating field $H_\perp$ is such that resonance saturation is far from being reached.

In reference 1 the present authors developed a theory of paramagnetic resonance, based on a solution of the equation for the density operator of electrons regarded as a gas of noninteracting quasi-particles with an arbitrary dispersion law $\epsilon(\mathbf{p})$. This theory is free of limitations on the direction of the constant field H_0 and the strength of the alternating field H_1. However, in the surface impedance of the metal was not obtained in that article. In addition to the case considered by Dyson, it is of interest to consider the dependence of surface impedance on the angle of inclination of the constant magnetic field to the metal surface, to determine the influence of dispersion upon impedance, and to study the case of alternating fields strong enough to produce resonance saturation. The present article is devoted to these questions.

We shall make a few preliminary remarks on the relation of impedance to dispersion and to the angle of inclination ψ of H_0 to the metal surface. First, it is clear that in specimens of thickness $d \ll \delta$ (δ is the skin thickness) the electron dispersion is quite unimportant. This is due to the fact that an electron is always in a field the amplitude and phase of which are identical at all points of the specimen, so that the probability of spin reversal per unit time does not have to depend on the character of electron motion. We shall not consider the question of the influence of dispersion on the spin relaxation time T_{sp}, which is always included in the theory as a parameter. It is also evident that impedance will not depend on the angle of inclination of H_0 to the surface.

The situation changes when we pass to bulk metal, where $\delta_{eff} \ll d$ (δ_{eff} is the electron diffusion depth; it will be shown below that for metals we almost always have $\delta \ll \delta_{eff}$). In a strong field H_0, when the radius r of the electron orbit is much shorter than the mean free path l, we can expect the impedance to depend on the angle ψ. Indeed, in a strong field ($r \ll l$) an electron can perform l/r revolutions between two successive collisions with the lattice. It is also easily seen that for a strong field the resonance frequency $\omega = \Omega_0$ is in the region of the anomalous skin effect. For all actually obtainable fields $r \gg \delta$. Therefore when the field H_0 is almost parallel to the metal surface ($\psi \ll r/l$) electrons which are close to the surface in a layer with thickness of the order of r will return l/r times to the skin layer, that is, they will remain in the skin layer l/r times longer than in the case of a perpendicular field. Correspondingly, the resonance amplitude will be enhanced by a factor of l/r compared with the effect when the field H_0 is perpendicular to the metal surface. Stronger resonance results from the fact that the probability of spin reversal increases with the time that an electron spends in the skin layer. In a weak magnetic field ($r \gg l$) the resonance is not enhanced because collisions with the lattice will prevent an electron from continually returning to the skin layer.

It must be noted that the picture of resonance which has just been given becomes somewhat complicated for the following reasons. We know that electron energy levels ϵ are isoenergetic surfaces $\epsilon(\mathbf{p}) = \epsilon$ in momentum space possessing a definite orientation with respect to the axes of the reciprocal lattice. Two kinds of surfaces can be distinguished—closed and opened surfaces. In the first case for any orientation of the constant magnetic field H_0 with respect to the crystal axes the electron trajectory in the momentum space (the cross section of the surface $\epsilon(p) = \epsilon$ with the plane $p_z = \text{const}$, where p_z is the conserved projection of the quasi-momentum on the direction of H_0) will be closed, that is, the electron will perform a finite (periodic) motion in a plane perpendicular to the field. For open surfaces both closed and open trajectories in momentum space are possible depending on the orientation of the magnetic field; in the latter case the electron will perform an infinite motion in a plane perpendicular to the field. We now note that because of the Fermi-Dirac distribution a contribution to resonance will not be given by all conduction electrons but only by those with energy in the range $\Delta\epsilon \sim kT$ close to the Fermi energy limit ϵ_0, where $kT \gg \mu H_0$ (or in the range $\Delta\epsilon \sim \mu H_0$, where $kT \lesssim \mu H_0$). Therefore the following cases are possible:

(a) In the interval $\Delta\epsilon$ there are no open surfaces. Then in a strong field H_0 parallel to the metal surface we can expect intensified resonance compared with the case of a field perpendicular to the surface.

(b) In the interval $\Delta\epsilon$ we have open and closed isoenergetic surfaces. Here also resonance will be intensified in a strong field H_0 parallel to the metal surface because of the electrons with closed trajectories in momentum space.

(c) In the interval $\Delta\epsilon$ there are only open isoenergetic surfaces. If the orientation of the metal surface plane is then such that in a field parallel to the surface the electron trajectories in momentum space are open, in any field H_0 the electrons cannot repeatedly return to the skin layer because of infinite motion in a plane normal to the metal surface; therefore the resonance cannot be intensified. This is to some extent a special case because of the strict conditions under which it occurs.

Thus we can almost always expect that in a strong magnetic field H_0 the surface impedance will depend essentially on the inclination of the field to the surface of the metal.

2. A GENERAL EXPRESSION FOR THE IMPEDANCE

Let the test specimen be a flat plate of thickness d which is infinite in the two other dimensions. We shall use two coordinate systems, $(\xi y \zeta)$ and (xyz), with the same origin. The ζ axis is directed into the metal normal to its surface; z is in the direction of H_0. The slope of the magnetic field H_0 with respect to the metal surface is given by the angle ψ between the ξ and z axes. The incident plane electromagnetic wave is normal to the metal surface.

In reference 1 it was shown that the field H_1 inside the metal can be represented in the form $H_1 \approx H_1^0 - 4\pi M$, that is, $B = H_1 + 4\pi M \approx H_1^0$. Here H_1^0 is the field in the absence of paramagnetic resonance (attenuated at the depth δ); M is the resonance magnetization, which is attenuated (near resonance) at the depth $\delta_{\text{eff}} \sim l(T_{sp}/t_0)^{1/2}$; t_0 is the mean free electron time. The relation $B \approx H_1^0$ holds true when the following inequality is satisfied:*

$$|\varkappa|\,\delta^2 \ll \delta^2_{\text{eff}}, \quad \varkappa = 1 - iT_{sp}(\omega - \Omega_0),$$

i.e., the frequency difference $\Delta\omega = \omega - \Omega_0$ is subject to the limitation $|\Delta\omega|\,T_{sp} \ll \delta^2_{\text{eff}}\ \delta^2$. However this limitation is not important since the resonance width is determined mainly by the spin relaxation time: $|\Delta\omega|\,T_{sp} \sim 1$, and the inequality $\delta \ll \delta_{\text{eff}}$ is almost always satisfied for metals. Indeed, in the anomalous skin effect $\delta \ll l$, while $\delta_{\text{eff}} \gg l$ for all actually attainable fields† H_0, so that obviously $\delta \ll \delta_{\text{eff}}$. In the normal skin effect $\delta/\delta_{\text{eff}} \lesssim 10^{-14}/t_0$ (for $\omega T_{sp} \gtrsim 10$), so that $\delta \ll \delta_{\text{eff}}$ fails to hold only at temperatures which are higher or of the order of room temperature, in which case $t_0 \lesssim 10^{-14}$ sec.

We shall now use the relation $B \approx H_1^0$ to determine the surface impedance of a metal under the given limiting conditions. The impedance when $\delta \gtrsim \delta_{\text{eff}}$ is found in Appendix (a). We define the surface impedance tensor z_{ik} by means of

---

*In reference 1 the interaction Hamiltonian $\hat{H} = \mu\boldsymbol{\sigma}\cdot\hat{H}$ ($\mu = -|e|\hbar/2mc$) did not take the sign of μ into account explicitly. When this is done and by μ we mean $|\mu|$, then in the final formulas for the magnetization we must make the substitutions $\Omega_0 \equiv 2\mu H_0/h \to -\Omega_0 \equiv -\frac{2|\mu|H}{\hbar}$ and $\omega \to -\omega$. These substitutions do not affect the results for nuclear polarization and the selective transparency of films. This comment will be taken into account in the present article.

†In a strong field H_0 the part of l is played by r, the radius of the electron orbit in a magnetic field.

$$E_i = (c/4\pi) Z_{ik} H_k \ (i, k = \xi, y).$$

(We perform a summation over repeated subscripts.) In the absence of resonance $E_i^0 = (c/4\pi) Z_{ik}^0 H_k^0$. Since $B \approx H_1^0$ and $E = E^0 + E'$, where $E' \sim cZ^0 (\delta/\delta_{\text{eff}}) M$, neglecting terms of the order of E', we have

$$E_i = \frac{c}{4\pi} Z_{ik}^0 B_k = \frac{c}{4\pi} Z_{ik}^0 (H_{1k} + 4\pi M_k). \tag{1}$$

Using the results obtained in reference 1, we can write

$$4\pi M_k = \alpha_{kn} E_n(0) = \alpha_{kn} Z_{nl}^0 H_{1l}^0.$$

Substituting this expression into (1), we obtain accurately to within linear terms in α:

$$E_i = \frac{c}{4\pi}\left(Z_{ik}^0 + \frac{c}{4\pi} Z_{in}^0 \alpha_{nl} Z_{lk}^0\right) H_{1k}.$$

Hence we obtain the surface impedance tensor in paramagnetic resonance (for $\delta \ll \delta_{\text{eff}}$):

$$Z_{ik} = Z_{ik}^0 + \frac{c}{4\pi} Z_{in}^0 \alpha_{nl} Z_{lk}^0, \tag{2}$$

where Z^0 is the impedance in the absence of resonance. In the present case

$$\alpha_{\xi\xi} = \alpha_{yy} = ia \sin\psi, \quad \alpha_{\xi y} = -a \sin^2\psi, \quad \alpha_{y\xi} = a.$$

For a specimen of thickness $d \gg \delta$ (far from resonance saturation)

$$a = -A 2\pi\chi \frac{\Omega_0 c T_{\text{sp}}}{\omega \delta_{\text{eff}} \sqrt{\varkappa}} \coth \frac{d}{\delta_{\text{eff}}} \sqrt{\varkappa}, \tag{3}$$

where A is a numerical coefficient of the order of unity which is associated with the conditions for electron reflection from the metal boundary (see Appendix b); $\delta_{\text{eff}} = \lambda (T_{\text{sp}}/t_0)^{1/2}$ is the distance traversed by an electron during diffusion in the time T_{sp}. The magnitude of λ depends essentially on the strength and inclination to the metal surface of the field H_0 and the electron dispersion law.

For closed Fermi surfaces

$$\lambda^2 = \frac{r_0^2\gamma}{2\int \theta dp_z} \int \frac{dp_z}{(e^{\gamma\theta} - 1)^3} \int_0^\theta d\tau \int_0^\theta d\tau' e^{\gamma\tau'} \{\widetilde{V}_\zeta^2 (e^{\gamma\theta} - 1)^2$$

$$- 2\widetilde{V}_\zeta \overline{V}_\zeta e^{\gamma\theta} (e^{\gamma\theta} - 1) + \overline{V}_\zeta^2 e^{\gamma\theta} (e^{\gamma\theta} + 1)\},$$

where

$$V_\zeta = \frac{v_\zeta}{v_0}, \quad v_\zeta = \frac{\partial \varepsilon(\mathbf{p})}{\partial p_\zeta}, \quad \widetilde{V} = \int_0^{\tau+\tau'} V d\tau'', \quad \overline{V} = \int_0^\theta V d\tau;$$

$$\gamma = T_0/t_0; \quad r_0 = v_0 T_0;$$

$$\theta = T(p_z)/T_0; \quad T(p_z) = \frac{c}{eH_0} \frac{\partial S(p_z)}{\partial \varepsilon} \equiv \frac{2\pi c m^*(p_z)}{eH_0};$$

$\tau = t/T_0$ is the dimensionless time which denotes the position of the electron in an orbit in momentum space; $T(p_z)$ is the orbital period of electrons with given p_z in the magnetic field H_0; $S(p_z)$ is the area of the intersection of the surface $\epsilon(\mathbf{p}) = \epsilon$ with the plane $p_z = \text{const}$; T_0 is the characteristic time of revolution of an electron in the magnetic field, say on the order of $\overline{T(p_z)}$; v_0 is the characteristic electron velocity on the Fermi surface. Specifically, for quadratic dispersion $\epsilon = m^* v^2/2$, $(2\pi)^{-1} \partial s/\partial\epsilon = m^*$, i.e., $m^*(p_z)$ is independent of p_z; therefore it is convenient to set $T_0 = T = 2\pi m^* c/eH_0$ and $v_0 = v$. It is easily seen that in actuality T_0 and v_0 do not enter into λ and are introduced only for convenience in obtaining values.

In the selected coordinate systems $V_\xi = V_z \sin\psi - V_x \cos\psi$. Therefore, remembering that $\overline{V}_x = 0$ in virtue of the periodic motion of electrons in the xy plane, we obtain

$$\lambda^2 = l^2 \sin^2\psi + s^2 \sin\psi \cos\psi + r^2 \cos^2\psi, \tag{4}$$

where

$$l^2 = \frac{r_0^2\gamma}{2\int \theta dp_z} \int \frac{dp_z}{(e^{\gamma\theta} - 1)^3} \int_0^\theta d\tau \int_0^\theta d\tau' e^{\gamma\tau'}$$

$$\times \{[(e^{\gamma\theta} - 1)\widetilde{V}_z - e^{\gamma\theta}\overline{V}_z]^2 + e^{\gamma\theta}\overline{V}_z^2\};$$

$$s^2 = \frac{r_0^2\gamma}{\int \theta dp_z} \int \frac{dp_z}{(e^{\gamma\theta} - 1)^2} \int_0^\theta d\tau \int_0^\theta d\tau' e^{\gamma\tau'} \widetilde{V}_x \{e^{\gamma\theta}\overline{V}_z - (e^{\gamma\theta} - 1)\widetilde{V}_z\};$$

$$r^2 = \frac{r_0^2\gamma}{2\int \theta dp_z} \int \frac{dp_z}{e^{\gamma\theta} - 1} \int_0^\theta d\tau \int_1^\theta d\tau' e^{\gamma\tau'} \widetilde{V}_x^2.$$

For weak magnetic fields H_0 ($\gamma \gg 1$):

$$l \sim s \sim r \sim r_0/\gamma = v_0 t_0,$$

so that for any angle ψ the magnitude of λ is of the order of the mean free electron path.

For strong fields H_0 ($\gamma \ll 1$):

$$l \sim r_0/\gamma, \quad s \sim r_0/\sqrt{\gamma}, \quad r \sim r_0, \tag{5}$$

so that for angles $\psi \gg \gamma$ the magnitude of λ is of the order of the mean free electron path and for $\psi \ll \gamma\lambda$ it is of the order of the radius of the electron orbit in the magnetic field.

For quadratic dispersion in any field H_0 (assuming $T_0 = T$ and $v_0 = v$) we have

$$l = \frac{r_0}{\gamma\sqrt{3}}, \quad s = 0, \quad r = \frac{r_0}{\sqrt{3(1+\gamma^2)}}$$

$$\text{or} \quad \lambda^2 = \frac{v^2 t_0^2}{3} \frac{\gamma^2 + \sin^2\psi}{\gamma^2 + 1}.$$

In the case of an open Fermi surface when the field H_0 is oriented with respect to this surface in such a way that the electron performs periodic motion in the xy plane, that is, $\overline{V}_x = 0$, a is also given by (3). When $\overline{V}_x \neq 0$, a is given by (3) with the following substitution for λ:

$$\lambda^2 = r_0^2 \frac{\gamma}{2} \lim_{\theta\to\infty} \frac{1}{\int \theta dp_z} \int dp_z \int_0^\theta d\tau \int_{-\infty}^{\tau} d\tau' e^{\gamma(\tau'-\tau)} \left\{ \int_\tau^{\tau'} V_\zeta d\tau'' \right\}^2 .$$

This expression is obtained for λ when we seek a solution of Eq. (30) in reference 1 which is aperiodic and bounded with respect to τ. Similarly to (4),

$$\lambda^2 = l^2 \sin^2\psi + s^2 \sin\psi \cos\psi + r^2 \cos^2\psi,$$

where, as is easily seen, for any field H_0 (with arbitrary γ)

$$l \sim s \sim r \sim r_0/\gamma = v_0 t_0.$$

If in $\Delta\epsilon \sim kT$ (or $\Delta\epsilon \sim \mu H_0$, with $kT \ll \mu H_0$) there are both closed and open surfaces $\epsilon(\mathbf{p}) = \epsilon$, then generally the magnetization can be represented in the form

$$M(\zeta) = M_1(\zeta) + M_2(\zeta), \tag{6}$$

where M_1 and M_2 are the contributions to the magnetization from the groups of electrons the energy levels of which are represented in momentum space by closed and open isoenergetic surfaces, respectively. Keeping in mind all that has been said above regarding resonance, we can infer that for a weak field H_0 $(\gamma \gg 1)$, independently of the angle ψ_1, M_1 and M_2 attenuate at the depth $\delta^0_{\text{eff}} \sim v_0 t_0 (T_{\text{sp}}/t_0)^{1/2}$, with $M_1 \sim M_2$. For a strong field H_0 $(\gamma \ll 1)$ and $\psi \gg \gamma$ we again have $M_1 \sim M_2$ and the attenuation depth of both expressions is of the order of δ^0_{eff}. For angles $\psi \ll \gamma$ when the field orientation with respect to open surfaces is such that $\overline{V}_x = 0$, the attenuation depth of M_1 and M_2 of the order of $\gamma\delta^0_{\text{eff}}$; if $\overline{V}_x \neq 0$, M_1 attenuates at the depth $\gamma\delta^0_{\text{eff}}$ and M_2 at the depth δ^0_{eff}. Then $M_1(0) \sim M_2(0)/\gamma \gg M_2(0)$.

When $\Delta\epsilon$ has only open surfaces $M(\zeta) = M_2(\zeta)$ and $M_2(\zeta)$ has the previous properties. It was stated above that the resonance part of the impedance is given by $M(0)$. We can therefore affirm that the specific form of the dispersion law does not essentially affect the dependence of the impedance on the angle ψ (with the exception of the "special" case). The presence of both closed and open surfaces in the interval $\Delta\epsilon$ when the magnetization is given by (6) could, for example, affect the selective transparency of films.[1]

We now note that for films with $d \ll \delta_{\text{eff}}$, as can easily be seen from (3), impedance is independent of ψ. Therefore the most interesting case is that of bulk metal $(d \gg \delta_{\text{eff}})$, which we shall consider hereafter.

3. SURFACE IMPEDANCE IN AN OBLIQUE FIELD

In the general case the formulas for surface impedance are very complicated. Therefore for simplicity we shall consider only the case in which the incident wave in linearly polarized (with non-vanishing components E_ξ and H_{1y}). Then the absorption of electromagnetic energy is given by the component $Z_{\xi y}$ of the impedance tensor:

$$P = (c/4\pi)^2 |H_1|^2 \operatorname{Re} Z_{\xi y}.$$

From (2) and (3) we have (omitting the subscripts ξ, y)

$$Z = Z^0 \left\{ 1 - Z^0 \frac{\chi \Omega_0 T_{\text{sp}} c^2}{\omega\lambda(\varkappa T_{\text{sp}}/t_0)^{1/2}} \right\}. \tag{7}$$

It is easily seen that Z will depend on ψ only in the anomalous skin effect. Equation (5) shows clearly that this requires a strong magnetic field H_0. For $\gamma \ll 1$ we have $H_0 \gg (3m^*/5m_0)10^{-7}/t_0$ oersteds, where m^*/m_0 is the ratio of the affective mass to the free electron mass; $\omega \gg 2\pi m^*/5m_0 t_0$ sec^{-1}. Thus for $t_0 \sim 2 \times 10^{-11}$ sec and $m^*/m \sim 1$ we must have fields $H_0 \gg 3000$ Oe and resonance frequencies $\omega \gg 2\pi \times 10^{10}$ sec^{-1}.

Two cases are conveniently distinguished: (a) An oblique field and (b) a parallel field.

(a) As shown in reference 5, the impedance Z^0 in a field H_0 inclined to the metal surface differs from the impedance for $H_0 = 0$ only in a very narrow range of angles $\psi < \psi_1 \sim (r_0/l)(\delta/r_0)^{2/3}$. Therefore when $\psi \gg \psi_1$ we use for Z^0 the familiar expression

$$Z^0 = \frac{C_1}{\sqrt{2}} \frac{(\delta^2 l)^{1/3}\omega}{c^2} (1 + i\sqrt{3}), C_1 = \frac{8}{9} (4\pi^2 \sqrt{6})^{1/3}. \tag{8}$$

From (7) and (8) we obtain

$$\begin{aligned} \operatorname{Re} Z &= \frac{C_1^2}{\sqrt{2}} \frac{\omega (\delta^2 l)^{1/3}}{c^2} \left\{ \frac{1}{C_1} + \frac{\chi\Omega_0 T_{\text{sp}} (\delta^2 l)^{1/3}}{\lambda (T_{\text{sp}}/t_0)^{1/2}} \frac{\alpha + \sqrt{3}\beta}{\sqrt{1 + T^2_{\text{sp}}\Delta\omega^2}} \right\}, \\ \operatorname{Im} Z &= \frac{C_1^2}{\sqrt{2}} \frac{\omega (\delta^2 l)^{1/3}}{c^2} \left\{ \frac{\sqrt{3}}{C_1} - \frac{\chi\Omega_0 T_{\text{sp}} (\delta^2 l)^{1/3}}{\lambda (T_{\text{sp}}/t_0)^{1/2}} \frac{\sqrt{3}\alpha - \beta}{\sqrt{1 + T^2_{\text{sp}}\Delta\omega^2}} \right\}, \end{aligned} \tag{9}$$

where

$$\begin{aligned} \alpha &= (\sqrt{1 + T^2_{\text{sp}}\Delta\omega^2} + 1)^{1/2}, \\ \beta &= \operatorname{sign}\Delta\omega (\sqrt{1 + T^2_{\text{sp}}\Delta\omega^2} - 1)^{1/2}. \end{aligned} \tag{10}$$

Equation (9) shows that the width of the resonance curve is independent of ψ while the resonance intensity changes considerably as ψ is varied from

0 to $\pi/2$ (for closed electron trajectories in momentum space). The ratio of the ordinate of the resonance curve at $\psi = \pi/2$ to the ordinate for arbitrary ψ will be

$$Y(\psi) = \frac{\operatorname{Re} Z_{\text{res}}(\pi/2)}{\operatorname{Re} Z_{\text{res}}(\psi)} = \frac{\operatorname{Im} Z_{\text{res}}(\pi/2)}{\operatorname{Im} Z_{\text{res}}(\psi)}$$

$$= \frac{1}{l}(l^2 \sin^2\psi + s^2 \sin\psi\cos\psi + r^2\cos^2\psi)^{1/2},$$

where Y varies between r/l and 1 (see the figure).

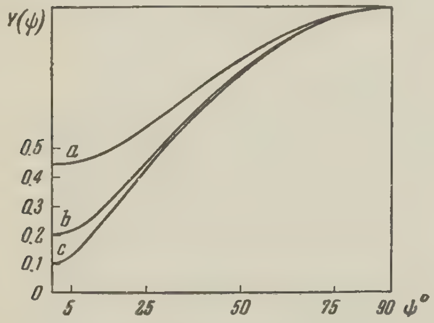

Y(ψ) for the quadratic dispersion law: a) – $\gamma = 0.5$; b) $\gamma = 0.2$; c) $\gamma = 0.1$.

(b) In a strong field H_0 ($\gamma \ll 1$) which is almost parallel ($\psi \ll \psi_1$) to the metal surface the impedance Z^0 depends on the magnetic field. We note that in such a field cyclotron resonance occurs at frequencies ω which are multiples of $2\pi/T_0$ and that this resonance depends essentially on the law of electron dispersion in the metal. Paramagnetic resonance occurs at frequencies $\omega = \Omega_0$ which generally do not coincide with the frequencies $2\pi/T_0$ since T_0 involves the effective electron mass while Ω_0 clearly involves the free electron mass. Therefore for $Z^0(H_0)$ we can use the expression for nonresonant impedance in a parallel field with quadratic dispersion (dispersion is not important far from resonance[6]):

$$Z^0(H_0) = (1+\omega^2 t_0^2)^{1/6}\left(\frac{2\pi H}{H_0}\right)^{1/3}\frac{16}{9}\left(\frac{\sqrt{3}\pi\omega l}{c^4\sigma}\right)^{1/3}\exp\left\{i\,\frac{\pi + \tan^{-1}\omega t_0}{3}\right\}.$$

Here

$$H = \frac{mc}{et_0}, \quad v_0\sqrt{2\pi mN}\left|1 + \frac{i}{\omega t_0}\right|^{-1/2} \gg H_0 \gg H\,|1 + i\omega t_0|.$$

When $\omega t_0 \ll 1$ the corresponding formulas for Re Z and Im Z are obtained from (9) after the substitution $l \rightarrow l2\pi H/H_0$ with $\lambda = r_0 = v_0 T_0$.

4. RESONANCE SATURATION

In the calculation of energy absorption in quite strong fields H_1 we must take resonance absorption into account. Here again we shall consider for simplicity the incident wave to be linearly polarized. For a specimen of thickness $d < \delta$ the expression for the resonance part of the absorption is analogous to the corresponding expression in the theory of nuclear resonance:

$$P_{\text{res}} = \frac{\omega H_1^2}{4}\frac{\Omega_0\chi T_{\text{sp}}}{|\varkappa|^2 + \Omega_1^2 T_{\text{sp}}^2}, \quad \Omega_1 = \frac{2\mu H_1}{\hbar}.$$

Resonance absorption occurs when $H_1 \gg 5 \times 10^{-8} \times T_{\text{sp}}^{-1}$ oersteds.

For bulk metal ($d \gg \delta_{\text{eff}}$) in the limiting case $\delta \gg \delta_{\text{eff}}$ the absorption is given by $P = (c/4\pi)^2 H_1^2 R$, where

$$Z \equiv R + iX = \frac{4\pi}{c}\frac{E(0)}{H_1(0)} \approx Z^0\left\{1 + \frac{4\pi M(0)}{H_1^0(0)}\right\}.$$

The magnetization $M(0)$ with resonance saturation taken into account will be[1]

$$M(0) = -\frac{\chi H_0 u}{1 + \operatorname{Re}(uu_r)}, \; u = \frac{c\Omega_0 T_{\text{sp}} E^0(0)}{\omega H_0 \delta_{\text{eff}}\sqrt{\varkappa}}, \quad u_r = u^*\Big|_{\omega=\Omega_0}$$

We shall now give the formulas for the resonance part of the impedance. For the normal skin effect

$$R_{\text{res}} = -4\pi^2\sqrt{2}\,\frac{\beta}{|\varkappa|}\frac{\chi\omega\Omega_0 T_{\text{sp}}\delta^2}{c^2\delta_{\text{eff}}}\left(1 + \frac{\alpha}{|\varkappa|}\frac{\sqrt{2}\,T_{\text{sp}}^2\omega\delta^2}{\Omega_0\delta_{\text{eff}}^2}\,\Omega_{1i}^2\right)^{-1},$$

$$X_{\text{res}} = -(\alpha/\beta)\,R_{\text{res}},$$

where α and β are given by (10); $\Omega_{1i} = 2\mu H_{1i}/\hbar$, H_{1i} is the strength of the wave impinging on the metal. We note that both far from resonance and at resonance $R_{\text{res}}/X_{\text{res}} = -\beta/\alpha$.

For the anomalous skin effect

$$R_{\text{res}} = \frac{C_1^2}{\sqrt{2}}\frac{\chi\Omega_0 T_{\text{sp}}(\delta^2 l)^{2/3}\omega}{c^2\delta_{\text{eff}}}\frac{\alpha + \sqrt{3}\beta}{|\varkappa|}$$

$$\times\left\{1 + \frac{C_1^2\sqrt{2}\,T_{\text{sp}}\,\omega\,(\delta^2 l)^{2/3}}{4\pi^2\Omega_0\delta_{\text{eff}}^2}\frac{\alpha}{|\varkappa|}\Omega_{1i}^2\right\}^{-1}, \quad X_{\text{res}} = -\frac{\sqrt{3}\alpha - \beta}{\alpha + \sqrt{3}\beta}R_{\text{res}}.$$

The ratio $R_{\text{res}}/X_{\text{res}}$ is independent of H_{1i} just as for the normal skin effect.

We note that for bulk metal resonance saturation requires considerably higher incident field strength than in the homogeneous case. Thus for the normal skin effect with $\omega \sim 10^8\ \text{sec}^{-1}$, $t_0 \sim 10^{-13}$ sec and $T_{\text{sp}} \sim 10^{-7}$ sec we have $H_{1i} \gg 5$ Oe, whereas in the homogeneous case under the same conditions we have $H_{1i} \gg 0.4$ oersteds.

APPENDIX

(a) The region where (2) can be applied is bounded by the inequality $\delta \ll \delta_{\text{eff}}$. $\delta \gtrsim \delta_{\text{eff}}$ refers entirely to the region of the normal skin effect ($j = \sigma E$), where without any special difficulty we can obtain an exact expression for the impedance through simultaneous solution of the equations[1]

$$\frac{\partial E}{\partial z} = \frac{\omega}{c}B_1; \quad \frac{\partial H_1}{\partial z} = -\frac{4\pi i\sigma}{c}E; \tag{1a}$$

$$v_z\frac{\partial u}{\partial z} + \frac{u}{t_0^*} = \frac{\bar{u}}{t_0} + \frac{2\mu B_1}{\hbar};$$

$$\dot{u}(v_z, 0) = qu(-v_z, 0) + (1-q)\bar{u}(0), \tag{2a}$$

where

$$B_1 = H_1 + 4\pi M, \; M = i\chi H_0 \bar{u},$$
$$1/t_0^* = 1/t_0 + 1/T_{\mathrm{sp}} - i(\omega - \Omega_0).$$

Equation (2a) applies to a field H_0 prependicular to the metal surface with quadratic dispersion. For simplicity we also assume $d = \infty$. Electron reflection from the metal boundary is characterized by the reflection coefficient q, with $q = 1$ for specular reflection and $q = 0$ for diffuse reflections.

Solving (2a) and averaging the solution over the Fermi surface, for the magnetization M with specular reflection we obtain the integral equation

$$M(z) = \frac{t_0^*}{t_0} \times \int_{-\infty}^{\infty} R(|z-\zeta|)\{(1 + 4\pi i\chi t_0\Omega_0) M(\zeta) + i\chi t_0\Omega_0 H_1(\zeta)\}\, d\zeta, \tag{3a}$$

where

$$R(z) = \frac{1}{2l_0}\int_1^{\infty} \exp\left(-\frac{zx}{l_0^*}\right)\frac{dx}{x}, \quad l_0 = vt_0, \quad l_0^* = vt_0^*.$$

Performing a Fourier transformation of (3a) and of the equation for H_1, we obtain

$$\begin{gathered} \frac{t_0}{t_0^*} M(k) = R(k)\{(1 + 4\pi i\chi t_0\Omega_0) M(k) + i\chi t_0\Omega_0 H_1(k)\}, \\ 2H_1'(0) + k^2 H_1(k) - 2i\delta^{-2} H_1(k) = 8\pi i\delta^{-2} M(k), \end{gathered} \tag{4a}$$

where

$$R(k) = \int_{-\infty}^{\infty} e^{ikz} R(|z|)\, dz = \frac{\tan^{-1} kl_0^*}{kl_0^*}, \tag{5a}$$
$$\delta = \frac{c}{\sqrt{2\pi\omega\sigma}}.$$

Hence

$$H_1(k) = \frac{2\delta^2 H_1'(0)}{k^2\delta^2 - 2i} \times \left\{-1 + \frac{8\pi\chi t_0\Omega_0 R(k)/(\delta^2k^2 - 2i)}{t_0/t_0^* - R(k)[1 + 4\pi i\chi t_0\Omega_0\delta^2k^2/(\delta^2k^2 - 2i)]}\right\}. \tag{6a}$$

The second term within square brackets in the denominator can always be neglected compared with unity since usually $t_0\Omega_0 \lesssim 1$, whereas $\chi \sim 10^{-6}$. Performing the inverse Fourier transformation of (6a) and remembering that $H_1^1(0) = -(4\pi i\sigma/c) \times E(0)$, for the impedance $Z = (4\pi/c)E(0)/H_1(0)$ we obtain

$$Z = Z^0\left\{1 - iZ^0\frac{2\chi t_0\Omega_0 c^2}{\pi\omega} \times \int_0^{\infty}\frac{R(k)\, dk}{[1 + t_0/T_{\mathrm{sp}} - it_0(\omega - \Omega_0) - R(k)][1 - \delta^2k^2/2i]^2}\right\}, \tag{7a}$$

where $Z^0 = 4\pi\omega\delta/ic^2\sqrt{2i}$. In deriving this expression we have assumed the second term in curly brackets to be small compared with unity. Equation (7a) agrees, as was to be expected, with (71) in Dyson's article[3] for $d = \infty$.

The integration in (7a) is easily performed if we note that for $t_0|\Delta\omega| \ll 1$ we can use the resolution $R(k) \approx 1 - k^2 l_0^{*2}/3$, since under this condition only small values of kl_0^* are significant in the integrand. The integral then becomes

$$\frac{3\delta_{\mathrm{eff}}^2}{l_0^{*2}}\int_0^{\infty}\frac{dk}{(\varkappa + \delta_{\mathrm{eff}}^2 k^2)(1 - \delta^2k^2/2i)^2}, \quad \delta_{\mathrm{eff}} = l_0\sqrt{\frac{T_{\mathrm{sp}}}{3t_0}}.$$

For $\delta \ll \delta_{\mathrm{eff}}$, subject to the condition $|\kappa| \ll (\delta_{\mathrm{eff}}/\delta)^2$, we obtain for the impedance:

$$Z = Z^0\left\{1 - iZ^0\frac{\chi\Omega_0 T_{\mathrm{sp}} c^2}{\omega\delta_{\mathrm{eff}}\sqrt{\varkappa}}\right\},$$

which agrees exactly with (7). (The appearance of the factor i in this and subsequent equations of the Appendix is associated with circular polarization of the incident wave.)

We note that for the magnetization M we obtain from (4a)

$$M(z) = \frac{1}{2\pi}\int_{-\infty}^{\infty} e^{-ikz} M(k)\, dk \approx -i\frac{\chi T_{\mathrm{sp}}\Omega_0 cE(0)}{\omega\delta_{\mathrm{eff}}\sqrt{\varkappa}}\exp\left\{-\frac{z\sqrt{\varkappa}}{\delta_{\mathrm{eff}}}\right\}. \tag{8a}$$

(b) We shall now show that the conditions for electron reflection from the metal boundary affect only the numerical coefficient in the magnetization (assuming that the electron spin does not change in collisions with the surface). For this purpose it is sufficient to obtain a solution of (2a) when $q = 0$ and to compare this solution with (8a). Solving (2a) and averaging the solution over the Fermi surface, we obtain for M the integral equation

$$M(z) = K(z)M(0) + \int_0^{\infty} R(z-\zeta)\{M(\zeta) + i\chi t_0\Omega_0 B_1(\zeta)\}\, d\zeta,$$

where

$$K(z) = \frac{1}{2}\int_1^{\infty}\exp\left\{-\frac{zx}{l_0^*}\right\}\frac{dx}{x^2}, \quad R(z) = \frac{1}{2l_0}\int_1^{\infty}\exp\left\{-\frac{zx}{l_0^*}\right\}\frac{dx}{x}.$$

Following Fock,[7] the solution of this equation can be written as

$$M(z) = M(0)J_2(z) + J_1(z), \tag{1b}$$

$$J_1(z) = \frac{1}{(2\pi)^2}\int_{b-i\infty}^{b+i\infty} e^{kz}\psi_1(k)\, dk \int_{-i\infty}^{i\infty}\psi_2(x)G(x)L(x)\frac{dx}{x-k}, \tag{2b}$$

$$J_2(z) = \frac{1}{(2\pi)^2}\int_{b-i\infty}^{b+i\infty} e^{kz}\psi_1(k)\, dk \int_{-i\infty}^{i\infty}\psi_2(x)N(x)\frac{dx}{x-k}, \quad \mathrm{Re}\, b > 0. \tag{3b}$$

Here

$$\ln\psi_1(k) = -\frac{k}{\pi}\int_0^\infty \frac{dx}{x^2+k^2}\ln\left(1-\frac{t_0^*}{t_0}\frac{\tan^{-1}l_0^*x}{l_0^*x}\right),$$

$$\psi_1(k) = \psi_2(-k),$$

$$L(k) = \int_{-\infty}^{\infty} e^{-kz}R(z)\,dz = \frac{t_0^*}{t_0}\frac{1}{2l_0^*k}\ln\frac{1+l_0^*k}{1-l_0^*k},$$

$$G(k) = i\chi t_0\Omega_0\int_0^\infty e^{-kz}B_1(z)\,dz,$$

$$N(k) = \int_0^\infty e^{-kz}K(z)\,dz = \frac{l_0^*}{2}\frac{l_0^*k+\ln(1+l_0^*k)}{l_0^{*2}k^2}.$$

The functions $\psi_2(k)$ and $\psi_1(k)$ have simple poles at the points

$$k = k_0 \equiv (1/l_0^*)\sqrt{3t_0\varkappa/T_{sp}} \equiv \sqrt{\varkappa}/\delta_{\text{eff}} \text{ and } k = -k_0$$

respectively. We shall now obtain the magnetization M. For calculation of the integrals in (1b) it is convenient to expand $\psi_1(k)$ in a series with respect to $\epsilon = (t_0/T_{sp})(1+iT_{sp}\Delta\omega)$ ($\epsilon \ll 1$, when $t_0|\Delta\omega| \ll 1$). We now have

$$\ln\psi_1(k_0) = -\frac{\sqrt{3\varepsilon}}{\pi}\int_0^\infty \frac{dx}{x^2+3\varepsilon}\ln\left(1+\varepsilon-\frac{\tan^{-1}x}{x}\right)$$

$$-\frac{\sqrt{3\varepsilon}}{\pi}\ln\frac{t_0}{t_0^*}\int_0^\infty\frac{dx}{x^2+3\varepsilon}.$$

By adding and subtracting the integral

$$\frac{\sqrt{3\varepsilon}}{\pi}\int_0^\infty \frac{dx}{x^2+3\varepsilon}\ln\left(\varepsilon+\frac{x^2}{3}\right) = \ln 2\sqrt{\varepsilon},$$

we obtain

$$\ln\psi_1(k_0) = -\ln 2\sqrt{\varepsilon}$$

$$+\frac{\sqrt{3\varepsilon}}{\pi}\int_0^\infty\frac{dx}{x^2+3\varepsilon}\ln\frac{\varepsilon+x^2/3}{1+\varepsilon-x^{-1}\tan^{-1}x}+\frac{1}{2}\ln(1+\varepsilon).$$

It can be shown that

$$\int_0^\infty\frac{dx}{x^2+3\varepsilon}\ln\frac{\varepsilon+x^2/3}{1+\varepsilon-x^{-1}\tan^{-1}x}$$

$$=\int_0^\infty\frac{dx}{x^2}\ln\frac{x^2/3}{1-x^{-1}\tan^{-1}x}-(3\varepsilon)^{1/2}\frac{9\pi}{20}$$

$$+3\varepsilon\int_0^\infty\frac{dx}{x^2}\left(\frac{5}{6}-\frac{1}{x^2}-\frac{1/3}{1-x^{-1}\tan^{-1}x}-\frac{1}{x^2}\ln\frac{x^2/3}{1-x^{-1}\tan^{-1}x}\right)$$

$$-(3\varepsilon)^{3/2}\frac{159\pi}{1120}+\dots$$

By numerical integration we find that

$$\int_0^\infty\frac{dx}{x^2}\ln\frac{x^2/3}{1-x^{-1}\tan^{-1}x}=\frac{2}{3}\pi\pm\eta$$

($\eta < 10^{-4}$; the requirement for resonance leads to $\eta = 0$). Thus, confining ourselves to terms of the expansion which are of the order of ϵ,

$$\ln\psi_1(k_0) = -\ln 2\sqrt{\varepsilon}+\frac{2}{\sqrt{3}}\sqrt{\varepsilon}-\frac{17}{20}\varepsilon$$

$$\approx\ln\left(\frac{1}{2\sqrt{\varepsilon}}+\frac{1}{\sqrt{3}}-\frac{17\sqrt{\varepsilon}}{40}\right). \tag{5b}$$

It can be shown similarly that for small k

$$\ln\psi_1(k) = -\ln\left[\sqrt{\varepsilon}\left(1+\frac{k}{k_0}\right)\right]$$

$$+k\left(\frac{2}{3}-\frac{9}{20}\sqrt{3\varepsilon}\right)+\frac{\varepsilon}{2}\operatorname{sign}k$$

$$\approx\ln\left\{\frac{1}{\sqrt{\varepsilon}}\left[1+k\left(\frac{2}{3}-\frac{9}{20}\sqrt{3\varepsilon}\right)+\frac{\varepsilon}{2}\operatorname{sign}k\right]\left(1+\frac{k}{k_0}\right)^{-1}\right\}. \tag{6b}$$

We shall now calculate the integrals $J_1(z)$ and $J_2(z)$. We apply the residue theorem to the inner integral in (2b). The integrand possesses poles in the right half plane at the points $x = k$ and $x = k_0$ because of the functions $1/(x-k)$ and $\psi_2(x)$. The function $G(x)$ has poles only in the left half plane. The "distant" pole $x = l/l_0^*$ of $L(x)$ can be neglected since $1/l_0^* \gg k$. Then

$$J_1(z) = \frac{i}{2\pi}\int_{b-i\infty}^{b+i\infty} e^{kz}\psi_1(k)\,dk$$

$$\times\left\{\psi_2(k)\,G(k)\,L(k)+\frac{G(k_0)\,L(k_0)}{k_0-k}\operatorname{Res}\psi_2(k_0)\right\}.$$

The residue theorem can also be applied to this integral. $G(k)$ has a pole at $k = -1/\delta$ and $\psi_1(k)$ has a pole at $k = -k_0$. If $\delta \ll 1/|k_0| = \delta_{\text{eff}}/|\sqrt{\kappa}|$ the pole at $G(k)$ like that of $L(k)$ can be neglected. Noting that $L(k_0) = L(-k_0) \approx 1$, we obtain

$$J_1(z) = e^{-k_0z}\left\{\psi_2(-k_0)\,G(-k_0)\right.$$

$$\left.+\frac{1}{2k_0}G(k_0)\operatorname{Res}\psi_2(k_0)\right\}\operatorname{Res}\psi_1(-k_0).$$

Hence, using (5b) and (6b) and retaining only zero order terms in (5), we obtain

$$J_1(z) = 2G(0)\,e^{-k_0z},\quad G(0) = -i\chi t_0\Omega_0cE(0)/\omega l_0. \tag{7b}$$

Similarly

$$J_2(z) = \left(1-\frac{211}{240}\sqrt{3\varepsilon}\right)e^{-k_0z}. \tag{8b}$$

From (1b), (7b) and (8b) we have

$$M(z) = -\frac{160}{211}\frac{i\chi T_{\text{sp}}\Omega_0cE(0)}{\omega\delta_{\text{eff}}\sqrt{\varkappa}}\exp\left\{-\frac{z\sqrt{\varkappa}}{\delta_{\text{eff}}}\right\},$$

which agrees with (8a) except for the coefficient. Thus the coefficient A in (3) equals unity for specular reflection of electrons from a metal boundary, while A = 160/211 for diffuse reflection.

[1] Azbel', Gerasimenko, and Lifshitz, J. Exptl. Theoret. Phys. (U.S.S.R.) **32**, 1212 (1957), Soviet Phys. JETP **5**, 986 (1957).

[2] Griswold, Kip, and Kittel, Phys. Rev. **88**, 951 (1952).

[3] F. J. Dyson, Phys. Rev. **98**, 349 (1955).

[4] Lifshitz, Azbel', and Kaganov, J. Exptl. Theoret. Phys. (U.S.S.R.) **30**, 220 (1956), Soviet Phys. JETP **3**, 143 (1956).

[5] M. Ia. Azbel' and E. A. Kaner, J. Exptl. Theoret. Phys. (U.S.S.R.) **32**, 896 (1957), Soviet Phys. JETP **5**, 730 (1957).

[6] M. Ia. Azbel', Doklady Akad. Nauk SSSR **100**, 437 (1955).

[7] V. A. Fock, Математическии сборник (Math. Collection) (new series) **14**, 3 (1944).

Translated by I. Emin
139

SOVIET PHYSICS JETP VOLUME 35(8), NUMBER 3 MARCH, 1959

MAGNETIC TRANSITIONS BETWEEN COLLECTIVE EXCITED STATES OF EVEN-EVEN NUCLEI

A. S. DAVYDOV and G. F. FILIPPOV

Moscow State University

Submitted to JETP editor April 3, 1958

J. Exptl. Theoret. Phys. (U.S.S.R.) 35, 703-706 (September, 1958)

The reduced probability for an M1 transition between two 2^+ states and the ratio of this probability to that for an E2 transition between the same states is calculated. The small value of this ratio is in agreement with the experimental data.

INTRODUCTION

In a previous paper,[1] assuming that the shape of the nucleus is not axially symmetric, the authors showed that various energy levels of nonaxial nuclei are satisfactorily explained if one assumes that they are assigned to be rotational states. The possibility of giving explicit expressions for wave functions of nuclear rotational states in terms of the parameters β and γ enables one to compute relative intensities of different transitions from a given excited state to other rotational states.

The intensity rules for transitions between rotational states of axial nuclei were investigated in a paper of Alaga, Alder, Bohr, and Mottelson.[2] In our paper,[1] we determined the probabilities of electric quadrupole transitions between rotational states of nonaxial even-even nuclei.

In the present paper we shall compute the probabilities of magnetic dipole transitions between rotational states having spins 2^+, 2^+. Such levels are observed in Se^{76}, Te^{122}, Os^{188}, Os^{186}, Pt^{192}, and other nuclides. As we have shown,[1] the knowledge of the ratio of the energy of the second 2^+ level to that of the first enables us to determine the parameter γ and the ratio of the reduced probabilities for the electric quadrupole transitions B(E2; 22→21)/B(E2; 22→0). However, according to the general selection rules, an M1 transition is possible between two states of spin 2 and the same parity, in addition to the E2 transition. As the experiments[3] show, the intensity ratio T(M1)/T(E2) is a few hundredths for the nuclei listed above. Such values are a definite indication that the lowest energy levels of spin 2 cannot be attributed to single-particle excitations, since in that case the ratio of the intensities of the competing magnetic dipole and electric quadrupole transitions can be given by the formula (cf. reference 4, Par. 31):

$$T(MJ)/T(E, J+1) \sim \{25(2J+1)/A^{2/3}(\hbar\omega)_{\mathrm{Mev}}\}^2;$$

from which one finds that this ratio is 10^4 for A ~ 30 and $\hbar\omega \sim 100$ kev, while it is ~10 for heavy nuclei and $\hbar\omega \sim 1$ Mev. Later we shall show that our picture of the rotational nature of the 2^+, 2^+ excited levels of even-even nuclei enables one to explain the experimentally observed value of T(M1)/T(E2).

1. THE MAGNETIC DIPOLE MOMENT OPERATOR IN THE UNIFORM NUCLEAR MODEL

The collective excitations of the nucleus are described in the uniform model of A. Bohr and Mottelson by wave functions depending on five coordinates α_μ, which determine (relative to a fixed coordinate system) the deviation of the nuclear shape from spherical:

$$R(\vartheta\varphi) = R_0\Big(1 + \sum_{\mu=-2}^{2} \alpha_\mu Y_{2\mu}\Big), \tag{1.1}$$

They can also be described by the two parameters β and γ, which determine the shape of the nucleus in the coordinate system fixed in the principal axes of the ellipsoid of inertia of the nucleus, and the three Euler angles which fix the orientation of these axes relative to a fixed system of coordinates.

If the equilibrium values of β and γ are different from zero, the lowest collective excited states of the nucleus correspond to energy levels of an asymmetric top (cf. reference 1). The wave functions of these states are eigenfunctions of the square of the total angular momentum. In classical theory the components of this angular momentum are expressed in terms of the coordinates α_μ and velocities $\dot{\alpha}_\mu$ by the formula

$$J_\nu = i\sqrt{6}(-1)^\nu B \sum_\mu (21, \nu+\mu, -\nu \,|\, 2\mu)\, \dot{\alpha}_\mu \overset{*}{\alpha}_{\mu+\nu}, \qquad \nu = 0, 1, -1, \tag{1.2}$$

where B is the mass parameter of the theory; $(21,\ \nu+\mu, -\nu\,|\,2\mu)$ are vector addition coefficients. In quantum theory the components of the angular momentum of the asymmetric top are operators acting on generalized spherical functions D^J_{MK} which depend on the Euler angles,

$$J_\nu D^J_{MK} = (-1)^\nu \sqrt{J(J+1)}\,(J1, M+\nu, -\nu\,|\,JM)\, D^J_{M+\nu, K}. \tag{1.3}$$

We now proceed to compute the magnetic dipole operator corresponding to collective motions in even-even nuclei. According to Bohr and Mottelson, this operator is given by the formula

$$\mathfrak{M}(1\mu) = \mu_0 g_R \int \mathbf{R}(\mathbf{r})\, \nabla (rY_{1\mu})\, d\tau, \tag{1.4}$$

where $\mu_0 = e\hbar/2Mc$ is the nuclear magneton; g_R is the gyromagnetic ratio corresponding to collective motion of the nucleons in the nucleus;

$$\mathbf{R}(\mathbf{r}) = BR_0^{-5} \sum_\lambda \dot{\alpha}_\lambda [\mathbf{r} \times \nabla (r^2 Y_{2\lambda})]$$

is the angular momentum density.

We write the operator ∇ as a sum of two terms:

$$\nabla = \frac{\mathbf{r}}{r}\frac{\partial}{\partial r} - \frac{i}{r^2}[\mathbf{r} \times \mathbf{L}],$$

where $\mathbf{L} \equiv -i[\mathbf{r} \times \nabla]$; we can then write

$$[\mathbf{r} \times \nabla (r^2 Y_{2\lambda})] = ir^2 \mathbf{L} Y_{2\lambda}.$$

Also noting that

$$\nabla (rY_{1\mu}) = (-1)^\mu \sqrt{3/4\pi}\, \mathbf{e}_\mu,$$

where the $\mathbf{e}_\mu$ are unit vectors which are given in terms of the unit vectors $\mathbf{e}_x$, $\mathbf{e}_y$, $\mathbf{e}_z$ of a Cartesian coordinate system by the relations $\mathbf{e}_0 = \mathbf{e}_z$, $\mathbf{e}_{1,-1} = \mp(\mathbf{e}_x \pm i\mathbf{e}_y)/\sqrt{2}$, and

$$(\mathbf{e}_\mu \cdot \mathbf{L})\, Y_{2\lambda} = (-1)^\mu \sqrt{6}\,(21\lambda+\mu, -\mu\,|\,2\lambda) Y_{2,\lambda+\mu},$$

we can write (1.4) in the form

$$\mathfrak{M}(1\mu) = \mu_0 g_R \frac{3B}{\sqrt{2\pi}} R_0^{-5} \times \sum_\lambda (21, \lambda+\mu, -\mu\,|\,2\lambda)\dot{\alpha}_\lambda \int d\Omega \int_0^{R(\vartheta\varphi)} dr r^4 Y_{2,\lambda+\mu}, \tag{1.5}$$

where $R(\vartheta\varphi)$ is defined in (1.1)

Carrying out the integration and using (1.2), we can write (1.5) as a series

$$\mathfrak{M}(1\mu) = \mathfrak{M}_0(1\mu) + \mathfrak{M}_1(1\mu) + \cdots, \tag{1.6}$$

where

$$\mathfrak{M}_0(1\mu) = \mu_0 g_R \frac{1}{2}\sqrt{\frac{3}{\pi}} J_\mu, \tag{1.7}$$

$$\mathfrak{M}_1(1\mu) = \mu_0 g_R \frac{5\sqrt{6}}{7\pi} \sum_\nu (21,\ \mu-\nu,\ \nu\,|\,1\mu)\, \overset{*}{\alpha}_{\mu-\lambda} J_\nu. \tag{1.8}$$

The matrix elements of the operator (1.7) between different rotational states are equal to zero. To obtain nonvanishing matrix elements, which determine the intensity of the magnetic dipole radiation between rotational states, one must include the operator (1.8) of the next approximation, which contains the collective coordinates α_μ and the projections J_ν of the total angular momentum.

2. PROBABILITY OF MAGNETIC DIPOLE TRANSITIONS BETWEEN ROTATIONAL STATES

We calculate the reduced probability for magnetic dipole transition between two rotational states having spin 2 and the same parity. According to reference 1, the wave functions of these states can be written as

$$\begin{aligned} \psi_{21m} &= (5/8\pi^2)^{1/2}[a_1 D^2_{m0} + b_1 (D^2_{m2} + D^2_{m,-2})/\sqrt{2}], \\ \psi_{22m} &= (5/8\pi^2)^{1/2}[a_2 D^2_{m0} + b_2 (D^2_{m2} + D^2_{m,-2})/\sqrt{2}], \end{aligned} \tag{2.1}$$

where

$$a_1 N_1 = -[\sin\gamma \sin 3\gamma + 3\cos\gamma\cos 3\gamma + \sqrt{9 - 8\sin^2 3\gamma}],$$

$$b_1 N_1 = 3\sin\gamma\cos 3\gamma - \cos\gamma \sin 3\gamma,$$

$$N_1^2 = 2\sqrt{9-8\sin^2 3\gamma} \times [\sqrt{9-8\sin^2 3\gamma} + \sin\gamma\sin 3\gamma + 3\cos\gamma\cos 3\gamma],$$

$$a_2 N_2 = \sqrt{9-8\sin^2 3\gamma} - \sin\gamma\sin 3\gamma - 3\cos\gamma\cos 3\gamma,$$

$$b_2 N_2 = 3\sin\gamma\cos 3\gamma - \cos\gamma\sin 3\gamma,$$

$$N_2^2 = 2\sqrt{9-8\sin^2 3\gamma} \times [\sqrt{9-8\sin^2 3\gamma} - \sin\gamma\sin 3\gamma - 3\cos\gamma\cos 3\gamma].$$

The reduced probability for magnetic dipole radiation in the transition from the 22 state to the 21 state is given by

$$B(M1;\ 22 \rightarrow 21) = \frac{1}{5}\sum_{m'\mu m} |(21m'|\mathfrak{M}(1\mu)|22m)|^2. \tag{2.2}$$

Substituting the values (1.8) and (2.1) in (2.2), we find

$$B(M1;\ 22 \rightarrow 21) = \frac{90}{49\pi^2}\mu_0^2 g_R^2 \beta^2 \frac{\sin^2 3\gamma}{9 - 8\sin^2 3\gamma}. \tag{2.3}$$

The reduced probability for magnetic dipole transition between the 22 and 21 states is equal to zero for an axial nucleus ($\gamma = 0$), and increases

Nucleus	$E_{22}-E_{21}$ (kev)	$T(M1)/T(E2)$	Percent of E2 transition (exptl)
Se^{76}	643	$9.8\cdot 10^{-2}$	98 ± 1
Te^{122}	693	$1.9\cdot 10^{-2}$	92 ± 4
Os^{186}	627	$6.5\cdot 10^{-3}$	99 ± 1
Os^{188}	480	$1.04\cdot 10^{-2}$	99.6

with increasing γ, reaching its maximum value for $\gamma = 30°$.

As we have previously shown,[1] the value of γ can be determined from the ratio of the energies E_{22}/E_{21} of the two 2^+ levels. Then the measurement of the reduced probability for magnetic dipole transition enables us, by means of (2.4), to compute the gyromagnetic ratio g_R for collective motion of the nucleons in the nucleus.

Using the formula for the reduced probability of electric quadrupole transition between these same levels[1]

$$B(E2;\ 22 \rightarrow 21) = (10e^2Q_0^2/7\pi)\sin^2 3\gamma/(9 - 8\sin^2 3\gamma),$$

we get the ratio of the reduced probabilities for magnetic dipole and electric quadrupole transitions:

$$\frac{B(M1;\ 22 \rightarrow 21)}{B(E2;\ 22 \rightarrow 21)} = \frac{144}{7\pi}\left(\frac{\mu_0 g_R \beta}{eQ_0}\right)^2 = \frac{80}{7}\left(\frac{\mu_0 g_R}{eZR_0^2}\right)^2, \quad (2.4)$$

where R_0 is the nuclear radius. It is interesting to note that this ratio is independent of γ and β.

The ratio of the γ-ray intensities emitted in the two types of radiation is determined from the ratio (2.4) of the reduced probabilities by the formula

$$T(M1)/T(E2) = (0.03k^2)^{-1}\frac{B(M1;\ 22 \rightarrow 21)}{B(E2;\ 22 \rightarrow 21)}, \quad (2.5)$$

where $k = (E_{22} - E_{21})/\hbar c$.

The table contains values of $T(M1)/T(E2)$ for 22 → 21 transitions in a few nuclei, as obtained from (2.5) using the values $\mu_0 = 5.05 \times 10^{-24}$ erg/Gauss, $g_R = 0.4$; $R_0 = 1.2\,A^{1/3} \times 10^{-13}$ cm. The last column gives the intensities of the 22 → 21 transition from the data of Lindquist and Marklund.[3]

---

[1] A. S. Davydov and G. F. Filippov, J. Exptl. Theoret. Phys. (U.S.S.R.) **35**, 440 (1958), Soviet Phys. JETP **8**, 303 (1959).

[2] Alaga, Alder, Bohr, and Mottelson, Kgl. Danske Videnskab. Selskab Mat. fys. Medd. **29**, No. 9 (1955).

[3] T. Lindqvist and I. Marklund, Nucl. Phys. **4**, 189 (1957).

[4] M. E. Rose, Multipole Fields, Wiley, 1955 (Russ. Transl. IIL, 1957).

Translated by M. Hamermesh
140

RADIATION CORRECTIONS TO BREMSSTRAHLUNG

P. I. FOMIN

Khar' kov State University

Submitted to JETP editor April 2, 1958

J. Exptl. Theoret. Phys. (U.S.S.R.) 35, 707-718 (September, 1958)

Radiation corrections to the differential cross section for bremsstrahlung are computed using the mass operator method. A general formula is obtained and some limiting cases are considered.

FOR the calculation of radiation corrections to cross sections one ordinarily makes use of Feynman techniques which are described in greatest detail by Brown and Feynman[1] as applied to the Compton effect. By comparison with the Compton effect an additional parameter appears in bremsstrahlung which is associated with the momentum transferred to the nucleus, and as a result of this the calculation of integrals by the Feynman method and also the evaluation of the traces of matrices becomes considerably more complicated. In the present article radiation corrections to bremsstrahlung are calculated by means of the mass operator method.[2,3] The main advantage of this method is the fact that in it one can make use of the expression for the mass operator obtained by Newton[3] in which the integration over the momenta of the virtual particles is carried out in a general way. This, in turn, facilitates the calculation of the traces of matrices. Moreover, it was also possible to develop a quite convenient technique for the evaluation of integrals which remain in the mass operator after the integrations over the momenta have been carried out.

1. GENERAL FORMULAS AND THE CROSS SECTION FOR THE FUNDAMENTAL PROCESS

As is well known,[2,3] single electron processes may be described taking radiation corrections into account, by means of the modified Dirac equation*

$$(\gamma p + m + V)\psi = 0 \tag{1}$$

where $V = e\gamma A + \Delta M$; ΔM is the regularized mass operator; A includes the radiation field A^r, the external field A^e and the regularized vacuum polarization field A':

$$A = A^r + A^e + A';$$

$$\gamma a = \gamma_\mu a_\mu = \gamma_1 a_1 + \gamma_2 a_2 + \gamma_3 a_3 + \gamma_4 a_4,$$

$$\gamma_\mu\gamma_\nu + \gamma_\nu\gamma_\mu = -2\delta_{\mu\nu}, \quad (\mu, \nu = 1, 2, 3, 4).$$

On the basis of Eq. (1) it is possible to obtain the following formula for the bremsstrahlung cross section averaged over the electron spins

$$d\sigma = \frac{\pi^2}{4}\frac{d\mathbf{p}_2 d\mathbf{k}}{\omega\varepsilon_2 |\mathbf{p}_1|} \times \mathrm{Sp}\,(p_2|H|p_1)(\gamma p_1 - m)(p_1|\gamma_4 H^+ \gamma_4|p_2)(m - \gamma p_2), \tag{2}$$

where

$$H = (1 + VG)^{-1} V = V - VGV + \cdots, \tag{3}$$

Here $G = (\gamma p + m)^{-1}$ is the Green's function of the Dirac equation; $(p_2|H|p_1)$ is the matrix element of H between the eigenfunctions of the momentum operator normalized in such a way that $(p_2|p_1) = \delta(p_2 - p_1)$; $p_1 = (\mathbf{p}_1, i\epsilon_1)$ and $p_2 = (\mathbf{p}_2, i\epsilon_2)$ are the initial and final electron momenta; $k = (\mathbf{k}, i\omega)$ is the photon momentum. It is assumed in formula (2) that one of the δ-functions with respect to energy arising here should be replaced by $(2\pi)^{-1}$ (cf., for example, Akhiezer and Berestetskii,[4] § 28).

The radiation field in (2) should be written in the form

$$A^r_\mu(x) = e_\mu e^{-ikx}, \quad e^2_\mu = 1. \tag{4}$$

The external field (the field of the nucleus at rest) satisfies the equation

$$\Box A^e_\mu(x) = -Ze v_\mu \delta(\mathbf{x}), \quad v_\mu = (0, 0, 0, i),$$

from which we obtain

$$A^e_\mu(k_1) = (2\pi)^{-2}\int A^e_\mu(x)\,e^{-ik_1x}dx = a(k_1)\,v_\mu, \tag{5}$$

where

$$a(k_1) = (Ze/2\pi)\,\delta(k_{10})/k_1^2.$$

The bremsstrahlung is described by the terms in H quadratic in the field A. By separating out in ΔM the terms ΔM_1 and ΔM_2 which are linear and quadratic in the field respectively, we can write on the basis of (3)

---

*We employ units in which $\hbar = c = 1$, $e^2/4\pi = 1/137$.

$$H = -e^2\gamma A G\gamma A + \Delta M_2 + e(\gamma A G\Delta M_1 + \Delta M_1 G\gamma A).$$

Newton[3] has shown [formula (2.19)] that the term $e(\gamma AG\Delta M_1 + \Delta M_1 G\gamma A)$ cancels with a part of ΔM_2 which is defined by formula (2.16). The remaining part of ΔM_2 which we shall denote by H_M is broken up into two terms [cf. Newton[3] (2.14) and (2.17)]:

$$H_M = \Delta M_2^1 + \Delta M_2^3.$$

In H one should make the substitution $A = A^r + A^e + A'$. However, the process which is of interest to us is described only by the cross terms:

$$\begin{gathered} H = H_0 + H_M + H_{A'}; \\ H_0 = -e^2(\gamma A^r G\gamma A^e + \gamma A^e G\gamma A^r), \qquad (6) \\ H_{A'} = -e^2(\gamma A^r G\gamma A' + \gamma A' G\gamma A^r), \end{gathered}$$

while in H_M one should also retain only the cross terms in A^r and A^e. H_0 describes the fundamental bremmstrahlung process:

$$d\sigma_0 = \frac{\pi^2}{4}\frac{d\mathbf{p}_2 d\mathbf{k}}{\omega\varepsilon_2|\mathbf{p}_1|} \times \operatorname{Sp}(p_2|H_0|p_1)(\gamma p_1 - m)(p_1|\gamma_4 H_0^+\gamma_4|p_2)(m - \gamma p_2). \qquad (7)$$

The radiation corrections $\sim e^2$ are determined by the interference of H_M and $H_{A'}$ with H_0:

$$d\sigma_R = \frac{\pi^2}{4}\frac{d\mathbf{p}_2 d\mathbf{k}}{\omega\varepsilon_2|\mathbf{p}_1|} 2\operatorname{Re}\operatorname{Sp}(p_2|H_M + H_{A'}|p_1) \times (\gamma p_1 - m)(p_1|\gamma_4 H_0^+\gamma_4|p_2)(m - \gamma p_2) \equiv d\sigma_M + d\sigma_{A'}. \qquad (8)$$

Taking (4) and (5) into account we can easily obtain

$$(p_2|H|p_1) = -(e/2\pi)^2 a(q) \times [\gamma e(\gamma p_3 + m)^{-1}\gamma v + \gamma v(\gamma p_4 + m)^{-1}\gamma e], \qquad (9)$$

where

$$q = p_2 + k - p_1, \quad p_3 = p_2 + k, \quad p_4 = p_1 - k. \qquad (10)$$

From this it follows that

$$(p_1|\gamma_4 H_0^+\gamma_4|p_2) = \gamma_4(p_2|H_0|p_1)^+\gamma_4 = (e/2\pi)^2 a(q)\,Q, \qquad (11)$$

where

$$Q = \gamma v(\gamma p_3 + m)^{-1}\gamma e + \gamma e(\gamma p_4 + m)^{-1}\gamma v. \qquad (12)$$

The evaluation of the traces of matrices in (7) is easily carried out after summing over the photon polarizations which, as is well known, consists of replacing $e_\mu \to \delta_{\mu\lambda}$ (and at the same time $\gamma e \ldots \gamma e \to \gamma_\lambda \ldots \gamma_\lambda$). As a result of this we obtain the Bethe-Heitler formula which may be conveniently written for future use in the following form [cf. Akhiezer and Berestetskii[4] (31.12)]*

$$d\sigma_0 = \frac{Z^2}{\pi^2}\left(\frac{e^2}{4\pi}\right)^3 \frac{d\mathbf{p}_2 d\mathbf{k}\,\delta(\varepsilon_1 - \varepsilon_2 - \omega)}{\omega\varepsilon_2|\mathbf{p}_1|\mathbf{q}^4} U_0, \qquad (13)$$

where

$$U_0 = T^2 - \rho S^2 - R^2/2\varkappa\tau, \qquad (14)$$

$$\mathbf{R} = \mathbf{R}_1 - \mathbf{R}_2, \quad \mathbf{S} = (\mathbf{R}_1/\tau + \mathbf{R}_2/\varkappa)/2\omega, \qquad (15)$$

$$\mathbf{T} = (\varepsilon_2\mathbf{R}_1/\tau + \varepsilon_1\mathbf{R}_2/\varkappa)/\omega, \quad \mathbf{R}_1 = 2[\mathbf{k}\times\mathbf{p}_1], \quad \mathbf{R}_2 = 2[\mathbf{k}\times\mathbf{p}_2],$$

$$\varkappa = p_3^2 + 1, \quad \tau = p_4^2 + 1, \quad \rho = \mathbf{q}^2, \qquad (16)$$

with

$$\begin{gathered} R_1^2 = 4\omega(\varepsilon_1\tau - \omega) - \tau^2, \quad R_2^2 = -4\omega(\varepsilon_2\varkappa + \omega) - \varkappa^2; \\ R_1R_2 = 2\omega(\varepsilon_1\tau - \varepsilon_2\varkappa - \omega\rho - 2\omega) + \varkappa\tau. \end{gathered} \qquad (17)$$

2. GENERAL EXPRESSION FOR THE RADIATION CORRECTIONS

Let us examine first the contribution to the cross section made by $H_{A'}$. It is determined by the second term in formula (8) and is denoted by $d\sigma_{A'}$. We note that $H_{A'}$ differs from H_0 merely by replacing A^e by A'. The Fourier components $\delta a(q)$ and $a(q)$ of the quantities $A_4'(x)$ and $A_4^e(x)$ are related in the static case by the following expression (Akhiezer and Berestetskii,[4] § 43):

$$\delta a(q) = -(e/2\pi)^2 a(q)\,W(x), \qquad (18)$$

where

$$W(x) = (1 - x\coth x)\left(1 - \frac{1}{3}\coth^2 x\right) - \frac{1}{9}, \qquad (19)$$

$$4\sinh^2 x = \mathbf{q}^2, \quad \mathbf{q} = \mathbf{p}_2 + \mathbf{k} - \mathbf{p}_1.$$

From this, after taking into account (6), (7), and (8), it follows that

$$d\sigma_{A'} = d\sigma_0[-(e/2\pi)^2 2W(x)]. \qquad (20)$$

Let us now write the sum $d\sigma = d\sigma_0 + d\sigma_R$ in the form

$$d\sigma = d\sigma_0[1 - (e/2\pi)^2(2W(x) + U/U_0)], \qquad (21)$$

where

$$U = \left(\frac{2\pi}{e}\right)^4 \frac{1}{4a(q)} \operatorname{Re}\operatorname{Sp}(p_2|H_M|p_1)(\gamma p_1 - m)\,Q\,(\gamma p_2 - m). \qquad (22)$$

According to Newton[3] [formula (2.10) and further],

$$H_M = \Delta M_2^1 + \Delta M_2^3 = \left(\frac{e^2}{4\pi}\right)^2 \int_0^\infty i\,ds \int_0^1 du \exp\{-is(u + \lambda^2/u)\} \times \int \frac{dk_1}{(2\pi)^2}\frac{dk_2}{(2\pi)^2} e^{ik_1x}[M_2^1(p, k_1, k_2) + M_2^3(p, k_1, k_2)]\,e^{ik_2x}, \qquad (23)$$

where M_2^1 and M_2^3 are given by Newton's formulas[3] (2.14) and (2.17). The factor $\exp(-is\lambda^2/u)$ added by us (λ is the fictitious photon mass) guarantees the convergence of the integrals over u at the lower limit. This factor arises if in the mass operator the photon Green's function is taken to be of the form $(k^2 + \lambda^2)^{-1}$, instead of k^{-2}, in order to eliminate the infrared divergence.

We shall illustrate the method of evaluating U on the example of one of the terms from M_2^3 which we shall denote by $B(p, k_1, k_2)$:

---

*We shall take m = 1 in all specific calculations and results.

$$B(p,\ k_1,\ k_2) = \int_0^1 dv_1 \int_0^{v_1} dv_2 \Phi(k_1,\ k_2)\,[f_B(v_1,\ v_2)\, i\gamma_\mu J_\mu(k_1)\, G(p) \times E(p^2)\, k_{1\nu} F_{\nu\lambda}(k_2)\,\gamma_\lambda \tag{24}$$

$$- f_B(1-v_2,\ 1-v_1)\, i\gamma_\lambda F_{\lambda\nu}(k_1)\, k_{2\nu} G(p)\, E(p^2)\,\gamma_\mu J_\mu(k_2)],$$

where

$$f_B(v_1,\ v_2) = -2isu(1-v_1)\,[2-u+u^2(1-2v_1)V],$$

$$V = v_1 - v_2,$$

$$\Phi(k_1,\ k_2) = \exp\{-isu\,[v_1(1-v_1)k_1^2 + v_2(1-v_2)k_2^2 + v_2(1-v_1)2k_1k_2]\},$$

$$E(p^2) = \exp\{-is(1-u)V(p^2+m^2)\};$$

$$J_\mu = J_\mu^r + J_\mu^e,\ F_{\mu\nu} = F_{\mu\nu}^r + F_{\mu\nu}^e,$$

in which, in accordance with (4) and (5),

$$\begin{aligned} F_{\mu\nu}^r(k_1) &= (2\pi)^{-2}\int F_{\mu\nu}^r(x)\, e^{-ik_1x}dx \\ &= i(2\pi)^2\delta(k_1+k)(e_\mu k_\nu - e_\nu k_\mu), \\ k_1^{-2}J_\mu^r(k_1) &= (2\pi)^2\delta(k_1+k)\, e_\mu,\ J_\mu^r(k_1) = 0, \\ F_{\mu\nu}^e(k_1) &= -ia(k_1)(v_\mu k_{1\nu} - v_\nu k_{1\mu}),\ J_\mu^e(k_1) = a(k_1)\, k_1^2 v_\mu. \end{aligned} \tag{25}$$

A contribution to bremsstrahlung will be made only by the terms

$$F^r(k_1)\ldots J^e(k_2) \text{ and } J^e(k_1)\ldots F^r(k_2).$$

Corresponding to this $B(p, k_1, k_2)$ will be broken up into two terms:

$$B = B^{re} + B^{er}. \tag{26}$$

We consider

$$H_B \equiv \left(p_2 \left| \int dk_1 dk_2 e^{ik_1x} B(p,\ k_1,\ k_2)\, e^{ik_2x} \right| p_1\right)$$

$$= \int dk_1 dk_2 dp\,\delta(p-p_1-k_2)\,\delta(p-p_2+k_1)\, B(p,\ k_1,\ k_2).$$

In accordance with (26) and (24) we can easily obtain

$$H_B = H_B^{re} + H_B^{er}, \tag{27}$$

where

$$H_B^{er} = (2\pi)^2 a(q)\, q^2 \int_0^1 dv_1 \int_0^{v_1} dv_2 \Phi(q,\ -k)$$

$$\times E(p_4^2)\, f_B(v_1,\ v_2)\,\gamma v(\gamma p_4 + 1)^{-1} \times [\gamma e(kq) - \gamma k(eq)],$$

$$H_B^{re} = (2\pi)^2 a(q)\, q^2 \int_0^1 dv_1 \int_0^{v_1} dv_2 \Phi(-k,\ q)\, E(p_3^2)$$

$$\times f_B(1-v_2,\ 1-v_1)\,[\gamma e(kq) - \gamma k(eq)]\,(\gamma p_3 + 1)^{-1}\gamma v.$$

We denote the contributions of H_B, H_B^{re} and H_B^{er} to U respectively by U_B, U_B^{re} and U_B^{er}. After the evaluation of traces U_B will be expressed only in terms of the quantities κ, τ, ρ, ϵ_1, and ϵ_2. Therefore

$$U_B = U_B^{re}(\varkappa,\ \tau,\ \rho,\ \varepsilon_1,\ \varepsilon_2) + U_B^{er}(\varkappa,\ \tau,\ \rho,\ \varepsilon_1,\ \varepsilon_2).$$

We shall now show that

$$U_B^{er}(\varkappa,\ \tau,\ \rho,\ \varepsilon_1,\ \varepsilon_2) = U_B^{re}(\tau,\ \varkappa,\ \rho,\ \varepsilon_2,\ \varepsilon_1). \tag{28}$$

Indeed, if in U_B^{er} we replace $k \to -k$, $q \to -q$, $p_1 \rightleftarrows p_2$ (and at the same time $p_3 \rightleftarrows p_4$), and if in the integrals we introduce new variables $v_1 \to 1 - v_2$, $v_2 \to 1 - v_1$ [with $\Phi(q, -k) \to \Phi(-k, q)$], we shall obtain under the trace sign in U_B^{er} the same factors as in U_B^{re}, but written out in inverted order. After the evaluation of the trace the two expressions will become the same. The replacement of the momenta indicated above is equivalent to the replacement $\kappa \rightleftarrows \tau$, $\epsilon_1 \rightleftarrows \epsilon_2$ in the final result, and this completes the proof of assertion (28). This property is common to all the terms in ΔM_2^3 and ΔM_2^1 and may be easily checked for each term. Thus

$$U = U^{re}(\varkappa,\ \tau,\ \rho,\ \varepsilon_1,\ \varepsilon_2) + U^{re}(\tau,\ \varkappa,\ \rho,\ \varepsilon_2,\ \varepsilon_1), \tag{29}$$

and therefore it is sufficient to evaluate only $U^{re}(\kappa, \tau, \rho, \epsilon_1, \epsilon_2)$.

The quantity U_B^{re} may be written in the form

$$U_B^{re} = J_B h_B / 16, \tag{30}$$

where

$$J_B = \mathrm{Re}\int_0^\infty ids \int_0^1 due^{-isu} \int_0^1 dv_1 \int_0^{v_1} dv_2 \Phi(-k,\ q) \times E(p_3^2)\, f_B(1-v_2,\ 1-v_1), \tag{31}$$

$$h_B = \mathrm{Sp}\, q^2\,[\gamma_\lambda(kq) \tag{32}$$

$$- q_\lambda(\gamma k)(\gamma p_3 + 1)^{-1}\gamma v(\gamma p_1 - 1)\, Q_\lambda(\gamma p_2 - 1),$$

$$Q_\lambda = \gamma v(\gamma p_3 + 1)^{-1}\gamma_\lambda + \gamma_\lambda(\gamma p_4 + 1)^{-1}\gamma v.$$

The evaluation of the trace of h_B leads to the result

$$\begin{aligned} h_B &= (2\rho/\varkappa)(2\rho b/\varkappa\tau + \tau\alpha) \\ &- 4\rho\,\{\rho\omega(\varepsilon_1/\tau + \varepsilon_2/\varkappa) + (2\rho/\varkappa)(\varepsilon_1^2 + \varepsilon_2^2) \\ &+ (\varepsilon_1/\varkappa + \varepsilon_2/\tau)\,[\varepsilon_1(1 + 4\alpha/\varkappa) - \varepsilon_2\tau]\}, \end{aligned} \tag{33}$$

where

$$\alpha = \varkappa + \tau,\ b = \alpha^2 + \varkappa\tau(\rho - \alpha).$$

With the aid of (15) and (17) this may be written in the form

$$h_B = 2\rho\,[2\tau U_0 + T(R_1 + R_2) - 2\omega RS]. \tag{34}$$

We introduce the notation

$$J[f(v_1, v_2)] = \int_0^\infty ids \int_0^1 du \exp\{-is(u + \lambda^2/u)\} \int_0^1 dv_1 \int_0^{v_1} dv_2 \times \Phi(q, -k) E(p_3^2) f(v_1, v_2), \qquad (35)$$

where

$$\Phi(q, -k) = \exp\{-is[v_1(1 - v_1)\rho - v_2(1 - v_1)\alpha]u\},$$

$$E(p_3^2) = \exp\{-is(1 - u)V\varkappa\}.$$

After introducing in (31) new variables $v_1 \to 1 - v_2$, $v_2 \to 1 - v_1$, (with $\Phi(-k, q) \to \Phi(q, -k)$, while $E(p_3^2)$ remains unchanged) we obtain:

$$J_B = J[(f_B(v_1, v_2)] = J\{-2isu(1 - v_1)[2 - u + u^2V(1 - 2v_1)]\}.$$

Making use of obvious properties of the integrals $J(f)$ we can easily rewrite J_B in the form

$$J_B = 2J[isu(u - 2)(1 - v_1)] + 2\frac{\partial}{\partial\alpha}J(u^2) + 2\frac{\partial}{\partial\rho}[J(u^2) - 2J(u^2V)].$$

It is shown in the Appendix [cf. (A.6) and (A.5)] that

$$J[isu^2(1 - v_1)] = -\varkappa\frac{\partial}{\partial\varkappa}J[isu(1 - v_1)],$$

$$2J(u^2) = \left(1 - \varkappa\frac{\partial}{\partial\varkappa}\right)J(u).$$

Thus it now remains to calculate $J(isu)$, $J(isuv_1)$, $J(u)$ and $J(u^2V)$. The method of carrying out these calculations is given in the Appendix.

It turns out that all the integrals appearing in ΔM_2^3 with the exception of $J(ise^{-is\lambda^2/u})$ can be expressed in a similar manner in terms of these four integrals and their derivatives with respect to the parameters κ, α and ρ. The integrals appearing in ΔM_2^1, and likewise $J(ise^{-is\lambda^2/u})$, may be evaluated directly; the results are given in the Appendix.

We have described the method of calculating the contribution to U^{re} of the term B. The contribution made by the remaining terms may be evaluated in an analogous manner. As a result of all these calculations the following result has been obtained for U^{re}

$$\begin{aligned}2U^{re}(\varkappa, \tau, \rho, \varepsilon_1, \varepsilon_2) &= T^2(2y/\sinh 2y) + U_0\{2(1 - 2y\coth 2y)\ln\lambda + 4y\coth 2y[h(2y) - h(y)] + 2 - y\coth y \\ &- (4 + \rho)y/\sinh 2y + 2\tau M + \text{antisymm. terms} - (\tau U_0 + S_1\partial/\partial\varkappa)J[u^2(1 - V)] + (S_2\partial/\partial\varkappa + S_3\partial/\partial\alpha \\ &+ S_4\partial/\partial\rho)J(u) + (S_5\partial/\partial\varkappa + S_6\partial/\partial\alpha + S_7\partial/\partial\rho)J(u^2) + (S_8\partial/\partial\alpha + S_9\partial/\partial\rho)J(u^2V) + (S_{10} - S_{11}\varkappa\partial/\partial\varkappa \\ &+ {}^1/_2 S_{12}\varkappa^2\partial^2/\partial\varkappa^2)J(isu) + (S_{13} - S_{14}\varkappa\partial/\partial\varkappa + {}^1/_2 S_{15}\varkappa^2\partial^2/\partial\varkappa^2)J(isuv_1),\end{aligned} \qquad (36)$$

where

$$2bJ(u) = [\varkappa(\alpha - \rho) - 2\alpha]L - \varkappa(\rho - \alpha)(\rho - \alpha + 4)M + \varkappa[(\rho - \alpha)(\rho - \varkappa + 4) + 2\alpha]N; \qquad (37)$$

$$2bJ(isu) = \alpha L + (\varkappa - \tau)(\rho - \alpha)M + [(\varkappa - \tau)(\alpha - \rho) + \alpha\tau]N, \qquad (38)$$

$$2bJ(isuv_1) = \tau L - [\tau(\rho - \alpha) + 2\alpha]M + [\tau(\rho - \varkappa) + 2\alpha]N, \qquad (39)$$

$$\begin{aligned}\alpha J(u^2V) &= (\rho - \alpha)\left[\varkappa\left(\frac{\partial}{\partial\alpha} + \frac{\partial}{\partial\rho}\right)J(u) - J(u^2)\right] - \frac{\varkappa^2}{4\rho}\left[(\rho - \varkappa)\frac{\partial N}{\partial\varkappa} - N + \frac{\ln|\varkappa|}{\varkappa - 1}\right] - \frac{1}{\varkappa}[F(\varkappa - 1) - F(-1)] \\ &- \frac{(\varkappa - 2)\ln|\varkappa|}{2(\varkappa - 1)} + x\coth x + \frac{2(\rho - \alpha)}{\alpha}(x\coth x - y\coth y);\end{aligned} \qquad (40)$$

$$L = 2(y^2 - x^2) + F(\varkappa - 1) - F(-1),$$

$$M = \int_0^1 \frac{dv}{1 + (1 - v)v(\rho - \alpha)} \ln\left|\frac{1 + (1 - v)v\rho}{\varkappa v}\right| = 2(\sinh 2y)^{-1}\{(y + x)h(y + x) + (y - x)h(y - x) - yh(y) - y\ln|\varkappa|\},$$

$$N = \int_0^1 \frac{dv}{1 + (1 - v)v\rho - \varkappa v} \ln\left|\frac{1 + (1 - v)v\rho}{\varkappa v}\right|; \quad yh(y) = \int_0^y u\coth u\,du, \quad F(x) = \int_0^x \frac{\ln|1 + u|}{u}du, \quad F(-1) = -\pi^2/6,$$

$$4\sinh^2 x = \rho, \quad 4\sinh^2 y = \rho - \alpha; \quad \alpha = \varkappa + \tau, \quad b = \alpha^2 + \varkappa\tau(\rho - \alpha)$$

and

$$S_1 = \varkappa\tau U_0 + R^2 + \varkappa RT + \varkappa\tau\alpha S^2 - 2\rho\omega SR_2, \quad S_2 = (\varkappa - 2)\tau U_0 - (\alpha/2\varkappa\tau)R^2 - 2RT - 2\varkappa\tau(T^2 + \varkappa S^2) + 4\rho\varepsilon_1 SR_2,$$

$$S_3 = -(\alpha/\varkappa\tau)R^2 - 6\varkappa\tau\rho S^2 + (\alpha - 4)RT + 2\rho TR_1 + 2\rho(\omega - 4\varepsilon_1)RS,$$

$$S_4 = S_3 + (1 + \alpha/\varkappa\tau)R^2 + 4RT + \varkappa\tau\alpha S^2 - \rho(R_1^2/\tau + R_2^2/\varkappa) - 2P,$$

$$S_5 = -2\tau U_0 + \varkappa\tau[T^2 + (\rho + \varkappa)S^2] - (1/\varkappa + \alpha/2\varkappa\tau)R^2 - 2RT - \rho[TR_1 + 2\varepsilon_1 S(R_2 - R)],$$

$$S_6 = \tau\rho U_0 - (1 + \alpha/\varkappa\tau)R^2 + \varkappa\tau(4\rho - \alpha)S^2 - (4 + \alpha)RT + \rho[2(\varepsilon_1 + \varepsilon_2)RS + R_1^2/\tau + R_2^2/\varkappa],$$

$$S_7 = S_6 + \alpha R^2/\varkappa\tau + 4RT - 2P, \qquad S_8 = 2\rho\omega RS + (\varkappa - \tau)RT, \qquad S_9 = -2\tau\rho U_0 + 2\rho[2\omega RS - T(R_1 + R_2)],$$

$$S_{10} = (3\varkappa - 2\rho - 2)\tau U_0 + \alpha R^2/2\varkappa\tau + 2RT, \qquad S_{11} = (\rho - \varkappa)\tau U_0 - R^2/\varkappa - (\rho/\varkappa\tau)RR_1 - 3TR - 4\tau\rho S^2 - P,$$

$$S_{12} = 2\tau U_0 + \frac{\alpha}{2\varkappa\tau}R^2 + 3RT + \frac{1}{\varkappa}\left(R^2 + \frac{\rho}{\tau}RR_1 + 4\varkappa\tau\rho S^2\right) - P,$$

$$S_{13} = 2\tau\rho U_0, \qquad S_{14} = -\tau\rho U_0 - S_{15} + 2P, \qquad S_{15} = -\rho\left(\frac{2}{\varkappa\tau}RR_1 + 4\tau S^2\right) + P,$$

$$P = \frac{\rho}{\varkappa}\left[\frac{1}{2}\left(\frac{1}{\tau} - \frac{1}{\varkappa}\right)R^2 - 2T(R_1 + R_2) - 2\tau U_0\right]. \tag{41}$$

The cross section for the fundamental process $d\sigma_0$ vanishes for zero angles when $\mathbf{k} \times \mathbf{p}_1 = \mathbf{k} \times \mathbf{p}_2 = 0$. At the same time the radiation corrections found by us also vanish, as should have been expected, since they are determined by interference with the matrix element of the fundamental process.

If the accuracy with which the energy is measured does not exceed a certain value $\Delta E \ll m$ then in actual fact the quantity which will be measured will be the total cross section of the ordinary bremsstrahlung of a single photon of momentum $\mathbf{k}$ and of processes in which additional soft photons are emitted whose total energy does not exceed ΔE. To the order in e^2 which we are at present considering we should also add to $d\sigma$ the cross section $d\sigma_D$ of double bremsstrahlung when the additional radiation consists of the emission of a single photon of low energy $\omega_1 < \Delta E$. According to the general rule[5]

$$d\sigma_D = d\sigma_0(e/2\pi)^2 D, \tag{42}$$

where

$$D = \frac{1}{4\pi}\int_0^{\Delta E}\frac{d\mathbf{k}_1}{\sqrt{\mathbf{k}_1^2 + \lambda^2}}\left(\frac{p_2}{p_2\cdot k_1} - \frac{p_1}{p_1\cdot k_1}\right)^2. \tag{43}$$

The expression for D may be written in the following form (Akhiezer and Berestetskii,[4] § 32.4):

$$D = 2(1 - 2y\coth 2y)\ln\frac{\lambda}{2\Delta E} \tag{44}$$

$$+ \frac{1}{2}\left[\frac{1}{v_1}\ln\frac{1 + v_1}{1 - v_1} + \frac{1}{v_2}\ln\frac{1 + v_2}{1 - v_2} - \coth 2y\cdot Y(y, \varepsilon_1, \varepsilon_2)\right],$$

where

$$v_1\varepsilon_1 = |\,p_1\,|, \quad v_2\varepsilon_2 = |\,p_2\,|,$$

$$Y(y, \varepsilon_1, \varepsilon_2) = \int_1^1 \frac{dz}{\coth^2 y - z^2\sinh^2 y}\,\frac{\varepsilon_z}{p_z}\ln\frac{\varepsilon_z + p_z}{\varepsilon_z - p_z}, \tag{45}$$

$$2\varepsilon_z = \varepsilon_1 + \varepsilon_2 + \omega z, \quad p_z^2 = \varepsilon_z^2 + z^2\sinh^2 y - \coth^2 y.$$

It may be easily seen that the term in $\ln\lambda$ cancels out in the total cross section $d\sigma + d\sigma_D$.

3. LIMITING CASES

On the basis of the general formulas (36) and (42) we can easily obtain certain limiting expressions for the radiation corrections to bremsstrahlung. Five independent parameters: ϵ_1, ω, $\theta_1 = \widehat{\mathbf{k}\mathbf{p}_1}$, $\theta_2 = \widehat{\mathbf{k}\mathbf{p}_2}$, and $\theta = \widehat{\mathbf{p}_1\mathbf{p}_2}$ appear in the cross section. All the other parameters may be expressed in terms of them:

$$\varkappa = -2\omega(\varepsilon_2 - p_2\cos\theta_2), \quad \varepsilon_2 = \varepsilon_1 - \omega,$$

$$\tau = 2\omega(\varepsilon_1 - p_1\cos\theta_1), \quad p_1 = \sqrt{\varepsilon_1^2 - 1},$$

$$\rho = -2 + \varkappa + \tau + 2(\varepsilon_1\varepsilon_2 - p_1p_2\cos\theta), \quad p_2 = \sqrt{\varepsilon_2^2 - 1}.$$

We consider four particularly interesting limiting cases in which the general formula can be considerably simplified. We write the total cross section $d\bar{\sigma} = d\sigma + d\sigma_D$ in the form

$$d\bar{\sigma} = d\sigma_0[1 - (e/2\pi)^2\delta], \tag{46}$$

where

$$\delta = U/U_0 + 2W(x) - D. \tag{47}$$

(1) The case of low frequencies ($\omega\epsilon_1 \ll 1$). In the limiting case of almost elastic scattering, i.e., for radiation of low frequencies, we should expect a simple relation between the radiation corrections to bremsstrahlung and the radiation corrections to elastic scattering.[6] Indeed, in the limit $\omega \to 0$ ($\mathbf{p}_2 \to \mathbf{p}_1 = \mathbf{p}$, $\epsilon_2 \to \epsilon_1 = \epsilon$) the bremsstrahlung cross section may be represented in the form of the product

$$d\sigma_0 = d\sigma_y^0\cdot w_\omega^0 \tag{48}$$

of the elastic scattering cross section

$$d\sigma_y^0 = \left(\frac{Ze^2}{8\pi pv}\right)^2\frac{1 - v^2\sin^2(\theta/2)}{\sin^4(\theta/2)}\,dO_2 \tag{49}$$

by the probability of radiation occurring during scattering

$$w^0_\omega = \frac{e^2}{2(2\pi)^3}\cdot\frac{v^2}{p^2}\,\frac{d\omega dO}{\omega V_1 V_2}\left(4p^2\sin^2\cdot\frac{\theta}{2}+2-\frac{V_1}{V_2}-\frac{V_2}{V_1}\right), \tag{50}$$

where

$$v = p/\varepsilon,\quad V_1 = 1 - v\cos\theta_1,\quad V_2 = 1 - v\cos\theta_2.$$

On taking radiation corrections into account

$$d\sigma^0_y \to d\sigma_y = d\sigma^0_y\,[1-(e/2\pi)^2\delta_y],$$

$$w^0_\omega \to w_\omega = w^0_\omega\,[1-(e/2\pi)^2\delta_\omega],$$

so that our formula (46) should in the limit $\omega \to 0$ reduce to

$$d\bar{\sigma} = d\sigma^0_y\cdot w^0_\omega\,[1-(e/2\pi)^2(\delta_y+\delta_\omega)], \tag{51}$$

where δ_y is determined by Schwinger's formula[6] (cf. also Akhiezer and Berestetskii,[4] § 45).

If we assume $\omega\epsilon_1 \ll 1$ [and at the same time $|\kappa|$, $\tau \ll 1$, $\rho = 4p^2\sin^2(\theta/2)$], we obtain the following value* for δ

$$\begin{aligned}\delta &= 2(1-2x\coth 2x)\ln 2\Delta E + x\tanh x\\ &+ 4x\coth 2x\,[h(2x)-h(x)] + 2W(x) + \frac{2x}{\sinh 2x}\,\frac{\rho}{4\varepsilon^2-\rho}\\ &+ \frac{1}{v}\ln\frac{1+v}{1-v} + \frac{(1-v^2)\coth 2x}{v\sin\theta/2}\,G(v_1\theta)\\ &+ O(\omega\varepsilon_1\ln\omega,\ \omega\varepsilon_1) = \delta_y + O(\omega\varepsilon_1\ln\omega,\ \omega\varepsilon_1).\end{aligned} \tag{52}$$

Here

$$G(v,\theta) = \int\limits_{\cos\theta/2}^{1}\frac{du}{(1-v^2u^2)(u^2-\cos^2(\theta/2))^{1/2}}\ln\frac{1+vu}{1-vu}.$$

Thus, $\delta_\omega = 0(\omega\epsilon,\ \ln\omega)$, i.e., it behaves like $\omega\ln\omega$ as $\omega \to 0$. In the non-relativistic limit (cf. below)

$$\delta_\omega = {}^4/_3\,(\mathbf{p}_1-\mathbf{p}_2)\,\mathbf{k}\ln\omega. \tag{53}$$

(2) Relativistic case (ϵ_1, $\epsilon_2 \gg 1$). At high energies, small angles (θ, θ_1, $\theta_2 \sim 1/\epsilon$) play the principal role in the cross section $d\sigma_0$. For these values of the angles the formula for the corrections is considerably simplified only if we assume $\omega \ll \epsilon_1$, in which case we may impose on the angles the less restrictive condition $\theta_1^2 \ll 1/\omega\epsilon_1$, $\theta_2^2 \ll 1/\omega\epsilon_2$. Under these conditions $|\kappa|$, $\tau \ll 1$, $\rho = \epsilon_1\epsilon_2\theta^2 \ll \epsilon_1/\omega$, and

$$\begin{aligned}\delta &= 2(1-2x\coth 2x)\left(\ln\frac{\Delta E}{\varepsilon_1}+1\right) + x\tanh x\\ &+ 2W(x) + O\left(\frac{\omega}{\varepsilon_1}\ln\varepsilon_1,\ \frac{\omega}{\varepsilon_1}\right).\end{aligned} \tag{54}$$

In order to estimate the order of magnitude of the corrections we take $\epsilon_1 = 100$, $x = 1$. In this case

$$(e/2\pi)^2\delta \simeq 0.02\,(1-0.25\ln 2\,\Delta E). \tag{55}$$

(3) Ultrarelativistic case. It is of interest to investigate the behavior of the corrections for angles which are not too small. In this case, to achieve simplification, we take energies so large that

$$\ln(\rho-\alpha),\ \ln\rho,\ \ln|\varkappa|,\ \ln\tau \gg 1,$$

but at the same time

$$\ln\frac{\rho-\alpha}{|\varkappa|},\ \ln\frac{\rho-\alpha}{\tau},\ \ln\frac{\rho}{|\varkappa|},\ \ln\frac{\rho}{\tau} \sim 1.$$

At the same time

$$\begin{aligned}\delta &= 2(1-2y)\ln 2\Delta E + 4y^2 - 3y - 2y\ln\frac{\rho-\alpha}{4\varepsilon_1\varepsilon_2} + \frac{4}{3}x\\ &- \ln\varepsilon_1\varepsilon_2 + O(1),\qquad 2x = \ln\rho,\ 2y = \ln(\rho-\alpha).\end{aligned} \tag{56}$$

From this it follows that, roughly speaking, the dependence on the energy is of the form

$$\delta = A\ln^2\varepsilon_1 + B\ln\varepsilon_1 + C.$$

Such behavior is characteristic in general for all the radiation corrections of order e^2 which we are at the moment discussing. At sufficiently high energies the correction may attain values of 10 to 20%.

(4) Nonrelativistic case ($p_1 \ll 1$). At low energies we obtain

$$\begin{aligned}\delta = -\frac{2}{3}\Big\{&(\mathbf{p}_1-\mathbf{p}_2)^2\left(\frac{19}{30}-\ln 2\Delta E\right)\\ &+ 2(\mathbf{p}_1-\mathbf{p}_2)\,\mathbf{k}\ln\omega\Big\} + O(p^3).\end{aligned} \tag{57}$$

The fact that the corrections tend to zero as $p_1 \to 0$ is a characteristic feature. We note that in the nonrelativistic limit corrections to the elastic scattering,[6] to the Compton effect,[1] and to the Møller scattering,[8] also vanish. The corrections to the two-photon pair annihilation[9] approach a finite limit as the relative velocity of the electron and the positron tends to zero. However, this limit is not a truly nonrelativistic one, but rather a threshold one, since in the inverse process of pair creation this will correspond to the threshold of the reaction. On the basis of these results we may apparently make a general assertion that the radiation corrections always vanish in the true nonrelativistic limit, while in the case of threshold reactions they approach a finite limit at the threshold.

The author takes this opportunity to express his gratitude to Prof. A. I. Akhiezer for suggesting the subject of the present investigation and for valuable aid, and also to V. G. Bar'iakhtar and S. V. Peletminskii for considerable aid in calculations at the earlier stages of the work, and to V. F. Aleksin and D. V. Volkov for valuable advice.

---

*cf. also Fomin.[7]

APPENDIX

We shall now present the method of evaluating the integrals. We shall first give the values of certain auxiliary integrals:

$$\int_0^1 [1 + v(1-v)\cdot 4\sinh^2 y]^{-1}\,dv = 2y/\sinh 2y; \qquad \int_0^1 dv_1 \int_0^{v_1} dv_2\,[1 + (1-v_1)\,v_2\cdot 4\sinh^2 y]^{-1} = y^2/2\sinh^2 y;$$

$$\int_0^1 \ln v\cdot[1 + (1-v)\,v\cdot 4\sinh^2 y]^{-1}\,dv = -2yh(y)\,(\sinh 2y)^{-1}; \tag{A.1}$$

$$\int_0^1 \frac{\ln|1 + (1-v)\,v\cdot 4\sinh^2 y|}{1 + (1-v)\,v\cdot 4\sinh^2 y}\,dv = \frac{4}{\sinh 2y}\int_0^y u\tanh u\,du = \frac{4y}{\sinh 2y}\,[h(2y) - h(y)].$$

We now consider J(isu). First of all, we note that the integral over the proper time s is defined in such a way that

$$\int_0^\infty i\,ds\,e^{-isa} = a^{-1} \text{and} \int_0^\infty i\,ds\,e^{-isa}\,is = a^{-2}.$$

In accordance with this, we have

$$J(isu) = \int_0^1 du \int_0^1 dv_1 \int_0^{v_1} dv_2\cdot u\,\{[1 + (1-v_1)(v_1\rho - v_2\alpha)]\,u + (1-u)\,V\varkappa]^{-2}.$$

After introducing the new variable $(1-u)u^{-1} = t$ the integration over v_2 and T may be easily carried out and leads to

$$J(isu) = \int_0^1 \frac{v_1\,dv_1}{1 + (1-v_1)\,v_1\rho - v_1\varkappa}\,\frac{1}{1 + (1-v_1)\,v_1(\rho-\alpha)}\ln\left|\frac{1 + (1-v_1)\,v_1\rho}{\varkappa v_1}\right|.$$

With the aid of the auxiliary integrals given above this integral may be easily brought to the final form (38). The evaluation of $J(isuv_1)$ is carried out in a completely analogous manner.

After integration over s and after the introduction of the new variable $(1-u)/u = t$ the integral J(u) takes on the form

$$J(u) = \int_0^\infty \frac{dt}{(1+t)^2}\int_0^1 dv_1 \int_0^{v_1} dv_2\,[1 + (1-v_1)(v_1\rho - v_2\alpha) + \varkappa Vt]^{-1}. \tag{A.2}$$

Integration by parts with respect to t gives

$$J(u) = 2(x^2 - y^2)/\alpha - \varkappa J(isuV). \tag{A.3}$$

By introducing the new variables $v_1 \rightarrow v_1$, $v_2 \rightarrow v_1 - V$ and by changing the order of integration over V and v_1 the integral J(isuv) may be brought to the form

$$J(isuV) = \frac{1}{\alpha}\int_0^\infty \frac{dt}{1+t}\int_0^1 dV \int_V^1 dv_1\,\frac{[V\alpha - (1-2v_1)(\rho-\alpha)] + (1-2v_1)(\rho-\alpha)}{\{1 + (1-v_1)\,[v_1(\rho-\alpha) + V\alpha] + \varkappa Vt\}^2}. \tag{A.4}$$

The part of the integral which corresponds to the last term in the numerator is evidently equal to $\frac{\rho-\alpha}{\alpha}$ $J[isu(1-2v_1)]$ and may be found directly with the aid of (38) and (39). The remaining part of the integral assumes the following form after integration over v_1 and t has been carried out:

$$\frac{1}{\alpha}\left\{\frac{1}{\varkappa}\cdot[F(\varkappa-1) - F(-1)] - N\right\}.$$

Finally we obtain the result (37) for J(u).

By means of differentiating (A.2) with respect to κ and then by means of integrating by parts with respect to t it can be shown that

$$\varkappa\frac{\partial}{\partial\varkappa}J(u) = J(u) - 2J(u^2),$$

from which it follows that

$$J(u^2) = {}^1/_2\,(1 - \varkappa\partial/\partial\varkappa)\,J(u). \tag{A.5}$$

In a similar way it can be shown that

$$\begin{gathered} J(isu^2) = -\varkappa\frac{\partial}{\partial\varkappa}J(isu),\quad J(isu^2v_1) = -\varkappa\frac{\partial}{\partial\varkappa}J(isuv_1),\\ J(isu^3) = \frac{1}{2}\Big(1-\varkappa\frac{\partial}{\partial\varkappa}\Big)J(isu^2) = \frac{\varkappa^2}{2}\frac{\partial^2}{\partial\varkappa^2}J(isu),\qquad J(isu^3v_1) = \frac{\varkappa^2}{2}\frac{\partial^2}{\partial\varkappa^2}J(isuv_1). \end{gathered} \tag{A.6}$$

We now consider the integral $J(u^2V)$. It can be shown in a manner similar to that used for deriving (A.3) that

$$J(u^2V) = \frac{1}{2}\int_0^1 dv_1\int_0^{v_1} dv_2\,\frac{V}{1+(1-v_1)(v_1\rho - v_2\alpha)} - \frac{\varkappa}{2}J(isu^2V^2).$$

The first integral can be easily evaluated. By carrying out a transformation similar to (A.4) we readily obtain for $J(isu^2V^2)$

$$\begin{aligned} J(isu^2V^2) = \frac{\rho-\alpha}{\alpha}J[isu^2(1-2v_1)V] &+ \frac{1}{\varkappa}\Big\{\frac{2}{\varkappa}[F(\varkappa-1) - F(-1)] + \frac{\varkappa-2}{\varkappa-1}\ln|\varkappa| - 2\Big\}\\ &+ \frac{\varkappa}{2\rho}\Big[(\rho-\varkappa)\frac{\partial N}{\partial\varkappa} - N + \frac{\ln|\varkappa|}{\varkappa-1}\Big]. \end{aligned}$$

Further, it can be easily checked that

$$J[isu^2(1-2v_1)V] = -2\Big(\frac{\partial}{\partial\alpha} + \frac{\partial}{\partial\rho}\Big)J(u) - J(isu^2V).$$

$$J(isu^2V) = J(isuV) - J[isu(1-u)V] = \frac{2}{\varkappa\alpha}(x^2-y^2) - \frac{1}{\varkappa}\Big(1-\varkappa\frac{\partial}{\partial\varkappa}\Big)J(u).$$

As a result we obtain for $J(u^2V)$ the value (40).

The evaluation of integrals appearing in ΔM_2^1 and also of $J(ise^{-is\lambda^2/u})$ may be easily carried out by means of the procedures outlined above. We now give the results:

$$J(ise^{-is\lambda^2/u}) = \frac{2}{\varkappa\sinh 2y}\Big[yh(y) - (y+x)h(y+x) - (y-x)h(y-x) - y\ln\frac{\lambda}{|\varkappa|}\Big];$$

$$I\{v(1-2v)[u^2 + 2isu(1-u)]\} = \frac{1}{\rho-\alpha}\Big\{1 - y\coth y + \frac{4y}{\sinh 2y}[h(2y) - h(y)] + \Big(1 - \frac{2y}{\sinh 2y}\Big)(1+\ln\lambda^2)\Big\}; \tag{A.7}$$

$$I[u(u-1)] = -y/\sinh 2y;\qquad I(2-u) = \frac{2y}{\sinh 2y}\{2[h(2y) - h(y)] - 1 - \ln\lambda^2\}.$$

Here we have introduced the notation

$$I[f(s,u,v)] = \int_0^\infty ids\int_0^1 du\int_0^1 dvf(s,u,v)\times\exp\{-isu[1+(1-v)v(\rho-\alpha)] - is\lambda^2/u\} \tag{A.8}$$

and in the course of the calculation we have neglected all those terms which vanish as $\lambda \to 0$.

---

[1] L. M. Brown and R. P. Feynman, Phys. Rev. **85**, 231 (1952).

[2] J. Schwinger, Proc. Nat. Acad. Sci. **37**, 455 (1951).

[3] R. G. Newton, Phys. Rev. **94**, 1773 (1954).

[4] A. I. Akhiezer and V. B. Berestetskii, Квантовая электродинамика (Quantum Electrodynamics), M. 1953, (Engl. transl. publ. by U. S. Dept. of Commerce).

[5] J. M. Jauch and F. Rohrlich, Helv. Phys. Acta. **27**, 613 (1954).

[6] J. Schwinger, Phys. Rev. **76**, 790 (1949).

[7] P. I. Fomin, J. Exptl. Theoret. Phys. (U.S.S.R.) **34**, 227 (1958), Soviet Phys. JETP **7**, 156 (1958).

[8] M. L. G. Redhead, Proc. Roy. Soc. **A220**, 219 (1953).

[9] I. Harris and L. M. Brown, Phys. Rev. **105**, 1656 (1957).

Translated by G. Volkoff
141

SOVIET PHYSICS JETP VOLUME 35(7), NUMBER 3 MARCH, 1959

ENERGY DEPENDENCE OF MULTIPLE-PRODUCTION REACTION CROSS SECTIONS NEAR THRESHOLD

A. F. GRASHIN

Moscow Engineering Physics Institute

Submitted to JETP editor April 3, 1958

J. Exptl. Theoret. Phys. (U.S.S.R.) **35**, 719-725 (September, 1958)

The energy dependence of multiple-production reaction cross sections near threshold is obtained, with account taken of effects of the Pauli principle and of the Coulomb interaction of the emitted particles with the residual nucleus. In the general case the recoil of the nucleus and the Coulomb interactions between the emitted particles were neglected. For the case in which not more than one charged particle is among those emitted the nuclear recoil is taken into account and the formulas obtained are exact.

THE functional dependence of the cross section on the energy near threshold for the reactions in question can be found in general form, independent of the concrete interaction mechanism. This has been shown by Wigner for reactions with two particles in the final state.[1] It is a very simple matter to obtain the threshold dependence for reactions in which the final stage is that of the simultaneous emission of N neutral particles with zero orbital angular momenta from an infinitely heavy complex (nucleus), i.e., under the conditions of short-range interaction and symmetry of the wave function in the coordinates of the particles.[2] Hart and others[3] have studied the special case $N = 2$ (emission of a charged particle and a neutral one) with arbitrary orbital angular momenta and with inclusion of effects of the nuclear recoil.

We shall consider the case of emission of N arbitrary particles with masses $\mu_\alpha \ll M_{\text{nuc}}$ (M_{nuc} is the mass of the residual nucleus), with inclusion of effects of the Pauli principle and of the Coulomb interactions of the emitted particles with the nucleus (of charge $Ze \gg e$).

It must be pointed out that for $N \geq 2$ the problem is considerably simplified by the use of the momentum representation, since this removes the necessity of finding the explicit form of the Green's functions in the coordinate representation.[2,3] Even the calculation of the asymptotic behavior of the Green's functions, which is needed for the construction of the reaction amplitude in the coordinate representation, involves considerable difficulty.[3] If there are groups of identical particles among those emitted, then in the determination of the threshold energy dependence the classification in terms of the permutation symmetry is often entirely sufficient for the choice of the allowed channels (including those in terms of the total angular momentum), and one avoids the necessity of examining arbitrary orbital angular momenta of the emitted particles.

1. NEUTRAL PARTICLES

In the center-of-mass system and in the variables $\mathbf{r}_\alpha = \mathbf{x}_\alpha (\mu_\alpha/M),^{1/2}$, $\mathbf{k}_\alpha = \mathbf{p}_\alpha (M/\mu_\alpha)^{1/2}$ the reaction amplitude (with nuclear recoil neglected) has the form*

$$F(\mathbf{k}_1 \ldots \mathbf{k}_N) = \int \exp\left\{-i \sum_{\alpha=1}^{N} \mathbf{k}_\alpha \cdot \mathbf{r}_\alpha\right\} U(r, q)\, \Psi(r, q)\, \varphi^*_{\text{nuc}}(q)\, dr dq, \tag{1}$$

where $U(r, q)$ is the total interaction energy of the emitted particles and the nucleus (it is essential that all the interactions are short-range ones), $\Psi(r, q)$ is the exact wave function, including all the reaction channels, and $\varphi_{\text{nuc}}(q)$ is the final state of the nucleus; the integration is taken over the entire set of particle coordinates r and nuclear variables q. As can be seen from the notation, the coordinates and momenta $\mathbf{r}_\alpha$, $\mathbf{k}_\alpha$ of the particles (relative to the nucleus) are measured in certain conventional units that depend on the arbitrary auxiliary mass M.

The amplitude (1) must be symmetrized in the $\mathbf{k}_\alpha$ in a definite way. Since we are interested in the functional dependence, the proportionality coefficients in the equations will be dropped. The reaction cross section is expressed in the form of an integral over the possible final states of the

---

*We take throughout $h = c = 1$.

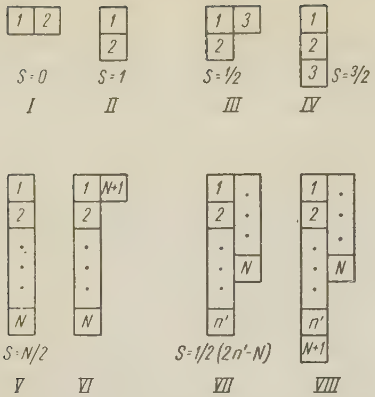

particles

$$\sigma_N = \int |F|^2 \prod_{\alpha=1}^{N} k_\alpha^2 dk_\alpha d\Omega_\alpha \delta(k^2 - K^2),$$

$$K^2 = 2ME,\quad k^2 = \sum_{\alpha=1}^{N} k_\alpha^2, \tag{2}$$

where E is the energy of the exit channel, i.e., the total kinetic energy in the c.m. system.

To obtain the dependence $\sigma_N(K)$ for $K \to 0$ it is enough to take the lowest power of k in the expansion of the expression (1). If the expansion begins with the m-th power, then

$$\sigma_N = K^{3N-2+2m}. \tag{3}$$

It is obvious that $U(r, q)\Psi(r, q)\varphi^*_{\text{nuc}}(q)$ is of zeroth order in k, and we have only to calculate the lowest term in the expansion of $\exp\{-i\sum \mathbf{k}_\alpha\cdot\mathbf{r}_\alpha\}$ in powers of $\sum \mathbf{k}_\alpha\cdot\mathbf{r}_\alpha$ which remains after the symmetrization in the $\mathbf{k}_\alpha$.

The symmetry of the wave function is given by the Young arrays (cf., e.g., reference 4); there exist several possible arrays for any prescribed set of N particles. For each Young array there is a definite lowest power $\left(\sum \mathbf{k}_\alpha\cdot\mathbf{r}_\alpha\right)^m$ which does not vanish identically through the symmetrization. Out of all the possible Young arrays for the given N particles there will be contributions to the reaction at threshold only from those which have the minimum value of m. We shall calculate this minimum exponent.

An identical vanishing of a symmetrized power term can occur only through alternations (antisymmetrizations) through the columns of an array, so that we shall not concern ourselves with symmetrization along the rows of an array. If an array is possible with a single row, not containing alternations, then m = 0. Thus for bosons or for identical fermions numbering $N \leq 2s + 1$ (s being the spin of the fermions) we get the previous result of reference 2.

We shall now consider the case of N identical fermions with spin $s = \frac{1}{2}$, and shall show by mathematical induction that $m = N - 2$ for $N \geq 2$. For N = 2, 3 the possible arrays are I, II, III, IV (see figure). It is easy to verify that $m_{\text{I}} = 0$, $m_{\text{II}} = m_{\text{III}} = 1$, $m_{\text{IV}} = 2$. It remains to show that when we go from N to N + 1 the minimum exponent increases from m to m + 1. We first note that, as in the passage from II to III, in going from the one-column array V to the array VI the lowest exponent does not change, so that the minimum exponent comes from arrays with the maximum number of columns (two in the case considered), and in the proof it suffices to examine transitions of the type VII → VIII, in which the new cell that is added does not form a new column. To begin with we shall show that the m-th power vanishes for the case of N + 1 particles.

We denote the complete alternation through all N + 1 momenta $\mathbf{k}_\alpha$ (array VIII) by the symbol $\underset{\alpha}{A}$. An index (or several indices) under an alternation symbol A will indicate the set of corresponding momenta through which the alternation is carried out. We note that the original alternated function can depend on an altogether different set of momenta. For example, it can depend on only part of the momenta through which the alternation is to be taken, or can even be a constant. After the alternation it will in the general case depend on all the momenta of the alternation. In the proof we have to break up the complete alternation into two stages: we first carry out the alternation through a certain part of the set of momenta, and then the remaining part of the alternation with the remaining momenta. For example, the complete alternation can be broken up into the alternation through the momenta $\mathbf{k}_\beta$ of the N particles ($\beta = 1, 2, \ldots N$) and the subsequent alternation through $\mathbf{k}_\beta$, $\mathbf{k}_{N+1}$ without alternation of the $\mathbf{k}_\beta$. We denote the second stage by the symbol $\underset{N+1,(\beta)}{A}$. Now separating the term $\mathbf{k}_{N+1}\mathbf{r}_{N+1}$ from the sum $\sum_{\alpha=1}^{N+1}\mathbf{k}_\alpha\cdot\mathbf{r}_\alpha$ and expanding the m-th power of this sum by the binomial theorem, we get

$$\underset{\alpha}{A}\left(\sum_{\alpha=1}^{N+1}\mathbf{k}_\alpha\cdot\mathbf{r}_\alpha\right)^m = \underset{N+1,(\beta)}{A}(\mathbf{k}_{N+1}\cdot\mathbf{r}_{N+1})^m\underset{\beta}{A}1 + \ldots$$

$$\ldots + m\underset{N+1,(\beta)}{A}(\mathbf{k}_{N+1}\cdot\mathbf{r}_{N+1})\underset{\beta}{A}\left(\sum_{\beta=1}^{N}\mathbf{k}_\beta\cdot\mathbf{r}_\beta\right)^{m-1}$$

$$+\underset{\alpha}{A}\left(\sum_{\beta=1}^{N}\mathbf{k}_\beta\cdot\mathbf{r}_\beta\right)^m.$$

All the terms of this expansion except the last vanish already on the alternation through the $\mathbf{k}_\beta$, since this alternation is equivalent to array VII, for which all powers of the sum $\sum\limits_{\beta=1}^{N} \mathbf{k}_\beta \cdot \mathbf{r}_\beta$ vanish up to the $(m-1)$st power inclusive (case of N particles).

We transform the last term in the following way: we break up the m-th power into a sum of N terms of a single type,

$$(\mathbf{k}_1 \cdot \mathbf{r}_1)\left(\sum_{\beta=1}^{N} \mathbf{k}_\beta \cdot \mathbf{r}_\beta\right)^{m-1}$$

$$+ (\mathbf{k}_2 \cdot \mathbf{r}_2)\left(\sum_{\beta=1}^{N} \mathbf{k}_\beta \cdot \mathbf{r}_\beta\right)^{m-1} + \ldots + (\mathbf{k}_N \cdot \mathbf{r}_N)\left(\sum_{\beta=1}^{N} \mathbf{k}_\beta \cdot \mathbf{r}_\beta\right)^{m-1}$$

In each term we single out from $\sum\limits_{\beta=1}^{N} \mathbf{k}_\beta \cdot \mathbf{r}_\beta$ the term that appears as the coefficient of the $(m-1)$st power, and corresponding to this we break up the alternation of each term into two stages:

$$\underset{\alpha}{A}\left(\sum_{\beta=1}^{N} \mathbf{k}_\beta \cdot \mathbf{r}_\beta\right)^{m}$$

$$= \underset{1,(\gamma, N+1)}{A} (\mathbf{k}_1 \cdot \mathbf{r}_1) \underset{\gamma,\, N+1}{A}\left(\mathbf{k}_1 \cdot \mathbf{r}_1 + \sum_{\gamma=2}^{N} \mathbf{k}_\gamma \cdot \mathbf{r}_\gamma\right)^{m-1} + \ldots \tag{4}$$

$$\ldots + \underset{N,\,(\gamma, N+1)}{A} (\mathbf{k}_N \cdot \mathbf{r}_N) \underset{\gamma,\, N+1}{A}\left(\mathbf{k}_N \cdot \mathbf{r}_N + \sum_{\gamma=1}^{N-1} \mathbf{k}_\gamma \cdot \mathbf{r}_\gamma\right)^{m-1}.$$

Let us take, for example, the first term of the sum (4) and show that it vanishes already in the alternation through γ, N+1 because of the vanishing of the factor

$$\underset{\gamma,\, N+1}{A}\left(\mathbf{k}_1 \cdot \mathbf{r}_1 + \sum_{\gamma=2}^{N} \mathbf{k}_\gamma \cdot \mathbf{r}_\gamma\right)^{m-1}. \tag{5}$$

We note that the expression (5) can be regarded as a homogeneous polynomial of degree $(m-1)$ in the coordinates $\mathbf{r}_1, \mathbf{r}_2, \ldots \mathbf{r}_N$ with coefficients depending on all N+1 momenta $\mathbf{k}_\alpha$. We now consider another polynomial

$$P_{m-1}(\mathbf{r}_1, \ldots \mathbf{r}_N, \mathbf{r}_{N+1})$$

$$= \underset{\gamma,\, N+1}{A}\left[\mathbf{k}_1 \cdot \mathbf{r}_1 + \left(\sum_{\gamma=2}^{N} \mathbf{k}_\gamma \cdot \mathbf{r}_\gamma + \mathbf{k}_{N+1} \cdot \mathbf{r}_{N+1}\right)\right]^{m-1},$$

which includes (5) as part of itself. If we expand this latter quantity in powers of $\left(\sum\limits_{\gamma=2}^{N} \mathbf{k}_\gamma \cdot \mathbf{r}_\gamma + \mathbf{k}_{N+1} \cdot \mathbf{r}_{N+1}\right)$, it can be seen that it vanishes identically, since we arrive at the array VII with the numbering of the cells changed. This means that the factor (5) also vanishes, since it is a particular value of the other polynomial for $\mathbf{r}_{N+1} = 0$.

Similarly one can show that each of the successive terms of the sum (4) vanishes, by going over to one of the arrays for N particles.

Finally, we convince ourselves that the $(m+1)$st power does not vanish:

$$\underset{\alpha}{A}\left(\sum_{\alpha=1}^{N+1} \mathbf{k}_\alpha \cdot \mathbf{r}_\alpha\right)^{m+1} = \underset{N+1,\,(\beta)}{A} (\mathbf{k}_{N+1} \cdot \mathbf{r}_{N+1})^{m+1} \underset{\beta}{A} 1 + \ldots$$

$$\ldots + \frac{(m+1)\,m}{2} \underset{N+1\,(\beta)}{A} (\mathbf{k}_{N+1} \cdot \mathbf{r}_{N+1})^2 \underset{\beta}{A}\left(\sum_{\beta=1}^{N} \mathbf{k}_\beta \cdot \mathbf{r}_\beta\right)^{m-1} \tag{6}$$

$$+ (m+1) \underset{N+1,\,(\beta)}{A} (\mathbf{k}_{N+1} \cdot \mathbf{r}_{N+1}) \underset{\beta}{A}\left(\sum_{\beta=1}^{N} \mathbf{k}_\beta \cdot \mathbf{r}_\beta\right)^{m}$$

$$+ \underset{\alpha}{A}\left(\sum_{\beta=1}^{N} \mathbf{k}_\beta \cdot \mathbf{r}_\beta\right)^{m+1}.$$

All the terms of this expansion except the last two vanish on the alternation with respect to β. In analogy with Eq. (4) we break up the next to last term of the expansion (6) into terms of the type

$$\underset{1,\, N+1,\,(\gamma)}{A} (\mathbf{k}_{N+1} \cdot \mathbf{r}_{N+1})(\mathbf{k}_1 \cdot \mathbf{r}_1) \underset{\gamma}{A}\left(\mathbf{k}_1 \cdot \mathbf{r}_1 + \sum_{\gamma=2}^{N} \mathbf{k}_\gamma \cdot \mathbf{r}_\gamma\right)^{m-1}.$$

After expanding the $(m-1)$st power in this term by the binomial theorem and alternating with respect to γ we have remaining

$$\underset{1,\, N+1,\,(\gamma)}{A} (\mathbf{k}_{N+1} \cdot \mathbf{r}_{N+1})(\mathbf{k}_1 \cdot \mathbf{r}_1) \underset{\gamma}{A}\left(\sum_{\gamma=2}^{N} \mathbf{k}_\gamma \cdot \mathbf{r}_\gamma\right)^{m-1}.$$

It is easy to see that the further alternation through 1, N+1, (γ), and combination of all analogous terms together with the last term in Eq. (6) does not lead to cancellation.

It is obvious from the proof that all arrays of two columns give the minimun degree $m = N - 2$, since it is immaterial to which column one adds a new cell. This means that all total spins $S \leq N/2 - 1$ give the same dependence $\sigma(K)$, and the cross-section for the largest total spin $S = N/2$ vanishes more rapidly at the threshold by a factor K^2.

In order to go over to the case of an arbitrary set of N particles, we note that the result just established can be formulated in the following way:

> The exponent of the lowest power of $\left(\sum\limits_{\alpha=1}^{N} \mathbf{k}_\alpha \cdot \mathbf{r}_\alpha\right)$ that does not vanish on alternation through a prescribed Young array is equal to the total number of cells in all rows of the array except the first, and in going from N to N+1 it increases by unity if the new cell does not form a new column. (7)

Noting that no use was made in the proof of the possible number of columns, and that consequently the result (7) is valid for arrays with an arbitrary number of columns, in the case of arbitrary spin s we get: $m = N - (2s + 1)$ for $N \geq 2s + 1$. For an arbitrary set of N particles the alternation must be carried out through a single common array, made up of the arrays for the different groups of identical particles written side by side. This gives for the minimum exponent:

$$m = \sum_i m_i, \quad m_i = \begin{cases} 0 & \text{for } N_i \leqslant 2s_i + 1, \\ N_i - (2s_i + 1) & \text{for } N_i \geqslant 2s_i + 1, \end{cases} \tag{8}$$

where the sum is taken over all groups of identical fermions; N_i is the number of fermions of the i-th group, and s_i is their spin.

It must be emphasized that Eq. (8) gives the minimum exponent in the expansion of the reaction amplitude that is possible according to the Pauli principle for the given set of emergent particles. In principle it is possible that there could be additional degrees of forbiddenness according to symmetry type, which could exclude the channels with the minimum m. In this case the degree m in Eq. (3) is given by Eq. (7) for the allowed arrays.*

Equation (3) represents the first term of an expansion in powers of kR_0 (R_0 is the radius of the nucleus, or more precisely the radius of the reaction zone). With increase of N the errors accumulate not faster than $N^{1/2}$, so that the region of applicability of Eq. (3) is limited by the inequality $N^{1/2} KR_0 \lesssim 1$.

2. CHARGED PARTICLES

Neglecting the Coulomb interactions between the emitted particles, we get for the reaction amplitude

$$F(\mathbf{k}_1 \ldots \mathbf{k}_N) = \int \prod_{\alpha=1}^{N} \psi^*(\mathbf{k}_\alpha, \mathbf{r}_\alpha) U(r, q) \Psi^*(r, q) \varphi^*_{\text{я}}(q)\, dr\, dq;$$

$$\psi(\mathbf{k}_\alpha, \mathbf{r}_\alpha) = \exp\left(-\frac{\pi a_\alpha}{2k_\alpha}\right) \Gamma\left(1 - i\frac{a_\alpha}{k_\alpha}\right) \tag{9}$$

$$\exp(i\mathbf{k}_\alpha \cdot \mathbf{r}_\alpha) F\left(i\frac{a_\alpha}{k_\alpha}, 1, -i(k_\alpha r_\alpha + \mathbf{k}_\alpha \cdot \mathbf{r}_\alpha)\right),$$

$$a_\alpha = \sqrt{M\mu_\alpha}\, Zz_\alpha e^2,$$

$z_\alpha e$ is the charge of the α-th particle. The amplitude (9) differs from Eq. (1) only in that for the charged particles the plane waves are replaced by Coulomb solutions with the asymptotic forms made up of plane and converging waves. Using the expansion of the confluent hypergeometric function, we get for small momenta

$$\psi(\mathbf{k}_\alpha, \mathbf{r}_\alpha) = \psi(\mathbf{k}_\alpha, 0)[1 + i\mathbf{k}_\alpha \cdot \mathbf{r}_\alpha + \ldots][f_0(r_\alpha + \mathbf{n}_\alpha \cdot \mathbf{r}_\alpha) + k_\alpha f_1(r_\alpha + \mathbf{n}_\alpha \cdot \mathbf{r}_\alpha) + \ldots] \approx \psi(\mathbf{k}_\alpha, 0) f_{0\alpha}, \tag{10}$$

where $\mathbf{n}_\alpha = \mathbf{k}_\alpha / k_\alpha$, and $f_1, f_2, \ldots$ are certain functions of the quantity $(r_\alpha + \mathbf{n}_\alpha \cdot \mathbf{r}_\alpha)$, the expansions for which contain arbitrarily high powers.

When the amplitude (9) is alternated through the group of neutral particles, according to Sec. 1, the contribution they give in the integrand is $\underset{\beta}{A}\left(\sum_\beta \mathbf{k}_\beta \cdot \mathbf{r}_\beta\right)^m$. The alternation through the charged particles does not change the functional dependence, since for an arbitrary Young array

$$\underset{\alpha}{A} \prod_\alpha \psi(\mathbf{k}_\alpha, 0) f_0(r_\alpha + \mathbf{n}_\alpha \cdot \mathbf{r}_\alpha) = \prod_\alpha \psi(\mathbf{k}_\alpha, 0)\, \underset{\alpha}{A} \prod_\alpha f_0(r_\alpha + \mathbf{n}_\alpha \cdot \mathbf{r}_\alpha) \not\equiv 0. \tag{11}$$

This means that arbitrary orbital angular momenta of the charged particles emitted give always the same threshold dependence.

If among the N particles there are n charged particles (n_+ positive and n_- negative) and n_0 neutral particles, then near the threshold

$$\sigma_N = \int \prod_{\alpha=1}^{n} |\psi(\mathbf{k}_\alpha, 0)|^2 f(\mathbf{k}_\beta, \mathbf{n}_\alpha) \prod_{\gamma=1}^{N} k_\gamma^2\, dk_\gamma\, d\Omega_\gamma \cdot \delta(k^2 - K^2),$$

where for the negative particles

$$|\psi(\mathbf{k}_\alpha, 0)|^2 = \frac{2\pi |a_\alpha|}{k_\alpha[1 - \exp(-2\pi |a_\alpha| / k_\alpha)]} \approx \frac{2\pi |a_\alpha|}{k_\alpha},$$

for the positive ones

$$|\psi(\mathbf{k}_\alpha, 0)|^2 = \frac{2\pi a_\alpha}{k_\alpha[\exp(2\pi a_\alpha / k_\alpha) - 1]} \approx \frac{2\pi a_\alpha}{k_\alpha} \exp\left(-\frac{2\pi a_\alpha}{k_\alpha}\right),$$

and

$$f(\mathbf{k}_\beta, \mathbf{n}_\alpha) = \left| \int \underset{\beta}{A} \left(\sum_\beta \mathbf{k}_\beta \cdot \mathbf{r}_\beta\right)^m \underset{\alpha}{A} \prod_\alpha f_{0\alpha} \cdot U \Psi \varphi^*_{\text{я}}\, dr\, dq \right|^2$$

is a certain function that is homogeneous of degree $2m$ in the momenta $\mathbf{k}_\beta$ of the neutral particles.

In computing the integral over the hypersphere $\sum_{\gamma=1}^{N} k_\gamma^2 = K^2$ in Eq. (11) we need obtain only the main contribution (method of steepest descent). For the exponential factors (from the positive particles) we have to find the position of the extremal point on the hypersphere under the condition $\sum_{\alpha=1}^{n_+} k_\alpha^2 = K^2$. Finally, setting $K = (2ME)^{1/2}$, we get

---

*The degree m also has the following further meaning: in a given channel the orbital angular momenta of the emergent particles obey $l_\alpha \leq m$ (at threshold).

$$\sigma_N = E^L \exp\left\{-\frac{2\pi Z}{137\sqrt{2E}}\left(\sum_{i=1}^{p} n_i z_i^{2/3}\mu_i^{1/3}\right)^{3/2}\right\},$$

$$L = \frac{1}{2}\left\{3N - 2 + 2m - n\right. \tag{12}$$

$$\left. + \frac{\varepsilon(n_+)}{2}(2m + 2n_0 + n_- + N - 1)\right\},$$

$$\varepsilon(n_+) = \begin{cases} 0 \text{ for } n_+ = 0, \\ 1 \text{ for } n_+ \geqslant 1. \end{cases}$$

n_i is the number of positive particles with mass μ_i and charge z_i, and p is the number of different masses of the positive particles. The exponent m from the group of neutral particles is determined as shown in Sec. 1.

The largest corrections to the threshold dependence (12) are those from the errors in the expansions (10), the subsequent terms of which give corrections $\sim KR_0$ and $\sim (KR_0)(Ze^2(M\mu)^{1/2}R_0)$. The main contribution to the integral is subject to corrections $\sim K(2\pi Ze^2(M\mu)^{1/2})^{-1}$. Smallness of all these parameters also limits the region of applicability of Eq. (12). If the particles have an actual or virtual energy level ϵ close to zero, there is the further condition* $E \lesssim |\epsilon|$.

Let us consider the special case $N = 2$, $n = 1$, treated in reference 3. The formula (12) gives

$$\sigma = E^{3/2+m} \qquad \text{for } n_- = 1, \quad n_+ = 0,$$

$$\sigma = E^{7/4+3m/2}\exp\{-2\pi Zze^2\sqrt{\mu/2E}\} \tag{13}$$

$$\text{for } n_- = 0, \quad n_+ = 1.$$

The minimum exponent is $m = 0$. If there is an additional forbiddenness from the orbital angular momentum of the neutral particle, then the lowest degree from the expansion of $\exp(-i\mathbf{k}\cdot\mathbf{r})$ in powers of kr is l, where l is the smallest allowed angular momentum. This means that in order to use the formulas (13) in the case of arbitrary orbital angular momentum l of the neutral particle we must take† $m = l$.

The results of reference 3 differ from Eq. (13) only by the inclusion of the motion of the nucleus. A comparison of the results shows that inclusion of the nuclear recoil does not change the threshold dependence in the case $n_+ = 0$, and changes the exponent in the case $n_+ = 1$ in the following way: $\mu \rightarrow \mu M_{nuc}/(\mu + M_{nuc})$. It is not hard to show that for $n = 0, 1$ with an arbitrary number of neutral particles the formula (12) is exact if we replace the mass of the charged particle by its reduced mass, $\mu \rightarrow \mu M_{nuc}/(\mu + M_{nuc})$. To do this one must reduce the kinetic energy in the exact Hamiltonian with recoil terms to the canonical form by the method of Jacobi, leaving the coordinate of the charged particle unchanged.*

In the case $n \geq 2$ the formula (12) is already an approximate one, and it makes sense to use it only under the conditions $\sum \mu_\alpha \ll M_{nuc}$, $\left|\sum z_\alpha\right| \ll Z$. It can be expected that under these conditions inclusion of the motion of the nucleus and the Coulomb interaction between the emergent particles will not change the threshold dependence for $n_+ = 0$, and will shift the exponent by amounts $\sim\sum_\alpha \mu_\alpha/M_{nuc}$ and $\lesssim\sum_\alpha |z_\alpha|/Z$ for $n_+ \geq 1$.

In conclusion I express my gratitude to Professor I. Ia. Pomeranchuk for suggesting the problem and for a discussion.

[1] E. Wigner, Phys. Rev. **73**, 1002 (1948).

[2] W. H. Guier and R. W. Hart, Phys. Rev. **106**, 296 (1957).

[3] Hart, Gray, and Guier, Phys. Rev. **108**, 1512 (1957).

[4] L. D. Landau and E. M. Lifshitz, Квантовая механика (Quantum Mechanics), Sec. 61, Gostekhizdat, Moscow-Leningrad, 1948.

Translated by W. H. Furry
142

---

*The effect of the interaction of the reaction products on the accuracy of the threshold dependence has been dealt with partly in reference 3.

†Similarly, we can take into account the raising of the lowest degree m owing to any additional forbiddenness in the group of neutral particles by finding the first term of the expansion of $\exp\{-i\sum \mathbf{k}_\beta\cdot\mathbf{r}_\beta\}$ in powers of kr.

*For the special case $n = n_0 = 1$, for example, this transformation was used in reference 3.

ON THE THEORY OF THE WEAK INTERACTIONS. II

Iu. A. GOL'FAND

P. N. Lebedev Physics Institute, Academy of Sciences, U.S.S.R.

Submitted to JETP editor April 3, 1958

J. Exptl. Theoret. Phys. (U.S.S.R.) **35**, 726-730 (September, 1958)

A scheme is constructed in which the non-Hermitian weak-interaction Hamiltonian H_w is a component part of the Hermitian total Hamiltonian operating in a "doubled" Hilbert space.

1. INTRODUCTION

In the writer's previous paper[1] the question was left open as to how the non-Hermitian Hamiltonian H_w can be included in a consistent quantum-mechanical scheme. One of the possible solutions of this question is proposed in the present paper. The essentials of the scheme are as follows.

The weak-interaction Hamiltonian H_w appears in the total Hamiltonian not simply added to the strong-interaction Hamiltonian H_s, but as one of the "blocks" of a Hermitian total Hamiltonian;

$$\hat{H} = \begin{pmatrix} H_s H_w \\ H_w^+ H_s \end{pmatrix}, \tag{1.1}$$

which acts in a Hilbert space with a doubled number of dimensions. In order to give a physical meaning to the doubling of the Hilbert space, we postulate as the form of the inversion operator the matrix

$$\hat{P} = \begin{pmatrix} 0 & P \\ P & 0 \end{pmatrix}.$$

With such a definition of the inversion the "second" Hilbert space is the mirror image of the "first" space.

The class of permissible Hamiltonians of the form (1.1) is restricted by the requirement that the operators $\hat{H}$ and $\hat{P}$ commute. In other words, in the theory developed here the inversion $\hat{P}$ is a constant of the motion.

Finally, we introduce a certain "condition of observation" that enables us to interpret physically the results of the theory. The condition of observation is not invariant with respect to the inversion $\hat{P}$; this corresponds to the experimentally known violation of the conservation of parity in the weak interactions.

It is curious to note that within the framework of the proposed theory the non-Hermitian character of the Hamiltonian H_w is necessary. If we replace H_w by a Hermitian operator, all the effects associated with the non-conservation of parity vanish. At the same time, the Hermitian character of the Hamiltonian H_s and the conservation of parity in the strong interactions are necessary consequences of the scheme.

2. THE EXPLICIT EXPRESSION OF THE HAMILTONIAN H_w

The Hamiltonian H_w is expressed extremely simply in terms of certain four-component field spinors describing pairs of charged particles. With the pair of leptons (e, μ) we associate the field

$$\chi_L = \begin{pmatrix} \varphi_a(\mu^-) + \varphi_c(e^+) \\ \dot{\varphi}_a(e^-) - \dot{\varphi}_c(\mu^+) \end{pmatrix}, \tag{2.1}$$

and with the pair of baryons (p, Σ^+) we associate the field

$$\chi_B = \begin{pmatrix} \varphi_a(\tilde{p}) + \varphi_c(\Sigma^+) \\ \dot{\varphi}_a(\tilde{\Sigma}^+) - \dot{\varphi}_c(p) \end{pmatrix} \tag{2.2}$$

(the notation is the same as in reference 1). We shall not include the other charged particles in the scheme of the direct Fermi interaction.

It is convenient to combine the fields χ_L and χ_B into a single χ-field. For this purpose we introduce explicitly the dependence of the field on the variable β canonically conjugate to the nucleonic charge N, and define the single field by the equation

$$\chi(x, t, \beta) = \chi_B(x, t)\, e^{i\beta} + \chi_L(x, t). \tag{2.3}$$

We introduce into the scheme the direct Fermi interaction of the following neutral particles: the neutrino, the Λ^0 particle, and their antiparticles. The neutral particles come into the theory in an essentially different way from the charged particles (the rule of polarization of lines[1] fixes the type of the φ-fields only for charged particles). Because of this the neutral particles have to be described by ordinary ψ-fields. We define the single ψ-field of the neutral particles by the equation

$$\psi(\mathbf{x}, t, \beta) = \{\psi_n(\mathbf{x}, t) + \psi_{\Lambda^0}(\mathbf{x}, t)\} e^{-i\beta} + \psi_\nu(\mathbf{x}, t). \tag{2.4}$$

We define the operation R as the interchange of the particles in the pairs (e, μ) and (p, Σ^+). The result of applying R will be written with an upper index. For the neutral particles we have by definition that R is the identical transformation: $\psi^R \equiv \psi$.

We can now write the weak-interaction Hamiltonian density $\mathcal{H}_W(x, t)$, satisfying all the rules formulated in reference 1, in the form

$$\mathscr{H}_w(\mathbf{x}, t) = (g/4\pi) \int_{-\pi}^{\pi} d\beta \{(\bar{\chi}\psi)^R (\bar{\psi}\chi) + (\bar{\psi}\chi)(\bar{\chi}\psi)^R\}. \tag{2.5}$$

In the expression (2.5) the integration with respect to β selects the terms corresponding to conservation of the nucleonic charge.

3. THE SYMMETRY OF THE THEORY WITH RESPECT TO INVERSIONS

Under proper Lorentz transformations the fields χ and ψ transform as bispinors. The behavior of the χ-fields under inversions is not obvious a priori and requires special consideration. We shall examine inversions of the following three types: spatial inversion P, charge conjugation C, and the transformation S, consisting of reflection of all four space-time axes and replacement of particles by antiparticles. All other inversions are expressible in terms of products of these "elementary" inversions.

We shall introduce the inversion operators acting in the state space in a way like that used in reference 2 for Lorentz transformations. We associate with the inversions P and C the unitary transformations U_P and U_C. To the inversion S, which involves time reversal, we assign an antiunitary transformation $U_S J$, where U_S is a unitary operator and J is the operation of complex conjugation. The forms of the operators U are given in the Appendix. The χ-field (2.3) transforms in the following ways under the elementary inversions:

$$\chi(\mathbf{x}, t, \beta) \rightarrow \begin{cases} U_P \chi U_P^+ = \gamma_4 \chi^R(-\mathbf{x}, t, \beta) & (P) \\ U_C \chi U_C^+ = C\chi^+(\mathbf{x}, t, -\beta). & (C). \\ U_S J \chi J U_S^+ = C\gamma_5 \chi^R(-\mathbf{x}, -t, -\beta) & (S) \end{cases} \tag{3.1}$$

In the right members of Eq. (3.1) C denotes the spinor conjugation matrix, which has the properties:

$$C\gamma_\mu C^{-1} = -\gamma_\mu^*, \quad C^* = C^T = C^+ = C; \quad C^2 = 1.$$

The appearance of the matrix C in the third of the equations (3.1) is due to the antilinear character of the transformation S. The ψ-field (2.4) also transforms by the formulas (3.1), the only difference being that for it R is the identical transformation

It is now easy to find the transformation law of the weak-interaction Hamiltonian. We give the result for the whole Hamiltonian H_W in the Schrödinger representation:

$$U_p H_w U_p^+ = U_c H_w U_c^+ = U_s J H_w J U_s^+ = H_w^+. \tag{3.2}$$

Under each of the elementary inversions H_W goes over into the Hermitian adjoint operator H_W^+. Under any combined inversion equal to the product of two elementary inversions H_W remains unchanged. This result has been obtained in a different way in the preceding paper.[1]

4. THE TOTAL HAMILTONIAN $\hat{H}$

Our further considerations are based on the hypothesis that the complete physical definition of the inversions must include, in addition to the transformations of the space of the state vectors Ψ discussed in the preceding section, also a transformation of a certain internal variable characterizing the properties of the space. We obtain a realization of this idea in the following scheme.

We shall regard the total state vector Ψ as a two-component quantity

$$\hat{\Psi} = \begin{pmatrix} \Psi_1 \\ \Psi_2 \end{pmatrix}, \tag{4.1}$$

where Ψ_1 and Ψ_2 are two Hilbert vectors for the state of the system. We define the scalar product of two vectors of the type (4.1) by

$$(\hat{\Psi}, \hat{\Phi}) = (\Psi_1, \Phi_1) + (\Psi_2, \Phi_2). \tag{4.2}$$

It is convenient to introduce matrices $\hat{\Lambda}_i$ acting on the vectors $\hat{\Psi}$, in analogy with the Pauli spin matrices:

$$\Lambda_1 = \begin{pmatrix} 0 & 1 \\ 1 & 0 \end{pmatrix}, \quad \Lambda_2 = \begin{pmatrix} 0 & -i \\ i & 0 \end{pmatrix}, \quad \Lambda_3 = \begin{pmatrix} 1 & 0 \\ 0 & -1 \end{pmatrix}.$$

Let I be any one of the elementary inversions. We define the complete inversion $\hat{I}$ by the equation

$$\hat{I} = I\Lambda_1. \tag{4.3}$$

Finally, let us define the total Hamiltonian H, containing both the strong and the weak interactions:

$$\hat{H} = H_s + \tfrac{1}{2}(H_w + H_w^+)\Lambda_1 + \tfrac{i}{2}(H_w - H_w^+)\Lambda_2. \tag{4.4}$$

The Hamiltonian $\hat{H}$ is Hermitian in the metric given by the scalar product (4.2). In virtue of the relation (3.2), the Hamiltonian H satisfies the relation

$$[\hat{H},\ \hat{I}] = 0. \tag{4.5}$$

In the derivation of Eq. (4.5) it has been assumed that there is conservation of all the inversion parities for the strong interactions, i.e., that we have the relations

$$[H_s,\ I] = 0. \tag{4.6}$$

The converse proposition is also true: the relations (4.6) and (3.2) are consequences of the relation (4.5) and the definitions (4.3) and (4.4).

5. THE PHYSICAL INTERPRETATION OF THE THEORY

Let us construct in our scheme the theory of the S matrix that gives the probabilities of transitions between unperturbed states. We subject the unperturbed states to the symmetry condition $\hat{\Psi} = \Lambda_1\hat{\Psi}$, or in terms of the components

$$\hat{\Psi} = \begin{pmatrix}\Psi\\ \Psi\end{pmatrix}. \tag{5.1}$$

Vectors of the form (5.1) can be regarded as eigenstates of either the strong-interaction Hamiltonian H_S or the free-particle Hamiltonian H_0. Let $\hat{S}$ be the S matrix related in the usual way to the Hamiltonian $\hat{H}$. We define the probability of transition from the symmetric state $\hat{\Psi}_0$ to the symmetric state $\hat{\Psi}_f$ by the equation

$$W(0\to f) = \left|\left(\hat{\Psi}_f,\ \frac{1+\Lambda_3}{2}\hat{S}\hat{\Psi}_0\right)\right|^2. \tag{5.2}$$

It is easy to see that the definition (5.2) of the probability goes over into the usual definition if we neglect the weak interactions.

On the basis of Eq. (5.2) the total transition probability is given by

$$\sum_f W(0\to f) = \left(\hat{\Psi},\ \frac{1+\Lambda_3}{2}\hat{\Psi}\right),\quad \hat{\Psi} = \hat{S}\hat{\Psi}_0. \tag{5.3}$$

In the derivation of Eq. (5.3) we have used only the completeness of the system of final states Ψ_f. In order for the definition (5.2) of the transition probability to be free from contradiction, the condition of conservation of the total probability must hold, that is,

$$\left(\hat{\Psi},\ \frac{1+\Lambda_3}{2}\hat{\Psi}\right) = \left(\hat{\Psi}_0,\ \frac{1+\Lambda_3}{2}\hat{\Psi}_0\right). \tag{5.4}$$

It can be shown that Eq. (5.4) is valid if the initial state $\hat{\Psi}_0$ has a definite intrinsic parity, i.e., satisfies the condition

$$P_0\Psi_0 = \lambda\Psi_0,\quad (\lambda = \pm 1).$$

By intrinsic parity we mean parity in the center-of-mass system. We define the intrinsic parity operator P_0 by the equation

$$P_0 = U_L U_P U_L^+,$$

where L is the Lorentz transformation from the laboratory coordinate system to the center-of-mass system, and U_L is the operator of the unitary representation of the Lorentz group discussed in reference 2.

if we apply l the definition (5.2) to the calculation in first-order perturbation theory of the transition probability occasioned by the weak interaction, we get the relation

$$W(0\to f) = \left|\left(\Psi_f,\ \int \mathscr{H}_w(x)\, d^4x\Psi_0\right)\right|^2,$$

from which it can be seen that in this case the transition probability is calculated by the usual rules, on the basis of the Hamiltonian $\mathscr{H}_W(x)$.

APPENDIX

It is easy to find the explicit forms of the operators U by the method discussed in reference 2:

$$U_p = \exp\Big\{-i\frac{\pi}{2}\sum a^+(\mathbf{p})\,[a(\mathbf{p}) - a(-\mathbf{p})] + b^+(\mathbf{p})\,[b(\mathbf{p}) + b(-\mathbf{p})]\Big\};$$

$$U_c = \exp\Big\{-i\frac{\pi}{2}\sum [a^+(\mathbf{p}) - b^+(\mathbf{p})]\,[a(\mathbf{p}) - b(\mathbf{p})]\Big\};$$

$$U_s = \exp\Big\{\frac{\pi}{2}\sum a^+(\mathbf{p})\,\varepsilon a(\mathbf{p}) - b^+(\mathbf{p})\,\varepsilon b(\mathbf{p})\Big\}.$$

All the operators (A.1) are unitary. The antiunitary transformation is $S = U_S J$, where J denotes complex conjugation. By definition the operator J does not change the vacuum state: $J\Phi_0 = \Phi_0$. Furthermore, J commutes with the operators for creation and annihilation of particles (since these operators are represented by real matrices): $JaJ = a$, $Ja^+J = a^+$.

Thus under the transformation S the creation operators do not go over into annihilation operators, and conversely. Our definition of S agrees with the definition of time reversal in nonrelativistic quantum mechanics (cf., e.g., reference 3).

---

[1] Iu. A. Gol'fand, J. Exptl. Theoret. Phys. (U.S.S.R.) **35**, 170 (1958), Soviet Phys. JETP **8**, 118 (1959).

[2] Iu. A. Gol'fand, J. Exptl. Theoret. Phys. (U.S.S.R.) **31**, 535 (1956), Soviet Phys. JETP **4**, 446 (1957).

[3] L. D. Landau and E. M. Lifshitz, **Квантовая механика** (Quantum Mechanics), Sect. 16. Gostekhizdat, Moscow-Leningrad 1948. [Engl. Transl. Addison-Wesley, 1958].

Translated by W. H. Furry
143

SOVIET PHYSICS JETP VOLUME 35(8), NUMBER 3 MARCH, 1959

THE STABILITY OF SHOCK WAVES IN MAGNETOHYDRODYNAMICS

A. I. AKHIEZER, G. Ia. LIUBARSKII, and R. V. POLOVIN

Physico-Technical Institute, Academy of Sciences, Ukrainian S.S.R.

Submitted to JETP editor April 4, 1958; resubmitted June 10, 1958

J. Exptl. Theoret. Phys. (U.S.S.R.) **35**, 731-737 (September, 1958)

The regions of instability of a stationary magnetohydrodynamic shock wave with respect to one-dimensional perturbations have been determined. It is shown that two types of stable shock waves exist. The types of shock waves that can follow each other are determined.

1. The purpose of the present paper is the investigation of the problem of the stability of plane magnetohydrodynamic shock waves with respect to small perturbations which depend only on the distance of the surface of discontinuity and on the time.

We shall show that magnetohydrodynamic shock waves can be unstable and must disintegrate into several shock waves if the total number of magnetohydrodynamic, magnetoacoustic, and entropy waves emanating from the front of the discontinuity is not equal to six.

2. The method that we shall employ consists of the following: we shall write down a set of equations of magnetohydrodynamics describing the perturbations in question in the form

$$\sum_{k=1}^{n}\left\{X_{ik}(u)\frac{\partial u_k}{\partial x}+T_{ik}(u)\frac{\partial u_k}{\partial t}\right\}=0;\ i=1,2,\ldots,n, \tag{1}$$

Where u_k represents any hydrodynamic quantity (the velocity v, the magnetic field H, the density ρ, the entropy s), $X_{ik}(u)$ and $T_{ik}(u)$ are certain functions of $u_1, u_2, \ldots, u_n$; x is the distance to the surface of discontinuity and t is the time (the direction of the x axis is chosen so that the projection of the velocities on it will be positive). These equations possess discontinuous solutions that satisfy the n given conditions on the surface of discontinuity. We denote the constant values of u_k on the two sides of the discontinuity by u_{1k} $(x < 0)$ and U_{2k} $(x > 0)$ (index 1 corresponds to the region in front of the shock wave, while index 2 corresponds to the region behind the shock). At the incident of time $t = 0$, let the quantities u_k undergo small perturbations $\delta u_k(x)$, which depend only on x; it is required to determine the functions $\delta u_k(x, t) = u_k(x, t) - u_k$ at all subsequent times. If the discontinuous solution is stable, then these quantities will remain small, and we can therefore linearize Eq. (1):

$$\begin{aligned}&\sum_{k=1}^{n}\left\{X_{ik}^{(1)}\frac{\partial\delta u_{1k}(x,t)}{\partial x}+T_{ik}^{(1)}\frac{\partial\delta u_{1k}(x,t)}{\partial t}\right\}=0,\\&\sum_{k=1}^{n}\left\{X_{ik}^{(2)}\frac{\partial\delta u_{2k}\,x,t)}{\partial x}+T_{ik}^{(2)}\frac{\partial\delta u_{2k}(x,t)}{\partial t}\right\}=0,\end{aligned} \tag{2}$$

where the indices (1) and (2) indicate the values of the function for $u_k = u_{1k}$ and $u_k = u_{2k}$. The resultant system of linearized equations can, however, fail to have a unique solution in a number of cases. On the other hand, since the Cauchy problem in hydrodynamics always has a unique solution, then the absence of a unique solution for the system (2) indicates the impossibility of replacing the exact equations (1) by the linearized equations (2). In turn, this means that the perturbations $\delta u_k(x, t)$, which are small at $t = 0$, are not small at any subsequent instant of time. Such a discontinuous change with the time of the quantities $\delta u_k(x, t)$ can take place only in the breaking up of the original shock wave into several waves, which are enclosed between the surfaces of discontinuity that are once again formed.

Therefore, the necessary condition for the stability of the shock wave relative to decomposition is the existence of a unique solution of the linearized Cauchy problem corresponding to the system (2). We shall make use of this criterion in what follows. The problem of the character of the breaking up of the shock wave is not considered in the present work.

3. Let us go on to the solution of Eq. (2). For this purpose we carry out a Laplace transformation in time:

$$\eta_k(x,z)=\int_0^\infty \delta u_k(x,t)\,e^{-zt}\,dt,\qquad \mathrm{Re}\,z>0,$$

which yields

$$\sum_{k=1}^{n}\left\{X_{ik}\frac{d\eta_k}{dx}+zT_{ik}\eta_k\right\}=\sum_{k=1}^{n}T_{ik}\delta u_k(x). \tag{3}$$

For a solution of these equations, we first consider the homogeneous set

$$\sum_{k=1}^{n}\left\{X_{ik}\frac{d\zeta_k}{dx}+zT_{ik}\zeta_k\right\}=0,$$

whose solution has the form

$$\zeta_k = A_{k\mu}e^{\lambda_\mu x}, \tag{4}$$

where λ_μ are the roots of the characteristic equation

$$|X_{ik}+T_{ik}z/\lambda_\mu|=0. \tag{5}$$

On the other hand, the phase velocities V_μ of the plane waves

$$\delta u_k(x,\ t)=C_k e^{i(k_\mu x-\omega t)}, \tag{6}$$

satisfying Eq. (2) are obviously determined from the equation

$$|X_{ik}-V_\mu T_{ik}|=0.$$

Therefore,

$$\lambda_\mu = -z/V_\mu. \tag{5'}$$

This relation shows that for $z > 0$ each plane wave of (6) moving in the positive direction corresponds to a negative λ_μ, while the wave moving in the negative direction corresponds to positive λ_μ.

We now turn to the solution of the inhomogeneous system (3). As is well known, this can be represented in the form

$$\eta_k=\sum_{\mu=1}^{n}A_{k\mu}e^{\lambda_\mu x}g_\mu(x),$$

where

$$g_\mu(x)=\sum_{\nu\gamma\sigma}(A^{-1})_{\mu\nu}(X^{-1})_{\nu\gamma}T_{\gamma\sigma}\int_0^x e^{-\lambda_\mu\xi}\,\delta u_\sigma(\xi)\,d\xi+g_\mu(0); \tag{7}$$

A^{-1}, X^{-1} are matrices inverse to the matrices $A = (A_{k\mu})$ and $X = (X_{ik})$. In order that the quantities $\eta_{2k}(x, z)$ be bounded for $x \to \infty$, the functions $g_{2\mu}(x)$ corresponding to positive $\lambda_{2\mu}$ must vanish for $x \to \infty$;

$$g_{2\mu}(+\infty)=0;\ \lambda_{2\mu}>0.$$

These conditions uniquely determine the constants of integration $g_{2\mu}(0)$ for $\lambda_{2\mu} > 0$; so far as the constants $g_{2\mu}(0)$ that correspond to $\lambda_{2\mu} < 0$ are concerned, the conditions at $+\infty$ do not impose any limitations on them. The number of these conditions is evidently equal to the number of types of plane waves (6) propagating in the positive x direction.

Thus, after consideration of the conditions at $+\infty$ in the solution (7), there remain as many arbitrary constants as there are forms of plane waves propagating to the right from the shock front.

Proceeding in exactly the same manner, it is easy to show that the number of arbitrary constants from among the $g_{1\mu}(0)$ is equal to the number of types of plane waves propagating to the left from the shock front.

Thus the total number m of arbitrary constants is equal to the number of solutions of Eq. (5) with $\lambda_{2\mu} < 0$ and $\lambda_{1\mu} > 0$, i.e., the number of waves propagating from the surface of discontinuity in the two directions.

On the other hand, on the surface of the discontinuity there are satisfied n conditions which relate the quantities u_{1k} and u_{2k}. The velocity of the wave front enters into these conditions. If it is eliminated, we obtain $(n-1)$ conditions connecting u_{1k} and u_{2k} at $x = 0$. We can now verify the fact that if the number of arbitrary constants is not equal to the number of these conditions, then the Cauchy problem either has no solution $(m > n-1)$ or it has an infinite number of solutions $(m < n-1)$. In this and in the other case, we must make some conclusion on the instability of the shock wave which is associated with its disintegration.

It is essential to note that neither boundary conditions nor considerations of thermodynamic stability (Zemplen theorem) exclude these conditions, generally speaking (see Sec. 5).

For stability of the shock wave it is necessary that the number of waves emanating from the discontinuity be equal to the number of boundary conditions on the discontinuity. If this condition is satisfied, it is still necessary to verify whether it is possible to satisfy the boundary conditions with the help of the remaining arbitrary constants.*

4. We now turn to the investigation of the stability of magnetohydrodynamic shock waves. As is well known,[2] there exist seven types of one-dimensional plane waves in magnetohydrodynamics: (1) Magnetohydrodynamic waves whose phase velocities are $v_x - V_x$, $v_x + V_x$) where $V_x = H_x/\sqrt{4\pi\rho}$. (2) Magnetoacoustic waves whose phase velocities are $v_x - u_-$, $v_x + u_-$, $v_x - u_+$, $v_x + u_+$, where

$$u_\pm^2=\frac{1}{2}\left[V^2+c^2\pm\sqrt{(V^2+c^2)^2-4c^2V_x^2}\right],\ \mathbf{V}=\mathbf{H}/\sqrt{4\pi\rho}$$

(c is the velocity of sound). (3) An entropy wave whose phase velocity coincides with the velocity of the liquid v_x. We note that

---

*This criterion is well-known for ordinary hydrodynamics (see reference 1, p. 405). However, we note that the considerations introduced in reference 1 cannot be applied in the case $m < n - 1$.

$$u_- \leqslant V_x \leqslant u_+. \qquad (8)$$

For stability of the shock wave, it is necessary (as was shown above) that the number of emergent waves should be one less than the number of boundary conditions, that is, it must be equal to six.

Waves having phase velocity $v_{1x} + V_{1x}$, $v_{1x} + u_{1+}$, $v_{1x} + u_{1-}$, and v_{1x}, are convergent, while the waves $v_{2x} + V_{2x}$, $v_{2x} + u_{2+}$, $v_{2x} + u_{2-}$, and v_{2x} are divergent. Therefore, in the case of stability of the remaining six waves with velocities $v_{1x} - V_{1x}$, $v_{1x} - u_{1+}$, $v_{1x} - u_{1-}$, $v_{2x} - V_{2x}$, $v_{2x} - u_{2+}$, and $v_{2x} - u_{2-}$, two must be divergent. Taking the inequalities (8) into account, it follows that the shock wave can be stable only under the following three conditions:*

$$\begin{aligned} &\text{A)}\ u_{-1} < v_{1x} < V_{1x},\ v_{2x} < u_{2-};\\ &\text{B)}\ V_{1x} < v_{1x} < u_{1+},\ u_{2-} < v_{2x} < V_{2x};\\ &\text{C)}\ u_{1+} < v_{1x}, \qquad V_{2x} < v_{2x} < u_{2+} \end{aligned} \qquad (9)$$

(see Fig. 1, in which the possible regions of stability are shaded).

We consider the particular case in which the magnetic field is parallel to the wave front: in this case $u_{1-} = u_{2-} = V_{1x} = V_{2x} = 0$; $u_{1+} = \sqrt{c_1^2 + V_1^2}$; $u_{2+} = \sqrt{c_2^2 + V_2^2}$, and therefore, in accord with Eq. (9), the shock wave can be stable on satisfaction of the inequalities

$$v_{1x} > \sqrt{c_1^2 + V_1^2};\ v_{2x} < \sqrt{c_2^2 + V_2^2} \qquad (10)$$

(see Fig. 2).

5. If the magnetic field is perpendicular to the shock front, then satisfaction of the conditions (9) is insufficient for stability of the wave with respect to the perturbations under consideration, since in this case the boundary conditions break up into three isolated groups. These conditions have the following form:

$$[\rho\delta v_x + v_x\delta\rho - \rho U] = 0, \quad [2\rho v_x\delta v_x + v_x^2\delta\rho + \delta p] = 0, \qquad (11)$$
$$[v_x\delta v_x + \delta w - v_x U] = 0;$$

$$\left[\rho v_x\delta v_y - \frac{H_x}{4\pi}\delta H_y\right] = 0,\ [v_x\delta H_y - H_x\delta v_y] = 0; \qquad (12)$$

$$\left[\rho v_x\delta v_z - \frac{H_x}{4\pi}\delta H_z\right] = 0,\ [v_x\delta H_z - H_x\delta v_z] = 0 \qquad (13)$$

(The set of coordinates is so chosen that $v_{1y} = v_{2y} = v_{1z} = v_{2z} = 0$, U is the velocity of the shock wave, w is the heat function.)

Of the four magnetoacoustic waves at $H_{1y} = H_{2y} = H_{1z} = H_{2z} = 0$, two are longitudinal and two are transverse. The longitudinal waves are ordinary sound waves whose velocities are equal to $v_x \pm c$. The transverse waves are ordinary magnetohydrodynamic waves considered earlier only in the direction of polarization.

In the consideration of the sound waves, it is necessary to take into account only the boundary conditions (11) since conditions (12) and (13) are satisfied identically for them. In the same fashion, in the consideration of the magnetohydrodynamic waves polarized along the y axis, we must take into account only the boundary conditions (12), while for waves polarized along the z axis we need only conditions (13).

Instead of investigating the stability relative to all three types of waves simultaneously, we must consider the stabilities for each type of wave individually. Let us begin with the magnetohydrodynamic waves. The number of boundary conditions for them is equal to 2 [see (12) or (13)]. Since these conditions do not contain the velocity of the wave front, then the presence of two diverging waves is necessary for stability. The wave with phase velocity $v_{2x} + V_{2x}$ diverges, while the wave

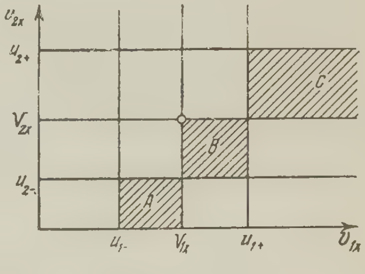

FIG. 1

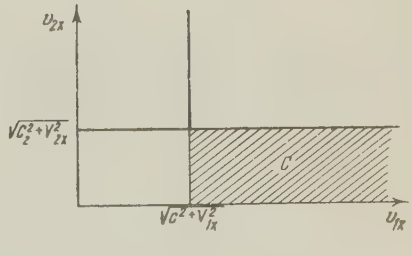

FIG. 2

---

*Note added in proof (August 6, 1958). Actually it must be considered that (as was pointed out to us by S. I. Syrovatskii) in the first approximation, the aggregate of boundary conditions in the case of shock waves (but not for rotational discontinuities) breaks up into two groups which contain quantities characterizing the magnetohydrodynamic waves (v_z, H_z) and magnetoacoustic waves (ρ, p, v_x, v_y, H_y; H lies in the xy plane). Therefore, computation of the number of diverging waves ought to be carried out not only for the entire aggregate of variables but also for each group separately. From this, we easily conclude that B is not a region of stability and is contracted to a point (small circle in Fig. 1; compare Secs. 5 and 6).

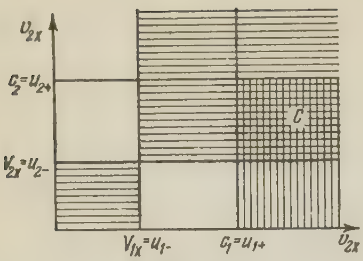

FIG. 3

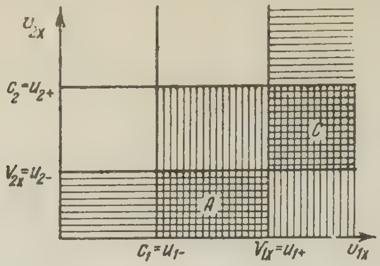

FIG. 4

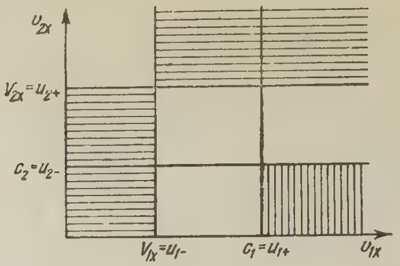

FIG. 5

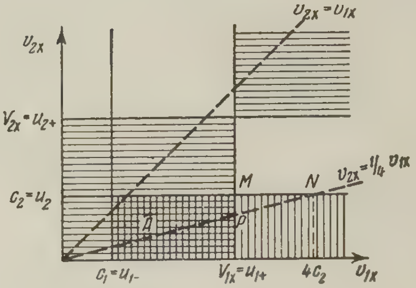

FIG. 6

with phase velocity $v_{1x}+V_{1x}$ converges. Of the remaining waves, with velocity $v_{1x}-V_{1x}$ and $v_{2x}+V_{2x}$, one must be diverging. This is possible in two cases: (1) $v_{1x}>V_{1x}$, $v_{2x}>V_{2x}$; (2) $v_{1x}<V_{1x}$, $v_{2x}<V_{2x}$ (see the horizontally shaded regions in Figs. 3 to 6).

Consideration of the sound waves leads to the following stability conditions:

$$v_{1x}>c_1, \quad v_{2x}<c_2$$

(see the vertically shaded regions in Figs. 3 to 6.)

The region of stability of shock wave relative to arbitrary single one-dimensional perturbations is the intersection of the regions of stability of the two separate waves. It is shown in Figs. 3, 4, and 6 by the doubly-shaded regions. In the case shown in Fig. 5, there is no region of stability. However, this cannot take place if

$$\left(\frac{\partial^2}{\partial p^2}\frac{1}{\rho}\right)_s>0.$$

We note that under the conditions in Figs. 3 to 6 the region for stability can be formally obtained from (9).

We emphasize that the inclusion of a magnetic field perpendicular to the wave front always leads to a decrease in the region of stability. This is explained by the fact that in such a field there are two independent transverse waves, which produce additional instability.

We note that in the case under consideration

$$V_{1x}>c_1,\ V_{2x}>c_2 \tag{14}$$

(see Fig. 6) the Cauchy problem corresponding to the system (2) has no solutions if

$$v_{1x}>V_{1x},\ v_{2x}<c_2 \tag{15}$$

(see the region of vertical shading in Fig. 6.)

One might think that the inequalities (14) and (15) are incompatible with Zemplen's theorem, by virtue of which

$$v_{2x}<v_{1x};\ \rho_2>\rho_1, \tag{16}$$

and with the boundary conditions. However, it is seen in the example of a monatomic ideal gas that this is not so. Actually the boundary conditions in this case can be written in the form

$$p_1=(4v_{2x}-v_{1x})\rho_1 v_{1x}/5,\ p_2=(4v_{1x}-v_{2x})\rho_1 v_{1x}/5,$$
$$\rho_2=\rho_1 v_{1x}/v_{2x},$$

from which it follows that

$$v_{2x}>{}^1/_4\,v_{1x};\ \rho_2<4\rho_1. \tag{17}$$

The inequalities (14) to (17) determine the triangle MNP (see Fig. 6). From this it is seen that for their simultaneous fulfilment it is necessary to have $V_{1x}<4c_2$ and $V_{2x}>c_2$. These inequalities are satisfied if the magnetic field H_x lies within the limits

$$c_2\sqrt{4\pi\rho_2}<H_x<4c_2\sqrt{4\pi\rho_2}, \tag{18}$$

which is always possible by virtue of (17).

6. Let us examine in particular Alfven rotational shock waves[2] which are the kind of shock waves most frequently considered. In these waves the velocities are characterized by the relations

$$v_{1x}=V_{1x}=v_{2x}=V_{2x}.$$

In Fig. 1, there corresponds to the Alfven wave a point surrounded by a circle. This point lies on the boundary of the region of stability. Therefore the problem of stability of the Alfven discontinuities requires additional consideration.

First we note that in our case two phase velocities vanish, namely, $v_{1x}-V_{1x}$ and $v_{2x}-V_{2x}$. With this, in accord with Eq. (5′), one of the roots λ of the characteristic equation becomes infinite. This means that the determinant $|X_{ik}|$ is equal to zero, i.e., the set (3) reduces to an $(n-1)$-fold differential equation and one algebraic relation among the quantities $u_1, u_2, \ldots, u_n$. Therefore the general solution of (3) contains $(n-1)$ constants of integration. Thus the presence of a "wave" with phase velocity equal to zero leads to the loss of a single arbitrary constant. Consequently, in the calculation of arbitrary constants, one must add such waves to the convergent ones.

Applying this conclusion to Alfven discontinuities, it is easy to see that they are stable relative to the perturbations being considered.

7. The necessary conditions that we have obtained for stability permit us to carry out a classification of shock waves. In the general case, when the magnetic field is inclined to the plane of the discontinuity, only three types of stable shock waves can exist, corresponding to the regions A, C of Fig. 1 and to a rotational discontinuity. If the jumps of all the quantities tend to zero on the surface of discontinuity, then the velocities of the shock waves approach the phase velocities of the linearized waves; in this case, the velocities of waves of type A tend to the phase velocity $v_x \pm u_-$ of the slow magnetoacoustic wave, the velocities of type C tend to the velocities $v_x \pm u_+$ of the fast magnetoacoustic wave. In this connection, it is appropriate to subdivide shock waves into slow and fast magnetoacoustic waves.

If the magnetic field is parallel to the plane of discontinuity, only the fast magnetoacoustic waves can be stable (see Fig. 2).

We note several consequences from the conditions for shock wave stability. If two shock waves of the same type follow one another, then the rear one overtakes the forward one. For example, let us consider two slow magnetoacoustic waves. The velocity of the forward wave, relative to the liquid contained between the waves is equal to v_{2x}, while the velocity of the rear wave is $-v_{1x}$. As follows from Fig. 1, for waves of this type, $v_{1x} > u_{1-}$ and $v_{2x} < u_{2-}$. Since the velocities u_{1-} and u_{2-} relate to the same region of space, then $u_{1-} = u_{2-}$ and, consequently, $v_{1x} > v_{2x}$.

So far as waves of different types are concerned, a rotational discontinuity will overtake a slow magnetoacoustic wave, while a fast magnetoacoustic wave will overtake all types of discontinuities. In the same way, we can show that a shock wave overtakes a weak discontinuity if it belongs to the same type as the shock wave itself, or to a slower type. A weak discontinuity overtakes a shock wave of the same type and shock waves of slower types.

The authors acknowledge their gratitude to L. D. Landau, A. S. Kompaneets, and G. I. Barenblatt for valuable discussions and advice.

---

[1] L. D. Landau and E. M. Lifshitz, Механика сплошных сред (The Mechanics of Continuous Media) (GITTL, Moscow, 1953).

[2] S. I. Syrovatskii, Usp. Fiz. Nauk **62**, 247 (1957).

Translated by R. T. Beyer
144

SOVIET PHYSICS JETP VOLUME 35(8), NUMBER 3 MARCH, 1959

THE DE HAAS-VAN ALPHEN EFFECT IN PULSED MAGNETIC FIELDS

A. M. KOSEVICH

Institute for Technical Physics, Academy of Sciences, Ukrainian S.S.R.

Submitted to JETP editor April 7, 1958

J. Exptl. Theoret. Phys. (U.S.S.R.) **35**, 738-741 (September, 1958)

Equations are obtained for the semi-classical quantization of the motion of an electron in a metal in an inhomogeneous magnetic field, the gradient of which is perpendicular to the direction of the field. The de Haas-van Alphen effect in a pulsed magnetic field is analyzed from the point of view of possibly using it to study the Fermi surface of the electron gas in a metal.

In reference 1 the author investigaged the de Haas-van Alphen effect in a sufficiently slowly changing magnetic field when one can start from the formulae for the quantization of the motion of an electron and the expression for the magnetic moment of an electron gas in a uniform magnetic field.[2] In the present note we obtain the equations for the quantization in an inhomogeneous magnetic field, the gradient of which is perpendicular to the direction of the field, and the role of the inhomogeneity of the field in a pulse method of investigating de Haas-van Alphen effect is elucidated.

1. We shall consider the motion of a particle with an arbitrary dispersion law $E = E(p_x, p_y, p_z)$ and charge e in an inhomogeneous magnetic field $\mathbf{H}$, directed along the z axis. If the y axis coincides with the direction* of grad $\mathbf{H}$, the classical motion of the particle proceeds according to

$$\mathscr{E}(P_x, P_y, p_z) = \varepsilon = \text{const}, \; p_x = \text{const}, \; p_z = \text{const}, \tag{1}$$

where the components of the kinetic momentum $\mathbf{P}$ are most conveniently expressed in the form

$$P_x = \frac{e}{c}\int\limits_{y_0(p_x)}^{y} H(y)\,dy, \; P_y = p_y, \; P_z = p_z, \tag{2}$$

where the function $y_0(p_x)$ is determined by the relation

$$p_x = -\frac{e}{c}\int\limits_{0}^{y_0(p_x)} H(y)\,dy. \tag{3}$$

We shall assume for the sake of simplicity that $H(y) > 0$. It is then clear from (1) and (2) that the classical motion of a particle corresponding to a closed surface $\mathscr{E}(p_x, p_y, p_z) = \epsilon$, is bounded along the y axis, and the coordinate $y_0 = y_0(p_x)$ plays the role of the center of the oscillations along this axis.

In the quantum case the components (2) of $\mathbf{P}$ correspond to operators with the following commutator relations

$$[\hat{P}_y, \hat{P}_x] = \frac{e}{c} H(\hat{y}), \; [\hat{P}_x, \hat{P}_z] = [\hat{P}_y, \hat{P}_z] = 0, \tag{4}$$

where $y = y(p_x, P_x)$ is determined from (2).

From (4) the semi-classical quantization condition

$$\oint [P_y / H(y)]\, dP_x = (n+\gamma)\, eh/c, \; (0 < \gamma < 1) \tag{5}$$

follows. The integration in (5) is performed along the closed curve (1).

Equation (5) determines implicitly the dependence of the energy levels ϵ on the quantum numbers n, p_z, p_x, or on the quantum numbers n, p_z, y_0, which is the same.

If the distance δ, over which the magnetic field $H(y)$ changes appreciably, is considerably larger than the radius r of the classical particle orbit in the magnetic field $H(y_0)$, we can for fixed p_z and $y_0(p_x)$ on the left hand side of the quantization equation (5) retain only the main terms in an expansion in powers of r/δ:

$$S(\varepsilon, p_z)\left\{1 - \frac{r_1}{H_0}\frac{dH}{dy_0} - \frac{1}{2}\frac{r_2^2}{H_0}\left[\frac{d^2H}{dy_0^2} - \frac{3}{H_0}\left(\frac{dH}{dy_0}\right)^2\right]\right\} = (n+\gamma)\frac{ehH}{c}; \tag{6}$$

$$r_1 S(\varepsilon, p_z) = (c/eH_0)\, J_{1y}, \; r_2^2 S(\varepsilon, p_z) = (c/eH_0)^2 J_{2y},$$

$$H_0 = H(y_0);$$

where $S(\epsilon, p_z)$ is the area of the cross section of the energy surface $\mathscr{E}(\mathbf{p}) = \epsilon$ with the plane $p_z = \text{const}$, $J_{1y}(\epsilon, p_z)$ the static moment, and $J_{2y}(\epsilon, p_z)$ the moment of inertia of the area $S(\epsilon, p_z)$ with respect to the p_y axis.

To conserve the quantization equations (5) and (6) in an electric field, produced by a non-static magnetic field (see reference 1) it is necessary that the energy, gained by a particle in the electrical field during a period of revolution in the classical orbit, be small compared to the distance between the quantized energy levels. We make a corresponding estimate in the case where Eq. (6) is justified, when the simple expression for the distance between the energy levels is well known to be

---

*Such an inhomogeneous magnetic field is necessarily solenoidal (curl $H \neq 0$) and can, therefore, not be purely magnetostatic.

$$\Delta\varepsilon = \hbar\omega^* \equiv \hbar\,(eH/m^*c) \equiv \mu^* H;$$

where m^* is the effective mass and μ^* the effective magnetic moment of the particle.

From an analysis of the Maxwell equations it follows that if T is a characteristic time of change of the magnetic field, the electrical field strength $E \sim H\delta/cT$. The above mentioned requirement leads thus to the inequality.

$$\omega^* T \gg \delta/\lambda, \tag{7}$$

where λ is the de Broglie wavelength of a particle with energy ϵ.

If the inhomogeneity of the magnetic field is vanishingly small, Eq. (6) goes over into the well-known quantization equations in a homogeneous field.[2,3] Corrections to the particle energy levels in a uniform magnetic field,[2,3] arising from taking the field inhomogeneity into account in Eq. (6), are meaningful, of course, only if they are considerably larger than the inaccuracy of the semi-classical approximation itself, i.e., when

$$r_1/\delta \gg (\lambda/r)^2 \quad\text{and}\quad r_2^2/\delta^2 \gg (\lambda/r)^2.$$

2. We shall consider the de Haas-van Alphen effect in a pulsed magnetic field. Let the external field which is directed parallel to the surface of the metal specimen increase from zero to a maximum value H_m in a time interval $(0, t_m)$ and the general duration of the pulse $T \sim t_m$. The magnetic field inside the metal is then a function of the y coordinate measuring the depth into the sample from its surface, and a characteristic measure along the y axis $\delta \sim (c^2T/\sigma_m)^{1/2}$, where $\sigma_m = \sigma(H_m)$ is the electrical conductivity of the metal in a magnetic field H_m.

The energy levels of an electron in such a sample are determined by Eqs. (5) or (6)* where y_0 changes within the limits 0 to L, where L is the length of the sample along the y axis.

As is well known,[2] the oscillations of the magnetic moment of the electron gas with a change of the magnetic field is determined by a change of the extreme value $n_m(H)$ — the integral quantum number n, corresponding to the limiting Fermi energy in a factor of the form $2\pi n_m(H)$. Since in a homogeneous field n is very simply connected with $S(\epsilon, p_z)$, an investigation of the periods of the oscillations in a uniform field enables one in principle to reconstruct the Fermi surface for the electrons in a metal.[4] In order that a study of the periods of the oscillations in a pulsed field can also give interesting information about the Fermi surface, it is necessary that n_m be directly connected with the cross sections of that surface. From the foregoing it is clear that this only takes place if $r \ll \delta$, when Eq. (6) is valid. In that case the relative change in period $P = \Delta(1/H_0)$ for the oscillations of the magnetic moment of a thin metal layer at a depth $y = y_0$ as compared to the period in a corresponding uniform field P_0 is, as to order of magnitude, equal to

$$\delta P/P_0 = |P - P_0|/P_0 \sim r_{1m}/\delta \div r_{2m}^2/\delta^2, \quad P_0 = eh/cS_m, \tag{8}$$

where S_m, r_{1m}, and r_{2m} are determined for the extremal cross section of the Fermi surface, corresponding to the given oscillations. If the center of gravity of the extremal cross section lies on the p_y axis (this will, for instance, be the case for a central cross section of the Fermi surface, possessing a center of symmetry), $r_{1m} = 0$ and the order of magnitude of the quantity $\delta P/P_0$ is determined by the second term on the right hand side of (8). Otherwise $\delta P/P_0 \sim r_{1m}/\delta$. We note that in magnetic fields $H_m \sim 10^5$ Oe for the basic electron groups $r_m \sim 10^{-4}$ to 10^{-5} cm.

From (8) it follows that if $r_m \ll \delta$ the above-mentioned periods are practically not changed, while the change in the phase of the oscillations compared with those in a uniform field can be appreciable, since it is of the order of magnitude $(\delta P/P_0)(\epsilon_0/\mu^* H)$ where ϵ_0 is the limiting Fermi energy.

Since the determination of the function $H = H(y)$ is a non-trivial mathematical problem for complicated pulses of the external field and when σ depends essentially on H in strong fields, quantita-

---

*Strictly speaking, if the external magnetic field vector and the normal to the surface of the sample do not coincide with the principal axes of the electrical conductivity tensor, the direction of the magnetic field inside the metal changes with depth. However, in the practically most interesting cases, considered below, this rotation of the H vector can be neglected when condition (7) is fulfilled. As to inequality (7) in metals, there is a sufficiently wide range of T for which it is satisfied. Indeed, if we take for λ an extreme estimate, $\lambda \sim 10^{-8}$ cm, and take into account that for the basic electron groups in metals at $H \approx 10^5$ Oe the Larmor frequency $\omega^* \sim 10^{12}$, we can write (7) in the form $T/\delta \sim (\delta_m T/c^2)^{1/2} \gg 10^{-4}$ sec/m.

tive conclusions about the Fermi surface based on results of an investigation of the oscillations by means of pulses is possible only in those cases when the measured periods are directly connected with the change in the external field. In reference 1 it was shown that those cases are (1) $\delta \gg L$, (2) $\delta \ll L$. If we take into account that an experimental measurement of the periods of the oscillations enables us to obtain directly the cross sectional area of the Fermi surface only if $r_m \ll \delta$ [see (8)] and $r_m < L$[5], it becomes logical to use in the same connection the following limiting cases (1) $\omega^* T\lambda \gg \delta \gg L > r_m$, (2) $L \gg \delta \gg r_m$; $\omega^* T\lambda \gg \delta$. The experimental conditions of Shoenberg[6] correspond to the first case.

In the first of the cases noted by us it is possible to observe the oscillations with the change in the external field practically during the whole duration of the pulse, but in the second case only for $t < t_0$, where $t = t_0$ corresponds to the moment when on the surface of the sample $dH/dy = 0$. One can show that always $t_0 > t_m$.[1]

The author expresses his thanks to I. M. Lifshitz and M. Ia. Azbel' for discussions.

---

[1] A. M. Kosevich, J. Exptl. Theoret. Phys. (U.S.S.R.) **33**, 735 (1957), Soviet Phys. JETP **6**, 564 (1958).

[2] I. M. Lifshitz and A. M. Kosevich, Dokl. Akad. Nauk SSSR, **96**, 963 (1954), J. Exptl. Theoret. Phys. (U.S.S.R.) **29**, 730 (1955), Soviet Phys. JETP **2**, 637 (1956).

[3] A. M. Kosevich, Укр. физ. журн. (Ukrain. Phys. J), **1**, 261 (1956).

[4] I. M. Lifshitz and A. V. Pogorelov, Dokl. Akad. Nauk SSSR, **96**, 1143 (1954).

[5] A. M. Kosevich and I. M. Lifshitz, J. Exptl. Theoret. Phys. (U.S.S.R.) **29**, 743 (1955), Soviet Phys. JETP **2**, 646 (1956).

[6] D. Shoenberg, Physica **19**, 791 (1953).

Translated by D. ter Haar
145

SOVIET PHYSICS JETP VOLUME 35(7), NUMBER 3 MARCH, 1959

ON THE SCATTERING OF "DRESSED" PARTICLES IN QUANTUM FIELD THEORY

Iu. V. NOVOZHILOV

Leningrad State University

Submitted to JETP editor April 10, 1958

J. Exptl. Theoret. Phys. (U.S.S.R.) **35**, 742-749 (September, 1958)

A scattering theory is considered in which the virtual "clouds" around the particles are always taken into account exactly. The theory is based on the representation of the basis functionals as products of single-particle functionals. In the absence of vacuum polarization the equations for the matrix elements are automatically renormalized, and the matrix elements can be expressed in terms of the single-nucleon matrix elements.

In scattering problems in quantum theory it is usually assumed that for $t = \pm\infty$ the particles do not interact with the vacuum. The adiabatic introduction of the interaction then includes both the interaction between the particles (by way of the field) and also the interaction with the vacuum. Since the particles always interact with the vacuum, it is interesting to consider the question of a scattering theory in which the interaction of the particles with the vacuum is at all times taken into account exactly (the scattering of "dressed" particles). This is also one of the possible approaches to a problem that has recently been much discussed, that of the construction of the S matrix on the basis of ideas about the physical particles, without the introduction of the concept of "bare" particles.[1]

As the first aspect of the problem of the scattering of "dressed" particles we can take the problem of constructing basis functionals Φ which asymptotically describe noninteracting dressed particles. In the present paper we consider from this point of view some problems of the scattering of dressed particles in the case in which the functionals Φ are represented in the form of products of single-particle functionals, which are solutions of the Schrödinger equation with interaction. Such functions have been discussed by Ekstein[2] and have been used by the present writer for the derivation of a two-nucleon potential depending on the phase shifts of the π-N scattering.

As soon as the system of basis functions Φ has been constructed, the apparatus of the formal scattering theory[2] at once leads to a system of nonlinear integral equations for the scattering amplitudes. A characteristic feature of this method is the presence in these equations of the matrix elements of the field operators between products of single-nucleon states. The method described below (in Sec. 2) for calculating such quantities is a generalization of the method we have proposed[3] earlier for the case of two bound nucleons.

The scattering scheme so developed takes proper-energy effects into account automatically; on the other hand it seems to be impossible to extend the scheme to the vacuum polarization without the explicit introduction of renormalization. This is a consequence of the assumption of the spatial localizability of the virtual field (only a "cloud" around the particles), which is the essential basis of the choice of the Φ. Therefore for practical calculations the method can be used for the treatment of the interaction of nucleons, mesons, and hyperons in the region of relatively low energies.

1. THE BASIS FUNCTIONS

Let us consider the case in which there is no vacuum polarization, and go over to the configuration space for the nucleons. The total Hamiltonian for n nucleons and antinucleons interacting with the meson field can be written in the form

$$H = H_\pi + \sum_i^n [H_N(i) + U_i], \tag{1}$$

where H_π is the Hamiltonian of the free meson field, $H_N(i)$ refers to the i-th "bare" nucleon, and U_i is the operator for the interaction of the i-th nucleon with the meson field, which we shall assume is linear in the meson creation operators a^+ and annihilation operators a:

$$U_i = \sum_q (V_{iq} a_q e^{i\mathbf{q}\cdot\mathbf{r}_i} + V_{iq}^+ a_q^+ e^{-i\mathbf{q}\cdot\mathbf{r}_i}\}. \tag{2}$$

Here q denotes all the quantum numbers of a meson. Let us consider the construction of the wave functions $\Phi(1, 2, \ldots n; \bar{a})$ of a system of n noninteracting dressed nucleons. Since the nucleons have meson clouds, Φ depends on the meson field variables $\bar{a}$, or

$$\Phi(1, 2 \ldots n; \bar{a}) = \Phi(1, 2 \ldots n; a^+)\Lambda_0,$$

where Λ_0 is the vacuum state vector. (Here the physical meson vacuum Λ_0 is the same as the mathematical state.) Strictly speaking, because of the identity of the mesons belonging to the meson clouds of different nucleons, one cannot define a state of noninteracting nucleons for arbitrary distances between them. Only for large distances R_{ij} between the nucleons does the effect of the identical nature of the mesons become negligible, so that the state of the noninteracting dressed nucleons can be defined only in the asymptotic sense for $R_{ij} \to \infty$.

It is easy to see that we cannot separate off from the Hamiltonian (1) any part corresponding to noninteracting dressed nucleons. Therefore $\Phi(1, 2, \ldots; \bar{a})$ must be a solution of the Schrödinger equation with the total Hamiltonian H for large relative distances,

$$\left\{H - \sum_i E(i)\right\}\Phi(1, 2, \ldots; a^+)\Lambda_0 \to 0, \quad R_{ij} \to \infty, \tag{3}$$

where E(i) is the energy of the i-th free nucleon. Moreover, asymptotically Φ must also be an eigenfunction of the total momentum. The wave function Φ is constructed from products of single-nucleon state vectors $F_\alpha(1, \bar{a})$ (α denotes all the quantum numbers of a nucleon), which are eigenvectors of the energy and momentum operators:

$$H_i F_\alpha(i, \bar{a}) = \{H_N(i) + H_\pi + U_i\} F_\alpha(i, \bar{a}) = E_\alpha(i) F_\alpha(i, \bar{a}), \tag{4}$$

$$\{\hat{\mathbf{p}}_N + \mathbf{u}\} F_\alpha(i, \bar{a}) = \mathbf{p}_i^\alpha F_\alpha(i, \bar{a}), \tag{5}$$

where $\mathbf{u}$ is the momentum of the meson field and $\hat{\mathbf{p}}_N$ is the momentum operator of a nucleon. Furthermore, $F_\alpha(i, \bar{a})$ is an eigenfunction of the total spin operator. The wave function of the system of noninteracting dressed nucleons is then

$$\Phi_a(1, 2 \ldots; a^+)\Lambda_0 = \sum_{\alpha\beta..} C^a_{\alpha\beta..} F_\alpha(1, a^+) F_\beta(2, a^+) \ldots \Lambda_0, \tag{6}$$

where the coefficients $C^a_{\alpha\beta\ldots}$ are such that asymptotically Φ_a has the required symmetry properties.

Such a method for constructing Φ has much in common with the construction of functions in the theory of molecules. The role of the electrons, in whose coordinates one has to antisymmetrize, is now played by the mesons, in whose coordinates Φ is symmetric. The antisymmetrization with respect to the electrons belonging to the various nuclei destroys the orthogonality of the basis functions. Here, in just the same way, because of the identity of the mesons in all the one-nucleon states F_α, the functions Φ_a and Φ_b are not orthogonal, and so on.

Let us verify that the conditions (3) are satisfied. We introduce the notation

$$U_i = U_i^{(+)} + U_i^{(-)}, \tag{7}$$

where $U^{(+)}$ contains the absorption operators and $U^{(-)}$ the emission operators. Since the operator $h = H_\pi + \sum U_i^{(+)}$ is linear in the absorption operators, the quantity $[h, F(i, a^+)]$ does not depend on the operators a and commutes with any other $F(j, a^+)$. Using the equations (4), we have

$$\begin{aligned}\left\{H - \sum_i E(i)\right\} F(1, a^+) F(2, a^+) \ldots \Lambda_0 \\ = \sum_{i \neq j} F(1, a^+) F(2, a^+) \ldots [U_i^{(+)}, F(j, a^+)]\Lambda_0.\end{aligned} \tag{8}$$

According to Eq. (5),

$$F(j, a^+)\Lambda_0 = \exp\{i(\mathbf{p}_j - \mathbf{u})\cdot\mathbf{r}_j\} F^0(j, a^+)\Lambda_0, \tag{9}$$

where F^0 does not depend on the coordinates. Therefore it follows from Eq. (4) that

$$\begin{aligned} U_i^{(+)} F_\alpha(j, a^+)\Lambda_0 \\ = -\sum_q \sum_n \exp\{i\mathbf{p}_x\cdot\mathbf{r}_j + i\mathbf{q}\cdot(\mathbf{r}_i - \mathbf{r}_j)\} \\ \times \frac{V_{iq} F^{(n)}(j)\,(F^{(n)}(j), V_{jq}^+ F_\alpha(j, \bar{a}))}{E_n + \omega_q - E_\alpha},\end{aligned} \tag{10}$$

where $F^{(n)}(j)$ is the eigenstate of the Hamiltonian H_j with the momentum $\mathbf{p}_n = \mathbf{p}_\alpha - \mathbf{q}$, and the energy $E_n = (M_n^2 + p_n^2)^{1/2}$, $M_n > M_N$; and $\omega_q = (1 + q^2)^{1/2}$. The denominator in Eq. (10) cannot vanish. For $|\mathbf{r}_i - \mathbf{r}_j| \to \infty$ the quantity (10) decreases exponentially. In a similar way one can verify that the function Φ is asymptotically an eigenfunction of the total momentum or angular momentum.

The basis functions Φ_A for states in which there are real mesons besides the nucleons are obtained from the expression (6) by multiplying by a suitable number of meson creation operators:

$$\Phi_A = a_{q_1}^+ a_{q_2}^+ \ldots \Phi_a; \quad A \equiv (q_1, q_2 \ldots; a). \tag{11}$$

To describe a meson spatially remote from the other particles one must take a wave packet, i.e., multiply Φ_a not by a_q^+, but by

$$f(r) = \sum_q c_q e^{-i\mathbf{q}\cdot\mathbf{r}} a_q^+.$$

Then asymptotically Φ_A will be a solution of the

Schrödinger equation. In fact, multiplying $\{H - \Sigma E(i) - \omega_q\} a_q^+ \Phi_a$ on the left by $\Sigma e^{-iqr} c_q$, we get on the right, in addition to terms of the type shown in Eq. (8), also terms that contain factors

$$\sum_i [U_i^{(+)}, f(r)] = \sum_i \sum_q e^{iq(\mathbf{r}_i - \mathbf{r})} V_{iq} c_q,$$

that vanish for $|\mathbf{r} - \mathbf{r}_i| \to \infty$ in virtue of the properties of the coefficients c_q of the wave packet. Because of the asymptotic character of the conditions imposed on Φ, there still remains some arbitrariness in the expression for Φ. The expression (6) can be multiplied by a function of the relative distances R_{ij} that goes to unity for $R_{ij} \to \infty$. This arbitrariness is of no importance when we deal with scattering by the methods of quantum field theory, and becomes important when we go over to the phenomenological treatment (see Sec. 3).

2. THE EQUATIONS FOR THE TRANSITION AMPLITUDES

In the case of scattering of "dressed" particles we cannot define[2] the scattering matrix S in terms of an operator acting on the asymptotic states of the "dressed" particles. In this case the S matrix is defined by the relation

$$S_{BA} = (\Psi_B^{(-)}, \Psi_A^{(+)}) = \delta_{BA} - 2\pi i \delta(E_B - E_A) R_{BA}^{(\pm)}, \tag{12}$$

where $\Psi^{(\pm)}$ are the eigenfunctions of the Hamiltonian H with the respective boundary conditions:

$$\Psi_A^{(\pm)} = \Phi_A - \frac{1}{H - E_A \mp i\varepsilon} [(H - E_A)\Phi_A]. \tag{13}$$

According to the formal scattering theory[2] the scattering amplitudes

$$R_{BA}^{(-)} \equiv R_{BA} = (\Psi_B^{(-)}, (H - E_A)\Phi_A) \tag{14}$$

satisfy a system of nonlinear integral equations. These equations have the form:

$$\begin{aligned} R_{BA} = (\Phi_B, (H - E_A)\Phi_A) - \sum_n \frac{R_{nB}^* R_{nA}}{E_n - E_B - i\varepsilon} \\ - \sum_d \frac{(\chi_d, (H - E_R)\Phi_B)^* (\chi_d, (H - E_a)\Phi_a)}{E_d - E_B}, \end{aligned} \tag{15}$$

where the χ_d refer to the bound states, and the first sum is taken over all states n of the continuous spectrum of H. In the case of a single nucleon Eq. (15) is nothing other than the Low equation. For a larger number of nucleons the formalism with the equations (15) departs from the usual formalism of the S matrix; this can be seen in particular from the fact that matrix elements with the wave functions Φ in the form of products of single-nucleon functions are not encountered in the usual theory of the S matrix.

Let us examine the inhomogeneous terms in the equations (15). According to Eq. (11)

$$\begin{aligned} R_{BA}^0 &= (\Phi_B, (H - E_A)\Phi_A) \\ &= (\Phi_b, a_{q_1'} a_{q_2'} \ldots (H - E_A) a_{q_1}^+ a_{q_2}^+ \ldots \Phi_a). \end{aligned} \tag{16}$$

In Eq. (16) let us displace all the creation operators to the left to Φ_b and all the annihilation operators to the right to Φ_a, and write R_{BA}^0 in the form

$$R_{BA}^0 = (\Phi_b, L(a, a^+)\Phi_a), \tag{17}$$

where the operator L contains only normal products of the creation and annihilation operators. Here the wave functions Φ_b and Φ_a, which describe noninteracting dressed nucleons (Eq. (6)) depend on the meson variables only in a small volume around a nucleon (the "meson cloud"). Therefore in calculating the expression (17) we may use the method of introducing individual coordinates for the mesons in the cloud of each nucleon.[3] We introduce a_{jq} and a_{jq}^+, the creation and annihilation operators for a meson in the cloud of the j-th nucleon,

$$[a_{jq}, a_{ik}^+] = \delta_{ij}\delta_{qk}; \; [a_{jq}, a_{ik}] = 0. \tag{18}$$

The state vector of a single nucleon is then written as $F(i, a_i^+)\Lambda_0$, and the state vector for n free nucleons (with neglect of the identical nature of the mesons in the clouds of different nucleons) has the form

$$\Phi_a^0 = \sum_{\alpha\beta\ldots} C_{\alpha\beta\ldots}^a F_\alpha(1, a_1^+) F_\beta(2, a_2^+) \ldots \Lambda_0. \tag{19}$$

The vectors Φ^0 are orthogonal. Asymptotically Φ_a coincides with Φ_a^0. Our problem is to reduce the matrix element (17) between the states Φ_b and Φ_a (i.e., with account taken of the identical nature of the mesons in the clouds of different nucleons) to matrix elements between states Φ_b^0 and Φ_a^0 (i.e., with only mesons belonging to the same nucleon treated as identical particles). This problem is solved in general form by Eq. (A.1) of the Appendix. We have

$$(\Phi_b, L(a, a^+)\Phi_a) = (\Phi_b^0, :[1 + \hat{N}] L(A, A^+): \Phi_a^0), \tag{20}$$

where :PT: denotes the normal product of the operators P and T, and A^+ and A are sums of creation and annihilation operators:

$$A_q = \sum a_{iq}; \; A_q^+ = \sum_i a_{iq}^+. \tag{21}$$

The weight operator $\hat{N}$ has the form

$$1 + \hat{N} = :\exp \sum_{i \neq j} \sum_q a_{iq}^+ a_{jq}:. \tag{22}$$

In Eq. (20) each of the meson operators occurring in $:L(1+\hat{N}):$ acts only on the state vector of a single nucleon. Therefore the matrix element (20) is expressed in terms of products of one-nucleon matrix elements of normal products of meson operators a, a^+ and vertex operators V:

$$(F_\alpha, a_q^+ \ldots a_k \ldots V_s \ldots F_\beta). \qquad (23)$$

We obtain the simplest matrix elements by omitting $\hat{N}$. Each successive term in the expansion of $1+\hat{N}$ adds one meson operator in the one-nucleon matrix elements (23), so that the inhomogeneous term (17) is represented as an infinite sum of products of one-nucleon matrix elements of the type (23). The operator $:(1+\hat{N})L:$ relates only to the interaction of the particles; all self-energy effects contained in L are eliminated automatically, since we are using functionals with the eigenfields F. The operator N itself describes the exchange of virtual mesons between the various nucleons ($i \neq j$ in Eq. (22)).

The rule (20) for calculating matrix elements of field operators between products of one-nucleon functionals completes the specification of the system of equations (15) for the transition amplitudes R_{BA}, in the sense that it expresses the inhomogeneous terms in the system in terms of quantities well known in the quantum field theory, the single-nucleon matrix elements. If the solution of the system (15) exists, we accordingly require, in order to find it, a knowledge of the one-nucleon problem, i.e., of the quantities (23). The charge renormalization also relates to the one-nucleon problem, since a knowledge of $(F_\alpha, V_s F_\beta)$ is required for the determination of the renormalized charge. All the one-nucleon matrix elements are already renormalized. In the static theory the quantities (23) can be related to the scattering amplitudes on the energy surface, and the charge renormalization is trivial.[4]

A possible method for the solution of the system (15) with the inhomogeneous terms in the form (20) is an expansion in terms of the number of mesons (if we disregard perturbation theory). We may assume that the larger the number of mesons by which a state n differs from the initial and final states A and B, the smaller is the part played by this state, and on this basis we can throw out some of the terms of the sum in Eq. (15). We must then break off the expansion of $1+\hat{N}$ in a similar way. When this is done, however, if we express the quantities (23) in terms of matrix elements $(F_\alpha, V_s F_\beta)$, $(F_\alpha^q, V_s F_\beta)$ (F_α^q is a state with one nucleon and one meson) and the other simplest one-nucleon quantities that can be taken as a basis, then in general each of the quantities (23) is a series involving summation over the eigenstates of the single-nucleon Hamiltonian. From this series also one must take only a suitable number of terms. The range of usefulness of such a method can be judged only from the results. We note that the series (22) that defines the operator $1+\hat{N}$ arose as a result of the expansion of the one-nucleon state vector $F(i, A^+)$ in a series in $A^+ - a_i^+$. The successive terms of the expansion will fall off rapidly in cases in which the meson clouds of the various nucleons "overlap" only slightly, so that the mesons in a cloud interact much more strongly with "their own" nucleon than with "a different" nucleon. Therefore it is to be expected that the higher the energy of the colliding nucleons (i.e., the greater the "overlapping" of the clouds) the more terms in the series (22) will have to be taken into account.

If the number and types of the particles do not change in the collision some simplification is possible. In this case one can use a treatment in which the methods of quantum field theory are used for the calculation of an effective potential, and the scattering amplitude is then determined by solving the Schrödinger equation with this potential. Such an approach is possible only for the region of moderate energies, in which the concept of a potential can be used and the polarization of the vacuum can be neglected.

3. DETERMINATION OF THE EFFECTIVE POTENTIAL

Let us denote by $K + W$ the total Hamiltonian in the phenomenological treatment, where W is the potential. For the eigenfunctions $\psi_a^{(\pm)}$ of the operator $K + W$ that belong to the continuous spectrum, the formal scattering theory gives

$$\psi_a^{(\pm)} = \psi_a^0 - \frac{1}{K - E_a \mp i\varepsilon} W \psi_a^{(\pm)} = \psi_a^0 - \frac{1}{K + W - E_a \mp i\varepsilon} W \psi_a^0,$$

where ψ_a^0 is an eigenfunction of the free-particle Hamiltonian K. For the scattering amplitude $R_{ba} = (\psi_b^{(-)}, W\psi_a^0)$ we can then write either the linear integral equation

$$R_{ba} = W_{ba} - \sum_c \frac{R_{bc} W_{ca}}{E_c - E_b - i\varepsilon}, \qquad (24)$$

or the nonlinear equation

$$R_{ba} = W_{ba} - \sum_c \frac{R_{cb}^* R_{ca}}{E_c - E_b - i\varepsilon} - \sum_d \frac{(\psi_d, W\psi_b^0)^* (\psi_d, W\psi_a^0)}{E_d - E_b}, \qquad (25)$$

where the summation goes over both the continuous spectrum c and the discrete spectrum d.

Here $W_{ba} = (\psi_b^0, W\psi_a^0)$ is the Born approximation to the scattering amplitude. Usually the potential is determined by solution of the linear equation (24). In the treatment we are considering it is more convenient to use the nonlinear equation (25). In addition one can generally avoid solving the equation connecting R_{ba} with W_{ba}.

Let us separate out from the whole sum over n in Eq. (15) the sum over the states c (of the continuous spectrum) with the same particles as there are in the states a and b (it is assumed that the collision does not change the types of the particles):

$$R_{ba} = (\Phi_b, (H - E_a)\Phi_a) - \sum_{n \neq c,d} \frac{R^*_{nb} R_{na}}{E_n - E_b - i\varepsilon} - \sum_c \frac{R^*_{cb} R_{ca}}{E_c - E_a - i\varepsilon} - \sum_d \frac{(\chi_d, (H - E_b)\Phi_b)^* (\chi_d, (H - E_a)\Phi_a)}{E_d - E_b}. \tag{26}$$

The last two terms in Eq. (26) are analogous in form to the last two terms in Eq. (25). Let us now determine the potential W from the requirement that the transition amplitudes between the two-nucleon states be equal to the corresponding amplitudes in the phenomenological treatment:

$$\begin{aligned} (\Psi_b^{(-)}, (H - E_a)\Phi_a) &= (\psi_b^{(-)}, W\psi_a^0), \\ (\chi_d, (H - E_a)\Phi_a) &= (\psi_d, W\psi_a^0). \end{aligned} \tag{27}$$

Then comparison of Eqs. (26) and (25) shows that

$$W_{ba} = (\Phi_b, (H - E_a)\Phi_a) - \sum_{n \neq c,d} \frac{R^*_{nb} R_{na}}{E_n - E_a - i\varepsilon}, \tag{28}$$

where the sum is over all states except the states with the original particles. This determination of the potential is valid also in the case in which nucleon-antinucleon pairs are taken into account.

As is well known,[5-7] the introduction of an effective potential by different methods can lead to different results. This ambiguity is due to the arbitrariness noted above in the choice of the basis functions Φ and arises from the fact that in quantum field theory the concept of noninteracting dressed nucleons is defined only asymptotically. In the phenomenological treatment, on the other hand, the wave function of the noninteracting nucleons is defined for all values of R_{ij}. Therefore the unique determination of the potential requires a knowledge of the state vector of the noninteracting dressed nucleons for arbitrary R_{ij}.

The formulas (27) and (28) for the potential W do not leave any ambiguity, but in these formulas it is assumed implicitly that one has chosen for Φ the wave function that "correctly" describes the noninteracting dressed nucleons for finite R_{ij} also. This assumption is included in the equations (27) outside the energy surface, since the replacement of the basis functions Φ by other functions Φ' (with the same asymptotic behavior) leaves Eq. (27) unchanged only on the energy surface.

In the case of two nucleons the adiabatic potential derived by Klein and McCormick[5] corresponds to the representation (6) for Φ without additional factors, and the potential obtained by Miyazawa[8] and the writer[3] corresponds to the choice of the function Φ with normalized amplitude

$$(\Phi_a | \Phi_a) = 1,$$

where (|) means that in the scalar product the integration over the space coordinates is not carried out.

APPENDIX

We shall derive the formula (20). We shift the operators a^+ to the left to Λ_0 and the absorption operators a to the right to Λ_0; then according to Eq. (6) a typical one of the quantities making up the left member of Eq. (20) will be

$$M = (F_1'(1, a^+) F_2'(2, a^+) \ldots \Lambda_0, F_1(1, a^+) F_2(2, a^+) \ldots \Lambda_0),$$

where F_i' and F_i can differ from F by the absence of one or more virtual mesons. We have

$$M = F_1'^*\left(1, \frac{\partial}{\partial \bar{a}}\right) F_2'^*\left(2, \frac{\partial}{\partial \bar{a}}\right) \ldots F_1(1, \bar{a}) F_2(2, \bar{a}) \ldots \Big|_{\bar{a}=0}$$

$$= F_1'^*\left(1, \frac{\partial}{\partial \bar{a}_1} + \frac{\partial}{\partial \bar{a}_2} + \ldots\right) F_2'^*\left(2, \frac{\partial}{\partial \bar{a}_1} + \frac{\partial}{\partial \bar{a}_2} + \ldots\right) \times \ldots F(1, \bar{a}_1) F(2, \bar{a}_2) \ldots \Big|_{\bar{a}_i=0}$$

Since $[\bar{\lambda}_i, \bar{a}_i] = 0$

$$F(i, \bar{\lambda}_i + \bar{a}_i) = \exp\left[\sum_q \bar{\lambda}_{iq} \frac{\partial}{\partial \bar{a}_{iq}}\right] F(i, \bar{a}_i).$$

From this, writing $\lambda_i = \sum_j \partial/\partial \bar{a}_j$ for $i \neq j$, we have

$$\begin{aligned} M &= F_1'^{*}\left(1, \frac{\partial}{\partial \bar{a}_1}\right) F_2'^{*}\left(2, \frac{\partial}{\partial \bar{a}_2}\right) \ldots : \prod_i \exp\left[\sum_q \lambda_{iq} \bar{a}_{iq}\right] : F_1(1, \bar{a}_1) F_2(2, \bar{a}_2) \ldots \Big|_{\bar{a}_i = 0} \\ &= \left(F_1'(1, a_1^+) F_2'(2, a_2^+) \ldots \Lambda_0, \; : \prod_i^n \exp\left[\sum_q \hat{\lambda}_{iq} a_{iq}^+\right] : F_1(1, a_1^+) F_2(2, a_2^+) \ldots \Lambda_0 \right), \quad \hat{\lambda}_{iq} = \sum_{i \neq j} a_{jq} = A_q - a_{iq}. \end{aligned} \tag{A.1}$$

Changing back from the quantities F_i and F_i' to the one-nucleon functions F, we get from this the formula (20).

---

[1] F. Low, Phys. Rev. **97**, 1392 (1955). Lehmann, Symanzik, and Zimmermann, Nuovo cimento **1**, 205 (1955). R. Haag, Kgl. Danske Vidensk, Selsk. Mat.-Fys. Medd. **29**, No. 12 (1955). N. N. Bogoliubov and D. V. Shirkov, **Введение в теорию квантованных полей** (Introduction to Quantum Field Theory), Sect. 47. Gostekhizdat 1957.

[2] H. Ekstein, Phys. Rev. **101**, 880 (1956); Nuovo cimento **4**, 1017 (1956).

[3] Iu. V. Novozhilov, J. Exptl. Theoret. Phys. (U.S.S.R.) **32**, 1262 (1957), **33**, 901 (1957); Soviet Phys. JETP **5**, 1030 (1957), **6**, 692 (1958).

[4] G. C. Wick, Revs. Modern Phys. **27**, 339 (1955).

[5] A. Klein and B. H. McCormick, Phys. Rev. **104**, 1747 (1956).

[6] Fukuda, Sawada, and Taketani, Prog. Theor. Phys. **12**, 156 (1954).

[7] Inoue, Machida, Taketani, and Toyoda, Prog. Theor. Phys. **15**, 122 (1956).

[8] H. Miyazawa, Phys. Rev. **104**, 1741 (1956).

Translated by W. H. Furry
146

SOVIET PHYSICS JETP VOLUME 35(8), NUMBER 3 MARCH, 1959

OPTICAL MODEL FOR THE INTERACTION OF NEUTRONS OF INTERMEDIATE ENERGY WITH NUCLEI

A. V. LUK'IANOV, Iu. V. ORLOV, and V. V. TUROVTSEV

Scientific Research Institute for Nuclear Physics, Moscow State University

Submitted to JETP editor April 11, 1958

J. Exptl. Theoret. Phys. (U.S.S.R.) **35**, 750-756 (September, 1958)

An optical nuclear model is investigated in which the nucleus is described by a complex potential with a fall-off given by a third-degree polynomial. Model parameters have been found which yield the best agreement between the theoretical cross sections σ_t, σ_r, and σ_s and the corresponding experimental values for 14-Mev neutrons. For nuclei heavier than chromium the agreement is quite satisfactory. The angular distributions of elastically scattered neutrons computed with these parameters are also in satisfactory agreement with experiment. A preliminary study of the low-energy region indicates that the parameters depend weakly on the energy over a comparatively wide range.

At present, the most convenient model for the description of the interaction between nucleons and nuclei over a wide energy range is the optical model, in which the nucleus is described by a complex potential. The square-well potential, investigated by Feshbach, Porter, and Weisskopf[1] for the case of neutron scattering, leads at least to qualitative agreement between theory and experiment. However, it cannot reconcile simultaneously the total neutron cross sections, the reaction cross sections, and the elastic scattering cross sections (the reaction cross sections come out too low).[2,3] In this connection Nemirovskii, and thereafter several other authors, were led to use a model with diffuse boundary, which had some definite success. To this time, however, the choice of the form of the potential and the values of its parameters, as well as the limits of applicability of the optical model, cannot be regarded as definitely established. Nemirovskii[4] considers mainly the optical model with diffuse boundary in the region of small neutron energies. The most recent of the papers published on this model (Beyster, Walt, and Salmi[5]) treats various energies up to 14 Mev. However, these authors base their choice of parameters on insufficiently complete experimental data (only for four nuclei).

In this paper we use a very simple diffuse boundary potential different from all previous ones. It satisfies the condition of smoothness. The boundary region of the potential is described by a third-degree polynomial. Our aim is to find the parameters, independent of the mass number, for which the proposed model gives the best fit to the experimental data on the total cross sections σ_t, the reaction cross sections σ_r, and the ratios between the scattering cross sections σ_s and the reaction cross sections for neutrons of energy $E_n = 14$ Mev.[6-9]

1. SOLUTION OF THE SCATTERING PROBLEM

We investigate the nuclear potential of form:

$$U(r) = V(r) + iW(r) = -U_0(1 + i\zeta) f(r), \qquad (1)$$

where

$$f(r) = \begin{cases} 1, & r \leqslant R - d \qquad (\mathrm{I}) \\ 1 + (r - R - 2d)(r - R + d)^2/4d^3, & R - d \leqslant r \leqslant R + d \qquad (\mathrm{II}) \\ 0, & r \geqslant R + d \qquad (\mathrm{III}) \end{cases}$$

(see Fig. 1).

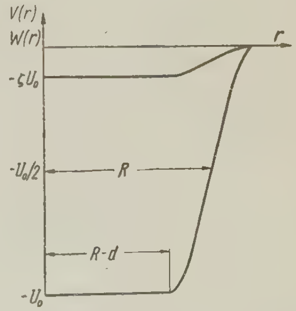

FIG. 1. Shape of the nuclear potential.

The equation for the radial part $u(r)$ of the wave function is solved analytically in regions I and III and numerically in region II. In the computation it is expedient to introduce the dimensionless independent variable $x_0 = k_0 r$ $(k_0 = \sqrt{2MU_0/\hbar^2})$. We also lower the order of the equation by going over to the logarithmic derivative. We separate the real and imaginary parts of the equation. After these transformations we obtain the following system of first order equations with real coefficients:

$$v_1' = v_2^2 - v_1^2 - a^2 + l(l+1)x^{-2} - f(x), \quad v_2' = -2v_1v_2 - \zeta f(x), \tag{2}$$

where

$$v_1 = \mathrm{Re}(u'/u), \; v_2 = \mathrm{Im}(u'/u), \; a^2 = E_n/U_0.$$

Knowing, at the point $x_2 = k_0(R + d)$, the solution of the system (2) satisfying the boundary conditions at the point $x_1 = k_0(R - d)$ obtained by the formulas of reference 1, we can calculate the amplitudes of the scattered waves η_l.* Using the recurrence relations for the Hankel functions of half odd-integer order, we obtain the following working formulas for the amplitudes η_l:

$$\begin{gathered}\mathrm{Re}\,\eta_l = \frac{D^2 - A^2 + B^2 - C^2}{(A+D)^2 + (B-C)^2}, \quad \mathrm{Im}\,\eta_l = \frac{2(AB + CD)}{(A+D)^2 + (B-C)^2}, \\ A = a\alpha_l - v_1(x_2)\gamma_l, \; B = a\beta_l - v_1(x_2)\delta_l, \; C = v_2(x_2)\gamma_l, \; D = v_2(x_2)\delta_l.\end{gathered} \tag{3}$$

Here the quantities α_l, β_l, γ_l, δ_l are computed by the recurrence formulas

$$\begin{gathered}\gamma_{-1} = \cos x, \; \gamma_0 = \sin y, \; \gamma_i = \frac{2i-1}{y}\gamma_{i-1} - \gamma_{i-2} \, (i = 1, 2, \ldots l), \\ \delta_{-1} = \sin y, \; \delta_0 = -\cos y, \; \delta_i = \frac{2i-1}{y}\delta_{i-1} - \delta_{l-2} \, (i = 1, 2, \ldots l), \\ \alpha_l = \gamma_{l-1} - l\gamma_l/y, \; \beta_l = \delta_{l-1} - l\delta_l/y,\end{gathered} \tag{4}$$

where $y = ax_2$.

The solution of the system (2) for many values of the parameters is quite laborious. These calculations can successfully be carried out only with the help of a high-speed computing machine. We used the "Strela" computer of Moscow State University. The whole computational procedure to obtain η_l as well as the cross sections was completely automatic. The numerical solution of system (2) was obtained by the Runge-Kutta method with automatic selection of the step. The constants determining the accuracy were chosen such that the amplitudes η_l were guaranteed to be correct within four places after the decimal. In the cross section formulas l was summed from 0 to l_0, where l_0 was automatically chosen by the machine from the condition

$$\max\{(1 - \mathrm{Re}\,\eta_{l_0}), |\mathrm{Im}\,\eta_{l_0}|\} \leqslant 10^{-4}.$$

It appeared that l_0 varies from 4 or 5 to 12 or 13, depending on the nuclear radius and on the neutron energy. As should be expected, l_0 increases with the nuclear radius and with the neutron energy. As a check, all results were computed twice.

2. METHOD OF SELECTION OF THE PARAMETERS

Our model contains four independent parameters U_0, ζ, d, and R. The simultaneous variation of all these parameters is a very complicated task. Therefore, in the first step, we fixed the parameter of the depth of the potential at $U_0 = 42$ Mev. The chief justification for this is the U_0-R ambiguity,[1,5] which, apparently, is independent of the form of the fall-off of the potential (the change in the quantity U_0 within reasonable limits can be compensated for by a corresponding change in R, such as to leave the cross sections essentially the same).

The nuclear radius is given by the formula $R = (r_0A^{1/3} + \delta) \times 10^{-13}$ cm.[5] The theoretical cross sections were computed for eight values of R ($10^{13}R = 3.75$, 4.05, 4.99, 5.39, 6.14, 6.63, 7.42, 8.01 cm) and various d and ζ. Thus it was possible to establish the dependence of $\sigma_t^{\text{theoret}}$ and $\sigma_r^{\text{theoret}}$ on the parameter d with various values ζ for each R. The cross section depends strongly on d: $\sigma_t^{\text{theoret}}$ and $\sigma_r^{\text{theoret}}$ increase with increasing d, where the rate of increase becomes faster as we go to heavier nuclei. In an analogous way the dependence of the cross sections on ζ for fixed values of the diffuseness parameter d was found. The reaction cross section increases, of course, with ζ. It is zero for $\zeta = 0$ and reaches an upper limit for sufficiently large ζ. A characteristic feature is the weak dependence of $\sigma_t^{\text{theoret}}$ on ζ for fixed d: the total cross sections increase slowly with increasing ζ for some values R, and decrease slightly for others.

The method used for the selection of the parameters was the following. For a given pair of values r_0 and δ ($1 \leq r_0 \leq 1.5$) each of the eight values of R was set in correspondence, by formula (5), to a definite value A, and hence, to a definite pair

---

*The quantities η_l are connected with cross sections by the well-known relations:

$$\sigma_t = 2\pi\lambda\!\!\!^{-2} \sum_{l=0}^{\infty} (2l+1)(1 - \mathrm{Re}\,\eta_l), \quad \sigma_r = \pi\lambda\!\!\!^{-2} \sum_{l=0}^{\infty} (2l+1)(1 - |\eta_l|^2).$$

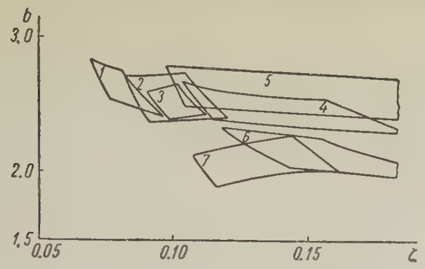

FIG. 2. Determination of the parameters $b = k_0 d$ and ζ for the given values $U_0 = 42$ Mev; $r_0 = 1.25$. $\delta = 0.42$ (the labels 1, 2, . . ., 7 refer, respectively, to $A = 220, 173, 121, 62, 19, 47, 24$).

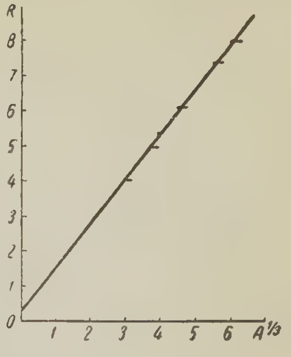

FIG. 3. Determination of the parameters r_0 and δ for fixed values $U_0 = 42$ Mev, $b = 2.5$, $\zeta = 0.12$.

of experimental cross sections $\sigma_t \pm \Delta\sigma_t$ and $\sigma_r \pm \Delta\sigma_r$ ($\Delta\sigma$ is the experimental error). In cases where there were no measurements, the cross sections were found by interpolation. This is possible on account of the sufficiently smooth change of the cross sections when going from one nucleus to the other, and the great number of nuclei investigated experimentally, particularly with respect to the total cross sections (54 nuclei in the region $2.08 \leq A^{1/3} \leq 6.2$). With the help of the curves representing the dependence of the cross sections on the parameters, figures (we call them "quadrangles") are then constructed in the ζd plane which define the region of values of the parameters d and ζ for which $\sigma_t^{\text{theoret}}$ and $\sigma_r^{\text{theoret}}$ agree with the experimental data within the limits of error. In order to fit the experimental data for the greatest possible number of nuclei by one and the same parameters, r_0 and δ have to be varied in this procedure until maximal closeness of the "quadrangles" is reached (see Fig. 2). In this case the common "center of gravity" of the "quadrangles" determines the required values of the parameters. During this operation a certain ambiguity was noted: several different sets of parameters r_0, δ, d, and ζ (d and ζ are restricted to a certain definite region) gave satisfactory agreement between the computed cross sections and the experimental data. A different method was used to choose the best among these sets of parameters. For given values of d and ζ in the above-mentioned region the dependence of R on $A^{1/3}$ was established. d and ζ were now fixed already in each single case, while r_0 and δ were to be determined. The given values R, d, and ζ determine the values of $\sigma_t^{\text{theoret}}$ and $\sigma_r^{\text{theoret}}$. Using, for example, the experimental curves for the total cross section, we determined the region of values of $A^{1/3}$ which correspond to a theoretical cross section such that $\sigma_t^{\text{theoret}} = \sigma_t^{\text{exptl}}$ within the experimental errors. The corresponding curve is represented in Fig. 3. Taking into account the weak dependence of $\sigma_t^{\text{theoret}}$ on ζ, we first chose the best d, based on the requirement that there be agreement between theoretical and experimental cross sections within the limits of error for the greatest possible number of values of R considered, i.e., that the short lines in the diagram $R = R(A^{1/3})$ lie on a straight line. The parameters of this straight line, determine, of course, the parameters r_0 and δ. The final choice of the parameter ζ was made by comparing the theoretical results using the obtained values of the parametrs d, r_0, and δ and various different values of ζ, with the experimental values of σ_r and $\sigma_0 = \sigma_t/\sigma_r - 1 = \sigma_s/\sigma_r$.

3. RESULTS AND DISCUSSION

The following parameter values were adopted as the best values as a result of this analysis:

$$U_0 = 42 \text{ Mev}, \; b = k_0 d = 2.5; \; \zeta = 0.12; \; r_0 = 1.27; \; \delta = 0.3 \tag{A}$$

However, after the cross sections for a great number of nuclei were calculated with these parameters, it appeared that better agreement with experiment could be achieved with

$$r_0 = 1.25, \; \delta = 0.4 \tag{B}$$

The comparison of the theoretical cross sections σ_t, σ_r, and σ_0 with the experimental results is shown in Figs. 4 and 5. The agreement is fully satisfactory for all intermediate and heavy nuclei, starting from chromium. The curve for $\sigma_0(A^{1/3})$ lies above the experimental values in the region of light nuclei. It could be lowered by increasing ζ, but this destroys the agreement for heavy nuclei. This discrepancy between theory and experiment for nuclei lighter than chromium may be connected with the dependence of the parameters on A in the region of light nuclei, or with the principal inapplicability of the proposed model in this region. This point requires special study.

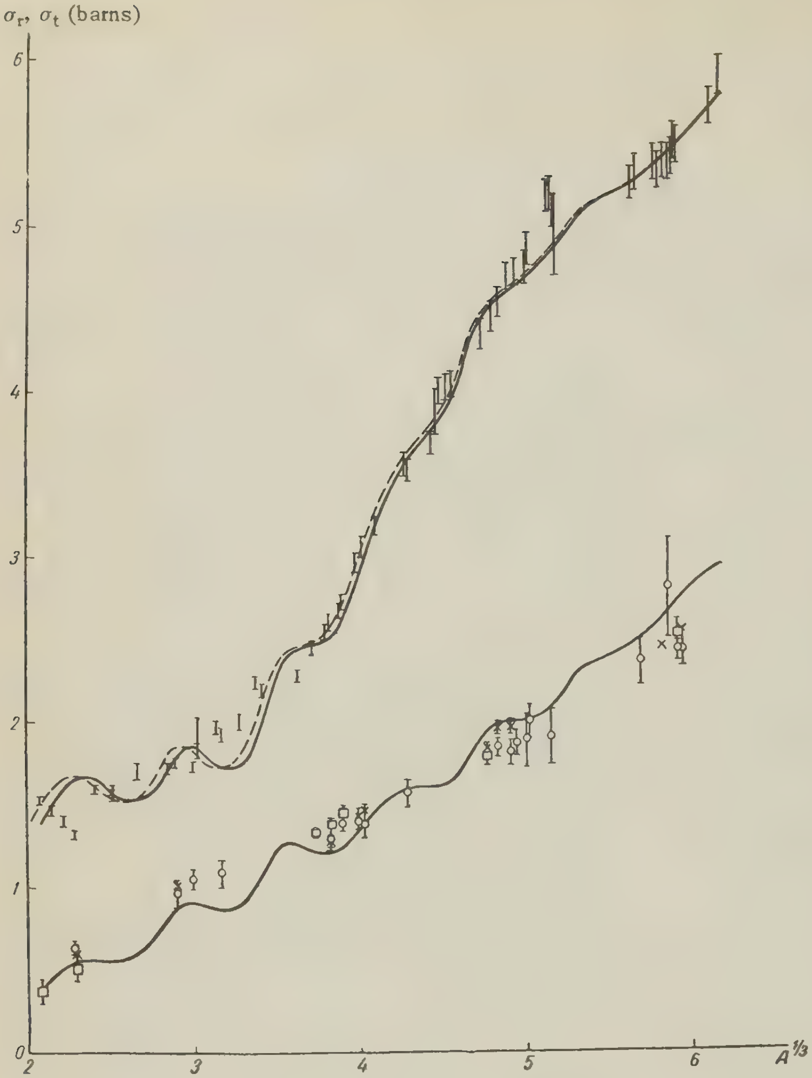

FIG. 4. Comparison of the theoretical and the experimental dependence of the cross section σ_t (upper curves) and σ_r (lower curve) on the mass number. Solid curve: theoretical cross sections computed with the parameter values (A); dotted curve: theoretical cross sections computed with the parameter values (B). Short lines: experimental data of reference 6; circles: reference 7; squares: reference 8; crosses: reference 9.

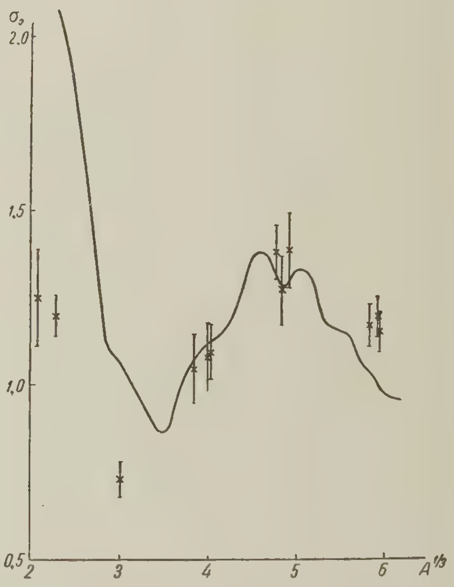

FIG. 5. Comparison of the theoretical and experimental[9] ratios between the scattering and reaction cross sections as a function of mass number (parameter A).

With the set of parameters (A) we calculated the differential cross sections for neutrons scattered elastically from the nuclei Al, S, Fe, Cu, In, Sn, Ta, Pb, and Bi ($E_n = 14.1$ Mev), and Mg, Ca, Cd, and Bi ($E_n = 14.6$ Mev) (see Fig. 6), for which the corresponding experimental data exist.[10,11] Although the parameters were chosen by studying only the values of σ_t, σ_r, and σ_0, the agreement between the angular distributions of the elastically scattered neutrons with the experimental data is not bad on the whole. The first maximum and the position of the maxima and minima are fitted rather well. For not too large angles the height of the maxima agrees well with experiment. The greatest discrepancey between theory and experiment shows up in the size of the minima, which are much deeper than the experimental data. This is independent of the character of the fall-off of the potential, since this occurs also for potentials of different type (see, for example, reference 5).

It is possible that there exist parameter values which yield an even better agreement between the differential cross sections and the experimental data without worsening the agreement for σ_t, σ_r, and σ_0 appreciably. The answer to this question requires a further careful analysis of the dependence of the theoretical differential cross sections on the model parameters. However, radical improvements can hardly be expected. In particular, the appearance of very deep minima in the theoretical angular distributions can apparently not be avoided. The same picture emerges for the most distinct values of d and ζ. Changing r_0 and δ also makes little difference. The dependence of the differential cross sections on $A^{1/3}$ was computed from 0° to 130° in steps of 10°, with $b = 2.3$ and $\zeta = 0.125$. The corresponding curves have, starting from 30°, deep and wide minima, while changes in r_0 and δ reduce the depth of the minimum for one nucleus, and increase it for another.

4. OTHER ENERGIES

The reasons for choosing the experimental cross sections for neutrons with energy $E_n = 14$ Mev as the basic data for the determination of the model parameters are, firstly, the great amount of published experimental material, and, secondly, the circumstance that, at this energy, one can neglect the compound elastic scattering cross section[1] and compare the experimental cross sections for elastic scattering and reactions with the theoretical values immediately. Taking d, r_0, and δ to be energy-independent parameters, we made several calculations for smaller energies. The comparison of the calculated cross sections with the experimental data[5,6] gives the possibility of determining the dependence of the parameters U_0 and ξ on the energy. Preliminary results indicate that the parameters U_0 and ξ stay practically the same when the neutron energy is lowered to ~7 Mev. The parameter ξ becomes smaller, while the parameter U_0 increases slowly. For 3.5 Mev, ξ decreases by ~30%, and U_0 increases by ~5%, as compared to their values at the energy 14 Mev. As in reference 5, the model parameters U_0 and ξ depend weakly on energy over a rather wide energy range.

The present investigation of the optical model shows that a great amount of experimental data on the scattering of neutrons from nuclei can be described by the model of a complex potential with a fall-off given by a very simple function.

In conclusion we take occasion to express our deep gratitude to Prof. I. S. Shapiro for suggesting the topic and interest in this work, and to Prof. A. N. Tikhonov, under whose guidance the numerical part of this work was carried out. The authors also thank G. A. Samoilova for her great help and initiative in the programming and in the treatment of the results of the computations.

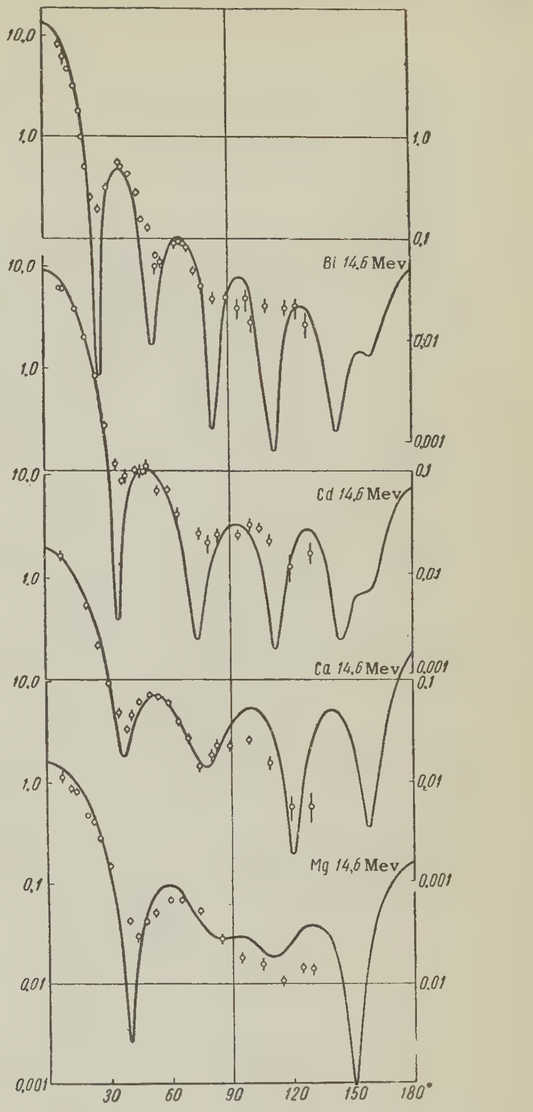

FIG. 6. Comparison of the theoretical angular distribution of the elastically scattered neutrons with the experimental data.[11] Abscissa: angle in dregees; ordinate: differential cross section in barns/sterad in logarithmic scale.

Translated by R. Lipperheide
147

---

[1] Feshbach, Porter, and Weisskopf, Phys. Rev. **96**, 448 (1954).

[2] Kawai, Ui, and Nagasaki, Progr. Theoret. Phys. **14**, 263 (1955).

[3] M. Walt and J. R. Beyster, Phys. Rev. **98**, 677 (1955).

[4] P. E. Nemirovskii, Reports of the Soviet Delegation to the International Conference on the Peaceful Use of Atomic Energy, Geneva, 1955, M., 1955, p. 287. J. Exptl. Theoret. Phys. (U.S.S.R.) 32, 1143 (1957); Soviet Phys. JETP **5**, 932 (1957).

[5] Beyster, Walt, and Salmi, Phys. Rev. **104**, 1319 (1956).

[6] Coon, Graves, and Barschall, Phys. Rev. **88**, 562 (1952).

[7] V. I. Strizhak, Атомная энергия (Atomic Energy) **2**, 68 (1957).

[8] Taylor, Loensjoe, and Bonner, Phys. Rev. **100**, 174 (1955).

[9] E. R. Graves and R. W. Davis, Phys. Rev. **97**, 1205 (1955).

[10] J. O. Elliot, Phys. Rev. **101**, 684 (1956).

[11] Culler, Fernbach, and Sherman, Phys. Rev. **101**, 1047 (1956).

SOVIET PHYSICS JETP VOLUME 35(8), NUMBER 3 MARCH, 1959

ON THE Λ-HYPERON CREATION CROSS SECTION NEAR THE Σ-HYPERON CREATION THRESHOLD

A. N. BAZ' and L. B. OKUN'

Submitted to JETP editor April 17, 1958

J. Exptl. Theoret. Phys. (U.S.S.R.) 35, 757-761 (September, 1958)

A singularity arises in the cross section of the $\pi^- + p \rightarrow K^0 + \Lambda^0$ reaction near the threshold of the $\pi^- + p \rightarrow K^0 + \Sigma^0$ reaction. An experimental study of this singularity affords a check on the validity of various models used to explain interactions between strange particles. The relative parity of the Λ and Σ hyperons can also be determined.

THE energy and angular dependences of elastic scattering of particles near the threshold of some inelastic process were investigated in many works (cf., e.g., references 1 and 2). It has been shown that a measurement of this dependence can yield information on the elastic-scattering phase shifts and on the spin and parity of particles created in the inelastic process. As will be shown below, analogous information can be obtained also by investigating the energy and angle dependences of one inelastic process near the threshold of another inelastic process. Such an analysis may prove particularly useful in the study of strange particles.

By way of an example, we examine the creation of strange particles through collisions between protons and π^- mesons with energies close to $E_0 = 890$ Mev. This energy is the threshold for the reaction*

$$\pi^- + p \rightarrow K^0 + \Sigma^0. \qquad (1)$$

Along with reaction (1), there occur also: (a) elastic scattering of π mesons, (b) processes involving creation of 2, 3, 4, and 5π mesons, and (c) creation of Λ hyperons in a reaction

$$\pi^- + p \rightarrow K^0 + \Lambda^0, \qquad (2)$$

whose threshold is 760 Mev. We shall investigate the cross section of reaction (2) near the threshold of reaction (1).

We shall assume henceforth that the K-meson spin is 0, and that the spins of the Λ and Σ hyperons is ½. We examine both possible values of the relative parity of the Λ and Σ hyperons.

It is quite clear that in the study of threshold effects it is enough to consider only those partial channels of reactions (1), (2a) and (2b) with identical total momenta, parities, and isotopic spins. Since reaction (1) is at the threshold, $\Sigma^0 + K^0$ are created in the S state, and the total momentum j is ½. The orbital momentum of $\Lambda^0 + K^0$ will at the same time be either 0 or to 1 in the channel of interest to us, depending on the relative parity of the Λ and Σ hyperons. Since reaction (2) proceeds only via a state with isotopic spin $T = \frac{1}{2}$, only this state will interest us in cases (a) and (b) of reaction (1).

We write the total S matrix of the channel with $j = \frac{1}{2}$ and $T = \frac{1}{2}$ and a given parity in the following form

$$S = \left| \begin{array}{ccccc} S_{11} & S_{12} \ldots & & S_{1N} & m_1 k^{1/2} \\ S_{21} & S_{22} \ldots & & S_{2N} & m_2 k^{1/2}. \\ \ldots & \ldots & \ldots & \ldots & \ldots \\ S_{N1} & S_{N2} \ldots & & S_{NN} & m_N k^{1/2} \\ m_1 k^{1/2} & m_2 k^{1/2} \ldots & & m_N k^{1/2} & x \end{array} \right|, \qquad (3)$$

where the matrix element at the intersection of the i-th column and j-th line is the transition from the j-th channel into the i-th one. We shall number the channels as follows: i = 1 corresponds to the $\pi^- + p$ pair; i = 2 corresponds to the $\Lambda^0 + K^0$ pair, and i = 3, 4, . . . , N corresponds to different states with several π mesons. Finally, the last channel (N + 1) corresponds to the $\Sigma^0 + K^0$ pair. The quantities $m_i k^{1/2}$ in the last column represent the amplitudes of creation of $\Sigma_0 + K^0$ in various channels. As a consequence of the symmetry of the S matrix, they equal the inverse processes listed in the lowest row.

We know that near the creation threshold of two neutral particles (in our case $\Sigma^0 + K^0$) their creation amplitudes are proportional to $k^{1/2}$ (k is the wave vector of the created particles, k =

---

*The existence of a reaction $\pi^- + p \rightarrow K + \Sigma^-$ the threshold of which should be several Mev below that of reaction (1), will barely affect the formulas derived below, since Coulomb attraction exists between the particles created in this reaction (see references 1 and 3 on this subject).

$\sqrt{2\mu(e-e_0)}$. We can therefore assume the m_i in (3) to be independent of the energy. The matrix element x describes elastic scattering of the K^0 meson by the Σ^0 hyperon; $x \to 1$ as $k \to 0$. The remaining matrix element can be rewritten

$$S_{ik} = s_{ik} + a_{ik} k + \ldots, \tag{4}$$

where s_{ik} is the value of S_{ik} at the threshold and a_{ik} are certain coefficients which will now be determined. The matrix S is unitary ($SS^+ = 1$) and symmetrical ($S = \tilde{S}$). Above the threshold this leads to the following relations between the matrix elements:

$$\sum_{l=1}^{N} (s_{il} a_{jl}^* + s_{jl}^* a_{il}) = -m_i m_j^*, \qquad \sum_{l=1}^{N} s_{il}^* m_l = -m_i^* x. \tag{5}$$

Below the threshold the channel $\Sigma^0 + K^0$ is closed, and the matrix S is reduced in rank from (N + 1) to N. In addition, the wave vector in (4) now becomes imaginary. Taking this into account we can readily obtain

$$\sum_{l=1}^{N} (-s_{il} a_{jl}^* + s_{jl}^* a_{il}) = 0. \tag{6}$$

Using (5), (6), and the condition $\sum_{l=1}^{N} s_{il} s_{kl}^* = \delta_{ik}$, which follows from the unitarity of the S matrix at the threshold, we obtain

$$a_{ik} = {}^1\!/_2\, m_i m_k, \tag{7}$$

where we took it into account that $x \to 1$ when $k \to 0$.

Having determined the energy dependence of the S matrix, we can now ascertain how reaction (2) behaves near E_0, which is the threshold of reaction (1).

The cross section for the creation of $\Lambda^0 + K^0$ is (in the c.m. system)

$$\sigma_\Lambda(\theta, E) = |g(\theta, E)|^2 + |h(\theta, E)|^2,$$

and the polarization of the Λ^0 hyperons is given by

$$P_\Lambda(\theta, E) = 2 \operatorname{Im} h(\theta, E)\, g^*(\theta, E) / \sigma_\Lambda(\theta, E),$$

where the amplitudes g and h are determined, as usual, by

$$g(\theta, E) = \frac{1}{2ik_1} \sum_l [(l+1) M_l^{l+1/2} + l M_l^{l-1/2}]\, P_l(\theta),$$

$$h(\theta, E) = \frac{1}{2ik_1} \sum_l [M_l^{l+1/2} - M_l^{l-1/2}]\, P_l^{(1)}(\theta). \tag{8}$$

Here k_1 is the wave vector of the colliding $p + \pi^-$, m_l^j the matrix element that describes the creation of $\Lambda^0 + K^0$ in a state with a total momentum j and an orbital momentum l, P_l and $P_l^{(1)}$ the ordinary and adjoint Legendre polynomials, θ the angle of emission of the Λ^0 hyperon, and E the total energy of the system.

Near the threshold of the $\Sigma^0 + K^0$ creation, as follows from formulas (5) and (7), all the elements M_l^j are independent of the energy, with the exception of the one characterized by the same quantum numbers as the state of $\Sigma_0 + K^0$. This last element is of the form

$$M_l^{1/2}(E) = M_l^{1/2}(E_0) + {}^1\!/_2\, m_1 m_2 k. \tag{9}$$

We can thus calculate the energy dependence of the cross section and of the polarization of reaction (2) near E_0, assuming that the entire dependence is contained in the matrix element (9).

If the Σ hyperon has the same parity as the Λ hyperon, then $l = 0$ in formula (9) and we obtain from (8)

$$g(\theta, E) = g(\theta) + \alpha k / 2ik_1, \quad h(\theta, E) = h(\theta), \quad \alpha = m_1 m_2 / 2.$$

Hereinafter $\varphi(\theta) \equiv (\theta, E = E_0)$, where φ is any quantity.

The cross section of reaction (2) and the polarization of the Λ hyperons are:

$$\sigma(\theta, E) = \sigma(\theta) + \frac{|k|}{k_1} \begin{cases} -\operatorname{Im} g(\theta)\alpha^* & E > E_0 \\ \operatorname{Re} g(\theta)\alpha^* & E < E_0 \end{cases},$$

$$P(\theta, E) = P(\theta) + \frac{|k|}{k_1} \begin{cases} \operatorname{Re} f(\theta)\alpha^* & E > E_0 \\ \operatorname{Im} f(\theta)\alpha^* & E < E_0 \end{cases}, \tag{10}$$

where $f(\theta) = (h(\theta) - iP(\theta) g(\theta)) / \sigma(\theta)$.

If the parity of the Σ hyperon opposes that of the Λ hyperon, we have $l = 1$ in formula (9) and

$$g(\theta, E) = g(\theta) + \frac{\alpha \cos\theta}{2ik_1} k, \quad h(\theta, E) = h(\theta) + \frac{\alpha \sin\theta}{2ik_1} k,$$

$$\sigma(\theta, E) = \sigma(\theta) + \frac{|k|}{k_1} \begin{cases} -\operatorname{Im} l(\theta)\alpha^* & E > E_0 \\ \operatorname{Re} l(\theta)\alpha^* & E < E_0 \end{cases}, \tag{11}$$

$$P(\theta, E) = P(\theta) + \frac{|k|}{k_1} \begin{cases} \operatorname{Re} f_1(\theta)\alpha^* & E > E_0 \\ \operatorname{Im} f_1(\theta)\alpha^* & E < E_0 \end{cases}$$

We have used here the following notation:

$$f_1(\theta) = (m(\theta) - iP(\theta)\, l(\theta)) / \sigma(\theta),$$
$$m(\theta) = h(\theta)\cos\theta - g(\theta)\sin\theta, \quad l(\theta) = g(\theta)\cos\theta + h(\theta)\sin\theta.$$

It is seen from (10) and (11) that near E_0 the cross section and the polarization are linear functions of $|k| \sim |E - E_0|^{1/2}$, and are singular near the threshold as functions of energy. The singularity may be a peak, a dip, or a step (for more details see references 1 to 3). On the basis of rather reasonable estimates we can expect the energy width of such a singularity to be on the order of $|k| \gtrsim \mu_\pi$. This singularity is proportional to $\alpha = m_1 m_2/2$, where m_2 is by definition the amplitude of the following reaction

$$K + \Lambda \rightarrow K + \Sigma \tag{12}$$

divided by $\sqrt{k}$. Consequently the greater the probability of reaction (12), the larger the singularity in the reaction (2) near E_0.

What can be predicted, on the basis of existing model representations of the interactions of strange particles, as regards the cross section of reaction (12) and, consequently, as regards the size of the singularity in reaction (2)^2?

In the model proposed by Gell-Mann,[4] π mesons interact strongly with baryons and moderately with K mesons. The amplitude of reaction (12), $m_2 k^{1/2}$, will be less in this model than the amplitude of reaction (1), $m_1 k^{1/2}$, since reaction (1) contains only one moderate interaction, while reaction (12) contains two, absorption and K-meson emission. Reaction (2), like reaction (1) contains one moderate interaction and the amplitudes of these reactions are apparently of the same order of magnitude. Using the language of perturbation theory, we can say that the quantity $\sigma(\theta)$ in formulas (10) and (11) is proportional to g^2, while the terms describing the singularity are proportional to g^4, where g is the constant of the moderate interaction. One can therefore expect on the basis of Gell-Mann's theory that the singularity of reaction (2) will be small in the vicinity of E_0.

An entirely different result is obtained by using the model considered by one of the authors.[5] According to this second model the creation of strange particles by collision between ordinary particles is due to the moderate interaction, while transitions of type (12) are due to the strong interaction. Consequently, within the framework of the second model, $m_2 > m_1$, the terms describing the singularity, like the cross section itself, are proportional to g^2, and the singularity in the cross section of reaction (2) would therefore be expected to be comparable with the value of the cross section of this reaction itself.

Thus, if the singularities predicted by formulas (10) or (11) are observed in the cross section for the creation of Λ hyperons and in their polarization, this would serve as an argument in favor of the second model.

It follows from formulas (10) and (11) that, by investigating reaction (2) near the threshold of reaction (1), it is possible to determine the relative parity of the Λ and Σ hyperons.* We shall demonstrate this by assuming, for the sake of being definite, that only S and P waves participate in reaction (2). This means that the amplitudes g and h do not contain higher powers of $\cos\theta$ and $\sin\theta$ than the first. On the other hand, it is seen from (10) and (11) that the angular distribution of the singularity in the cross section is determined by the value of $g(\theta)$ if the Λ and Σ hyperons have the same parity, and by the quantity $g(\theta)\cos\theta + h(\theta)\sin\theta$ if the parities are opposite. The first quantity does not contain $\cos^2\theta$ but the second does contain it. Therefore, by measuring experimentally the angular distribution of the singularity in reaction (2) and then expanding it in powers of $\cos\theta$, it is possible to determine the relative parity of the Λ and Σ hyperons. Similar reasoning can be applied if D waves also participate in the reaction along with the S and P waves. The actual number of partial waves in reaction (2) can be determined from the angular distribution of this reaction.

It also follows from formulas (10) and (11) that with sufficiently accurate measurements it is possible to find (with accuracy to within a common phase factor) the amplitudes $g(\theta)$ and $h(\theta)$. The possibility of total determination of the amplitudes $g(\theta)$ and $h(\theta)$ becomes evident from a count of the number of equations obtained for these amplitudes from experiment, comparing it with the number of unknown parameters in $g(\theta)$ and $h(\theta)$ (see reference 2). It must be noted that at present there is no other method whatever for the determination of the amplitudes $g(\theta)$ and $h(\theta)$, since it is essential to know, for an ordinary phase-shift analysis of reaction (2), not only the cross section and polarization in this reaction, but also in all other reactions occurring during $\pi^- + p$ collisions at this energy.

The above argument can be extended to include other cases of strange-particle creation. In particular, it would be interesting to investigate the reactions $\bar{K} + p \rightarrow \Lambda(\Sigma) + \pi$ near the threshold of creation of a cascade hyperon $\bar{K} + p \rightarrow \Xi + K$.

---

*Professors Flowers and Chinovskii have communicated to the authors that the possibility of determining the relative parity of Λ and Σ hyperons by investigating reaction (2) near the threshold of reaction (1) has been indicated by Adair.

[1] E. P. Wigner, Phys. Rev. **73**, 1002 (1948).

[2] A. N. Baz', J. Exptl. Theoret. Phys. (U.S.S.R.) **33**, 923 (1957), Soviet Phys. JETP **6**, 709 (1958).

[3] G. Breit, Phys. Rev. **107**, 1612 (1957).

[4] M. Gell-Mann, Phys. Rev. **106**, 1296 (1957).

[5] L. B. Okun', J. Exptl. Theoret. Phys. (U.S.S.R.) **34**, 469 (1958), Soviet Phys. JETP **7**, 322 (1958).

Translated by J. G. Adashko
148

SOVIET PHYSICS JETP VOLUME 35(8), NUMBER 3 MARCH, 1959

STATIONARY RELATIVISTIC MOTIONS OF A GAS IN A CONDUCTING MEDIUM

K. P. STANIUKOVICH

Bauman Moscow Technical College

Submitted to JETP editor April 19, 1958

J. Exptl. Theoret. Phys. (U.S.S.R.) 35, 762-765 (September, 1958)

Quasi-unidimensional relativistic stationary flow of a gas is considered in a medium with infinite conductivity and with a magnetic field perpendicular to the velocity. Particular attention is devoted to cylindrically symmetric flow. We calculate the total momentum which an expanding gas can acquire per unit time (equal to the "reactive" force), both with a field and without it. This calculation is performed, in particular, for escape of an ultrarelativistic gas.

CONSIDER the quasi-unidimensional stationary flow of a gas in a magnetic field, assuming the conductivity to be infinite.

By quasi-unidimensional flow we mean a flow with a smoothly varying cross section containing given flow lines. In particular, we shall treat the cylindrically symmetric case.

The basic equations, assuming adiabatic flow, are[1]

$$w^*/\theta = w_0^* = \text{const}; \tag{1}$$

$$\Delta s a/\theta V = \Delta\dot{M} = \text{const}, \tag{2}$$

$$\theta = (1 - a^2/c^2)^{1/2}; \quad w^* = pV + \rho V c^2 + \mu H^2 V/4\pi,$$

where a is the velocity, w_0^* is the rest heat content, p is the pressure, V is the specific volume, ρ is the density of the medium (including the microscopic energy), H is the magnetic field strength (we consider H to be perpendicular to a) which, for infinite conductivity, is related to the specific volume by the expression

$$HV = b = \text{const}; \tag{3}$$

and $\Delta\dot{M}$ is the amount of mass crossing the area Δs per unit time. (The area Δs is a function of r.)

For cylindrical symmetry, we have

$$s = 2\pi r; \quad \dot{M} = 2\pi r a/\theta V; \ HV = br. \tag{4}$$

If there is no field, we can assume point symmetry, and then

$$\rho = 4\pi r^2; \quad \dot{M} = 4\pi r^2 a/\theta V.$$

In general,

$$\Delta\dot{M}/\Delta s = f(r). \tag{5}$$

The energy equation for adiabatic flow gives σ = const (where σ is the entropy), or isoentropic flow.

Let us now write Eqs. (1) and (2) in the form

$$(pV + \rho V c^2 + b_0/V)/\theta = p_0 V_0 + \rho_0 V_0 c^2 + b_0/V_0 = w_0; \qquad \Delta\dot{M} = a\Delta s/\theta V, \tag{6}$$

where $b_0 = \mu b^2/4\pi$.

If the equation of state of a gas

$$pV = RT, \tag{7}$$

(where T is the temperature) and the constant-entropy equation

$$pV^k = A = \text{const}, \tag{8}$$

are satisfied, then

$$w = pV + \rho V c^2 = \alpha c^2 + kpV/(k-1), \tag{9}$$

where

$$\alpha = \rho_a V_a - p_a V_a/(k-1)c^2; \quad w^* = w + b_0/V.$$

For an ordinary gas $\alpha = 1$, while for an ultrarelativistic gas $\alpha = 0$, and

$$pV = RT = (k-1)\rho V c^2. \tag{10}$$

The first equation of (6) then becomes

$$\alpha c^2 + \frac{k}{k-1} A V^{1-k} + \frac{b_0}{V} = w_0\theta, \tag{11}$$

thus relating V and a. Further, from the second equation of (6) we have

$$(a/V)\Delta s = \theta\Delta\dot{M}. \tag{12}$$

Relations (11) and (12) lead to equations which can be used to find a and V as functions of r. These are

$$\alpha c^2 + \frac{kA}{k-1}\left(\frac{\theta\Delta\dot{M}}{a\Delta s}\right)^{k-1} + b_0\frac{\theta\Delta\dot{M}}{a\Delta s} = \theta w_0; \tag{13}$$

$$\left(\alpha c^2 + \frac{kA}{k-1}V^{1-k} + \frac{b_0}{V}\right)^2\left[1 + \frac{V^2(\Delta\dot{M})^2}{c^2(\Delta s)^2}\right] = w_0^2. \tag{14}$$

In the cylindrically symmetric case $\Delta\dot{M}/\Delta s = \dot{M}/2\pi r$. Using this, it is a simple matter to find $a(r)$ and $V(r)$ both for an ordinary gas with high energy and for an ultrarelativistic gas. In the classical limit the cylindrically symmetric flow becomes the same as that given by ordinary gas dynamics.

Since $\Delta s a/V\theta = \Delta\dot{M} = \text{const}$, we have

$$-\frac{d\Delta s}{\Delta s} = -\frac{dV}{V} + \frac{da}{a(1-a^2/c^2)}. \tag{15}$$

Since

$$dw^*/w^* = -(a^2/c^2)\,da/\theta^2 a, \tag{16}$$

Eq. (15) becomes

$$\frac{d\Delta s}{\Delta s} = -\frac{da}{a\theta^2} + \frac{dV}{V} = \frac{dw^*}{w^*}\frac{c^2}{a^2} + \frac{dV}{V}. \tag{17}$$

We also have

$$-(c^2/\omega^{*2})\,dw^*/w^* = dV/V, \tag{18}$$

where

$$\omega^{*2}/c^2 = dp^*/c^2 d\rho^*, \tag{19}$$

and ω^* is the magnetohydrodynamic velocity of sound. Comparing (16), (17), and (18), we arrive at

$$-\frac{d\Delta s}{\Delta s} = \left(1 - \frac{a^2}{\omega^{*2}}\right)\frac{da}{a(1-a^2/c^2)}. \tag{20}$$

At the minimum (critical) cross section, when $d\Delta s = 0$, we have $\omega^* = \pm a$, indicating critical flow in which the velocity of the medium is equal to the velocity of sound.

In the more general case, as in classical gas flow, one can have motion with $a \geq \omega^*$ if $d\Delta s \geq 0$, or motion with $a \leq \omega^*$ if $d\Delta s \leq 0$.

Let us now calculate the momentum that the flow can attain in escaping into a rarefied volume (this is the case with $a \geq \omega^*$ and $d\Delta s \geq 0$).

The time rate of change of momentum (or the reactive force acting on an area Δs) is given by

$$\Delta F = \Delta\dot{J} = \Delta s\left[\frac{a^2}{c^2\theta^2}\left(p + \rho c^2 + \frac{\mu H^2}{4\pi}\right) + p + \frac{\mu H^2}{4\pi}\right]. \tag{21}$$

(In the cylindrical case the total momentum in all directions over a circle vanishes.) Let us write (21) in a different form. Since

$$(p + \rho c^2 + \mu H^2/4\pi)/\theta = w^*/\theta V = \overset{*}{w}_0/V; \quad a\Delta s/\theta V = \Delta\dot{M},$$

we have

$$\Delta s\,(p + \rho c^2 + \mu H^2/4\pi)(a/c^2\theta^2) = \overset{*}{w}_0 a\Delta\dot{M}/c^2;$$

further

$$(p + \mu H^2/8\pi)\,\Delta s = (\Delta\dot{M}\theta/a)(pV + b_0/2V),$$

so that

$$\Delta F = a\Delta\dot{M}\left[\frac{\overset{*}{w}_0}{c^2} + \frac{\theta}{a^2}\left(pV + \frac{b_0}{2V}\right)\right], \tag{22}$$

or

$$\Delta F = \Delta\dot{M}a\left[\alpha + \frac{kAV_0^{1-k}}{(k-1)c^2} + \frac{b_0}{c^2V_0} + \frac{\theta}{a^2}\left(AV^{1-k} + \frac{b_0}{2V}\right)\right]. \tag{23}$$

For the ordinary case we have $\alpha = 1$, and since $\rho_0 V_0 = 1$, we may write

$$\Delta F = \Delta\dot{M}a\left[1 + \frac{kAV_0^{1-k}}{(k-1)c^2} + \frac{b_0V_0^{-1}}{c^2} + \frac{\theta}{a^2}\left(AV^{1-k}(a) + \frac{b_0}{2V(a)}\right)\right]; \tag{24}$$

as $p \rightarrow 0$, we have $V \rightarrow \infty$, $pV = 0$, and

$$\Delta F_\infty = \Delta\dot{M}a_\infty\,[1 + kAV_0^{1-k}/(k-1)c^2 + b_0V_0^{-1}/c^2], \tag{25}$$

where

$$a_\infty = c\,\{1 - [1 + kAV_0^{1-k}/c^2(k-1) + b_0V_0^{-1}/c^2]^{-2}\}^{1/2}; \tag{26}$$

Therefore

$$\Delta F_\infty = \Delta\dot{M}c\,[(1 + kAV_0^{1-k}/(k-1)c^2 + b_0V_0^{-1}/c^2)^2 - 1]^{1/2}. \tag{27}$$

In the classical limit we have

$$\Delta F = \Delta\dot{M}a\,[1 + a^{-2}(AV^{1-k} + b_0/2V)]; \tag{28}$$

$$a = \left[\frac{2kA}{k-1}(\rho_0^{k-1} - \rho^{k-1}) + 2b_0(\rho_0 - \rho)\right]^{1/2}. \tag{29}$$

As $V \rightarrow \infty$,

$$\Delta F_\infty = \Delta\dot{M}a_\infty = \Delta\dot{M}\,[2kp_0/(k-1)\rho_0 + 2b_0\rho_0]^{1/2}. \tag{30}$$

In the ultrarelativistic case with $\alpha = 0$ we have $p_0 = (k-1)\rho_0 c^2$ and

$$\Delta F = \Delta\dot{M}a\,[k\rho_0V_0 + b_0/c^2V_0 + \theta a^{-2}(AV^{1-k} + b_0/2V)]. \tag{31}$$

From Eq. (11) we find that for an ultrarelativistic gas V and a are related by

$$\frac{k}{k-1}AV^{1-k} + \frac{b_0}{V} = \theta\overset{*}{w}_0 = \theta\left[kc^2\rho_0V_0 + \frac{b_0}{V_0}\right]. \tag{32}$$

this gives

$$AV^{1-k} = \frac{k-1}{k}\left[\theta\left(kc^2\rho_0V_0 + \frac{b_0}{V_0}\right) - \frac{b_0}{V}\right],$$

so that

$$\Delta F = \Delta\dot{M}a\left[\left(1 + (k-1)\frac{c^2}{a^2}\right)\left(\rho_0V_0 + \frac{b_0}{kc^2V_0}\right) + \frac{2-k}{2k}\frac{b_0\theta}{a^2V(a)}\right]. \tag{33}$$

Equation (33) is more convenient to write in the form

$$\Delta F = \Delta\dot{M}c\left[\left(\frac{a}{c} + (k-1)\frac{c}{a}\right)\left(\rho_0V_0 + \frac{b_0}{kc^2V_0}\right) + \frac{2-k}{2k}\frac{b_0\theta}{caV(a)}\right]. \tag{34}$$

As $V \rightarrow \infty$ and $a \rightarrow c$,

$$\begin{aligned}\Delta F_{\infty} &= \Delta\dot{M}c\,(k\rho_0 V_0 + b_0 / c^2 V_0)\\ &= \Delta\dot{M}c\,(k\rho_0 V_0 + \mu H_0^2 V_0 / 4\pi c^2).\end{aligned} \tag{35}$$

If there is no field $(b_0 = 0)$,

$$\Delta F = \Delta\dot{M}c\,[a / c + (k - 1)\,c / a]\,\rho_0 V_0. \tag{36}$$

In the limit, $\Delta F_{\infty} = k\Delta\dot{M}c\rho_0 V_0$. If there is no gas $(A = 0$ and $p = 0)$ but there exists only a field, we write (22) in the form

$$\Delta F = \Delta\dot{M}c\left(\frac{\mu H_0^2}{4\pi\rho_0 c^2}\,\frac{a}{c} + \frac{\mu b^2\theta}{8\pi c^2 V}\,\frac{c}{a}\right). \tag{37}$$

Since $(1 - a^2/c^2)^{1/2} = w^*/w_0^* = H^2V/H_0^2V_0 = H/H_0$, we find that $a/c = (1 - H^2/H_0^2)^{1/2}$, so that (37) becomes

$$\Delta F = \frac{\mu H_0^2 \Delta\dot{M}}{4\pi c^2 \rho_0}\,\frac{1 - H^2 / 2H_0^2}{(1 - H^2 / H_0^2)^{1/2}}. \tag{38}$$

As $p \rightarrow 0$, however, with $a = c$, these relations have meaning only if $V \rightarrow \infty$ and $H = 0$; then $F_{\infty} = \mu H_0^2 \Delta\dot{M}/4\pi c_0^2 = \Delta\dot{E}/c$, where $\Delta\dot{E} = (\mu H_0^2/4\pi\rho_0)\,\Delta\dot{M}$ is the mean energy flux.

The expressions given in the present paper can be used in studying the interaction of bodies emitting either streams of gas or fields.

---

[1] K. P. Staniukovich, Dokl. Akad. Nauk SSSR **119**, 251 (1958), Soviet Phys. "Doklady" **3**, 299 (1958).

Translated by E. J. Saletan
149

SOVIET PHYSICS JETP VOLUME 35(8), NUMBER 3 MARCH, 1959

CERENKOV RADIATION IN THE PASSAGE OF A CHARGED PARTICLE THROUGH A FERRITE

V. G. BAR'IAKHTAR and M. I. KAGANOV

Physico-Technical Institute, Academy of Sciences, U.S.S.R.

Submitted to JETP editor April 1, 1958

J. Exptl. Theoret. Phys. (U.S.S.R.) **35**, 766-770 (September, 1958)

The Cerenkov radiation produced by a charged particle which moves through a medium with gyrotropic magnetic permeability is considered. Losses due to spin-wave excitation by the particle are computed.

1. The electromagnetic radiation produced by the motion of a charged particle in a ferrite (ferrodielectric) is distinguished by a number of features which derive from the dispersion properties of the ferrite. In the gyrotropic magnetic permeability tensor $\hat{\mu}$, which characterizes the ferrite

$$\hat{\mu} = \begin{pmatrix} \mu_1, & i\mu_2 & 0 \\ -i\mu_2, & \mu_1 & 0 \\ 0 & 0 & \mu_3 \end{pmatrix}, \tag{1}$$

the components μ_1 and μ_3 approach unity as the frequency increases, whereas μ_2 approaches zero at relatively low frequencies.[1] For this reason the above-mentioned features can be observed only in the low-frequency region ($\omega \sim 10^{10}$ to 10^{11} sec^{-1}). Under these conditions the gyrotropic effects and the anisotropic effects[2] can lead to Cerenkov radiation at low particle velocities.

The tensor $\hat{\mu}$ does not give a complete description of the dispersion properties of a ferrite medium, because it does not take account of the possible propagation of spin waves. Spin-wave excitation can occur at almost any particle velocity. The energy losses associated with this excitation are of the same nature as polarization losses but are considerably smaller in magnitude.

It is the purpose of this note to investigate the effect of the gyrotropic properties of the magnetic permeability tensor on energy loss in the motion of a charged particle through a ferrite. For simplicity we assume that the motion takes place along the gyrotropic axis (z axis).

The radiation of a charged particle in a gyrotropic medium has been considered by Kolomenskii and Sitenko[3] who treated the gyrotropic electrical effects rather than the magnetic effects. Magnetic effects in the Cerenkov radiation have been examined in references 4 and 5. In reference 4 the magnetic premeability was assumed isotropic; in reference 5 it was characterized by an anisotropic symmetric tensor.

2. We shall assume that the ferrite is electrically isotropic. In point of fact the gyrotropic electrical effects generally found in ferrites should be manifest at frequencies associated with the electronic dispersion of the dielectric permittivity $\hat{\epsilon}$. As a rule, the electronic dispersion in $\hat{\epsilon}$ and the gyrotropic effect in $\hat{\mu}$ occur in different frequency regions so that in the present work we shall consider the gyrotropic magnetic effect only. These results, however, do not apply in the optical region. On the other hand, $\mu_{ik} \rightarrow \delta_{ik}$ in the optical region and the results obtained by Kolomenskii and Sitenko[3] can be used to calculate losses at these frequencies.

We calculate the intensity of the Cerenkov radiation in the usual way (cf. reference 1):

$$\begin{aligned} \frac{dW}{dz} = {} & -\frac{e^2}{c^2}\int\limits_{I} \mu_1\left(1-\frac{1}{\beta^2\varepsilon\mu_1}-\frac{\mu_2^2}{\mu_1^2}\right)\omega d\omega - \frac{e^2}{2c^2}\int\limits_{II}\left\{\mu_1\left(1-\frac{1}{\beta^2\varepsilon\mu_1}-\frac{\mu_2^2}{\mu_1^2}\right)\right. \\ & + \frac{1}{\beta^2\varepsilon|\mu_1|}\{(\beta^2\varepsilon\mu_1-1)^2(\mu_1-\mu_3)^2+2\beta^2\varepsilon\mu_2^2[(1+\beta^2\varepsilon\mu_1)\mu_3-\mu_1(\beta^2\varepsilon\mu_1-1)]+\beta^4\varepsilon^2\mu_2^4\}^{1/2} \\ & \left. + \frac{\mu_3\{(\beta^2\varepsilon\mu_1-1)^2(\mu_1-\mu_3)-\beta^2\varepsilon\mu_2^2(1+\beta^2\varepsilon\mu_1)\}}{\beta^2\varepsilon|\mu_1|\{(\beta^2\varepsilon\mu_1-1)^2(\mu_1-\mu_3)^2+2\beta^2\varepsilon\mu_2^2[(1+\beta^2\varepsilon\mu_1)\mu_3-\mu_1(\beta^2\varepsilon\mu_1-1)]+\beta^4\varepsilon^2\mu_2^4\}^{1/2}}\right\}\omega d\omega, \end{aligned} \tag{2}$$

where the region of integration is given in the table for $\mu_3 > 0$.

Region	$\mu_1<0$	$\mu_1>0$	Number of cones
I	$\beta^2\varepsilon\lvert\mu_1\rvert+1<\beta^2\varepsilon\lvert\mu_2\rvert$	$\beta^2\varepsilon\mu_1-1>\beta^2\varepsilon\lvert\mu_2\rvert$	2
II	$\beta^2\varepsilon\lvert\mu_1\rvert+1>\beta^2\varepsilon\lvert\mu_2\rvert$	$-\beta^2\varepsilon\lvert\mu_2\rvert<\beta^2\varepsilon\mu_1-1<\beta^2\varepsilon\lvert\mu_2\rvert$	1

The conditions given in the table do not take account of the fact that macroscopically we are not actually considering short waves.[2] This limitation must be taken into account close to points at which the integrand diverges. By introducing a finite attenuation we avoid the divergence and obtain a determinate result.

When $\mu_2 = 0$ the integral vanishes in region II and we obtain the result given by Sitenko:[4]

$$\frac{dW}{dz} = -\frac{e^2}{c^2}\int\limits_{\beta^2\varepsilon\mu_1>1}\mu_1\left(1-\frac{1}{\beta^2\varepsilon\mu_1}\right)\omega d\omega. \tag{3}$$

3. In considering Cerenkov radiation in the radio-frequency region (wavelengths greater than 0.1 to 1 mm) we use a simplified model in which the ferrite is characterized by a spontaneous magnetization M. Then, following reference 7, the quantities μ_1 and μ_2 are given by

$$\mu_1 = \frac{\omega_1^2-\omega^2+2i\omega\lambda(H_e+2\pi M)/M}{\omega_0^2-\omega^2+2i\omega\lambda H_e/M};$$

$$\mu_2 = \frac{\omega}{\omega_0}\frac{\omega_1^2-\omega_0^2}{\omega_0^2-\omega^2+2i\omega\lambda H_e/M}; \quad \mu_3 = 1; \tag{4}$$

$$\omega_0 = gH_e, \quad \omega_1 = g\sqrt{H_eB}; \quad B = H_e+4\pi M, \; H_e = H+\beta M$$

where H is the magnetic field applied along the axis of easiest magnetization, β is the anisotropy constant and λ is the relaxation frequency in the Landau-Lifshitz equation.

Substitution of Eq. (4) in Eq. (2) (with $\lambda \ll \omega_0$) yields

$$\begin{aligned}\frac{dW}{dz} = &-\frac{e^2}{c^2}\int\limits_{\mathrm{I}}\left(1-\frac{1}{\beta^2\varepsilon}+\omega_1^2\frac{\mu_0-1}{\omega_1^2-\omega^2}\right)\omega d\omega\\ &-\frac{e^2}{2c^2}\int\limits_{\mathrm{II}}\left\{1-\frac{1}{\beta^2\varepsilon}+\omega_1^2\frac{\mu_0-1}{\omega_1^2-\omega^2}\right.\\ &\left.+\frac{\omega_1^2(\beta^2\varepsilon\mu_0-1)^2-\omega^2[(\beta^2\varepsilon-1)^2\mu_0-(\mu_0-1)(1+\beta^2\varepsilon)]}{2\beta^2\varepsilon\left[\beta^2\varepsilon\mu_0\frac{\omega^2}{\omega_1^2}+\frac{1}{4}(\beta^2\varepsilon\mu_0-1)^2\right]^{1/2}\lvert\omega_1^2-\omega^2\rvert}\right\}\omega d\omega,\end{aligned} \tag{5}$$

where μ_0 is the value of $\mu_1(\omega)$ at $\omega = 0$.

The limits of the regions of integration which are determined by the radiation conditions (cf. table), can be obtained by using the explicit forms of $\mu_1(\omega)$ and $\mu_2(\omega)$. A characteristic feature of Cerenkov radiation in a ferrite is the existence of a low-frequency spectrum at small particle velocities. In terms of the velocity of the charged particle, $\beta = v/c$, the limits of the low-frequency radiation region are given by

$$\begin{aligned}&\text{for} \quad 0<\beta n\leqslant 1: && \Omega<\omega<\omega_1\\ &\text{for} \quad 1\leqslant\beta n\leqslant\mu_0^{1/4}: && 0<\omega<\omega_1\\ &\text{for} \quad \mu_0^{1/4}\leqslant\beta n\leqslant\mu_0^{1/2}: && 0<\omega<\Omega.\end{aligned}$$

Here

$$n = \sqrt{\mu_0\varepsilon_0}, \; \varepsilon_0 = \varepsilon\rvert_{\omega=0}, \; \Omega = \omega_0\lvert\beta^2n^2-1\rvert/\lvert\beta^2\varepsilon_0-1\rvert.$$

The integral in Eq. (5) must be computed before we can obtain the total intensity of the low-frequency radiation. Computing this integral we obtain the following results:

for $0 < \beta n < 1$:

$$\begin{aligned}\frac{dW}{dz} &= -\frac{e^2}{2c^2}\omega_1^2(\mu_0-1)\\ &\times\left[\ln\frac{\omega_1}{2\lambda}\frac{(\mu_0-1)(1+\beta^2\varepsilon_0\mu_0)}{\mu_0(1-\beta^2\varepsilon_0)}-1-\frac{\mu_0-1}{2\mu_0(1-\beta^2\varepsilon_0)}\right],\end{aligned} \tag{6}$$

for $1 < \beta n < \mu_0^{1/4}$:

$$\begin{aligned}\frac{dW}{dz} = &-\frac{e^2}{2c^2}\omega_1^2(\mu_0-1)\ln\frac{\omega_1}{2\lambda}\frac{(1-\beta^2\varepsilon_0)(1+\beta^2\varepsilon_0\mu_0)}{\beta^2\varepsilon_0(\mu_0-1)}\\ &-\frac{e^2}{4c^2}\omega_1^2\frac{2(\mu_0-1)(\beta^6\varepsilon_0^3\mu_0-1)+2\mu_0(\beta^2\varepsilon_0-1)^2-(\beta^4\varepsilon_0^2\mu_0-1)^2}{\beta^4\varepsilon_0^2\mu_0(1-\beta^2\varepsilon_0)},\end{aligned} \tag{7}$$

for $\mu_0^{1/4} < \beta n < \mu_0^{1/2}$:

$$\begin{aligned}\frac{dW}{dz} = &-\frac{e^2}{2c^2}\omega_1^2(\mu_0-1)\ln\frac{\omega_1}{2\lambda}\frac{(1-\beta^2\varepsilon_0)(1+\beta^2\varepsilon_0\mu_0)}{\beta^2\varepsilon_0(\mu_0-1)}\\ &-\frac{e^2}{4c^2}\omega_1^2\frac{4\beta^2\varepsilon_0(\beta^2\varepsilon_0-1)+2\beta^6\varepsilon_0^3(\mu_0-1)+\frac{1}{\mu_0}(1-\beta^8\varepsilon_0^4\mu_0^4)}{\beta^4\varepsilon_0^2(1-\beta^2\varepsilon_0)}.\end{aligned} \tag{8}$$

We have not considered the Cerenkov-radiation intensity for particle velocities which satisfy the condition $\beta n > \mu_0^{1/2}$ because in this case there is no separate low-frequency region (isolated in terms of frequency) and it is necessary to introduce the actual frequency dependence of ϵ to obtain the integrated intensity.

4. In deriving Eqs. (5) to (8) we used Eq. (4) which was derived assuming a simplified model for the ferrite. Actually, a ferrite must be considered as a system of magnetized sub-lattices. Analyzing the motion of the magnetic moments of each of these sub-lattices in a high-frequency magnetic field, we find the following expressions for μ_1 and μ_2:

$$\mu_1 = (\omega^2 - \omega_{1a}^2)(\omega^2 - \omega_{2a}^2) / (\omega^2 - \omega_1^2)(\omega^2 - \omega_2^2), \ \mu_2 = -4\pi\omega (g_1 M_1 + g_2 M_2)(\omega^2 - \omega_{3a}^2) / (\omega^2 - \omega_1^2)(\omega^2 - \omega_2^2), \ \mu_3 = 1;$$
$$\omega_1 = g_1 g_2 (M_2 H_{A1} + M_1 H_{A2}) / (g_1 M_1 + g_2 M_2), \ \omega_{1a}^2 = \omega_1 [\omega_1 + 4\pi (g_1 M_1 + g_2 M_2)],$$
$$\omega_2 = -\alpha (g_1 M_2 + g_2 M_1) + \frac{g_1^2 M_2 H_{A1} + g_2^2 M_1 H_{A2}}{g_1 M_2 + g_2 M_1} - 2 \frac{g_1 g_2 M_1 M_2 (g_1 H_{A1} - g_2 H_{A2})^2}{\alpha (g_1 M_2 + g_2 M_1)^3}, \tag{9}$$
$$\omega_{2a}^2 = \omega_2^2 + 4\pi (g_1 - g_2)^2 | \alpha M_1 M_2, \quad \omega_{3a}^2 = \omega_2^2 + (g_1 - g_2)^2 | \alpha M_1 M_2 | (\omega_1 + \omega_2) / (g_1 M_1 + g_2 M_2),$$

where $H_{A_j} = \beta_j M_j + H$ and M_j, β_j and g_j are respectively the magnetic moment per unit volume, the anisotropy constant and the gyromagnetic ratio for the j-th sub-lattice. The dimensionless parameter α characterizes the exchange reaction between the sub-lattices. In Eq. (9) it is assumed that the axes of easiest magnetization of the sub-lattices are parallel to each other and that the magnetic field H is along this direction.

It is apparent from Eq. (9) that "magnetic" Cerenkov radiation should be observed in the region of the high-frequency resonance $(\omega \sim \omega_2)$* as well as in the region of the usual ferromagnetic resonance $(\omega \sim \omega_1)$. This result is of interest because ω_2 is a sensitive function of temperature; thus it is possible to obtain Cerenkov radiation in different regions of the spectrum (from radio frequencies to the infrared) at low particle velocities.

5. Up to this point we have not considered the possibility that spin waves can be excited by the particle. In other words, we have not taken account of the spatial dispersion in the tensor $\hat{\mu}$; this dispersion is a result of the exchange interaction between the spins.

Inasmuch as the coupling between the electromagnetic waves and the spin waves is weak,[9] we can compute the intensity of the spin-wave excitation by successive approximations, assuming zero electric field in the first approximation.

The following expressions, which give the loss due to spin-wave excitation, can be obtained by some rather laborious computations:

$$\frac{dW}{dz} = -\frac{1}{4\pi} \frac{e^2}{c^2} gM \frac{\Theta_c}{\hbar} \left(\frac{\Theta_c}{\mu M}\right)^2 \left(\frac{v}{v_s}\right)^4 \times \left[\ln \left(\frac{\Theta_c}{\mu M} \frac{v^2}{v_s^2}\right) - 1\right], \quad \sqrt{\frac{\mu M}{\Theta_c}} v_s \gg v; \tag{10}$$

$$\frac{dW}{dz} = -\pi \cdot \frac{e^2}{c^2} gM \frac{\Theta_c}{\hbar} \left(\frac{v}{vs}\right)^2, \quad v_s \gg v \gg \sqrt{\frac{\mu M}{\Theta_c}} v_s; \tag{11}$$

$$\frac{dW}{dz} = -\pi^5 \frac{e^2}{c^2} gM \frac{\Theta_c}{\hbar} \left(\frac{v_s}{v}\right)^2, \quad v \gg v_s, \tag{12}$$

where Θ_c is on the order of the Curie temperature and $v_s = \Theta_c a/h$ is the maximum $(k = 1/a)$ phase velocity for the spin waves. Equation (10) to (12) are obtained under the assumption that $H \ll M$.

It is interesting to note that conservation of energy and conservation of momentum (the radiation conditions) permit excitation of spin waves at almost any particle velocity.

Comparing Eqs. (10) to (12) with the polarization losses in a dielectric, one is easily convinced that the excitation of spin waves by the charged particle is responsible for only a small part of the total energy loss. The polarization losses are of order $dW/dz \approx (e^2/c^2)\omega_p^2$ where $\omega_p^2 = 4\pi Ne^2/m$ $(\omega_p \sim 10^{15} \text{ sec}^{-1})$. Hence the ratio of spin-wave loss to polarization loss is of order $(gM/\omega_p) \times (\Theta_c/\hbar\omega_p) \ll 1$.

The authors are indebted to A. I. Akhiezer for suggesting this problem and for discussion of the results.

---

[1] L. D. Landau and E. M. Lifshitz, Электродинамика сплошных сред (Electrodynamics of Continuous Media) GITTL, M. 1957.

[2] A. G. Sitenko and M. I. Kaganov, Dokl. Akad. Nauk SSSR 100, 681 (1955).

[3] A. G. Sitenko and A. A. Kolomenskii, J. Exptl. Theoret. Phys. (U.S.S.R.) 30, 511 (1956); Soviet Phys. JETP 3, 410 (1956).

[4] A. G. Sitenko, Dokl. Akad. Nauk SSSR 98, 377 (1954).

[5] V. E. Pafomov, J. Exptl. Theoret. Phys. (U.S.S.R.) 30, 761 (1956); Soviet Phys. JETP 3, 597 (1956).

[6] N. Bohr, The Passage of Atomic Particles Through Matter (Russ. Transl.) IIL, M. 1950.

[7] L. D. Landau and E. M. Lifshitz, Sow. Physik 8, 153 (1935).

[8] L. Neel, Ann. phys. 3, 137 (1948).

[9] Akhiezer, Bar' iakhtar, and Peletminskii, J. Exptl. Theoret. Phys. (U.S.S.R.) (in press).

Translated by H. Lashinsky
150

---

*The high-frequency resonance in ferrites will be considered in detail in a separate paper.

SOVIET PHYSICS JETP VOLUME 35(8), NUMBER 3 MARCH, 1959

SPIN WAVES IN A FERROMAGNETIC METAL

A. A. ABRIKOSOV and I. E. DZIALOSHINSKII

Institute for Physical Problems, Academy of Sciences, U.S.S.R.

Submitted to JETP editor April 22, 1958

J. Exptl. Theoret. Phys. (U.S.S.R.) 35, 771-775 (September, 1958)

Using the theory of a Fermi liquid, developed by Landau,[1] we consider spin waves in a ferromagnetic metal.

It is well known that the energy spectrum of a ferromagnetic contains elementary excitations corresponding to oscillations of the magnetic moment. These are called spin waves and have a characteristic dispersion law $\epsilon \sim k^2$. The spin waves were first obtained by Bloch[2] starting from the Heisenberg model of a ferromagnet. Later Landau and Lifshitz[3,4] constructed a phenomenological theory of spin waves and showed that the quadratic dispersion law is by no means particular to the Heisenberg model, but arises from the general properties of the exchange interaction.

Both the Bloch and the Landau-Lifshitz theories considered a ferromagnet as a system of spins, rigidly fixed to the crystalline lattice. This is at any rate not the case in metals where the electrons can freely move through the crystal. It is thus of interest to consider how the motion of the electrons influences the general conclusions of the phenomenological theory. In the present paper we shall consider this problem, using the theory of a Fermi liquid, constructed by Landau.[1]

The electron spectrum of a metal is described by means of quasi-particles, obeying Fermi statistics, conventionally called "electrons." Since the energy of these quasi-particles depends on the orientation of their spin, we shall introduce, in accordance with Landau's theory, the energy operator of the quasi-particles $\epsilon(\mathbf{p}, \sigma)$ (where $\mathbf{p}$ is the quasi-momentum and σ the spin operator) by the formula

$$\delta E = \frac{1}{2} \mathrm{Sp}_{\sigma} \int \varepsilon(\mathbf{p}, \sigma)\, \delta n(\mathbf{p}, \sigma)\, d\tau,$$

$$d\tau = 2dp_x\, dp_y\, dp_z / (2\pi\hbar)^3,$$

where E is the energy per unit volume, n the distribution function occurring in the spin statistical operator relation. The quantity $\epsilon(\mathbf{p}, \sigma)$ is in general a complicated function of the quasi-momentum and is an operator, as is n, depending on the spin operators (here and henceforth we shall mean by σ_i the Pauli matrices). The electrons in a metal interact with one another and form the so-called electron Fermi liquid. According to Landau's theory, their interaction displays itself in particular in the fact that the energy $\epsilon(\mathbf{p}, \sigma)$ of each electron depends on the state of the other electrons and is a functional of the distribution function.

If the distribution function is slightly changed the electron energy is increased by

$$\delta\varepsilon(\mathbf{p}, \sigma) = \frac{1}{2} \mathrm{Sp}_{\sigma'} \int f(\mathbf{p}, \sigma;\ \mathbf{p}', \sigma')\, \delta n(\mathbf{p}', \sigma')\, d\tau', \tag{1}$$

where the function

$$f(\mathbf{p}, \sigma; \mathbf{p}', \sigma') = \delta\varepsilon(\mathbf{p}, \sigma) / \delta n(\mathbf{p}', \sigma')$$

is symmetrical with respect to an interchange of $\mathbf{p}$, σ with $\mathbf{p}'$, σ' and in general can be written in the form

$$f(\mathbf{p}, \sigma; \mathbf{p}', \sigma') = \psi(\mathbf{p}, \mathbf{p}') + \psi(\mathbf{p}, \mathbf{p}')(\sigma + \sigma') + \psi_{ik}(\mathbf{p}, \mathbf{p}')\, \sigma_i \sigma'_k. \tag{2}$$

In a ferromagnetic metal where basically the electron interaction is purely an exchange interaction, the energy operator will depend only on the orientation of the spin with respect to the total magnetic moment. The electron energy is thus of the form

$$\varepsilon(\mathbf{p}, \sigma) = \alpha(\mathbf{p}) - \beta(\mathbf{p})(\mathbf{m}\cdot\sigma), \tag{3}$$

where $\mathbf{m}$ is a unit pseudovector in the direction of the magnetic moment of the crystal. Expression (3) does not take the anisotropy energy into account. However, in view of the smallness of the latter, we shall neglect the anisotropy terms, since they have no special interest for us.

According to Eq. (3) the energy of electrons with σ parallel to $\mathbf{m}$ is equal to $\alpha - \beta$ and the corresponding equilibrium distribution function is $n^+ = n_F(\alpha - \beta)$ (n_F is the usual Fermi function). The energy of electrons with σ antiparallel to $\mathbf{m}$ is equal to $\alpha + \beta$ and their equilibrium distribution function is $n^- = n_F(\alpha + \beta)$. One sees easily that the eigenvalues $n_F(\alpha \pm \beta)$ belong to the operator

$$n_0 = {}^1/_2\,(n^+ + n^-) + {}^1/_2\,(n^+ - n^-)(\mathbf{m}\cdot\sigma), \tag{4}$$

which also follows from considering the equilibrium distribution function.

Neglecting anisotropy effects, Eq. (2) also simplifies and takes on the form

$$\begin{aligned} f(\mathbf{p}, \sigma; \mathbf{p}', \sigma') = {} & \psi(\mathbf{p}, \mathbf{p}') + \varphi(\mathbf{p}, \mathbf{p}')\, \mathbf{m}\cdot(\sigma+\sigma') \\ & + \zeta(\mathbf{p}, \mathbf{p}')(\sigma\cdot\sigma') + \xi(\mathbf{p}, \mathbf{p}')(\mathbf{m}\cdot\sigma)(\mathbf{m}\cdot\sigma'). \end{aligned} \tag{2'}$$

There is a connection which determines β of Eq. (3) from ζ in (2′). To establish this connection* we consider how the electron energy changes when the magnetic moment is rotated over an angle $\delta\boldsymbol{\theta}$ with respect to the crystalline axes. Then $\delta\mathbf{m} = [\delta\boldsymbol{\theta} \times \mathbf{m}]$ and we have according to (3)

$$\delta\varepsilon = -\beta\,[\mathbf{m}\times\sigma]\,\delta\boldsymbol{\theta}. \tag{5}$$

On the other hand, the equilibrium distribution function n_0 changes also when $\mathbf{m}$ changes:

$$\delta n_0 = {}^1/_2\,(n^+ - n^-)\,[\mathbf{m}\times\sigma]\,\delta\boldsymbol{\theta},$$

and with it, according to (1), the energy; namely,

$$\delta\varepsilon = {}^1/_2\,\mathrm{Sp}_{\sigma'} \int f\,\frac{n^+ - n^-}{2}\,[\mathbf{m}\times\sigma']\,\delta\boldsymbol{\theta}\,d\tau'. \tag{6}$$

Comparing Eqs. (5) and (6) for arbitrary $\delta\boldsymbol{\theta}$ we get

$$-\beta\,[\mathbf{m}\times\sigma] = {}^1/_2\,\mathrm{Sp}_{\sigma'} \int f\,\frac{n^+ - n^-}{2}\,[\mathbf{m}\times\sigma']\,d\tau',$$

whence we find

$$\beta(\mathbf{p}) = -{}^1/_2 \int \zeta(\mathbf{p}, \mathbf{p}')(n^+ - n^-)\,d\tau'. \tag{7}$$

To obtain the magnetic spectrum we shall consider the oscillations of a system of electrons. They are described by the transport equation

$$\frac{\partial n}{\partial t} + \frac{\partial\varepsilon}{\partial\mathbf{p}}\frac{\partial n}{\partial\mathbf{r}} - \frac{\partial\varepsilon}{\partial\mathbf{r}}\frac{\partial n}{\partial\mathbf{p}} + i\,[\varepsilon, n] = 0. \tag{8}$$

Here $[\epsilon, n]$ denotes a commutator and we have put $\hbar = 1$. The difference between Eq. (8) and the usual transport equation consists in the fact that ϵ is here a functional of the distribution function. This must be taken into account when one differentiates ϵ with respect to $\mathbf{p}$ and $\mathbf{r}$.

Let $n = n_0 + \delta n$ where n_0 is the equilibrium function (4) and where δn depends on the coordinates and the time in the form $\exp\{i[(\mathbf{k}\cdot\mathbf{r}) - \omega t]\}$. We shall write δn as a sum of a term depending on and one independent of the spin,

$$\delta n = \nu(\mathbf{p}) + (\boldsymbol{\nu}(\mathbf{p})\cdot\sigma), \tag{9}$$

Substituting (9) into (8) and taking into account that according to (1) the energy of the excitations is equal to

$$\varepsilon + \frac{1}{2}\,\mathrm{Sp}_{\sigma'} \int f\,\delta n\,d\tau',$$

with ϵ from (3), we get after a simple transformation, retaining only the terms of first order in δn a set of equations for ν and $\boldsymbol{\nu}$.

This set of equations falls into two parts.* The first one corresponds to oscillations of the electron density and the oscillations of the spin component along the direction of the magnetic moment, $\nu_z = (\boldsymbol{\nu}\cdot\mathbf{m})$ connected with them. However, since oscillations of this kind are accompanied by a change in charge density, their occurrence will be connected with the appearance of strong electrostatic forces. Consequently excitation of such oscillations requires in actual fact a large energy and we need not consider them. Only the second set of equations is of interest to us; it corresponds to oscillations of the transverse components of the total spin.

We note that in non-ferromagnetic metals when the terms in $\mathbf{m}$ are absent, oscillations of the quantity $\boldsymbol{\nu}$ are not connected with density oscillations and satisfy the equation found by Landau[5]

$$-i\omega\boldsymbol{\nu} + i(\mathbf{k}\cdot\mathbf{u})\,\boldsymbol{\nu} + i(\mathbf{k}\cdot\mathbf{u})\,\delta(\alpha - \eta) \int \zeta\boldsymbol{\nu}\,d\tau' = 0,$$

where $\mathbf{u} = \partial\alpha/\partial\mathbf{p}$ and η is the limiting Fermi energy. From this equation it is clear that in such metals the magnetic spectrum is described by excitations with a dispersion law $\epsilon \sim k$.

Instead of the transverse components ν_x and ν_y we introduce the quantities $\nu_\pm = \nu_x \pm i\nu_y$. From the set of equations for ν_x and ν_y we get then for ν_+

$$\begin{aligned} -\omega\nu_+ + (\mathbf{k}\cdot\mathbf{u})\nu_+ + {}^1/_2\,\{ & \mathbf{k}\cdot(\mathbf{u}-\mathbf{v})\,\delta(\alpha - \beta - \eta) + \mathbf{k}\cdot(\mathbf{u}+\mathbf{v}) \\ & \times \delta(\alpha + \beta - \eta)\} \int \zeta\nu_+ d\tau' - 2\beta\nu_+ - (n_+ - n_-) \int \zeta\nu_+ d\tau' = 0, \end{aligned} \tag{10}$$

where $\mathbf{v} = \partial\beta/\partial\mathbf{p}$. The spectrum of this equation gives the dispersion law for the magnetic excitations of a ferromagnetic metal (the equation for ν_- differs in the sign of the least two terms and leads to the same spectrum).

We shall solve Eq. (10) by successive approximations. For $\mathbf{k} = 0$ we have

$$\omega^{(0)}\nu^{(0)} + 2\beta\nu^{(0)} + (n_+ - n_-) \int \zeta\nu^{(0)} d\tau' = 0. \tag{11}$$

Integrating (11) over $d\tau$ and taking the connection (7) between β and ζ into account we get $\omega^{(0)} = 0$ and

$$\nu^{(0)} = A\,(n_+ - n_-),$$

---

*The idea of the derivation given here stems from L. D. Landau.

*It was shown by Silin[6] that the same situation occurs when one considers spin waves in a Fermi liquid when an external magnetic field is present.

where A is a constant. The change in the distribution function is in this order thus proportional to $(n^+ - n^-)\sigma_x$, or $(n^+ - n^-)\sigma_y$. Comparing this with Eq. (4) we see easily that in this case the oscillations lead to a rotation of the total magnetic moment.

We now write down the equation for the next approximation

$$A\omega^{(1)}(n^+ - n^-) + 2\beta\nu^{(1)} + (n^+ - n^-)\int \zeta\nu^{(1)}d\tau'$$
$$= A(\mathbf{k}\cdot\mathbf{u})(n^+ - n^-) - A\beta\{\mathbf{k}\cdot(\mathbf{u}-\mathbf{v})\delta(\alpha - \beta - \eta) \qquad (12)$$
$$+ \mathbf{k}\cdot(\mathbf{u}+\mathbf{v})\delta(\alpha + \beta - \eta)\}.$$

We integrate this over $d\tau$, using again condition (7) and the fact that α and β are even functions of the quasi-momentum. This leads to $\omega^{(1)} = 0$, i.e., ω is at least of second order in k.

According to Eq. (12), the change in the distribution function consists of three parts. One differs from zero in the same interval as $n_+ - n_-$, and the other two are different from zero only on the corresponding Fermi surface and are proportional to $\delta(\alpha - \beta - \eta)$ and $\delta(\alpha + \beta - \eta)$, respectively. If we denote the quantity $\nu^{(1)}/A$ (this quantity does not depend on A) by ν_1 and write ν_1 in the form

$$\nu_1 = B(\mathbf{p})(n_+ - n_-) - {}^1/_2\{\mathbf{k}\cdot(\mathbf{u}-\mathbf{v})\delta(\alpha - \beta - \eta)$$
$$+ \mathbf{k}\cdot(\mathbf{u}+\mathbf{v})\delta(\alpha + \beta - \eta)\}, \qquad (13)$$

we get for the function $B(\mathbf{p})$ the equation

$$2\beta B + \int \zeta B'(n^+ - n^-)\,d\tau'$$
$$= \mathbf{k}\cdot\mathbf{u} + \frac{1}{2}\int\left[\zeta(\mathbf{p}, \mathbf{p}')\mathbf{k}\cdot(\mathbf{u}'-\mathbf{v}')\frac{d\tau'}{d\varepsilon'}\right]_{\alpha'-\beta'=\eta} \qquad (14)$$
$$+ \frac{1}{2}\int\left[\zeta(\mathbf{p}, \mathbf{p}')\,\mathbf{k}\cdot(\mathbf{u}'+\mathbf{v}')\frac{d\tau'}{d\varepsilon'}\right]_{\alpha'+\beta'=\eta}.$$

In the case where $\zeta(\mathbf{p}, \mathbf{p}')$ is an arbitrary function of the quasi-momenta $\mathbf{p}$ and $\mathbf{p}'$, the last equation cannot be solved explicitly for $B(\mathbf{p})$.

To find the connection between ω and $\mathbf{k}$ we write down the equation for $\nu^{(2)}$ and integrate it over $d\tau$; this leads to

$$\omega^{(2)} = \Big\{\int \mathbf{k}\cdot\mathbf{u}\,\nu_1 d\tau + \frac{1}{2}\int\int[\mathbf{k}\cdot(\mathbf{u}-\mathbf{v})\delta(\alpha - \beta - \eta)$$
$$+ \mathbf{k}\cdot(\mathbf{u}+\mathbf{v})\,\delta(\alpha + \beta - \eta)]\,\zeta\nu_1' d\tau d\tau'\Big\} \Big/ \int (n^+ - n^-)\,d\tau. \qquad (15)$$

Substituting Eq. (13) into this expression and transforming it by means of Eq. (14) we get

$$\omega^{(2)} = \Big\{\int \mathbf{k}\cdot\mathbf{u}\,(n^+ - n^-)B(\mathbf{p})\,d\tau - \int\left[\beta B(\mathbf{p})\mathbf{k}\cdot(\mathbf{u}-\mathbf{v})\frac{d\tau}{d\varepsilon}\right]_{\alpha-\beta=\eta}$$
$$- \int\left[\beta B(\mathbf{p})\mathbf{k}\cdot(\mathbf{u}+\mathbf{v})\frac{d\tau}{d\varepsilon}\right]_{\alpha+\beta=\eta}\Big\} \Big/ \int (n^+ - n^-)\,d\tau. \qquad (16)$$

In view of the fact that B is of first order in $\mathbf{k}$ and clearly an odd function of the quasi-momentum it is evident that ω is a quadratic function of $\mathbf{k}$.

We have thus come to the rather natural conclusion that the model considered leads to the usual quadratic dispersion law.

Equations (14) and (16) determine completely the dependence $\omega(\mathbf{k})$. In the simplest case, $\zeta = \text{const}$, Eq. (14) can be solved for B. Indeed, in view of the fact that B is an odd function of the quasi-momentum and that n^+ and n^- are even functions, all integrals in Eq. (14) tend to zero. It is thus shown that $B = (\mathbf{k}\cdot\mathbf{u})/2\beta$. Substituting this into Eq. (16) and taking into account the fact that according to Eq. (7) for $\zeta = \text{const}$, β is also a relative constant and $\mathbf{v} = \partial\beta/\partial\mathbf{p} = 0$, we find

$$\omega = \Big\{\int (\mathbf{k}\cdot\mathbf{u})^2(n^+ - n^-)\,d\tau - \frac{\beta}{2}\int\left[(\mathbf{k}\cdot\mathbf{u})^2\frac{d\tau}{d\varepsilon}\right]_{\alpha=\eta+\beta}$$
$$- \frac{\beta}{2}\int\left[(\mathbf{k}\cdot\mathbf{u})^2\frac{d\tau}{d\varepsilon}\right]_{\alpha=\eta-\beta}\Big\} \Big/ 2\beta\int (n^+ - n^-)\,d\tau. \qquad (17)$$

In conclusion we express our gratitude to academician L. D. Landau for valuable advice and a discussion for the results obtained.

---

[1] L. D. Landau, J. Exptl. Theoret. Phys. (U.S.S.R.) **30**, 1058 (1956), Soviet Phys. JETP **3**, 920 (1956).

[2] F. Bloch, Z. Physik, **61**, 206 (1930).

[3] L. D. Landau and E. M. Lifshitz, Physik. Z. Sowjetunion **8**, 153 (1935).

[4] E. M. Lifshitz, J. Exptl. Theoret. Phys. (U.S.S.R.) **15**, 97 (1945), J. Phys. (U.S.S.R.) **8**, 337 (1944).

[5] L. D. Landau, J. Exptl. Theoret. Phys. (U.S.S.R.) **32**, 59 (1957), Soviet Phys. JETP **5**, 101 (1957).

[6] V. P. Silin, J. Exptl. Theoret. Phys. (U.S.S.R.) **33**, 1227 (1957), Soviet Phys. JETP **6**, 945 (1958).

Translated by D. ter Haar

UNIDIMENSIONAL MOTION IN MAGNETOHYDRODYNAMICS

G. S. GOLITSYN

Institute of Physics of the Atmosphere, Academy of Sciences, U.S.S.R.

Submitted to JETP editor April 23, 1958

J. Exptl. Theoret. Phys. (U.S.S.R.) **35**, 776-781 (September, 1958)

The motion of a perfectly conducting gas in a magnetic field is investigated. The Riemann invariants for a number of gases are computed and some nonstationary problems are solved. A new method is proposed for obtaining an approximate general solution of the magnetohydrodynamic equations. Some types of motion involving shock waves are considered.

THE qualitative picture of unidimensional motion in magnetohydrodynamics is fairly clear. It appears to be useful to develop methods for solving unidimensional problems in order to be able to evaluate quantitatively those new features that the introduction of a field adds to the dynamics of a conducting gas.

We shall restrict ourselves to the case of infinite conductivity, since only in this case, and even then not always, can we obtain solutions in analytic form. Moreover, this case is of interest as a limiting case in the sense that here the influence of the field is particularly pronounced. The effect of finite conductivity can be estimated qualitatively by treating classical gas dynamics as another limiting case.

1. NONSTATIONARY MOTION

The principal results in this field were obtained by Kaplan and Staniukovich,[1] who found the characteristics and a particular solution of the magnetohydrodynamic equations. However, their formulas are in a form that cannot yet be applied to the solution of specific problems.

For the case of isentropic motion the magnetohydrodynamic equations can be written as

$$\frac{\partial v}{\partial t} + v\frac{\partial v}{\partial x} + \frac{1}{\rho}\frac{\partial p^*}{\partial x} = 0; \qquad (1.1)$$

$$\frac{\partial p^*}{\partial t} + v\frac{\partial p^*}{\partial x} + \rho c_m^2\frac{\partial v}{\partial x} = 0. \qquad (1.2)$$

Here $p^* = p + h^2/2$, $h\sqrt{4\pi} = H$ is the intensity of the magnetic field such that $\mathbf{H}\perp\mathbf{v}$; $c_m^2 = c^2 + V_a^2$, where $c^2 = (\partial p/\partial\rho)_S$ is the speed of ordinary sound, while $V^2 = H^2/4\pi\rho$ is the Alfven velocity. Equation (1.2) can be obtained from the equation of continuity if we take into account that

$$\partial\rho/\partial z = (\partial\rho/\partial p^*)_S\partial p^*/\partial z = c_m^{-2}\partial p^*/\partial z,$$

where $z = x$ or t.

After dividing (1.2) by ρc_m, adding and subtracting (1.1), we can write the result in the form

$$[\partial/\partial t + (v \pm c_m)\partial/\partial x]J_\pm = 0,$$

where we have denoted

$$J_\pm = v \pm \int dp^*/\rho c_m = v \pm \int c_m d\ln\rho. \qquad (1.3)$$

The quantities $J_\pm$ are conserved along the characteristics $dx/dt = v \pm c_m$ and go over into the classic Riemann invariants as $h \to 0$. The integral in (1.3) may be conveniently written in the form

$$\frac{2c_0}{\gamma-1}\int(1 + \eta y^{2(2-\gamma)/(\gamma-1)})^{1/2}dy. \qquad (1.4)$$

Here $\gamma = c_p/c_v$, $\eta = V_{a0}^2/c_0^2$; $y = c/c_0$; the subscript 0 refers to quantities defined for $v = 0$. The integral (1.4) is a Chebyshev differential binomial and can be evaluated as a whole only in the cases $\gamma = (4n + 1)/(2n + 1)$ and $\gamma = 2 - 1/2n$, where $n = 1, 2, 3 \ldots$ In the first case when $n = 1$ we have the practically important case $\gamma = 5/3$. All other values of n can be used only for approximations. This does not include the case of isothermal motion[2] of interest for certain applications which is given by $\gamma = 1$. In this case we must start with (1.3). We state the results of integration for certain values of γ which are of practical interest:

$$\gamma = 1,\ J_\pm = v \pm \left[2(c_T^2 + b^2\rho)^{1/2} + b^2\ln\frac{(c_T^2 + b^2\rho)^{1/2} - b}{(c_T^2 + b^2\rho)^{1/2} + b}\right];$$

$$\gamma = \frac{3}{2},\ J_\pm \qquad (1.5)$$

$$= v \pm 2c_0[y(1 + \eta y^2)^{1/2} + \eta^{-1/2}\ln(y + (y^2 + 1/\eta)^{1/2}];$$

$$\gamma = \frac{5}{3},\ J_\pm = v \pm (2c_0/\eta)(1 + \eta y)^{3/2}.$$

Here C_T is the isothermal speed of sound, while

$b = h/\rho = \text{const.}$

We shall deal henceforth only with a monatomic gas. We obtain the constant $J_\pm$ from the condition that $y = 1$ when $v = 0$. Then

$$v = \mp (2c_0/\eta)\,[(1+\eta y)^{3/2} - (1+\eta)^{3/2}], \tag{1.6}$$

from which it follows that

$$c = c_0 y = (c_0/\eta)\,\{[(1+\eta)^{3/2} \pm \eta v/2c_0]^{2/3} - 1\}. \tag{1.7}$$

By using the Poisson adiabatic we can determine the dependence on v and on the other parameters of the gas. Formulas (1.6) and (1.7) may be used for the description of self-similar motion and for unidimensional running waves given by the special solution[1] $x = (v \pm c_m)t + f(v)$ which can now be written in the following form convenient for practical purposes:

$$x = t\left\{\frac{3}{2}v \pm \frac{c_0}{\eta}\left[(1+\eta)^{3/2} - \left((1+\eta)^{3/2} \pm \frac{\eta v}{2c_0}\right)^{1/3}\right]\right\} + f(v). \tag{1.8}$$

By using this formula we can solve, for example, the problem of a piston entering with a speed $U = at$ into a tube which contains a perfectly conducting gas in a magnetic field ($a = \text{const}$).

This solution is completely analogous to the case $h = 0$, although it is more awkward. The shock wave is formed at the instant

$$t = \frac{c_0}{a}\,\frac{6\,(1+\eta)^{3/2}}{8+\eta}, \tag{1.9}$$

which in the case $\eta = 0$ reduces to the well known result[3a] for $\gamma = 5/3$: $t = 3c_0/4a$. As the field increases, the shock wave is formed at progressively later times and progressively further away from the piston, since the field decreases the compressibility of the medium, the perturbations are propagated with greater speed, and it is more difficult for a compression wave to develop in this case than in a medium in the absence of the field and for the same piston speed. One can arrive at the same conclusion by investigating graphically the system of characteristics for this problem.

The condition $c > 0$ enables us to determine from (1.7) the maximum rate of nonstationary efflux of monatomic gas into a vacuum where there is also no field:

$$v \leqslant 2c_0\,[(1+\eta)^{3/2} - 1]\,/\,\eta. \tag{1.10}$$

From the Bernoulli equation of magnetohydrodynamics we can obtain the rate of stationary efflux:

$$v = [2\,(i_0 + b^2\rho_0)]^{1/2} = \sqrt{2}\,c_0\left(\frac{1}{\gamma-1} + \eta\right)^{1/2}. \tag{1.11}$$

Both rates given by (1.10) and (1.11) increase as the field increases. The limit of their ratio approaches $\sqrt{2}$ as $\eta \to \infty$, and is equal to $\sqrt{3}$ for $\eta = 0$ in the case $\gamma = 5/3$.

The magnetohydrodynamic equations for isentropic flows can be reduced in the usual way[3b] to a single second order linear equation with variable coefficients, and in doing so we must take t and x as the dependent variables, while v and ρ or c should be taken as the independent variables. However, the equation which is obtained as a result of this does not have an analytic solution for any value of γ. In order to obtain an approximate general solution we can approximate the equation of state as follows[1]

$$p = A\rho^{(2n+3)/(2n+1)} + B - {}^1/_2\, b^2\rho^2,$$

where A, n, B are arbitrary constants. However, such an approximation is not convenient in the case when the magnetic pressure is greater than the thermodynamic pressure. We shall give the equation of state in a different form which is convenient in the majority of cases for obtaining the general solution:

$$p^* = A\rho^\gamma + {}^1/_2\, b^2\rho^2 = (A + {}^1/_2\, b^2\rho_1^{2-\gamma})\,\rho^\gamma = C\rho^\gamma, \tag{1.12}$$

where ρ_1 is the constant value of the density defined in a suitable manner. In the case $\gamma = (2n+3)/(2n+1)$, where n is an integer, we can obtain the exact solution of the corresponding Darboux equation. If we interpret p^* as the ordinary pressure, then all the equations in terms of whatever variables are employed, and all the thermodynamic relations will be of exactly the same form as in ordinary gas dynamics, only the velocity of sound will be greater in the present case. Therefore all the results of Landau and Lifshitz[3b] and of Staniukovich[4] may be carried over to this case without any changes.

2. MOTION INVOLVING SHOCK WAVES

We shall consider in detail a number of problems where the presence of a shock discontinuity plays an essential role. The front of the discontinuity is parallel to the magnetic field and is perpendicular to the velocity of the flow. The relations between the parameters of different types of discontinuity have been investigated in detail by Helfer[5] and by Lust.[6] We shall discuss a number of topics ab initio, having in mind the solution of certain problems.

In the system of coordinates associated with the surface of discontinuity the following conditions must be fulfilled:

$$\rho_1 u_1 = \rho_2 u_2; \tag{2.1}$$

$$\rho_1 u_1^2 + p_1 + h_1^2/2 = \rho_2 u_2^2 + p_2 + h_2^2/2; \tag{2.2}$$

$$i_1 + u_1^2/2 + h_1^2/\rho_1 = i_2 + u_2^2/2 + h_2^2/\rho_2; \tag{2.3}$$

$$h_1 u_1 = h_2 u_2. \tag{2.4}$$

The subscripts 1 and 2 refer to the two sides of the surface of discontinuity.

The taking into account of finite conductivity alters only the last relation[7] by smearing out the front of the discontinuity. However, formulas (2.1) to (2.4) will hold at large distances from the front. Therefore, the formulas which we obtain below should also hold in the case of finite conductivity.

By introducing the specific volume $V = 1/\rho$ and the energy per unit volume of the field $\epsilon = H^2/8\pi$ we can obtain the equation of the shock adiabatic:

$$\begin{gathered} i_1 - i_2 + \frac{1}{2}(V_1 + V_2)(p_2 + \varepsilon_2 - p_1 - \varepsilon_1) \\ + 2(\varepsilon_1 V_1 - \varepsilon_2 V_2) = 0. \end{gathered} \tag{2.5}$$

We now introduce $\rho_2/\rho_1 = x = V_1/V_2$ representing the discontinuity in the density of the medium. As a result of the field being frozen-in $\epsilon_2 = \epsilon_1 x^2$. After taking into account the fact that $i = \gamma pV/(\gamma - 1)$ we shall obtain from (2.5) after a number of transformations:

$$\begin{gathered} \alpha x - 1 - (\alpha - x)\, p_2/p_1 + \eta_1 (x - 1)^3 = 0, \\ \alpha = (\gamma + 1)/(\gamma - 1), \quad \eta_1 = \varepsilon_1/p_1 = H_1^2/8\pi p_1. \end{gathered} \tag{2.6}$$

In the case $\eta_1 = 0$ we obtain the usual Hugoniot adiabatic. The parameter η_1 differs by the factor $\gamma/2$ from the parameter η of the preceding section.

We note that although Eq. (2.6) is cubic in x, it is linear in p_2/p_1, and η_1. Therefore, by fixing one of the parameters we can easily calculate the dependence of the other parameter on x. Figure 1 shows the Hugoniot adiabatics in the presence of the field in the case $\gamma = 5/3$ in the system of coordinates p_2/p_1 and $V_2/V_1 = 1/x$. They lie progressively higher than the usual adiabatic as the initial field H_1 increases, i.e., the compressibility of the medium decreases. The adiabatics in the presence of the field are fourth order curves with two asymptotes:

$$\begin{gathered} V_2/V_1 = 1/\alpha = (\gamma - 1)/(\gamma + 1), \\ p_2/p_1 = -(1 + \eta_1)/\alpha. \end{gathered} \tag{2.7}$$

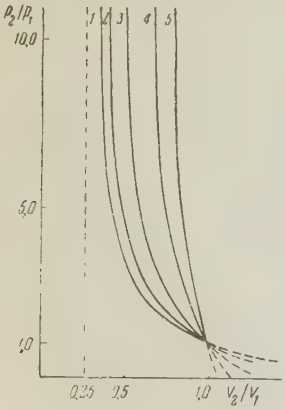

FIG. 1. Curve 1 – $\eta_1 = 0$; 2 – $\eta_1 = 1$; 3 – $\eta_1 = 10$; 4 – $\eta_1 = 10^2$; 5 – $\eta_1 = 10^3$.

A rarefaction shock wave cannot exist also in the case of magnetohydrodynamics in consequence of the principle of increase of entropy at a discontinuity of the type under investigation,[8] therefore states represented by points of the adiabatics below the point (1, 1) are not realized.

Due to the occurrence of "freezing-in" in order to specify completely the state of the medium beyond the discontinuity we must know in addition to the initial parameters only any one of the three quantities p_2, ρ_2, h_2.

The discontinuity in the temperature is determined by the equation of state, from which it follows that $T_2/T_1 = p_2/xp_1$. Since $1/x$ increases with η_1 for a given value of the ratio p_2/p_1, the temperature discontinuity must also increase. Although in actual fact the problem cannot be stated so simply, nevertheless we must not forget the possibility of such an increase in temperature, since it could occur in the case of some nonstationary introduction of a field into a medium which already contains a discontinuity and when p_2/p_1 remains constant or decreases insignificantly.

In order to obtain an evaluation as to which wave is more advantageous from the point of view of obtaining a higher temperature — the wave in a medium with a field, or without a field — we shall solve the problem of the piston moving with a constant velocity U into an unbounded tube. A shock wave is formed in the gas which at the initial moment coincides with the position of the piston and then moves away from it. In the region between the wave and the piston the gas moves with velocity U. From (2.1) and (2.2) we can obtain the following formula:

$$u_1 - u_2 = [(p_2^* - p_1^*)(V_1 - V_2)]^{1/2}. \tag{2.8}$$

Since the gas is at rest ahead of the discontinuity we obtain from (2.8):

$$U = [(p_2^* - p_1^*)(V_1 - V_2)]^{1/2}. \tag{2.9}$$

This equation can be conveniently rewritten in the form

$$U = c_1 \left\{\frac{1}{\gamma}\left(1 - \frac{1}{x}\right)\left[\frac{p_2}{p_1} - 1 + \eta_1 (x^2 - 1)\right]\right\}^{1/2}. \tag{2.10}$$

We can easily calculate the speed of the discontinuity front by expressing it in terms of the density

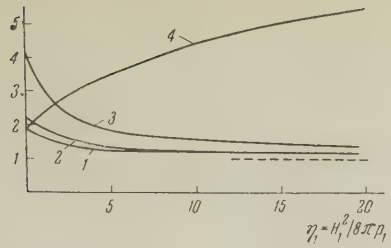

FIG. 2. Curve $1 - T_2/T_1$; $2 - x = \rho_2/\rho_1$; $3 - p_2/p$; $4 - v/c_1$.

discontinuity:

$$\frac{v}{c_1} = \left\{\frac{x}{\gamma}\,\frac{\eta\,[(\alpha-3)\,x^2+4x-(\alpha+1)]+(\alpha+1)\,(x-1)}{x-1}\right\}^{1/3}. \quad (2.11)$$

With the aid of (2.10), (2.11), and (2.8) we can find for any specific value of U/c, the discontinuities in the pressure, the temperature, the density, and the value of v/c_1. Figure 2 shows the variation with η_1 of these parameters in the case $\gamma = 5/3$ and $U/c_1 = 1$. As the field increases all the discontinuities tend to 0, while v/c_1 increases, however the value of $v/c_{m_1} = v/c_1(1+\eta)^{1/2}$ approaches 1, i.e., the shock wave degenerates into a weak discontinuity. This result is physically clear: as the field increases the compressibility of the medium decreases, while progressively larger masses of gas are involved in the motion and progressively larger fractions of the work done must be expended in increasing the energy of the field. Therefore the discontinuities in p, ρ, T must decrease and tend to 0 as $\eta_1 \to \infty$. In a medium in which $p \ll H^2/8\pi$ with all the other conditions remaining the same, the shock wave has a low efficiency from the point of view of heating the gas. This should be taken into account in many astrophysical problems.

Let us consider the reflection of a shock wave from an absolutely rigid wall. Since the gas is at rest in the space between the wall and the shock wave, the relative velocities of the gas on the two sides of the discontinuity are the same for the incident and for the reflected wave. Therefore, by making use of (2.8), we obtain

$$(p_2^* - p_1^*)(V_1 - V_2) = (p_3^* - p_2^*)(V_2 - V_3),$$

where the subscript 3 denotes the region between the wall and the shock wave. This condition may be brought into the form:

$$\begin{aligned}(x_1-1)\left[\frac{p_2}{p_1} - 1 + \eta_1(x_1^2-1)\right] \\ = \frac{p_2}{p_1}\left(1-\frac{1}{x_2}\right)\left[\frac{p_3}{p_2} - 1 + \eta_1\frac{x_1^2}{p_2/p_1}(x_2^2-1)\right]\end{aligned} \quad (2.12)$$

Here $x_1 = \rho_2/\rho_1$; $x_2 = \rho_3/\rho_2$. The equations of the adiabatics for the incident and the reflected shock waves are given by:

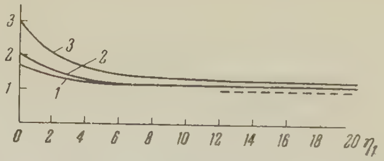

FIG. 3. Curve $1 - T_3/T_2$; $2 - x_2$; $3 - p_3/p_2$.

$$\alpha x_1 - 1 - (\alpha - x_1)\,p_2/p_1 + \eta_1(x_1-1)^3 = 0; \quad (2.6')$$

$$\alpha x_2 - 1 - (\alpha - x_2)\,p_3/p_2 + \eta_1 x_1^2 (p_1/p_2)(x_2-1)^3 = 0. \quad (2.6'')$$

Here, just as in the case of the problem of the piston, we have not succeeded in finding an analytic solution, but the numerical solution of equations (2.12), (2.6′), and (2.6″) does not present any difficulties.

The results of the calculation are given in Fig. 3. For the sake of simplicity we have taken the wave of the preceding problem as the incident wave.

The use of the above results to investigage the decay of an arbitrary discontinuity in the medium considered by us, containing a field perpendicular to the velocity, also presents no difficulties in principle. Such an investigation can be carried out in exactly the same way as in the case of ordinary gas dynamics,[3c] and we can obtain the same qualitative results with somewhat altered estimates for the velocities.

In conclusion, I express my deep gratitude to K. P. Staniukovich for a discussion of the above results.

---

[1] S. A. Kaplan and K. P. Staniukovich, Dokl. Akad. Nauk S.S.S.R. **95**, 769 (1954).

[2] S. A. Kaplan, Астрономич. журн. (Astronomy Journal) **31**, 358 (1954).

[3] L. D. Landau and E. M. Lifshitz, Механика сплошных сред (The Mechanics of Continuous Media), GITTL, 1954; (a) § 94, problem 1; (b) § 98, (c) § 93.

[4] K. P. Staniukovich, Неустановившиеся движения сплошной среды (Unsteady Motion of a Continuous Medium), GITTL, 1955, §§ 13, 18.

[5] H. F. Helfer, Astrophys. Jour. **117**, 177 (1953).

[6] R. Lust, Z. Naturforsch. **10a**, 125 (1955).

[7] G. S. Golitsyn and K. P. Staniukovich, J. Exptl. Theoret. Phys. (U.S.S.R.) **33**, 1417 (1957), Soviet Phys. JETP **6**, 1090 (1958).

[8] F. Hoffman and E. Teller, Phys. Rev. **80**, 692 (1950).

Translated by G. Volkoff
152

Letters to the Editor

WAVE-FRONT VELOCITY IN ELECTRODYNAMICS CONTAINING HIGHER DERIVATIVES

L. G. IAKOVLEV

Uzbek State University

Submitted to JETP editor April 7, 1958

J. Exptl. Theoret. Phys. (U.S.S.R.) **35**, 782-783 (September, 1958)

THE wave-front velocity in Maxwell-Lorentz electrodynamics and in nonlinear electrodynamics has been the subject of several studies.[1,2] Some of the references cited used the method of Levi-Civita, which is the simplest and clearest. We propose to use this method to analyze electrodynamics with higher derivatives. We shall restrict our considerations to fourth-order differential equations for the potential.

First we use the Lagrangian formalism to obtain the general form of the equations of electrodynamics with higher derivatives. Since the correspondence principle must always remain fulfilled, let us assume that the Lagrangian density L depends on the two invariants $I_1 = H_{ik}H_{ik}/2$ and $I_2 = H_{ik,l}H_{ik,l}$, where, as usual,

$$H_{ik} = A_{k,i} - A_{i,k}. \tag{1}$$

This last expression gives us the first group of equations, namely*

$$H_{ik,l} + H_{kl,i} + H_{li,k} = 0. \tag{2}$$

The second group is obtained from the variationally derived Euler-Lagrange equations

$$\frac{\partial}{\partial x_k}\frac{\partial L}{\partial A_{i,k}} - \frac{\partial^2}{\partial x_k \partial x_l}\frac{\partial L}{\partial A_{i,kl}} = 0. \tag{3}$$

Writing out Eq. (3) using the relations

$$\frac{\partial L}{\partial A_{i,k}} = \frac{\partial L}{\partial I_1}\frac{\partial I_1}{\partial A_{i,k}}$$

etc., we obtain the general form of the second group of equations, namely

$$\begin{aligned} &AH_{ik,k} + BH_{ik,kll} + CH_{ik}H_{lm}H_{lm,k} + D\,(H_{ik}H_{lm,n}H_{lm,nk} + 2H_{mn}H_{mn,l}H_{ik,kl} + 2H_{mn}H_{mn,k}H_{ik,ll} + 2H_{mn}H_{ik,l}H_{mn,kl} \\ &+ 2H_{ik,l}H_{mn,k}H_{mn,l}) + \mathscr{E}\,(H_{mn,p}H_{mn,lp}H_{ik,kl} + H_{mn,p}H_{mn,kp}H_{ik,ll} + H_{ik,l}H_{mn,pk}H_{m,npl} + H_{ik,l}H_{mn,p}H_{mn,klp}) \qquad (4) \\ &+ GH_{mn}H_{pr}H_{mn,k}H_{pr,l}H_{ik,l} + K\,(H_{mn}H_{mn\,k}H_{ik,l}H_{ns,p}H_{ns,pl} + H_{mn}H_{mn,l}H_{ik,l}H_{rs,p}H_{rs,pk}) + MH_{ik,l}H_{mn,p}H_{rs,t}H_{mn,pl}H_{rs,tk} = 0 \\ &(A = \partial L/\partial I_1, \quad B = 2\partial L/\partial I_2, \quad C = \partial^2 L/\partial I_1^2, \quad D = \partial^2 L/\partial I_1 \partial I_2, \\ &\mathscr{E} = 2\partial^2 L/\partial I_2^2, \quad G = \partial^3 L/\partial I_1^2 \partial I_2, \quad K = \partial^3 L/\partial I_1 \partial I_2^2, \quad M = 2\partial^3 L/\partial I_2^3). \end{aligned}$$

The wave front is a surface of weak discontinuity. In the present case all the H_{ik} and all but their very highest derivatives are continuous on the wave front, that is, all but the $H_{ik,lmn}$. According to the method we are using, we must find the differences which occur in Eqs. (2) and (4) when passing through the wave front. Writing $h_{ik,lmn}$ for the nonvanishing differences of the $H_{ik,lmn}$, Eqs. (2) and (4) give

$$\begin{gathered} h_{ik,lmm} + h_{kl,imm} + h_{li,kmm} = 0, \\ Bh_{ik,kll} + \mathscr{E}H_{ik,l}H_{mn,p}h_{mn,pkl} = 0. \end{gathered} \tag{5}$$

Let us consider a plane front. Let $E = E_x(z, t)$ and $H = H_y(z, t)$, which means that $H_{14}(x_3, x_4)$ and $H_{13}(x_3, x_4)$ do not vanish. Writing the relations

$$\begin{aligned} &H_{ik,lm}(x_3 + \Delta x_3, x_4 + \Delta x_4) \\ &= H_{ik,lm}(x_3, x_4) + H_{ik,lm3}\Delta x_3 + H_{ik,lm4}\Delta x_4 \end{aligned}$$

for points in front of and behind the wave front and taking the differences, we find that the discontinuities in the second derivatives give

$$\begin{gathered} h_{ik,lm4} = iv h_{ik,lm3} \\ v = \lim\,(i\Delta x_3/\Delta x_4) \ \text{ as } \ \Delta x_4 \to 0. \end{gathered} \tag{6}$$

It can be shown, using (2), (5), and (6), that the index 4 in Eq. (5) can be replaced by 3 if the additional factor iv is added (for instance, $h_{14,444} = v^4 h_{13,333}$). Then dividing by $h_{13,333}$ and writing the result in three-dimensional vector form, Eq. (5) gives

$$\begin{aligned} &(1 + 2\alpha E_{x,t}^2)\,v^4 - 4\alpha E_{x,t}E_{x,z}v^3 - 2\,(1 + 2\alpha E_{x,t}H_{y,z} \\ &- 4\alpha E_{x,z}^2)\,v^2 - 8\alpha H_{x,z}H_{y,z}v + 1 + 2\alpha H_{y,z}^2 = 0, \end{aligned} \tag{7}$$

where $\alpha = \mathscr{E}/B$.

Thus in electrodynamics with higher derivatives, as in nonlinear electrodynamics, a wave front has in general four velocities of propagation different from the velocity of light in vacuo.

A special case is $\mathscr{E} = 0$ (or $\alpha = 0$), i.e., $L = f(I_1) + bI_2/2$ (the electrodynamics of Bopp and Podolsky is of this kind). It is easily seen that in this case (7) yields $v = 1$, which is the velocity of light in vacuo.

The author expresses his gratitude to Professor D. Ivanenko for discussing the work.

---

*Here A_k is the four-vector whose components are A_x, A_y, A_z, and $i\varphi$, and $A_{k,l} = \partial A_k/\partial x_l$; we set $c = 1$.

---

[1] A Sommerfeld, Ann. Physik **44**, 177 (1914); L. Brillouin, Ann. Physik **44**, 203 (1914).

[2] M. S. Svirskii, Вестник МГУ (Bulletin Moscow State Univ.) **3**, 43 (1951); D. I. Blokhintsev, Dokl. Akad. Nauk SSSR **82**, 553 (1952); D. I. Blokhintsev and V. V. Orlov, J. Exptl. Theoret. Phys. (U.S.S.R.) **25**, 513 (1953); V. I. Skobelkin, J. Exptl. Theoret. Phys. (U.S.S.R.) **27**, 689 (1954); L. G. Iakovlev, J. Exptl. Theoret. Phys. (U.S.S.R.) **28**, 246 (1955), Soviet Phys. JETP **1**, 181 (1955).

Translated by E. J. Saletan
153

SELECTION RULES IN REACTIONS INVOLVING POLARIZED PARTICLES

CHOU KUANG-CHAO

Joint Institute for Nuclear Research

Submitted to JETP editor April 23, 1958

J. Exptl. Theoret. Phys. (U.S.S.R.) **35**, 783-785 (September, 1958)

SIMON and Welton[1] and Shirokov[2] have obtained the selection rules for a reaction of the type $a + b \rightarrow c + d$ in the form of relations between the polarization vectors and tensors. They assume that the initial state is not polarized. The present communication gives a derivation of the selection rules for any arbitrarily-polarized initial state. We shall use Shirokov's notation[2] and assume that all the particles have nonvanishing rest mass.

Consider the statistical tensors of the final state in the $a + b \rightarrow c + d$ reaction,

$$\rho'(q_c, \tau_c, q_d, \tau_d;\ g_c g_a^{-1}), \tag{1}$$

which depend essentially on the parameters of the rotation $g_c g_a^{-1}$ which carries the z_a, y_a, x_a coordinate system into the z_c, y_c, x_c coordinate system. The first of these systems is associated with the initial state, the z_a axis being parallel to n_a, and the y_a axis being perpendicular to the production plane of particle a. The second of these systems has z_c parallel to n_c, and y_c in the direction of the cross product $n_a \times n_c$. Here n_i is the unit vector along the direction of motion of particle i, and q is the rank of the statistical tensors. The spin indices τ are defined in terms of these particular coordinate systems. With this choice of coordinate systems, the Euler angles for the rotation $g_c g_a^{-1}$ are $\{-\pi,\ \theta_c,\ \pi - \varphi_c\}$, where θ_c and φ_c are the spherical angles of the unit vector n_c in the z_a, y_a, x_a coordinate system (see Shirokov[2]).

Let the state obtained from the initial one by space reflection be characterized by the statistical tensor ρ_I'. Under the reflection the z_a and z_c axes, chosen along the momenta of particles a and c, change direction, while the y_a and y_c axes remain invariant. The spherical angles θ_{cI} and φ_{cI} of the reflected $-n_c$ vector in the reflected $\{z_a, y_a, x_a\}_I$ coordinate system are

$$\vartheta_{cI} = \vartheta_c, \quad \varphi_{cI} = -\varphi_c. \tag{2}$$

The spin operators remain invariant under reflection. If θ_c and φ_c are replaced by θ_{cI} and φ_{cI} in Eq. (1), we obtain the ρ_I' statistical tensors from ρ'; the spin indices τ of the new ρ_I' tensors must be quantized with respect to the old nonreflected z_c, y_c, x_c system. Since the reflected $\{z_c, y_c, x_c\}_I$ coordinate system differs from the initial one only by rotation through an angle π about the y_c axis, the transformation properties of the statistical tensors[2] lead to the equations

$$\rho_I'(q_c, \tau_c, q_d, \tau_d; \vartheta_c, -\varphi_c) = \sum_{\tau_c'\tau_d'} D^{q_c}_{\tau_c\tau_c'}(0, \pi, 0)\, D^{q_d}_{\tau_d\tau_d'}(0, \pi, 0) \times \rho'(q_c, \tau_c', q_d; \tau_d'; \vartheta_c, \varphi_c). \tag{3}$$

Here the spin indices τ are quantized with respect to their own proper coordinate systems. Since $D^q_{\tau\tau'}(0, \pi, 0) = (-1)^{q+\tau}\delta_{\tau,-\tau'}$ (see Shirokov[2] and Gel'fand and Shapiro[3]), Eq. (3) leads to

$$\rho_I'(q_c, \tau_c, q_d, \tau_d; \vartheta_c, -\varphi_c) = (-1)^{q_c+\tau_c+q_d+\tau_d}\rho'(q_c, -\tau_c, q_d, -\tau_d; \vartheta_c, \varphi_c). \tag{4}$$

The law of parity conservation may be stated in the following way: if the initial statistical tensors ρ are replaced by the reflected tensors ρ_I, the tensors ρ'' of the products of the reaction are the tensors ρ_I' which are obtained from ρ' by Eq. (4). In other words, if the statistical tensors ρ' are written $\rho' = F(\rho)$, then

$$\rho_I' = F(\rho_I). \tag{5}$$

Equations (4) and (5) together give the most general selection rules in the form of a relation between the statistical tensors.

Let us now consider some simple examples. If the initial state of the $a + b \rightarrow c + d$ reaction is unpolarized, then $\rho = \rho_I$. Then according to (4) and (5) $\rho' = \rho'_I$, or

$$\rho'(q_c, \tau_c, q_d, \tau_d; \vartheta_c) = (-1)^{q_c+\tau_c+q_d+\tau_d}\rho'(q_c, -\tau_c, q_d, -\tau_d; \vartheta_c). \tag{6}$$

In our case the ρ' tensors do not depend on φ_c Equations (6) are the same selection rules as Simon and Welton obtained for $q = 1$ and the same as those obtained by Shirokov.*

Let us now consider a cascade of the form $a + b \rightarrow c + d$ followed by $c + e \rightarrow f + g$ (the incident beam a, the target b, and e are unpolarized). According to (6), $\rho = \rho_I$ in the initial state of the second reaction, and we obtain

$$\rho'(q_f, \tau_f, q_g, \tau_g; \vartheta_f, -\varphi_f) = (-1)^{q_f+\tau_f+q_g+\tau_g}\rho'(q_f, -\tau_f, q_g, -\tau_g; \vartheta_f, \varphi_f). \tag{7}$$

For the special case in which $q_f = q_g = 0$, Eq. (7) becomes

$$\sigma(\vartheta_f, -\varphi_f) = \sigma(\vartheta_f, \varphi_f). \tag{8}$$

Since φ_f is the azimuth angle of n_f in the coordinate system in which the y_c axis is directed along $n_a \times n_c$, Eq. (8) states the well known fact that the angular distribution is symmetric about the production plane of the incident particle in the second reaction of the cascade. Equations (7) may be regarded as a generalization of this assertion.

In conclusion, we remark that our selection rules can also be obtained by Shirokov's method, but the present approach is simpler.

The author expresses his gratitude to Professors M. A. Markov, M. I. Shirokov, and L. G. Zastavenko for interest and discussion of the results.

---

*We remark that the first and second selection rules given by Shirokov are actually two different ways of stating the same rule.

[1] A. Simon and T. A. Welton, Phys. Rev. 90, 1036 (1953).

[2] M. I. Shirokov, J. Exptl. Theoret. Phys. (U.S.S.R.) 32, 1022 (1957), Soviet Phys. JETP 5, 835 (1952).

[3] M. I. Gel'fand and Z. Ia. Shapiro, Uspekhi Mat. Nauk 7, 3 (1952).

Translated by E. J. Saletan

ON THE QUESTION OF THE UNIQUENESS OF PHASE ANALYSIS

L. G. ZASTAVENKO

Joint Institute for Nuclear Research

Submitted to JETP editor May 5, 1958

J. Exptl. Theoret. Phys. (U.S.S.R.) 35, 785-787 (September, 1958)

MINAMI[1] has given a transformation of the scattering matrix which leaves the differential cross section invariant for the case in which the colliding particles have spins 0 and $\frac{1}{2}$. The present note gives an analog of this transformation for all spins s_1 and s_2 of the colliding particles.

We express the scattering matrix in terms of the functions ${}_{s_1s_2}Y^{jM}_{\alpha_1\alpha_2}(\mathbf{n})$ describing the state of a system of two particles whose total angular momentum is j. The component of j and the components of the spins of the two particles along the direction given by $\mathbf{n}$ are M, α_1, and α_2, respectively. In terms of these functions, the scattering matrix is[2,3]

$$M(\mathbf{n}_f, \mathbf{n}) = \sum_{\alpha jM} Y^{jM}_{\alpha_1\alpha_2}(\mathbf{n}_f)\,[Y^{jM}_{\alpha'_1\alpha'_2}(\mathbf{n}_i)]^*\,A^j_{\alpha_1\alpha_2\alpha'_1\alpha'_2},$$

$${}_{s_1s_2}Y^{jM}_{\alpha_1\alpha_2}(\mathbf{n}) = \sum_{s,l}\langle s_1\alpha_1s_2\alpha_2\,|\,s_1s_2sa\rangle \times \langle sal0\,|\,slja\rangle\sqrt{\frac{2l+1}{2j+1}}\;{}_{s_1s_2}Y^{jM}_{sl}(\mathbf{n})$$

Let $S(\mathbf{n})$ be a rotation that carries the vector $\mathbf{n}$ into the third axis, and consider the functions $\varphi_{\sigma_1\sigma_2}(\mathbf{n})$ whose components are

$$[\varphi_{\sigma_1\sigma_2}(\mathbf{n})]_{\alpha_1\alpha_2} = D^{s_1}_{\alpha_1\sigma_1}(S^{-1}(\mathbf{n}))\,D^{s_2}_{\alpha_2\sigma_2}(S^{-1}(\mathbf{n})),$$

where $D^j_{m_1m_2}(S)$ are the matrix elements of an irreducible representation of the three-dimensional rotation group.[4] These functions describe a state in which the first and second particles have spins whose components are σ_1 and σ_2, respectively, along $\mathbf{n}$.

The functions $Y^{jM}_{\alpha_1\alpha_2}(\mathbf{n})$ satisfy the relation

$$Y^{jM}_{\alpha_1\alpha_2}(\mathbf{n}) = \varphi_{\alpha_1\alpha_2}(\mathbf{n})\sqrt{\frac{2j+1}{4\pi}}\,D^j_{\alpha_1+\alpha_2,M}(S(\mathbf{n})),$$

so that the matrix element for the transition from the state $\varphi_{\alpha'_1\alpha'_2}(\mathbf{n}_i)$ to the state $\varphi_{\alpha_1\alpha_2}(\mathbf{n}_f)$ is*

$$(\alpha_1\alpha_2\,|\,M\,|\,\alpha'_1\alpha'_2) = \sum_j A^j_{\alpha_1\alpha_2\alpha'_1\alpha'_2} \times\sqrt{\frac{2j+1}{4\pi}}\,D^j_{\alpha_1+\alpha_2,\alpha'_1+\alpha'_2}(S(\mathbf{n}_f)\,S^{-1}(\mathbf{n}_i)). \tag{1}$$

Since $Y^{jM}_{\alpha_1\alpha_2}(-\mathbf{n}) = (-)^{s_1+s_2-j} Y^{jM}_{-\alpha_1-\alpha_2}(\mathbf{n})$, the condition that the matrix element be invariant under reflection requires that

$$A'^{j}_{\alpha_1\alpha_2\alpha'_1\alpha'_2} = A^{j}_{-\alpha_1-\alpha_2,\,-\alpha'_1-\alpha'_2}.$$

It is easily seen that the coefficients

$$A'^{j}_{\alpha_1\alpha_2\alpha'_1\alpha'_2} = \lambda_{\alpha_1\alpha_2}\lambda_{\alpha'_1\alpha'_2}A^{j}_{\alpha_1\alpha_2\alpha'_1\alpha'_2}, \qquad (2)$$

where each of the λ's are either +1 or −1, and satisfy the same unitary and symmetry conditions as do the $A^{j}_{\alpha_1\alpha_2\alpha'_1\alpha'_2}$.[5]

If, in addition, $\lambda_{-\alpha_1-\alpha_2} = k\lambda_{\alpha_1\alpha_2}$, where $k = \pm 1$ (if s_1 and s_2 are integers, $k = -1$ must be excluded, since the combinations of α's include one in which $\alpha_1 = \alpha_2 = 0$), the A′ coefficients can be used to construct the scattering matrix. It is seen from (1) that this matrix, although different from M, gives the same scattering cross section. It is easily shown that $M'(\mathbf{n}_f\mathbf{n}_i) = A(\mathbf{n}_f)M(\mathbf{n}_f\mathbf{n}_i)A^*(\mathbf{n}_i)$, where $A(\mathbf{n})$ is diagonal and has matrix elements $\lambda_{\alpha_1\alpha_2}$ in the coordinate system whose third axis lies along $\mathbf{n}$. Let us consider double scattering given by

$$\rho_{f2}(\mathbf{n}_{f2}\mathbf{n}_{i2}) = M(\mathbf{n}_{f2}\mathbf{n}_{i2})\,\rho_{i2}(\mathbf{n}_{i2})\,M^*(\mathbf{n}_{f2}\mathbf{n}_{i2}).$$

The M matrix is given on the center-of-mass coordinate system, so that the density matrix $\rho_{i2}(\mathbf{n}_{i2})$ of the initial state before the second scattering must also be given in this system, since it is obtained from the density matrix of the particle after the first scattering by the transformation $\rho_{i2}(\mathbf{n}_{i2}) = S\rho_{f1}(\mathbf{n}_{f1})S^*$. Here S is some rotation in the plane of the first scattering,[6] and $\mathbf{n}_{i2}$ and and $\mathbf{n}_{f1}$ are vectors related in the usual way. Now consider the density matrices ρ′ obtained from the scattering matrix by

$$M' = A(\mathbf{n}_f)\,M(\mathbf{n}_f\mathbf{n}_i)\,A^*(\mathbf{n}_i),$$
$$\rho'_{2f} = M'\rho'_{2i}M'^*,\ \ \rho'_{2i} = S\rho'_{1f}S^*,$$
$$\rho'_{1f}(\mathbf{n}_{f1}) = A(\mathbf{n}_{f1})\,\rho_{f1}(\mathbf{n}_{f1})\,A^*(\mathbf{n}_{f1}).$$

The cross section for double scattering is then given by

$$\sigma_2 \sim \mathrm{Sp}(MS\rho_{1f}S^*M^*);\ \ \sigma'_2 \sim \mathrm{Sp}(MS'\rho_{f1}S'^*M^*),$$

where $S' = A^*(\mathbf{n}_{i2})SA(\mathbf{n}_{f1})$.

If the spins of the particles involved are no greater than $\frac{1}{2}$, the transformations of Eq. (2) contain one for which $S'\rho_{f1}S'^* = \rho_{f1}$.[7] If at least one of the particles has spin greater than $\frac{1}{2}$, however, there is no such transformation among those given by (2). Thus for processes involving particles of spin greater than $\frac{1}{2}$, there is in general no arbitrariness such as that given by (2). An obvious exception is scattering by an infinitely heavy target, when $\mathbf{n}_{i2} = \mathbf{n}_{f1}$ and $S = 1$; in this case there is no multiplicity of scattering which can be used to differentiate between the set of phases given by (2).

In conclusion, I express my gratitude to Professor M. A. Markov, Professor Ia. A. Smorodinskii, R. M. Ryndin, M. I. Shirokov, and Chou Kuang-Chao for discussion of the work and valuable comments.

---

*We note that the cross section and tensor moments are easily expressed in terms of the parameters $A^{j}_{\alpha_1\alpha_2\alpha'_1\alpha'_2}$ and generalized spherical functions[4] without the use of Racah coefficients.

---

[1] S. Minami, Progr. Theoret. Phys. **11**, 213 (1954).

[2] Berestetskii, Dolginov, and Ter-Martirosian, J. Exptl. Theoret. Phys. (U.S.S.R.) **20**, 527 (1950).

[3] R. Van Wageningen and H. J. Groenewold, Physica **23**, 720 (1957).

[4] I. M. Gel'fand and Z. Ia. Shapiro, Usp. Matem. Nauk **7**, 3 (1952).

[5] J. Blatt and V. Weisskopf, Theoretical Nuclear Physics (Russian Translation)(IIL, M., 1954), p. 415. [N. Y., Wiley, 1952.]

[6] M. I. Shirokov and Chou Kuang Chao, J. Exptl. Theoret. Phys. (U.S.S.R.) **34**, 1230 (1958), Soviet Phys. JETP **7**, 851 (1958).

[7] Zastavenko, Ryndin, and Chou Kuang-Chao, J. Exptl. Theoret. Phys. (U.S.S.R.) **34**, 526 (1958), Soviet Phys. JETP **7**, 363 (1958).

Translated by E. J. Saletan
155

COMPUTING THE SPECTRA OF FISSION NEUTRONS

V. P. KOVALEV, V. S. STAVINSKII

Submitted to JETP editor May 10, 1958

J. Exptl. Theoret. Phys. (U.S.S.R.) 35, 787-789 (September, 1958)

USACHEV,[1] Watt,[2] Fraser,[3] and Gurevich and Mukhin[4] have studied the theoretical interpretation of fission neutron spectra. These authors used a model in which the neutrons are assumed to be evaporated from the moving fission fragments. In the center-of-mass system the spectrum of neutrons evaporated from a fragment whose excitation energy is E_0 is of the form

$$n(\varepsilon) \sim \sigma(\varepsilon, E_0)\,\varepsilon\omega(E_0 - \varepsilon).$$

Here ϵ is the kinetic energy of the neutron, $\sigma(\epsilon, E_0)$ is the cross section for capture of a neutron with energy ϵ by fragments whose energy is $E_0 - \epsilon$, and $\omega(E_0 - \epsilon)$ is the energy level density of a fragment at an excitation energy of $E_0 - \epsilon$. In the works cited above the level density was assumed proportional to $\exp(-\epsilon/\tau)$, where τ is the temperature of the fragment. Satisfactory agreement with experiment was attained by properly choosing the value of τ, Watt[2] and Gurevich and Mukhin[4] assuming that $\sigma(\epsilon, E_0) \sim 1/\sqrt{\epsilon}$, while Usachev[1] and Fraser[3] assume $\sigma(\epsilon, E_0)$ to be independent of both ϵ and E_0. Such a choice of $\sigma(\epsilon, E_0)$ is valid, however, only when the neutrons are captured by unexcited nuclei.

In the present note we calculate the fission neutron spectra taking account of the energy dependence of the neutron capture cross section. The energy dependence of $\sigma(\epsilon, E_0)$ was calculated by the complex-potential method,[5] which gives a satisfactory description of the total cross section and capture cross section for low energy neutrons interacting with nuclei. It was assumed that the imaginary part of the potential increases when ϵ is decreased, since to low values of ϵ correspond large excitation energies of the target nucleus, so that the Pauli principle, which weakens the energy exchange between the incident neutrons and the target nuclei, plays a lesser role. Further, since the fragments are so overloaded with neutrons, we may assume that the imaginary part of the potential for fission fragments is greater than the experimentally observed value for ordinary nuclei. Therefore $\sigma(\epsilon, E_0)$ may be evaluated by using the model of a "black" nucleus.[6]

In calculating $\sigma(\epsilon, E_0)$ we must make sure that the potential varies smoothly at the boundary of the nucleus. This can be done by using the approximate expression $\sigma(\epsilon) = \sigma_0(\epsilon) T_d(\epsilon)/T_0(\epsilon)$. Here $\sigma(\epsilon)$ is the cross section we wish to obtain, $\sigma_0(\epsilon)$ is the neutron capture cross section by a "black" nucleus with a sharp potential change[6] at the boundary, $T_0(\epsilon)$ is the penetration transmission coefficient of the neutron wave for this potential, and $T_d(\epsilon)$ is this coefficient for a smoothly varying potential of the form

$$V(x) = -V_0/[1 + \exp(-2x/d)],$$

where $-\infty < x < \infty$, $v_0 = 42$ Mev, and $d = 1.4 \times 10^{-13}$ cm.

The table gives $T_d(\epsilon)/T_0(\epsilon)$ and $\sigma(\epsilon)\epsilon^{1/2}$, which characterizes the deviation of $\sigma(\epsilon)$ from the $1/\sqrt{\epsilon}$ law.

ε, Mev	$T_d(\varepsilon)/T_0(\varepsilon)$	$\sigma(\varepsilon)\,\varepsilon^{1/2}$ barn-Mev$^{1/2}$
0.1	2.55	1.83
0.2	2.50	1.83
0.3	2.40	1.99
0.4	2.30	2.05
0.5	2.20	2.12
0.75	2.02	2.28
1.0	1.89	2.44
1.5	1.74	2.59
2.0	1.63	2.68
2.5	1.55	2.94
3.0	1.49	3.19
5.0	1.34	4.03
10.0	1.18	5.70

It is interesting to note that the energy dependence obtained for the inverse process is close to the $1/\sqrt{\epsilon}$ law up to an energy of about 1 Mev. which is a qualitative verification of this ϵ dependence chosen by Usachev[1] and Fraser.[3]

In calculating the spectra it was assumed that the most probable fission mode occurs, that the neutrons are emitted isotropically in the center-of-mass system of the moving fragments,[1–4] and that the level density obeys Weisskopf's law $\omega(\epsilon) \sim \exp(2\sqrt{aE})$ over the whole interval of excitation energy,[6] with $a = 0.1\,A$, where A is the atomic weight of the fragment.

The mean excitation energy $E_{L,H}$ was calculated using the relation[7,8] $d\nu/dE = 0.12$ Mev^{-1} and Fraser's[3] relation $\nu_L/\nu_H = 1.3$. Here ν_L and ν_H are the mean numbers of neutrons emitted by the light and heavy fragments, respectively. The mean energy of the accompanying gammas was taken as 7.8 Mev, and was distributed equally between the two fragments.[9]

These assumptions were used to calculate the fission neutron spectra of U^{235} and Cf^{252} The spectra of the "first" and "second" neutrons from an individual fragment in the laboratory system were calculated using the formula

$$N_{L,H}(E) \sim \int_{E(1-\sqrt{\omega_{L,H}/E})^2}^{E(1+\sqrt{\omega_{L,H}/E})^2} \sigma_{L,H}(\varepsilon)\,\varepsilon^{1/2}$$

$$\times \exp\{2\sqrt{a_{L,H}[\bar{E}_{L,H} - E^B_{L,H} - \varepsilon]}\}\,d\varepsilon.$$

Here $\omega_{L,H}$ is the mean kinetic energy per nucleon of a fragment, and $E^B_{L,H}$ is the neutron binding energy in the fragment.[9,10] The mean excitation energy of a fragment after emission of the first neutron is given by $\bar{E}'_{L,H} = \bar{E}_{L,H} - E^B_{L,H} - \bar{\epsilon}_{L,H}$, where $\bar{\epsilon}_{L,H}$ is the mean kinetic energy of the first neutron. The theoretical calculations for U^{235} are in good agreement with the experimental data.[8,11] Comparing our results with the curve given by $N(E) \sim \exp(-E/0.965)\sinh\sqrt{2.29E}$, which is the best approximation of the observed[8] fission neutron spectrum from U^{235}, we find no deviations greater than 7 per cent up to an energy of about 7 Mev. The agreement with experiment is also satisfactory for Cf^{252}, although the experimental accuracy is not high.[12] Similar results can be obtained assuming that $\omega(\epsilon) \sim \exp(-\epsilon/\tau_{L,H})$, where $\tau_{L,H}$ are the temperatures of the fragments which correspond to their mean excitation energies. These temperatures can be calculated using the formula

$$\tau_{L,H} = \left[\frac{\bar{E}_{L,H} - E^{B}_{L,H} - \bar{\varepsilon}_{L,H}}{a_{L,H}}\right]^{1/2},$$

and for U^{235} fragments we obtain $\tau_L \sim 1$ Mev and $\tau_H \sim 0.8$ Mev.

The authors express their gratitude to A. I. Leipunskii for his interest in the work and discussion of the results, to I. I. Bondarenko and L. N. Usachev for many critical remarks, and to V. P. Kharin for performing the numerical calculations.

---

[1] L. N. Usachev, Отчет АН СССР, 1950 (Report, Acad. Sci. U.S.S.R., 1950).

[2] B. Watt, Phys. Rev. **87**, 1037 (1952).

[3] J. S. Fraser, Phys. Rev. **88**, 536 (1952).

[4] I. I. Gurevich and K. N. Mukhin, Отчет АН СССР, 1951 (Report, Acad. Sci. U.S.S.R., 1951). See Supplement No. 1 to Атомная энергия (Atomic Energy) (1957).

[5] Feshbach, Porter, and Weisskopf. Phys. Rev. **96**, 448 (1955).

[6] J. Blatt and V. Weisskopf, Theoretical Nuclear Physics (Russian Translation)(M., IIL, 1954) Ch. 8, Sections 4-6. [N.Y., Wiley, 1952].

[7] Smirenkin, Bondarenko, Kutsaeva, Mishchenko, Prokhorova, and Shemetenko, Атомная энергия (Atomic Energy) **4**, No. 2, 188 (1958).

[8] R. B. Leachman, Report No. 592 to the Conference on the Peaceful Uses of Atomic Energy, Geneva, 1955.

[9] R. B. Leachman, Phys. Rev. **101**, 1005 (1956).

[10] Smith, Fields, and Friedman, Phys. Rev. **106**, 779 (1957).

[11] V. P. Kovalev, J. Exptl. Theoret. Phys. (U.S.S.R.) **34**, 501 (1958), Soviet Phys. JETP **7**, 345 (1958).

[12] Hjalmar, Slätis, and Thompson, Phys. Rev. **100**, 1542 (1955).

Translated by E. J. Saletan
156

THE POSSIBILITY OF ESTIMATING THE MEAN LIFETIME OF ALPHA PARTICLES WITHIN NUCLEI

Iu. I. SEREBRENNIKOV

Leningrad Polytechnic Institute

Submitted to JETP editor May 21, 1958

J. Exptl.Theoret. Phys. (U.S.S.R.) **35**, 789-791 (September, 1958)

It has often been shown[1-6] that α-particle substructures and others exist within the nucleus. According to the references cited, these substructures participate in nuclear cascade processes and can be knocked out of a nucleus by a fast particle passing through it. Cuër, Combe, and Samman[1-5] assumed that these substructures are unstable in nuclei. Combe[4] considers their lifetimes to be probably of the order of 10^{-22} sec. If this is so, it may be possible to obtain experimental indications as to their mean lifetimes. Let us consider knockout of α particles from nuclei.

If the α particles are stable within the nucleus, then the energy spectrum with which they are knocked out will be given by $N(E) = f(E)P(E)$, where $f(E)$ is the recoil-energy distribution function of the α-particles within the nucleus for positive E, and $P(E)$ is the Coulomb barrier penetration factor for the α particles. If the α particles are unstable within the nucleus with a mean lifetime τ_α of the order of 10^{-22} sec, the expression for $N(E)$ should contain a factor which accounts for their disintegration during the time they move within the nucleus. If this disintegration can be described by an exponential law of the form $N = N_0 \exp(-t_{\text{eff}}/\tau_\alpha)$, the knockout α-particle energy spectrum will be of the form

$$N(E) = f(E)P(E) \exp\{-[m_\alpha/2(E+U)]^{1/2} l/\tau_\alpha\}, \tag{1}$$

where $t_{\text{eff}} = l/v$ is the time it takes an α-particle which attains the velocity v at the point of collision to move through the shortest distance l to the surface of the nucleus. This distance l should be chosen from the condition that in a spherical shell of thickness l low-energy recoil α particles can be produced efficiently and can leave the nucleus with the least possible losses due to disintegration. In the above equation m_α

is the mass of the α particle, and U is the depth of the potential well.

Let us evaluate the exponent of Eq. (1) with $\tau_\alpha = 10^{-22}$ sec and for an energy E equal to the height of the Coulomb barrier U_c; we shall treat nuclei in which U is known. For C^{12} nuclei,[5] $U \approx 11$ Mev. For different nuclei the distance l can be chosen about equal to the α-particle diameter. For C^{12} we have $l \approx R = 1.4 \times 10^{-13} A^{1/3}$ cm and $U_c \approx 4$ Mev. With these assumptions the exponent for C^{12} is 1.2. For silver nuclei, we again set $E = U_c$ and assume that $l(\mathrm{Ag}) = l(C^{12})$ and $U(\mathrm{Ag}) \approx U(C^{12})$; the exponent is then -0.8.

These values of the exponents indicate that if $\tau_\alpha = 10^{-22}$ sec, the α-particle spectrum given by (1) should be measurably weakened in the energy region around $E = U_c$.

The situation changes drastically if τ_α is actually somewhat less than 10^{-22} sec. A lifetime smaller by a factor of 2 or 2.5 is sufficient to decrease the exponent for C^{12}, for instance, to 0.05 for $E = U_c$. Then for this energy there should be practically no α-particles knocked out, and they should appear in measurable quantities only for $E \geq E_{\alpha\,\mathrm{eff}} > U_c$.

Now 10^{-22} sec is the time it takes a 20-Mev nucleon in the nucleus to pass entirely through a C^{12} nucleus. It is very probable that internal α-particles can be destroyed in collisions with fast nuclei located in their vicinity when they are formed. There is therefore reason to suppose that τ_α is considerably less than 10^{-22} sec. If this is so, experiment should observe almost the complete absence of α particles knocked out in the energy region $U_c(A) < E < E_{\alpha\,\mathrm{eff}}$. An experimental determination of $E_{\alpha\,\mathrm{eff}}$ could be used to estimate τ_α.

It should be noted that this effect is more probably observable for nuclei with A around 12 or 20 than for nuclei with A around 100, since there may be quite a large number of α particles produced in the latter in a shell with low l.

Deuteron knockout will be observed if τ_d is less than τ_α, for if we consider deuterons with energy $E = U_c$ and set $U \approx 30$ Mev,[6] $l(d) = l(\alpha)$, and $\tau_d = 10^{-22}$ sec, the exponent in Eq. (1) becomes -0.6.

---

[1] P. Cüer and J. Combe, J. phys. et radium **16**, 29 (1955).

[2] J. Combe, J. phys. et radium **16**, 445 (1955).

[3] Cüer, Combe, and Samman, Compt. rend. **240**, 75, 1527 (1955).

[4] J. Combe, Suppl. No. 2, Nuovo cimento **3**, 182 (1956).

[5] A. Samman, Compt. rend. **242**, 2232, 3062 (1956).

[6] Azhgirei, Vzorov, Zrelov, Meshcheriakov, Neganov, and Shabudin, J. Exptl. Theoret. Phys. (U.S.S.R.) **33**, 1185 (1957), Soviet Phys. JETP **6**, 1911 (1958).

Translated by E. J. Saletan
157

NONLOCAL EFFECTS IN WEAK INTERACTIONS OF FERMIONS

S. G. MATINIAN

Physics Institute, Academy of Sciences,
Georgian SSR

Submitted to JETP editor May 23, 1958

J. Exptl. Theoret. Phys. (U.S.S.R.) **35**, 791-793 (September, 1958)

RECENTLY Lee and Yang[1] have studied the nonlocal four-Fermion interactions as applied to μ decay. Phenomenologically these interactions can be described using a Lagrangian corresponding to the interaction of pairs of fermions separated by a space-like interval of the order of 10^{-13} to 10^{-14} cm.

The present communication gives a similar treatment of nonlocal effects in μ^- capture by a proton. The neutrino is described by the two-component theory.[2-4]

1. The nonlocal Lagrangian for the interaction which gives rise to the $\mu^- + p \rightarrow n + \nu$ reaction is

$$L = \sum_i g_i \int [\bar{\psi}_n(x) O_i \psi_p(x)] K_i(x - x') \times [\bar{\psi}_\nu(x') O_i \psi_\mu(x')] d^4x d^4x'; \; \psi_\nu = -\gamma_5 \psi_\nu. \tag{1}$$

In this expression the summation is taken over all possible S, V, T, P, and A couplings; the O_i are the appropriate Dirac matrices, and $K_i(x - x')$ is an invariant function of $x - x'$ which accounts for the nonlocal extension of the interaction. Assuming that the space-time extension of $K_i(x - x')$ is smaller than the inverse of the energy momentum transfer involved in the process, we can write

$$K_i(x - x') = \delta^4(x - x') + \frac{\varkappa_i}{m^2} \frac{\partial^2}{\partial x_\lambda^2} \delta^4(x - x') + \ldots, \tag{2}$$

$$(i = S, V, T, P, A; \; \hbar = c = 1),$$

where m is the mass of the μ meson, and $|\kappa_i / m^2|^{1/2}$ is the length characterizing the nonlocal effect.* Using Eq. (2) and treating the case of the μ meson and proton at rest, we obtain

$$L = \sum_i g_i \int [1 + \varkappa_i (1 - 2p_\nu / m)] [\bar{\psi}_n O_i \psi_p] [\bar{\psi}_\nu O_i \psi_\mu] \, d^4x, \tag{3}$$

where p_ν is the neutrino momentum.

From this we immediately obtain an expression for $1/\tau$, the probability of μ^- capture by hydrogen, and an expression for $w(\theta)$, the angular distribution of the neutrons in the capture of polarized μ^- mesons.[6-8] These expressions are

$$1/\tau = p_\nu^2 \xi / 2\pi^2 a^3, \quad w(\theta) = 1 + \alpha \cos\theta, \tag{4}$$

where a is the Bohr radius of the muonium atom, θ is the angle between the spin of the μ^- meson and the neutron momentum, and

$$\begin{aligned} \xi &= |f_S + f_V|^2 + 3|f_A + f_T|^2, \\ \alpha\xi &= -|f_S + f_V|^2 + |f_A + f_T|^2, \\ f_i &= g_i [1 + \varkappa_i (1 - 2p_\nu / m)]. \end{aligned} \tag{5}$$

For the $\mu^- + p \rightarrow n + \tilde{\nu}$ reaction, ξ by ξ', and $\alpha\xi$ are replaced by $-\alpha'\xi'$.

2. Let us assume the existence of a universal AV interaction.[9] As is known, it is then possible to choose the coupling constant G for β decay so as to obtain excellent agreement with experiment for the μ meson lifetime.

It is easily shown, however, that nonlocal effects in β decay are quite negligible. If such effects actually exist, they should be observed in μ decay, by a definite change in the coupling constant.

For the universal AV interaction in μ decay, Feynman and Gell-Mann take the expression

$$8^{1/2} G (\bar{\psi}_\mu \gamma_\lambda a \psi_\nu)(\bar{\psi}_\nu \gamma_\lambda a \psi_e), \tag{6}$$

where $a\psi$ is a two-component wave function, and $G = (1.01 \pm 0.01) 10^{-5}/M^2$ (where M is the mass of the nucleon). The μ-meson lifetime is then given by

$$1/\tau_\mu = G^2 m^5 / 192\pi^3.$$

The nonlocal interaction corresponding to (6), namely

$$8^{1/2} G (\bar{\psi}_\mu \gamma_\lambda a \psi_\nu (x)) K (x - x') (\bar{\psi}_\nu \gamma_\lambda a \psi_e (x')) \tag{7}$$

(this corresponds to Lee and Yang's[1] Lagrangian L_{II}) gives

$$1/\tau_\mu = (G^2 m^5 / 192\pi^3)(1 + {}^3/_5 \bar{\zeta}_2),$$

for the μ-meson lifetime, where ζ_2 is a parameter characterizing the nonlocal effects, introduced by Lee and Yang.[1] Bearing in mind the experimental uncertainty in the determination of G, we obtain an upper limit for $|\bar{\zeta}_2|$ compatible with the universality of G. This is

$$|\bar{\zeta}_2| \leqslant 0.07. \tag{8}$$

Lee and Yang (using the nonlocal Lagrangian L_{II}) have found the value of $\bar{\zeta}_2$ for which the two-component theory will give a Michel parameter ρ in agreement with experiment. This value is $\bar{\zeta}_2 = -0.21$, which is too large by a factor of three.

It should be noted that if the nonlocal effects (with $\bar{\zeta}_2 > 0$) are attributed to the propagation of a heavy virtual particle, its mass M_0 must, according to (8), satisfy the inequality $M_0 \geq \sqrt{14}\, m$.

The formulas given in Sec. 1 for the nonlocal interaction in the capture of a μ^- meson by a proton may be useful in establishing the magnitude of κ, which characterizes the length involved in the nonlocal effects, if there exists a universal AV interaction.

Radiative μ^- capture $(\mu^- + p \rightarrow n + \nu + \gamma)$ may in general be helpful in establishing κ_i.

In conclusion, I take this opportunity to express my gratitude to Professor G. R. Khutsishvili for interest in the work and to Iu. G. Mamaladze for discussion of the results.

---

*We note that if the nonlocal effects are assumed to be caused by virtual π mesons, the capture probabilities obtained fail to agree with experiment.[5]

[1] T. D. Lee and C. N. Yang, Phys. Rev. **108**, 1611 (1957).

[2] L. Landau, Nuclear Phys. **3**, 127 (1957).

[3] A. Salam, Nuovo cimento **5**, 299 (1957).

[4] T. D. Lee and C. N. Yang, Phys. Rev. **105**, 1671 (1957).

[5] J. Lopes, Phys. Rev. **109**, 509 (1958).

[6] B. L. Ioffe, J. Exptl. Theoret. Phys. (U.S.S.R.) **33**, 308 (1957), Soviet Phys. JETP **6**, 240 (1958).

[7] Shapiro, Dolinsky, and Blokhintsev, Nuclear Phys. **4**, 273 (1957).

[8] Huang, Yang, and Lee, Phys. Rev. **108**, 1340 (1957).

[9] R. P. Feynman and M. Gell-Mann, Phys. Rev. **109**, 193 (1958).

Translated by E. J. Saletan
158

EQUATIONS OF MOTION FOR A SYSTEM CONSISTING OF TWO TYPES OF INTERACTING SPINS

G. V. SKROTSKII

Ural' Polytechnic Institute

Submitted to JETP editor May 26, 1958

J. Exptl. Theoret. Phys. (U.S.S.R.) 35, 793-794 (September, 1958)

SOLOMON[1] has found the equations of motion describing the magnetization of a system consisting of two types of interacting magnetic moments in parallel fields. Kurbatov and the author[2] have investigated the thermodynamic properties of a two-spin system, including the spin-spin and spin-lattice relaxations. The present note gives a simple thermodynamic derivation of the equations describing the behavior of such a system in a constant field H_0 arbitrarily oriented with respect to an alternating field $\mathbf{h}$.

We shall start with the equations

$$\dot{M}_k^{(1)} = L_{ik}^{11}(H_l - H_l^{(1)}) + L_{ik}^{12}(H_l - H_l^{(2)}),$$
$$\dot{M}_k^{(2)} = L_{ik}^{21}(H_l - H_l^{(1)}) + L_{ik}^{22}(H_l - H_l^{(2)}), \tag{1}$$

where $\mathbf{H}^{(1)}$ and $\mathbf{H}^{(2)}$ are related to the magnetizations $\mathbf{M}^{(1)}$ and $\mathbf{M}^{(2)}$ of the spin subsystems by

$$\mathbf{M}^{(1)} = \chi_{01}\mathbf{H}^{(1)}, \quad \mathbf{M}^{(2)} = \chi_{02}\mathbf{H}^{(2)}. \tag{2}$$

The L_{ik} satisfy the Onsager relations. Assuming that in the absence of a field the medium is isotropic, we write

$$L_{ik}^{11} = \frac{\chi_{01}}{\tau_1}\delta_{ik} + \gamma_1\chi_{01}\varepsilon_{ikl}H_0; \quad L_{ik}^{12} = \frac{\chi_{02}}{\tau}\delta_{ik},$$
$$L_{ik}^{21} = \frac{\chi_{01}}{\tau}\delta_{ik}; \quad L_{ik}^{22} = \frac{\chi_{02}}{\tau_2}\delta_{ik} + \gamma_2\chi_{02}\varepsilon_{ikl}H_0, \tag{3}$$

where γ_1 and γ_2 are the gyromagnetic ratios for the spin subsystems, ϵ_{ikl} is the unit antisymmetric tensor, and $\mathbf{H} = \mathbf{H}_0 + \mathbf{h}(t)$. Equations (1) now become*

$$\dot{\mathbf{M}}_1 + \mathbf{M}_1/\tau_1 + \mathbf{M}_2/\tau = (\chi_{01}/\tau_1 + \chi_{02}/\tau)\mathbf{H} + \gamma_1[\mathbf{M}_1\times\mathbf{H}],$$
$$\dot{\mathbf{M}}_2 + \mathbf{M}_2/\tau_2 + \mathbf{M}_1/\tau = (\chi_{01}/\tau + \chi_{02}/\tau_2)\mathbf{H} + \gamma_2[\mathbf{M}_2\times\mathbf{H}]. \tag{4}$$

In the absence of a transverse rf field in the steady state, as may have been expected, these equations lead to the relations given by (2).

For parallel fields, i.e., if $[\mathbf{H}_0 \times \mathbf{h}(t)] = 0$, Eqs. (4) are the same as those obtained by Solomon. If the second subsystem is missing, they become

$$\dot{\mathbf{M}} + \mathbf{M}/\tau = (\chi_0/\tau)\mathbf{H} + \gamma[\mathbf{M}\times\mathbf{H}].$$

Let us now require that $\mathbf{M}^{(1)}$ and $\mathbf{M}^{(2)}$ are of equal magnitudes; then multiplying Eqs. (4) by $\mathbf{M}^{(1)}$ and $\mathbf{M}^{(2)}$, respectively, we obtain

$$\frac{\mathbf{M}_1^2}{\tau_1} + \frac{(\mathbf{M}_1\cdot\mathbf{M}_2)}{\tau} = \left(\frac{\chi_{01}}{\tau_1} + \frac{\chi_{02}}{\tau}\right)(\mathbf{M}_1\cdot\mathbf{H}),$$
$$\frac{\mathbf{M}_2^2}{\tau_2} + \frac{(\mathbf{M}_1\cdot\mathbf{M}_2)}{\tau} = \left(\frac{\chi_{01}}{\tau} + \frac{\chi_{02}}{\tau_2}\right)(\mathbf{M}_2\cdot\mathbf{H}). \tag{5}$$

Eliminating χ_{01} and χ_{02} from (4) and (5), we obtain

$$\dot{\mathbf{M}}_1 = \gamma_1[\mathbf{M}_1\times\mathbf{H}] - \frac{\lambda_{11}}{M_1^2}[\mathbf{M}_1\times[\mathbf{M}_1\times\mathbf{H}]] - \frac{\lambda_{12}}{(\mathbf{M}_1\cdot\mathbf{M}_2)}[\mathbf{M}_1\times[\mathbf{M}_2\times\mathbf{H}]],$$
$$\dot{\mathbf{M}}_2 = \gamma_2[\mathbf{M}_2\times\mathbf{H}] - \frac{\lambda_{22}}{M_2^2}[\mathbf{M}_2\times[\mathbf{M}_2\times\mathbf{H}]] - \frac{\lambda_{21}}{(\mathbf{M}_1\cdot\mathbf{M}_2)}[\mathbf{M}_2\times[\mathbf{M}_1\times\mathbf{H}]], \tag{6}$$

where

$$\lambda_{11} = M_1^2/\tau(\mathbf{M}_1\cdot\mathbf{H}); \quad \lambda_{12} = (\mathbf{M}_1\cdot\mathbf{M}_2)/\tau(\mathbf{M}_1\cdot\mathbf{H});$$
$$\lambda_{21} = (\mathbf{M}_1\cdot\mathbf{M}_2)/\tau(\mathbf{M}_2\cdot\mathbf{H}); \quad \lambda_{22} = M_2^2/\tau(\mathbf{M}_2\cdot\mathbf{H}). \tag{7}$$

If $\lambda_{12} = \lambda_{21} = 0$ (that is in the limit as $\tau \to \infty$), Eqs. (6) go over into the Landau-Lifshitz equations for two noninteracting spin systems. They can be used to describe relaxation processes and resonance phenomena in antiferromagnets.

---

*Henceforth we shall write the indices denoting the subsystems as subscripts.

---

[1] I. Solomon, Phys. Rev. 99, 559 (1955).

[2] G. V. Skrotskii and L. V. Kurbatov, Izv. Akad. Nauk SSSR, Ser. Fiz. 21, 833 (1957) [Columbia Techn. Transl. 21, 833 (1957)].

[3] G. V. Skrotskii and V. T. Shmatov, Изв. высших учебн. завед., физика (Bulletin of the Higher Inst. of Study, Physics) 2, 138 (1958).

Translated by E. J. Saletan
159

CLEBSCH-GORDAN EXPANSION FOR INFINITE-DIMENSIONAL REPRESENTATIONS OF THE LORENTZ GROUP

A. Z. DOLGINOV and I. N. TOPTYGIN

Leningrad Physics and Engineering Institute, Academy of Sciences, U.S.S.R.

Submitted to JETP editor May 29, 1958

J. Exptl. Theoret. Phys. (U.S.S.R.) 35, 794-796 (September, 1958)

ONE of the authors has given[1] the explicit form of the Clebsch-Gordan coefficients for the expansion of the finite-dimensional representations of the Lorentz group. If one choose the basis functions of the finite-dimensional representation to be

$$\psi_{Nlm}(\alpha\vartheta\varphi)=\frac{\sinh^{l}\alpha}{\sqrt{N^2(N^2-1^2)\ldots(N^2-l^2)}}\frac{d^{l+1}\cosh N\alpha}{d\cosh^{l+1}\alpha}Y_{lm}(\vartheta\varphi),$$

$$t=\rho\cosh\alpha,\ r=\rho\sinh\alpha,\ 0\leqslant\alpha\leqslant\infty,$$

$$-\infty\leqslant\rho\leqslant\infty,\ N=0,1,2,\ldots,\tag{1}$$

the expansion has the form

$$\psi_{N_1l_1m_1}\psi_{N_2l_2m_2}=\sum_{N,l}\sqrt{\frac{N_1N_2}{4\pi N}}A(N_1l_1N_2l_2Nl)C^{lm}_{l_1m_1l_2m_2}\psi_{Nlm},\tag{2}$$

$$A(N_1l_1N_2l_2Nl)\equiv N\sqrt{(2l_1+1)(2l_2+1)}X(j_1j_1l_1,\ j_2j_2l_2,\ jjl);$$

$2j_i + 1 = N_i$, and X are the Fano functions.[2] It was mentioned that if one replaces N by in, where n is real and $0 \le n \le \infty$, Eq. (1) gives the basis functions of one of the irreducible unitary infinite-dimensional representations of the Lorentz group:

$$\psi_{nlm}(\alpha,\vartheta,\varphi)=\frac{\sinh^{l}\alpha}{\sqrt{n^2(n^2+1)\ldots(n^2+l^2)}}\frac{d^{l+1}\cos n\alpha}{d\cosh^{l+1}\alpha}Y_{lm}(\vartheta,\varphi).\tag{3}$$

The functions ψ_{nlm} are orthogonal and are normalized by the condition

$$\int\limits_0^\infty\sinh^2\alpha d\alpha\int d\Omega\psi^*_{n_1l_1m_1}(\alpha,\vartheta,\varphi)\psi_{n_2l_2m_2}(\alpha,\vartheta,\varphi)$$
$$=\frac{\pi}{2}\delta(n_1-n_2)\delta_{l_1l_2}\delta_{m_1m_2}.\tag{4}$$

Let us find the Clebsch-Gordan expansion for the ψ_{nlm}. We shall look for an expansion of the form

$$\psi_{n_1l_1m_1}\psi_{n_2l_2m_2}=\sum_l\int\limits_0^\infty dni^{l-l_1-l_2}\sqrt{in_1n_2/4\pi n}\,C^{lm}_{l_1m_1l_2m_2}$$
$$\times B(n_1n_2n,\ l_1l_2l)A(n_1l_1n_2l_2nl)\psi_{nlm}.\tag{5}$$

$A(n_1l_1n_2l_2nl)$ is expressed in terms of j_1, j_2 and j exactly as in the case of Eq. (2), except that instead of using integer or half-integer values of j_1, j_2 and j, we must take

$$j_1={}^1/_2(in_1-1),\ j_2={}^1/_2(in_2-1)\ \text{and}\ j={}^1/_2(in-1).$$

The recursion relations for the ψ_{nlm} enable us to obtain equations relating the $B(n_1n_2n,\ l_1l_2l)$ for different values of l_1, l_2 and l. These equations are satisfied if $B(n_1n_2n,\ l_1l_2l) \equiv B(n_1n_2n)$ does not depend on l_1, l_2 and l:

$$B(n_1n_2n)=\sinh\pi n_1\sinh\pi n_2\sinh\pi n\Big[\cosh\frac{\pi}{2}(n_1+n_2+n)$$
$$\times\cosh\frac{\pi}{2}(n_1-n_2-n)\cosh\frac{\pi}{2}(n_1+n_2-n)\tag{6}$$
$$\times\cosh\frac{\pi}{2}(n_1-n_2+n)\Big]^{-1}.$$

Using the fact that

$$\sum_{l_1l_2}A(n_1l_1n_2l_2nl)A(n_1l_1n_2l_2n'l)=\delta(n-n'),$$
$$A(n_10n_20n0)=\sqrt{n/in_1n_2},\tag{7}$$

we get the inverse Clebsch-Gordan series:

$$\psi_{nlm}=\sqrt{4\pi n/in_1n_2}[B(n_1n_2n)]^{-1}\sum_{l_1l_2m_1m_2}i^{l_1+l_2-l}$$
$$\times A(n_1l_1n_2l_2nl)C^{lm}_{l_1m_1l_2m_2}\psi_{n_1l_1m_1}\psi_{n_2l_2m_2}.\tag{8}$$

For complex n, formula (3) gives the basis functions of an infinite-dimensional irreducible non-unitary representation. Such functions occur in the expansion of the product of (1) and (3) in a Clebsch-Gordan series:

$$\psi_{nl_1m_1}\psi_{Nl_2m_2}=\sum_{l,\nu}i^{l_1-l}\sqrt{nN/4\pi\nu}A(n_1l_1Nl_2\nu l)C^{lm}_{l_1m_1l_2m_2}\psi_{\nu lm},\tag{9}$$
$$\nu=n_1-i\varkappa;\ \varkappa=-N+1,\ -N+2,\ldots,N-1;$$
$$i\nu=2j+1,\ N=2j_2+1.$$

Using Eqs. (22) and (29) of reference 1 and Eq. (9), one can obtain the expansion of derivatives of the ψ_{nlm} in terms of irreducible representations:

$$\partial_{\alpha\beta}G_n(\rho)\psi_{nlm}=\sum_{\nu,f,L}i^{l-L}\sqrt{(2f+1)n/2\nu}\,C^{\frac{1}{2}\alpha}_{\frac{1}{2}\beta f-\varphi},$$
$$\times C^{L\Lambda}_{lmf\varphi}A(nl,2f,\nu L)\left[\frac{\partial}{\partial\rho}-\varkappa\frac{in-\varkappa}{\rho}\right]G_n(\rho)\psi_{\nu L\Lambda},\tag{10}$$

$i\nu = in + \kappa$, $\kappa = \pm 1$, $G_n(\rho)$ depends only on ρ, $\partial_{\pm1/2,\pm1/2} = \partial/\partial t \mp \partial/\partial z$, $\partial_{\pm1/2,\mp1/2} = \pm(\partial/\partial x \mp i\partial/\partial y)$.

All the formulas given here apply to the case where $\rho^2 = t^2 - r^2 > 0$, i.e., when all the basis functions are timelike. To go over to the case of $r = \rho\cosh\alpha$, $t = \rho\sinh\alpha$, $-\infty \le \alpha \le \infty$, $0 \le \rho \le \infty$, one should make the substitution $\alpha \to \alpha - i\pi/2$ in all the formulas.

---

[1] A. Z. Dolginov, J. Exptl. Theoret. Phys. (U.S.S.R.) 30, 746 (1956), Soviet Phys. JETP 3, 589 (1956).

[2] M. Matsunobu and H. Takebe, Progr. Theor. Phys. 14, 589 (1955).

Translated by M. Hamermesh
160

BETA DECAY OF A SPIN-$^3/_2$ PARTICLE

R. A. ASANOV

Joint Institute for Nuclear Research

Submitted to JETP editor May 31, 1958

J. Exptl. Theoret. Phys. (U.S.S.R.) **35**, 796-798 (September, 1958)

It is of some interest, in connection with the possible existence of hyperons with spin greater than $^1/_2$, to consider the decay of a spin-$^3/_2$ particle. Let us consider the β decay of such a particle according to the decay scheme $Y \rightarrow p + e + \tilde{\nu}$, in analogy with the neutron-decay scheme, in the first approximation of perturbation theory. We shall assume that the decay products are described by the Dirac equation and that the decaying particle is described by an equation of Rarita-Schwinger type.[1]

We write the interaction leading to decay in the form

$$H_{\text{int}} = (\bar{\psi}_p B^\mu)(C_V \bar{\psi}_e \gamma_\mu \psi_\nu + C'_V \bar{\psi}_e \gamma_\mu \gamma_5 \psi_\nu) + (\bar{\psi}_p \gamma_5 B^\mu)(C_A \bar{\psi}_e \gamma_\mu \gamma_5 \psi_\nu + C'_A \bar{\psi}_e \gamma_\mu \psi_\nu) + (\bar{\psi}_p \gamma_\mu B^\sigma)(C_T \bar{\psi}_e \gamma_\mu \gamma_\sigma \psi_\nu + C'_T \bar{\psi}_e \gamma_\mu \gamma_\sigma \gamma_5 \psi_\nu) + \text{compl. conj.} \quad (1)$$

Here B^μ, the wave function of the spin-$^3/_2$ particle, is a four-vector each of whose components is a bispinor. This function (when there is no interaction) satisfies the equation[1]

$$(i\gamma p + m) B^\mu = 0, \quad \gamma_\mu B^\mu = 0. \quad (2)$$

We sum over the states of the decay products in the usual way, and average over initial states of the spin-$^3/_2$ particle using the relations

$$\sum_{i=1}^{4} {}^{(i)}B^\mu_\rho(\pm \mathbf{p})\, {}^{(i)}B^{\nu *}_\sigma(\pm \mathbf{p}) = (\Lambda^{\mu\nu}\Lambda^\pm)_{\rho\sigma}. \quad (3)$$

The upper and lower signs correspond to summing over positive and negative energy states, respectively, $\Lambda^\pm$ is the usual projection operator of Dirac theory, and the operator $\Lambda^{\mu\nu}$ is given by

$$\Lambda^{\mu\nu} = \delta_{\mu\nu} + \frac{2}{3m^2} p_\mu p_\nu - \frac{1}{3}\gamma_\mu\gamma_\nu - \frac{1}{3m^2}(\gamma_\mu p_\nu - \gamma_\nu p_\mu)(\gamma p). \quad (4)$$

The resulting averaged and summed square of the matrix element for decay at rest is

$$|M_0|^2 = L_1 + \frac{1}{3} L_2 \frac{\mathbf{p}_e\mathbf{p}_\nu}{E_e E_\nu} + L_3 \left(\frac{\mathbf{p}_e}{E_e} + \frac{\mathbf{p}_\nu}{E_\nu}\right)\frac{\mathbf{p}_p}{E_p} + L_4 \left(\frac{\mathbf{p}_e}{E_e} - \frac{\mathbf{p}_\nu}{E_\nu}\right)\frac{\mathbf{p}_p}{E_p} + L_5 \frac{m_p}{E_p}\left(1 - \frac{1}{3}\frac{\mathbf{p}_e\mathbf{p}_\nu}{E_e E_\nu}\right) + L_6 \frac{m_e m_p}{E_e E_p} + L_7 \frac{m_e}{E_e}\left(1 - \frac{1}{3}\frac{\mathbf{p}_p\mathbf{p}_\nu}{E_p E_\nu}\right), \quad (5)$$

where the L coefficients depend only on the coupling constants and are given by

$$L_{1,2} = \frac{1}{2}[\pm(|C_V|^2 + |C'_V|^2 + |C_A|^2 + |C'_A|^2) + 2(|C_T|^2 + |C'_T|^2)],$$
$$L_3 = -\frac{1}{3}(|C_T|^2 + |C'_T|^2), \quad L_4 = -\frac{1}{6}(C_V C_A^* + C_V^* C_A + C'_V C'^*_A + C'^*_V C'_A), \quad (5')$$
$$L_5 = \frac{1}{2}(|C_V|^2 + |C'_V|^2 - |C_A|^2 - |C'_A|^2), \quad L_{6,7} = \frac{1}{2}[(C_V \pm C_A)C_T^* + (C_V^* \pm C_A^*)C_T + (C'_V \pm C'_A)C'^*_T + (C'^*_V \pm C'^*_A)C'_T].$$

These calculations are performed on the assumption that the neutrino rest mass vanishes. Equation (5) is written in a form analogous to that obtained for the β decay of a spin-$^1/_2$ particle (see, for instance, Michel[2]). From this equation we easily obtain the known[3] expressions for "pure" V, A, or T coupling.

Equation (5) for the spin-$^3/_2$ particle is not the same as the corresponding equation in the β decay of a Dirac particle. The difference is, among other things, that the β-ν correlation coefficient cannot have an absolute value greater than $^1/_3$. This, in turn, leads to a difference in the shape of the decay-electron energy spectrum, which we give below:

$$w(E_e) = \frac{m_Y^2 (W - E_e)^2 \sqrt{E_e^2 - m_e^2}}{6(2\pi)^3 z_1^3} [L_1 E_e \{z_2 [3m_Y (W - E_e) + E_e^2 - m_e^2] + 3m_p^4\}$$
$$- \frac{L_2}{3} z_2 (m_Y - E_e)(E_e^2 - m_e^2) - L_3 \{z_2 [m_Y E_e (W - E_e) + (m_Y - 2E_e)(E_e^2 - m_e^2)]$$
$$+ 4m_Y^2 E_e (W - E_e)^2\} + L_4 \{z_2 m_Y [E_e (W - E_e) - E_e^2 + m_e^2] + 4m_Y^2 E_e (W - E_e)^2\} \quad (6)$$
$$+ L_5 2z_1 m_p (3m_Y E_e - 2E_e^2 - m_e^2) + L_6 6z_1 m_p m_e (m_Y - E_e) + L_7 \frac{m_e}{3}\{z_2 [12m_Y (W - E_e) + 2(E_e^2 - m_e^2) - 3m_p^2] + 18m_p^4\}].$$

Here

$$z_1 = m_Y(W - E_e) + {}^1/_2 m_p^2, \quad z_2 = 2(z_1 + m_p^2), \quad W = (m_Y^2 - m_p^2 + m_e^2)/2m_Y.$$

The present considerations can be used for μ-meson decay[4] of spin-$^3/_2$ particles according to the scheme $Y \rightarrow p + \mu + \tilde{\nu}$, as well as for the electron decay scheme considered above.

I wish to acknowledge the guidance provided by Professor M. A. Markov and to thank B. N. Valuev and I. V. Polubarinov for discussions.

---

[1] W. Rarita and J. Schwinger, Phys. Rev. **60**, 61 (1941).

[2] L. Michel, Proc. Phys. Soc. (London) **A63**, 514 (1949).

[3] E. R. Caianiello, Phys. Rev. **83**, 735 (1951).

[4] M. A. Markov, Гипероны и *K*-мезоны (Hyperons and K-mesons) M., 1958 (in press).

Translated by E. J. Saletan
161

ELECTRONIC PARAMAGNETIC RESONANCE IN ALLOYS OF ALKALI METALS

N. C. GARIF'IANOV and M. A. STARIKOV

Physico-Technical Institute, Kazan' Branch, Academy of Sciences, U.S.S.R.

Submitted to JETP editor May 31, 1958

J. Exptl. Theoret. Phys. (U.S.S.R.) **35**, 798-799 (September, 1958)

REFERENCES 1 to 3 report on the influence of impurities on resonance absorption in metals due to conductive electrons.

We have investigated the 290-Mcs resonance absorption in alloys of sodium at T = 90°K and 300°K, as a function of the concentration of components. The following metals served as components: Li, K, Hg, Pb and Woods' alloy.

The measurement procedure was described previously.[4] The original sodium was 99.5% pure and contained approximately 0.4% of potassium. The alloys were produced under a layer of paraffin or in an argon atmosphere. To prevent skin effect from distorting the shape of the absorption lines,[5] the alloy was dispersed in paraffin; the average size of metal particles was approximately 4 μ. The width ΔH in the original sodium measured between the half-intensity points of the resonance-absorption curve, has a maximum of 16 Oe at room temperature and equals 9 Oe at 90°K.

Our data on the width coincide with the results of Gutovsky and Frank.[6] The measurements of paramagnetic resonance in alloys indicate that the metals used as alloy components can be divided into two groups. The first group includes Li and K, which have little effect on ΔH, and consequently on T_1 and T_2.

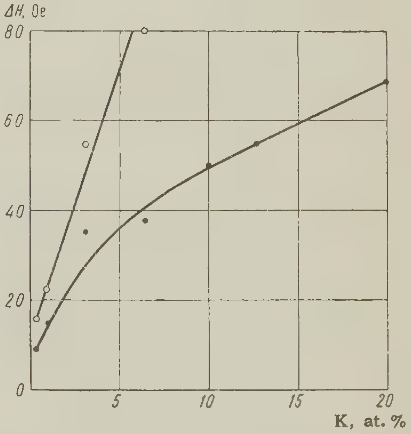

FIG. 1. Alloys Na – K. ● – T = 90°K, ○ – T = 300°K.

In Na-K alloys ΔH has a greater temperature dependence than in the original sodium (Fig. 1).

The second group contains the heavy metals Hg, Pb and Wood's alloy, which increase ΔH almost 10^4 times more than the metals of the first group. (Fig. 2). In the alloys of these metals ΔH is independent of the temperature.

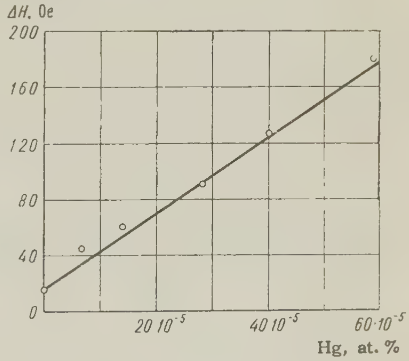

FIG. 2. Alloy Na – Hg. T = 300°K.

We have also investigated paramagnetic resonance in lithium alloys. The alloying components used were Na, K, Hg, Pb and Wood's alloy.

The effect of the alkali metals Na and K on paramagnetic resonance in lithium is just as weak as in the case of sodium. However, even 0.001% of a heavy component such as Hg, Pb, or Wood's alloy broaden the line to such an extent that it becomes impossible to observe absorption in these alloys. We offer no quantitative data on these alloys, because the purity of the original lithium was only 98%. Furthermore, lithium alloys very poorly with sodium or potassium.[7]

Our results agree with Elliot's theory,[8] from which it follows that impurity metals with strong spin-orbit interaction greatly shorten the spin-lattice relaxation time. This results in such a broadening of the lines in the Li and Na alloys with insignificant admixtures of heavy metals. On the other hand, the alkali metals (Li, Na and K) have relatively weak spin-orbit interactions and therefore have a weak influence on the width ΔH.

The shift of the g-factor of the line can be used as a measure of the spin-orbit interaction of the impurity atoms. We propose to conduct measurements of g-factors at 10,000 Mcs in alloys with smaller metal-particle dimensions. We also plan to measure the Knight shift for the resonance lines of Na^{23} and Li^7. These experiments will permit a detailed comparison with the theory.

In conclusion, the authors express their gratitude to K. A. Valiev for his review of the results.

---

[1] G. Feher and A. F. Kip, Phys. Rev. **95**, 1343 (1954).

[2] G. Feher and A. F. Kip, Phys. Rev. **98**, 337 (1955).

[3] N. C. Garif'ianov, J. Exptl. Theoret. Phys. (U.S.S.R.) **32**, 149 (1957), Soviet Phys. JETP **5**, 111 (1957).

[4] N. C. Garif'ianov and B. M. Kozyrev, J. Exptl. Theoret. Phys. (U.S.S.R.) **30**, 272 (1956), Soviet Phys. JETP **3**, 255 (1956).

[5] N. Blombergen, J. Appl. Phys. **23**, 1379 (1952).

[6] H. S. Gutowsky and P. J. Frank, Phys. Rev., **94**, 1067 (1954).

[7] F. I. Shamrai, Литий и его сплавы (Lithium and its Alloys) Acad. Sci. Press, M. 1952.

[8] R. J. Elliott, Phys. Rev. **96**, 266 (1954).

Translated by E. Vinogradov
162

THE FIRST EXCITED STATE OF Tb^{159}

Iu. A. NEMILOV, A. N. PISAREVSKII and L. D. SOSHIN

Radium Institute, Academy of Sciences, U.S.S.R.

Submitted to JETP editor June 4, 1958

J. Exptl. Theoret. Phys. (U.S.S.R.) **35**, 800-801 (September, 1958)

In a scintillation-spectrometer study of the γ radiation of Dy^{159}, which decays entirely via K capture, a weak line at twice the energy was observed in the pulse distribution in addition to the K radiation of Tb^{159} (44.5 kev). Measurements with varying distances from source to crystal, and using filters showed that this line is the result of full summing of 44.5-kev quanta. For the 1.5-microsec resolving time of our apparatus (a 128-channel analyzer[1]), the chance-coincidence rate would be two orders of magnitude smaller than that actually observed in the sum peak. From this one is naturally led to the assumption that the observed 90-kev line is the result of summing two cascade quanta of half the energy, the first of which is the K radiation of Tb^{159} after K capture, while the second is the result of decay of the first excited state of Tb^{159}.

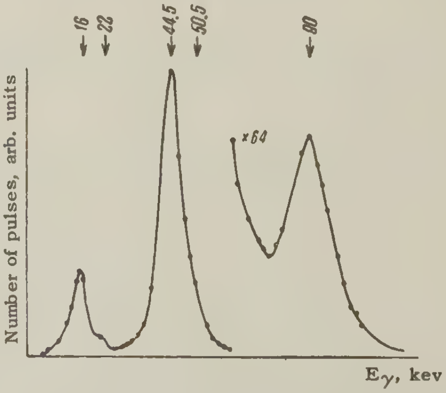

FIG. 1. γ spectrum of Dy^{159}, using NaI (Tl) crystal. The 16-kev peak is due to K_α radiation of iodine, the 22-kev peak to K_β radiation of iodine.

A suggested value of the energy of the first excited state of Tb^{159} (57.5 kev) was given on the basis of Coulomb excitation of Tb.[2] The conversion electrons corresponding to this excited state have been observed.[3] Gamma rays from deexcitation of this state have never been observed. Our experiments show that if such a line does exist, its intensity does not exceed 1% of the 44.5-kev peak.

An additional check was made using a "sum" spectrometer with a CsI (Tl) crystal (diameter

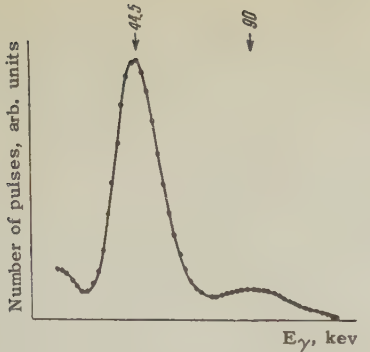

FIG. 2. γ spectrum of Dy^{159} taken with a sum spectrometer.

50 mm, h = 20 mm). The pulse distribution is shown in Fig. 2. A computation of the efficiency from the areas of the main and sum peaks,[4] on the assumption that the latter is produced by the same number of 44.5-kev quanta in cascade, is in good agreement with the efficiency computed by an independent method.

Thus the deexcitation of the first excited state of Tb^{159} also occurs with emission of Tb K radiation, in view of the strong conversion of the 57.5-kev line. The conversion coefficient is $\geq 99\%$.

In conclusion the authors thank A. N. Murin and B. K. Preobrazhenskii for their preparation of the pure source.

---

[1] V. O. Viazemskii and V. V. Trifonov, Report at the Conference on Analyzers, Moscow, 1956.

[2] N. P. Heydenburg and G. M. Temmer, Phys. Rev. 100, 150 (1955).

[3] Mihelich, Harmatz and Handley, Phys. Rev. 108, 989 (1957).

[4] P. Shapiro and R. W. Higgs, Rev. Sci. Instr. 28, 939 (1957).

Translated by M. Hamermesh
163

STUDY OF γ-RAYS FROM As^{78} *DECAY*

Iu. A. NEMILOV, A. N. PISAREVSKII, and L. D. SOSHIN

Radium Institute, Academy of Sciences, U.S.S.R.

Submitted to JETP editor June 4, 1958

J. Exptl. Theoret. Phys. (U.S.S.R.) 35, 801-802 (September, 1958)

It is known that in the decay of As^{78} (T = 90 min) two groups of β^- particles are emitted ($E_\beta = 4.1$ Mev, 70% branch; $E_\beta = 1.4$ Mev, 30%). γ rays with energies of 0.27 Mev[1] and 0.615 Mev[2] are also observed in the decay. It is impossible, on the basis of the available data, to attempt even a decay scheme for this isotope.

We obtained As^{78} from bombardment of separated Se^{78} isotope with 14-Mev neutrons, via the (np) reaction.

The measurements were carried out on a scintillation spectrometer with a 128-channel analyzer.[3] We used the geometry of the standard single-crystal spectrometer (with FEU-S photomultiplier and a NaI (Tl) crystal, diameter 30 mm, h = 40 mm), and the geometry of a 4π summing spectrometer (FEU-13 with CsI (Tl) crystal, diameter 50 mm, h = 40 mm).

The following γ lines were observed in the singles spectrometer geometry: 500 kev with T = 5 to 6 min; γ lines with T = 90 ± 10 min: 270, 610, 800, 1280, 2680 kev (all intense lines), 80, 345, 690, 1200, 1620, 1880, 2020, and 2160 kev (weak lines). There was a suspicion of the existence of a line with very low intensity at ~ 2400 kev.

In the summing spectrometer geometry, the following sum lines were definitely observed (all with period 90 ± 10 min): 420, 2700, and 1650 kev. The transitions with a period of 90 min can be assigned to the $As^{78} \rightarrow Se^{78}$ β^- decay.

The γ line at 500 kev (T = 5 to 6 min) is interesting. It is not the result of annihilation of positrons from some β^+ decay, since careful measurements with the summing spectrometer showed no sum line at $E_\gamma = 1$ Mev. We also observed no other γ lines with T = 5 to 6 min. This suggests that this line is the result of deexcitation of some metastable state which is formed in the interaction of neutrons with Se^{78}

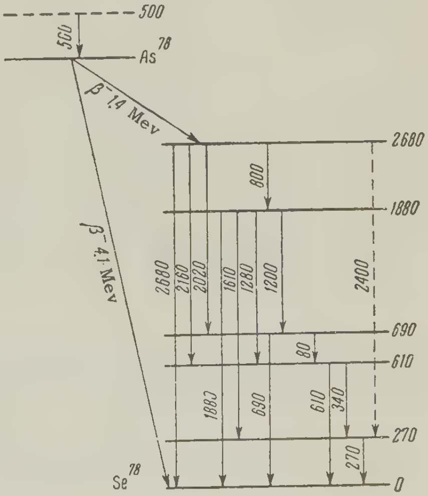

Decay Scheme of As^{78}.

(since this line was not found in experiments with other separated isotopes of Se).

Running through the other possible reactions on Se^{78} (n2n, n2p, nα, npn), one finds that the isomers of products of such reactions have been well investigated and that no isomer has been found which has the observed state (T = 5 to 6 min; E = 500 kev). We can therefore assume that As^{78} has a metastable state with an energy of 500 kev.

A possible decay scheme for As^{78} is shown in the figure.

In conclusion, the authors thank A. N. Protopopov and his colleagues for neutron irradiation of the samples.

---

[1] Hollander, Perlman, and Seaborg, Revs. Modern Phys. **25**, 469 (1953).

[2] B. S. Dzhelepov and L. K. Peker, **Схемы распада радиоактивных изотопов** (Decay Schemes of Radioactive Isotopes), Acad. Sci. Press, 1957.

[3] V. O. Viazemskii and V. V. Trifonov. Report to the Conference on Analyzers, Moscow, 1956.

Translated by M. Hamermesh
164

LOW TEMPERATURE POLYMORPHISM OF METALS

I. A. GINDIN, B. G. LAZAREV, Ia. D. STARODUBOV, and V. I. KHOTKEVICH

Physico-Technical Institute, Academy of Sciences, Ukrainian S.S.R.

Submitted to JETP editor June 7, 1958

J. Exptl. Theoret. Phys. (U.S.S.R.) **35**, 802-804 (September, 1958)

THE existence of a so-called low-temperature modification of tin (α-Sn), stable below 18°C, is well known. Spontaneous transformation of white tin into gray, however, does not occur in practice even upon substantial holding times at low temperatures. It can be brought about by means of plastic deformation at temperatures below the transformation point.[1]

Works of recent years have established the existence of low-temperature allotropic transformations which proceed also in lithium and sodium[2,3] upon plastic deformation under conditions of strong supercooling. One can surmise that this phenomenon is characteristic of many non-close-packed metals. At the same time, on account of the small diffusion mobility of the atoms, there is practically no reorganization of the lattice into a new more dense structure stable at low temperatures. Plastic deformation facilitates the process, helping surmount the activation barrier.

In contrast to the preceding investigations, we used in the present work a method of mechanical tests, which consisted of studying the compression diagrams of specimens of lithium, sodium, cesium, bismuth, and beryllium with subsequent warming and registration of the volume changes during the reverse transformation. The bismuth and beryllium were monocrystals of 99.98% purity; the lithium, sodium, and cesium were chemically-pure polycrystals. The tests were run on a one-ton machine with a stiff dynamometer, adapted for measurements at helium temperatures.[4,5] The rate of deformation was constant at 0.03 mm/sec. The deformation and warming curves were recorded on photographic film.

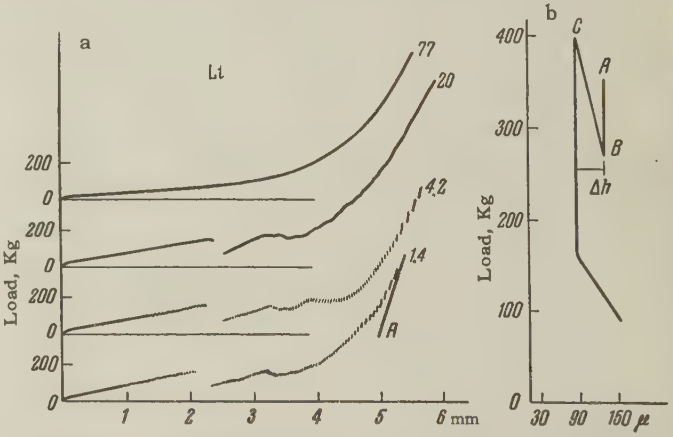

FIG. 1. a – Machine compression diagrams for specimens of chemically pure lithium at temperatures from 77 to 1.4°K; b – Dilatometric curve taken during warming of the lithium specimen deformed at a temperature of 1.4°K.

A typical deformation diagram in "load vs. absolute compression" coordinates is shown in Fig. 1a for lithium (the polymorphic transformation of which has been well studied by x-rays[2,3]). At 77°K it is a smooth curve with a hardening shape at high degrees of reduction, without any singular points indicative of the occurrence of a transformation. It should be noted here, however, that x-ray investigations under these conditions recorded a partial transformation from body-centered cubic modification to face-centered. On reducing the deformation temperature to 20°K and lower (down to 1.4°K), a characteristic disruption appears on the curve with a sharp drop in resistance to deformation, in response to allotropic transformation in a considerable portion of the volume of the deformed metal.*

The most direct demonstration of a polymorphic transformation in our experiments is the occurrence of volume changes during the reverse transition in the course of warming the deformed specimen (Fig. 1b). After deformation, the specimen was unloaded to a stress corresponding to the point A on the curve (temperature 1.4°K) and then it was warmed. At first, with increase in temperature, the load falls on account of the thermal behavior of the testing machine (branch AB). This circumstance was verified by separate experiments without specimens. On reaching the point B (corresponding to a temperature of 143°K) the load begins to increase sharply with a simultaneous growth in length of the specimen, which in a well defined manner can be related to the start of the reverse transformation. The temperature corresponding to the end of the transition (point C) is 167°K. On further increase of the temperature, the load again begins to fall. Thus, the size of the gap Δh represents the absolute extension of the specimen in the process of transformation and allows one to estimate a lower limit for the relative change in density during the transitions. For lithium $\Delta\rho/\rho$ amounts to about 15%. The size of Δh falls with increasing temperature of deformation indicating a decrease in completeness of the transition, and at 77°K is not registered by this method.

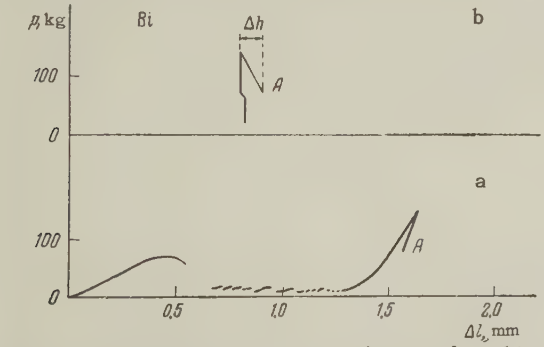

FIG. 2. a – Machine compression diagram for a bismuth specimen at a temperature of 77°K; b – Dilatometric curve taken during warming of a bismuth specimen deformed at 77°K.

Analogous curves were obtained for sodium. In this case, a clearly expressed allotropic transformation is observed only at temperatures of 4.2°K and below. The temperature for the start of the transformation during the reverse transition is 73°K and the value of $\Delta\rho/\rho$ is approximately 8%.

In cesium, no polymorphic transformation is recorded on the deformation diagram even at 1.4°K, although the shape of the warming curve allows one to come to a conclusion about the existence of a transition in an insignificant volume.

Such behavior of these three alkali metals must apparently be associated with the substantial decline of the characteristic temperature (474, 192 and 50°K for lithium, sodium, and cesium respectively) and permits us to surmise the presence of polymorphism in the entire group of alkali metals.

In Figs. 2a and b, a deformation diagram and warming curve are presented for bismuth deformed at 77°K. This diagram permits a definite conclusion to be drawn about the presence in this case of also a polymorphic transformation with a reorganization of the lattice in the direction of an increase in density with a transformation temperature ~ 80°K.

The phenomenon of disruption of the load on the compression diagram is also observed for beryllium at temperatures of 4.2°K and below.

Thus, a conclusion can be drawn about the widespread prevalence of low-temperature polymorphism which is observed in tin, sodium, lithium, cesium, bismuth and beryllium.†

---

*An interesting feature of the deformation curves is the discontinuous character of the deformation at helium temperatures, noted by the authors in aluminum,[5] one of the possible causes of which is mechanical twinning.

†The possibility is not excluded that the superconductivity of bismuth and beryllium condensed on cold substrates[6] is connected with the low-temperature modifications of these metals.

---

[1] E. S. Hedges and J. Y. Higgs, Nature **169**, 621 (1952).

[2] C. S. Barrett, Phys. Rev. **72**, 245 (1947).

[3] V. I. Khotkevich, J. Tech. Phys. (U.S.S.R.) **22**, 477 (1952).

[4] Garber, Gindin, Konstantinovskii, Poliakov, and Startsev, Заводск. лабор. (Plant Laboratory) **7**, 857 (1953).

[5] Gindin, Khotkevich and Starodubtsov, Физика металлов и металловедение (Phys. of Metals and Metal Research) 1958 (in press).

[6] Lazarev, Sudovtsov, and Smirnov, J. Exptl. Theoret. Phys. (U.S.S.R.) **33**, 1059 (1957), Soviet Phys. JETP **6**, 816 (1958).

Translated by R. Eisner
165

THE INFLUENCE OF PLASTIC DEFORMATION ON THE ANOMALOUS BEHAVIOR OF THE RESISTANCE OF GOLD AT LOW TEMPERATURES

N. E. ALEKSEEVSKII and Iu. P. GAIDUKOV

Institute for Physical Problems, Academy of Sciences, U.S.S.R.

Submitted to JETP editor June 14, 1958

J. Exptl. Theoret. Phys. (U.S.S.R.) 35, 804-806 (September, 1958)

WE have noted earlier[1] that the depth of the minimum of the resistance r_T vs. temperature curve for gold is decreased when the measurement is performed in a constant magnetic field, and for some value of the field H_k becomes equal to zero. An investigation of the dependence of the Hall emf on the magnitude of the magnetic field and also a measurement of the magnetic susceptibility have shown that for a field equal to H_k the Hall constant and the diamagnetic susceptibility of the samples investigated increase discontinuously.[2]

For a further investigation of the causes influencing the resistance minimum of gold, we performed experiments to determine the influence of elastic and plastic deformations both on the depth of the minimum and on the value of the "critical" field H_k. To study the influence of elastic deformations, we experimented on some samples of gold possessing a resistance minimum. The measurement proceeded with a uniform compression, produced by freezing water in a beryllium-bronze bomb[3] in which the gold sample was placed. A measurement of the dependence of $(r_{1.4} - r_{\min})/r_{\min}$ at pressures of $p = 0$ and $p = 1600$ atmos in the temperature range from 4.2 to 1.4°K showed that under a uniform compression the depth of the minimum decreased slightly by an amount which is less than the limits of the experimental accuracy, while the resistivity also changes slightly.

To investigate the influence of plastic deformations on the behavior of the resistivity curves we took two sets of experiments.* In the first experiments the deformation of the specimen was produced at liquid-helium temperature. To produce the deformation we used a special press in which a wire prepared from the gold batch Au-1 or Au-6 (length ≈ 9 mm, diameter ≈ 0.4 mm) was squashed between two horizontal plates of agate. The degree of deformation was estimated from the magnitude of the relative change in the resistivity $\alpha = \rho_{4.2}^{\text{def}}/\rho_{4.2}^{0}$ produced by the deformation at 4.2°K. In Fig. 1 we give the results of the measurements.

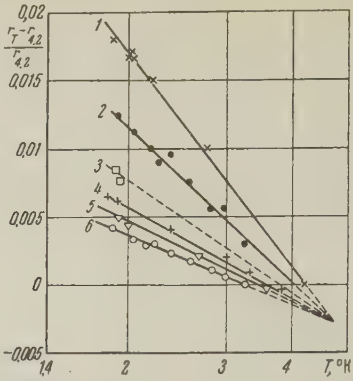

FIG. 1. Specimen Au – 1. Dependence of the anomalous increase of the resistivity on the temperature (the abscissa axis is logarithmic). Values of α: 1) 1, 2) 1.8, 3) 2.5, 4) 3.9, 5) 6.2, 6) 8.

The deformations obtained at liquid-helium temperature were relatively small (wire of 0.4 mm diameter was squashed into a plate not less than 0.20 mm thick).

To investigate the influence of stronger deformations we performed experiments with wires deformed at room temperature in a hydraulic press. In that case the degree of deformation was estimated from the quantity $\beta = r_{295}/r_{4.2}$. In Figs. 2 and 3 the results are given of the measurements of the depth of the minimum and of H_k for deformed samples of Au-1 and Au-6. Analogous measurements were performed on a number of other gold samples.

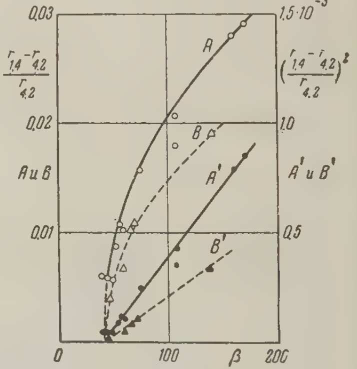

FIG. 2. Dependence of the depth of the resistivity minimum on deformation: ●, ○) specimen Au-1; ▲, △) specimen Au-6.

From all results given it is clear that the depth of the minimum and the magnitude of the "critical" field depend strongly on the deformation. From Figs. 2 and 3 it follows that for a well determined value of the deformation the depth of the minimum tends to zero and the critical field tends to infinity. If the deformed specimens are annealed for 30 minutes at a temperature of 800 to 900°C the anomalous properties of the specimens are restored. One must note that within the limits of

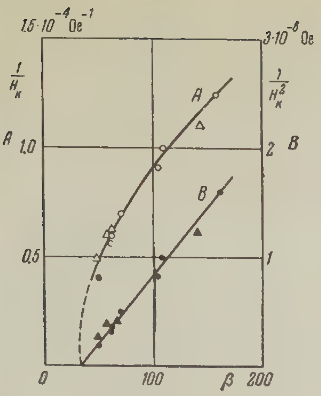

FIG. 3. Dependence of the critical field on the deformation: ●, ○) specimen Au-1; ▲, △) specimen Au-6.

the experimental accuracy the value of T_{min} is not changed by the deformation and lies for all specimens in the range 4 to 6°K. Earlier we have already reported[1] that specimens prepared from Au-4 do not show a resistance minimum. A spectral analysis performed on these samples showed that gold of the two batches (both Au-1 and Au-4) does not differ essentially in their impurity contents. On the basis of the data given in the present paper, it was assumed that specimens prepared from Au-4 after careful annealing would also, like those from Au-1, have a minimum in the r(T) curve. Experiments performed by us confirmed this assumption.

Comparing all results obtained we can conclude that the cause responsible for the appearance of a resistance minimum is the scattering of conduction electrons by impurities of some well defined elements. A decrease of the mean free path of the conduction electrons (for instance, due to the deformation) leads to a decrease of the probability for scattering of the electrons by those impurities, and as a result the anomalous properties also disappear. From this point of view, the crystal boundaries and the grain size are not responsible for the appearance of the resistance minimum.

In conclusion we consider it a pleasant duty to express our gratitude to academician P. L. Kapitza for a discussion of the results obtained.

---

*We should remark Schmitt[4] has noted the influence of deformation on the behavior of the resistance curves in the case where a minimum is present for copper.

---

[1] N. E. Alekseevskii and Iu. P. Gaidukov, J. Exptl. Theoret. Phys. (U.S.S.R.) **31**, 947 (1956), Soviet Phys. JETP **4**, 807 (1957).

[2] N. E. Alekseevskii and Iu. P. Gaidukov, J. Exptl. Theoret. Phys. (U.S.S.R.) **32**, 1589 (1957), Soviet Phys. JETP **5**, 1301 (1957).

[3] B. Lazarev and L. Kan, J. Exptl. Theoret. Phys. (U.S.S.R.) **14**; 439 (1944); J. Phys. (U.S.S.R.) **8**, 193 (1944).

[4] R. W. Schmitt and M. D. Fiske, Phys. Rev. **96**, 1445 (1954).

Translated by D. ter Haar
166

THE SCATTERING OF SPIN 3/2 PARTICLES BY A COULOMB FIELD

A. A. KOMAR

P. N. Lebedev Institute of Physics, Academy of Sciences, U.S.S.R.

Submitted to JETP editor June 14, 1958

J. Exptl. Theoret. Phys. (U.S.S.R.) **35**, 806-807 (September, 1958)

In studying the spin of new particles it may be of interest to describe how their interaction with an electro-magnetic field depends upon their spin. This spin dependence appears clearly in such phenomena as Compton scattering, bremsstrahlung, and pair production of particles of spin 0, $^1/_2$, 1, and $^3/_2$ and has been considered by a number of authors.

In the present note we consider the scattering of particles of spin $^3/_2$ by the Coulomb field of a nucleus.

The matrix element for the process looks as follows in the Born approximation:

$$\mathcal{M} = -e\int \overline{B}^i(x)\,A_k(x)\,\gamma_k B^i(x)\,d^4x,$$

where $B^i(x)$ is the spin vector describing the particles of spin $^3/_2$, and obeys the following equation and subsidiary conditions:

$$(\gamma_k\partial/\partial x_k + M)\,B^i(x) = 0, \quad \gamma_i B^i = 0, \quad \partial B^i/\partial x_i = 0;$$

$A_k(x)$ is the 4-potential describing the nuclear field [for a static field, $A(x) = (0, 0, 0, A_4(\mathbf{x}))$]. In the p representation

$$\mathcal{M} = -2\pi e a_4(\mathbf{q})\,\overline{B}^i(p_f)\,\gamma_4 B^i(p_i)\,\delta(E_f - E_i), \quad \mathbf{q} = \mathbf{p}_f - \mathbf{p}_i.$$

Making use of the following formula in summing over the polarizations

$$\sum_m [B^i_m(p)]_\nu\,[\overline{B}^k_m(p)]_{\nu'} = (1/6E_pM)\,[(M - i\gamma p)\,(2p_ip_k/M + 3M\delta_{ik} + i\gamma_ip_k - i\gamma_kp_i - M\gamma_i\gamma_k]_{\nu\nu'}$$

(ν, ν' are spinor indices) we obtain the differential cross section

$$d\sigma = \frac{e^2}{(2\pi)^2}\frac{p^2}{v^2}\,|\,a_4(\mathbf{q})\,|^2\,d\Omega\left\{1 + \frac{v^2}{3}\left(1 + \frac{8}{3}\frac{p^2}{M^2}\right)\sin^2\frac{\theta}{2} + \frac{8}{9}\frac{v^2p^4}{M^4}\sin^4\frac{\theta}{2}\cos^2\frac{\theta}{2}\right\},$$

where θ is the scattering angle and $q = 2p\sin(\theta/2)$.

For a pure Coulomb field $a_4(\mathbf{q}) = -i4\pi Ze/q^2$ and the factor preceding the curly brackets yields $(Ze^2/2pv)^2 d\Omega = d\sigma_{\text{Ruth.}}$, the Rutherford cross section.

Thus the expression in the curly brackets specifically gives the spin correction. We recall for the sake of comparison the cross section for particles of spin ½ (reference 1)

$$d\sigma = d\sigma_{\text{Ruth}}[1 - v^2\sin^2\theta/2]$$

and for spin 1:[2]

$$d\sigma = d\sigma_{\text{Ruth}}[1 + (v^2p^2/6M^2)\sin^2\theta].$$

It can be seen that for spin 1 and $3/2$ the correction grows with energy, this is especially marked in the case of spin $3/2$ as it includes a factor p^4. At sufficiently high energies this may yield differences from the usual scattering picture even at relatively small angles. It should however be noted that if $q > 1/R$ where R is the nuclear radius, it is necessary to include the effect of the spread out nuclear charge.

---

[1] N. F. Mott, Proc. Roy. Soc. **124**, 425 (1929).

[2] H. S. W. Massey and H. C. Corben, Proc. Cambr. Phil. Soc., **35**, 463 (1939).

Translated by M. A. Melkanoff
167

USE OF CYCLOTRON RESONANCE IN SEMICONDUCTORS FOR THE AMPLIFICATION AND GENERATION OF MICROWAVES

A. S. TAGER and A. D. GLADUN

P. N. Lebedev Physics Institute, Academy of Sciences, U.S.S.R.

Submitted to JETP editor June 14, 1958

J. Exptl. Theoret. Phys. (U.S.S.R.) 35, 808-809 (September, 1958)

As is well known,[1-3] when cyclotron resonance occurs in certain semiconductors (Ge or Si), additional lines are observed along with the main absorption lines at frequencies that are integral multiples of the fundamental cyclotron frequency. This effect is associated with the anharmonic nature of the motion of holes, which leads to the breakdown of the usual selection rules $\Delta n = \pm 1$ for the Landau levels and to the appearance of nonvanishing dipole moments for transitions with $\Delta n = \pm 2$ or 3.

This phenomenon can be utilized for the construction of regenerative amplifiers or generators at microwave frequencies, for example, by using the following method. The semiconductor sample, placed into a constant magnetic field H_0, is acted upon by the high-frequency electric "pumping" field E_p of frequency $\omega_p = n\omega_c = neH_0/m^*c$ ($n = 1, 2, 3, \ldots$, m^* is the effective mass of the hole (m_h^*) or of the electron (m_e^*)) polarized in the plane perpendicular to H_0.

If the intensity of the field E_p is sufficiently great, so that during a thermal relaxation time τ a sufficiently large number of carriers goes over into the upper energy levels, then in this system excitation (or amplification) can occur at frequencies given by $\omega_s = l\omega_p/n = l\omega_c$, $l = 1, 2, \ldots,$ which can be both less than ($l < n$) and greater than ($l > n$) the "pumping" frequency. The excitation of such oscillations is facilitated by placing the semiconductor into a resonator for which ω_p and ω_s are eigenfrequencies.

According to Basov and Prokhorov,[4] in order to excite a maximum number of carriers at the frequency ω_p it is necessary to expend per unit volume of the semiconductor an amount of power given (in order of magnitude) by: $P_p \approx (10^{-7} \times 3\hbar^2\omega_p/4\pi\tau^2\,|\,d_n\,|^2 Q_p)$ w/cm³, where $h = 2\pi\hbar$ is Planck's constant, $|\,d_n\,|$ and Q_p are the dipole moment for the transition and the figure of merit of the resonator at the frequency $\omega_p = n\omega_c$.

In the special case $\omega_s = \omega_c = \omega_p/2$ (corresponding to the resonance of the second kind in a nonlinear oscillating system) at a temperature $T \approx 2$ to 4°K we have $\tau \approx 6 \times 10^{-11}$ sec, $|\,d_2\,| \approx 10^{-15}$ cgs Esu,[2,3] from which we obtain $P_p \approx (10^{-11}\,\omega_p/Q_p)$ w/cm³.

For the excitation (or amplification) of oscillations of frequency $\omega_s = \omega_c = \omega_p/2$ it is necessary that the density of active carriers attain the value $N_{\text{act}} \approx 3\hbar/4\pi Q_1\tau\,|\,d_1\,|^2$. In the case under discussion $|\,d_1\,| \approx 10^{-14}$ cgs Esu (reference 3) and $N_{\text{act}} \approx (3 \times 10^{10}/Q_1)$ cm⁻³. The maximum radiated power is

$$P_s = N_{\text{act}}\hbar\omega_s/2\tau \ll P_p,$$

which in the case $N_{\text{act}} \approx 10^{10}$ cm^{-3} and $\omega_s = 2\pi \times 10^{11}$ cps will amount to approximately 5 mw/cm³, i.e., to a significantly greater value than in the usual molecular or paramagnetic generators. This effect is due to the fact that the electric dipole moment for the transition in the case of cyclotron resonance exceeds approximately by a factor of 10^6 the magnetic moment of the electron, and by a factor of 10^4 the electric dipole moment of the molecule.

An important advantage of cyclotron resonance in comparison with paramagnetic resonance is the possibility of generating microwaves of shorter wavelengths, in the millimeter and the submillimeter ranges, since the low values for the effective mass of the carriers compared to the electron rest mass m_0 allow us to use lower magnetic fields. Thus, for example, in Ge $m_h^* \approx 0.04\, m_0$, and at a frequency of 1×10^{12} cps, the resonance value of the magnetic field is approximately 1.4×10^4 Oe instead of the 3.5×10^5 Oe in paramagnetic resonance.

If the anharmonicity of cyclotron oscillations of the carriers is not strongly pronounced or is completely absent, it is possible to achieve amplification or frequency conversion of the oscillations by the following method. A linearly polarized electromagnetic wave of frequency $\omega_p = 2\omega_c/n$, in which the vector $\mathbf{H}_p$ is oriented parallel to the constant field while its amplitude is somewhat less than H_0, is incident on a semiconductor sample situated in the constant magnetic field H_0. Such a system is potentially unstable with respect to the high-frequency signal of cyclotron frequency polarized in the plane perpendicular to the constant magnetic field. Parametric amplification or generation of high frequency oscillations is possible at this frequency. The power of the "pumping" signal depends on the value of m^*. In the case $\omega_c = 2\pi \times 3 \times 10^9$ cycles/sec and $m^* \approx 0.01\, m_0$ (for example, in the case of InSb) the resonance value of the magnetic field is given by $H_0 \approx 10$ Oe and $P_p \approx 10^4/Q_p$ watts.

---

[1] Dresselhaus, Kip, and Kittel, Phys. Rev. **98**, 368 (1955).

[2] Dexter, Zeiger, and Lax, Phys. Rev. **104**, 637 (1956).

[3] Zeiger, Lax, and Dexter, Phys. Rev. **105**, 495 (1957).

[4] N. G. Basov and A. M. Prokhorov, J. Exptl. Theoret. Phys. (U.S.S.R.) **27**, 431 (1954).

[5] Dresselhaus, Kip, and Kittel, Phys. Rev. **98**, 556 (1955).

Translated by G. Volkoff

SEVERAL POSSIBILITIES ASSOCIATED WITH THE SEPARATION OF CHARGED PARTICLES IN AN INHOMOGENEOUS HIGH-FREQUENCY ELECTROMAGNETIC FIELD

M. A. MILLER

Gor'kii State University

Submitted to JETP editor June 17, 1958

J. Exptl. Theoret. Phys. (U.S.S.R.) **35**, 809-810 (September, 1958)

THE nonrelativistic motion of charged particles in an inhomogeneous electromagnetic field $\mathbf{E}(\mathbf{r})e^{i\omega t}$, $\mathbf{H}(\mathbf{r})e^{i\omega t}$ has been investigated,[1-5] and it was shown that by means of high-frequency potential wells

$$\Phi(\mathbf{r}) = (\eta/2\omega)^2 |\mathbf{E}(\mathbf{r})|^2$$

(η is the ratio of charge to mass) it is possible to control within wide limits the average (over the period $2\pi/\omega$) motion of the particles: reflection from potential barriers, focusing of beams, acceleration of plasma blobs, confinement in a bounded region of space, and so forth. The field, however, had been considered as given, i.e., the reaction of the motion of the particles upon the magnitude and shape of the potential $\Phi(\mathbf{r})$ had been ignored, which is permissible only for low charge densities and if the particles do not leave the interaction region. Taking into account the finite charge density leads to the introduction of the effective dielectric constant of the region occupied by charges, which can markedly change the structure[6] of the potential $\Phi(\mathbf{r})$. Sometimes the second factor is also important; associated with it are a series of interesting new possibilities which are illustrated below on a simple example of sufficient generality.

Let a rectilinear beam of particles move with velocity $\dot{z} = v_0$ into the side of a potential $\Phi(z)$, monotonically increasing from zero and produced by an inhomogeneous high-frequency field. If the period $2\pi/\omega$ of this field is much less than the particle transit time over a distance $L \sim E/|\nabla E|$, along which the amplitude of E changes substantially, then the kinetic energy of a particle, being composed of the energy of the average (over the period $2\pi/\omega$) motion and of the average energy of the oscillatory motion (of frequency ω), remain constant.[1,2] Consequently the particles advance only up to the plane $z = z_0$, such that $\Phi(z_0) = v_0^2/2$, whereupon in the turning point of the beam the energy of forward motion is completely transformed into energy of oscillatory motion: $|\dot{r}_1|^2/4 = \Phi(z)$, $\dot{r}_1 = -(\eta/\omega^2)Ee^{i\omega t}$. Now we assume that the particles leave the interaction region when the total velocity vanishes $[\dot{z}(t) + \dot{r}_1(t) = 0]$ at the plane $z = z_0$. Such a separation of particles can be achieved, for example, with an arrangement of conducting walls at a distance $r_{1\,max} = |\eta E(\dot{r}_0)|/\omega^2$ from the average trajectory of the beam. Then the kinetic energy of the particles is returned completely to the field. Moreover, if the system forming the high-frequency field is tuned to resonance and has a high Q, then, as is not difficult to show,[7] a stable oscillatory regime is always attained for a specific choice of the parameters.

Thus it appears to be possible to use the separation of particles for maintaining a given level of high-frequency power in a system. For instance, in containing a plasma blob in a high-frequency potential well inside a resonant cavity, the separation of fast particles at the walls can ensure the required level of high-frequency field for confining the slower particles, if the plasma temperature is kept constant (i.e. if the plasma is heated by some external source). For these purposes it is also possible to introduce an auxiliary beam of particles, i.e., to combine within a single cavity a source of high-frequency oscillations and a confined plasma blob. A similar combination might prove to be useful for several types of the accelerators that employ a high-frequency electromagnetic field to transfer energy from one beam to another.

The separation of particles interacting with an inhomogeneous field also has a quite independent importance as one of the possible methods of generating and amplifying microwaves.

---

[1] M. A. Miller, Report at the Second Conference MVO on Radioelectronics, Saratov, 1957; Изв. высших учебных заведений, Радиофизика (News of Higher Educational Institutions, Radiophysics) No. 3, 1958 (in press).

[2] A. V. Gaponov and M. A. Miller, J. Exptl. Theoret. Phys. (U.S.S.R.) **34**, 242 (1958), Soviet Phys. JETP **7**, 168 (1958).

[3] H. A. H. Boot and R. B. R.-S.-Harvie, Nature **180**, 1187 (1957).

[4] M. A. Miller, Dokl. Akad. Nauk SSSR **119**, 478 (1958), Soviet Phys. "Doklady" **3**, 322 (1958); J. Exptl. Theoret. Phys. (U.S.S.R.) **35**, 299 (1958), Soviet Phys. JETP **8**, 206 (1959).

[5] A. V. Gaponov and M. A. Miller, J. Exptl. Theoret. Phys. **34**, 751 (1958), Soviet Phys. JETP **7**, 515 (1958).

[6] F. B. Knox, Austral. J. Phys. **10**, 565 (1957).

[7] M. A. Miller, Изв. высших учебных заведений, Радиофизика (News of the Higher Educational Institutions, Radiophysics) No. 4, 1958 (in press).

Translated by J. Heberle
169

CIRCULAR POLARIZATION OF INTERNAL γ-BREMSSTRAHLUNG IN β-DECAY AND TIME REVERSAL INVARIANCE

R. Iu. VOLKOVYSKII

Leningrad State Pedagogical Institute

Submitted to JETP editor June 21, 1958

J. Exptl. Theoret. Phys. (U.S.S.R.) **35**, 811-812 (September, 1958)

THE continuous γ-radiation which accompanies β-decay is of current interest in connection with parity nonconservation in weak interactions. A number of authors[1-3] have indicated that instead of observing the electron polarization it may be possible to observe the circular polarization of the γ-photons. The experiments which have been carried out[4] verify parity nonconservation in weak interactions.

In the present note, we present a theoretical analysis of the bremsstrahlung effect in β-decay in connection with the problem of invariance under time reversal.

A pseudoscalar with respect to time reversal can be formed from the electron momentum, the photon momentum, and the neutrino momentum (using the recoil of the nucleus) or from the electron momentum, the photon momentum and the angular momentum of the nucleus. In the first case we obtain the following expression for the distribution over direction of the electron and the neutrino and energy of the electron and γ-photon (in units in which $\hbar = c = 1$):

$$dw = \frac{e^2}{2(2\pi)^7}\frac{(\varepsilon - E - k)^2}{(p\cos\vartheta - E)^2}\,p\,dE\,d\Omega\,d\Omega_\nu\frac{dk}{k}\,\xi\left\{p^2\sin^2\vartheta\left(E + a\frac{\mathbf{p}_\nu}{E_\nu}\mathbf{p} + bm\right) + (1 \mp G)\,I_1 + (a \mp H)\frac{\mathbf{p}_\nu}{E_\nu}\mathbf{I}_2 \pm K\frac{\mathbf{p}_\nu}{E_\nu}\mathbf{I}_3 \pm L\frac{m\,[\mathbf{p}\times\mathbf{p}_\nu]\,\mathbf{k}}{E_\nu}\right\}. \tag{1}$$

Here m, E, $\mathbf{p}$, and Θ are respectively the rest mass, energy, and momentum of the electron and the angle formed by it and the γ-photon, ϵ is the difference in mass for the initial and final nucleus, E_ν and $\mathbf{p}_\nu$ are the energy and momentum of the neutrino, k and $\mathbf{k}$ are the energy and momentum of the photon, and n is a unit vector in the $\mathbf{k}$ direction. The upper sign refers to right-handed circular polarization of the γ-photon, the lower sign refers to left-handed polarization. Further,

$$I_1 = kp^2\sin^2\vartheta + k^2E - k^2p\cos\vartheta,$$
$$\mathbf{I}_2 = k(E - p\cos\vartheta)\,\mathbf{p} + (p^2 + Ek - pk\cos\vartheta - Ep\cos\vartheta)\,\mathbf{k},$$
$$\mathbf{I}_3 = m(\mathbf{k}\,p\cos\vartheta - k\mathbf{p});$$
$$H\xi = 2\mathrm{Re}\,[\mp|M_{\mathrm{F}}|^2(C_SC_S'^* + C_VC_V'^*) \pm \tfrac{1}{3}|M_{\mathrm{GT}}|^2(C_TC_T'^* + C_AC_A'^*)];$$
$$K\xi = 2\mathrm{Re}\left[-|M_{\mathrm{F}}|^2(C_SC_V'^* + C_S'C_V^*) + \tfrac{1}{3}|M_{\mathrm{GT}}|^2(C_TC_A'^* + C_T'C_A^*)\right];$$
$$L\xi = 2\mathrm{Im}\left[|M_{\mathrm{F}}|^2(C_SC_V^* + C_S'C_V'^*) - \tfrac{1}{3}|M_{\mathrm{GT}}|^2(C_TC_A^* + C_T'C_A'^*)\right].$$

The upper sign in the last three expressions refers to electron decay, the lower sign refers to positron decay. The remaining notation is the same as that used by Jackson, Treiman, and Wyld.[5] The appearance of a term proportional to L is inconvenient because of the fact that the Fierz interference terms are contained in L.

The following expression for the probability of internal bremsstrahlung in β-decay of oriented nuclei is obtained when we integrate over direction of neutrino emission:

$$dw = \frac{e^2}{2(2\pi)^7}\frac{(\varepsilon - E - k)^2}{(p\cos\vartheta - E)^2}\,p\,dE\,d\Omega\frac{dk}{k}\,\xi\left\{p^2\sin^2\vartheta\left(E + A\frac{\langle\mathbf{J}\rangle}{J}\mathbf{p} + bm\right) + (1 \mp G)\,I_1 + \frac{\langle\mathbf{J}\rangle}{J}(A \mp N)\,\mathbf{I}_2 \pm \frac{\langle\mathbf{J}\rangle}{J}(Q\mathbf{I}_3 + Rm\,[\mathbf{p}\times\mathbf{k}])\right\}. \tag{2}$$

$\langle\mathbf{J}\rangle$ is the expectation value for the angular momentum of the initial nucleus,

$$N\xi = 2\mathrm{Re}\left[|M_{\mathrm{GT}}|^2\lambda_{J'J}\tfrac{1}{2}(|C_T|^2 + |C_A|^2 + |C_T'|^2 + |C_A'|^2) \pm \delta_{J'J}|M_{\mathrm{F}}||M_{\mathrm{GT}}|\left(\frac{J}{J+1}\right)^{1/2}(C_SC_T^* + C_VC_A^* + C_S'C_T'^* + C_V'C_A'^*)\right];$$
$$Q\xi = 2\mathrm{Re}\left[\pm|M_{\mathrm{GT}}|^2\lambda_{J'J}(C_TC_A^* + C_T'C_A'^*) + \delta_{J'J}|M_{\mathrm{F}}||M_{\mathrm{GT}}|\left(\frac{J}{J+1}\right)^{1/2}(C_SC_A^* + C_VC_T^* + C_S'C_A'^* + C_V'C_T'^*)\right];$$
$$R\xi = 2\mathrm{Im}\left[\pm|M_{\mathrm{GT}}|^2\lambda_{J'J}(C_TC_A'^* + C_T'C_A^*) + \delta_{J'J}|M_{\mathrm{F}}||M_{\mathrm{GT}}|\left(\frac{J}{J+1}\right)^{1/2}(C_SC_A'^* + C_S'C_A^* - C_VC_T'^* - C_V'C_T^*)\right].$$

Expressions containing the imaginary parts of the coupling constants are also obtained in an analysis of electron polarization in β-decay of oriented and nonoriented nuclei in the same cases as in ordinary β-decay.[5] The results of calculations of β-decay with the emission of γ-photons will be published in Изв. высших учебных заведений (News of the Higher Educational Institutions). Here we present the probability for transition into a state in which the electron has an energy in the interval dE, the γ-photon has an energy in the interval dk, the electron momentum $\mathbf{p}$ lies in the solid angle dΩ, and the polarization of the electron is given by the unit vector ξ (the polarization directions for the γ-photon are summed and the nuclei are nonoriented):

$$dw = \frac{2e^2}{(2\pi)^6}\frac{(\varepsilon - E - k)^2}{(p\cos\vartheta - E)^2}\,p\,dE\,d\Omega\frac{dk}{k}\,\xi\Big\{k^2(E - p\cos\vartheta) + (E + k)\,p^2\sin^2\vartheta$$
$$+ bmp^2\sin^2\vartheta + G\left[(\boldsymbol{\zeta}\cdot\mathbf{p})\left(p^2\sin^2\vartheta + \frac{kp^2}{E+m}\sin^2\vartheta + k^2 + mk + \frac{k^2p}{E+m}\cos\vartheta\right) - m(\boldsymbol{\zeta}\cdot\mathbf{k})(k + p\cos\vartheta)\right]\Big\}. \tag{3}$$

We wish to express our thanks to S. V. Izmailov for his constant interest.

---

[1] G. W. Ford, Phys. Rev. **107**, 321 (1957).

[2] R. E. Cutkosky, Phys. Rev. **107**, 330 (1957).

[3] A. Pytte, Phys. Rev. **107**, 1681 (1957).

[4] H. Schopper and S. Galster, Nucl. Phys. **6**, 125 (1958).

[5] Jackson, Treiman and Wyld, Phys. Rev. **106**, 517 (1957).

Translated by H. Lashinsky
170

NEW MEASUREMENTS OF THE NEUTRON SPECTRUM IN THE BOMBARDMENT OF Be BY 680-Mev PROTONS

V. S. KISELEV, K. O. OGANESIAN, R. A. POZE, and V. B. FLIAGIN

Joint Institute for Nuclear Research

Submitted to JETP editor June 21, 1958

J. Exptl. Theoret. Phys. (U.S.S.R.) 35, 812-814 (September, 1958)

AN investigation of the neutron spectrum obtained in the bombardment of a beryllium target by 680-Mev protons has been reported earlier;[1] in that work the measurements were performed by measuring the absorption curves for the recoil protons emitted in elastic np scattering. The energy distributions obtained in this way contained a sizeable charged-pion component (20%) in the high-energy region; these mesons are products of the reactions

$$n + p \rightarrow \pi^+ + n + n, \quad (1)$$

$$n + p \rightarrow \pi^- + p + p. \quad (2)$$

The absence of any experimental data for the spectra of charged pions formed in these reactions leaves an element of uncertainty in the reliability of the corrections which are applied to take account of this contamination.

By using a magnetic field for momentum analysis of the recoil protons in the present work, it has been possible to avoid completely any charged-pion contamination over the entire energy range investigated. The measurements carried out with the new method were performed at a neutron emission angle of 0°. Special attention was paid to the high-energy region of the spectrum, since this region is important in most of the work carried out with the neutron beam.

A diagram of the experimental arrangement is shown in Fig. 1. The neutron beam strikes either a polyethylene or a carbon target. The effect due to hydrogen is taken as the difference in the results obtained with these two targets. The scintillation counters 1, 2, 3, which record the recoil protons, are connected in coincidence. Counter 1 is very thin (0.1 g/cm^2) in order to minimize multiple scattering; counters 2 and 3 are long (15 cm) in the direction perpendicular to the plane of the figure in order to detect the majority of particles which diverge in the vertical plane as a result of defocusing. The spectrometer is calibrated by the well-known method in which a current-carrying wire is used to "mark" the magnetic field. The absolute energy scale is determined with an accuracy of approximately 1%.

In computing the spectrum, corrections were made for the proton energy loss in the targets and in air and for the astigmatism of the magnetic system. Corrections for the energy dependence of the cross section for elastic np scattering were taken from work on the differential cross sections for np scattering reported in the literature.[2-8]

In Fig. 2 are shown the corrected results of these measurements. In the same figure are shown the data obtained earlier,[1] which have been adjusted (corrections < 10%) in accordance with the new measurements on the yield of charged pions in np collisions.[9] The results of the two measurements were combined in such a way as to make the integrated spectra the same between 300-Mev and the maximum energy. The errors denoted by the vertical lines in Fig. 2 are the statistical uncertainties; these do not include the errors in the n-p scattering cross sections. The latter are not important because we consider only a small energy range and need be taken into account only in comparing the far regions of the spectra. The horizontal spreads indicate the calculated resolving power of the instrument.

It should be kept in mind that the portion of the spectrum between 100 and 500 Mev contains a small admixture of protons emitted in the reaction $n + p \rightarrow \pi^0 + n + p$ and in reaction (2). This admixture is estimated as approximately 10%; this figure

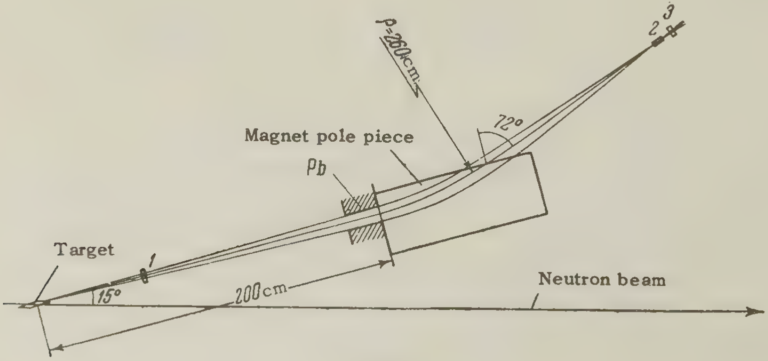

FIG. 1.

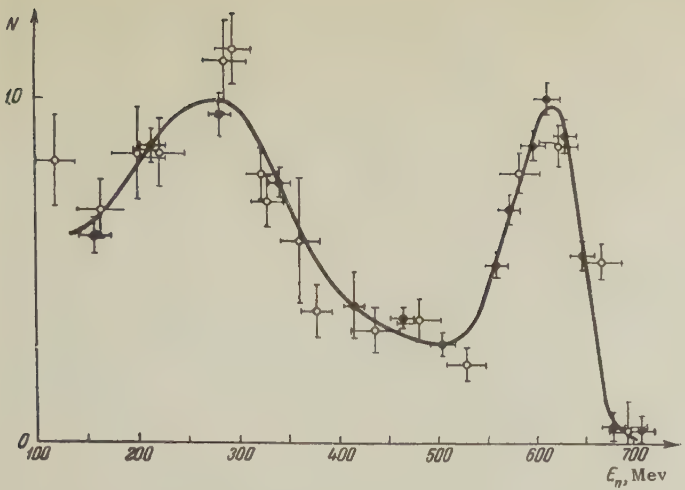

FIG. 2. Neutron energy spectrum. The black dots refer to the data of the present measurements. The circles refer to the data of reference 1 with the corrections indicated in the text.

has not been determined experimentally because of the great difficulty involved.

The present measurements, which were made with a high-resolution detector and in which there was no pion contamination, indicate that the maximum at 610-Mev has a smaller half-width (approximately 100-Mev) than that given in reference 1.

The origin of the two maxima in the neutron spectrum has been discussed in reference 1, to which the reader is referred.

In conclusion the authors wish to thank V. P. Zrelov for a number of valuable comments in connection with the present work.

---

[1] V. S. Kiselev and V. B. Fliagin, J. Exptl. Theoret. Phys. (U.S.S.R.) **32**, 962 (1957), Soviet Phys. JETP **5**, 786 (1957).

[2] Randle, Taylor, and Wood, Proc. Roy. Soc. (London) **A213**, 392 (1952).

[3] Guernsey, Mott, and Nelson, Phys. Rev. **88**, 15 (1952).

[4] Kelly et al., Phys. Rev. **79**, 96 (1950).

[5] J. De Pangher, Phys. Rev. **95**, 578 (1954).

[6] A. J. Hartzler and R. T. Siegal, Phys. Rev. **95**, 185 (1954).

[7] V. P. Dzhelepov et al., Izv. Akad. Nauk SSSR, Ser. Fiz. **19**, 573 (1955) [Columbia Techn. Transl. **19**, 514 (1955)].

[8] Iu. M. Kazarinov and Iu. N. Simonov, J. Exptl. Theoret. Phys. (U.S.S.R.) **31**, 169 (1956); Soviet Phys. JETP **4**, 161 (1957).

[9] Iu. M. Kazarinov and Iu. N. Simonov, J. Exptl. Theoret. Phys. (U.S.S.R.) **35**, 78 (1958); Soviet Phys. JETP **8**, 56 (1959).

Translated by H. Lashinsky
171

RELATIVE YIELDS OF DELAYED NEUTRONS IN FISSION OF U^{238}, U^{235} *AND* Th^{232} *BY FAST NEUTRONS*

B. P. MAKSIUTENKO

J. Exptl. Theoret. Phys. (U.S.S.R.) **35**, 815-816 (September, 1958)

MEASUREMENTS have been made of the relative yields of delayed neutrons in fission of natural uranium, U^{235} (90% enriched) and Th^{232} by neutrons with energies of 15.0 ± 0.9, 3.3 ± 0.7, and 2.4 ± 0.3 Mev.

The 15.0-Mev neutrons were obtained from a thick tritium target which was bombarded by 440-kev deuterons. The 3.3 and 2.4-Mev neutrons were obtained from the $D(d, n)He^3$ reaction. A target of heavy ice was bombarded by 920-kev deuterons.

The thermal neutrons were also recorded. The latter were obtained by slowing down fast neutrons from the $Be^9(d, n)B^{10}$ reaction in a paraffin block which surrounded the target. The number of delayed neutrons for a sample enclosed in cadmium was less than 5% of the number of the delayed neutrons without the cadmium.

In order to determine the effect of target thickness on the delayed-neutron yield ratio measurements were made using U^{235} samples of different thickness in fission by 15.0-Mev neutrons. The U^{238}, Th^{232} and U^{235} samples were 35 mm in diameter and 9, 10, and 8 mm thick respectively.

The detector was a bank of four BF_3 counters connected in parallel and surrounded by paraffin.

The samples of fissile material were irradiated by the fast-neutron flux for a given time interval and then dropped into the counter block, located at a distance of approximately 1.5 meters below the target. When the sample was located the ion source of the accelerator and the high voltage power supply were switched off. The time required to move the sample was 0.20 to 0.30 sec.

The neutron detection circuit was switched on when the sample reached the center of the counter. The pulses from the counter bank were amplified and then recorded in a time analyzer. The channels in the time analyzer record in sequence the time required for a predetermined number of pulses.

Two series of exposures were made, 300 and 30 sec. The corresponding measurement times were 360 and 270 sec. There was essentially no background during the measurements; the background was checked by using a steel sample in place of the fissile material.

Group Number	Decay time	Relative yield	Group Number	Decay time	Relative yield
	U^{235} Thermal			U^{238}(2.4 Mev)	
1	55.55	0.039	1	54.88	0.012
2	22.02	0.245	2	21.41	0.152
3	6.06	0.206	3	5.47	0.176
4	2.25	0.418	4	1.95	0.440
5	0.462	0.092	5	0.568	0.220
	U^{235}(2.4 Mev)			U^{238}(3.3 Mev)	
1	56.09	0.037	1	53.51	0.014
2	22.27	0.221	2	20.34	0.153
3	5.46	0.217	3	5.66	0.169
4	2.17	0.409	4	2.10	0.423
5	0.435	0.116	5	0.590	0.241
	U^{235}(3.3 Mev)			U^{238}(15 Mev)	
1	55.16	0.043	1	56.11	0.022
2	21.63	0.219	2	21.92	0.167
3	6.32	0.210	3	5.20	0.171
4	2.24	0.428	4	2.27	0.412
5	0.650	0.100	5	0.600	0.228
	U^{235}(15 Mev; 8 mm)			Th^{232}(2.4 Mev)	
1	54.70	0.052	1	53.32	0.038
2	20.93	0.182	2	19.63	0.127
3	6.27	0.206	3	6.37	0.195
4	2.27	0.396	4	2.08	0.408
5	0.646	0.164	5	0.651	0.232
	U^{235}(15 Mev; 4 mm)			Th^{232}(3.3 Mev)	
1	53.98	0.058	1	54.97	0.037
2	20.60	0.201	2	21.64	0.137
3	5.60	0.209	3	6.61	0.190
4	2.23	0.366	4	2.07	0.423
5	0.659	0.166	5	0.664	0.213
	U^{235}(15 Mev; 2.3 mm)			Th^{232}(15 Mev)	
1	55.15	0.051	1	53.80	0.044
2	22.32	0.181	2	19.07	0.154
3	6.29	0.203	3	6.42	0.169
4	2.17	0.402	4	2.15	0.428
5	0.638	0.163	5	0.553	0.205

The decay curves for a given element and the corresponding energy obtained in different experiments were combined. In combining these results use was made of the fact that the ratio of the counting rates at any instant of time for the decay curves obtained with different irradiation intensities is equal to the ratio of the total counts (i.e., the total number of pulses) for the same curves over equal time intervals (in the present case these intervals are 360 and 270 sec for exposures of 300 and 30 sec). Five groups of delayed neutrons were resolved. The relative yields of 55- and 22-sec decays were determined from the decay curves obtained using the 300-sec exposure. These two groups were resolved using a method of successive approximations. The three later groups (with shorter periods) were determined from the decay curve obtained with the 30-sec exposure. A sixth decay time could not be resolved because of its low intensity and short lifetime.

The contribution of the first and second delayed-neutron groups in short exposures was determined for each individual decay curve appearing in the total from the integrated pulse count over a time interval of approximately 60 sec (when the contribution of the short-lived decays was negligibly small) to 270 sec (end of count), using the intensity ratio for the first two groups as obtained from an analysis of the curves for the 300-sec exposures. In computing the contributions of the first two groups we used the mean value of the initial counting rate in the individual measurements carried out at the same exposure intensities.

All curves were computed by a least-squares method. The results are shown in the table.

The author is indebted to O. D. Kazachkovskii for valuable comments.

Translated by H. Lashinsky
172

RADIATION OF A MULTILEVEL SYSTEM MOVING IN A MEDIUM WITH A VELOCITY GREATER THAN THE VELOCITY OF LIGHT

V. L. GINZBURG and V. M. FAIN

Gor'kii State University

Submitted to JETP editor June 30, 1958

J. Exptl. Theoret. Phys. (U.S.S.R.) **35**, 817-818 (September, 1958)

THE formula for the complex ("superlight") Doppler effect, in which the radiator moves with a velocity $v > c/n$ in a transparent medium characterized by a refractive index $n(\omega)$, is of the form[1]

$$\omega(\theta) = \omega_{ik}\sqrt{1-\beta^2}/|1-\beta n(\omega)\cos\theta|, \qquad (1)$$

where ω_{ik} is the frequency in the system in which the radiator is at rest, $\beta = v/c$, and θ is the angle between **v** and the wave normal. In a quantum-mechanical analysis Eq. (1) is obtained (cf. reference 2) from the laws of conservation of energy and momentum where the energy and momentum of the photon in the medium are respectively $\hbar\omega$ and $\hbar\omega n/c$. In the quantum-theory formulation, the Cerenkov condition $\beta n \cos\theta_0 = 1$ is obtained in a similar way (cf. reference 3). In the normal Doppler effect [when $\beta n(\omega)\cos\theta < 1$] the radiating system makes a transition from an upper state with energy ϵ_i to a lower state with energy $\epsilon_k = \epsilon_i - \hbar\omega_{ik}$. In the complex Doppler effect, however, [when $\beta n(\omega)\cos\theta > 1$, i.e., inside the Cerenkov cone] the radiation is characterized by transitions of the system in the upward direction — from a level ϵ_k to a level $\epsilon_i = \epsilon_k + \hbar\omega_{ik}$.[2] As a result, even in the absence of any other interaction, the system does not radiate and the probability of its remaining at the levels ϵ_i and ϵ_k is determined by the total probability of radiation at the normal and complex Doppler frequencies. Two points must be kept in mind in considering the possibility of observing the complex Doppler effect. First, if the radiator does not move in the medium itself but in an empty channel or in a slit of width smaller than the wave length of the radiated waves the characteristic features of the "superlight" radiation still obtain.[4,5] The complex Doppler effect can be important in motion of electrons in a magneto-active plasma when the losses are small; this case is of special interest in practice (cf. below). It is the purpose of the present note to point out the interesting possibilities associated with the faster-than-light motion of a multilevel system. If the system is initially at one level, say the ground state, in the course of time it may be found in all states to which it can make a transition as a result of direct or multiple radiative transitions (transitions upward with the radiation of frequency ω are possible only if the relation in (1) obtains with $\beta n(\omega)\cos\theta > 1$). The level populations are determined by the equations:

$$dN_i/dt = -\sum_k A_{ik}N_i + \sum_k B_{ik}N_k,$$

where A_{ik} is the probability for a radiative transition from level i to level k while B_{ik} is the probability for transition from level k to level i (this scheme, similar to that used to describe radioactive decay, can be obtained from the quantum theory of radiation, using certain justifiable assumptions[6]). In the dipole transitions between any states, i and k, the radiation intensity at the normal and complex Doppler frequencies can be determined from the classical formulas[1,2] by replacing the square of the amplitude of the dipole moment by $4|\mathbf{p}_{ik}|^2$. For example, with $n = \text{const}$ and a moment $\mathbf{p}_{ik}$ oriented along the velocity vector **v**, the energy radiated per unit time into unit solid angle is

$$W(\theta) = \omega_{ik}^4(1-\beta^2)^3|\mathbf{p}_{ik}|^2\sin^2\theta/2\pi c^3|1-\beta n\cos\theta|^5, \qquad (2)$$

where the angle θ is related to ω by Eq. (1) and $\mathbf{p}_{ik}$ is the matrix element for the rest system.

When $\beta n\cos\theta \to 1$, it is obviously impossible to neglect dispersion. In a number of cases, however, a reasonable approximation can be obtained by taking n as a step function: $n(\omega) = n$ for $\omega < \omega_c$ and $n = 1$ for $\omega > \omega_c$. This behavior for the refractive index n is reasonable in the case of weak dispersion for motion in a channel or in a slit as well as for an extended radiating system (in this case when $\cos\theta_0 \sim 1$ the frequency $\omega_c \sim 2\pi v/l$ where l is the radius of the channel, the width of the slit or a typical dimension of the system). If the angle θ_c is close to the Cerenkov angle θ_0, it is clear from Eq. (2) that the intensity (or probability) of the radiation is approximately the same at the normal and complex frequencies [basically, frequencies are radiated which are close to $\omega_c(\theta_c)$]. Under these conditions, the populations of levels i and k will be the same in the stationary state.

In a number of multilevel systems we deal with bunches of atoms or molecules with two appropriate levels. The radiation from a bunch which is smaller than the wavelength of interest is coherent and similar to the radiation of a spin system placed in a magnetic field.[7] However, the faster-than-light radiation of such bunches or of individual atoms and molecules or paramagnetic or ferromagnetic particles is scarcely of practical interest (even with $n \sim 30$ the hydrogen atom can acquire a velocity $v > c/n$ only when its kinetic energy is 5×10^6 ev). On the other hand, it is completely feasible to consider faster-than-light radiation of electrons which move along a magnetic field in which the role of the medium is played by a metal slow-wave structure, a dielectric, or a plasma located near the beam. If the velocity component perpendicular to the field $\mathbf{v}_\perp$ is zero only Cerenkov radiation is possible. If, however, $\mathbf{v}_\perp \neq 0$ and the condition $v_\perp/v_\parallel \ll mc^2/E \ll 1$ is fulfilled the electrons radiate in the same way as two perpendicular oscillators which lie in the plane of $\mathbf{v}_\perp$ and move through the field with a velocity $v_\parallel$. The faster-than-light Doppler radiation, which appears when $v_\parallel > c/n(\omega)$, causes electron transition to higher levels, i.e., the excitation of transverse oscillations. As a result the velocity $v_\parallel$ is reduced and, for example, with $n = \text{const}$ the excitation stops when $v_\parallel = c/n$. In a case of great practical interest, namely, the sporadic radio waves from the sun,[8] the motion of the electrons in the magneto-active plasma medium is anisotropic. Hence in Eq. (1) we must replace n by $n_j(\theta, \omega)$ where j denotes the type of proper wave (ordinary or extraordinary). Dispersion cannot be neglected and the expression for the radiated energy is strongly divergent.[9] The author proposes to consider faster-than-light Doppler electron radiation in detail in a subsequent paper.

---

[1] I. M. Frank, Izv. Akad. Nauk SSSR, Ser. Fiz. **6**, 3 (1942); J. Phys. (U.S.S.R.) **7**, 49 (1943).

[2] V. L. Ginzburg and I. M. Frank, Dokl. Akad. Nauk SSSR **56**, 583 (1947).

[3] V. L. Ginzburg, J. Exptl. Theoret. Phys. (U.S.S.R.) **10**, 589 (1940); J. Phys. (U.S.S.R.) **2**, 441 (1940).

[4] V. L. Ginzburg and I. M. Frank, Dokl. Akad. Nauk SSSR **56**, 699 (1947).

[5] V. L. Ginzburg, Dokl. Akad. Nauk SSSR **56**, 145 (1947); V. L. Ginzburg and V. Ia. Eidman, J. Exptl. Theoret. Phys. (U.S.S.R.) (in press).

[6] L. D. Landau, Z. Physik **45**, 430 (1927); F. Bloch, Physik. Z. **29**, 58 (1958); V. Weisskopf and E. Wigner, Z. Physik **63**, 54 (1930); **65**, 18 (1930).

[7] R. H. Dicke, Phys. Rev. **93**, 99 (1954); V. M. Fain, Usp. Fiz. Nauk **64**, 273 (1958).

[8] G. G. Getmantsev and V. L. Ginzburg, Dokl. Akad. Nauk SSSR **87**, 187 (1952); V. V. Zhelezniakov, Usp. Fiz. Nauk **64**, 113 (1958).

[9] V. Ia. Eidman, J. Exptl. Theoret. Phys. (U.S.S.R.) **34**, 131 (1958), Soviet Phys. JETP **7**, 91 (1958).

Translated by H. Lashinsky
173

CHANGE IN WIDTH OF BOUNDARY LAYER IN FERROMAGNETS BY MEANS OF THE MAGNETO-OPTICAL KERR EFFECT

L. V. KIRENSKII and V. V. VETER

Physics Institute of the Siberian Division, Academy of Sciences, U.S.S.R.

Submitted to JETP editor July 11, 1958

J. Exptl. Theoret. Phys. (U.S.S.R.) 35, 819 (September, 1958)

ATTEMPTS to measure the width of the boundary layer between ferromagnetic domains have been heretofore by the method of powder patterns with the use of an electron microscope.[1] In the final analysis, however, this method determines not the true width of the boundary layer, but the width of the path occupied by the magnetic suspension. In this work we employ in principle a method proposed by Krinchik,[2] based on the use of the polar magneto-optical Kerr effect.[3] This method permits direct measurement of the width of the boundary layer.

It can be shown that the average normal component of magnetization of the boundary layer is represented by the quantity $2j_S/\pi$, where J_S is the saturation magnetization of the ferromagnetic region. A photomultiplier (FEU-18) was used to measure the variation, due to the rotation of the plane of polarization, in light reflected from the boundary layer, and to measure the change in the light flux from the studied portion of the ferromagnetic region, magnetized normal to the surface to a value $2J_S$. The direct proportionality between the two measured quantities leads to the ratio

$$\Delta\Phi / \Delta\Phi' = ld / S',$$

where $\Delta\Phi$ is the change in the light flux from the boundary layer, $\Delta\Phi'$ is the change in the light flux from the studied section of the specimen normally magnetized to a value $2J_S/\pi$, l is the length of the boundary layer bounded by the area of the section considered, d is the width of the boundary layer, and S' is the area of the studied portion of the specimen.

As can be seen from this expression, d is determined by comparing the light fluxes and the areas.

We used an integral-balance circuit in conjunction with the FEU-18 photomultiplier[4] and a compensating setup, the MBI-6 microscope, and the SI-1 pulse synchroscope. The variation of the light flux reflected from the boundary layer was estimated from the value of the capacitor-charging photocurrent at the instant when the boundary layer was brought into the field of view of the microscope and the system was unbalanced. The variation of the light flux from the section of the ferromagnetic region normally magnetized to a value $2J_S/\pi$ was estimated from the value of the flux as measured directly by the galvanometer.

The area of the studied region was measured under the microscope with an ocular micrometer and an object micrometer.

The width of the boundary layer was determined for single crystals of iron silicide containing 3% silicon. The longitudinal measurements give a value of 0.8 microns for the width of the boundary layer.

---

[1] D. J. Craig, Proc. Phys. Soc. B69, 438 (1956).

[2] G. S. Krinchik, Физика металлов и металловедение (Physics of Metals and Metal Research) 3, 549 (1956).

[3] A. V. Sokolov, Usp. Fiz. Nauk 50, 161 (1953).

[4] L. A. Kubetskii, Вторично-электронныеxx приборы (Secondary-Emission Devices), 1951.

Translated by J. G. Adashko

NEGATIVE IONS OF IRON, COBALT, AND NICKEL

V. M. DUKEL'SKII and V. M. SOKOLOV

Leningrad Physico-Technical Institute,
Academy of Sciences, U.S.S.R.

Submitted to JETP editor July 5, 1958

J. Exptl. Theoret. Phys. (U.S.S.R.) 35, 820 (September, 1958)

In all cases known at present, it is possible to attribute formation of atomic negative ions to the penetration of an additional electron into an incomplete outer group of equivalent electrons. It appeared to us that an electron affinity could be possessed also by such atoms that have an "open position" not on the periphery of the electron cloud but in its deeper portions. In connection with this, we undertook a search for negative ions of iron, cobalt, and nickel. In these elements there are two outer 4s electrons and an incompletely filled 3d group. We chose these elements also because we found mention made in the work of Schaefer and Walcher[1] of weak nickel lines in the spectrum of the negative ions emitted by an oxide cathode with a nickel core.

In our experiments we used a magnetic mass spectrometer with a resolving power of about 100. We obtained negative ions by exposing molecules containing the investigated atoms to the action of an intense beam of electrons. For working substances we chose the anhydrous dichlorides $FeCl_2$, $CoCl_2$ and $NiCl_2$. Analysis of the composition of the negative ions obtained upon introduction of vapors of these substances into the ion source of the mass spectrometer gave the following results:

$FeCl_2$. With operation of the ion source as usual for mass-spectroscopic determinations, lines for Cl^-, Cl_2^-, $FeCl^-$ and $FeCl_3^-$ were observed in the negative ion spectrum. For a higher temperature of the oven which contained the $FeCl_2$, lines appeared corresponding to Fe^- ions (masses 54 and 56). Pushing the operation of the source (25 ma, 70 v), the current of Fe_{56}^- ions could be raised to 5×10^{-13} amp (along with which the current of $FeCl^-$ and $FeCl_2^-$ ions was of the order of 10^{-10} amp).

$CoCl_2$. With ordinary operation of the ion source, ions of Cl^-, Cl_2^-, $CoCl^-$, $CoCl_2^-$ and also a weak line of Co_{59}^- were observed. By increasing the intensity of the electronic current and the density of the $CoCl_2$ fumes in the source, we could drive the current of Co^- ions to 3×10^{-13} amp.

$NiCl_2$. In the spectrum of negative ions, the lines Cl^-, Cl_2^-, $NiCl^-$, $NiCl_2^-$ and also weak Ni^- lines (masses 58 and 60) were observed. With forced operation of the ion source, the intensity of the Ni_{58}^- and Ni_{60}^- lines substantially increased and a Ni_{62}^- line became noticeable. The current of Ni_{58}^- ions was successfully raised to 1×10^{-12} amp.

We have thus discovered the existence of Fe^- and Co^- ions and have confirmed the existence of Ni^- ions.

One can make two different hypotheses about the electronic structure of the Fe^-, Co^- and Ni^- ions. Either the additional electron starts a new 4p group in these ions, or, upon its penetration, a rearrangement of the electronic shell proceeds which results in one of the electrons going into the 3d group. The second hypothesis seems to us the more probable. If it is correct, then the Fe^- ion should have the structure $1s^2 \ldots 3d^7\,4s^2$, differing from the structure of the Fe atom ($1s^2 \ldots 3d^6\,4s^2$) by an odd electron in the 3d group. Analogously, a Co^- ion must have the structure $1s^2 \ldots 3d^8\,4s^2$, and a Ni^- ion the structure $1s^2 \ldots 3d^9\,4s^2$. In connection with this, one should note that according to spectroscopic data,[2] upon the removal of one of the outer 4s electrons from atoms of Co and Ni the second 4s electron goes over into the 3d group.

---

[1] H. Schaefer and W. Walcher, Z. Physik **121**, 679 (1943).

[2] Ch. E. Moore, Atomic Energy Levels **2**, 83, 151 (1952) [U. S. Govt. Printing Off.].

Translated by R. Eisner
175

THE UNIVERSAL FERMI INTERACTION AND THE CAPTURE OF THE μ MESON BY THE PROTON

Ia. B. ZEL' DOVICH and S. S. GERSHTEIN

Leningrad Physico-Technical Institute, Academy of Sciences, U.S.S.R.

Submitted to JETP editor July 26, 1958

J. Exptl. Theoret. Phys. (U.S.S.R.) **35**, 821-823 (September, 1958)

GELL-MANN and Feynman,[1] and independently Suderman and Marshak,[2] proposed principles leading to a definite form of the interaction between four fermions. Depending on whether the A, B, C, D are "particles" or "antiparticles," these principles yield two distinct possibilities: the interaction (V − A), which is invariant under different pairings of the particles,

$$H_1 = 8^{1/2} G (\overline{\Psi}_A \gamma_\mu a \Psi_B)(\overline{\Psi}_C \gamma_\mu a \Psi_D) \qquad (1)$$

[where Ψ_A, Ψ_B, Ψ_C, Ψ_D are the wave functions of the "particles," $a = (1 + \gamma_5)/2$], or the interaction (V + A),

$$H_2 = 8^{1/2} G (\overline{\Psi}_A \gamma_\mu \bar{a} \Psi_B)(\overline{\Psi}_C \gamma_\mu a \Psi_D) \qquad (2)$$

[where Ψ_A, Ψ_B are the wave functions of the "antiparticles," $\bar{a} = (1 - \gamma_5)/2$], which for a different pairing of the particles[3] has the form (S − P):

$$H_2 = 2 \cdot 8^{1/2} G (\Psi_A a \Psi_D)(\overline{\Psi}_C \bar{a} \Psi_B). \qquad (2')$$

In all formulas we consider here one and the same process A + C = B + D and, by convention, call "particles" all those particles which have a left longitudinal polarization for $v/c = 1$; their antiparticles have the opposite sign of polarization.

The difference between the interactions (1) and (2) is particularly clear when we look at the formula (2′). Gell-Mann and Feynman note the extremal properties of (V − A) and (V + A) from the point of view of the asymmetry of the decay of the polarized neutron. We note that even before the discovery of parity non-conservation one of us has shown[4] that the difference of the Fermi and Gamow-Teller interactions with equal coefficients of (S − T) and (V − A) (which does not satisfy the Tolhoek-de Groot symmetry[5]) yields full polarization of the slow electron, whereas the sum yields complete depolarization of the slow electron in the β decay of the polarized neutron. The capture of the μ meson by a proton from a definite state of the hyperfine structure is evidently the reverse process to the emission of a slow particle. Expressions for the capture probability of the μ meson in different states of the hyperfine structure are given in reference 6. It follows from these expressions that in the variant (V + A), which goes over into (S − P) when written as $(\overline{P}0\nu)$ $(\bar{\mu}^- 0N)$, the (S − P) probabilities for the capture in the states F = 0 and F = 1 (F is the combined spin of the proton and μ meson) are exactly the same, while in the variant (V − A) the probability for capture from F = 1 is zero, and the probability for capture from $F = 0$ is four times larger than the value averaged over the spins. This result can be obtained immediately, when we write the interactions $(\mu\nu PN)$ (1) and (2) in spinor components for the case when the neutron, proton, and μ meson are described by nonrelativistic wave functions:

$$H_1 = -2G\,(N_1^*\nu_2^* - N_2^*\nu_1^*)\,(P_1\mu_2 - P_2\mu_1); \qquad (3)$$

$$\begin{aligned} H_2 = -2G\Big\{ & N_1^*\nu_1^*P_1\mu_1 + N_2^*\nu_2^*P_2\mu_2 \\ & + \frac{1}{2}\,(N_1^*\nu_2^* + N_2^*\nu_1^*)\,(P_1\mu_2 + P_2\mu_1) \\ & - \frac{1}{2}\,(N_1^*\nu_2^* - N_2^*\nu_1^*)\,(P_1\mu_2 - P_2\mu_1)\Big\}, \end{aligned} \qquad (4)$$

where the wave functions of the neutron (N), proton (P), μ meson (μ), and neutrino (ν) have the form (we use a representation in which γ_4 is diagonal):*

$$N = \begin{pmatrix} N_1 \\ N_2 \\ 0 \\ 0 \end{pmatrix}; \qquad P = \begin{pmatrix} P_1 \\ P_2 \\ 0 \\ 0 \end{pmatrix}; \qquad \mu = \begin{pmatrix} \mu_1 \\ \mu_2 \\ 0 \\ 0 \end{pmatrix};$$

$$\nu = \frac{1}{\sqrt{2}}\begin{pmatrix} \nu_1 \\ \nu_2 \\ -\nu_1 \\ -\nu_2 \end{pmatrix}.$$

As was shown in reference 7, the capture of a μ meson by a proton occurs, because of the possibility of the "jumping" of the μ meson from one proton to another, from the hyperfine structure state $F = 0$, i.e., from the state in which the μ meson and the proton have opposite spins. The probability for the capture of the μ meson by the proton is four times greater for $(V - A)$ than for $(V + A)$. Hence, it is possible to determine the relative sign of V and A in the fundamental interaction law $(\mu\nu PN)$ by a measurement of the absolute yield of the reaction $\mu^- + P \rightarrow N + \nu$ in hydrogen for capture from the state $F = 0$.

Allowing for the possibility that strong interaction corrections may change the value of the axial vector constant, we may write the Hamiltonian for the interaction of the real nucleons with $(\mu\nu)$ in the form

$$H = \frac{1+\lambda}{2}\,H_1 + \frac{1-\lambda}{2}\,H_2$$

(where $\lambda = C_A/C_V$). The absolute yield of the reaction $\mu^- + P \rightarrow N + \nu$ from the state $F = 0$ is then equal to

$$W = \frac{8}{\pi^2}\cdot\left(\frac{e^2}{\hbar c}\right)^3\left(\frac{\hbar q_{\nu\,\max}}{m_\mu c}\right)^2\frac{G^2 m_\mu^5 c^4}{\hbar^7} \times \frac{1}{(1+v_N/c)(1+m\ \ /M_p)^3}\left(\frac{1+3\lambda}{4}\right)^2;$$

its ratio with the decay probability for $\mu \rightarrow e + \nu + \tilde{\nu}$ ($W_{\text{decay}} = G^2 m_\mu^5 c^4/192\pi^3\hbar^7 = 1/2.2 \times 10^{-6}\ \text{sec}^{-1}$) is

$$W/W_{\text{decay}} \approx 1.1 \cdot 10^{-3}\left(\frac{1+3\lambda}{4}\right)^2.$$

For $(V - A)$ $(\lambda = 1)$ $W/W_{\text{decay}} \approx 11 \times 10^{-4}$, while for $(V + A)$ $(\lambda = -1)$ $W/W_{\text{decay}} \approx 2.7 \times 10^{-4}$. If $|\lambda| = 1.13$, as in β decay,† $W/W_{\text{decay}} \approx 13 \times 10^{-4}$ (for $\lambda = +1.13$) and $W/W_{\text{decay}} \approx 4 \times 10^{-4}$ (for $\lambda = -1.13$).

Since the formation of the meson molecular ions $(pp)_\mu^+$ in liquid hydrogen complicates the picture of the capture of μ mesons by protons,[8] the experiments have to be carried out with hydrogen of a density 1/20 or 1/30 of the density of liquid hydrogen at 20°K. It is also necessary to use hydrogen purified from deuterium, since in natural hydrogen 25% of the mesons manage to "jump" to the deuterons.[9]

In conclusion we note that the spin correlations of the μ meson (or the electron) with the proton are easily obtained under the assumption that the β decay (or the μ decay) goes through a heavy intermediate particle with spin zero.[10,11] The interaction $(V - A)$ corresponds to a neutral particle (ζ): $N \rightarrow \zeta + \tilde{\nu}$; $\zeta \rightarrow p + e^-$, and the interaction $(V + A)$ corresponds to a charged particle (ζ'): $N \rightarrow \zeta' + e^-$; $\zeta' \rightarrow p + \tilde{\nu}$.

---

*The neutrino is described by the two-component function $\begin{pmatrix}\nu_1 \\ \nu_2\end{pmatrix}$; $|\nu_1|^2 + |\nu_2|^2 = 1$.

†If C_A is renormalized owing to strong interactions, C_A/C_V for the $(\mu\nu PN)$ interaction may, of course, be different from C_A/C_V for the $(e\nu PN)$ interaction (through the influence of the direct decay $\pi \rightarrow \mu + \nu$ alone).

---

[1] R. P. Feynman and M. Gell-Mann, Phys. Rev. **109**, 193 (1958).

[2] R. E. Marshak and E. C. G. Suderman, Nuovo cimento (Preprint).

[3] M. Fierz, Z. Physik **104**, 553 (1936).

[4] Ia. B. Zel'dovich, Izv. Akad. Nauk SSSR, Ser. Fiz., 1954.

[5] S. R. de Groot and H. A. Tolhoek, Physica **16**, 456 (1950).

[6] Bernstein, Lee, Yang, and Primakoff, Phys. Rev. (Preprint).

[7] S. S. Gershtein, J. Exptl. Theoret. Phys. (U.S.S.R.) **34**, 463 (1958), Soviet Phys. JETP **7**, 318 (1958).

[8] Ia. B. Zel'dovich and S. S. Gershtein, J. Exptl. Theoret. Phys. (U.S.S.R.), **8**, 649 (1958), this issue, p. 451.

[9] Alvarez et al., Phys. Rev. **105**, 1127 (1957).

[10] Ila. B. Zel'dovich, Dokl. Akad. Nauk SSSR **89**, 33 (1953).

[11] Tanikawa, Phys. Rev. **10**, 1615 (1958).

Translated by R. Lipperheide
176

NUCLEONIC INTERACTION WHICH PRODUCES A SUPERFLUID STATE OF THE NUCLEUS

V. G. SOLOV' EV

Joint Institute for Nuclear Research

Submitted to JETP editor July 29, 1958

J. Exptl. Theoret. Phys. (U.S.S.R.) **35**, 823-825 (September, 1958)

WE shall consider the possible appearance of superfluid states among medium and heavy nuclei, i.e., states which are energy wise more advantageous than the state of completely degenerate Fermi gas (normal state). In order to do this we shall apply the variational principle of Bogoliubov[1] as it arises from generalizing the method of Fock,[2] and mathematical techniques developed in the theory of superconductivity.[3]

Basing ourselves on the shell model of the nucleus, we shall examine the weak interaction[4] existing among protons (or neutrons) of the same shell with equal and opposite values of the projection of their angular momenta upon the axis of symmetry of the nucleus. Assuming that the shell is characterized by a set of quantum numbers s, the model Hamiltonian may be written in the following form:

$$H=\sum_{s,\,m}\{[E(s,m)-E_F]\,a^{+}_{m+}(s)\,a_{m+}(s)+[E(s,-m)-E_F]\,a^{+}_{-m-}(s)\,a_{-m-}(s)\}+\frac{1}{N}\sum_{\substack{s,\,m,\,m'\\ m\neq m'}}J_0(s\,|\,m,m')\,a^{+}_{m+}(s)\,a^{+}_{-m-}(s)\,a_{-m'-}(s)\,a_{m'+}(s), \tag{1}$$

where N is the number of levels and the other quantities are described in reference 4. Let us make the following canonical transformations.

$$a_{m+}(s)=u_m(s)\,\alpha_{m0}(s)+v_m(s)\,\alpha^{+}_{m1}(s),\qquad a_{-m-}(s)=u_m(s)\,\alpha_{m1}(s)-v_m(s)\,\alpha^{+}_{m0}(s), \tag{2}$$

$$\eta_m(s)=u_m(s)^2+v_m(s)^2-1=0. \tag{3}$$

We shall find the average value of $\overline{H}=\langle C_0^{*}HC_0\rangle$ in the new vacuum $\alpha_{m_1}C_0=\alpha_{m_0}C_0=0$. We then find the functions $u_m(s)$, $v_m(s)$ from the requirement that $\overline{H}$ have a minimum value with the additional condition (3). As a result we obtain the following equation for the new unknown function $C_m(s)$:

$$C_m(s)=-\frac{\dfrac{1}{2N}\sum\limits_{m'}J_0(s\,|\,m,m')\,C_{m'}(s)}{\sqrt{\{\overline{E}(s,m)-E_F\}^2+C_{m'}(s)^2},} \tag{4}$$

thus

$$u_m(s)^2=\frac{1}{2}\left[1+\frac{\overline{E}(s,m)-E_F}{\varepsilon_m(s)}\right]$$

$$v_m(s)^2=\frac{1}{2}\left[1-\frac{\overline{E}(s,m)-E_F}{\varepsilon_m(s)}\right], \tag{5}$$

$$\varepsilon_m(s)=\sqrt{\{\overline{E}(s,m)-E_F\}^2+C_m(s)^2},$$

$$\overline{E}(s,m)=\frac{1}{2}\{E(s,m)+E(s,-m)\}.$$

When the energy is close to the Fermi surface energy we obtain the following approximate solution to Eq. (4) for small values of J

$$C_m(s_0)=\omega\frac{J_0(s_0\,|\,m,m_0)}{J_0(s_0\,|\,m_0,m_0)}\exp\left\{\frac{(m_2-m_1)\,d\overline{E}(s_0,m_0)/dm_0}{J_0(s_0\,|\,m_0,m_0)}\right\},$$

$$\ln\frac{\omega}{\mu}=\frac{1}{2}\int_{m_1}^{m_2}dm'\,\frac{d\overline{E}(s_0,m_0)}{dm_0}\ln\frac{|\overline{E}(s_0,m'-E_F|}{\mu}\times\frac{d}{dm'}\left[\frac{J_0(s_0\,|\,m_0,m')}{J_0(s_0\,|\,m_0,m_0)}\,\frac{1}{d\overline{E}(s,m')/dm'}\right], \tag{6}$$

where $\overline{E}(s_0,m_0)=E_F$. The functions $u_m(s)$ and $v_m(s)$ of the superfluid state are obtained from Eq. (5) and (6), while for the normal state $u_m(s)=1-\theta_F(s,m)$, $v_m(s)=\theta_F(s,m)$ where $\theta_F(s,m)=1$ if $E(s,m)<E_F$, and $\theta_F(s,m)=0$ if $\overline{E}(s,m)>\overline{E}_F$.

We shall now compute the difference ΔE^{I} between the ground and the first excited superfluid states in such a way as to avoid departing from even-even nuclei to odd ones, and we find

$$\Delta E^{I}_m(s)=\langle C_s^{*}\alpha_{m0}(s)\,\alpha_{m1}(s)\,H\alpha^{+}_{m1}(s)\,\alpha^{+}_{m0}(s)\,C_s\rangle-\langle C_s^{*}HC_s\rangle=2\varepsilon_m(s), \tag{7}$$

and for $s=s_0$, $m=m_0$

$$\Delta E^{I}_{m_0}(s_0)\approx 2\omega\exp\left\{\frac{(m_2-m_1)\,d\overline{E}(s_0m_0)/dm_0}{J_0(s_0/m_0,m_0)}\right\}. \tag{7'}$$

It can be seen from this that the first excited state is separated from the ground state by a gap (7′). Note that there is no energy splitting when the normal state is perturbed.

We can find the difference ΔE between the superfluid and normal states in the form

$$\Delta E_m(s) = \langle C^*_{(s)} HC_{(s)}\rangle - \langle C^*_{(n)} HC_{(n)}\rangle$$
$$= -\frac{1}{2}\varepsilon_m(s) - \frac{\{\overline{E}(s, m) - E_F\}^2}{2\varepsilon_m(s)} \qquad (8)$$
$$+ \{\overline{E}(s, m) - E_F\}\{1 - 2\theta_F(s, m)\},$$

and for $s = s_0$, $m = m_0$

$$\Delta E_{m_0}(s_0) = -C_{m_0}(s_0)/2. \qquad (8')$$

From this it may be seen that the superfluid state turns out to be more advantageous energy wise than the normal state and is separated from it.

Thus the interaction among protons of the same shell having equal and opposite z components of angular momentum gives rise to a superfluid state of the atomic nucleus. The presence of an energy split between the first excited and ground superfluid states confirm the considerations of Bohr, Mottelson, and Pines on the possibility of explaining in this way the energy split in heavy even-even nuclei.

In conclusion the author wished to express his profound gratitude to academician N. N. Bogoliubov for his constant interest in this work and for very valuable remarks.

---

[1] N. N. Bogoliubov, Dokl. Akad. Nauk SSSR **119**, 244 (1958), Soviet Phys. "Doklady" **3**, 292 (1958).

[2] V. Fock, Z. Physik **61**, 126 (1930).

[3] Bogoliubov, Tolmachev, and Shirkov, Новый метод в теории сверхпроводимости (New Approach to the Theory of Superconductivity), Acad. Sci. Press, 1958.

[4] V. G. Solov'ev, Dokl. Akad. Nauk SSSR (in press).

[5] Bohr, Mottelson, and Pines (in press).

Translated by M. A. Melkanoff
177

PRODUCTION OF PIONS IN CONDENSED MEDIA BY COSMIC RAYS IN THE STRATOSPHERE

D. K. KAIPOV, V. N. SHAKHOROSTOV, and Iu. G. KOSIAK

Institute for Nuclear Physics, Academy of Sciences, Kazakhstan S.S.R.

Submitted to JETP editor May 16, 1958

J. Exptl. Theoret. Phys. (U.S.S.R.) **35**, 825-826 (September, 1958)

EXPERIMENTS designed to study the dependence of the cross section for meson production by low energy particles on the atomic weight A have shown that this dependence is not stronger than the $A^{2/3}$ law for elements up to aluminum, and somewhat weaker than $A^{2/3}$ for heavy nuclei.[1,2] For primary protons with an energy of 3 Bev the cross section for meson production increases as A for elements up to aluminum and somewhat faster than $A^{2/3}$ for heavier elements.[3]

We report here data on production of very slow π mesons in condensed media by cosmic rays in the stratosphere. Unbounded photoemulsions of 10 cm diameter and 400 μ thickness were used to detect the slow mesons; 12×12 cm aluminum and lead plates of varying thicknesses were used as targets. The photoemulsions were pressed between two plates of aluminum or lead, lifted into the stratosphere in balloon probes and irradiated by cosmic

TABLE I

Substances surrounding the emulsion	Thickness in g/cm²	Number of mesons per cm² including prongless stars		Total number of π-mesons in a g/cm² of the substance and in a cm² of the emulsion after geometric correction	Upper limit of meson energy E_0 in Mev, estimated from the thickness of the target substance
		π^+	π^-		
Packing material		0.17±0.06 *	0.53±0.12		
Aluminum	1.62	0.58±0.09	1.28±0.15	0.75±0.13	13.5
	2.7	0.84±0.12	1.68±0.21	0.73±0.11	18
	5.4	1.79±0.17	3.19±0.25	0.94±0.07	27.5
Lead	2.27	0.34±0.07	1.90±0.19	0.68±0.1	12
	4.54	0.92±0.13	3.96±0.32	0.94±0.08	18
	6.80	1.51±0.16	4.30±0.32	0.80±0.06	23
	11.34	2.04±0.20	4.84±0.37	0.59±0.05	31

*The errors shown are purely statistical.

rays for 12 hours at an altitude of 28 to 30 km. The developed photoemulsions were scanned under microscope and $\pi \rightarrow \mu$ decays and σ captures were noted. Table I shows the results of the study.

In order to allow conclusions about the π-meson production cross section to be drawn from the table, we calculated and included corrections for the geometry of the experiment. As can be seen, the geometry of the experiment significantly affects the results, particularly when the target substance and detector are of comparable dimensions.

Assuming that the energy spectrum of the mesons produced in aluminum and lead in the energy region under study is of the form $n(E)dE = kE^{0.6}dE$ (E is the kinetic energy of produced mesons),[4] the total number of mesons with energy less than E_0 is given by

$$N(< E_0) = aE_0^{1.6}$$

Using this relation and the data of Table I we calculated lead to aluminum ratios of cross sections for production of mesons for various thicknesses of the target substance. They are given in Table II together with values of the coefficient a.

TABLE II

Target substance	Thickness (cm)	$a \cdot 10^{-4}$	σ_{Pb}/σ_{Al}
Al Pb	0.6 0.2	186.6±32.6 128 ±19	5.30±0.22
Al Pb	0.6 0.4	186.6±32.6 147.0±12.7	6.03±0.51
Al Pb	0.6 0.6	186.6±32.6 84.8± 6.6	3.70±0.88
Al Pb	1 1	147.7±15.7 38.8± 2.5	2.60±0.46

As can be seen from Table II, the lead-to-aluminum meson production cross section ratio increases with decreasing E_0 and, probably, becomes larger than the geometric $\sigma_{Pb}/\sigma_{Al} = 3.9$ for low-energy mesons.

The authors express gratitude to R. Suzhikova for help in emulsion scanning.

---

[1] R. Sagane and W. Dudziak, Phys. Rev. **92**, 212 (1953).

[2] Meshkovskii, Pligin, Shalamov, and Shebanov, J. Exptl. Theoret. Phys. (U.S.S.R.) **31**, 987 (1956), Soviet Phys. JETP **4**, 842 (1957).

[3] D. Berley and G. Collins, Bull. Am. Phys. Soc. **1**, 320 (1956).

[4] H. Jagoda, Phys. Rev. **85**, 891 (1952).

Translated by A. Bincer

METHOD FOR DETERMINING HYPERON POLARIZATION IN THE REACTION $\pi + p \rightarrow Y + K$

S. M. BILEN'KII and R. M. RYNDIN

Joint Institute for Nuclear Research

Submitted to JETP editor July 26, 1958

J. Exptl. Theoret. Phys. (U.S.S.R.) **35**, 827-828 (September, 1958)

THE polarization of hyperons is one of the main features of the interactions that lead to the production of strange particles. On the other hand, the asymmetry in the subsequent decay of the polarized hyperons is specified by the product of the polarization and the asymmetry coefficient;[1,2] for the determination of the latter quantity, the polarization of the hyperon has to be known.

In the present note we propose a method for determining the polarization of the hyperon in the reactions

$$\pi + p \rightarrow (\Sigma, \Lambda) + K, \quad K + p \rightarrow (\Sigma, \Lambda) + \pi. \qquad (1)$$

The method consists of measuring the asymmetry of the K or π mesons produced in the reactions (1) with a polarized proton target. We shall show that in this case the asymmetry gives directly the polarization of the hyperon in the reaction with an unpolarized proton target.

The matrix for a reaction of type (1) in the most general form can be written as

$$M = a + \mathbf{b} \cdot \sigma \qquad (2)$$

(the hyperon spin is ½, the K-meson spin is zero). The density matrix of the initial state is

$$\rho_0 = (1 + \mathbf{P}_0 \cdot \sigma)/2, \qquad (3)$$

where $\mathbf{P}_0$ is the polarization of the target protons.

Using (2) and (3) we obtain the following expression for the differential cross section

$$\sigma(\theta, \varphi) = (aa^* + \mathbf{b} \cdot \mathbf{b}^*)\left(1 + \mathbf{P}_0 \frac{a^*\mathbf{b} + a\mathbf{b}^* + i[\mathbf{b}^* \times \mathbf{b}]}{aa^* + \mathbf{b} \cdot \mathbf{b}^*}\right). \qquad (4)$$

Now we compute the polarization of the hyperon for the case of the unpolarized proton target and obtain

$$\mathbf{P} = \frac{a\mathbf{b}^* + a^*\mathbf{b} + i[\mathbf{b} \times \mathbf{b}^*]}{aa^* + \mathbf{b} \cdot \mathbf{b}^*}. \qquad (5)$$

Two cases arise according to the intrinsic parity of the particles involved in the reaction.

1. The intrinsic parity does not change, i.e., $I_\pi I_p = I_Y I_K$. Here the matrix (2) is scalar and $\mathbf{b} = b_0 \times [\mathbf{k} \times \mathbf{k}']$, where $\mathbf{k}$ and $\mathbf{k}'$ are unit vec-

tors in the directions of the relative momenta of the initial and final states. From (4) and (5) we have

$$\sigma = \sigma_0(1 + \mathbf{P}_0 \cdot \mathbf{P}); \quad \mathbf{P} = \frac{ab_0^* + a^* b_0}{aa^* + bb} [\mathbf{k} \times \mathbf{k}'], \qquad (6)$$

where σ_0 is the cross section of the unpolarized protons.

2. The intrinsic parity changes, i.e., $I_\pi I_p = -I_Y I_K$. The matrix (2) is pseudoscalar with $a = 0$ and $\mathbf{b} = b_1\mathbf{k} + b_2\mathbf{k}'$. In this case we have

$$\sigma = \sigma_0(1 - \mathbf{P}_0 \cdot \mathbf{P}); \quad \mathbf{P} = i\,\frac{b_1 b_2^* - b_2 b_1^*}{\mathbf{b} \cdot \mathbf{b}^*} [\mathbf{k} \times \mathbf{k}']. \qquad (7)$$

Finally we obtain

$$\sigma(\theta, \varphi) = \sigma_0(1 \pm P_0 P \sin(\delta - \varphi)), \qquad (8)$$

where δ is the azimuth of the initial polarization vector ($\mathbf{P}_0$ is in the plane perpendicular to $\mathbf{k}$). Hence the asymmetry is equal to

$$e(\theta) = \pm P_0 P \sin \delta. \qquad (9)$$

Thus a measurement of the reaction (1) with a polarized target would permit a determination of the polarization P of the hyperon in the reaction with an unpolarized target. If the parity (KY) relative to (πp) is known, then this experiment would also allow one to determine the sign of the polarization. On the other hand, if the sign of the polarization is determined from the hyperon decay, then the proposed experiment would afford a possibility to determine the relative parity (KY).

---

[1] F. S. Crawford et al., Phys. Rev. **108**, 1102 (1957).

[2] T. D. Lee et al., Phys. Rev. **106**, 1367 (1957).

Translated by J. Heberle
179

SOME REMARKS ON THE STRUCTURE OF SHOCK WAVES

G. S. GOLITSYN and K. P. STANIUKOVICH

Bauman Higher Technical School

Submitted to JETP editor June 9, 1958

J. Exptl. Theoret. Phys. (U.S.S.R.), **35**, 828-830 (September, 1958)

1. The behavior of entropy in the transition zone of a not very strong shock wave is described by the general heat-transfer equation. Ia. B. Zel'dovich has shown that in a gas with a high thermal conductivity and negligible viscosity the entropy goes through a maximum and in that case the speed of sound in the system of coordinates associated with the discontinuity is equal to the local speed of sound.[1] We shall show that this coincidence also occurs in other cases. For a maximum to exist we must have a non-hydrodynamic energy flux associated above all with the thermal conductivity, since the viscosity alone can only increase the entropy. If we differentiate with respect to V (specific volume) the condition of the conservation of momentum flux at the point $dS = 0$ we obtain:

$$\left(\frac{dp}{dV}\right)_S = -m^2 + \left(\frac{4}{3}\mu + \zeta\right)\frac{d}{dV}\left(\frac{du}{dx}\right)$$

$$= -m^2 + \left(\frac{4}{3}\mu + \zeta\right)\frac{d^2u}{dx^2} \Big/ \frac{dV}{dx}. \qquad (1)$$

The last term is equal to zero since at the point $S = S_{max}$ the velocity has a point of inflection, which can be shown to exist both in the case of weak waves,[2] and also in the case of waves of arbitrary intensity. At the same time $(dp/dV)_S = -m^2 = -\rho^2 u^2$, from which it follows that $\pm u = c_0$.

If we now turn to magnetohydrodynamics, then finite conductivity (Joule heat) alone can only increase the entropy. It may go through a maximum if we take thermal conductivity into account. Then, by investigating the conditions for the conservation of momentum flux and of the magnetic field perpendicular to the flow of gas,[3] it can be shown that a maximum exists when $\pm u = c_m = (c_0^2 + H^2/4\pi\rho)^{1/2}$, if the field has a point of inflection at this point.

If the influence of thermal conductivity or of any kind of diffusion is predominant while the viscosity and the Joule heat can be neglected, then the coincidence noted above can be easily established even in the relativistic case. It is of interest to note that under these circumstances, in the case of detonation, the process passes through the Jouguet point twice: the first time when the medium undergoes shock compression, but subsequently the removal of heat due to thermal conductivity lowers the entropy, and the process arrives at a point on the Hugoniot adiabatic, and from there the initiated detonation again brings the process to the Jouguet point.

2. We shall investigate qualitatively some aspects of the physical picture of the structure of a normal shock wave in magnetohydrodynamics. In this case a new type of dissipation, Joule heat, appears and manifests itself in the formula for the entropy discontinuity in a weak wave:[4]

$$T\Delta S = \frac{1}{12}\left(\frac{\partial^2 V}{\partial p^2}\right)_S (\Delta p)^3 - \frac{1}{16\pi}\left(\frac{\partial V}{\partial p}\right)_S \Delta p\,(\Delta H)^2 = \frac{\gamma+1}{12}\,c_0^2\left(\frac{\Delta\rho}{\rho}\right)^3\left(1+\frac{3\eta}{\gamma+1}\right), \tag{2}$$

where $\eta = H^2/4\pi\rho c_0^2$ is the ratio of the Alfven velocity to the velocity of sound. The Joule dissipation predominates for $\eta > 1$. It can also be estimated directly:

$$T\Delta S = \int \frac{j^2}{\rho\sigma}\,dt = \frac{c^2}{(4\pi)^2\sigma}\int\limits_0^L \left(\frac{dH}{dx}\right)^2 \frac{dx}{m} \approx \frac{\nu_m}{4\pi}\,\frac{(\Delta H)^2}{mL}, \tag{3}$$

where, for example, $L = \Delta H\,(dH/dx)_{\mathrm{max}}$. On comparing (3) and the last term in (2) we obtain:

$$L \approx -\frac{4\nu_m}{(\partial V/\partial p)_S\,\Delta p m} = \frac{4\rho^2 c_0^2 \nu_m}{m\Delta p} = \frac{4\rho}{\Delta\rho}\,\frac{\nu_m}{c_m}. \tag{4}$$

This result depends somewhat on the method of averaging, but in order of magnitude we always have $L \approx \nu_m/c_m$. If we measure the variation of the field in the shock wave by some kind of induction method, we can estimate the conductivity of the medium.

As σ increases $(\nu \to 0)$ the width of the front decreases, but the field gradients increase in such a way that the discontinuity in the entropy depends only on the discontinuity in the field. While the problem is formulated with the conductivity considered infinite everywhere, this is not the case inside the transition zone. In a reference system associated with the discontinuity front, there exists throughout the whole space an electric field given by $\mathbf{E} = (\mathbf{u}_1 \times \mathbf{H}_1)/c$. Behind the front both the magnetic field and the velocity vary and currents appear:

$$-dH/dx = 4\pi j/c = (E - uH/c)\,4\pi\sigma/c = (H' - H)\,u/\nu_m, \tag{5}$$

where

$$H' = \frac{c}{u}E = \frac{c}{u}\,\frac{u_1}{c_1}\,H_1 = \frac{\rho}{\rho_1}\,H_1.$$

Thus H' is the field which exists at the given point under the condition of being "frozen in." The equation shows that the field gradually approaches its "frozen-in" equilibrium value. The conductivity determines only the method of relaxation.

We give also the coefficient of absorption for sound propagated at right angles to the field in a medium of sufficiently high conductivity,

$$\alpha = (\omega^2/2c_m^3)\,[{}^4/_3\nu + \zeta/\rho + (\gamma-1)\chi/c_p + \nu_m H^2/4\pi\rho c_m^2] = a\omega^2, \tag{6}$$

where ω is the frequency, ν and ξ are the kinematic and the volume viscosities of the medium, and $\chi\rho$ is the coefficient of thermal conductivity. In the case $H = 0$ formula (6) reduces to the usual formula for the damping coefficient of a sound wave.[2] In classical gas dynamics the corresponding parameter a determines, for a given Δp, the smearing of the front of a weak shock wave.[2] As the field increases the value of our quantity a decreases, and this shows that the dimensions of the transition zone decrease, while everything else remains the same. This can also be seen from (4).

In conclusion, we express our thanks to Ia. B. Zel'dovich and S. B. Pikel'ner for discussions which were useful to the authors.

---

[1] Ia. B. Zel'dovich, Теория ударных волн и введение в газодинамику (Theory of Shock Waves and Introduction to Gas Dynamics) Acad. Sci. Press, 1946, § XII.

[2] L. D. Landau and E. M. Lifshitz, Механика сплошных сред (Mechanics of Continuous Media), GITTL, 1954, §§ 77, 87.

[3] G. S. Golitsyn and K. P. Staniukovich, J. Exptl. Theoret. Phys. (U.S.S.R.) **33**, 1417 (1957), Soviet Phys. JETP **6**, 1090 (1958).

[4] L. D. Landau and E. M. Lifshitz, Электродинамика сплошных сред (Electrodynamics of Continuous Media), Moscow, Gostekhizdat, 1957, § 54.

Translated by G. Volkoff
180